Conf-801128

NEWARK PUBL'C LIBRARY

FEB 10 1981

U. S. GOVT. PUBS.
DEPOSITORY 376

Proceedings of

Mechanical, Magnetic, and Underground Energy Storage 1980 Annual Contractors' Review

Prepared for:
U.S.Department of Energy
Assistant Secretary for
Conservation and Solar Energy
Office of Advance Conservation
and Technologies

Under Contract No. AC06-76RL01830

E1.10:

NOTICE

This report was prepared as an account of work sponsored by the United States Government. Neither the United States nor the United States Department of Energy, nor any of their employees, makes any warranty, express or implied, or assumes any legal liability or responsibility for the accuracy, completeness, or usefulness of any information, apparatus, product, or process disclosed, or represents that its use would not infringe privately owned rights. Reference herein to any specific commercial product, process, or service by trade name, mark, manufacturer, or otherwise, does not necessarily constitute or imply its endorsement, recommendation, or favoring by the United States Government or any agency thereof. The views and opinions of authors expressed herein do not necessarily state or reflect those of the United States Government or any agency thereof.

Available from:

National Technical Information Service (NTIS)
U.S. Department of Commerce
5285 Port Royal Road
Springfield, Virginia 22161

Price: Printed Copy: $33.50
Microfiche: $4.00

Conf-801128
Dist. Categories UC 94,94b,94E

Proceedings of

Mechanical, Magenetic, and Underground Energy Storage 1980 Annual Contractors' Review

Prepared by:
MCC Associates, Inc.
Batelle/Pacific Northwest Laboratories
Richland, Washington 99352
Under Contract No. AC06-76-RL01830

Prepared for:
U.S. Department of Energy
Assistant Secretary for
Conservation and Solar Energy
Washington D.C. 20585

blank page

MECHANICAL, MAGNETIC, and UNDERGROUND ENERGY STORAGE 1980 ANNUAL CONTRACTORS' REVIEW

Washington, D.C.
November 10-13, 1980

INTRODUCTION i

TABLE OF CONTENTS iii

SEASONAL THERMAL ENERGY STORAGE PROGRAM

SEASONAL THERMAL ENERGY STORAGE PROGRAM
James E. Minor (Pacific Northwest Laboratory) 5

AQUIFER THERMAL ENERGY STORAGE PROGRAM MANAGEMENT (Summary)
Kenneth Fox (Pacific Northwest Laboratory) 9

BETHEL, ALASKA, ATES PROJECT
Jack Cherne (TRW) 10

AQUIFER THERMAL ENERGY STORAGE SYSTEM AT THE UNIVERSITY OF MINNESOTA
Warren E. Soderberg (University of Minnesota) 17

CONCEPTUAL DESIGN-ATES DEMONSTRATION PROJECT, S.U.N.Y., STONY BROOK, N.Y.
Louis I. Stern (Dames & Moore) 27

TECHNICAL SUPPORT PROGRAM MANAGEMENT (Summary)
Jay R. Eliason (Pacific Northwest Laboratory) 34

LEGAL AND REGULATORY ISSUES APPLICABLE TO AQUIFER THERMAL ENERGY STORAGE
Paul L. Hendrickson (Pacific Northwest Laboratory) 35

ECONONIC ASSESSMENT OF AQUIFER THERMAL ENERGY STORAGE
R. W. Reilly, D. R. Brown, & H. D. Huber
(PACIFIC NORTHWEST LABORATORY) 38

DEVELOPMENT OF A METHODOLOGY FOR CONCEPTUAL DESIGN AND EVALUATION OF ATES SYSTEMS
Charles F. Meyer, Walter Hausz (General Electric Company) 42

ENVIRONMENTAL ASSESSMENT
George E. Wukelic and Jon C. Zuck (Pacific Northwest Laboratory) 47

PROGRAMMATIC ENVIRONMENTAL ASSESSMENT (DOCUMENTATION)
Donald W. Lee (Oak Ridge National Laboratory) 52

ENVIRONMENTAL ANALYSIS/CONSULTING-ATES DEMONSTRATIONS
Heather McCartney (Resource Management and Assessment) 56

FIELD TEST FACILITY
David A. Myers (Pacific Northwest Laboratory) 62

MOBILE, ALABAMA FIELD TEST FACILITY
F. Molz, A. David Parr and Joel G. Melville (Auburn University) 64

SITE EXPLORATION AND CHARACTERIZATION NEAR BELLINGHAM, WASHINGTON (Summary)
Carl A. Johnson (Fugro, Inc.) 71

COMPENDIA OF EXISTING INFORMATION TASK
Leigh S. Prater (Pacific Northwest Laboratory) 72

STES TECHNICAL INFORMATION SYSTEM
Viktor E. Hampel (Lawrence Livermore Laboratory) 77

MAINTENANCE AND DEVELOPMENT OF THE SEASONAL THERMAL ENERGY STORAGE (STES) LIBRARY (Summary)
Charles H. Lee (Midwest Research Institute) 83

PUBLICATION OF THE SEASONAL THERMAL ENERGY STORAGE (STES) NEWSLETTER (Summary)
Chin Fu Tsang (Lawrence Berkeley Laboratory) 84

SURVEY OF GROUND-WATER REINJECTION EXPERIENCE IN AIR CONDITIONING APPLICATIONS (Summary)
Charles H. Lee (Midwest Research Institute) 85

REGIONAL AQUIFER ASSESSMENT STUDY (Summary)
Dorothy Stoffel (Century West Engineering) 86

DOCUMENT ON AQUIFER THERMAL ENERGY STORAGE SITE CHARACTERIZATION METHODS (Summary)
David D. Hostetler (Consulting Engineer) 87

SURVEY OF GROUND-WATER SOURCE HEAT PUMP OPERATIONS IN THE PORTLAND AREA (Summary)
Gordon Reistad (Oregon State University) 88

PHYSICOCHEMICAL PROPERTIES ANALYSES IN SUPPORT OF THE SEASONAL THERMAL ENERGY STORAGE PROGRAM
James A. Stottlemyre (Battelle, Pacific Northwest Laboratory) 89

FLOW FACILITY DEVELOPMENT AND LABORATORY ANALYSIS
C. H. Cooley, Lawrence B. Owen, C. Kim Blair and Gary J. BaniK (Terra Tek, Inc.) 96

NUMERICAL SIMULATION OF AQUIFER THERMAL ENERGY STORAGE FACILITIES
C. T.Kincaid (Pacific Northwest Laboratory) 103

EXTENSION OF ISOTHERMAL SIMULATION CODE TO THE NON-ISOTHERMAL REGIME (Summary)
Sumant K. Gupta (George Maddox & Associates) 107

MATHEMATICAL STUDIES IN AQUIFER THERMAL ENERGY STORAGE
Chin Fu Tsang (Lawrence Berkeley Laboratory) 108

STUDY OF COUPLED ENERGY AND MASS TRANSPORT IN GEOLOGIC MEDIA (Summary)
Stuart Childs (Oregon State University) 115

HYDROLOGIC STUDIES SUPPORT (Summary)
J. W. Crosby III, Vernon Ichimura (Washington State University) 116

NON-AQUIFER SEASONAL THERMAL ENERGY STORAGE CONCEPTS
Donald E. Blahnik (Pacific Northwest Laboratory) 117

READEX FICHE best copy available

COMPRESSED AIR ENERGY STORAGE (CAES) PROGRAM

CAES AND UPHS PROGRAM OVERVIEW
Walter V. Loscutoff (Pacific Northwest Laboratory) 125

PNL SECOND-GENERATION CONCEPTS STUDIES
M.K. Drost, R.W. Reilly, J.K. Young and F.R. Zaloudek
(Pacific Northwest Laboratory) 131

AES/FBC STUDIES
Robert D. Lessard and William A. Blecher
(United Technologies Research Center) 137

ADIABATIC CAES IN HARD ROCK
C.L. Driggs (Acres American Incorporated) 147

ANALYTICAL MODELING OF THE CHAMPAGNE EFFECT
D.S. Rowe and C.A. McMonagle (Rowe & Associates) 177

RESERVOIR STABILITY STUDIES
T.J. Doherty (Pacific Northwest Laboratory) 184

NUMERICAL STUDIES OF SALT CAVITIES
Shosei Serata and J. McNamara (Serata Geomechanics, Inc.) 192

LABORATORY STUDIES OF ROCK SALT
R.L. Thoms (Louisiana State University) 199

NUMERICAL MODELING TO PREDICT BEHAVIOR OF UNDERGROUND HARD ROCK CAVERNS USED FOR COMPRESSED AIR ENERGY STORAGE
Arlo F. Fossum (RE/SPEC Inc.) 206

LABORATORY STUDIES OF HARD ROCK FOR CAES
Arlo F. Fossum (RE/SPEC Inc.) 213

AIR/WATER/ROCK INTERACTIONS IN A CAES POROUS ROCK RESERVOIR
J.A. Stottlemyre (Pacific Northwest Laboratory) 220

FIELD STUDIES OF POROUS ROCK RESERVOIRS
Neil Rudd (Dames & Moore) 227

MAGNETIC ENERGY STORAGE PROGRAM

MAGNETIC ENERGY STORAGE PROGRAM OVERVIEW
Mitchell O. Hoenig (Massachusetts Institute of Technology) 237

WIRE ROPE SUPERCONDUCTING CABLE FOR DIURNAL LOAD LEVELING SMES
George Costello (University of Illinois) 243

EFFECTS OF SMES UNITS ON POWER SYSTEM STABILITY
J.A. Juves and R.T. Byerly (Westinghouse Electric Company) 249

30MJ SUPERCONDUCTING MAGNETIC ENERGY STORAGE FOR BPA TRANSMISSION LINE STABILIZER
Robert I. Schermer (Los Alamos Scientific Laboratory) 255

30MJ SUPERCONDUCTING COIL DESIGN AND FABRICATION
John Purcell (General Atomic Company) 263

DIURNAL SUPERCONDUCTIVE ENERGY STORAGE SYSTEM DESIGN
Y.M. Eyssa and R.W. Boom (University of Wisconsin) 270

CONDUCTOR AND STRUCTURAL COMPONENT STUDIES FOR DIURNAL ENERGY STORAGE
S.W. Van Sciver, K.S. Han, K.T. Hartwig, G.F. McIntosh and W.C. Young (University of Wisconsin) 279

CONDUCTOR DESIGN AND DEVELOPMENT FOR SUPERCONDUCTING MAGNETIC ENERGY STORAGE MAGNETS
D.C. Larbalestier, K.T. Hartwig, A.W. West, and D.L. Moffat (University of Wisconsin) 287

FLYWHEEL ENERGY STORAGE PROGRAM

AN OVERVIEW OF THE MECHANICAL ENERGY STORAGE TECHNOLOGY (MEST) PROJECT
Thomas M. Barlow (Lawrence Livermore Laboratory) 299

MECHANICAL ENERGY STORAGE TECHNOLOGY APPLICATION TO ELECTRIC VEHICLES
E.P. Cornell (General Electric Corp.) 307

FLYWHEEL/HEAT ENGINE VEHICLE APPLICATIONS ANALYSIS
Norman H. Beachley and Andrew Frank (University of Wisconsin) 315

FLYWHEEL/HEAT ENGINE VEHICLE DESIGN AND ANALYSIS
I. Kalns (Eaton Engineering & Research Center) 324

REGENERATIVE BRAKING THROUGH ELASTOMERIC ENERGY STORAGE
Lyle O. Hoppie (Eaton Engineering & Research Center) 328

PHOTOVOLTAIC ENERGY SYSTEM APPLICATIONS OF FLYWHEEL TECHNOLOGY
P.O. Jarvinen
(Massachusetts Institute of Technology/Lincoln Laboratory) 340

DEVELOPMENT AND ASSESSMENT OF STATIONARY FLYWHEEL STORAGE TECHNOLOGIES
David B. Eisenhaure (The Charles Stark Draper Laboratory) 346

CONTINUED DEVELOPMENT OFTHE BAND-TYPE VARIABLE INERTIA FLYWHEEL
David Ullman (Union College) 355

APPLICATIONS OF CELLULOSIC MATERIALS IN FLYWHEEL ROTORS
David L. Hagen, Arthur G. Erdman and Scott A. Gaff (University of Minnesota) 363

THE ALPHA-PLY LAMINATED-DISC FLYWHEEL ROTOR
Ronald P. Nimmer (General Electric Company) 370

THE TAPERED-THICKNESS-DISC FLYWHEEL ROTOR (Summary)
Satish V. Kulkarni (Lawrence Livermore Laboratory) 379

EVALUATION OF COMPOSITE FLYWHEEL MATERIALS CONSTRUCTION
Alan D. Sapowith (AVCO Systems Division) 380

FLYWHEEL TECHNOLOGY DEVELOPMENT AT APL
D.W. Rabenhorst
(The Johns Hopkins University Applied Physics Laboratory) 385

COMPRESSION MOLDED LOW-COST COMPOSITE ROTORS
J.F. Kay (Owens Corning) 393

FABRICATION OF HIGH PERFORMANCE, FILAMENT-WOUND FIBER COMPOSITE RINGS
Alan J. Hannibal (Lord Kinematics) 407

REVIEW OF FLYWHEEL CONTAINMENT TECHNOLOGY
Alan D. Sapowith and Emmett A. Witmer (AVCO Systems Division) 414

FLYWHEEL CONTAINMENT TECHNOLOGY ASSESSMENT
Anthony P. Coppa and Carl H. Zweben (General Electric) 419

FIBER COMPOSITE MATERIALS TECHNOLOGY DEVELOPMENT
T.T. Chiao (Lawrence Livermore Laboratory) 428

ENGINEERING PROPERTIES DETERMINATION FOR FIBER COMPOSITE MATERIALS
H. Thomas Hahn and W.K. Chin (Washington University) 435

FLYWHEEL TESTS AT THE OAK RIDGE FLYWHEEL EVALUATION LABORATORY
Robert S. Steele and E. F. Babelay (Union Carbide) 443

PROGRAM AGENDA 452

LIST OF ATTENDEES 456

Dr. James H. Swisher, Acting Director of DOE's Division of Thermal and Mechanical Energy Storage Systems, welcomes participants to the Contractors' Review.

BETHESDA
rriott Hotel

Dr. Theodore B. Taylor delivers the banquet address, "The Need for Annual Storage of Heat and Cold."

ELECTRONIC COMMUNICATIONS
DISTRIBUTED NETWORK
Technology Information System

William A. Frier, Project Manager of the Seasonal Thermal Energy Storage Program, reviews an exhibition of Lawrence Livermore Laboratory's Technology Information System.

INTRODUCTION

The Mechanical, Magnetic, and Underground Energy Storage Programs of the Office of Advanced Conservation Technologies of the Department of Energy (DOE) are developing reliable, efficient and economic energy storage technologies to support other DOE end-use divisions in their energy substitution and energy-savings missions. The technologies being developed will contribute to the reliability of renewable energy systems such as solar and wind energy. By load leveling and reduction of seasonal peak load they will reduce capital and operating expense in conventional systems and accelerate load shifting to coal, nuclear, or solar thermal electric systems. The mechanical storage technologies, applicable to vehicle shaft power, will contribute to fuel savings in individual vehicles and mass transport systems.

Implementation of the Mechanical, Magnetic and Underground Energy Storage Programs under the direction of Saul Strauch has been assigned to lead laboratories and universities. These lead assignments and program elements for FY 1980 are as follows:

UNDERGROUND ENERGY STORAGE PROGRAM

Lead Laboratory: Pacific Northwest Laboratory

Seasonal Thermal Energy Storage (STES)
James E. Minor, Program Manager

The goals of the STES Program are to demonstrate the economic storage and retrieval of energy on a seasonal basis, using heat or cold available during a surplus period to reduce peak period demand; reduce electric utilities peaking problems; and contribute to the establishment of favorable economics for solar heating and cooling systems.

Seasonal storage in aquifers will be evaluated in the Aquifer Thermal Energy Storage (ATES) Demonstration Program. A parallel Technical Support Program will provide data on aquifer behavior, data from field tests and economic and mathematic modeling data. Previous work on earth storage, and work under the International Energy Agency on pond, lakes, tanks, and constructed caverns will be evaluated and additional field tests or demonstrations recommended, if appropriate.

Compressed Air Energy Storage (CAES)
Landis D. Kannberg, Program Manager

The goals of the CAES Program are to develop design and stability criteria for long-term operation of underground reservoirs used for CAES in order to accelerate the commercialization of the concept; and to develop and assess second-generation technologies for CAES that require little or no supplementary firing by petroleum fuels in order to eliminate the dependence of CAES on these fuels.

SUPERCONDUCTING MAGNETIC ENERGY STORAGE PROGRAM (SMES)

Technical Consultant: Francis Bitter National Magnet
Laboratory (MIT)

T. M. Barlow, Program Manager

The goals of the MEST Program are to develop, demonstrate, and evaluate mechanical energy storage technology for vehicular and fixed-base applications and to carry out the research, development and demonstration activities in a manner that maximizes the commercialization potential of the technology.

This proceedings volume for the Annual Mechanical, Magnetic and Underground Energy Storage Review Meeting contains the program overviews and contractor summaries and reports presented at the meetings. The summaries and reports were prepared by the responsible individuals/organizations. No technical editing or evaluation has been performed by PNL or DOE.

James E. Minor, Chairman
Mechanical, Magnetic and Underground Storage Review Meeting

SEASONAL THERMAL

ENERGY STORAGE PROGRAM

blank page

PROJECT SUMMARY

Project Title: Seasonal Thermal Energy Storage Program

Principal Investigator: James E. Minor

Organization:
Pacific Northwest Laboratory
P.O. Box 999
Richland, Washington 99352
(509) 376-0694 (FTS: 444-0694)

Project Goals: Demonstrate the economic storage and retrieval of energy on a seasonal basis, using heat or cold available during a surplus period to reduce peak period demand; reduce electric utilities peaking problems; and contribute to the establishment of favorable economics for solar heating and cooling systems.

Seasonal storage in aquifers will be evaluated in the Aquifer Thermal Energy Storage (ATES) Demonstration Program. A parallel Technical Support Program will provide data on aquifer behavior, data from field tests and economic and mathematic modeling data. Previous work on earth storage, and work under the International Energy Agency on pond, lakes, tanks, and constructed caverns will be evaluated and additional field tests or demonstrations recommended, if appropriate.

Project Status: Conceptual design studies, including aquifer characterization, have been initiated at three sites. This Phase I work will be completed in FY-1982.

Eight technical support tasks have been initiated. Contracted work under these tasks is discussed individually. The field test site for lower temperature tests (55-125°C) has been redesigned and completion of the modified well field is in progress.

Evaluation of existing data for other methods of seasonal storage is proceeding, and IEA work on seasonal storage methods is being monitored.

Contract Number: DE-AC06-76RLO 1830

Contract Period: Continuing

Funding Level: FY-1980 $5,190K BO/$5,729K BA

Funding Source: U.S. Department of Energy, Office of Advanced Conservation Technologies

SEASONAL THERMAL ENERGY STORAGE PROGRAM

James E. Minor
Pacific Northwest Laboratory
P.O. Box 999
Richland, Washington 99352

INTRODUCTION

The Pacific Northwest Laboratory (PNL) was assigned management of the Seasonal Thermal Energy Storage Program (STES) by the DOE Office of Advanced Conservation Technologies in April, 1979. PNL formed the Seasonal Thermal Energy Storage Program Office for this purpose. STES Program plans have been formulated; work breakdown structures developed and modified as planning proceeded, and a matrix of external contracts have been placed. The research and demonstration work of the STES Program is being performed by industry, universities, and PNL and other DOE laboratories.

In this overview, the STES Program incentives, objectives, and long-range implementation plan for achieving program goals are described. Procurements in progress in the Demonstration Program will be described in subsequent papers. Specific projects contributing to technical studies will be discussed by contractor representatives supplemented by PNL and other DOE laboratory staff.

PROGRAM INCENTIVES

Storage of thermal energy is expected, in the near term, to provide a significant contribution toward achieving the goals of the National Energy Plan. This contribution will encourage a shift from use of insufficient or costly fuels such as oil and natural gas to more abundant or available energy sources such as coal, solar, and nuclear power. Thermal energy storage, when incorporated in energy supply and conservation systems, permits efficient and economical use of intermittent energy sources such as solar or off-peak electrical power. Thermal storage also may allow use of waste heat from industrial and utility sources.

The STES Program is designed to demonstrate the storage and retrieval of energy on a seasonal basis, using heat or cold available from waste or other sources during a surplus period to reduce peak period demand, reduce electric utility load problems, and contribute to the establishment of favorable economics for district heating and cooling systems for commercialization of the technology. Aquifers, ponds, earth, and lakes have potential for seasonal storage. The initial thrust of the STES Program is toward utilization of ground-water systems (aquifers) for thermal energy storage.

During the last decade, the storage of thermal energy in aquifers has received considerable attention. The motivations for storing large quantities of thermal energy on a long-term basis have been identified, including: a) the need to store solar heat that is collected in the summer for use in the winter months; b) the cost effectiveness of utilizing heat now wasted in electrical generation plants; c) the need to profitably use industrial waste heat; and d) the need to more economically provide summer cooling for buildings. Seasonal aquifer storage should make significant contributions to the satisfaction of these needs. Most geologists and ground-water hydrologists agree that heated and chilled water can be injected, stored, and recovered from aquifers. Geologic materials are good thermal insulators, and there are potentially suitable aquifers distributed throughout the United States. Recent studies and small-scale field experiments have reported energy recovery rates above 70 percent for seasonal storage. The U.S. Department of Energy predicts that, by the year 2000, seasonal aquifer storage could replace or conserve up to 350 million barrels of oil per year. However, demonstration of large-scale aquifer thermal energy storage is under initial study and the concept's economic feasibility and institutional acceptability have yet to be established.

Many potential energy sources exist for use in an aquifer thermal energy storage system. These include solar heat, power plant cogeneration, winter chill, and industrial waste heat sources such as aluminum plants, paper and pulp mills, food processing plants, garbage inceneration units, cement plants, and iron and steel mills. For heating, energy sources ranging from 50°C to over 150°C are available. Potential energy uses include space heating on an individual or district scale, heating for industrial or institutional plants and heat for processing/manufacturing.

PROGRAM OBJECTIVES

The objective of the Seasonal Thermal Energy Storage (STES) Program is to demonstrate the economic storage and retrieval of energy on a seasonal basis, using heat or cold available from waste sources or other sources during a surplus period to reduce peak period demand; reduce electric utilities peaking problems; and contribute to the establishment of favorable economics for district heating and cooling systems. Aquifers, ponds, earth, and lakes have potential for seasonal storage. The initial thrust of the STES Program is toward utilization of ground-water systems (aquifers) for thermal energy storage.

The program has the further objective of evaluating other methods of seasonal storage, both from existing literature and by following current work in other countries. New program thrusts may be recommended as a result of these studies.

PROGRAM IMPLEMENTATION

The STES Program organization provides for two major subprograms -- the Aquifer Thermal Energy Storage (ATES) Program and the Technical Support Program. Seasonal storage in aquifers will be evaluated in the ATES Demonstration Program. The first phase of this program is now in progress in the field.

At Bethel, Alaska, the retrieval of waste heat from a diesel electric utility for use in space heating is under study by TRW. The potential aquifer to be utilized is being characterized. Phase I will include aquifer characterization, conceptual design of the storage and heat transport system will be completed together with estimated Phase II costs; and a cost sharing proposal for Phase II prepared.

At the Stony Brook campus of the University of New York, Dames & Moore are studying the use of a cooling tower in the winter to chill aquifer water. This water will be stored until summer and retrieved for summer cooling of campus buildings. Phase I activities will cover the same activities described above.

At the St. Paul campus of the University of Minnesota, the storage of 150°C water is being evaluated. The energy source will be the St. Paul campus coal fired heating plant; the end use building heating. The end objective is to store heat during low demand periods, and reduce the load on the St. Paul plant during the peak heating season. The scope of Phase I activities is the same as for the prior two activities.

The overall schedule for the ATES program is shown in Figure I. The schedule as planned in FY 1979 has been met to this point. The number of Phase I contracts placed has, however, been reduced to three because of limitations imposed by prospective FY 1981 funding. Should aquifer characteristics at any site be found to be inadequate or should any one of the Phase I contracts be unsuccessful for any other reason, demonstration of one of the temperature zones (high, medium, or chill) will be delayed until an alternate effort can be initiated.

Using the conceptual designs and aquifer characterization information gained from Phase I work, contractors will prepare cost sharing proposals for Phase II. Phase II will include the detailed design, construction, startup, and operation of ATES Demonstrations. Timing of this task is shown in Figure I.

The Technical Support Program is designed to evaluate nonaquifer methods of seasonal thermal energy storage; provide technical and environmental information in support of ATES demonstrations; and provide technical, institutional, economic and technology transfer support for commercialization of aquifer storage.

This program is organized around the following tasks:

Legal/Institutional Assessment
Economic Assessment
Environmental Assessment
Field Test Facilities
Compendia
Laboratory Analysis
Numerical Simulation
Nonaquifer STES Concepts

Activities in each of these tasks are covered in individual papers.

The field test activities at Auburn University are continuing. The well field has been redesigned to provide a true doublet, and planned experiments include storage and retrieval of water injected at 55°, 95°, and 125°C.

No contract is in place at this time for field test work at injection temperatures of 150°C. Every effort must be made to place such a contract during FY 1981.

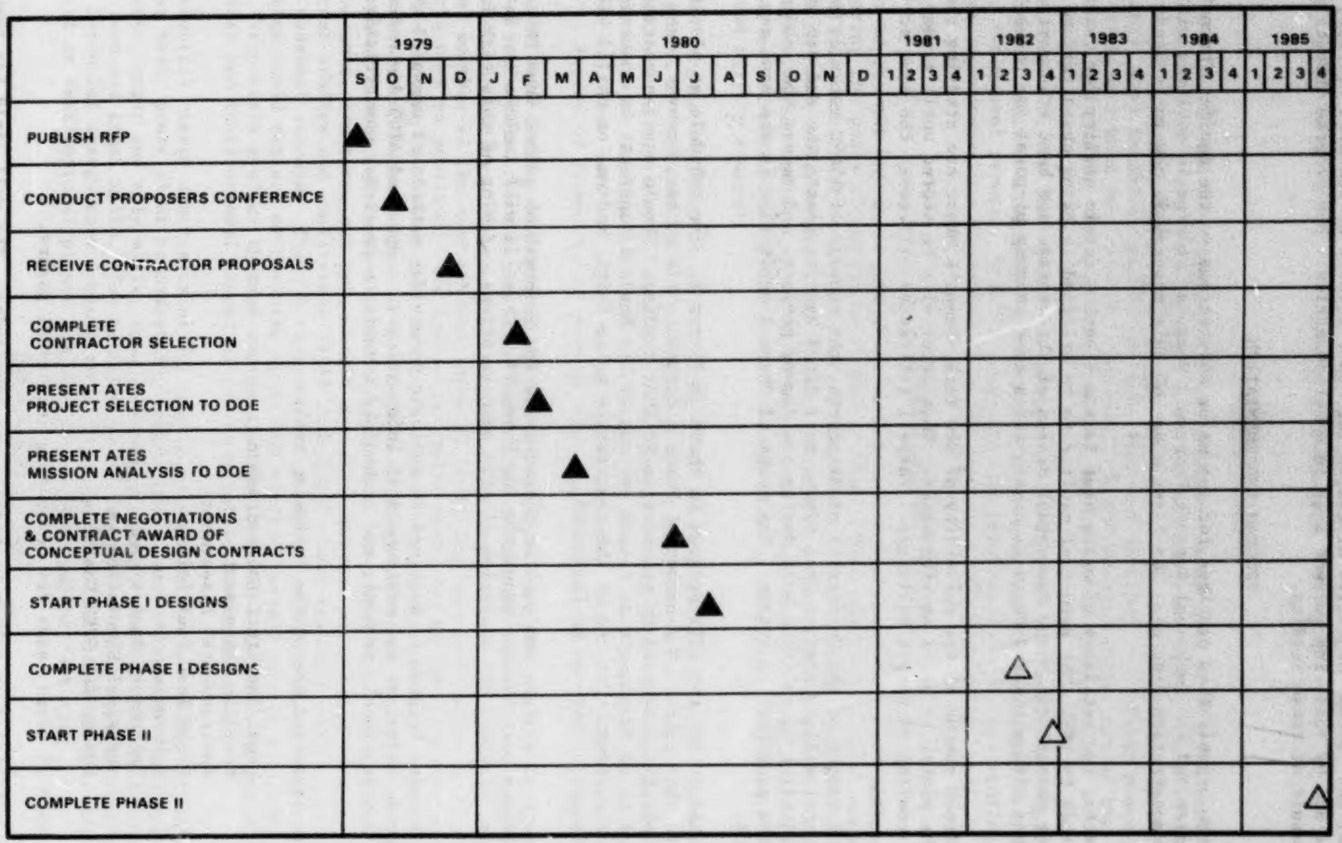

Figure I. Aquifer Thermal Energy Storage Demonstration Program

PROJECT SUMMARY

Project Title: Aquifer Thermal Energy Storage Program Management

Principal Investigator: Kenneth Fox

Organization:
Pacific Northwest Laboratory
P.O. Box 999
Richland, Washington 99352
(509) 376-0891 (FTS: 444-0891)

Project Goals: The initial goal of this program is to establish conceptual design contracts with the maximum number of potential demonstration contractors. After these contracts are in place the principal task in Phase I is the characterization of the aquifers for conceptual designs. The functional design criteria for the above ground portions will then be added to complete the conceptual designs.

From the Phase II proposals submitted at the end of Phase I we will establish the maximum number of Phase II contracts allowed by funding and technical considerations. During Phase II we will design, construct, startup, and operate the aquifer demonstrations to demonstrate aquifer storage feasibility (economic, technical, environmental and institutional) in operating demonstrations.

Project Status: Three conceptual designs are in place. The initial plans for management, aquifer characterization, environmental and institutional work are complete.

Aquifer characterization is in progress at all three sites.

Functional design criteria are being prepared.

Contract Number: DE-AC06-76RLO 1830

Contract Period: Continuing

Funding Level: $371,000, FY-1980, B/O

Funding Source: U.S. Department of Energy, Office of Advanced Conservation Technologies

PROJECT SUMMARY

Project Title:	Bethel, Alaska, Aquifer Thermal Energy Storage Project
Principal Investigator:	Jack M. Cherne
Organization:	TRW One Space Park Redondo Beach, California 90278 (213) 535-4321
Project Goals:	The first goal is to identify and characterize a viable aquifer. Concurrently, a conceptual design for an ATES system will be developed, including an energy source, thermal transport, storage aquifer and users. During the study, the economic viability of the conceptual system will be established, and the institutional and environmental concerns for future development will be identified. The products of Phase I will be a complete conceptual design for Phase II and a plan for a Phase II program.
Project Status:	All plans, management, environmental, institutional, and aquifer characterization have been written and approved by PNL. All environmental and institutional requirements for obtaining permits for drilling and testing the wells for aquifer characterization have been accomplished. Roads and pads for well drilling have been designed and construction started. A well driller has been selected and the drilling has started. Drilling is expected to be complete by mid-November 1980. A test transfer loop using the Bethel Utility Corporation diesel cooling water has been designed for use in the injection tests. A contractor to build this system has been selected. All instrumentation for the test wells has been procured. Testing the wells (production, injection and measurement of temperatures, pressures and flows) will be started in November and completed in December.
Contract Number:	DE-AC06-76RLO 1830, Subcontract B-68264-A-G
Contract Period:	1 May 1980 through 31 January 1982
Funding Level:	$1,888,126
Funding Source:	U.S. Department of Energy through Pacific Northwest Laboratory

BETHEL, ALASKA
AQUIFER THERMAL ENERGY STORAGE PROJECT

Jack Cherne
Manager, ATES Project
TRW Energy Systems
One Space Park
Redondo Beach, CA 90278

ABSTRACT

TRW Energy Systems Group, under contract to Battelle Pacific Northwest Laboratories, is developing the conceptual design of a seasonal thermal energy storage system in Bethel, Alaska, using an aquifer for storage. The system consists of a diesel electric generating plant as the source of the thermal energy, an aquifer beneath the property of the utility, and an energy transport system to take the energy from the utility, store it in the aquifer, and provide it to the city for space heating and hot water of the local hospital, municipal buildings, schools and residences.

This paper will describe the progress made this year in characterizing the aquifer and the development of a system design criteria for use in the conceptual design.

INTRODUCTION

TRW's Aquifer Thermal Energy Storage System project is located in the Town of Bethel, Alaska. Bethel, 450 miles west of Anchorage, on the Kuskokwim River, in the Yukon-Kuskokwim River delta and is at 30 feet above sea level. Bethel has a population of 4,000 and is the regional center for trade, transportation, administration, health care and education for the 80,000 square mile, 20,000 population of southwestern Alaska.

Bethel, like many isolated communities in Alaska, uses diesel generators for electric power. Hot water and space heating are normally supplied by oil fired units. The waste heat from the diesel power plants will be stored in the aquifer and will be used on a seasonal basis in a district heating system for many of the buildings in the community. The town of Bethel is well suited for this demonstration for the following reasons:

- Source of surplus heat is available
- Seasonal variation of surplus heat in summer and deficit in winter
- Rising costs of fossil fuel in region
- Expectation of finding a useable aquifer is strong
- A preliminary economic analysis indicates system would produce energy to users at one-third present cost.

The Phase I of the project includes site analysis, well drilling, aquifer characterization, conceptual design of the system and preparation for a Phase II design and implementation of the design.

TRW assembled a team of subcontractors and participants who are expert in each aspect of the project. These team members are:

- Harding-Lawson Associates have unique capabilities in thermal aquifer modeling and analysis, and are geologists with Alaskan soils test laboratory.
- R & M Consultants is an Architectural and Engineering firm with Alaskan experience in design of systems in permafrost and logistics of Alaskan construction.
- HMS, Inc. have expertise in Alaskan construction costs and general cost analyses capabilities.
- Calista Corporation is the native corporation, covering southwest region of Alaska, established by the Alaska Native Claims Settlement Act. They are the owner of the subsurface rights in the Bethel area.

- City of Bethel is the owner of present district heated water and sewage system and surface access rights to property. They are the proposed lead organization for Phase II and are a major user of energy in Bethel.
- Bethel Utility Corporation is the owner of source of energy.
- State of Alaska, Division of Energy and Power Development will assist in the coordination of all institutional and environmental interfaces.
- University of Alaska, Institute of Water Resources will provide independent quality assurance surveillance of the project.

TRW is managing and integrating the expertise and ownership rights of the team members into the demonstration of the potential for using a thermal aquifer for seasonal energy storage.

SITE ANALYSIS

Owing to its isolated location and lack of mineral resources, limited subsurface exploratory work has been conducted in the Bethel area. The terrain is very gently sloping with the land surface covered by low growing wet tundra vegetation and numerous lakes. The city is within the zone of "discontinuous" permafrost as classified in the National Atlas, 1970. The permafrost is characterized as "warm" with measured temperatures of about 31.8°F. The natural active layer, or near-surface layer subject to annual freezing and thawing, is about 10 feet thick. Permafrost thickness, obtained from drilling, indicates a thickness of about 400 to 500 feet. Soils in the Bethel area consist of fairly uniform fine sands, silty sands and sandy silts of deltaic origin and may be a few hundred feet thick. Coarser alluvial and beach sand deposits have been verbally verified at depth. Moisture content of near surface soils is high and numerous shallow thaw and ox bow lakes are present in the Bethel area. They apparently do not migrate significantly and have historically remained rather stable.

AQUIFER CHARACTERIZATION

The objectives of the aquifer characterization task are to:

- Identify and characterize a suitable aquifer hot water storage zone to establish the functional design parameters required for ATES System design
- Ensure that the source of hot water is in balance with the ability to store and use the energy
- Ensure that projected economics of thermal aquifer storage are based on sound principles
- Obtain sufficient information such that aquifer performance may be transferred to other aquifers in other locations and environments.

The identification of a suitable storage zone will be accomplished via five test holes drilled through the permafrost (about 400 feet thick at Bethel) to a depth of 800 feet. See Figure 1. A borehole soil sample log and an electric log (caliper, self-potential, resistivity and Gamma) will be made for each test hole. Borehole soil samples will be taken for laboratory measurement and analysis of grain size, bulk density, moisture content, permeability, thermal conductivity, specific heat, and thaw consolidation behavior. The borehole soil sample logs, electric logs, and results of laboratory measurements will be correlated to define aquifer horizons and their properties throughout the potential aquifer zone. A suitable storage zone will be identified using these data as applied to requirements and storage zone selection criteria.

The characterization of the aquifer storage zone - obtaining information on the physical, geophysical, mechanical, hydraulic, and thermal properties of the aquifer - will be accomplished by a laboratory measurements program and a field measurements program. Characterization data will be used as input for a numerical model of the aquifer storage zone. The two field tests planned are on isothermal well test and a hot water injection test. Three test holes will be used as observation wells to determine pressure and temperature response. Two larger diameter test holes will be completed as supply and injection water wells and will be in a doublet configuration in which water pumped from the aquifer supply zone by one well will be injected back into the zone through the other well. Isothermal well test pressure data will be obtained during circulation of near-freezing water in the well doublet. The hot water injection test will directly follow the isothermal test with a significant increase in the temperature of the injected water. Temperature data from this test will be used to calibrate the numerical model.

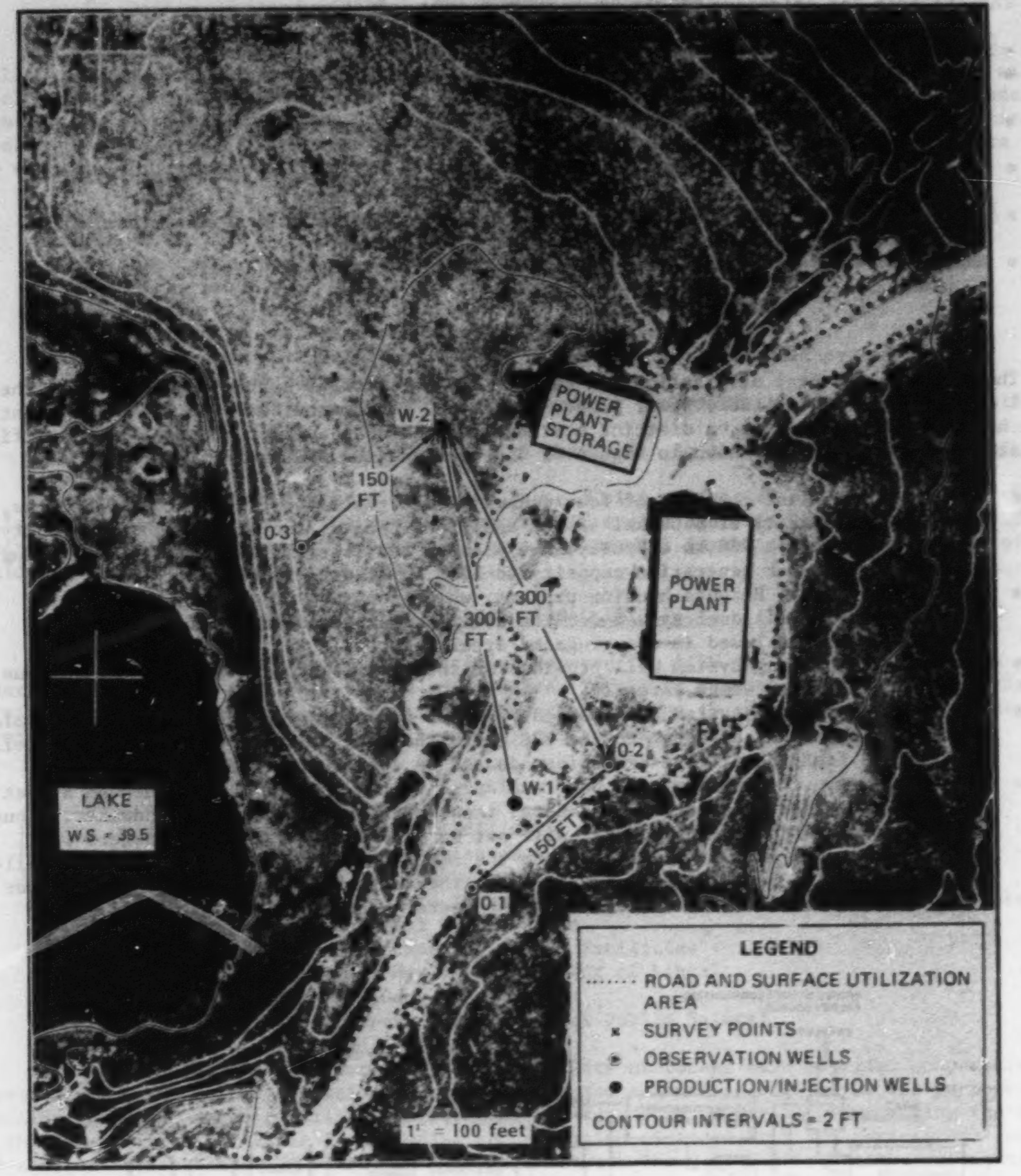
POWER PLANT STORAGE
W-2
150 FT
0-3
300 FT
300 FT
POWER PLANT
0-2
W-1
150 FT
0-1
LAKE
W.S. = 39.5
LEGEND
ROAD AND SURFACE UTILIZATION AREA
SURVEY POINTS
OBSERVATION WELLS
PRODUCTION/INJECTION WELLS
CONTOUR INTERVALS = 2 FT
1" = 100 feet

Figure I. Well Field Layout

The criteria for selection of the storage zone are:

- Be bounded on top by a low permeability, insulating soil layer
- Be permeable enough throughout its volume to accept design injection flow rates without danger of hydraulic rupture
- Be of sufficient height relative to permeability and anisotropy to limit buoyancy tilting
- Have a lateral extent sufficient to contain the injected water volume and prevent comingling of hot and cold water of a doublet well system(s)
- Have a small regional aquifer zone water velocity (hydraulic gradient) to minimize the possibility of lateral displacement of stored water
- Have a particle size distribution such that well plugging and sanding problems are minimal.

SYSTEM DESCRIPTION

The Bethel waste heat utilization and thermal aquifer storage system is composed of the Bethel Utility Corporation (BUC) power plant, a duct for the transmission of the power plant waste heat to user facilities, a district heating system and an aquifer storage. A simplified schematic of this system is shown in Figure 2. The system is summarized as follows:

- The BUC power plant consists of four diesel engine generators, type S16-EMW-2100 kw, with a peak capacity of 8400 kw. Three additional units, two with a 600 kw capacity each and one with a 900 kw capacity, are planned for installation during 1981, bringing the total power generation capacity to 10.5 Mw electric power.
- The present Bethel Heights housing project, which consists of 180 single family dwellings use a utiliduct system for the domestic water and sewage and consist of insulated pipes enclosed in a corrugated steel pipe.
- The district heating system will provide for the distribution of heat to the various users and establish usage rates.
- The Phase II storage system will consist of four wells (two doublets) in a rectangular pattern in the field adjacent to the BUC where the test wells were drilled. The wells will be 600 feet apart. The dimensions depend on the aquifer characteristics.
- The energy from the utility will be transferred to the aquifer fluids through a heat exchanger in order to separate the energy transport fluid from the groundwater. Thus, chemical composition of the aquifer will not be altered. The heat exchangers will operate in a dual mode providing heat to the aquifer when excess waste heat is available and removing heat from the aquifer when the waste heat available from the power plant is insufficient to provide all of the users' requirements.

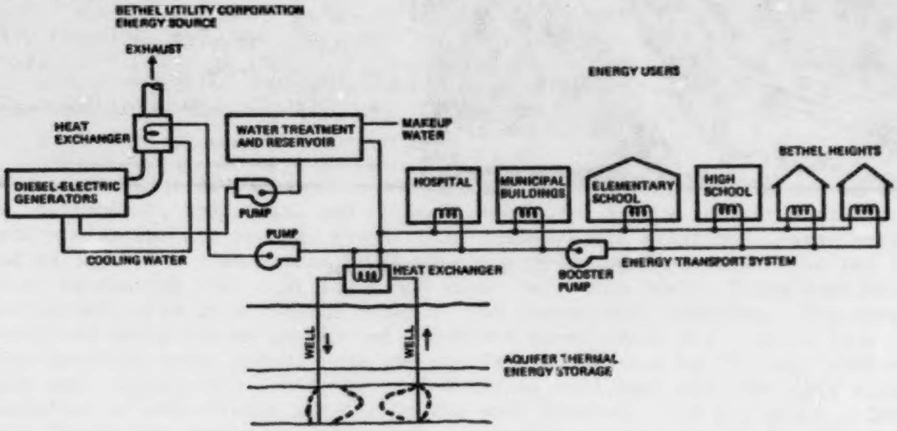
BETHEL UTILITY CORPORATION
ENERGY SOURCE
EXHAUST
ENERGY USERS
HEAT EXCHANGER
WATER TREATMENT AND RESERVOIR
MAKEUP WATER
BETHEL HEIGHTS
DIESEL-ELECTRIC GENERATORS
HOSPITAL
MUNICIPAL BUILDINGS
ELEMENTARY SCHOOL
HIGH SCHOOL
PUMP
PUMP
COOLING WATER
HEAT EXCHANGER
BOOSTER PUMP
ENERGY TRANSPORT SYSTEM
WELL
WELL
AQUIFER THERMAL ENERGY STORAGE

Figure 2. Simplified Schematic ATES

PHASE I ENVIRONMENTAL ASSESSMENT

The potential impact on the environment that may be caused by site preparation, test well drilling, and aquifer measurement during Phase I has been assessed and these activities will be closely monitored for their effect. Site preparation activities during Phase I include construction of gravel roads and drill pads, the drilling of two production wells and three observation wells, and the movement of associated heavy equipment. The potential impacts to the existing environment as a result of these activities can include:

- Contamination of groundwater by infiltration through weak formations or ruptured borehole casings
- Subsidence as a result of permafrost thaw due to improper drilling or extensive vegetation removal
- Soil erosion due to vegetation removal and subsequent flooding
- Expansion due to increased pressure in aquifer formation
- Contamination of surface water due to uncontrolled spill of heat system water
- Induced seismicity due to permafrost subsidence
- Aquifer clogging due to precipitation because of incompatibility of heated injection fluids with subsurface lithologies
- Groundwater and/or surface water quality change due to thermal/chemical interaction

A major consideration in the planning of Phase I site activities and the design of the wells and other components of the aquifer measurement system has been the incorporation of practices and design features which reduce the environmental impact and the possibility of accidents which could damage the environment.

PHASE I INSTITUTIONAL INTERFACES

There are several institutional interfaces between the ATES project and city, state and federal agencies, and the local native corporation. At TRW's request, the State of Alaska's Permit Coordination Center held a Permit Conference on 13 May to establish state and federal permit requirements for Phase I. The agencies involved included:

U.S. Corps of Engineers
U.S. Environmenatl Protection Agency
Alaska Office of Coastal Management (Office of the Governor)
Alaska Oil and Gas Conservation Commission (Office of the Governor)
Alaska Division of Minerals and Energy Management (Department of Natural Resources)
Alaska Division of Forest, Land and Water Management (Department of Natural Resources)
Alaska Department of Environmental Conservation
Alaska Department of Transportation and Public Facilities
Alaska Occupational Safety and Health (Department of Labor)
Alaska Department of Fish and Game
Division of Alaska State Troopers (Department of Public Safety)

Both the Calista (native) Corporation and the City of Bethel have provided cooperative agreements regarding the permission to use the land and subsurface rights for the purposes of the ATES project. Bethel Utilities Corporation has agreed to cooperate by providing the use of their facilities for Phase I, including the provision of waste heat and certain equipment for aquifer characterization work. An agreement between the U.S. Public Health Service and Bethel Utilities Corporation regarding participation in waste heat utilization for the local hospital.

PHASE I ANTICIPATED ECONOMICS

The proposed aquifer thermal storage system will be used to supply space and water heating to residences and buildings in the Bethel area. Currently, such heating is obtained primarily from individual oil-fired furnaces. Oil and other fuels are now transported to Bethel by barge (for about three months of the year) and by air. Hence, minimization of oil consumption is of particular importance to Bethel residents. Among the potential system advantages are:

- High potential for recoverable waste heat due to the rather low efficiency (around 30 percent) of the diesel generators currently used by BUC
- High replacement value of energy saved due to the relatively high cost of transporting heating oil to the Bethel area
- High ratio of winter heat demand to summer heat demand due to climatic conditions. The supply of waste heat is in excess of demand in the summer while the reverse is true in the winter
- Possible low incremental cost of distributing heat through an insulated water pipe system

Some preliminary calculations were made using assumptions on system cost, O & M cost, thermal customers charged for all capital and O & M, system is owned by the City of Bethel, and fuel cost escalates at 12% per year. Using a 20 year system life, the price per 10^6 Btu supplied is \$2.70, compared to \$5.80/10^6 Btu for No. 2 oil which becomes \$7.25/10^6 Btu taking into account the 80% efficiency of local user's boilers.

PROJECT CURRENT STATUS

As of October, 1980, the permits for drilling have been obtained with little difficulty. The management plans, environmental and institutional plans and the aquifer characterization plans have been written and approved by Battelle Pacific Northwest Laboratories. The drilling pads and access roads have been designed and constructed. Well drilling has started on the observation wells. Design of the mechanical and electrical systems of the hot water test system which interfaces with the utility have been completed and construction started. The difficulties of operating in remote areas of Alaska has had its toll on project schedules, however, the overall schedule for the project will not be affected. Preliminary work has been performed on the development of system design criteria and the conceptual design of the system. The bulk of this activity will be performed as the characteristics of the aquifer are established.

CONCLUSION

A waste heat-powered district heating system in Bethel will directly benefit the City of Bethel, the local utility company, and the residential and commercial users of the waste heat. The benefits are generally economic in nature:

- The Bethel Utility Corporation, as the operator, will be able to offset some, if not all, of the cost of fuel by charging a fee for the waste heat it will provide to the new district heating system customers; it is possible that electricity costs in the area could be adjusted to reflect this new source of revenue. Subsequent to amortization of the Phase II capital costs, the electricity rates and the district heating rates could balance with the fuel costs, overhead/maintenance costs and profits, in accordance with a future plan to be negotiated with the Public Utilities Commission.
- The City of Bethel will benefit in several ways, including increased employment of the local native labor, the integration of the entire city into a central heating system and reduced heating cost.
- The Department of Energy will benefit by a demonstration of ATES in a geographically dispersed site. Participation via the Calista Corporation in a DOE demonstration program will benefit a minority group.
- The major benefit, however, is to the local community who will obtain a reliable auxiliary source of heat with reduced annual energy costs.

TRW envisions that the commercial use of the Phase II demonstration facility will be by the City of Bethel, who are negotiating the purchase of the utility. The intended primarty use is for residential and municipal space heating, followed by commercial and industrial space heating, and possibly agricultural and fish hatchery applications which would represent real economic expansion due to the availability of hot water in larger quantity than is presently available. The demonstration of the concept in a permafrost region opens up many potential opportunities in Alaska that a demonstration in the lower 48 might not provide. There are a number of small towns, villages and a portion of Fairbanks which currently have warm water distribution systems which can be readily upgraded to accommodate this technology.

PROJECT SUMMARY

Project Title: Aquifer Thermal Energy Storage System at the University of Minnesota

Principal Investigator: Warren E. Soderberg

Organization:

University of Minnesota
319 15th Avenue S.E.
Minneapolis, Minnesota 55455
(612) 373-2001

Project Goals: The first goal is to identify and characterize a viable aquifer. Concurrently, a conceptual design for an ATES system will be developed, including an energy source, thermal transport, storage aquifer and users. During the study, the economic viability of the conceptual system will be established, and the institutional and environmental concerns for future development will be identified. The products of Phase I will be a complete conceptual design for Phase II and a plan for a Phase II program.

Project Status: The project is in its initial stages of construction and design. A contract to core three (3) holes was awarded in August 1980 to provide a complete core sample for laboratory testing and analysis, and to log the entire stratigraphic sections.

Plans and specifications for six (6) monitoring wells and the two (2) pumping wells (300 gpm) as well as above ground mechanical and electrical equipment necessary to perform the testing of the aquifer storage theory will be issued in September for bidding. Construction is planned for completion by March 31, 1981. Heat injection testing is planned to start April 15, 1981.

The testing will involve heating the aquifer water from supply well at an ambient temperature of (12°C) to 100°C and injection into the aquifer at a distance of 240 meters for a period of eight (8) days, rest eight (8) days, and then the flow reversed for eight (8) days. Upon removal, the injected water will be passed through heat exchangers lowering the temperature to 80°C prior to reinjecting into the supply well. This procedure is repeated using the supply well water temperature of 80°C to 125°C through a heat exchanger prior to injection into the injection well and the cycle repeated as above.

The next cycle will take the supply water at 80°C and raise it to 150°C. At least two additional cycles will be run at this design condition and all taken, recorded and analyzed, thus completing the test phase from which an aquifer characterization plan will be made. From this a Phase II design concept will be developed.

Contract Number: DE-AC06-76RLO 1830, Subcontract B-97601-A-G

Contract Period: 21 May 1980 through 1 July 1982

Funding Level: $1,936,431

Funding Source: U.S. Department of Energy through Pacific Northwest Laboratory

CONCEPT DESIGN OF
AQUIFER THERMAL ENERGY STORAGE SYSTEM
UNIVERSITY OF MINNESOTA
ST. PAUL CAMPUS

Prime Contractor
University of Minnesota

ABSTRACT

In May, 1980 a field test began, consisting of construction of a well doublet and monitor wells for storing 150°C hot water in a regional aquifer under the St. Paul Campus of the University of Minnesota. The purpose of this test is to define the characteristics of an aquifer with hot water and to define the environmental, institutional, economic and technical feasibility of a full scale demonstration incorporating a heat source for the aquifer, a transport system for hot water, an end-use system for the stored energy, and an integration of above ground heat exchanger equipment between the transport system, the end-use system and the aquifer. The results of the tests will be used to provide a concept design and proposal for construction of a full scale thermal energy storage system for Phase II of this demonstration.

INTRODUCTION

The University of Minnesota and Battelle/Pacific Northwest Laboratories, assisted by Orr-Schelen-Mayeron & Associates, Inc., Minnesota Geological Survey, U.S. Geological Survey, Minnesota Energy Agency, Honeywell Technology Strategy Center, General Electric-TEMPO, and the U of M Institute of Technology, are proud to present their participation in the Aquifer Thermal Energy Storage demonstration project located on the St. Paul Campus of the University of Minnesota.

The Aquifer Thermal Energy Storage Project (ATES) is a two-phased energy project designed to store and utilize heat on a seasonal basis from the University of Minnesota's Central Heating Plants. The baseline concept ultimately involves the integration of an aquifer into the University's co-generation system by linking up the Minneapolis Campus with the St. Paul Campus through a hot water system. Heated groundwater from the Franconia and Ironton-Galesville (FIG) aquifer will be injected into the source aquifer for storage during times of low thermal demand and the stored heat will be extracted during times of high thermal demand on a seasonal basis. By storing heat, the University can postpone addition of coal fired thermal production in their heating system, increase cogeneration of electricity thereby offsetting greater fuel requirements by the local utility, improve plant load factors, and reduce air pollution. The concept design is a closed loop system in which only heat is introduced or removed from the aquifer.

Phase I ATES, a scaled down feasibility test is designed to evaluate 150°C hot water storage and recovery in the FIG aquifer. In Phase I, system testing, aquifer characterization, engineering, and environmental and institutional assessment will take place. Seven monitoring wells surrounding a one-quarter scale high temperature water injection-withdrawal doublet will enable assessment of the project in terms of economic and engineering feasibility, aquifer impacts and water quality.

The present full scale concept involves interconnection of the St. Paul and Minneapolis Campus heating plants. The Minneapolis Campus cogeneration plant, known as the Grid Integrated Community Energy System (Grid-ICES), consists of the Minneapolis

Campus, St. Mary's Hospital, Fairview Hospital, and Augsburg College. It is planned to be connected to the St. Paul ATES System by a high temperature, hot water transport loop.

Program management is the responsibility of the University of Minnesota (U of M), with the Minnesota Energy Agency (MEA) coordinating the environmental review. The Minnesota Geological Survey (MGS) will provide aquifer characterization and site management. The United States Geological Survey (USGS) will perform aquifer field tests and modeling studies. General Electric-TEMPO will perform concept studies (G.E.TEMPO). System engineering is to be provided by the Honeywell Technology Strategy Center (TSC). Orr-Schelen-Mayeron & Associates, Inc. (OSM) will oversee the technical coordination, construction design, and Phase II concept design. National Biocentric (ERG) will prepare the environmental assessment.

CONCEPT DESIGN

The baseline concept proposal for construction shown in Figure I consists of a number of subsystems: (1) heat source, (2) end-uses for heat, (3) transport, (4) aquifer thermal storage, (5) instrumentation and control. Since these systems interact it is the purpose of the conceptual design of the full scale system to combine their individual subsystem characteristics into an integrated operation. The emphasis of this demonstration is on seasonal thermal storage and withdrawal, with diurnal storage and withdrawal a distinct possibility. Other concepts will be explored for optimum cost effectiveness as a beginning stage to the final baseline concept.

The cogeneration source at the Southeast Steam Plant will deliver high pressure (180 psig) and low pressure (20 psig) steam to a set of heat exchangers which will produce 150°C water. A transport pipeline for the hot water will be constructed between the University plant heat exchangers and the St. Paul Campus. The pipeline will terminate at either the aquifer storage or the St. Paul Campus heating plant where hot water allocation is made to either storage or end-use. The University Heating Plant and the St. Paul Heating Plant will provide peaking capacity only, as it is economically desirable to base load the Southeast Steam Plant and maximize electric generation. Current aquifer parameters suggest that up to 20 MW_t rates of 150°C charging and discharging are possible. However, that assumption is only credible if the aquifer permeability does not decrease with time.

If aquifer energy storage appears feasible, a detailed proposal will be prepared during Phase I work which will describe aquifer characteristics, an optimized concept design for Phase II, and a preliminary environmental and institutional assessment. Life cycle costing and financial considerations will be included. The above ground design work will be coupled with the below ground aquifer characterization resulting in an optimum concept design or alternative concepts prepared for Phase II.

PROGRAM DESCRIPTION

Concept Study - Through concept analysis, standard engineering criteria and computer study, a thermal source end usage time dependent (seasonal) profile will be developed to determine the best economic aquifer thermal storage. Alternatives will be examined based upon constant volume transport sizing, variable volume - variable temperature hot water transport sizing, economic cogeneration, and/or staged construction of the baseline concept. This work will be performed by GE-TEMPO.

System Engineering - The baseline conceptual study will be optimized through system engineering and computer modeling to determine the optimum source, transport, end-use and aquifer interface design criteria such as pressure ranges, temperature ranges, flow rates, and capacity. Primary characteristics of the aquifer characterization will be input to the system model for optimization. This work will be performed by Honeywell TSC.

Hot Water Technology - This work will be devoted to the modeling and development of advanced heat exchanger technology and application of sacrificial particles. This work is being performed by Dr. P. Blackshear of the U of M's Institute of Technology.

Economic and Energy Assessments - This work involves developing economic models of the system to determine the economic and energy sensitivity to construction costs, fuel costs, M & O costs; and to provide life cycle analysis. This work is assigned to Dr. M. Riaz of the U of M's Institute of Technology.

Aquifer Characterization - The aquifer will be characterized through actual construction of a well doublet and a system of monitoring wells. Hot water will be injected as previously described, and the aquifer characterized by the results of hydrological, geological, chemical, biological and petrological analysis. In-situ samples of water and rock will be laboratory analyzed to determine the resultof hot water on the chemical reactions.

The results of the various tests will be mixed by computer modeling with in-situ temperature-pressure measurements to develop an aquifer model. This work will be jointly developed by the MGS and the USGS. The site plan is shown on Figure 2 for the test well doublet at Site A injection and withdrawal well, and Site B water supply well, with site C one of seven monitoring wells.

The FIG aquifer to be used for feasibility testing and characterization was selected because of its isolation from other heavily used aquifers both above and below. The Upper St. Lawrence and lower Eau Claire confining beds will provide the isolation required from other groundwater sources. The formation consistency and lower permeability than other formations was also considered when selecting the FIG aquifer for storing hot water. See Figure 3.

Under the U of M's St. Paul Campus, the FIG formation ranges from fine to coarse grained sandstone. It is approximately 200 feet thick, and ranges in depth from 600 to 880 feet from the surface. Because of the influence of shaly zones in the sandstone, the effect may approach a multiple-aquifer system. Testing of the FIG aquifer will reveal the effect from irregularities in the formation on the thermocline.

The heat injection testing consists of a well doublet approximately 800 feet apart with four monitoring wells at Site A, two at Site B and one at Site C to record data for the aquifer characterization. See Figures 4 and 5 for heat injection and heat recovery cycles.

Above ground heat exchangers will provide the heat for injection and recovery by interconnection with the heating plant steam distribution system.

The testing will consist of three cycles of heat injection and heat recovery at 300 GPM. The aquifer water temperature will be increased from 11°C to 150°C in three steps of 100°C, 125°C and 150°C respectively. Each test cycle will be 24 days in duration. During all testing, the information collected will be carefully analyzed for the proper operation of all elements before continuation of the testing program. The end-user heat loads will be simulated during testing by the use of an air cooled heat exchanger. Upon completion of the previously described tests, 2 additional 24 day cycles will be repeated at 150°C for the heat injection- withdrawal well and the supply well temperature will be at 80°C.

Upon successful completion of the 5 test cycles, further tests may be conducted for extended periods of 120 days for each cycle and will provide further data for the conceptual design for the Phase II demonstration. Figure 6 illustrates a hypothetical thermocline and how the thermocline might look in the FIG aquifer.

Concept Design and Phase II Proposal - Development of a concept design will be based upon results of the foregoing work. One-line flow diagrams and schematics, outline equipment specification, and budget will be used in developing a Phase II proposal for construction and demonstration. Environmental-institutional analysis will be integrated into the design for the proposal. Design and specification of the well doublet and monitoring well system for the Phase 1 test are also part of this effort. This work is being done by Orr-Schelen-Mayeron, a consulting branch of the Kidde Corporation.

Environmental and Institutional Assessments - The environmental and institutional assessments will be jointly analyzed by National Biocentrics, the University of Minnesota and the Minnesota Energy Agency. The preliminary environmental assessment for above and below ground impacts will be made by National Biocentrics, and institutional analysis by the University of Minnesota. Coordination of regulatory requirements and community conflict appraisal will be by the Minnesota Energy Agency.

Prime Contractor - The University Physical Plant will provide prime contractors and program management roles. All construction design review, construction management, and cost control will be provided by Physical Plant. Final decisions of program management and direction rests in the Physical Plant.

Quality Assurance - Aquifer characterization assurance will be primarily controlled by the MGS and the USGS. Primary quality assurance and control in other areas is provided for in the technical, environmental, institutional and construction activities.

Technical and Institutional Review - Participating in review will be invited knowledgeable technical members to act as an ad-hoc review panel.

PROGRAM STATUS

Phase 1 started non-contractually, in March, 1980 by application to the regulatory agencies for variance and permits for heat injection, well construction, and water appropriation from the FIG aquifer. Phase 1 began contractually in May, 1980 and will end during July, 1982. To date, variances and permits for well construction and heat injection have been received for the field testing. Management plans, site control plans, aquifer characterization plans, data acquisition, instrumentation and calibration plans, and environmental and institutional plans have been prepared and documented. The well systems and above ground systems for the field test have been designed and specified. Well boring and logging is being done on-site at present. If economic and environmental feasibility can be proven with this one-quarter scale system, a full scale storage demonstration is to be conceptualized and analyzed during Phase I for construction during Phase II.

The well doublet and monitoring well construction is expected to be completed for heat injection testing in the FIG aquifer in April, 1981. Preliminary modeling of the aquifer and a preliminary concept study report have been completed. Environmental and institutional analyses have begun.

Where permanent additional casing pipe was required, State regulations became another factor to deal with. The design and completion of core drillings finished as monitoring wells required adherance to the Water Well Construction Code. This directly affected the design of additional monitoring wells and their resulting costs.

GENERAL BENEFITS

1. Postpone the addition of coal fired boilers to heating system.
2. Increase cogeneration of electricity.
3. Improve plant load factors.
4. Reduce air pollution.
5. Allow solar heating to become more cost effective.

CONCLUSIONS AND RECOMMENDATIONS

It is still too early to make conclusive judgments or recommendations. One tentative conclusion that has been reached, however, is that general commercialization of aquifer thermal storage would not be probable in Minnesota because of stringent standards on the use of the ground water aquifers. Barrier removal of regulatory requirements for a Phase II demonstration will depend heavily on the aquifer characterization and subsequent impact assessment. Nothing has changed that has lessened the initial high optimism that ATES will become acceptable after completion of Phase 1 testing.

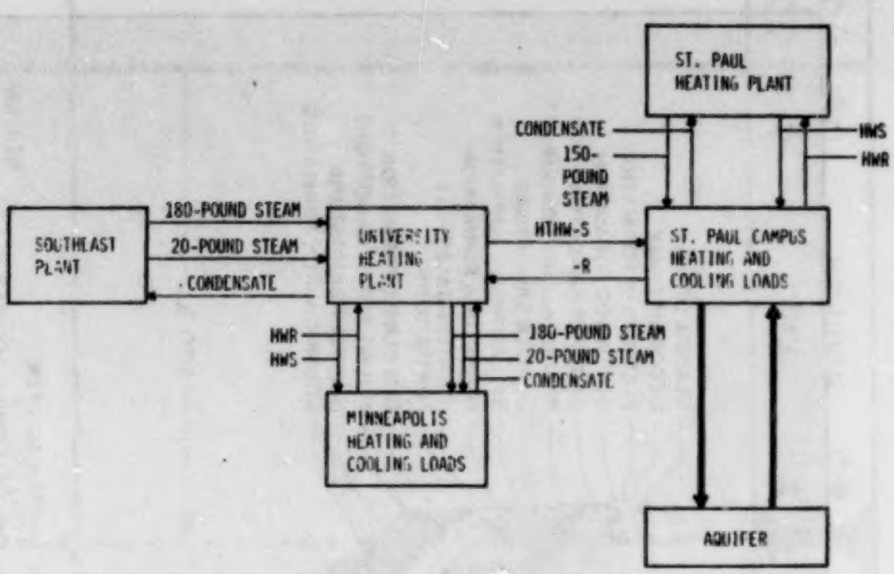
ST. PAUL HEATING PLANT
CONDENSATE
150-POUND STEAM
HWS
HWR
SOUTHEAST PLANT
180-POUND STEAM
20-POUND STEAM
CONDENSATE
UNIVERSITY HEATING PLANT
HTHW-S
-R
ST. PAUL CAMPUS HEATING AND COOLING LOADS
HWR
HWS
180-POUND STEAM
20-POUND STEAM
CONDENSATE
MINNEAPOLIS HEATING AND COOLING LOADS
AQUIFER

Fig. 1 BASELINE SYSTEM SCHEMATIC

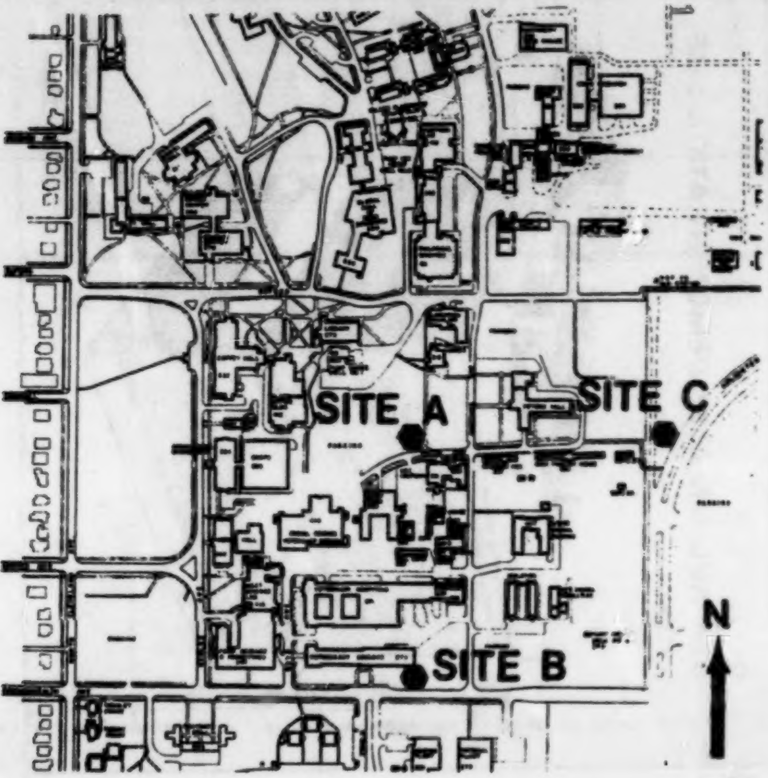
SITE A
SITE C
SITE B
N

Fig. 2 SITE PLAN

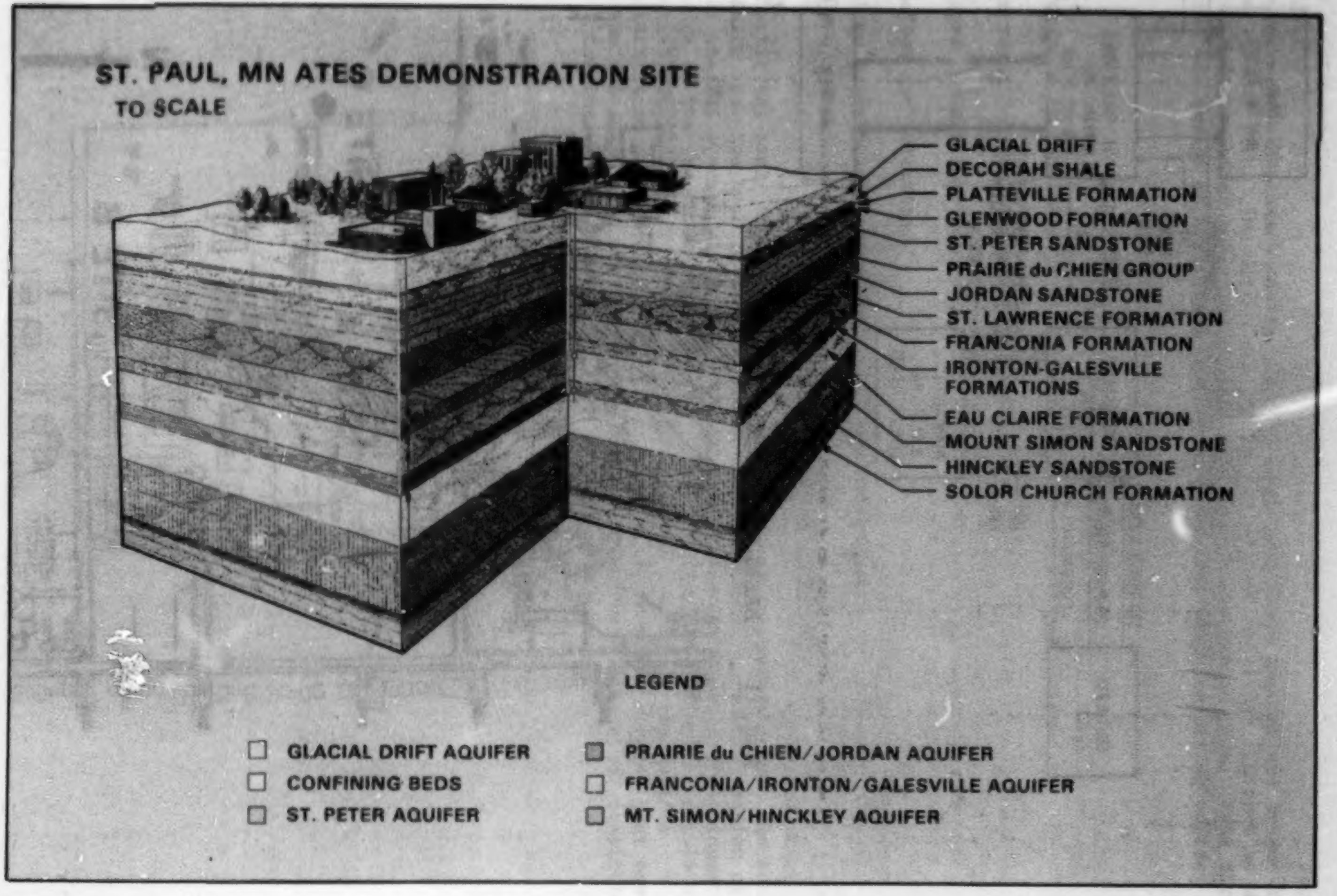
ST. PAUL, MN ATES DEMONSTRATION SITE
TO SCALE
GLACIAL DRIFT
DECORAH SHALE
PLATTEVILLE FORMATION
GLENWOOD FORMATION
ST. PETER SANDSTONE
PRAIRIE du CHIEN GROUP
JORDAN SANDSTONE
ST. LAWRENCE FORMATION
FRANCONIA FORMATION
IRONTON-GALESVILLE FORMATIONS
EAU CLAIRE FORMATION
MOUNT SIMON SANDSTONE
HINCKLEY SANDSTONE
SOLOR CHURCH FORMATION
LEGEND
☐ GLACIAL DRIFT AQUIFER
☐ CONFINING BEDS
☐ ST. PETER AQUIFER
▨ PRAIRIE du CHIEN/JORDAN AQUIFER
☐ FRANCONIA/IRONTON/GALESVILLE AQUIFER
☐ MT. SIMON/HINCKLEY AQUIFER

FIG. 3

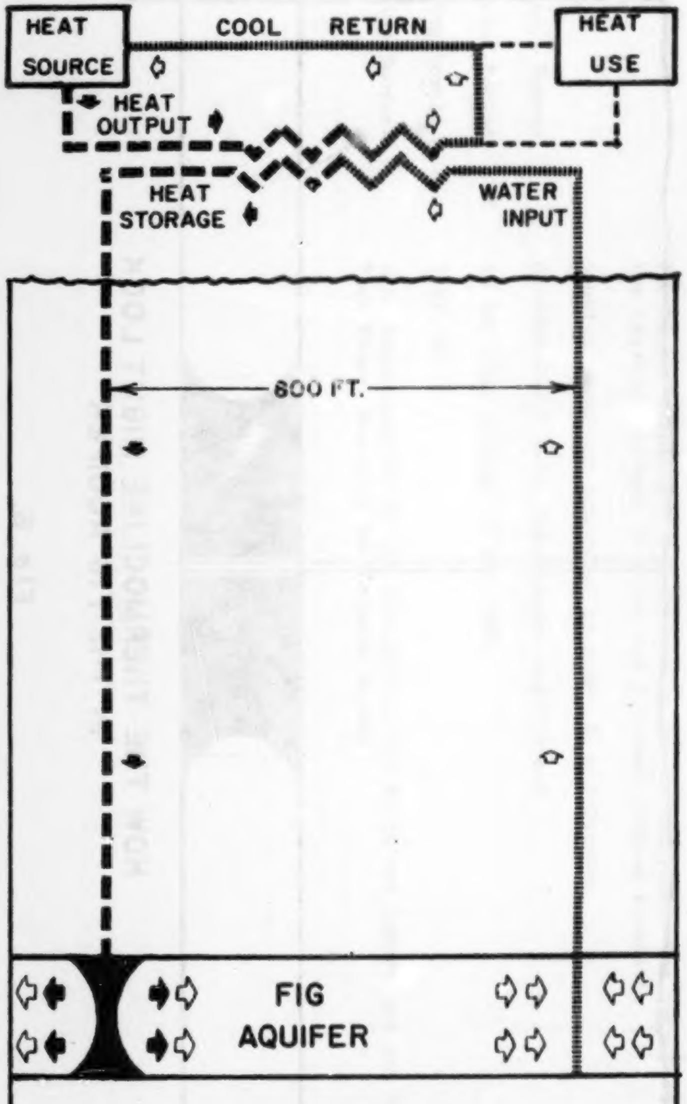
HEAT SOURCE
COOL RETURN
HEAT USE
HEAT OUTPUT
HEAT STORAGE
WATER INPUT
800 FT.
FIG AQUIFER

Fig. 4. HEAT INJECTION

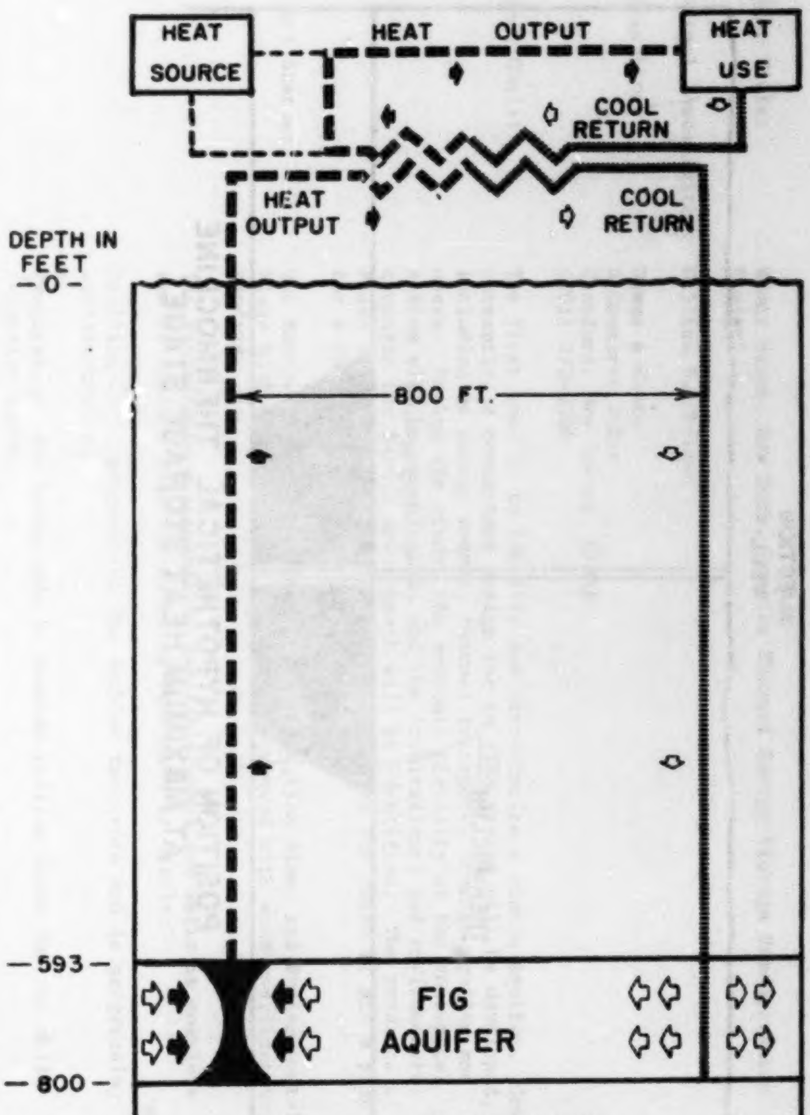
HEAT SOURCE
HEAT OUTPUT
HEAT USE
COOL RETURN
HEAT OUTPUT
COOL RETURN
DEPTH IN FEET
— 0 —
800 FT.
— 593 —
FIG AQUIFER
— 800 —

Fig. 5. HEAT WITHDRAWAL

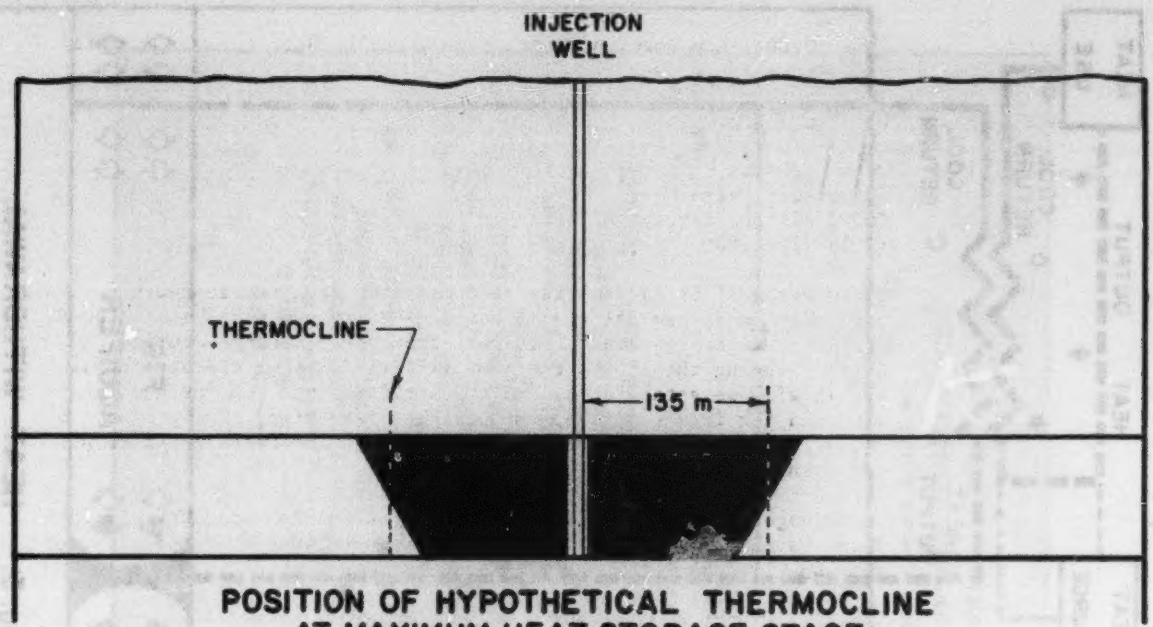
INJECTION WELL
THERMOCLINE
135 m

POSITION OF HYPOTHETICAL THERMOCLINE AT MAXIMUM HEAT STORAGE STAGE

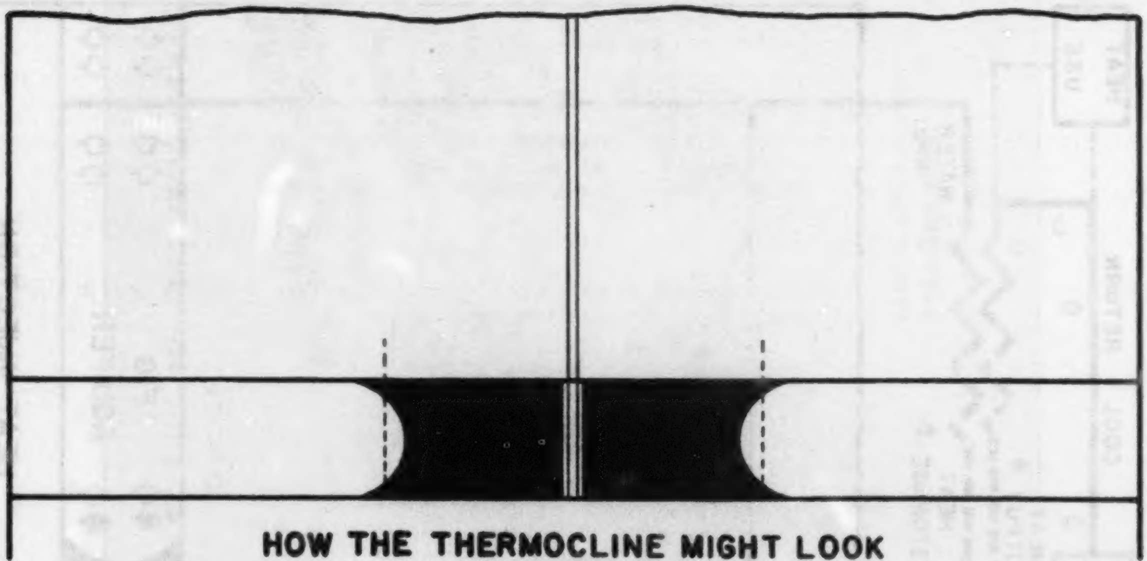

HOW THE THERMOCLINE MIGHT LOOK IN THE FIG AQUIFER

Fig. 6.

PROJECT SUMMARY

Project Title: Stony Brook, New York, Aquifer Thermal Energy Storage Demonstration Project

Principal Investigator: William V. Skinner

Organization:
Dames & Moore
6 Commerce Drive
Cranford, New Jersey 07016
(201) 272-8300

Project Goals: The first goal is to identify and characterize a viable aquifer. Concurrently, a conceptual design for an ATES system will be developed, including an energy source, thermal transport, storage aquifer and users. During the study, the economic viability of the conceptual system will be established, and the institutional and environmental concerns for future development will be identified. The products of Phase I will be a complete conceptual design for Phase II and a plan for a Phase II program.

Project Status: The Management Plan, Aquifer Characterization Plan, and Environmental Plans have been submitted to PNL and approved with some modifications pending.

The preliminary assessment of available pumps and wells is complete and it appears that the existing equipment is usable.

Drilling is in progress at the doublet test site and is progressing satisfactorily.

Preparations are being made to provide chilled water for the chill injection tests.

Facilities assessment and evaluation are in progress. The survey of the existing systems is about two (2) weeks behind schedule.

Doublet tests are scheduled to start in mid-October.

Contract Number: DE-AC06-76RLO 1830, Subcontract B-67775-A-G

Contract Period: 16 May 1980 through 31 May 1982

Funding Level: $797,594

Funding Source: U.S. Department of Energy through Pacific Northwest Laboratory and New York Energy Research Development Agency

CONCEPTUAL DESIGN OF AQUIFER THERMAL ENERGY STORAGE SYSTEM DEMONSTRATION STATE UNIVERSITY OF NEW YORK STONY BROOK CAMPUS, LONG ISLAND

Louis I. Stern
Dames & Moore
6 Commerce Drive
Cranford, New Jersey 07016

ABSTRACT

This is a summary of work to date on the Conceptual Design (Phase I) of an aquifer thermal energy storage system to store winter chilled water for summer air conditioning use. The two-phase Program is to demonstrate the technical, economic, environmental, and institutional feasibility of aquifer thermal energy storage systems. Phase II, which is dependent upon Phase I results, is the detailed design, construction, start-up, and test operation of the system before turning it over to the State University of New York (SUNY).

To date, the above and below ground conditions appear favorable.

INTRODUCTION

Aquifers are used as sources for cooling water, with the warmed waters frequently injected into the aquifer. There are, however, no known large-scale projects for which winter chilled cold water is stored in an aquifer for later use. One potential storage site is the State University of New York, Stony Brook Campus, on Long Island, 50 miles east of New York City (see Fig. 1). The Campus appears ideal: there are extensive above ground facilities which can be retrofitted, and there is an underlying aquifer system. The Upper Glacial and Magothy aquifers (see Fig. 2) are part of an extensive aquifer system which provides drinking and industrial water to Long Island. (In fact, the Environmental Protection Agency has determined that the Long Island aquifer system is the sole or principal source of drinking water which, if contaminated, would create a significant hazard to health.)

Originally (1962) ground water was used for Campus cooling, but a significant rise in ground water temperature resulted in the system being abandoned, although a number of the wells and pumps are still in place.

EVALUATION OF AQUIFER THERMAL ENERGY STORAGE AT STONY BROOK

Phase I is divided into three parts--above ground, below ground, and the coupling of the above and below ground studies to prepare the conceptual design and proposal for Phase II. Dames & Moore is managing the work and performing the Phase I below ground and environmental studies. Ambrosino & DePinto is performing the above ground studies, as a subcontractor.

ABOVE GROUND

The existing chilled water production facilities include a high pressure boiler plant, two 450 psi steam turbine driven centrifugal chillers (4,500 tons each), and 13,000 ton induced draft cooling towers for heat rejection. Chilled water and higher temperature hot water are distributed campus-wide via pipelines in an extensive network of 15 foot by 15 foot utility tunnels.

In the systems being considered, water would be pumped from the aquifer during the winter, piped through the distribution network, chilled by the towers, and then injected back into the aquifer. During the cooling season the stored chilled water would be retrieved, distributed to the cooling units, and then injected into the aquifer. The design factors include the chilled water requirements in terms of tonnage, temperature, and flow; the ability of the existing towers to meet these needs; the need for a closed system with heat exchangers to isolate the water from possible contamination (an open system would be less expensive and more efficient); potential changes in water chemistry; potential corrosion of the existing piping and mechanical equipment; and the energy needed to operate the system(s). Conceptual designs must be evaluated in terms of first cost and potential energy cost savings.

BELOW GROUND

The hydraulic and thermal properties which characterize the aquifer system must be evaluated. The most important parameter is permeability (a measure of how rapdily water can flow through the aquifer); the faster water can move through the aquifer the more economically chill energy can be stored. The direction and rate of ambient ground water flow must be determined, to estimate the movement of stored chilled water (which might affect the amount of energy which can be recovered later), and to evaluate migration of chilled or heated water beyond the Campus. The heat capacity of the aquifer, a measure of how much heat energy can be stored (and later retrieved), must also be estimated; as must the thermal conductivity, which is a measure of how rapidly heat energy moves through the aquifer. The overall thermal efficiency of the storage system, i.e., how much of the chill energy injected into the aquifer will be available for cooling, must be evaluated.

The aquifer characterization program includes literature review, field exploration, field and laboratory testing to obtain hydraulic and thermal properties, a well doublet test with appropriate hydraulic and thermal monitoring, and computer simulation of the doublet test to calibrate a model of the aquifer. The calibrated computer model will be used to compare, analytically, alternative below ground energy storage systems. The results of the studies will be coupled with the above ground work and conceptual designs prepared.

Environmental considerations and constraints, including regulatory requirements, must be evaluated. An understanding of the existing aquifer chemistry is essential, to evaluate possible changes with time and potential adverse effects. Potential problems of using the sole source aquifer system for other than drinking water must be addressed, and a system developed which is acknowledged to be environmentally, as well as economically, sound.

COMBINED ABOVE AND BELOW GROUND

The above and below ground work must be coupled. If aquifer energy storage is feasible, a conceptual design and detailed proposal are to be prepared for the Phase II work.

PROGRAM DESCRIPTION

ABOVE GROUND

Define User Needs, and Existing Production and Transport Capabilities - Computer modeling will be used to determine the total chilled water flow, and temperature and use profile, for the Campus as a whole and for certain major buildings (individual building needs differ, the system must be capable of meeting the worst case, not just the average). The winter production capabilities of the cooling towers and associated problems must be documented on both theoretical and empirical bases. The feasibility of an alternative approach to chill production, the use of existing 100% outside air fan systems on a building

ABOVE GROUND TASKS

It was found that the chilled water system did not operate as designed; and that recent conservation efforts have resulted in higher supply water temperatures and valving-off of certain unused buildings during the summer. SUNY is planning additional conservation measures; their impacts on the thermal energy storage system design criteria are being evaluated. Three of the 40 buildings use 40% of the load; buildings with the large 100% outside air fan systems. If winter chilled ground water could be produced and used in these buildings as a supplemental source, significant energy savings could result at the central plant. There are also potential savings by preheating cold air with water being chilled and stored for summer use (see Figs. 4 and 5). Aquifer storage systems dedicated to only one or two buildings thus look promising, and are being evaluated.

Based on preliminary manufacturer's data, and review of a winter tower installation at Princeton University, the existing cooling towers are capable of producing most of the Campus' chilled water requirements. To minimize environmental problems, cooling towers would only be used with a closed system to prevent ground water from being exposed to the air. For similar reasons the use of heat exchangers between the ground water and the existing chilled water distribution system is being evaluated.

BELOW GROUND TASKS

Available site data and facilities, and the local environment, were the basis for locating the well doublet test, which includes one existing and one new pumping/injection well. The new well, nine observation wells, and the chiller installation, have been completed. In situ thermal conductivity and pumping tests; and baseline determinations of ground water temperature, piezometric levels, and ground water chemistry; are almost completed.

Preliminary two-dimensional computer modeling work has been certified, including comparisons with published works.

Environmental evaluations are proceeding. No permits are required for the Phase I doublet test. The Environmental Protection Agency and New York State Department of Environmental Conservation personnel, as well as county and local governmental organizations, have been contacted and are aware of the proposed program. However, because there are no substantive results to report to date, no significant additional contacts have been made.

COMBINED ABOVE AND BELOW GROUND TASKS

No work has been performed on these tasks.

CONCLUSIONS AND RECOMMENDATIONS

Substantive conclusions or recommendations would be premature. One tentative conclusion has emerged, however. Some existing 100% outside air facilities, coupled with local aquifer thermal energy storage systems, may be suitable for providing significant portions of the chilled water requirements during the summer, as well as for preheating air during the winter.

Nothing has been learned which changes the initial optimism that aquifer thermal energy storage is feasible at Stony Brook.

ACKNOWLEDGMENT

The New York State Energy Research and Development Agency (NYSERDA) was instrumental in identifying Stony Brook as a potential site for aquifer thermal energy storage, and is providing financial support.

by building basis, will be evaluated. The capabilities of the existing distribution system in terms of pipe capacity, tunnel capacity (space for new pipes), and location with respect to new well fields and existing pumping ability must be assessed.

Develop Above Ground Schemes and Economic Analyses - Above and below ground data will be integrated to develop systems for preliminary economic testing. Systems may include direct ground water injection with straining; direct heat exchange using a plate and frame exchangers; open system chilled water production using cooling towers; closed system chilled water production using air systems; central source distribution or individual building wells; once-through systems, and/or condenser water use; the reuse of all or part of the distribution system; the addition of new piping; etc.

BELOW GROUND

Aquifer Characterization - Suffolk County and site specific well data must be evaluated. The well doublet test to obtain site specific field hydraulic, thermal and chemical data, and the computer modeling program, must be designed. Necessary production/injection wells, observation wells, and monitoring appurtenances are to be installed for the doublet test. During the well doublet test (see Fig. 3) ground water will be pumped from one well, through a chiller, and injected into a second well for 45 days to simulate winter. There will be a 30 day quiet period. The chilled water injected into the ground during the first 45 day period will be pumped from the second well, piped through a heater, and then injected into the first well, to simulate the summer air conditioning cycle. During the test measurements of water levels and temperatures will be taken, and changes in the water chemistry evaluated.

Two-dimensional computer modeling will be used to simulate the doublet test, based upon geologic, hydrologic, piezometric, temperature, and water flow data collected prior to and during the doublet test. The model will be calibrated to develop hydrogeologic and thermal parameters for use in modeling and evaluating alternative conceptual schemes.

Development of Conceptual Alternatives - Using the calibrated parameters, and specific selected well configurations, two-dimensional computer models will be used to predict the behavior of alternative below ground schemes. The energy versus time and flow versus time requirements will be input; output will be projected piezometric levels and temperature, versus time. Thermal efficiences will be estimated, and the economics of feasible alternatives compared.

Environmental Evaluations - Above and below ground environmental effects of the conceptual alternatives will be evaluated. Concurrent with other work baseline data will be collected vis-a-vis compliance with regulatory and other environmental constraints. Permitting requirements of Phase II will be determined.

COUPLING OF BELOW AND ABOVE WORK

Economic evaluations of several combinations of above ground and below ground systems will be made. One or more alternatives will be selected for preparation of conceptual designs. Conceptual above and below ground plans, specifications, outline drawings, instrumentation, and cost estimates and schedules will be prepared for the selected system(s). A detailed proposal will be prepared for Phase II work.

RESULTS

Phase I started in mid-May, 1980 and will be completed in March, 1982. Campus energy needs, existing equipment, and distribution facilities have been evaluated. Subsurface data have been evaluated; the wells, and the above ground chiller system, have been completed for the well doublet test, which is to start in November, 1980. Environmental and computer modeling work are progressing.

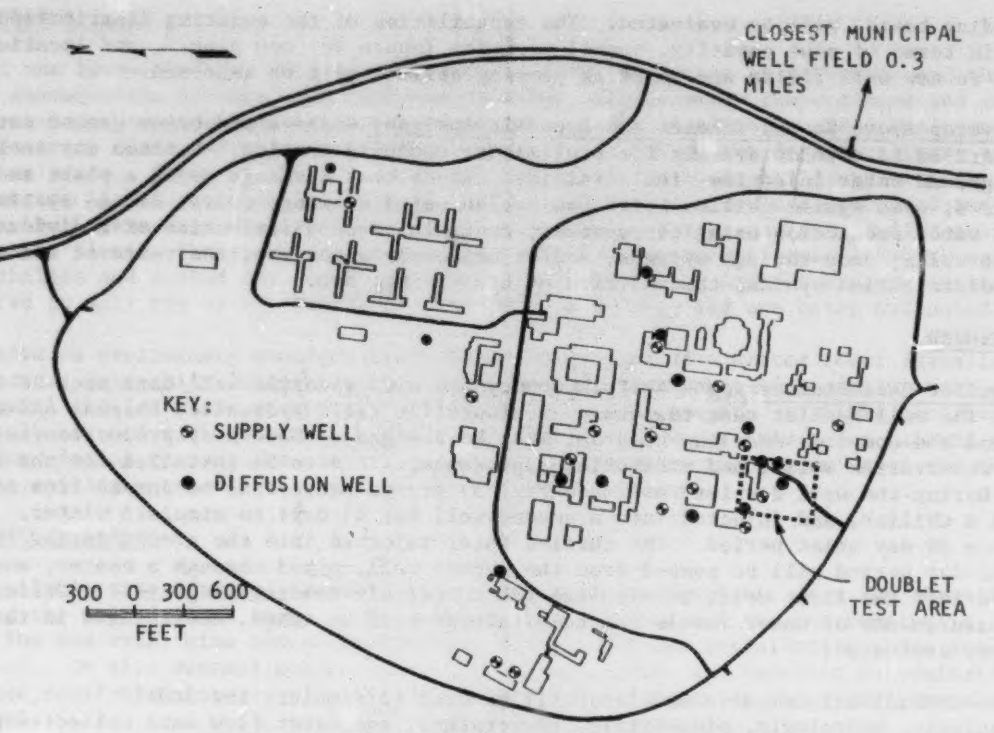
CLOSEST MUNICIPAL
WELL FIELD 0.3
MILES
KEY:
SUPPLY WELL
DIFFUSION WELL
DOUBLET
TEST AREA
300 0 300 600
FEET

MAP OF STONY BROOK'S MAIN CAMPUS
LOCATION OF SUPPLY AND DIFFUSION WELLS

FIGURE 1

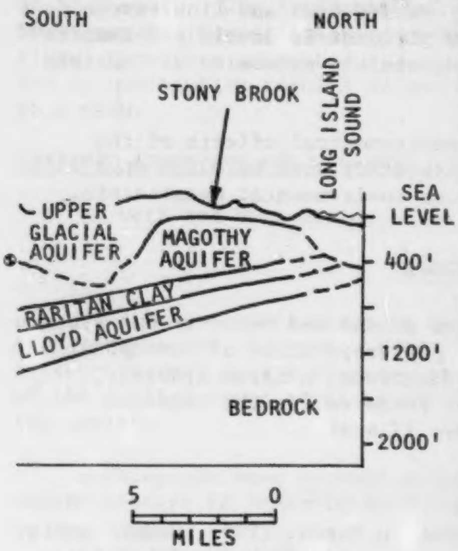
SOUTH
NORTH
STONY BROOK
LONG ISLAND SOUND
SEA LEVEL
UPPER GLACIAL AQUIFER
MAGOTHY AQUIFER
400'
RARITAN CLAY
LLOYD AQUIFER
1200'
BEDROCK
2000'
5 0
MILES

HYDROGEOLOGIC
CROSS SECTION

FIGURE 2

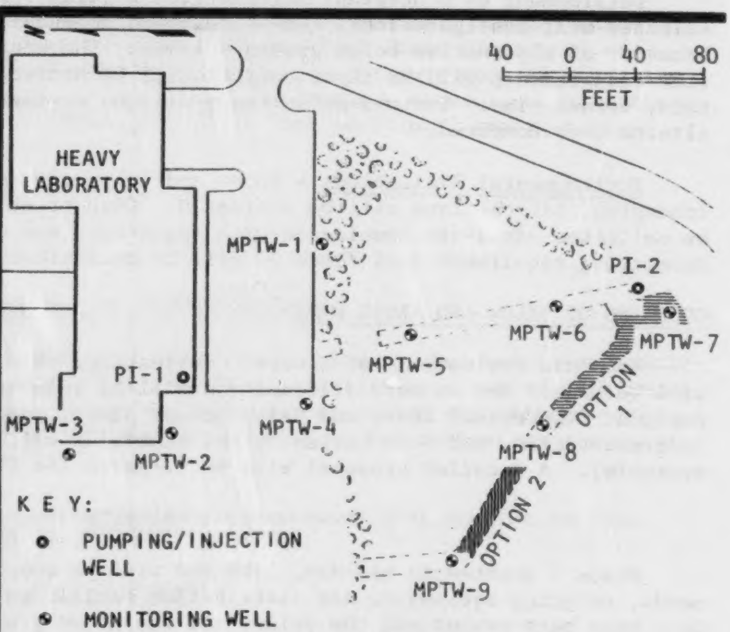
40 0 40 80
FEET
HEAVY
LABORATORY
MPTW-1
PI-2
MPTW-6
MPTW-7
MPTW-5
PI-1
MPTW-4
OPTION 1
MPTW-3
MPTW-2
MPTW-8
OPTION 2
MPTW-9
KEY:
PUMPING/INJECTION WELL
MONITORING WELL

WELL DOUBLET TEST LAYOUT

FIGURE 3

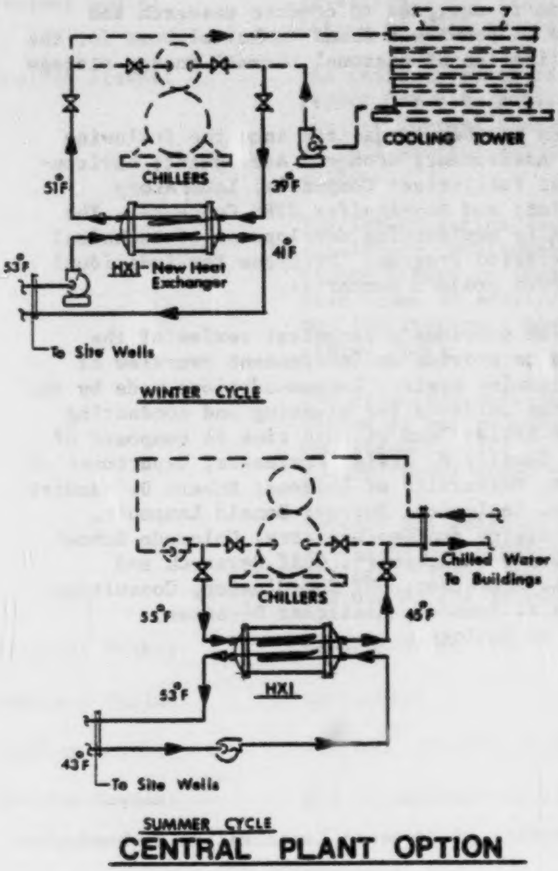
COOLING TOWER
CHILLERS
51°F
39°F
53°F
HX1 New Heat Exchanger
41°F
To Site Wells
WINTER CYCLE
Chilled Water To Buildings
CHILLERS
55°F
45°F
53°F
HX1
43°F
To Site Wells
SUMMER CYCLE
CENTRAL PLANT OPTION

FIGURE 4

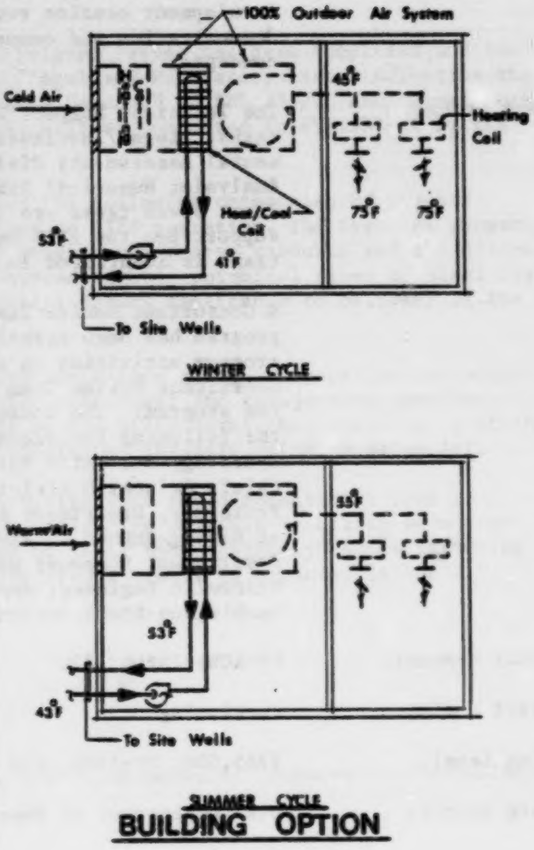
100% Outdoor Air System
Cold Air
45°F
Heating Coil
75°F
75°F
Heat/Cool Coil
53°F
41°F
To Site Wells
WINTER CYCLE
Warm Air
55°F
53°F
43°F
To Site Wells
SUMMER CYCLE
BUILDING OPTION

FIGURE 5

PROJECT SUMMARY

Project Title:	Technical Support Program Management
Principal Investigator:	Jay R. Eliason
Organization:	Pacific Northwest Laboratory P.O. Box 999 Richland, Washington 99352 (509) 376-0115 (FTS: 444-0115)
Project Goals:	The Technical Support Program is designed to conduct research and development studies required to provide a sound technical base for the demonstration and commercialization of seasonal thermal energy storage concepts.
Project Status:	The Technical Support Program has been organized into the following tasks: Legal/Institutional Assessment; Economic Assessment; Environmental Assessment; Field Test Facilities; Compendia; Laboratory Analysis; Numerical Simulation; and Non-Aquifer STES Concepts. The first seven tasks are initially emphasizing development of technical support for the ATES Demonstration Program. Progress for individual tasks is identified in separate project summaries. A Consultant Review Team which provides a technical review of the program has been established to provide an independent overview of program activities on a continuing basis. Recommendations made by the Consultant Review Team provide guidance for planning and conducting the program. The Consultant Review Team at this time is composed of the following individuals: Stanley N. Davis, Professor, Department of Hydrology and Water Research, University of Arizona; Robert D. MacNish, Chief, Arizona District, U.S. Geological Survey; Donald Langmuir, Professor, Department of Chemistry and Geochemistry, Colorado School of Mines; Arthur C. Riese, Senior Geochemist, Gulf Research and Development Company; David L. Schreiber, CRT Coordinator, Consulting Hydraulic Engineer; and John F. Spencer, Assistant Director, Washington State Department of Ecology.
Contract Number:	DE-AC06-76RLO 1830
Contract Period:	Continuing
Funding Level:	$265,000, FY-1980, B/O
Funding Source:	U.S. Department of Energy, Office of Advanced Conservation Technologies

PROJECT SUMMARY

Project Title: Legal/Institutional Assessment

Principal Investigator: Paul L. Hendrickson

Organization: Pacific Northwest Laboratory
P.O. Box 999
Richland, Washington 99352
(509) 376-4253 (FTS: 444-4253)

Project Goals: Investigate the legal and regulatory issues that will affect implementation of STES concepts.

Project Status: The initial review of ATES related issues has been completed and the report has been published, "Legal and Regulatory Issues Affecting the Aquifer Thermal Energy Storage Concept" as PNL 3437. Additional work in this general subject area will be conducted in FY-1981-82 by the author.

The investigation focused on the following categories of issues: regulatory requirements prior to ATES operation, the types of property rights needed to store and recover the energy resource and the alternative means to acquire the needed rights, potential areas of liability, and institutional and financial issues applicable to delivery of the stored energy.

The principal regulatory considerations prior to operation are acquisition of needed ground-water withdrawal and reinjection permits. Requirements will be mainly at the state level, but could occur at the Federal level under the authority of the Safe Drinking Water Act.

Surface and subsurface activities that could potentially lead to liability and approaches to mitigating possible liability were considered. The investigation of legal and regulatory issues affecting end use of the stored energy resource will be expanded in 1981.

Contract Number: DE-AC06-76RLO 1830

Contract Period: Continuing

Funding Level: $46,000, FY-1980, B/O

Funding Source: U.S. Department of Energy, Office of Advanced Conservation Technologies

LEGAL AND REGULATORY ISSUES APPLICABLE TO AQUIFER THERMAL ENERGY STORAGE

Paul L. Hendrickson
Pacific Northwest Laboratory
P.O. Box 999
Richland, Washington 99352

ABSTRACT

This paper summarizes research conducted during FY 1980 at the Pacific Northwest Laboratory on the subject of legal and regulatory issues affecting the aquifer thermal energy storage (ATES) concept. The investigation considered issues in four subject categories: 1) regulatory requirements prior to operation, 2) potential liability from ATES operations and available means to mitigate possible liability, 3) issues related to storage and recovery of the energy resource, and 4) institutional and financial issues applicable to delivery of the stored energy resource.

The results of the investigation have recently been published.(1) Additional related work is planned in coming years as part of the Seasonal Thermal Energy Storage (STES) Program managed by the Pacific Northwest Laboratory for the Division of Energy Storage Systems, U.S. Department of Energy.

INTRODUCTION

Most work to date on the ATES concept has appropriately been devoted to studies on technical feasibility and potential problems. A period of field testing and demonstration of the concept under the STES Program has now begun. The projects will help determine technical feasibility, environmental impact, and energy storage costs through actual applications. If the test results are favorable and the costs of delivered energy are sufficiently attractive in comparison with other energy sources, it is likely that commercial application will follow. Accordingly, it seems desirable to examine the significant legal and regulatory issues that can influence successful implementation of the concept.

REGULATORY REQUIREMENTS PRIOR TO OPERATION

Initiation of an ATES project will necessarily involve compliance with certain permits and regulatory requirements. In most western states and some eastern states, a permit to withdraw ground water will be required from the appropriate state water resources agency. Most states have requirements related to well drilling, construction, and abandonment. In many states, a separate permit to reinject the thermally altered ground water will be required from the appropriate pollution control agency. A few states prohibit such reinjection, and a variance will be necessary if an ATES project is to be implemented. Eventually, a permit from a state agency or the U.S. Environmental Protection Agency under the Underground Injection Control (UIC) Program established by the Safe Drinking Water Act of 1974 will be required. This requirement will supersede existing underground injection requirements. Final UIC requirements for the well classification likely to include ATES wells will probably not be issued for several years. An ATES project may also trigger the need for an environmental impact statement (EIS) under the National Environmental Policy Act (NEPA) if a significant Federal action is involved in licensing or construction. Even if an EIS under NEPA is not required, about 20 states require an EIS for projects with significant environmental impacts. Table 1 summarizes potential regulatory requirements.

POTENTIAL LIABILITY

An ATES operator should be aware of several possible sources of liability. Liability is most likely for interference with the property rights of others in the storage aquifer. Interference with existing users of an aquifer as a potable water source is of greatest concern. Alleged interference would most likely be for increased water temperature, although it is also possible that an ATES operation could lead to some chemical or biological contamination of ground water. Liability is also possible to other existing ground-water users, to potential ground-water users in states (principally eastern states) recognizing overlying ground-water rights, and to mineral rights holders if mineral interests (including oil and gas) are interfered with. Subsurface storage rights and/or mineral rights may have to be purchased if significant liability is foreseen.

Surface drilling and injection activities can also potentially lead to liability through such things as noise, vibrations and fluid spills. Proper care in surface operations can minimize these possibilities.

TABLE 1. Areas of Regulation Potentially Applicable to an ATES Project

Activity	Level of Control		
	Federal	State	Local
EIS	Required by NEPA for projects with significant Federal activity and environmental impacts.	Required in about 20 states, requirements can often be satisfied by a NEPA EIS.	
Land Use		Permit may be needed in certain states that regulate key facilities.	Compliance with applicable zoning and land use plans.
Well Drilling		Most states have requirements.	
Ground Water Withdrawal		Permit needed in most western and some eastern states.	Units of local government regulate withdrawal in a few states, e.g., Calif.
Ground Water Reinjection	By about 1984, UIC permit will be needed from EPA in states without UIC program authority.	Permit currently needed in about half of states. By about 1984, permit required under UIC program from states that receive UIC program authority from EPA.	Certain local governments (e.g., Kern County, Calif.) have injection requirements.

STORAGE AND RECOVERY

A central concern of the ATES operator will be assurance of the ability to store, protect, and recapture the thermal energy when desired. At a minimum, the ATES operator will need to purchase or when necessary condemn (assuming statutory authority) sufficient surface property rights to provide site access, drill needed wells and provide adequate spacing from nearby land use activities. Acquisition of a subsurface energy storage easement may be needed if significant liability is foreseen or if intentional interference with the ATES operation by a surface owner/user is considered possible. Both of these contingencies are more likely if a relatively shallow aquifer is utilized for storage, although the likelihood of each can be rendered very small by careful aquifer selection. The possibility that someone could drill with impunity into the energy storage bubble with the major purpose of capturing stored energy and/or interfering with an ATES operation is remote. This is true even if the ATES operator has not acquired any property interests.

ENERGY DELIVERY

Many legal, institutional, and regulatory issues will occur at the stage of heat or chill delivery. A principal issue is locating an entity with sufficient incentive to construct and operate an ATES and delivery system. It may be difficult to find an investor-owned entity with sufficient economic incentive; consequently, the responsibility may fall to a public body. A variety of other issues related to financing, rate setting, service areas, taxation, and other areas will require resolution. These issues are likely to be most complex for a residential district heating system.

CONCLUSIONS

A variety of legal and regulatory issues will affect implementation of the ATES concept. The most important regulatory issue is likely to be restrictions and related permit requirements for re-injection of thermally altered ground water into an aquifer. Acquiring needed permits will be most difficult when the aquifer is used as a potable water source.

Property rights and liability concerns are also important, but will likely prove less critical than regulatory concerns. It seems possible to conclude that an ATES operator can assure the right to store, protect, and recapture the energy and to adequately limit the possibility of future liability. It is also likely that this assurance can be provided at a reasonable cost, especially in relation to total ATES costs.

REFERENCE

1. Hendrickson, P. L., "Legal and Regulatory Issues Affecting the Aquifer Thermal Energy Storage Concept," PNL-3437, October 1980, Pacific Northwest Laboratory, Richland, WA 99352.

PROJECT SUMMARY

Project Title: Economic Assessment

Principal Investigator: Raymond Wm. Reilly

Organization:
Pacific Northwest Laboratory
P.O. Box 999
Richland, Washington 99352
(509) 376-4359 (FTS: 444-4359)

Project Goals: Conduct economic analyses and related investigations for all phases of the Seasonal Thermal Energy Storage (STES) Program.

Project Status: The project consisted of four major activiites. The first two are complete, and the second two will be completed during FY-1981.

A literature search was made to document the technical, environmental, economic, and institutional aspects of the Aquifer Thermal Energy Storage (ATES) technology. The results were published in A Descriptive Analysis of Aquifer Thermal Energy Storage Systems, June 1980.

A work statement was designed and an external contract was let to develop Guidelines for Conceptual Design and Evaluation of Aquifer Thermal Energy Storage Systems. The document was published in October 1980.

A computer code has been developed and is operational for analysis of the economics of ATES systems. The code: AQUASTOR, simulates the development and operation of an aquifer storage system (including transmission and distribution systems) to develop a life-cycle cost for delivered thermal energy (heat or chill). AQUASTOR will undergo refinement, through checkout, and documentation during FY-1981, and will then be made available for public use.

Preliminary investigations were made into the economics of chill storage in aquifers (in conjunction with development of AQUASTOR). In-depth, site-specific analyses of chill storage will be conducted during FY-1981.

Contract Number: DE-AC06-76RLO 1830

Contract Period: Continuing

Funding Level: $99,000, FY-1980, B/O

Funding Source: U.S. Department of Energy, Office of Advanced Conservation Technologies

ECONOMIC ASSESSMENT OF AQUIFER THERMAL ENERGY STORAGE

R. W. Reilly/D. R. Brown/H. D. Huber
Seasonal Thermal Energy Storage Program
Pacific Northwest Laboratory
P.O. Box 999
Sigma 4 Building/3000 Area
Richland, Washington 99352

ABSTRACT

This paper describes the FY 1980 economic assessment program undertaken at PNL in support of the Seasonal Thermal Energy Storage (STES) Program. The effort was composed of four major activities: 1) summary of the existing state of the Aquifer Thermal Energy Storage (ATES) technology, 2) development of a techno-economic computer code for in-depth economic analysis of ATES systems, 3) initial investigations into the cost of heat and chill storage, and 4) development of a methodology for conceptual design and evaluation of ATES systems.

The first three activities were performed in-house, and form the basis for continuing economic analysis of ATES at PNL. The results of these activities will be discussed in this paper. The fourth activity was subcontracted to General Electric TEMPO, and is discussed in a separate paper.

The first activity is complete and the results are published in A Descriptive Analysis of Aquifer Thermal Energy Storage Systems, June 1980 (PNL-9238). The techno-economic computer code, AQUASTOR, is operational, and is presently undergoing refinement. It will be made available to the general public in March 1982, after completion of testing and documentation. Initial work on chill storage economics was presented in a paper at the 15th Intersociety Energy Conversion Engineering Conference in a paper entitled, "The Economics of Aquifer Storage of Chilled Water for Air Conditioning." This paper will present initial findings on heat storage economics. The fourth activity has resulted in Guidelines for Conceptual Design and Evaluation of Aquifer Thermal Energy Storage Systems, a document now in the final stages of publication.

INTRODUCTION

The Seasonal Thermal Energy Storage (STES) Program is a large scale effort to demonstrate the technical and economic feasibility of storing significant amounts of thermal energy on a seasonal basis. The program is managed by Pacific Northwest Laboratory for the Office of Advanced Conservation Technologies, U.S. Department of Energy.

The program is composed of two major parts: the demonstration subprogram and the technical support subprogram. The former is supporting a number of Aquifer Thermal Energy Storage (ATES) demonstration installations to illustrate the commercial potential for ATES storage. The technical support subprogram is seeking ways to reduce technological and other barriers to development of energy storage systems (with an emphasis on ATES) prior to widespread investment in demonstration and/or commercial facilities.

The economic assessment effort is an integral part of the technical support subprogram, with the responsibility for assessing the economic feasibility of seasonal thermal energy storage technologies. The major objectives are: 1) to determine whether a storage technology has adequate economic promise to warrant further technical investigation, 2) to provide economic information which will enable optimization of storage applications and implementation, 3) to guide technical research into the most fruitful areas, and 4) to provide support to the ATES demonstration subprogram. All of the FY 1980 economic assessment effort was expended in support of the ATES technology.

PROGRAM DESCRIPTION

SUMMARY OF THE EXISTING STATE OF THE ATES TECHNOLOGY

At the onset of the STES Program it was recognized that, although there existed a body of scientific literature on ATES, there was no document which presented an overall picture of the nascent technology. Since a major intent of the STES Program is technology transfer to the commercial sector, such a document was needed as an introduction to more technical information, and to serve as a general marketing document. Further, such a document could serve to focus program activities upon the most pressing issues facing the technology.

Generation of the document was assigned to the economics assessment effort. After an extensive literature search through the STES library, A Descriptive Analysis of Aquifer Thermal Energy Storage Systems was published in June 1980.

The 71-page document presents an overall picture of the ATES technology, citing the major issues facing the technology, and investigating its potential. The major areas investigated include: storage applications, technical feasibility, environmental considerations, aquifer availability, energy source availability, systems economics, potential markets, and legal and institutional issues. The overall result of the investigation was that there appear to be no major impediments to widespread ATES implementation, although there are a number of significant unknowns. Perhaps the most difficult issues facing the technology are institutional in nature: providing impetus for initiation of ATES systems, and procuring the funding required for construction of the capital-intensive energy delivery systems.

As part of the market research effort for the document, a brief investigation was made to estimate the energy savings that could accrue through widespread implementation of ATES systems. It was found that up to 7.5% of the total national energy demand could be supplied by ATES in the year 2000. This is purely a technical limitation based upon type of use, temperature restrictions, delivery restrictions, and aquifer availability. It does not consider the cost-effectiveness of ATES, the need for collocation of energy sources and users, nor the enormous capital budget that would be required for such widespread implementation. Because of these factors, the realized energy savings in the year 2000 will be considerably less than is indicated by technical constraints.

THE AQUASTOR CODE

The major tool employed in the investigation of ATES economics is AQUASTOR, a computer code developed at PNL specifically for evaluation of the economics of heating and cooling using energy supplied by an ATES installation. AQUASTOR provides the capability to individually or collectively evaluate the impact of various technical and economic conditions upon the cost of cooling. It consists of two major parts. The supply submodel calculates the unit cost of energy production by simulating the exploration, development, and operation of an ATES system, and the transmission of this energy to a distribution center. The distribution submodel calculates the unit cost of delivered energy by simulating the development and operation of district and/or point demand heating (cooling) systems.

AQUASTOR can simulate nearly any financial and tax structure by varying the rates of return on equity and debt, the debt-equity ratio, tax rates, investment credits, and depreciation schedules. Both municipal utility and private ownership can be simulated. The supply submodel and the distribution submodel may have the same or different financial structures and costs of capital.

The code calculates the cost of energy delivery by actually designing thermal collection and delivery systems and simulating cash flows over the lifetime of the system. Piping, insulation, pumps, and other capital items are optimized in the design, based upon capital, operation, and maintenance costs.

AQUASTOR does not attempt to simulate fluid or thermal flow within the aquifer. Rather it captures the relevant aquifer characteristics in three input parameters: fluid recovery fraction, thermal storage efficiency, and in-situ aquifer temperature. The fluid recovery factor is simply the ratio of the water recovered from the storage well field to the previously injected water. It can vary from a fractional value to greater than one, depending upon the nature of the aquifer being simulated, the temperature differential between the injected water and the in-situ water, and the energy delivery system's response to temperature degradation of the delivery fluid. (Some users may shut down when the temperature of the water starts to degrade; others may be able to continue operation by increasing the flow rates, or by employing supplemental energy sources.) The thermal efficiency factor is similarly the ratio of energy recovered to energy injected, both defined with respect to the in-situ water temperature. Defining storage efficiency in this manner isolates aquifer storage efficiency from the characteristics of the above-ground equipment.

The code operates on an average-year performance basis. In an actual ATES development, aquifer efficiency is expected to rise dramatically over the first several years of operation as the aquifer is conditioned to the temperature of storage by lost thermal energy, and it is expected to approximate a steady state afterwards. In the present configuration of AQUASTOR, only the steady state situation is modelled.

During FY 1981 the code will be streamlined, validated, and documented. It will be made available to the general public by March of 1982 through the Argonne code center, and through the DOE/STOR Technical Management Information System (TMIS).

INITIAL INVESTIGATIONS INTO THE COST OF AQUIFER STORAGE

During the year initial cost studies were made for both heat and chill storage in aquifers, using the AQUASTOR code as the primary tool.

The intent of the chill study was to evaluate the effect of a number of technical and economic parameters on the cost of chill storage. These included: system size, load factor, transmission distance, load reject temperature, source availability, source temperature, aquifer thermal efficiency, well cost, electricity cost, and the cost of capital. The major result of the investigation is that the cost of chill storage is extremely dependent upon site-specific conditions. Under appropriate demand, supply, and geologic conditions ATES cooling can be competitive with both electric compression and absorption chiller devices. Under less favorable conditions, the cost of cooling could be an order of magnitude too high.

A few implications can be drawn for all ATES cooling systems. It will be uneconomical to pump chilled water for very long distances due to the low energy density of the fluid. Hence, a typical ATES cooling system will be located on or near a suitable aquifer with the energy supplied by a nearby chill source (such as winter air collected at the site). Another implication of the study is that temperature gain of the cooling water at the load must be maximized, since that determines the energy delivered per unit of fluid delivered. A few degrees variance in the delivery water temperature can markedly affect the cost of cooling, and so equipment components must be chosen carefully to maximize this delta T. A major consideration is choice of heat exchanger approach temperature; it is likely that rather low approach temperatures (on the order of 2-5°F) will be optimum.

Initial heat storage studies have indicated that seasonal storage in aquifers can be very cost effective. A brief investigation was made to determine storage costs (with no cost for stored thermal energy and no distribution or end-use costs). Most of the assumptions made were highly favorable for an ATES system, thereby providing best-case cost performance estimates. Under these best-case assumptions (including an 80% aquifer thermal recovery efficiency, a 30% load factor, and 10% municipal utility financing), the results below were generated. All costs are levelized costs in $/MBtu, January 1979 price levels.

150°C ENERGY SOURCE

	1 MW_t Peak Load	10 MW_t Peak Load	100 MW_t Peak Load
150-ft deep aquifer	8.37	1.62	0.97
1000-ft deep aquifer	10.28	2.31	1.78

90°C ENERGY SOURCE

	1 MW_t Peak Load	10 MW_t Peak Load	100 MW_t Peak Load
150-ft deep aquifer	9.23	2.66	2.04
1000-ft deep aquifer	11.89	4.81	4.29

PROJECT SUMMARY

Project Title:	Development of a Methodology for Conceptual Design and Evaluation of Aquifer Thermal Energy Storage (ATES) Systems. (Short Title: ATES Guidelines.)
Principal Investigator:	Charles F. Meyer, Walter Hausz
Organization:	General Electric Company GE-TEMPO Santa Barbara, California 93102 (805) 965-0551
Project Goals:	To develop and present guidelines as a tool for those considering use of a new technology, ATES. The guidelines will assist in the conceptual design and the evaluation of technical and economic feasibility of systems employing ATES.
Project Status:	The project has been completed. Chapters 1 and 2 of the Guidelines, totaling seven pages, describe the potential benefits of ATES, give an overview of the technology and its application, and provide rules of thumb for quickly judging whether a proposed project has sufficient promise to warrant detailed conceptual design and evaluation. The balance of the document discusses the characteristics of sources and end uses for heat and chill which are seasonally mismatched and may benefit from ATES (industrial waste heat, solar heat, winter chill, and cogeneration, for space heating and air conditioning); describes storage and transport subsystems and their expected performance and cost, as best these parameters are now known; presents a 10-step methodology for conceptual design of an ATES system and evaluation of its technical and economic feasibility, with examples; and applies the methodology to a hypothetical proposed ATES system, to illustrate its use.
Contract Number:	DE-AC06-76RLO 1830, Subcontract B-67764-A-O
Contract Period:	12 February 1980 through 30 September 1980
Funding Level:	$95,357
Funding Source:	U.S. Department of Energy through Pacific Northwest Laboratory

DEVELOPMENT OF GUIDELINES FOR CONCEPTUAL DESIGN AND EVALUATION OF AQUIFER THERMAL ENERGY STORAGE SYSTEMS

Charles F. Meyer
Walter Hausz
General Electric Company-TEMPO
P.O. Drawer QQ
Santa Barbara, California 93102

ABSTRACT

This paper summarizes and discusses briefly a 10-step methodology which has been developed for conceptual design of an ATES system and evaluation of its technical and economic feasibility.

INTRODUCTION

Relatively few studies of system applications of ATES have been published, compared to the numerous reports on worldwide investigations of ATES phenomenology which have appeared since descriptions of the potential benefits of ATES were first published in the U.S. literature.(1,2)

DOE predicts that, by the year 2000, seasonal aquifer storage could replace or conserve up to 350 million barrels of oil per year. DOE's Office of Advanced Conservation Technologies, placing a high priority on ATES, has established a Seasonal Thermal Energy Storage Program managed by its Pacific Northwest Laboratory.

PNL has awarded contracts for three projects to demonstrate the commercial potential of ATES and stimulate interest in its use. The STES Program library has collected approximately 1400 articles on STES with main emphasis on ATES.(3) PNL has written a brief description of ATES technology for the layman.(4) A need was recognized for a manual on the design and evaluation of ATES systems, to be used as a tool by utilities, municipalities, industry, and other entities considering application of ATES.(5) PNL awarded a contract to TEMPO for this work. The project was completed on 30 September 1980.

Highlights illustrating the contents of the *ATES Guidelines* follow.

INITIAL SCREENING

An Executive Summary gives an overview of ATES and its potential benefits, and provides some rough rules of thumb for early screening to judge quickly whether a proposed ATES system has sufficient promise to warrant spending the time and effort required for detailed conceptual design and evaluation.

Use of ATES can correct large-scale mismatches between thermal energy supply and demand — between seasonal loads, such as space heating and air conditioning, and the availability of inexpensive supplies of heat or chill, such as solar heat, byproduct or waste heat, and winter chill. ATES has a significant potential for

- Conserving energy
- Reducing energy costs
- Permitting substitution of coal or nuclear heat for oil and gas
- Improving the dependability of low to medium temperature heat supply or of chill supply
- Abatement of air and water pollution.

Criteria suggested for early screening are: a seasonal mismatch exists between the availability and the use of heat or chill; high temperature water rather than steam is a satisfactory heat-transport medium; hot water needs to be stored at a rate of at least 3 MW thermal for 90 days or more, cold water at a rate of at least 1 MW, for good recovery efficiency; a suitable aquifer may be available; and the cost of ATES, including exploratory drilling and aquifer testing if needed, is acceptable.

STEPS IN CONCEPTUAL DESIGN AND EVALUATION

1. Describe expected thermal energy load as a function of time.
2. Describe prospective energy source as a function of time.
3. Compare source and load:
    a. Quantify mismatch as a function of time.
    b. Select supply and storage temperatures.
    c. Estimate ATES capacity needed, and location.
    d. Estimate transport capacity and length needed.

4. Estimate losses in ATES and transport. Add these to the thermal load to find the annual total energy demand, production required, and maximum hourly peak. Adjust estimates of ATES and transport capacity needed.
5. Develop operating schedules for production, transport, ATES charge, and ATES discharge, to supply the demand.
   a. Evaluate effect of temperature drop across ATES heat exchangers.
   b. Evaluate effect of temperature loss as stored water is withdrawn.
   c. Plan for mitigation of temperature losses, if necessary (blending, add trim heat, increase supply temperature during storage).
   d. Iterate earlier steps to incorporate mitigation.
6. Evaluate the potential benefits of ATES: Assume ATES at zero cost. Subtract the other costs and the fuel consumption of the system using ATES from those of the reference system without ATES. The difference is the breakeven cost and the fuel savings of ATES. If the difference is negative, ATES is not beneficial for the proposed application.
7. Repeat above procedure to develop alternative conceptual ATES system designs covering variations in energy sources, uses, and ATES employment.
8. Make rough estimate of the expected cost of ATES facilities and their operation.
9. If the prospective benefits found in step 6 are
   a. Substantially less than the expected cost of ATES facilities (including exploratory drilling and aquifer testing, if needed): Defer or abandon investigation.
   b. Substantially greater than the expected cost of ATES facilities: Proceed with exploratory drilling and aquifer testing if needed, or utilize existing information if available, to ascertain hydrogeological and geochemical parameters of candidate aquifers. Prepare preliminary design of ATES facilities to develop budgetary estimate of performance and cost.
   c. Roughly equal to the expected cost of ATES facilities: Evaluate secondary benefits (environmental, reliability, fuel substitution) and disbenefits (regulatory problems, risk that no suitable aquifer will be available). Decide whether secondary benefits outweigh disbenefits sufficiently to justify proceeding as in step 9(b).
10. If step 9(b) is performed, use the improved performance and cost data to repeat steps 4 through 9.

DISCUSSION

To evaluate the possible benefits of ATES in making feasible the use of inexpensive thermal energy sources, a basis for comparison is needed — a reference system with no ATES, which supplies thermal energy for the same end use in some other way. The reference system may be quite different from the ATES system; for example, space heating with boilers instead of solar heat. It may be quite similar: a cogeneration-district heating system, already quite energy efficient, using boilers rather than ATES for standby and peaking purposes. The reference system may already exist, or it may be an alternative conceptual design.

In the design and evaluation steps given above, it will be noted that the approach is to defer estimating the cost and performance of ATES facilities until it has been established (steps 1 through 7) that ATES has a potential payoff in cost and fuel savings. This sequence is suggested so that relatively well-known system design procedures and components can be dealt with before undertaking the more speculative steps of ATES design and predictions of cost and performance. As in the early screening, the objective is to save time and expense if seasonal storage is not sufficiently promising.

The starting point is information about the thermal energy source and the end use being considered:

- *Source or sources of heat or chill:* Amount, quality (temperature), cost, and constraints on availability, all versus time. Location.
- *End use or uses for heat or chill:* Amount, temperature, and dependability of thermal energy supply required, versus time. Flexibility of requirements. Location. Allowable price or cost of supply (usually that of a reference or alternative supply such as natural gas).

To quantify mismatch between supply and demand, estimate ATES charge and discharge capacity required, and develop operating schedules, projections will be needed of total annual energy production and demand in energy units (gigajoules or megawatt-hours); of monthly production and demand in both energy and power units (GJ, MW); of hour-by-hour production and demand for typical weeks in the year, in power units; and of peak hourly production and demand, in power units.

A basic configuration of ATES is shown in Fig. 1. The two wells of the doublet comprise a closed hydraulic system. Water pumped from one well is injected into the companion well. No water is consumed.

Heat is stored in the porous rock comprising the aquifer, in the water filling the pores, and in the relatively impervious aquifer cap and bottom. When heat is to be stored, hot water from the sendout pipeline flows through the counterflow heat exchanger as shown by the open arrows in Fig. 1. Groundwater is pumped from the warm well, flows through the heat exchanger where it picks up heat, and

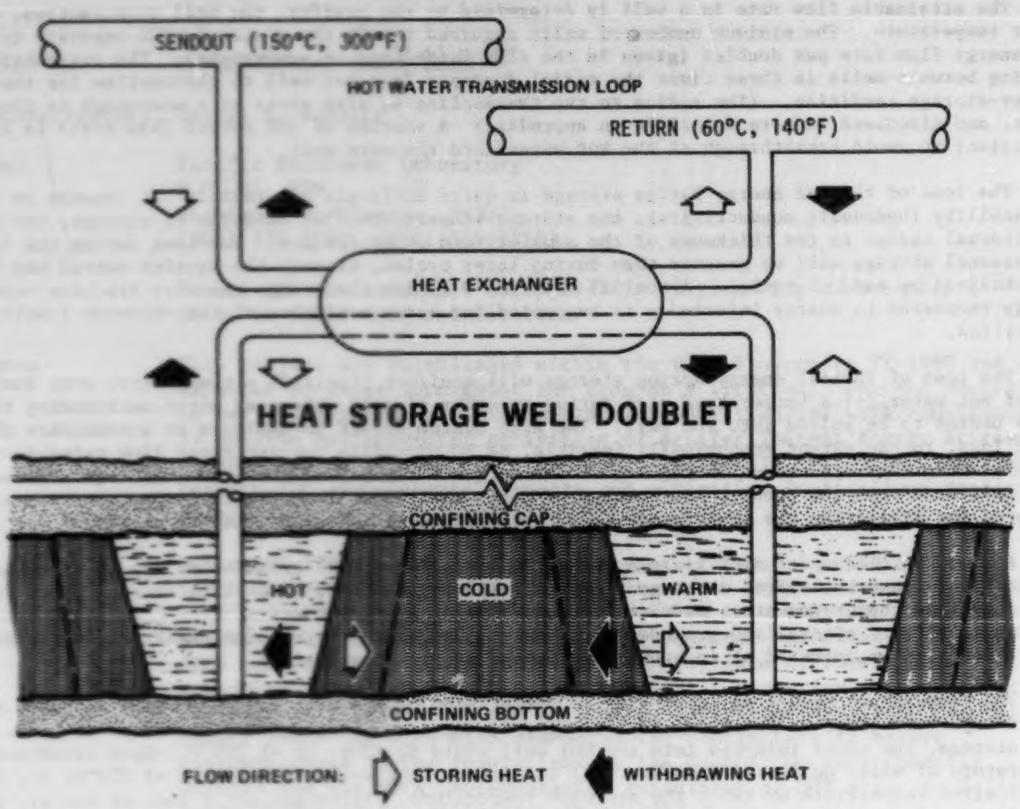

Fig. 1. Schematic diagram of Heat Storage Well doublet operation.

is injected into the hot well. As shown by the open arrows, the thermocline between warm and cold water moves inward toward the warm well, and the thermocline between hot and cold water moves radially outward from the hot well. When heat is to be recovered from storage, water flow and thermocline movement are reversed as shown by the solid arrows.

If the stored water is at a temperature above the local boiling point, it must be maintained in its liquid phase by keeping it at all times under a pressure higher than its saturation pressure. A reasonable expectation is that a confined aquifer at a depth of 100 to 300 meters (350 to 1000 feet), not heavily pumped for other purposes, will have sufficient natural pressure (artesian head) to exceed the saturation pressure of water at 150°C (300°F): 375 kPa gauge pressure at sea level (54 psig), corresponding to 38 meters (126 feet) of artesian head at normal aquifer water temperature. This temperature is expected to be about the economic maximum storage temperature. Because of the rapid increase in saturation pressure of water above 150°C, water at higher temperatures is likely to have an immediate surface use more beneficial than storage; and containing higher pressures would require such deep, tightly-confined aquifers that the cost of wells could be prohibitive.

The amount of ATES capacity needed, to a first approximation, is the difference (mismatch) between the peak load and the maximum dependable output of the energy source at the time of peak load. The energy source supplies as much as it can, and withdrawal from ATES supplies the rest. If peaks in energy-source output need to be smoothed (eg, captured waste heat, or winter chill), ATES stores whatever the load does not need at the time and delivers it later. (Note that ATES is capable of also smoothing short term fluctuations in addition to seasonal fluctuations.) In contrast to use of tanks for storing hot water, the capacity required and the cost of ATES are determined almost entirely by the maximum rate of storage or discharge, not by the amount of energy to be stored. The storage media (water and rock), the containment (layers of clay or shale), and the insulation (rock and sand) are all provided by the aquifer formation. The only significant capital cost elements are the land, the wells, and the surface equipment for handling the hot (or cold) water.

The attainable flow rate in a well is determined by the aquifer, the well construction, and the water temperature. The minimum number of wells required equals the required ATES capacity divided by the energy flow rate per doublet (given in the *ATES Guidelines* by nomographs). The suggested minimum spacing between wells is three times the radial distance from hot well to thermocline for the maximum energy-storage condition. (The radius to the thermocline is also given by a nomograph in the *ATES Guidelines,* and discussed in more detail in an appendix.) A spacing of 200 meters (650 feet) is likely to be sufficient to avoid breakthrough of the hot water into the warm well.

The loss of thermal energy during storage is quite difficult to predict. It depends on the aquifer permeability (hydraulic conductivity), the storage temperature, the duration of storage, the ratio of the thermal radius to the thickness of the aquifer, and other factors. The loss during the first cycle of seasonal storage will be greater than during later cycles, because the aquifer matrix has been warmed (or chilled) by earlier cycles. A nominal value of 0.75 for the energy recovery fraction — ratio of energy recovered to energy injected — is suggested for early estimates of the recovery fraction after a few cycles.

The loss of thermal energy during storage will manifest itself in a temperature drop during recovery of hot water, or a temperature rise during recovery of cold water, as water surrounding the thermocline begins to be pulled into the well. The ATES system should be designed to accommodate this temperature loss, to the extent economically feasible, as by providing for increased flow rates in the sendout pipeline when they are needed. Blending of water from a primary heat source (eg, cogeneration) with that delivered from the doublet heat-exchanger often may reduce the effect of the temperature loss. Measures for mitigating the temperature loss, such as adding trim heat, may be needed.

In some chilled-water ATES systems, direct circulation of the groundwater may be feasible. In most applications, however, a heat exchanger (Fig. 1) will be required, to isolate treated water in the pipeline loop from the groundwater, prevent contamination of the groundwater, keep possible corrosion and scaling effects of mineralized groundwater out of the pipeline system, and permit the pipeline and the well systems to be operated at independent flow and pressure conditions.

The temperature drop from input side to outlet side of the heat exchanger (the approach temperature) has an important effect. Referring back to Fig. 1, suppose the approach temperature is 15°F. During heat storage, the water injected into the hot well would be (300 - 15 =) 285°F. Upon withdrawal, the temperature of water delivered from hot well to sendout line would be (215 - 15 =) 270°F; ie, lower than the pipeline temperature by twice the approach temperature. (Although not a loss of energy, this is a degradation of energy.) To cut the approach temperature in half requires doubling the heat exchange area. An economic tradeoff must be made. The ATES system should be designed to accommodate this temperature drop, as well as that lost during storage. Mitigating measures also should be evaluated.

The life-cycle cost of the reference system and the ATES system(s) should be used for economic evaluation of the possible benefits of ATES. Recognizing that other criteria such as payback time may also be a part of the decisionmaking process of some entities, and will be employed, it is recommended that life-cycle costing also be employed. The "required-revenue" approach, a special form of the present worth method, is in common use by electric utilities for evaluating and comparing alternative energy systems which may differ significantly in their makeup. This approach, as described by the Electric Power Research Institute(6), is suggested. It is summarized in the *ATES Guidelines;* supporting equations and tables are given in an appendix.

The final chapter in the *ATES Guidelines* is an illustrative example of the application of the suggested methodology, going from an existing urban situation to conceptual cogeneration-district heating systems with and without ATES, and comparing them.

REFERENCES

1. Kazmann, Raphael G., "Exotic Uses of Aquifers," Proceeding Paper 8352, *ASCE Journal of the Irrigation and Drainage Division,* Vol. 97, No. IR3, pp 515-522, September 1971.
2. Meyer, C.F., and D.K. Todd, "Conserving Energy with Heat-Storage Wells" (General Electric-TEMPO Paper P-623), *Environmental Science and Technology,* Vol. 7, No. 6, pp 512-516, June 1973.
3. Prater, L.S., *Aquifer Thermal Energy Storage Reference Manual,* PNL-3471; US DOE Contract DE-AC06-76 RLO 1830; Pacific Northwest Laboratory, Battelle Memorial Institute, Richland, Washington, 1980.
4. Reilly, R.W., *A Descriptive Analysis of Aquifer Thermal Energy Storage Systems,* PNL-3298; US DOE Contract DE-AC06-76RLO 1830; Pacific Northwest Laboratory, Battelle Memorial Institute, Richland, Washington, June 1980.
5. Minor, J.E., *Seasonal Thermal Energy Storage Program Progress Report, April 1979 - December 1979,* PNL-3322; US DOE Contract DE-AC06-76RLO 1830; Pacific Northwest Laboratory, Battelle Memorial Institute, Richland, Washington, March 1980.
6. Electric Power Research Institute, *Technical Assessment Guide,* Special Report EPRI PS-1201-SR, The Technical Assessment Group of The EPRI Planning Staff, Palo Alto, California, July 1979.

PROJECT SUMMARY

Project Title: Environmental Assessment

Principal Investigator: George E. Wukelic

Organization:
Pacific Northwest Laboratory
P.O. Box 999
Richland, Washington 99352
(509) 376-5860 (FTS: 444-5860)

Project Goals: Ensure the environmental acceptability of promising STES concepts prior to their commercialization.

Project Status: This project was established within the STES Program in FY-1980 and is expected to exist throughout the program's lifetime. Current emphasis is on: 1) developing environmental documentation for NEPA compliance, 2) guiding environmental activities of Aquifer Thermal Energy Storage (ATES) testing and demonstration projects, and 3) evaluating research results for environmental impacts and mitigation implications pertinent to commercialization feasibility.

During FY-1980, intra and interagency environmental coordination was initiated to clarify the type and contents of NEPA documentation required and external contracts established to assist PNL in their preparation. A preliminary draft Environmental Assessment (EA) for ATES has been completed, reviewed by appropriate offices and is scheduled for publication in early FY-1981. Plans for site-specific environmental assessment and monitoring activities have been cooperatively developed with ATES demonstration contractors to ensure responsiveness to the regulations of the Council on Environmental Quality and the NEPA implementation guidelines of DOE prior to full-scale demonstration activities in FY-1983.

Contract Number: DE-AC06-76RLO 1830

Contract Period: Continuing

Funding Level: $95,000, FY-1980, B/O

Funding Source: U.S. Department of Energy, Office of Advanced Conservation Technologies

ENVIRONMENTAL ASSESSMENT

George E. Wukelic and Jon C. Zuck
Pacific Northwest Laboratory
P. O. Box 999
Richland, Washington 99352

ABSTRACT

This paper summarizes the Environmental Assessment task of the Seasonal Thermal Energy Storage (STES) Technical Support Program that has been established to ensure the environmental acceptability of promising STES concepts prior to their commercialization. The task emphasizes (1) developing environmental documentation required for NEPA compliance, (2) guiding environmental activities for field testing and demonstration projects, and (3) evaluating technical information generated from research and development activities for environmental implications.

To date, the task has successfully initiated the necessary DOE and non-DOE coordination to clarify NEPA environmental documentation requirements in support of the STES Program's emphasis on aquifer thermal energy storage (ATES) research, development, and demonstration. This task, assisted by external contractors, has recently completed the draft programmatic Environmental Assessment for the ATES Subprogram (to be published in FY 81) and has guided the development of comprehensive environmental assessment and monitoring plans for the ATES Demonstration Projects.

Future efforts will stress (1) analyzing data provided through ATES research, development, and demonstration activities to refine estimates of environmental impacts and to identify necessary environmental control measures, and (2) educating the general public and responsible regulatory agencies about the environmental concerns pertaining to the ATES technology.

INTRODUCTION

The Environmental Assessment (EA) task was established within the STES Program in FY 80 and is expected to continue throughout the Program's lifetime (FY 85). As is the case for the entire STES Program, current emphasis of the EA task is directed at aquifer thermal energy storage (ATES). The activities of this task are being performed by a combination of PNL staff members and external contractors. During FY 80, EA task contractors included the Oak Ridge National Laboratory, Oak Ridge, Tennessee and Resource Management and Assessment, Seattle, Washington.

Environmental Assessment subtask activities include the following:

1. NEPA environmental coordination and documentation
2. environmental support to ATES demonstration projects
3. environmental data acquisition and evaluation
4. environmental advisory assistance

TASK DESCRIPTION

NEPA Environmental Coordination and Documentation

Environmental coordination and documentation is the primary support area of the EA task. Its purpose is to identify, coordinate, and prepare environmental documentation (environmental assessments and/or impact statements) required to ensure STES Program compliance with the National Environmental Policy Act (NEPA)/Council on Environmental Quality Regulations (40 CFR 1500-1508) and DOE Implementation Guidelines (10 CFR 1021). This comprehensive effort requires extensive coordination with the various organizational components of the Department of Energy (DOE) including the Office of Environment, NEPA Affairs Division (EV), Office of the General Counsel (OGC), Office of Advanced Conservation Technologies (OACT), Assistant Secretary for Conservation and Solar Energy (CS), and DOE Richland Operations (RL) as well as with other concerned governmental agencies (federal, state, and local). The scope of this effort includes preparation of appropriate environmental documents, Environmental Assessments (EA), Environmental Impact Reports(EIR), or Environmental Impact Statements

(EIS), necessary to meet programmatic and site-specific requirements.

Environmental Support to ATES Demonstration Projects

The Environmental Assessment task activities in support of the ATES demonstration projects involve four main thrust areas. First, as noted in the previous section, the EA task has the basic responsibility for identifying and developing site-specific environmental documentation for NEPA compliance. Second, the EA task is responsible for guiding the development and execution of the site-specific environmental assessment and monitoring plans for Phase I demonstration activities. The challenge is to maintain consistency among the various projects, while preserving the flexibility needed to scope site-specific environmental issues. Third, continuous, direct contact must be maintained with the contractors' environmental specialists to discuss potentially relevant site-specific environmental concerns and to ensure that initiatives are taken to inform the general public and local regulatory agencies about the demonstration projects' environmental assessment and monitoring activities currently in progress. And, lastly, the EA task has provided assistance in reviewing contractors' Aquifer Characterization Plans to ensure consistency with the Environmental Plans so that data sharing opportunities between the environmental and technological efforts are realized.

Environmental Data Acquisition and Evaluation

Acquisition of environmental data is an important activity of the Environmental Assessment task. STES research and development activities and the environmental concerns and regulatory requirements must be integrated. The objective is to ensure that appropriate environmental data are acquired and fully evaluated during the research feasibility testing and demonstration activities. This thrust is undertaken in concert with test facility activities, the demonstration projects, and other technical support tasks. The information generated in this support area will be used in preparing NEPA environmental reports, identifying environmental control needs, and educating regulatory personnel and the general public.

Environmental Advisory Assistance

The Environmental Assessment task provides environmental advisory assistance as needed to the STES Program. The EA staff answer internal and external queries concerning environmental matters, assist STES personnel in evaluating the environmental components of demonstration proposals, evaluate contractor environmental documents, and assist in preparing program-level reports and technical and educational publications.

RESULTS

During FY 80, the EA task began discussions with appropriate DOE and non-DOE agencies/personnel to determine the requirements of NEPA compliance associated with STES/ATES activities. These agencies are noted in Figure 1; EA staff will have additional contact in FY 81 with those organizations designated by an asterisk.

As a consequence of these discussions, a tentative environmental documentation plan for STES/ATES activities has been developed, (see Figure 2). As shown in the figure, a programmatic Environmental Assessment for the ATES Subprogram(1) is in final review stage and will be published during FY 81. The scope, contents and conclusions of this assessment are described in a paper by D.W. Lee (ORNL) entitled "Programmatic Environmental Assessment (Documentation)"(2). This Programmatic Environmental Assessment will serve as a tier document for the three demonstration (site-specific) environmental impact reports (EIR). The EIRs are scheduled to be completed in FY 81-82 prior to initiation of Phase II demonstration activities scheduled for FY 83. Plans to prepare a Programmatic Environmental Assessment for the overall STES Program as well as for several non-aquifer seasonal storage concepts are more tentative.

During FY 80, the EA task coordinated the development and implementation of comprehensive Environmental Assessment and Monitoring Plans for the three ATES Demonstration Projects. This effort will not only help ensure NEPA compliance, but also will assist in the acquisition and evaluation of site-specific environmental data. The details of these efforts are discussed in a paper by H.E. McCartney (Resource Management and Assessment) entitled, "Environmental Analysis/Consulting ATES Demonstrations Environmental Assessment".(3)

Conclusions and Recommendations

The STES program through the Environmental Assessment task is analyzing the environmental needs associated with new energy technology development, demonstration, and commercialization. The program is actively identifying and responding to environmental documentation and regulatory requirements for its ATES demonstration projects as well as providing programmatic documentation. The program is also incorporating environmental data collection and analysis needs within its ongoing research, development (testing), and demonstration activities.

Recently, national attention has focused concern on the misuse and increasing contamination of valuable groundwater resources. This misuse has created an air of skepticism and perhaps resistance on the part of the general public about any future developments involving groundwater use. Since a number of STES concepts, in particular ATES, use ground water, an important recommendation is that future task efforts stress water use/public acceptance issues. In particular, the public and regulatory agency personnel need to be educated about the nominal environmental consequences of developing energy storage technologies.(4)

ACKNOWLEDGEMENT

Reported task progress is due to the combined contributions of participating PNL staff, contractor personnel, STES Program Office staff and several DOE Headquarter representatives.

REFERENCES

1. Draft, Environmental Assessment: Aquifer Thermal Energy Storage Subprogram, Oct. 1980.
2. Lee, D. W., 1980. "Programmatic Environmental Assessment (Documentation)", Annual Contractor Review Meeting, Bethesda, Maryland.
3. McCartney, H.E., 1980. "Environmental Analysis/Consulting - ATES Demonstration Environmental Assessment", Annual Contractors Review Meeting, Bethesda, Maryland.
4. STES Consultant Review Team, 1980. "Review Report on the Seasonal Thermal Energy Storage Program". Pacific Northwest Laboratory, Battelle, Richland, WA, 16 pp.

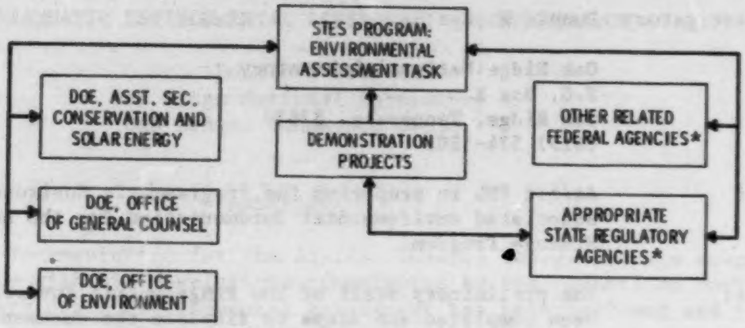
STES PROGRAM: ENVIRONMENTAL ASSESSMENT TASK
DOE, ASST. SEC. CONSERVATION AND SOLAR ENERGY
DEMONSTRATION PROJECTS
OTHER RELATED FEDERAL AGENCIES*
DOE, OFFICE OF GENERAL COUNSEL
APPROPRIATE STATE REGULATORY AGENCIES*
DOE, OFFICE OF ENVIRONMENT

*Increased Coordination Planned for FY 81

FIGURE 1: AGENCIES/ORGANIZATIONS RELEVANT TO STES ENVIRONMENTAL ASSESSMENT ACTIVITIES

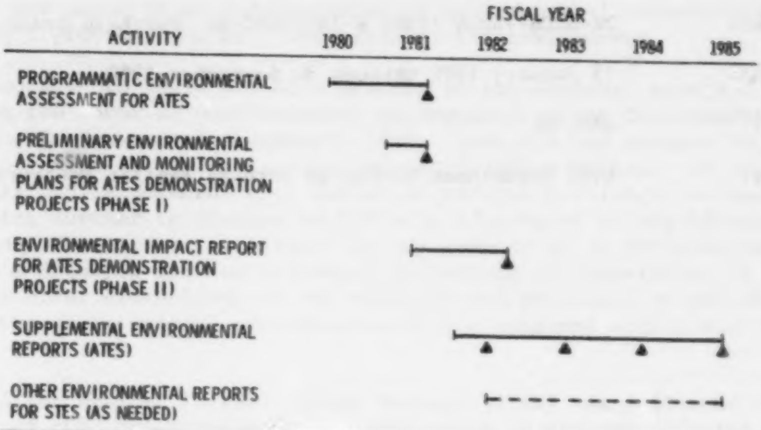

FIGURE 2: TENTATIVE ENVIRONMENTAL DOCUMENTATION PLAN FOR THE STES PROGRAM

PROJECT SUMMARY

Project Title:	Programmatic Environmental Assessment (Documentation)
Principal Investigator:	Donald W. Lee
Organization:	Oak Ridge National Laboratory P.O. Box X Oak Ridge, Tennessee 37830 (615) 574-5803
Project Goals:	Assist PNL in preparing the Programmatic Environmental Assessment and associated environmental documentation for the Aquifer Thermal Energy Storage Program.
Project Status:	The preliminary draft of the Programmatic Environmental Assessment has been completed and steps to finalize the document are progressing. The document is intended to be responsive to the regulations of the Council on Environmental Quality and the NEPA implementation guidelines of DOE. The scoping process, prior to document preparation was directed towards identifying the alternatives to ATES, the significant environmental issues related to ATES and its alternatives, and the assessment methodology to be used in the document's preparation. Preliminary conclusions indicate that ATES technology is more developed to support testing and demonstration that its alternatives. Assessment of initially planned field activities identified no significant adverse environmental impacts. Potential environmental consequences are site-specific, and the implementation of a monitoring program with associated initiatory procedures is recommended to reduce the occurrence of any adverse environmental impact.
Contract Number:	DE-AC06-76RLO 1830, W-7405-ENG-26, Purchase Order B-93958-A-O
Contract Period:	15 January 1980 through 30 September 1980
Funding Level:	$60,000
Funding Source:	U.S. Department of Energy through Pacific Northwest Laboratory

PROGRAMMATIC ENVIRONMENTAL ASSESSMENT (DOCUMENTATION)

Donald W. Lee
Oak Ridge National Laboratory
Oak Ridge, Tennessee 37830

ABSTRACT

The environmental documentation for the Aquifer Thermal Energy Storage subprogram is being prepared to comply with the regulations promulgated by the Council on Environmental Quality. The preliminary draft Environmental Assessment has been reviewed and revisions have been incorporated into a revised draft Environmental Assessment. Environmental consequences of the Aquifer Thermal Energy Storage subprogram are expected to be site-specific.

INTRODUCTION

The National Environmental Policy Act (NEPA, 1969) requires that environmental values be incorporated into any major Federal action which may significantly affect the quality of the human environment. The procedural provisions of NEPA were implemented by the Council on Environmental Quality in 1978 as final regulations (40 CFR parts 1500-1508). The Department of Energy (DOE) has prepared guidelines for implementing these regulations as part of agency decision making (10 CFR part 1021).

The principal objectives of the NEPA process are to incorporate an appropriate and careful consideration of the environmental aspects of proposed actions before decisions are made and actions are taken. The process is intended to help public officials in making decisions that are based on an understanding of environmental consequences and in taking actions that will protect, restore, and preserve the environment.

Agencies are encouraged to begin the NEPA process at the earliest possible time. The NEPA process relies on two forms of environmental documentation, the Environmental Impact Statement (EIS) and the Environmental Assessment (EA). Agencies may prepare an environmental assessment at any time to assist in planning and decision-making. An environmental assessment is a concise public document that serves to provide sufficient evidence and analysis for determining whether to prepare an EIS or a finding of no significant impact (FONSI). An EA is also intended to facilitate the preparation of an EIS when one is necessary. An EIS is a detailed written statement satisfying all provisions of NEPA whereas an EA includes brief discussions of the need for the proposal, of the alternatives to the proposal, and the environmental consequences of the proposed action and its alternatives.

A programmatic EA for Aquifer Thermal Energy Storage (ATES) was initiated to comply with the requirements of the NEPA process at an early stage in program planning and to determine if an EIS was required before demonstration of the ATES concept began. The purpose of the EA was to determine whether an EIS or a FONSI should be prepared for the ATES subprogram. After the programmatic environmental documentation is completed, site-specific environmental reviews of the individual ATES demonstration projects are planned. For the site-specific reviews, the programmatic EA serves as a tiering document, allowing the demonstration projects to reference the programmatic aspects of their activity, thus, focusing on the specific issues related to the individual project.

BACKGROUND

The Oak Ridge National Laboratory (ORNL) was requested to assist Pacific Northwest Laboratory (PNL) in preparing the programmatic EA for the ATES subprogram. The format of the EA was planned to conform with the new regulations of CEQ and to facilitate an EIS should it be necessary. This activity was an extension of an earlier activity at ORNL to prepare an EA for the ATES concept. The disciplines of hydrology, geology, ecology, sociology, and economics were to be incorporated into the EA by the use of an interdisciplinary team of authors. At the onset of the project, several issues were unresolved. Although the team of authors was familiar with the ATES concept, only limited information on alternative technologies was available. Environmental documentation for seasonal thermal energy storage or the more encompassing programs had not been released or prepared and the scope of activities to be included in the ATES subprogram was being prepared. The economics of ATES and the legal and institutional questions that will influence the commercial potential of ATES had received limited attention. The greatest unresolved issue was the preparation of a programmatic EA under the final CEQ regulations.

PROJECT DESCRIPTION

The preparation of the programmatic EA was separated into two phases. During Phase I the scope of the EA, the format of the EA, and a workplan for the EA were to be devised. During Phase II the EA was to be prepared utilizing the information developed in Phase I.

Phase I was to result in a finalized definition of alternatives to be considered in the assessment, an annotated outline for the preparation of the EA, and the preparation of the workplan for Phase II. The outline and workplan required PNL approval. The finalization of alternatives was to be achieved by agreement between representatives of ORNL, PNL, and DOE.

Phase II was to result in a preliminary draft EA to be distributed for comment to PNL and DOE. Prior to release of the preliminary draft EA, approval by PNL was necessary. Extensive comments were anticipated and a revised draft of the EA was planned prior to the finalization of the document.

RESULTS

Phase I work resulted in a finalized list of technological alternatives to ATES that included insulated pond storage, wet earth storage, natural lake or pond storage, metal tank storage, rock bed storage, and solar pond storage. The programmatic alternatives to be assessed were no action, an accelerated program and a deferred program. These programmatic alternatives were modified later to be no action, an accelerated or expanded program and a delayed or limited program. Priorities were established for the various subject areas to be assessed. Finally, an annotated outline and workplan were prepared and agreed upon.

Phase II work resulted in a preliminary draft Environmental Assessment that was released for comment by the PNL program office, DOE/EV, DOE/OGC, and DOE/OACT. By the completion of Phase II, the economics of ATES and the legal and institutional issues of ATES had received further clarification. The environmental consequences of the technological alternatives to ATES were more thoroughly understood and the role of an EA in the CEQ regulations clarified.

The environmental consequences of the ATES subprogram were assessed to be site-specific in nature. Potential adverse environmental impacts could occur which may reduce aquifer permeability, alter groundwater quality, and groundwater microbiology. These impacts can be mitigated if careful aquifer selection and site-specific mitigatory strategies are included in a project's design and operation. Site-specific institutional issues related to water use are expected to be important for ATES demonstration projects. Adverse impacts to surface water hydrology, aquatic ecology, terrestrial ecology, air quality and the host communities are not anticipated. Site-specific monitoring programs, which are comprehensive in scope, must be developed to ensure that mitigatory measures are adequate and to detect any unforeseen impacts. Potential environmental benefits are anticipated from reducing the amount of waste heat discharged to the environment and from reducing dependence on conventional energy sources for space heating and cooling. The ATES technology was assessed to be more developed for demonstration than its alternatives. The environmental consequences of the programmatic alternatives are not expected to differ from the proposed action to a great extent.

The comments received on the preliminary draft EA were extensive, as was anticipated. Revisions to the document in response to the comments were prepared and have been incorporated into a revised EA. As of the time of this writing, a revised EA is being prepared for release.

CONCLUSIONS AND FUTURE ACTIVITY

The preparation of a preliminary draft Environmental Assessment of the Aquifer Thermal Energy Storage Subprogram has been completed. Comments on the assessment have been received and a revised draft will be released soon. Future activity will include finalizing the EA and providing additional assistance to PNL in the preparation of environmental documentation for the ATES subprogram.

Level of Funding $70,000

PROJECT SUMMARY

Project Title: Environmental Analysis/Consulting

Principal Investigator: Heather E. McCartney

Organization: Resource Management and Assessment
P.O. Box 981
Everett, Washington 98201
(206) 258-1980

Project Goals: To provide environmental consulting services in connection with the development of environmental documentation and research efforts required to support PNL's STES Program.

Project Status: This project was established in the last quarter of FY-1980. To date, services have been provided relating to: 1) preparation of the draft programmatic environmental assessment of ATES (jointly with ORNL and PNL) and 2) development of environmental assessment and monitoring plans for the ATES demonstration projects.

In addition to the general Environmental/Institutional Plans required for each of the three demonstration projects (Bethel, Alaska; Minneapolis, Minnesota; and Stony Brook, New York), separate environmental assessment and monitoring plans for Phase I (Aquifer Characterization and Preliminary Testing) activities have been developed to identify and minimize potential environmental problems, to facilitate accumulation of needed environmental information and to fulfill NEPA requirements, CEQ regulations, and DOE guidelines for compliance with NEPA. Site-specific environmental issues are identified; monitoring plans and mitigating strategies are presented to address these issues.

Contract Number: DE-AC06-76RLO 1830, Subcontract B-B2411-A-O

Contract Period: 5 August 1980 through 15 February 1981

Funding Level: $15,000

Funding Source: U.S. Department of Energy through Pacific Northwest Laboratory

ENVIRONMENTAL ANALYSIS/CONSULTING - ATES DEMONSTRATIONS ENVIRONMENTAL ASSESSMENT

Heather E. McCartney
Resource Management and Assessment
P. O. Box 981
Everett, Washington 98206

ABSTRACT

This paper summarizes the environmental activities related to the Aquifer Thermal Energy Storage (ATES) demonstration projects. These activities are being performed by a combination of PNL, ORNL, and Resource Management and Assessment staff. Environmental activities for the ATES demonstration projects include: environmental input during the procurement process; and coordination with the demonstration contractors during the preparation of the environmental assessment and monitoring plans for Phase I and during the preparation of environmental impact reports for Phase II.

Separate environmental assessment and monitoring plans for Phase I (conceptual design) activities have been developed and environmental impact reports are being prepared for Phase II activities (final design, construction and operation). The purpose of these documents is to identify and minimize potential environmental problems, to facilitate accumulation of needed enviromental information, and to fulfill NEPA requirements. Site-specific environmental issues are identified; monitoring plans and mitigating strategies are presented to address these issues.

INTRODUCTION

The objective of Resource Management and Assessment's responsibility is to provide environmental consulting services in connection with the development of environmental documentation and research efforts required to support PNL's STES Program. The main thrust at this time and the subject of this paper is the environmental activities in support of the ATES demonstration projects. Experience gained in undertaking demonstration projects and evaluating accumulated environmental information will help determine the environmental acceptability of the ATES concept.

BACKGROUND

The three initial ATES demonstration projects commenced during FY 80, and their programmatic characteristics are noted in Table I. These projects provide the focal point in the ATES Subprogram for testing technical feasibility, economic attractiveness, and environmental acceptability. The ATES demonstration projects will also impact on technology transfer in that the combination of research, testing, and demonstration will help to determine future demonstrations, and moreover, the more successful demonstrations will become operational facilities.

The ATES demonstration projects are divided into two phases. Phase I is the conceptual design phase begun in 1980 which will provide the basis for determining if a full demonstration (Phase II) is feasible. The three demonstration projects are scheduled to complete Phase I by mid-1982. Phase II demonstration activities will be determined by the results of the conceptual design phase (including aquifer characterization) completed in Phase I. The feasible sites will proceed with final design, construction, and operation on a cost sharing basis between DOE and the operating entity. The actual demonstration activities under Phase II are scheduled to start in late 1982 and operate to the end of 1985.

The STES Environmental Assessment task has the responsibility for guiding environmental considerations on the ATES demonstrations projects to ensure assessment consistency and NEPA compliance.

A DESCRIPTION OF ENVIRONMENTAL ACTIVITIES FOR THE ATES DEMONSTRATIONS

The environmental activities in support of the three ATES demonstration projects include: environmental considerations during the procurement process, the development and implementation of an environmental assessment and monitoring plan for Phase I, and the preparation of an environmental impact report for Phase II.

Description of Environmental Activities During Procurement

Environmental concerns were first initiated with the procurement process for the ATES demonstration projects in 1980. The Request for Proposals (RFP) required respondees to address potential, site-specific environmental concerns. The proposers had to identify major environmental concerns directly associated with their proposed scope of demonstration activities. Each proposer was also required to develop a preliminary Environmental and Institutional Plan describing environment support functions, including the identification of environmental permits required and planned procedures for obtaining permits or approvals. Among the initial requirements for the three selected demonstration contractors, was the finalization of this Environmental and Institutional Plan to include specifically

- an environmental assessment and monitoring plan for Phase I (conceptual design and aquifer characterization) activities, and
- a description of their plan for preparing an environmental impact report (EIR) for Phase II demonstration activities.

Description of Environmental Assessment and Monitoring Activities for Phase I (1980-1982)

The environmental activities related to Phase I for each demonstration project include; a preliminary environmental assessment, development of a monitoring plan, the preparation of an environmental report on Phase I activities, and the preparation of an environmental impact report (EIR) for the proposed Phase II activities. Figure 1 is an example of the scope, timing and inter-relationship of environmental tasks and non-environmental tasks for a typical demonstration project. The two stages of environmental assessment indicate the activities that will take place in Phase I of the demonstrations during conceptual design and aquifer characterization.

The preliminary environmental assessment provides for the initial identification and evaluation of potential site-specific issues. In most cases, this assessment was basically an amplification of potential environmental concerns originally addressed in the ATES proposals. Although the demonstration contractors were not required to follow a specific format in the preparation of their preliminary environmental assessments, they had to be comprehensive in assessing site-specific environmental concerns in order to support the formulation of a Phase I monitoring plan. In all cases, the preliminary environmental assessments were required to identify potential environmental impacts likely to occur during site preparation, construction and operational (testing) stages of Phase I activities and corresponding monitoring/mitgating procedures planned for implementation. Typical scope of impact areas considered in these assessments includes: groundwater, surface water, geologic, terrestrial ecology, air quality, noise and institutional. Logically, assessment emphasis was on potential ground-water impacts.

Environmental monitoring (and data analysis) activities during Phase I will serve three project functions. First, they will provide the baseline and real-time data necessary to identify an environmental impact so that appropriate mitigation measures can be taken. Second, they will provide relevant field data to support the comparative environmental assessment of the various Phase II system design alternatives. And third, they will provide the quantitative data necessary to prepare the comprehensive Environmental Impact Report (EIR) for planned Phase II (demonstration) activities.

Preparation of Environmental Assessment for Phase II (1982-1985)

A comprehensive Environmental Impact Report (EIR) of planned Phase II activities is required of all ATES demonstration contractors. The EIRs are to be completed during the Phase I conceptual design stage so that they can be used to make an DOE determination as to whether an Environmental Assessment (EA) or an Environmental Impact Statement (EIS) will be required for the proposed Phase II site-specific actions.

Specific scope, format and content guidelines for the EIRs have been given to the demonstration contractors which resemble those required by NEPA/CEQ for federal agency compliance documents. This requirement will accelerate the preparation of an EIS, if one is required, in that no major format transition in going from the EIR to the EIS will be necessary.

During the actual demonstration (Phase II), environmental assessment activities will involve the refinement of data from continued monitoring of expanded construction activities and the first real operation of complete ATES systems. The actual scope and priority of environmental monitoring and data analysis activities during Phase II will depend upon the technological and environmental results of Phase I. Most likely, Phase II environmental concerns will emphasize considerations relative to the type and availability of environmental controls required to support the commercialization of successfully demonstrated ATES systems.

RESULTS

With STES Program Office guidance, the three demonstration contractors have (1) finalized their Environmental and Institutional Plans, (2) completed their preliminary environmental assessments, and (3) implemented monitoring procedures as appropriate for Phase I site preparation and construction activities undertaken.

These environmental actions, which were all completed and approved during FY 80, are considered to be important to the overall success of the demonstrations for several reasons. First, the early inclusion of environmental concerns has resulted in the functional integraton of the environmental and technology teams. This consolidation, during the planning stages, has resulted in a single field monitoring and data collection effort for site preparation, construction and testing activities that serves both environmental and technological objectives. Second, early environmental initiatives have minimized potential complexities associated with local environmental regulatory permitting requirements. Third, early environmental interactions directed toward educating the public and regulatory personnel should help prepare for the local environmental acceptance of expanded Phase II activities. And lastly, environmental activities throughout the program should ensure the development of environmental documentation and control technology to support commercialization needs.

CONCLUSIONS

The initiation of environmental activities early in the ATES Demonstration Program has played an important role in planning and implementing Phase I actions which will provide data relevant to both technological and environmental needs. Planned environmental activities should quantify the environmental impacts and support the timely development of NEPA documentation and control measures required for ATES commercialization.

TABLE 1 ATES Demonstration Projects (Phase I)

LOCATION	Bethel, Alaska	Stony Brook, New York	Minneapolis, Minnesota
CONTRACTOR	TRW, Inc.	Damec and Moore	University of Minnesota
ENVIRONMENTAL SPECIALIST	A. Takata	P. Buchinsky	G. Riedesal (National Biocentric)
STORAGE TEMPERATURE	Low Temperature ~ 95°C	Chill ~ 5°C	High Temperature ~ 150°C
ENERGY SOURCE	Diesel Exhaust and Cooling Water	Cooling Tower	Cogeneration Steam
END USE	District Heating	Building Air Conditioning	Campus Heating

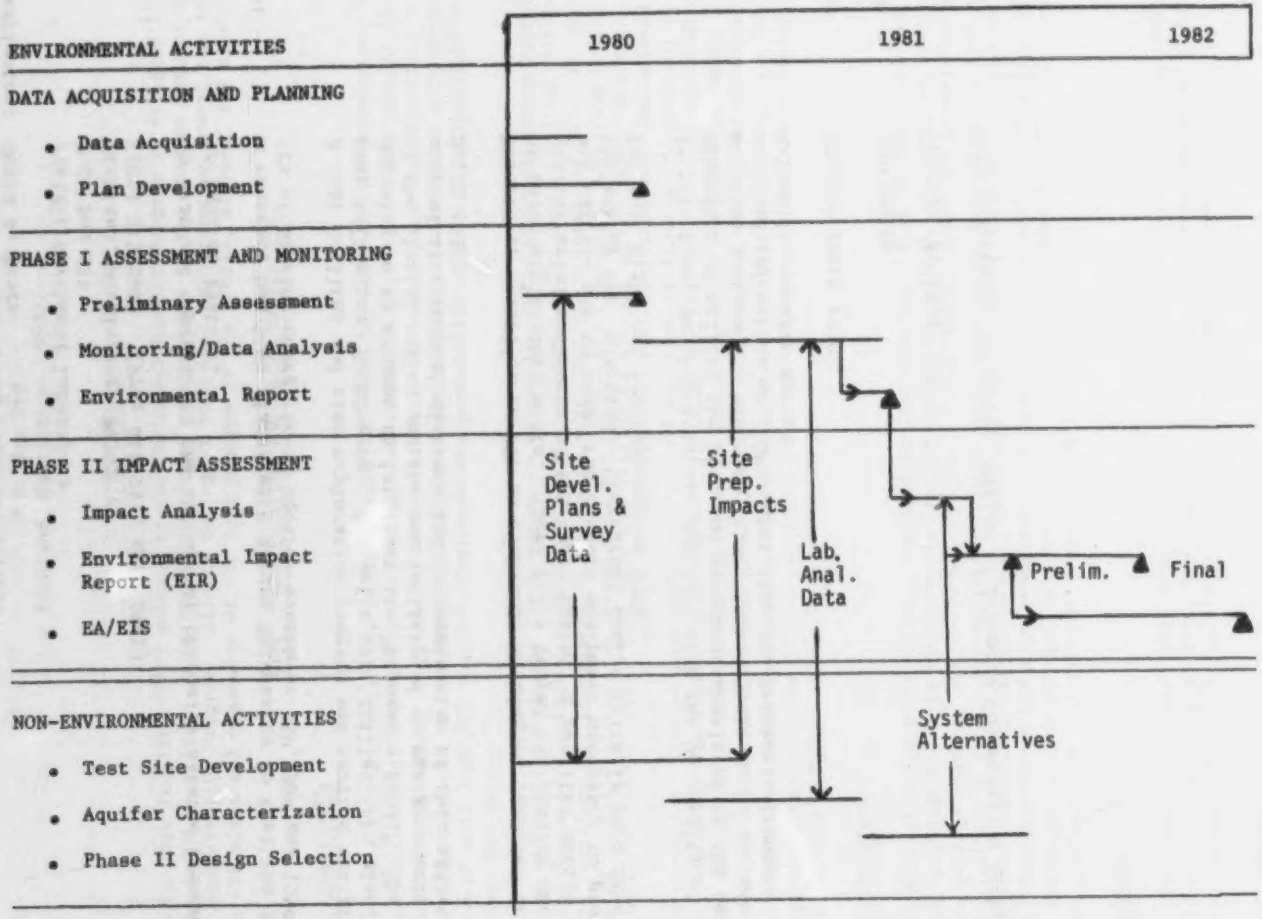

FIGURE 1 ATES Demonstration Projects Environmental - Non-Environmental Relationship

PROJECT SUMMARY

Project Title: Field Test Facility

Principal Investigator: David A. Myers

Organization:
Pacific Northwest Laboratory
P.O. Box 999
Richland, Washington 99352
(509) 375-2462 (FTS: 444-7511 ext. 2462)

Project Goals: To test and demonstrate the storage of thermally altered ground water in aquifer systems.

Project Status: A contract has been placed with Auburn University to test the feasibility of storing energy in an aquifer system at 55°, 90° and 125°C.

A test drilling and site exploration program was carried out at a site near Bellingham, Washington. Two wells were drilled into glacial deposits in an attempt to interrupt the "Esperance Sand." The nature of the glacial valley and the availability of an energy source within economical transport distance led to termination of this effort in April 1980.

Efforts to establish an FTF at Richland, Washington included drilling of seven exploratory wells. These wells tapped the shallow unconfined glaciofluvial sediments of the Pasco Basin. A parallel design effort was carried out to cover the surface equipment necessary to provide the energy for injection. Conceptual design criteria were developed for both high- and low-temperature FTFs.

At this time, negotiations are underway with the University of Minnesota to utilize the site and equipment developed by the demonstration program for extended field tests. Tests would include extended injections of 150°C water into the Franconia-Ironton-Galesville aquifer system.

Contract Number: DE-AC06-76RLO 1830

Contract Period: Continuing

Funding Level: $70,400, FY-1980, B/O

Funding Source: U.S. Department of Energy, Office of Advanced Conservation Technologies

FIELD TEST FACILITY

David A. Myers
Pacific Northwest Laboratory
P.O. Box 999
Richland, Washington 99352

INTRODUCTION

The Field Test Facility (FTF) subtask of the Technical Support Program is designed to provide actual field tests to provide operational experience and guidance to the Aquifer Thermal Energy Storage (ATES) Demonstration Program. Efforts during FY 1980 have been directed toward the identification of suitable FTF sites and expansion of the test program at the Mobile, Alabama, FTF site.

SITE IDENTIFICATION AND CHARACTERIZATION

BELLINGHAM, WASHINGTON

A contract with Fugro Engineers of Long Beach, California, and Seattle, Washington, was let to identify and characterize a potential saline aquifer system in the Puget sound glacial flurial basin near Bellingham, Washington. A potential source of waste thermal energy was identified at a garbage burning facility operated by the Thermal Reduction Company (TRC) of Bellingham. Literature searches and a review of well logs for the area indicated the probability of an appropriate aquifer lying at a depth of about 800 feet.

Drilling was initiated on the TRC property in September, 1979, after obtaining appropriate permits from the State of Washington and Whatcom County officials. The first well was drilled to a depth of 505 feet. Drilling was terminated in this well after the bit entered bedrock. No suitable aquifer was penetrated during drilling. A second hole was initiated at Hovander Homestead County Park, about 1.5 miles north of the TRC site. This hole was drilled to a depth of 650 feet. Numerous small water bearing units were penetrated at this site. Flowing artesian conditions were encountered, necessitating that casings be grouted into place to seal off the flow. Following the grouting of the casing at 650 feet, the drill was lowered into the bore to clean out the casing before proceeding. The drill bit was lost during this operation and proved to be nonrecoverable, forcing abandonment of the well. The bore hole was logged and then backfilled with drill cuttings and cement and abandoned according to Washington State standards. The economics and environmental concerns associated with long distance transport of hot water from the TRC to alternate sites dictated termination of consideration of the Bellingham site for a FTF.

RICHLAND, WASHINGTON

A potential site for a FTF in an unconfined aquifer was identified in the Pasco Gravels formation at Richland, Washington. Site characterization was initiated with the drilling of several exploration wells. The average depth of the wells was 70 feet. Water bearing sands and gravels were penetrated at a depth of about 30 feet. The aquifer materials were composed of predominately fine sand with some gravel. Aquifer conditions varied markedly over short distances, indicating that buried channels of the ancient Columbia River had been penetrated. A pump test of one well showed a drawdown of 0.15 feet at a discharge rate of 200 gallons per minute. This site has been reserved for a potential experiment in gradient and flow control in unconfined aquifer systems.

MOBILE, ALABAMA

A contract has been placed with Auburn University to alter the existing site at Mobile to accommodate injection experiments at 55°C, 90°C and 125°C. This round of experiments calls for the use of a true doublet system. Detailed laboratory and field experiments are planned.

ST. PAUL, MINNESOTA

Negotiations are underway with the University of Minnesota to expand the experimental efforts of the Demonstration Program effort. This expansion of effort would include additional monitoring wells, post test coring and an extended period of injection. The tests would utilize facilities and equipment provided by the demonstration program. Sixty day periods of injection/storage/recovery are planned for this test.

PROJECT SUMMARY

Project Title: Mobile, Alabama Field Test Facility

Principal Investigator: Fred J. Molz, A. David Parr and Joel G. Melville

Organization: Water Resources Research Institute
Auburn University, Alabama 36830
(205) 826-4320

Project Goals: To investigate the feasibility of storing thermal energy in confined aquifers by designing, developing, operating and analyzing data for a doublet well system.

Project Status: Work on the construction of a new well field at the Mobile field site is nearly complete. When completed, the well field will consist of 28 observation wells of various types (hydraulic head, temperature, and tracer) and three pumping wells. The new supply and injection wells will be screened in the same aquifer and separated by approximately 800 feet.

Three, 6-month, injection-storage-recovery cycles are planned. Tentative injection temperatures are 55°, 90° and 125°C, respectively. Ground-water temperatures in the storage formation will be monitored at six locations in each of 13 observation wells and at two locations in the upper and lower aquitard.

During the injection phase of each cycle, water will be pumped from the supply well, heated and injected approximately 800 feet away. After a minimum of 2 months of storage, recovery pumping will begin and water will be pumped from the injection well and returned to the supply well so that as much heat as possible can be saved between cycles.

During the first injection-storage-recovery cycle a tracer experiment will be performed. Sodium-Bromide will be injected with the heated water at a constant concentration and monitored in four tracer observation wells. Tracer concentration and temperature profiles can then be compared. In addition, land surface elevation measurements will be made along with aquifer matrix and ground-water sampling.

It is expected that the first cycle will begin in early January of 1981.

Contract Number: DE-AC06-76RLO 1830, Subcontract B-67770-A-O

Contract Period: 26 March 1980 through 31 December 1982

Funding Level: $1,087,097

Funding Source: U.S. Department of Energy through Pacific Northwest Laboratory

FIELD STUDIES OF THE AQUIFER THERMAL ENERGY STORAGE CONCEPT

A. David Parr, Fred J. Molz and Joel G. Melville
Department of Civil Engineering
Auburn University
Auburn, Alabama 36849

INTRODUCTION

The possibility of using confined aquifers for the temporary storage of heat has received in-depth study for the past five years. In the United States, experimental study of the concept was started by Auburn University in the summer of 1976 (Molz, Warman and Jones, 1978). The data generated by this experiment enabled the U. S. Geological Survey and others to make preliminary tests of several mathematical models designed to model the simultaneous transport of water and heat in an aquifer (Papadopulos and Larson, 1978).

In March of 1978, a second round of experiments was begun at the field test site in Mobile, Alabama. Two six-month injection-storage-recovery cycles were performed wherein approximately 55,000 cubic meters (14.5 million gallons) of water were pumped from a shallow supply aquifer, heated to an average temperature of 55°C (131°F), and injected into a deeper confined aquifer with an ambient temperature of 20°C (68°F). After a storage period of about 2 months, the water was recovered from the confined aquifer (Molz, et al., 1980). The resulting data formed the basis for a computer study performed by the Lawrence-Berkeley Laboratory.

Clogging of the injection-production well during injection was an important negative result of the Mobile experiments. The present writers (Molz, et al., 1978) and others have suggested that using water from the storage aquifer as supply water for the boiler or other heating system would minimize clogging problems. Drilling the supply well and the injection-production well in the same formation leads to what is called the doublet configuration. If aquifer storage of thermal energy becomes feasible on a commercial scale, it seems likely that a system based on the doublet configuration will offer distinct advantages. Therefore, there is a real need to study this concept experimentally so that potential advantages and disadvantages can be identified clearly before major amounts of money are invested in the concept.

In order to test a doublet supply-injection well configuration, a third round of experiments consisting of 3 injection-storage-recovery cycles are scheduled to begin in January, 1980, at the Mobile site. A schematic of the doublet system is shown in Figure 1. The injection and supply wells fully penetrate the confined aquifer and are separated by 244 m (800 ft). High injection temperatures will be used during the last two cycles in order to investigate the effect of increased buoyancy on energy recovery. This paper will discuss the design and planned procedures for the upcoming experiments and will present the results of a preliminary anisotropy pumping test which was performed recently.

EXPERIMENTAL DESIGN

Figure 2 shows the location of the supply well, injection well and boiler with respect to the 28 observation wells to be used to measure temperature, hydraulic head and tracer concentration. The different types of observation wells are indicated on the figure.

Observation wells that will be used to measure temperature in the storage formation are constructed as shown in Figure 3. Thermistors will be used to measure temperature at six locations in each well. Two thermistors will be installed at each location to provide a backup array. The wells will be backfilled with sand in order to minimize unrepresentative thermal convection within the well bores. Temperature will also be measured in the upper and lower aquitards. One well is screened in each of these formations and temperature will be measured at two locations in each well. The observation wells that will be used to measure hydraulic head are constructed like the temperature wells but, of course, will not be backfilled with sand.

A tracer experiment will be performed during the first cycle to compare the movements of solute and heat in the aquifer. A chemical feed system will be used to inject sodium-bromide into the hot water pipeline at a constant rate throughout the first injection. Water samples will be taken from four observation wells constructed as shown in Figure 4. There will be two wells of each type. Water will be withdrawn through a 1.5-m (5-ft) screened section at the middle of the confined aquifer for one pair of wells and through similar screened sections near the top and bottom of the aquifer for the other two wells.

Hot water pumped from the injection well during the recovery phase of each cycle will be returned to the confined aquifer through the supply well in order to minimize the amount of energy needed to heat water for subsequent injections. This procedure may create clogging problems, however, since the concentration of clay particles in the pumped water may tend to increase with repeated cycles. In order to control clogging and to maintain acceptable injection rates, a rapid sand filtering system has been installed. The filtering system can either be used or bypassed during injection and recovery phases.

EXPERIMENTAL PROCEDURES

The three injection-storage-recovery cycles that are planned are depicted in Figure 5. The tentative injection temperatures for the first, second and third cycles are 55°C (131°F), 90°C (194°F) and 125°C (257°F), respectively. The injection volume for each of the cycles will be approximately 57,000 cubic meters (15 million gallons) and the injection rate will be about 12.6 liters per second (200 gpm). After two-month storage periods, hot water will be produced from the confined aquifer through the injection well and reinjected at the supply well, at least during the first two cycles. Energy recovery will be determined from continuous temperature and flow measurements.

An anisotropy pumping test was performed during the construction phase of the project. Figure 6 shows the temporary partially-screened injection and observation wells used to perform the test. The injection well was located in the bore hole for the permanent, fully-screened, injection well. Water was pumped from the confined aquifer for 12 hours at a constant rate of 9.5 liters per second (150 gpm). Drawdowns measured in each of the three observation wells are shown in Figure 7. The procedure given by Weeks (1969) was used to analyze the data. The transmissibility and storage coefficient determined for each of the observation wells are listed in Table 1. A value of approximately 7 was determined for the ratio of horizontal to vertical permeability in the confined aquifer.

A leaky aquifer pumping test will also be performed to further evaluate the aquifer and aquitard hydraulic parameters. A method described by Neuman and Witherspoon (1972) will be used to analyze the pumping test.

PROJECT STATUS

As of October 10, 1980, construction of the well field and piping system has been completed and the anisotropy pumping test has been performed and analyzed. Core samples of the storage formation and the upper and lower aquitards have been obtained. These samples were delivered to the Battelle Pacific Northwest Laboratories where they will be analyzed in detail.

The following tasks must be completed before the injection-storage-recovery cycles can begin

1. Instrumentation and backfilling of temperature observation wells,
2. Installation of supply and injection well pumps,
3. Performance of leaky aquifer pumping test,
4. Installation of tracer sampling system.

REFERENCES

1. Molz, F. J., J.C. Warman, and T. E. Jones, "Aquifer Storage of Heated Water: Part I - A Field Experiment," Ground Water, Vol. 16, pp. 234-241, 1978.

2. Molz, F. J., A. D. Parr, and P. F. Andersen, "Experimental Study of the Storage of Thermal Energy in Confined Aquifers," Final Report for ORNL/Sub-7338/1, Contract No. W-7405-eng-26, NTIS, 5285 Port Royal Road, Springfield, VA 22161, 1980.

3. Neuman, S. P., and P. A. Witherspoon, "Field Determination of the Hydraulic Properties of Leaky Multiple Aquifer Systems," Water Resources Research, Vol. 8, No. 5, pp. 1284-1298, October, 1972.

4. Papadopulos, S. S., and S. P. Larson, "Aquifer Storage of Heated Water: Part II - Numerical Simulation of Field Results," Ground Water, Vol. 16, pp. 242-248, 1978.

5. Weeks, E. P., "Determining the Ratio of Horizontal to Vertical Permeability by Aquifer-Test Analysis," Water Resources Research, Vol. 5, No. 1, pp. 196-214, February, 1969.

Observation Well No.	Distance from Pumped Well (m)	Transmissibility (m^2/day)	Storage Coefficient
1	7.6	1,170	0.00046
2	15.2	1,120	0.00052
3	22.9	1,140	0.00049

Table 1. Values of Transmissibility and Storage Coefficient for Anisotropy Pumping Test.

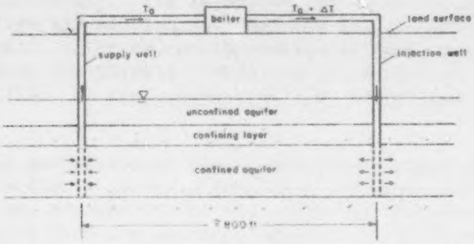

T_0
boiler
$T_0 + \Delta T$
land surface
supply well
injection well
unconfined aquifer
confining layer
confined aquifer
≈ 800 ft

Fig. 1. Schematic of Doublet Supply-Injection Well Configuration.

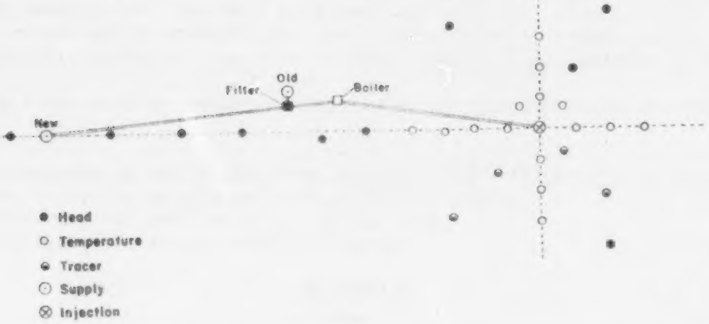

Old
Filter
Boiler
New
● Head
○ Temperature
● Tracer
⊙ Supply
⊗ Injection

Fig. 2. Top View of Well Field, Boiler, and Sand Filter at Mobile Site.

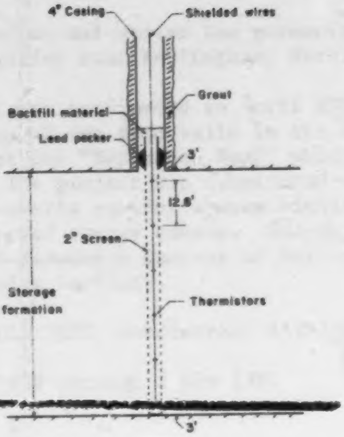
4" Casing
Shielded wires
Grout
Backfill material
Lead packer
3'
12.8'
2" Screen
Storage formation
Thermistors
3'

Fig. 3. Side View of Temperature Observation Well Showing Details of Well Construction and Positions of Thermistors.

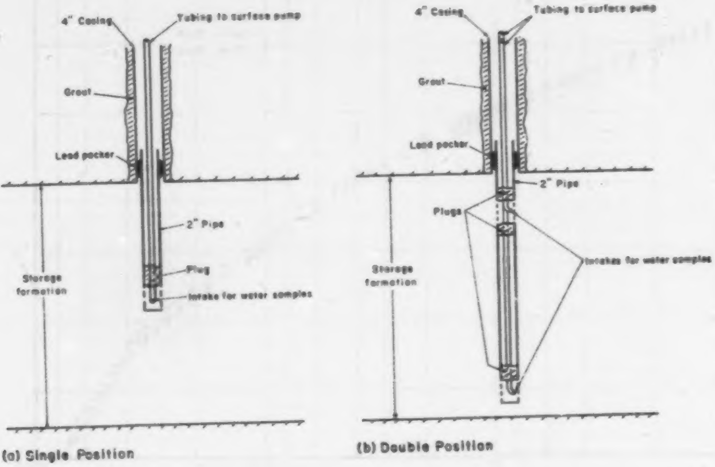
4" Casing
Tubing to surface pump
Grout
Lead packer
2" Pipe
Plug
Storage formation
Intake for water samples
4" Casing
Tubing to surface pump
Grout
Lead packer
2" Pipe
Plugs
Intakes for water samples
Storage formation

(a) Single Position

(b) Double Position

Fig. 4. Side View of Observation Wells Designed to Measure Tracer Concentration and Hydraulic Head.

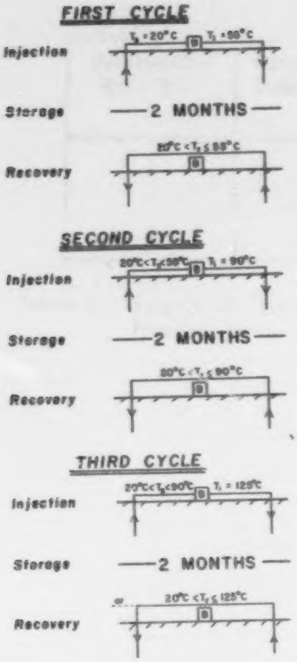
FIRST CYCLE
Injection
T_s = 20°C
T_i = 90°C
Storage
2 MONTHS
Recovery
20°C < T_r ≤ 90°C
SECOND CYCLE
Injection
20°C < T_s < 90°C
T_i = 90°C
Storage
2 MONTHS
Recovery
20°C < T_r ≤ 90°C
THIRD CYCLE
Injection
20°C < T_s < 90°C
T_i = 125°C
Storage
2 MONTHS
Recovery
20°C < T_r ≤ 125°C

Fig. 5. Planned Injection-Storage-Recovery Cycles.

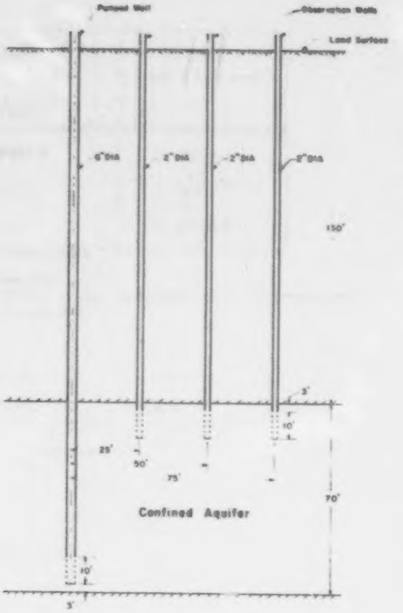
Pumped Well
Observation Wells
Land Surface
6" DIA
2" DIA
2" DIA
2" DIA
130'
3'
10'
25'
50'
75'
70'
Confined Aquifer
10'
3'

Fig. 6. Side View of Partially-Screened Wells Used for Anisotropy Pumping Test.

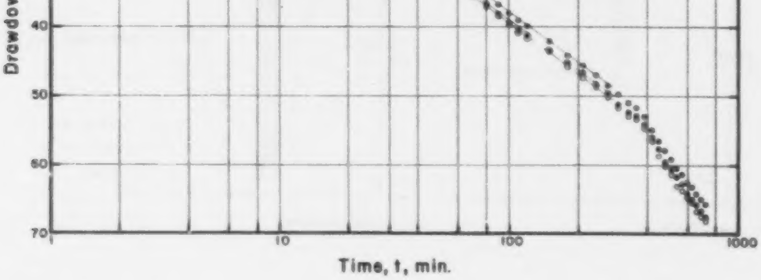

Fig. 7. Observation Well Drawdowns for Anisotropy Pumping Test at Mobile Site.

PROJECT SUMMARY

Project Title: Site Exploration and Characterization near Bellingham, Washington

Principal Investigator: Carl A. Johnson

Organization:
Fugro, [illegible].
3777 Long Beach Blvd.
Long Beach, California 90807
(213) 595-6611

Project Goals: To characterize and assess the potential energy storage capability of a saline aquifer near Bellingham, Washington.

Project Status: This effort was terminated in April 1980. FY-1980 activities included the drilling of two deep wells in the Nooksak River Basin in an attempt to intercept the "Esperance Sand" which is thought to be present in the area. The project was terminated after drilling efforts failed to identify a usable aquifer system within economical transport distances of the proposed energy source. Energy was to have been supplied by the Thermal Reduction Company of Bellingham, Washington from their refuse burning facility.

Contract Number: DE-AC06-76RLO 1830, Subcontract B-93156-A-Z

Contract Period: 15 August 1979 through 1 May 1980

Funding Level: $159,766

Funding Source: U.S. Department of Energy through Pacific Northwest Laboratory

PROJECT SUMMARY

Project Title: Compendia of Existing Information Task

Principal Investigator: Leigh S. Prater

Organization:
Pacific Northwest Laboratory
P.O. Box 999
Richland, Washington 99352
(509) 376-4870 (FTS: 444-4870)

Project Goals: Collect, summarize, and transmit information related to Seasonal Thermal Energy Storage (STES), and maintain key data in an interactive data base.

Project Status: A useful STES library has been established. It now contains about 1400 articles with a wide range of key references on topics related to thermal energy storage.

Literature reviews and topical reports are being prepared. The topics are as follows: ATES site characterization methods, regional aquifer assessments, thermal fatigue of reservoir materials, energy and mass transport in geologic media, energy uses and sources, and reinjection experience in ground-water cooling applications.

A newsletter containing brief reports about STES projects around the world is being published quarterly by Lawrence Berkeley Laboratory.

A STES data base is being established. It will contain bibliographic information and data files generated by the STES Program components. The data base is being established on the Technology Information System (TIS) at Lawrence Livermore Laboratory.

Contract Number: DE-AC06-76RLO 1830

Contract Period: Continuing

Funding Level: $105,300, FY-1980, B/O

Funding Source: U.S. Department of Energy, Office of Advanced Conservation Technologies

COMPENDIA OF EXISTING INFORMATION TASK

Leigh S. Prater
Pacific Northwest Laboratory
P.O. Box 999
Richland, Washington 99352

ABSTRACT

The Compendia of Existing Information Task is a technical support task of the Seasonal Thermal Energy Storage (STES) Program. The task goal is to collect, summarize and transmit STES-related information. The task consists of five subtasks: Library Establishment, Maintenance, and Development; Literature Reviews and Summary Papers; STES Newsletter Publication; Production and Maintenance of the Aquifer Thermal Energy Storage Reference Manual; and Development of the STES Data Base.

Highlights of technical progress include the following:

- The STES Library has been established and now contains over 1500 articles with a wide range of key references on topics related to thermal energy storage.
- Literature reviews and topical reports on subjects of importance to the STES Program are being prepared.
- A newsletter containing brief reports about STES projects around the world is being published quarterly.
- The Aquifer Thermal Energy Storage Reference Manual has been issued.
- A computerized STES data base is being established.

INTRODUCTION

The Compendia of Existing Information Task is a technical support task of the Seasonal Thermal Energy Storage (STES) Program. The objective of the Compendia Task is to collect, summarize, and transmit STES-related information to other program components. This goal is being met by the following activities: 1) development of a library of STES-related information; 2) production of selected literature reviews and topical reports; 3) publication and distribution of the quarterly STES Newsletter; 4) production and maintenance of the Aquifer Thermal Energy Storage Reference Manual; and 5) development of the computerized STES data base. These activities are intended to support the future development of STES technology.

Many of the Compendia Task activities are carried out under subcontracts. The FY 1980 subcontractors are listed below.

Midwest Research Institute	Charles H. Lee, Principal Investigator
Lawrence Livermore Laboratory	Viktor Hampel, Principal Investigator
Oregon State University, Department of Soil Science	Stuart Childs, Principal Investigator
Century West Engineering	Dorothy Stoffel, Principal Investigator
Oregon State University, Department of Mechanical Engineering	Gordon Reistad, Principal Investigator
Lawrence Berkeley Laboratory	Chin Fu Tsang, Principal Investigator
David D. Hostetler, Consulting Engineer	D. D. Hostetler, Principal Investigator

TASK DESCRIPTION

The Compendia Task has five subtasks:

Subtask 1 - Library Establishment, Maintenance, and Development. This subtask involves all efforts necessary to provide a useful library of STES-related literature. These efforts include identifying and procuring new literature, indexing library articles, distributing updated bibliographies and maintaining library operation.

Subtask 2 - Literature Reviews and Summary Papers. This subtask will result in the production of papers covering topics pertinent to STES. These papers are intended to support STES Program efforts by providing information on topics that are of major concern to various program elements.

Subtask 3 - STES Newsletter Publication. This subtask involves compiling, editing, publishing and distributing a quarterly STES Newsletter.

Subtask 4 - Production and Maintenance of the Aquifer Thermal Energy Storage Reference Manual. The objective of this subtask is to produce and maintain a reference manual for the STES Program. The subtask involves efforts needed to compile, edit, publish, distribute and update the Aquifer Thermal Energy Storage Reference Manual.

Subtask 5 - Development of the STES Data Base. This subtask involves all activities needed to develop a computerized STES data base utilizing the Technology Information System at Lawrence Livermore Laboratory.

TECHNICAL PROGRESS

SUBTASK 1

As a result of work done during FY 1979 and FY 1980, Compendia Task staff members have assembled a useful STES Library. The library contains approximately 1500 articles with a wide range of key references on topics related to thermal energy storage. Although the library contains articles pertaining to many types of seasonal thermal energy storage, the main emphasis is on the storage of thermal energy in aquifers.

During FY 1979 and FY 1980, efforts were made to identify and procure STES-related articles. Customized searches were run on computerized data bases (including DIALOG and RECON), reference lists were obtained from the Compressed Air Energy Storage and the Geothermal Program libraries at PNL, and several national laboratories, including Lawrence Berkeley Laboratory (LBL) and Oak Ridge National Laboratory (ORNL). These reference lists and data base searches were used to procure STES-related articles. Staff members working on the STES Program identified additional references for the library.

Bibliographic information from the library is being entered into the STES data base. Each reference is represented by a citation, which includes an abstract, keywords and bibliographic information. On-line, customized literature searches can be conducted.

The STES Library bibliography is regularly updated and periodically distributed so that researchers on the STES Program will be informed about the contents of the library. Library maintenance and development is now being conducted via subcontract with Midwest Research Institute.

SUBTASK 2

The objective of this subtask is to summarize and reference work on selected topics. This subtask will produce papers covering various topics pertinent to STES. These papers are intended to support other STES Program efforts by providing information on topics of concern.

Topics currently being investigated include: Aquifer Thermal Energy Storage (ATES) site characterization methods, regional aquifer assessments, energy and mass transport in geologic media, reinjection experience in ground-water cooling operations, thermal fatigue of reservoir materials, and energy uses and sources. All of these studies except the last two have been subcontracted. Progress on these studies is discussed in the following paragraphs.

A document on ATES site characterization methods was prepared by Mr. David Hostetler, a consulting engineer. This document contains information on the following: site selection and ambient temperature characterization; preoperational thermal characterization and site evaluation; and subsurface facility design and development. The report was submitted to the Pacific Northwest Laboratory (PNL) on September 30, 1980.

Century West Engineering is conducting a regional aquifer assessment study. The objective of this study is to qualitatively describe the ATES potential of major aquifers throughout the United States. Century West Engineering has collected existing hydrogeological information for major U.S. aquifers. This information has been used to characterize each aquifer system. On the basis of its characteristics, each aquifer has been evaluated for its ATES potential. This project will be completed in January, 1981. Century West Engineering will submit to PNL a report containing evaluations of major United States aquifers.

The Department of Soil Science of Oregon State University is conducting a study of energy and mass transport in geologic media. This study will examine the physical principles of energy and mass transport in unsaturated porous media. This project is intended to strengthen existing theoretical knowledge and to provide information on engineering design and site evaluation for ATES systems. Research will focus primarily on energy transport mechanisms in the unsaturated zone of the unconfined aquifer system. The overall objective of this project is to identify soil and environmental conditions or parameters influencing aquifer thermal energy storage efficiency. Definition of these important parameters will provide needed technical support to the STES Program. The scope of research includes a thorough literature review, laboratory work, and limited computer modeling. The research is divided into two phases. The first phase consists of a literature review and a parametric analysis of important transport mechanisms pertinent to mass and energy transport in unconsolidated, unsaturated porous media. In the second phase the research will further characterize transport mechanisms through laboratory experimentation. An annotated bibliography and a preliminary interpretive report on the main facets of energy and mass transport were submitted to PNL in September, 1980.

Midwest Research Institute has conducted a survey of ground-water reinjection experience in air-conditioning operations. Basically, the work consisted of three tasks: site identification, documentation of selected sites, and analysis of site data. The site identification task involved identifying sites across the United States where reinjection of cooling water is practiced. Selection of sites was based on availability of information and geographic location. The reinjection sites chosen for documentation were representative of different geographic locations and hydrogeologic environments. The second task involved site documentation. Documentation consisted of three parts: well system design, operational performance history, and analysis of the reinjection experience. The third task, data analysis, involved the identification of actual and potential problems with the reinjection operations of each site. The results of the study are contained in MRI's final report, which was submitted to PNL in September, 1980.

A survey of ground-water source heat pump operations in the Portland, Oregon, area is being conducted by the Department of Mechanical Engineering of Oregon State University. This study is intended to assess the use of ground-water source heat pumps for large-scale heating and cooling operations in the Portland area. It is scheduled to be completed in early FY 1981. Basically, the survey of ground-water source heat pump operations consists of the following tasks: 1) identification of sites, 2) documentation of system design, operational procedures, operational problems and overall system performance of each site, and 3) analysis of the heat pump operations. All of this information will be contained in a report that Oregon State University (OSU) will submit to PNL. OSU will also assess the potential benefit of using aquifer thermal energy storage in conjunction with ground-water source heat pumps. As part of this effort, OSU will study potential heat pump designs that can efficiently use ground water in a wide temperature range. The information from this effort will also be summarized in a report.

The topics of thermal fatigue of reservoir materials and energy uses/sources are being studied within PNL. Reports will be written on each of these topics.

SUBTASK 3

Lawrence Berkeley Laboratory has been responsible for producing the Seasonal Thermal Energy Storage (STES) Newsletter. The newsletter contains brief reports about STES projects around the world. The STES Newsletter is now being published quarterly and has an international distribution list. It has proven to be a valuable means for disseminating current information about STES projects.

SUBTASK 4

The Aquifer Thermal Energy Storage (ATES) Reference Manual was issued in August, 1980. This manual is the primary document for the transfer of technical information from the STES Program. It has been issued in preliminary form and will be updated periodically to include more technical data and results of research. As the program progresses and new technical data become available, sections of the manual will be revised to incorporate these data. The revised sections will be distributed to all individuals holding a copy of the manual.

SUBTASK 5

The objective of this subtask is to establish a STES data base utilizing the Technology Information System (TIS). Lawrence Livermore Laboratory (LLL) is assisting PNL in this endeavor. The data base will provide easy access to bibliographic information from the library and to data files generated by the STES Technical Support Program and the ATES Demonstration Program. The STES data base will utilize the TIS, which was developed by LLL for DOE's Office of Advanced Conservation Technologies. The TIS is a computer-based hierarchy of technical, econometric, and other data bases and models. These include physical and chemical properties of energy storage materials, characterization data for energy storage components and systems, and modeling programs for energy storage applications. Bibliographic information and numeric test data are also included. The TIS has been established for the use of program managers and project personnel under contract to DOE's Office of Advanced Conservation Technologies. Authorized users can achieve access to TIS from remote computer terminals by telephone dial-up.

PROJECT SUMMARY

Project Title:	Seasonal Thermal Energy Storage Technical Information System
Principal Investigator:	Viktor E. Hampel
Organization:	Lawrence Livermore Laboratory P.O. Box 808 Livermore, California 94550 (415) 422-4357 (FTS: 532-4357)
Project Goals:	To establish a comprehensive Technical Information and Communication System for the Seasonal Thermal Energy Storage (STES) Program.
Project Status:	The project started in June 1980. An overall hierarchical STES data base structure has been developed. This includes the administrative, organizational, and technical description of the STES Program, its demonstration projects, and supportive activities. The bibliography of the STES Library has been added to the data base and is available for on-line access. Over 1400 citations are contained in the bibliographic data files. On-line, customized literature searches can be conducted. Computer equipment has been installed at the Pacific Northwest Laboratory. This equipment is being used to support the development of the STES data base. A user's manual for the STES Technical Information System has been drafted and will be completed in FY-1981. The STES Program staff and STES contractor personnel are being trained in the use of the system.
Contract Number:	DE-AC06-76RLO 1830, Subcontract B-97602-A-O
Contract Period:	Continuing
Funding Level:	$122,700, FY-1980,
Funding Source:	U.S. Department of Energy through Pacific Northwest Laboratory

STES-TIS — TECHNICAL INFORMATION SYSTEM*

Viktor E. Hampel and William G. Rabe+
Lawrence Livermore Laboratory
University of California
P.O. Box 808
Livermore, California 94550

ABSTRACT

This paper summarizes a project conducted by Transportation Systems Research (TSR) at Lawrence Livermore National Laboratory (LLNL) to provide a centralized information and communications system for the "Seasonal Thermal Energy Storage" (STES) and Aquifer Thermal Energy Storage (ATES) Programs for Battelle Pacific Northwest Laboratory (BPNL).

The key to effective R&D program decision-making is the development and availability of accurate and timely information. The STES Technology Information System (STES-TIS) is an informational tool which can be used to make information accessible to STES staff and contractors using a remote terminal via the commercial dial-up telephone network. Because of the system's capability to handle numeric and bibliographic data bases, STES-TIS is well suited to satisfying the informational storage and retrieval needs of STES libraries and model development/field test data programs.

The project consists of three tasks: Task I - Define and implement the overall STES hierarchial data base structure; Task II - Assist in the incorporation of existing or planned data bases and models into the STES Technical Information System; Task III - Procure terminal hardware and build software interfaces to increase communications efficiency. Progress to date, in each of these task areas is discussed.

INTRODUCTION

The STES-Technology Information System (STES-TIS) is being developed using the Technology Information System (TIS) developed at the Lawrence Livermore National Labratory (LLNL) under the sponsorship of DOE/ACT. TIS is designed to provide standardized information for use in research and development efforts addressing energy storage systems. TIS provides a computer-based hierarchy of technical, econometric, and other data bases and models. These include physical and chemical properties of energy storage materials; characterization data for energy storage components and systems; and modeling programs for energy storage applications. Bibliographic references and numeric test data serve to authenticate information and to validate models. Highly interactive and self-guided, TIS can be used by R&D program managers, engineers, and researchers without previous computer experience.

TIS can be accessed from remote computer terminals by telephone dial-up and over the ARPA national computer network. The system provides an expedient means for electronic communication and acts as an automated gateway for connection to other computers and information centers.

As designed TIS provides a sound base upon which a centralized information and communications system for STES and ATES can be developed. When completed, the STES-TIS can be

---

+ Control Data Corporation, under contract to Lawrence Livermore National Laboratory.

* Work performed under the auspices of the U.S. Department of Energy by the Lawrence Livermore Laboratory under contract number W-7405-ENG-48.

of significant benefit to the STES program's research and development work. It can be an efficient means of disseminating results to other staff and contractors. Furthermore, the system can provide feedback on project progress to project leaders through STES-TIS' capability to provide user selected and defined reports of data from the data base.

The main emphasis of the STES-TIS is to provide remote access to technological information relating to aquifer/non-aquifer energy storage systems. This will be accomplished through the use of data base structures containing bibliographic information from the STES and other libraries: DOE/RECON, NASA/RECON, and NTIS to mention afew; and from data accumulated by the STES Technical Support Program and the ATES Demonstration Programs.

TIS BACKGROUND

The TIS Project was initiated at LLNL midyear in FY 1976 under DOE/ACT sponsorship. Following a period of definition and interaction with the prospective user community, the computer-based system was planned and procured as an integrated information system, combining in one central mini-computer the relevant up-to-date information and data required for accessing the value of energy storage devices and systems, and making this information available to the energy storage community.

Communications facilities were added to allow access from remote terminals by telephone dial-up and over the ARPANET. The link to ARPA, which is cosponsored by DOE, brought TIS into high-speed communications with other national laboratories, universities, and some industrial organizations programmatically related to DOE/ACT. A user interface was designed to store and display in a hierarchical manner the large number of data files and models required. Self-guiding and self-prompting, this user interface permits those not intimately familiar with computer operations to work effectively with the system. User-to-user communications capabilities were added to TIS to permit communications directly and indirectly to other users through: "write", which allows one user to write directly to another user's terminal; "link", which interconnects two terminals together on a one-to-one basis, in a teacher-student mode; and electronic mail, which permits all users to send mail to another user or users.

During FY-80, the information content of TIS and its capabilities were substantially extended. The number of programmatic data bases was increased from 13 to 57 while the number of models grew from 9 to 14.

The primary concept embodied in TIS is a novel approach to information management. Unlike other information systems or computational facilities that specialize in bibliographic, financial, numerical, or computational services, TIS combines all these resources into one central information system. This is made possible through state-of-the-art software and hardware designed and developed specifically for that purpose.

PROJECT DESCRIPTION

The STES-TIS project consists of three major tasks. The following is a description of the tasks and supporting activities.

Task I — DEFINE AND IMPLEMENT STES DATA BASE STRUCTURE

Three data files have been identified for implementation at this time: the STES library, the conference schedules, and the STES organizational structure. Creation of the schema and sub-schema for these data bases, then creating and loading the data itself is the primary activity during this task. Specifically:

1) The STES library activity entails automating the existing STES card catalogue of the publications in the library. The card catalogue consists of approximately 1300 publications.

2) The conference data base will consist of a list of conferences of interest to the STES programs and will include all pertinent information pertaining to past and scheduled conferences, i.e., attendees, names of speakers and topics, and a schedule of up-coming conferences.

3) The STES organizational data will consist of charters, plans, and progress of all STES and ATES related programs. The STES organizational data serves as the master menu used to navigate through the other STES data files. It is this data that provides the hierarchial structure for STES-TIS. The menu is the device which allows the inexperienced user to obtain the information desired without intimate knowledge of the data base structures or the operating system's command language.

Training of STES staff and sub-contractors is an essential activity during this task. Although the system is highly interactive, formal training is essential so that the optimum value can be derived from its use. Training will be accomplished through manuals and personal training. Hotline support is also included in this task although it applies equally to all tasks. Hotline support is available to all users and is available during normal business hours. Provisions are made to allow communications with the LLNL staff at any time through "electronic mail" (em) and "comment".

Task II — INCORPORATE EXISTING OR PLANNED DATA BASES AND MODELS

During this task other numerical and bibliographic data bases and models will be evaluated for appropriateness and applicability on STES-TIS. The LLNL staff will assist STES personel and sub-contractors in determining which present or planned data bases and models are suited to the STES-TIS system environment and within its capabilities. Various data bases exist within the energy community which would be useful to the STES program and its staff.

The DOE/RECON, NASA/RECON, and NTIS systems have bibliographic data which has been identified for use in the aquifer and non-aquifer programs. In this task, an automated mechanism will be developed in which these data bases would be searched for citations which are related to the STES program and transfered to the STES-TIS data base. This search would be automatically conducted periodically, thereby ensuring an up-to-date library of new technologies in "Thermal Energy Storage" and related diciplines.

LLNL staff will assist in the conversion of aquifer and non-aquifer models to make them interactive and interface with the STES-TIS data base. These models need not reside on the STES-TIS system, in fact, where models are too complex or require extremely long execution times, it may be appropriate to have them reside on other computer resourses. In these cases, STES-TIS can still be used as a centralized gateway machine to control access to the remote computer resource.

To aid in the evaluation and validation of models and data, the LLNL staff will generate reports and plots of on-line data tailored to the needs of the STES programs. Plots are especially useful in data analysis and evaluation. Special reports will be generated at the request of STES.

Task III — PROCUREMENT OF REMOTE TERMINAL EQUIPMENT

This task is primarily concerned with terminal equipment procurement software development to support that equipment, and enhancement of the communications capability to increase the reliability of transmission and the development of new communications tools.

Assistance will be given to STES in the evaluation and selection of terminal hardware to interface with TIS. LLNL will also provide necessary software to support the selected equipment. When special application programs are required to simplify use of said hardware, LLNL staff will provide them.

STATUS

All three tasks in currently in progress. Some of the task activities were started in FY-80 with all due for completion in FY-81.

Task I — DEFINE AND IMPLEMENT STES DATA BASE STRUCTURE

Library data was originally entered onto a Wang text-processing system and then transferred to the STES Technology Information System data bank. As the data was transferred, it was checked for validity and converted to the proper data base format. Verification and correction of the catalogue data is completed. The library data base is now established and is currently being updated to reflect new entries. The citation extracts data file is currently being designed. LLNL will assist in the transfer of the extracts when they become available.

The conference data base and the STES organizational data file structure are in the final stages of design. A temporary organizational structure has been implemented to permit updating and access of data on STES-TIS.

Training on the use and maintenance of the STES library system is complete. The LLNL staff has written a User's Maintenance Manual for the library system. It has been delivered to BPNL. The STES staff and Library subcontractor personnel have been provided with private tutoring on the use and maintenance of the Library system. Like training will be provided to key personnel for other data bases as well as providing appropriate user's manuals. User's manuals for the TIS system and "Electronic Mail" (em) have been delivered.

Task II — INCORPORATE EXISTING OR PLANNED DATA BASES AND MODELS

Current activity in this task is primarily in the area of enhancing the plot and report capabilities. A device independent driver has been written to enable the use of the four-color plotter and increase the flexibility of the report writer's capability to output to either plotter or printer. A self-guiding user application program has also been written which supports the device independent driver allowing the user to select various options of report writing and plotting, i.e., color selection, line drawing type, report formatting, and etc.

Task III — PROCUREMENT OF REMOTE TERMINAL EQUIPMENT

LLNL assisted STES in the evaluation of terminal requirements and procured the necessary equipment to communicate with TIS. The following Hewlett Packard terminal equipment has been ordered by LLNL staff: 2-HP2648 terminals with line-drawing set, 2-HP7310 high-speed printers, and 1-HP7221 four-color plotter. Associated Vadic modems and error correction units were also ordered. These equipment items satisfy the STES requirement of 1200 baud transmission rates. The procurement and delivery of the terminal, printers, plotter, and the necessary communications modems and error correction equipment is complete. One additional 1200 baud Modem is yet to be delivered. This modem will be used as a spare.

Software drivers and application programs existed for all but the four-color plotter. A software development activity was started here at LLNL to provide a device-independent driver and applications to allow users to fully utilize the plotter. Besides plotting in color, this package will allow users to generate multiple line plots as well as histogram and pie-plots. The software driver for the color plotter is essentially completed and in the final stages of quality assurance.

LLNL has also undertaken several projects to enhance the TIS communications capability. Two areas of enhancement are currently underway, the first to increase user-to-user communications capabilities; the second to increase computer-computer capabilities. The electronic mail (em) capability has been redesigned to including such features as, mail forwarding, mail answering, group routing, conferencing, and composing and editing mail. The enhanced electronic mail is currently available. To enhance the computer-to-computer capability, LLNL developed a capability to allow input of text data from Wang Text Processors. A project has been started which would allow similar entry from other processors like the Qyx Text Processor.

REMARKS

STES-TIS can provide a valuable service to STES program managers, developers, and sub-contractors by making information readily available and accessible in an interactive environment.

The completed STES-TIS tasks have presented no serious obstacles; the planned tasks are not expected to pose any problems either. LLNL is confident that the remaining tasks will be completed on schedule.

PROJECT SUMMARY

Project Title: Maintenance and Development of the Seasonal Thermal Energy Storage (STES) Library

Principal Investigator: Charles H. Lee

Organization:
Midwest Research Institute
425 Volker Boulevard
Kansas City, Missouri 64110
(816) 753-7600

Project Goals: Perform activities necessary for library maintenance and development, including technical abstracting and assignment of keywords.

Project Status: Operation of the STES Library is being implemented by Midwest Research Institute (MRI). One of MRI's employees, their librarian, is stationed at Battelle and is maintaining library operation. Technical support is being provided by personnel at their main office.

Contract Number: DE-AC06-76RLO 1830, Subcontract B-97521-A-O

Contract Period: 5 August 1980 through 30 September 1981

Funding Level: $147,815

Funding Source: U.S. Department of Energy through Pacific Northwest Laboratory

PROJECT SUMMARY

Project Title: Publication of the Seasonal Thermal Energy Storage (STES) Newsletter

Principal Investigator: Chin Fu Tsang

Organization:
Lawrence Berkeley Laboratory
Berkeley, California 94720
(415) 486-4000 ext. 5782

Project Goals: To organize, solicit, edit, and publish a quarterly International ATES Newsletter.

Project Status: The International ATES quarterly Newsletter is published as scheduled. Much enthusiasm both in the United States and abroad is apparent from the many contributions to and the requests for this publication. After much consideration and discussion with Pacific Northwest Laboratory, the DOE Field Manager for this project, we have decided, beginning with the September 1980 issue, to expand the Aquifer Thermal Energy Storage (ATES) Newsletter to the Seasonal Thermal Energy Storage (STES) Newsletter so that research into other means of seasonal storage will be included.

Contract Number: DE-AC06-76RLO 1830, Subcontract B-67762-A-Z

Contract Period: 1 October 1979 through 30 September 1980

Funding Level: $25,000

Funding Source: U.S. Department of Energy through Pacific Northwest Laboratory

best copy available

PROJECT SUMMARY

Project Title: Survey of Ground-Water Reinjection Experience in Air Conditioning Applications

Principal Investigator: Charles H. Lee

Organization: Midwest Research Institute
425 Volker Boulevard
Kansas City, Missouri 64110
(816) 753-7600

Project Goals: Conduct a nation-wide survey of air conditioning operations that use ground-water reinjection.

Project Status: The survey has been completed. Basically, the work consisted of three tasks: site identification, documentation of selected sites, and analysis of site data.

A final report containing results of the survey was submitted to PNL during August 1980. This report has information on 45 sites. The site analysis showed that operational problems were caused by plugging and thermal pollution. Plugging problems were caused by oxidation of Fe and Mn.

Contract Number: DE-AC06-76RLO 1830, Subcontract B-78986-A-O

Contract Period: 25 March 1980 through 15 September 1980

Funding Level: $29,490

Funding Source: U.S. Department of Energy through Pacific Northwest Laboratory

PROJECT SUMMARY

Project Title:	Regional Aquifer Assessment Study
Principal Investigator:	Dorothy Stoffel
Organization:	Century West Engineering North 1010 Washington Spokane, Washington 99201 (509) 326-4227
Project Goals:	Qualitatively describe the Aquifer Thermal Energy Storage (ATES) potential of major aquifers throughout the United States.
Project Status:	Century West Engineering has collected existing geohydrologic data for major U.S. aquifers. These data have been used to evaluate the ATES potential of each aquifer. A report containing the aquifer evaluations is currently being prepared.
Contract Number:	DE-AC06-76RLO 1830, Subcontract B-93966-A-O
Contract Period:	29 March 1980 through 22 September 1980
Funding Level:	$38,317
Funding Source:	U.S. Department of Energy through Pacific Northwest Laboratory

PROJECT SUMMARY

Project Title: Document on Aquifer Thermal Energy Storage Site Characterization Methods

Principal Investigator: David D. Hostetler

Organization: David D. Hostetler, Consulting Engineer
P.O. Box 151
Cannon Beach, Oregon 97110
(503) 436-2650

Project Goals: Produce a document outlining site characterization methods for an aquifer thermal energy storage facility.

Project Status: The draft report is being prepared and will be completed by September 12, 1980. The final report is due on September 30, 1980.

Contract Number: DE-AC06-76RLO 1830, Subcontract B-93986-A-O

Contract Period: 1 August 1980 through 30 September 1980

Funding Level: $8,840

Funding Source: U.S. Department of Energy through Pacific Northwest Laboratory

PROJECT SUMMARY

Project Title: Survey of Ground-Water Source Heat Pump Operations in the Portland Area

Principal Investigator: Gordon Reistad

Organization:
Department of Mechanical Engineering
Oregon State University
Corvallis, Oregon 97331
(503) 754-2575

Project Goals: Assess the use of ground-water source heat pumpts for large-scale heating and cooling operations in the Portland area, and assess the potential benefit of using aquifer thermal energy storage in conjunction with heat pumps.

Project Status: The survey of heat pump operations in the Portland area has been completed. Thirteen installations were identified, and six of them were selected for documentation. Information on these six installations is contained in a report submitted to PNL during August 1980.

An assessment of the benefit of using aquifer thermal energy storage in conjunction with heat pumps is in progress and will be completed in November 1980.

Contract Number: DE-AC06-76RLO 1830, DE-AM06-76RL02227, Task Order DE-AT06-79RL10121

Contract Period: 26 September 1979 through 30 September 1980

Funding Level: $30,000

Funding Source: U.S. Department of Energy, Richland Operations Office

PROJECT SUMMARY

Project Title:	Laboratory Analysis
Principal Investigator:	James A. Stottlemyre
Organization:	Battelle, Pacific Northwest Laboratory P.O. Box 999 Richland, Washington 99352 (509) 375-2733 (FTS: 444-7511 ext 2733)
Project Goals:	Investigate the potential for the causes of significant STES-induced changes in reservoir physical and chemical properties. Primary emphasis is on permeability, injectivity, and water quality. Develop equipment and procedures necessary to support drafting of site specific reservoir design and operating criteria and environmental assessment reports.
Project Status:	The project is only partially completed. Activity has focused on three tasks including laboratory equipment development, mobile field equipment development, and laboratory analysis of the effects of temperature on sand and sandstone permeability. A contract has been awarded to Terra Tek, Inc. to design and construct a laboratory scale apparatus capable of testing reservoir materials and associated ground waters under simulated STES operating conditions, e.g., time-varying temperatures, stresses and flow rates. Emphasis is on permeability, porosity, strain (sample deformation), mineralogy, particle carry-over, and water quality. Completion of the equipment is scheduled for June 1981. A contract has been awarded to Terra Tek, Inc., to develop a mobile, inline, injectivity-impairment test stand for use at field sites. This equipment is designed to permit evaluation of injection well longevity as a function of injection water quality and reservoir injection parameters. Completion of the equipment is tentatively scheduled for December 1980. A report covering the motivations for and techniques of injection well impairment testing has been drafted and is undergoing PNL/DOE review. Several experiments have been conducted at Terra Tek and PNL concerning the effects of temperature on sand and sandstone permeability to water. Preliminary observations are that significant permeability reductions can be expected, damage may be confined to near wellbore zones, degradation is time dependent and transient in nature, and particulate plugging appears to be the principle cause. Experiments are continuing and a draft report will be issued this fall.
Contract Number:	DE-AC06-76RLO 1830
Contract Period:	Continuing
Funding Level:	$66,000, FY-1980, B/O
Funding Source:	U.S. Department of Energy, Office of Advanced Conservation Technologies

PHYSICOCHEMICAL PROPERTIES ANALYSES
IN SUPPORT OF THE SEASONAL THERMAL ENERGY STORAGE PROGRAM

James A. Stottlemyre
Pacific Northwest Laboratory
P.O. Box 999
Richland, Washington 99352

Craig H. Cooley
Terra Tek Inc.
University Research Park
Salt Lake City, Utah 84108

Gary J. Banik
Terra Tek Inc.
University Research Park
Salt Lake City, Utah 84108

ABSTRACT

This paper summarizes FY 1980 activities concerning the physical and chemical stability of aquifers subjected to Seasonal Thermal Energy Storage (STES) operating conditions. Subtasks include the development of laboratory and field equipment, an assessment of geochemical modeling, and laboratory-scale investigations of the permeability/creep compaction stability of quartz sands.

Terra Tek Inc. is in charge of developing equipment, namely, a laboratory-scale flow loop that simulates several STES reservoir conditions, and a water well injectivity impairment test stand that can be used for inline testing of functional STES injection streams in the field.

The geochemical modeling assessment has resulted in a preliminary selection of the model most pertinent to STES and in recommendations for FY 1981 refinements.

The effects of temperature and time on permeability and the compressibility of unconsolidated sands are being studied at Pacific Northwest Laboratory and Terra Tek. Preliminary results indicate that significant permeability reductions might be expected at elevated temperatures. Particulate plugging may be responsible for this lowered permeability, but additional study is required before final conclusions can be made.

INTRODUCTION AND SUBTASK DESCRIPTIONS

Being able to predict and understand the physical and chemical stability of aquifer materials and associated ground waters is important to Seasonal Thermal Energy Storage projects from the standpoints of developing site-specific design and operating guidelines and protecting the environment. Although site-specific field analyses are very important, valuable information can be expediently generated from laboratory-scale investigations based on simulated STES operating reservoir conditions, mathematical modeling, and limited field analyses.

When conducting experiments on aquifers in the lab, actual samples of aquifer materials and ground waters should be used, and an attempt should be made to replicate the aquifer conditions as regards temperature, confining (lithostatic) stess, interstitial fluid pressure, flow direction, and flow rate. Dependent variables of primary interest include porosity, permeability, compactability, and water quality. The use of automated equipment would facilitate testing over long periods of time until parameter equilibrium is attained. Such experimental equipment, which must also be corrosion resistant,(1,2) is presently being developed by Terra Tek for the STES Program.

Another tool that has recently been designed at Terra Tek is a portable field unit for conducting water well injectivity impairment studies. These analyses have been shown to predict, within a factor of two, the longevity or impairment potential of reinjection wells exposed to a variety of suspended particles common in many reinjection schemes.(3,4,5) Potential particle sources include: pre-existing aquifer fines, disaggregated sand grains, corrosion products, mineral scale products, atmospheric dust particles, chemical additives, and particulates associated with any dilution or makeup waters.

Geochemical modeling is another potentially powerful tool available to STES site managers. Dr. Evert Jenne, PNL, an international expert in the area of aqueous geochemistry and modeling, has assessed available models, associated data bases, current limitations, and costs. A specific code is being recommended based on its thermodynamic data base and solid phases pertinent to STES. Certain modifications are, in addition, being suggested for FY 1981.

A laboratory-scale investigation is in progress concerning the potential effects of temperature on unconsolidated sand permeability and creep compaction potential. These experiments are being conducted at Terra Tek and Pacific Northwest Laboratory and were motivated by previous investigations at Stanford, Texas A&M, and the University of California at Berkeley. Results from previous studies showed that for Berea, Bandera, and Boise sandstones, permeability to liquid water may decrease by more than 60% over the temperature range of 25 to 150°C.(6) Similar decreases have been recorded for Massillon Sandstone and unconsolidated Ottawa sand (Figures 1 and 2).(7,8) No such perturbations have been systematically observed when dry gas or mineral oil were used as the working fluids, however.

In the present study, two explanations are being considered to explain permeability degradation with liquid water: 1) the decrease is actually a time-dependent (fluid volume handled) phenomenon, which previous researchers may have mistakenly attributed to temperature, because equilibrium conditions were not attained during the experiment; or 2) permeability is really temperature dependent and caused by one or more factors. These factors may include thermal expansion of quartz grains into pore throats, material consolidation with or without chemical weakening, anomalous fluid viscosities, pre-existing fines, water sensitivity (clay swelling and dispersion), temperature-induced particle disaggregation (cement dissolution or particle spalling), particles introduced with the inlet fluid (corrosion products or other contaminants), and mineral scaling.

RESULTS AND CONCLUSIONS

Equipment development results are reported separately (Craig Cooley, Larry Owen). With respect to geochemical modeling, it is being recommended that the code WATEQ(4) be emphasized. This code appears to have the best thermodynamic data base and the greatest number of environmentally important solid phases pertinent to STES of all the codes evaluated. Some code modifications are recommended for FY 1981: the aqueous speciation and equilibrium calculations at temperatures up to 150°C should be incorporated, as should the mass transfer capabilities for specific minerals at equilibrium, and some degree of kinetic control on mineral precipitation due to temperature decreases. In the long term (post FY 1981), should also be added to the code.

Preliminary results have been obtained about the permeability versus temperature problem (Figures 3, 4, and 5). Tests were run on Ottawa sand (150/170 mesh) at room and elevated temperatures using doubly dionized and prefiltered water, confining pressure (150 bars), median pore fluid pressure (60 bars), and flow rate (16 ml/min). Darcian permeability data are presented in two formats: 1) the ratio K_T/K_{25}, which is defined as the ratio of the final (steady state) permeabilities at temperature T and 25°C, respectively (Figure 6); and 2) the ratio K_f/K_i, which is defined as the ratio of the final permeability and the initial permeability at any given temperature (Figure 7). These formats permit a decoupled evaluation of the importance of temperature and time. Although significant data scatter exists, it appears that, at least for Ottawa sand, the permeability to distilled water may be sensitive to both temperature and time (fluid volume handled).

The effects of reduced pore volume (bulk consolidation and/or sand grain thermal expansion) have been analyzed based on the volumetric strain (deformation) data recorded during the permeability runs. Volume strain data for Ottawa sand, two sandstones, and a zero porosity quartz aggregate are shown in Figure 8.

By comparing the deformational response (net expansion or compaction) of the porous materials with the zero porosity quartz aggregate, the decrease in available pore space due to sample consolidation and the expansion of sand grains into pore throats can be estimated. For Ottawa sand, the total reduction in pore space between 25°C and 150°C was about 0.8%, roughly half of which is attributable to grain expansion, and the other half to bulk compaction. The modified Kozeny-Carman Equation can then be used for a very rough approximation of the permeability reduction. Table 1 shows the results of comparing calculated and measured permeability reductions, where the calculated value is based on pore volume reduction alone, but the measured value includes all potential damage mechanisms. It appears that pore volume reduction due to bulk compaction and/or expansion of matrix constituents into pore throats does not explain observed permeability decreases with time and temperature.

Although insufficient data have been collected to warrant definitive conclusions, preliminary observations appear to support the following: 1) the increased total dissolved solids (TDS) level in the experiments has no measurable effect on viscosity; 2) a significant quantity of fine particulates (quartz and clay minerals) adheres to the sand grains, and the mobility of these particles appears to be temperature sensitive; 3) prefiltering the fluid just prior to its entry into the sand sample is necessary to prevent face plugging; 4) stopping the flow generally results in a partial but temporary permeability recovery; 5) the grain size distribution of the sample is biased towards smaller particles subsequent to a test indicating some grain fragmentation; and 6) based on washed sand tests and $CaCl_2$ test results, virgin Ottawa sand may be somewhat water sensitive (clay particle dispersion).

TABLE 1. Results for Pore Volume Reduction Analysis

Temperature 150°C
Confining Load 150 Bars
Pore Fluid Pressure 60 Bars
Distilled, Deareated Water

Sample Type	Incremental Volume Strain	Porosity Change Measured	Permeability Ratio K_f/K_i	
			Calculated*	Measured**
	(10^{-3})	(%)		
Quartz	5.50	-	-	-
Ottawa Sand	-2.10 ± 1.30	0.80 ± 0.10	0.91 ± 0.04	0.49 ± 0.19
Massillon S.S.	-0.5 ± 0.2	0.40 ± 0.03	0.95 ± 0.02	0.26 ± 0.11

* Calculation: Modified Kozeny Carman EqN for pore volume reduction only.
** Measured: Includes all potential damage mechanisms.

Research in FY 1981 should lead to a better understanding of the physical and chemical response of sand and sandstones under simulated STES operating conditions. More information about the causes and magnitude of potential permeability degradation and material compaction will assist in STES aquifer selection, design, and operating criteria and environmental reports.

ACKNOWLEDGEMENT

This work was supported by the Office of Advanced Conservation Technologies, U.S. Department of Energy, under Contract DE-AC06-76RLO 1830.

REFERENCES

1. Potter, J., W. Dibble, and A. Nur. 1980. "The Effect of Temperature and Fluid Composition on the Permeability of Quartz Sandstones." Journal of Petroleum Technology Forum.

2. Erikson, R. L., J. A. Stottlemyre, and R. P. Smith. 1980. "An Experimental Study of the Response of the Galesville Sandstone to Simulated CAES Conditions," PNL-3399, Pacific Northwest Laboratory, Richland, Washington.

3. Barkman, J. H. and D. H. Davidson. 1972. "Measuring Water Quality and Predicting Well Impairment." J. Petrol. Tech. 24(7):865-873.

4. Owen, L. B. 1979. Evaluating Brine Reinjection for DOE's Strategic Petroleum Reserve Program. Resource Applications. Lawrence Livermore Laboratory, Livermore, California.

5. Shannon, D. W. and R. P. Smith. 1980. "Field Evaluation of Sampling Methods for Pressurized Geothermal Liquids, Gases, and Suspended Solids." PNL-3412, Pacific Northwest Laboratory, Richland, Washington.

6. Casse, F. J. 1974. The Effect of Temperature and Confining Pressure on Fluid Flow Properties of Consolidated Rocks. Ph. D. Dissertation, Stanford University.

7. Muhammadu, A. 1976. "The Effects of Temperature and Pressure on Absolute Permeability of Sandstones." Ph. D. Dissertation, Stanford University.

8. Danesh, A. and H. J. Ramey. 1978. "The Effect of Temperature Level on Absolute Permeability of Unconsolidated Silica and Stainless Steel." TRANSACTIONS. Geothermal Resources Council, Vol. 2.

9. Sydansk, R. D. 1980. "Discussion of the Effect of Temperature and Confining Pressure on Single-Phase Flow in Consolidated Rocks." Society of Petroleum Engineers Journal.

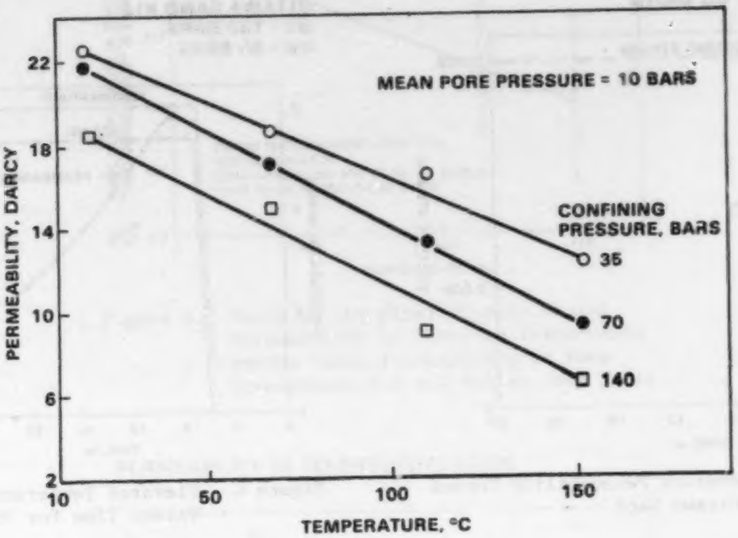

Figure 1. Permeability Versus Temperature for Ottawa Sand(7)

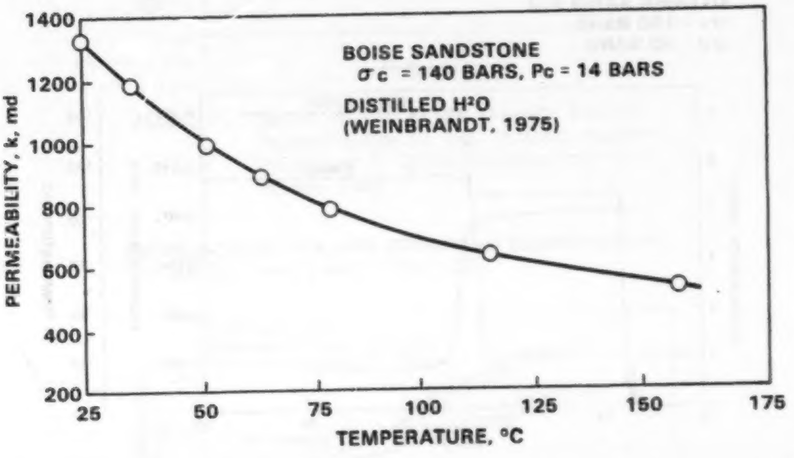

Figure 2. Permeability Versus Temperature for Massillon Sandstone(6)

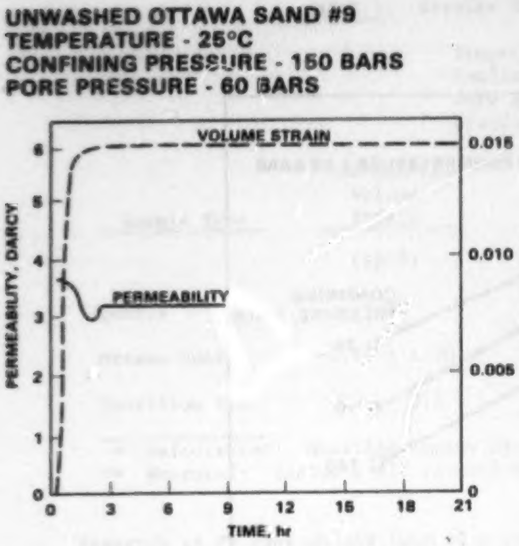

Figure 3. Room Temperature Permeability Versus Time for Ottawa Sand

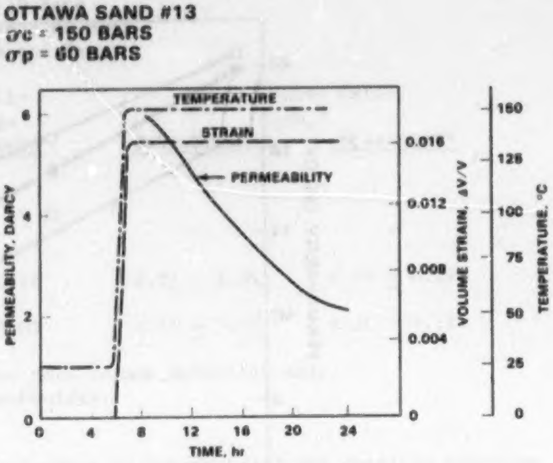

Figure 4. Elevated Temperature Permeability Versus Time for Ottawa Sand

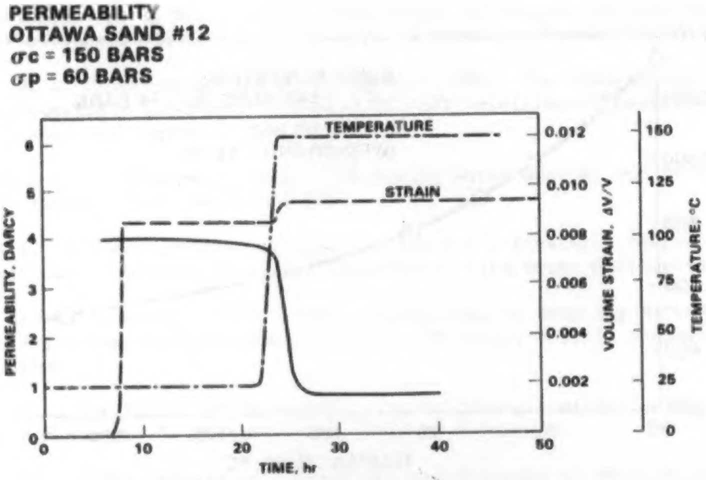

Figure 5. Elevated Temperature Permeability Versus Time for Ottawa Sand

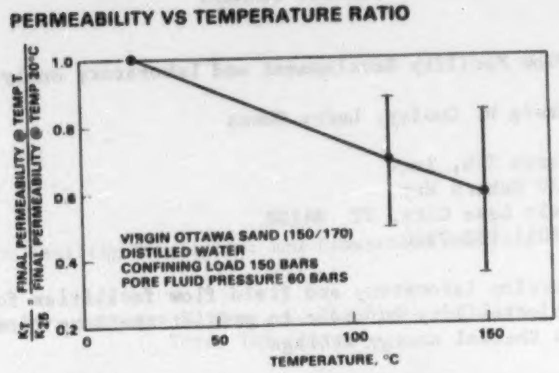

Figure 6. Ratio of the Final (Steady State) Permeability at Elevated Temperature to the Final Permeability at Room Temperature for all Ottawa Sand Tests

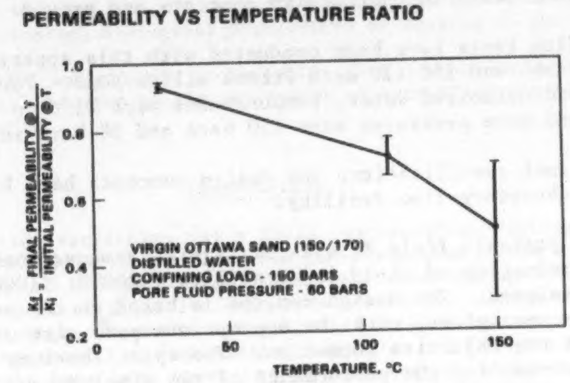

Figure 7. Ratio of the Final (Steady State) Permeability to the Initial Permeability at a Given Temperature for Ottawa Sand

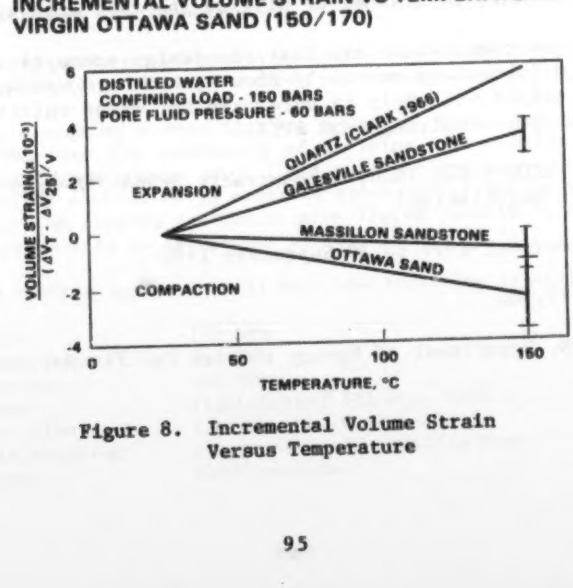

Figure 8. Incremental Volume Strain Versus Temperature

PROJECT SUMMARY

Project Title: Flow Facility Development and Laboratory Analysis

Principal Investigator: Craig H. Cooley, Larry Owens

Organization:
Terra Tek, Inc.
420 Wakara Way
Salt Lake City, UT 84108
(801) 582-2220

Project Goals: Develop laboratory and field flow faciiities for evalaution of water injectability in order to predict the long term response of aquifers to thermal energy storage.

Project Status: This project is on-going. A combined laboratory and field program has been designed. The laboratory flow facility will be built to test core under simulated ATES reservoir conditions. A field flow apparatus will be built to evaluate the injectability of fluids.

Modification of an existing Terra Tek laboratory flow facility was undertaken to test design concepts and provide early data.

Flow tests have been conducted with this apparatus on Massillon sandstone and 150/170 mesh Ottawa silica sand. Pore fluids included brine and deionized water, temperatures were 25°C to 150°C, and confining and pore pressures were 150 bars and 60 bars respectively.

Final specifications and design concepts have been determined for the laboratory flow facility.

A portable field flow facility with semi-automated apparatus for the evaluation of fluid injectability ($\leq$200°C; $\leq$1000 psi) has been designed. The design concept is based on the use of membrane filters or core plugs, with the appropriate pore size distribution, as analogs of the injection formation. The specifications for the test apparatus provide for the performance of two simultaneous tests to permit evaluation of the effects of ATES thermal cycling on injectability.

Standard operating procedures will be developed. HP-67-compatible software will be developed to permit field analysis of test data by the Barkman and Davidson water quality method. Field tests will be performed at one ATES test site and the operation's personnel at that site will be trained to utilize the test apparatus on a routine basis.

Major conclusions are that the design concepts and specifications for the laboratory and field flow systems are valid, and the early data obtained will help in understanding water injectability and production changes resulting from ATES.

Contract Number: DE-AC06-76RLO 1830, Subcontracts B-96462-A-D; B-82282-A-H; 78992 AD (in negotiation)

Contract Period: 1 October 1979 to 30 September 1980

Funding Level: $115,000

Funding Source: U.S. Department of Energy through Pacific Northwest Laboratory

Flow Facility Development and Laboratory Analysis

Craig H. Cooley, Lawrence B. Owen, C. Kim Blair and Gary J. Banik
Terra Tek, Inc.

Abstract

A key element in the assessment of Aquifer Thermal Energy Storage (ATES) processes is the determination of aquifer response to cyclical production and injection of hot water. There is also a need to establish baseline injectability data, in conjunction with pilot demonstration projects, and to determine the impairment potential of factors such as thermal cycling, time-dependent water chemistry changes and the impact of any chemical treatment schedules that may be required to control corrosion, biological degradation or scaling of the ATES system.

Terra Tek, Inc., under subcontract to Battelle, PNL, is developing laboratory and field testing equipment that will be used in the assessment of subsurface storage reservoir response to long-term ATES utilization.

Introduction

Laboratory core testing facilities and a field injectability testing apparatus are being developed for Battelle, PNL by Terra Tek, Inc. for the evaluation of the response of subsurface aquifers to long term thermal energy storage. Aquifer Thermal Energy Storage (ATES) refers to processes which involve cyclical injection and production of hot fluids used in surface direct heating applications. Storage reservoirs are subjected to elevated temperatures which lead to increased in-situ stresses resulting from thermal expansion of the porous medium. Since temperature and stress effects have been shown to severely degrade the permeability of sandstone and unconsolidated sands, there is a need to critically assess these impacts on the feasibility of typical ATES operations. It can also be anticipated, that repeated cycling of process waters may ultimately lead to degradation of process water quality through generation of corrosion-induced particulates, particulates derived from the storage aquifers and, perhaps, formation of precipitates as the chemistry of process water changes in response to hydrothermal alteration effects.

Laboratory Core Testing Facility Development

In order to accurately assess the potential impairment mechanisms that may impact ATES feasibility, it is desirable to perform laboratory core tests at simulated in-situ conditions.

Terra Tek, Inc., is designing a core testing apparatus similar to the apparatus shown in Figure 1 for Battelle, PNL with the capability of exposing core samples to simulated in-situ ATES conditions of stress, temperature, pore fluid pressure and pore fluid chemistry. These parameters must be carefully controlled in order to accurately simulate in-situ permeabilities and core volume strains. The ability to sample pore fluids permits an unambiguous evaluation of the effects of fluid properties on impairment of core permeability.

The laboratory core testing apparatus will have the following capabilities:

Axial stress:	172 MPa
Hydrostatic stress:	103 MPa
Pore pressure:	103 MPa
Pore fluids:	light brine, 10% wtg, NaCl
Pore fluid flow rate:	1 ml/sec to 16 ml/sec
Pore fluid sampling:	via pressurized sampling bomb
Temperature:	200°C maximum

Temperature cycle: 100°C amplitude
Filters: 0.45 μm - before sample
Material: Titanium-for those parts that see 200°C
Measurements: permeability: 100 micro darcy to 10 darcy
volume strain: 30% strain; 0.03% strain resolution

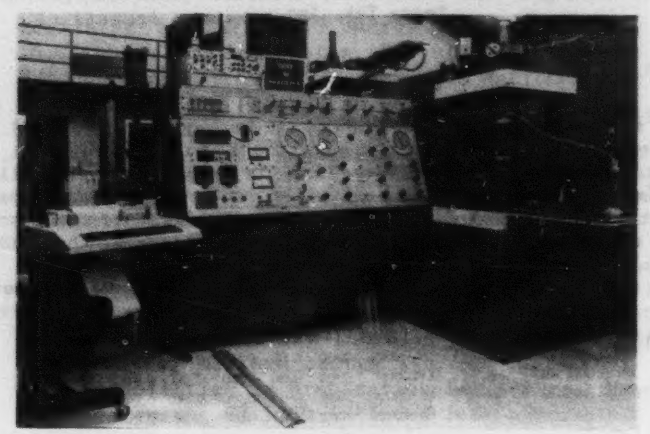

Figure 1. Laboratory Core Testing Facility

Hydrostatic confining pressures to 103 MPa are controlled via a gas backed hydraulic accumulator that will maintain pressure within ±2% of the desired value. Axial stress on 5.40 cm diameter (NX) core to 172 MPa is servo-controlled to within 0.9 MPa. Temperature control to 200°C and temperature cycling of 100°C amplitude is achieved with band heaters and a cooling jacket placed around the triaxial pressure vessel. A microprocessor controls temperature to ±2°C.

Reliable permeability measurements from 10.0 darcies to 100 micro darcies require that clean (filtered to 0.45 μm) pore fluid be flowed through the sample at ATES in-situ pore pressures and pore fluid temperatures. Flow must also be free of large pressure pulses as the differential pressure drop across a 10.0 darcy core (typical permeability value for unconsolidated sands) may be less than 0.01 bars. Figure 2 depicts a simplified schematic of the flow system designed to meet the above criteria. The variable flow rate piston pump in conjunction with the servo-controlled pore pressure provides smooth pore fluid flow. The pore fluid is heated after volume flow rate is measured with a turbine flow meter. Differential pressure across the sample length is measured at the sample end caps to minimize errors due to line pressure drops.

Effluent pore fluid chemistry and suspended particle load determinations will help in understanding the relationship between permeability and water quality changes. A pore fluid sampling bomb immediately after the core permits sampling of pore fluid without disturbing the sample pore pressure. After pore fluid is collected in the sampling bomb, it is allowed to cool to 95°C (to prevent flashing) and then drained into a container for subsequent laboratory analysis.

Anomalously high pore fluid viscosities at elevated temperatures have been propounded as a possible cause of permeability reduction. A hot viscometer directly downstream of the sample will measure pore fluid viscosities at test conditions. Core pore space reduction due to creep compaction will be measured with low drift strain transducers. Volume strain resolution will be approximately ±0.03% strain.

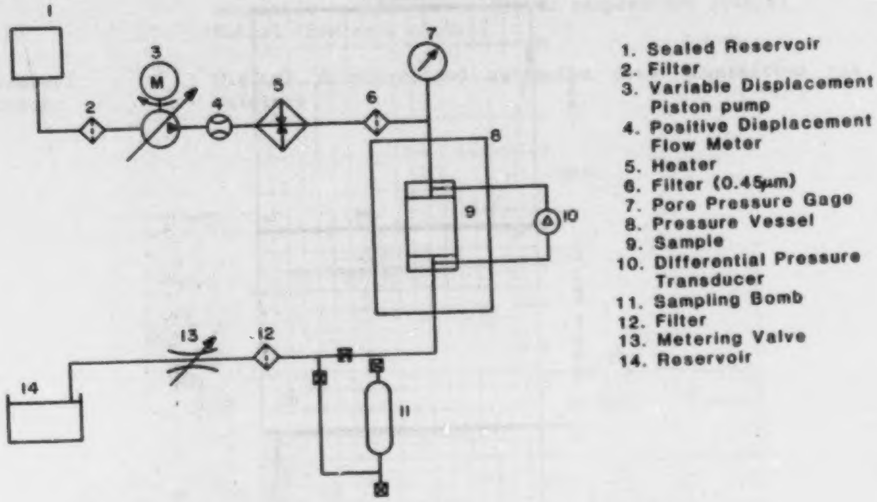
1
3
M
2
4
5
6
7
8
9
10
11
12
13
14
1. Sealed Reservoir
2. Filter
3. Variable Displacement Piston pump
4. Positive Displacement Flow Meter
5. Heater
6. Filter (0.45μm)
7. Pore Pressure Gage
8. Pressure Vessel
9. Sample
10. Differential Pressure Transducer
11. Sampling Bomb
12. Filter
13. Metering Valve
14. Reservoir

Figure 2. Simplified Laboratory Flow System Schematic

Titanium alloys will be used for those parts of the flow loop subjected to 200°C to minimize corrosion. To ensure that the core is not contaminated by extraneous suspended solids, a 0.45 μm silver membrane filter is placed between the heater and the core.

Terra Tek, Inc. modified an existing test system to prove design concepts and provide some preliminary data to the ATES program. The pore fluid flow loop concept was tried and proven amenable to manual control. Flow is smooth enough to measure differential pressures of less than 0.01 bars with pore pressure equal to 80 bars and pore fluid temperatures equal to 150°C. Pore fluid sampling techniques and the appropriate apparatus allowed samples to be taken with pore pressure disturbances of less than 1.0 bar. Low drift strain transducers operated satisfactorily at temperatures to 150°C.

Temperature cycle tests require precise control of heating and cooling functions not attainable with the existing manual Terra Tek system. Verification of the temperature cycling design, therefore, awaits the completion of the automated apparatus.

Experiments have been conducted on Massillon sandstone and 150/170 mesh Ottawa sand. An example of data obtained on Massillon sandstone is given in Figure 3 where permeability, volume strain and temperature are plotted against time. In general, permeability was found to decrease with time and temperature in both materials and sufficient time-dependent strain was observed in some Ottawa sand samples to impact permeability. Understanding the phenomena responsible for these observed permeability changes will help in maintaining satisfactory ATES performance.

Field Injectability Apparatus

The most reliable method of establishing water quality in conjunction with full-scale injection tests is based on the use of membrane filters and cores as analogs of the injection formation. The permeability of a representative core sample or a membrane filter (with the appropriate pore size distribution) to injected water is continuously monitored. Observed permeability variations can then be interpreted in terms of the performance characteristics of a typical injection well. Membrane filtration data resolve the impairment potential of injected water resulting from scale formation or deposition of suspended solids. Core tests provide similar data and are also useful in establishing whether detrimental water-rock interactions are important.

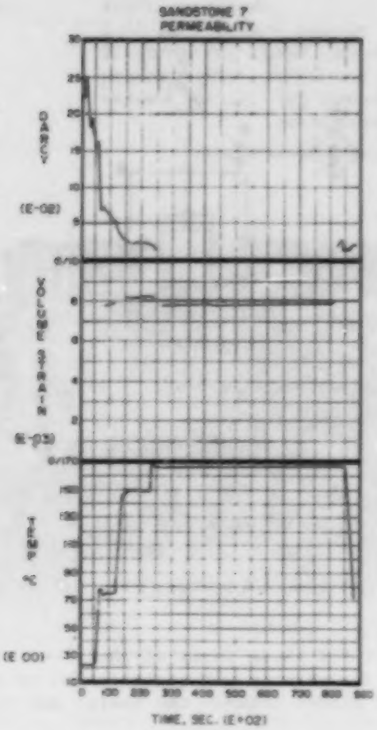

Figure 3. Permeability of Massillon Sandstone to Simulated Brine (7 ppm silica in deionized H_2O)

Terra Tek, Inc. will develop a field test apparatus for evaluating the injectability of ATES waters. The semi-automated apparatus (Figure 4), with provisions for conducting either membrane filtration or core tests, will have the capability of performing two simultaneous tests to permit evaluation of the injectability of waters before and after passage through ATES heaters. A capability for mounting up to three membrane filter holders in series will also be provided to permit determination of the size distribution of suspended solids.

The field injectability apparatus has the following specifications:

Apparatus Capabilities:

A. Simultaneous operation of either two membrane filter test loops or one membrane filter and one core test loop.

B. Particle size determinations using three in-series membrane filters.

Design Pressure: 7 MPa

Design Temperature: 150°C (200°C with inclusion of heat exchangers upstream of flowmeters).

Materials of Construction:

Flowmeter Bodies - 316 Stainless Steel
Pressure Transducer Bodies - 300 Series Stainless Steel
Isolation Valves - Inconel 600
Control Valves - Inconel 600
Fittings - Inconel 600
Tubing - Inconel 600

Control Modes: Automatic valve selection for flow options
Automatic core/membrane filter temperature control
Manual flow rate control

Data Display/ Acquisition: Digital displays and automated data acquisition via thermal printers

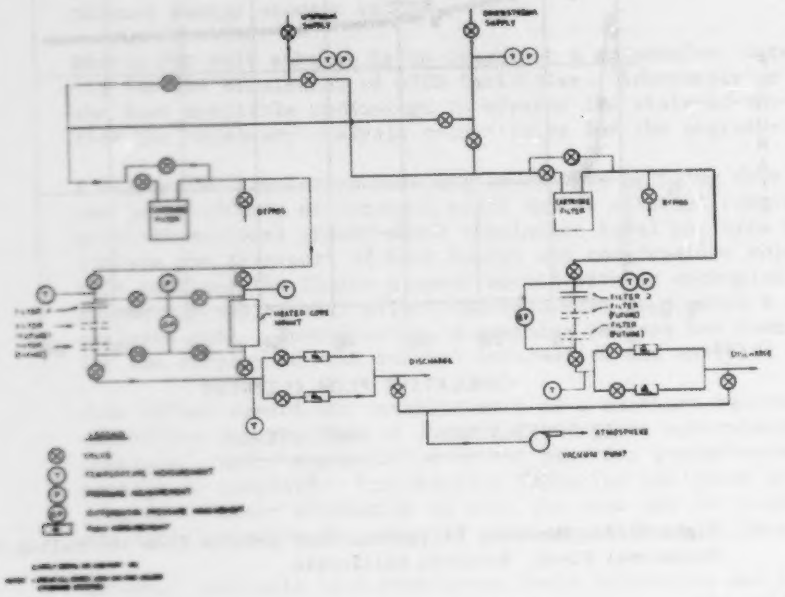
UPSTREAM SUPPLY
DOWNSTREAM SUPPLY
BYPASS
CARTRIDGE FILTER
BYPASS
FILTER 2
FILTER (FUTURE)
FILTER (FUTURE)
HEATED CORE MOUNT
DISCHARGE
DISCHARGE
ATMOSPHERE
VACUUM PUMP
LEGEND
VALVE
TEMPERATURE MEASUREMENT
PRESSURE MEASUREMENT
DIFFERENTIAL PRESSURE MEASUREMENT
FLOW MEASUREMENT

Figure 4. Flow System Schematic of the Field Injectability Apparatus

The injectability test frame is connected, as a bypass system, to the main flowline via a suitable electrically-controlled manifold that permits simultaneous testing of input and output streams from the ATES heat exchangers. Injectability tests are carried out at constant differential pressure. Coarse and fine control valves are used to initially set and maintain differential pressure. Cumulative flow and instantaneous flow rate are obtained via turbine flowmeters and their associated output devices. Thermal printers are used to record all data. The system will also be equipped with a high pressure cartridge filter to permit prefiltration of water prior to passage through the membrane filter or core sample. The latter capability is used to establish the benefit to be derived from pre-injection treatment systems, if the injectability of raw effluent is low.

An auxiliary vacuum system is employed to quickly degas the test system prior to a run in order to eliminate entrained air that might adversely affect permeability measurements. The vacuum system is also used to bleed residual fluid from the system after each run. A temperature controller and clam-shell heating jacket are used to maintain epoxy-mounted core samples at constant temperature. The same temperature controller and heating jacket are also used to maintain membrane filters at constant temperature.

All of the hardware shown in Figure 4 is mounted on a single test frame that includes a small integral bench. A separate instrument rack will be used to house the electronic readout and control devices. The design of the test apparatus will permit locating the equipment in either permanent enclosures (i.e. buildings, large trailers, etc.) or in small trucks or vans.

Figure 5 presents an example of the type of data that can be obtained with a suitably designed injectability apparatus. In this example, hypersaline brine from the Salton Sea geothermal field is shown to be highly injectable following prefiltration whereas the raw brine is not suitable for direct subsurface disposal.

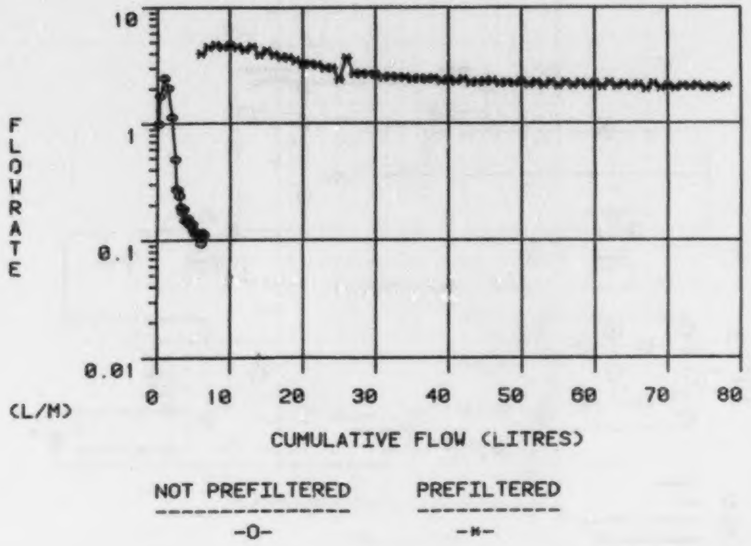

Figure 5. Eight Micron Membrane Filtration Test Results From the Salton Sea Geothermal Field, Southern California.

PROJECT SUMMARY

Project Title: Numerical Simulation

Principal Investigator: Charles T. Kincaid

Organization:
Battelle, Pacific Northwest Laboratory
P.O. Box 999
Richland, Washington 99352
(509) 375-2867 (FTS: 444-7511 ext 2867)

Project Goals: Provide technical support in the form of numerical simulation techniques capable of assessing the performance and impacts of aquifer thermal energy storage (ATES).

Within PNL this subtask is to establish a responsive, internal capability for the simulation of ATES facilities. Externally we are utilizing the best available technology to advance the state-of-the-art and provide the necessary analysis capabilities for the engineering community.

Project Status: A responsive simulation modeling capability is being developed through the joint efforts of internal staff and an external contractor. A multi-dimensional ground-water simulation model has been broadened to include the transport of both energy and conservative solute. The code combines the finite element method with an uncoupled solution scheme. A substantial effort has been made to produce a user oriented analysis tool. Specifically, a graphics package has been developed for the display of both initial information and analysis results.

This effort toward the establishment of a confined aquifer modeling capability for the flow of fluid and energy is approximately 80% complete. Major augmentation to the previous ground-water analysis package is complete. Verification employing published solutions is in progress. Minor alteration to both the code and its graphics package are anticipated in the areas of mesh generation and time step control.

External contracts with Washington State University and Lawrence Berkeley Laboratory compliment this work through the utilization of presently available computing methods. WSU is nearing completion of a version of Intera's DWDM code which will be appropriate for use on restricted word size machines. Several simulation modeling tasks are being conducted by LBL.

Contract Number: DE-AC06-76RLO 1830

Contract Period: Continuing

Funding Level: $65,000, FY-1980, B/O

Funding Source: U.S. Department of Energy, Office of Advanced Conservation Technologies

NUMERICAL SIMULATION OF AQUIFER THERMAL ENERGY STORAGE FACILITIES

Charles T. Kincaid
Pacific Northwest Laboratory
P.O. Box 999
Richland, Washington 99352

ABSTRACT

This paper is a review of progress for that portion of the Seasonal Thermal Energy Storage (STES) Program which involves the numerical simulation of aquifer thermal energy storage (ATES) systems. The Pacific Northwest Laboratory (PNL) has been involved in the modification of an isothermal ground-water code to include energy transport. Washington State University personnel are involved in modification and application of Intera's Deep Well Disposal Model (DWDM).

Means are being sought to quantify the adequacy of mesh and time discretizations for the finite element model of coupled fluid, energy, and solute transport (CFEST). Meshes developed from flow net grids appear to be promising and will be pursued during FY 1981. Both CFEST and Intera's DWDM codes will be applied to the Auburn University experiment(6) during FY 1981.

INTRODUCTION

The STES Program, directed by Battelle's Pacific Northwest Laboratory (PNL) for the Department of Energy (DOE), has the overall objective of developing the necessary technical support for, and demonstrating the feasibility of seasonal thermal energy storage. Currently the most viable application of this concept is to the ground-water or aquifer environment. Fundamental to the eventual acceptance of this technology by industry is not only its economic feasibility, but also the development of knowledge which will allow the engineering community to design facilities and provide users with efficient operational scenarios for controlling the storage and recovery of the energy resource.

Over the 5-year life of the STES Program it is the objective of the numerical simulation subtask to direct the work which will lead to a predictive capability for the engineering community. In the foreseeable future, the objective of this subtask is to evaluate competitive technologies, and provide the STES Program Office with a responsive, independent simulation capability for the purpose of evaluating the design and operational scenarios of proposed aquifer thermal energy storage (ATES) facilities. Toward this end, several computational methodologies have been examined.

During the past decade, research dealing with geothermal resources(5) and deep well disposal(1) has yielded models applicable to situations very similar to those of an ATES facility. The physical and energy phenomena of these models are believed to be the same as those required for ATES, and simulations of the Auburn University experiments directed by Dr. C. F. Tsang have provided encouraging results.

Efforts during the first year of the STES Program have been directed toward (1) providing the STES Program with a responsive simulation capability, (2) applying alternative technologies to experimental problems for evaluation purposes, (3) developing sensitivity and parametric analyses, and 4) initiating the development of a numerical simulation capability for unconfined aquifers. A portion of item (2) and items (3) and (4) are included in external contracts awarded to Lawrence Berkeley Laboratory (LBL). Review of LBL contracts will be provided by Dr. Chin Fu Tsang. The review of item (1) involves a joint effort from PNL staff and Dr. S. K. Gupta. Dr. Gupta is a consultant to PNL for the modification, verification, and application of numerical simulation codes. Due to the intimacy of this work, no effort will be made to distinguish contributions by individuals. An external contract with Washington State University involves the modification and application of Intera's Deep Well Disposal Model (DWDM).(1) Funding during FY 1980 for this subtask, excluding awards to LBL, amounted to one hundred seventy-five thousand dollars ($175K).

PROGRAM DESCRIPTION

The development of a responsive, independent analysis and evaluation capability is being pursued by both PNL staff and a consultant, Dr. S. K. Gupta. CFEST, a model of coupled fluid, energy, and solute transport, is an extension of a multi-dimensional model(4) which was developed for and applied to large natural ground-water systems. Equations for the conservation of energy and solute mass have been included and reduced to an algebraic system via the finite element method. Nonisothermal influences enter the computation through temperature dependent properties including density and viscosity.

This effort toward the establishment of a confined aquifer modeling capability for the flow of fluid and energy is approximately 80% complete. While major modifications to the code are completed, it is expected that minor modification may be necessary prior to achieving a final product. A substantial effort has been made to produce a user oriented analysis tool. Specifically, a graphics package is being developed for the display of both initial information and analysis results.

Alteration of the Intera Deep Well Disposal Model (DWDM) code by Washington State University personnel for its use on restricted word size machines serves two purposes. It allows PNL staff the opportunity to test and become familiar with the code, while producing a product which will be of use to the engineering community, where restricted word length machines are more common. Modifications to this code and its verification utilizing published results(1,2) are near completion.

RESULTS

Verification of the CFEST code has necessitated the development of analytical solutions from the literature. Of particular importance have been those of Avdonin(2) and Gringarten and Sauty.(3) Each has served to define the adequacy of both time step and mesh discretization.

Avdonin presents a one-dimensional solution to the problem of forced convection within a confined aquifer with conductive transport through overburden and underburden. Solutions of temperature as a function of radial or linear distance and time are given. Comparison of numerical and analytical solutions revealed that mesh discretizations of widely varying character yield good results when time step is adequately refined. A definition of adequacy is currently being investigated.

Gringarten and Sauty provide an uncoupled treatment of fluid and energy transport in a vertically uniform aquifer of infinite extent. This two-dimensional, horizontal model of injection/recovery for heat pump application presents an excellent opportunity to test the simulative ability of the CFEST code. Test problems to date have revealed that mesh and time step discretization are not nearly as easily defined for the two-dimensional case. A series of automatically generated meshes have been employed, and it has been determined that the mesh must be altered gradually from a fine radial structure near the wells to a coarse rectangular structure in the far field where a uniform natural gradient dominates.

Two mesh generation schemes are currently being evaluated. The first is an automatic generation package which embeds a gradually varied radial mesh into a rectangular mesh. A second generation scheme employs the flow net of the steady-state approximation to flow as a pattern from which to take the near well mesh discretization. This near field mesh is then embedded in the far field rectangular mesh. Each of these mesh generation schemes is expected to generate acceptable solutions. However, the latter one is particularly attractive since it generates a physically meanful grid and hence would be expected to produce less noticeable numerical dispersion.

CONCLUSIONS AND RECOMMENDATIONS

A multi-dimensional numerical simulation capability has been developed and is in the process of being verified against published solutions. Means of determining the adequacy of mesh refinement and time step size are continuing. The code has been verified for one-dimensional linear and axi-symmetric analysis. Work is continuing on the two-dimensional verification. Completion of verification for this multi-dimensional code, CFEST, is scheduled for the first quarter of FY 1981. Documentation of this code and a companion code, FILTER, employed in the processing of field data for simulation, are currently being prepared for publication during FY 1981.

Following verification and documentation, the CFEST code will be employed in a numerical simulation of the Auburn experiment. This will give PNL personnel experience with an ATES facility simulation and will prepare them for subsequent requests for analysis by the STES Program management (e.g., field test facility and demonstration site analyses). The Intera DWDM code will also be applied to the Auburn experiment. Comparison of CCC, DWDM, and CFEST results should provide valuable insight into the simulative abilities of these competitive methods.

During FY 1981 it is anticipated that some funding will be devoted to geochemical modeling under nonisothermal conditions. This will be the initial effort toward the eventual development of a coupled nonisothermal geochemical, ground-water simulation capability. Other efforts planned for the coming year include the initial phase of long-term, far-field estimates of impact from an ATES facility and the publication of a state-of-the-art paper on: the physical, thermal, and chemical phenomena; their numerical analogues; and the numerical simulation methods available to potential users of ATES technology.

REFERENCES

1. "A Model for Calculating Effects of Liquid Waste Disposal in Deep Saline Aquifer," Intercomp Resource Development and Engineering, Inc., PB-256903, (June 1976).

2. Avdonin, N. A., "Some Formulas for Calculating the Temperature Field of a Formation During Thermal Injection," Neft'i Gaz, Vol. 7, No. 3, pp. 37-41, (1964).

3. Gringarten, A. C. and J. P. Sauty, "A Theoretical Study of Heat Extraction from Aquifers with Uniform Regional Flow," Journal of Geophysical Research, Vol. 80, No. 35, pp. 4956-4962, (December 10, 1975).

4. Gupta, S. K., C. R. Cole and F. W. Bond, "Methodology for Release Consequence Analysis - Part III, Finite-Element Three-Dimensional Ground-Water (FE3DGW) Flow Model," PNL-2939, Pacific Northwest Laboratory, (September 1979).

5. Lippmann, M. J., C. F. Tsang, and P. A. Witherspoon, "Analysis of the Response of Geothermal Reservoirs Under Injection and Production Procedures," Society of Petroleum Engineers, SPE 6537, (April 1977).

6. Molz, F. J., A. D. Parr, and P. F. Andersen, "Experimental Study of the Storage of Thermal Energy in Confined Aquifers," Final Report, Contract: Union Carb 7338, Water Resources Research Institute, Auburn University, (January 1980).

PROJECT SUMMARY

Project Title:	Extension of Isothermal Simulation Code to the Non-isothermal Regime
Principal Investigator:	Sumant K. Gupta
Organization:	George Maddox & Associates W. 601 Mallon Spokane, Washington 99201 (509) 326-7515
Project Goals:	Extend the current ground-water analysis capability of the FE3DGW (finite element three-dimensional ground water) code to include energy and conservative solute transport. Verify the analysis through the use of published solutions to simplified analyses, and hypothetical problems of a more complex nature.
Project Status:	Major modifications to the isothermal code have been completed. Current efforts focus upon the verification of the computational package. Equations for the conservation of mass, energy, and solute mass have been reduced to an algebraic system via the finite element method. The non-isothermal influence is introduced through the density and viscosity terms. A solution is achieved via a sequential, uncoupled methodology. Study of the mass conserving character of this analysis reveals that local conservation may be best used to judge the adequacy of mesh refinement and length of time step. Interactive programs designed for the creation of input files have been developed. Graphics capabilities are utilized to review input as well as display output. Present efforts focus upon verification and the determination of adequate mesh and time step resolution for accurate simulation.
Contract Number:	DE-AC06-76RLO 1830, Consultant Agreement B-29028-A-L
Contract Period:	1 October 1979 through 30 September 1980
Funding Level:	$110,000
Funding Source:	U.S. Department of Energy through Pacific Northwest Laboratory

PROJECT SUMMARY

Project Title: Mathematical Studies in Aquifer Thermal Energy Storage

Principal Investigator: Chin Fu Tsang

Organization: Lawrence Berkeley Laboratory
Berkeley, California 94720
(415) 486-4000 ext. 5782

Project Goals: To perform ATES generic studies, improve modeling techniques, and carry out field-specific planning and simulation studies.

Project Status: Considerable generic studies have been done during this fiscal year to study the dependence of the energy recovery factor and the recovery temperature as a function of aquifer properties, storage period, partial and full penetration, storage volume and temperature. The general conclusion is that with a proper selection of an aquifer and a carefully designed system, a good recovery can be realized. Lumped parameter groups are also identified and evaluated to be used for optimization of the system.

Work has also been initiated to improve our numerical model "CCC" so that it can more effectively handle saturated-unsaturated flow problems. This is expected to be completed during the next fiscal year.

The two-cycle Auburn field experiments (1978-1979) have been successfully simulated with the LBL numerical model "CCC". Observed and calculated recovery factors are within 2% of each other and the production temperatures are reproduced within 2°C. No adjustable parameter was used. One may conclude that a) we understand the physical processes involved in an ATES system at the Auburn field site, thus giving us confidence in dealing with confined aquifers of a similar type, and b) the LBL numerical model "CCC" is a satisfactory code that may be useful for further applications. Further calculations have been performed with this numerical model to help in the design of the next series of experiments by the Auburn University.

Contract Number: DE-AC06-76RLO 1830, Subcontract B-67762-A-Z, W-7405-ENG-48

Contract Period: 1 October 1979 through 30 September 1980

Funding Level: $235,000

Funding Source: U.S. Department of Energy through Pacific Northwest Laboratory

AQUIFER THERMAL ENERGY STORAGE STUDIES AT LBL IN 1980

Chin Fu Tsang
Earth Sciences Division
Lawrence Berkeley Laboratory
University of California
Berkeley, California 94720

ABSTRACT

The paper reviews the Aquifer Thermal Energy Storage (ATES) program at Lawrence Berkeley Laboratory during 1980. The four major lines of work were: (1) To solicit appropriate articles and edit them for a quarterly International ATES Newsletter; (2) to perform ATES generic studies; (3) to carry out field-specific planning and simulation studies; and (4) to improve modeling techniques. These four tasks formed a well-balanced program of work to stimulate interest and information exchange in this field, to provide technical support to field projects, and to develop techniques that may be useful for industrial applications of this concept.

INTRODUCTION

Lawrence Berkeley Laboratory (LBL) began working on seasonal thermal energy storage in aquifers in 1976. Initial studies included comprehensive generic calculations based on a numerical model to calculate the coupled heat and fluid flows in a three-dimensional, complex-geometry aquifer system. Proof-of-concept calculations were made for a number of hypothetical situations, the results of which have been published in a series of papers [for example, 1-3].

In 1978, LBL organized and hosted the First International Workshop on Aquifer Thermal Energy Storage. Active workers from nine countries participated in this workshop and their contributions were published in the workshop proceedings [4]. Since the workshop, a periodic newsletter [5] has kept researchers abreast of the current status of various projects worldwide. Many of these projects are reviewed in two survey papers published in 1979 [6,7].

During fiscal year 1979, major LBL work involved the numerical modeling of the recently completed hot water storage field experiments at Auburn University. A paper was prepared in the current fiscal year and submitted to the Journal of Water Resources Research for publication [8]. A summary version was presented at the Intersociety Energy Conversion Engineering Conference and was included in the conference proceedings [9].

The LBL 1980 ATES project includes four main tasks: (a) to solicit appropriate articles and to edit them for a quarterly International ATES Newsletter; (b) to perform ATES generic studies; (c) to carry out field-specific planning and simulation studies; and (d) to improve modeling techniques. Following is a description of the accomplishments and status of each of these four tasks.

INTERNATIONAL ATES NEWSLETTER

The International ATES quarterly Newsletter is published regularly as scheduled. Much enthusiasm both in the United States and abroad is evident from the many contributions to and requests for this publication. Currently we have a mailing list of over 300 representing researchers, developers, and program managers in 16 countries including China and Japan. Vibrant exchange of information and ideas becomes possible through this Newsletter and we are able to keep in touch with researchers and developers at the forefront of this new technology.

Since the initiation of this newsletter in 1978, a number of methods have evolved that utilize underground containments other than natural aquifers for storage. These include storage in buried pipes, shallow man-made aquifers, rock caverns, and natural or man-made lakes.

The common factor among these methods of aquifer and nonaquifer storage is their application to long-term or seasonal storage. In light of this expanding methodology and at the suggestion of the U. S. Department of Energy and the Pacific Northwest Laboratory, we have formally broadened the scope of the Newsletter to include all types of seasonal thermal energy storage. Reflecting this, beginning with the September 1980 issue, the name of the newsletter has been changed to the Seasonal Thermal Energy Storage (STES) Newsletter.

ATES GENERIC STUDIES

Generic studies during 1980 emphasize the understanding of the energy recovery factor (i.e., the ratio of energy recovered to energy stored) as a function of aquifer properties and storage parameters. The goal is to arrive at optimal choices of aquifer and storage arrangements. Dimensionless parameter groups that will be useful in the planning and design of practical projects are being studied and validated.

So far in our studies we have neglected buoyancy flow. This is the case for low permeability aquifers or for storage of low-temperature water. Hellstrom, Tsang, and Claesson [10] recently studied the problem and from their work a criterion may be used to verify the applicability of this assumption. On the other hand, the results obtained for the functional dependence of the recovery factor may be still true for cases of significant buoyancy flow.

Since many computations have to be made for a study of functional dependence, a simple numerical model [11] is used. Besides assuming no buoyant flow, this model also assumes a steady-state fluid flow field in a laterally infinite, uniform aquifer. The recovery factor is calculated for a series of values of aquifer thickness, storage volume, aquifer and aquitard thermal conductivity, caprock thickness, cycle time period, velocity-dependent dispersion, and the number of cycles. In all cases, equal volumes of fluid are injected and produced. As illustrations, some of the results are shown in Figures 1-4.

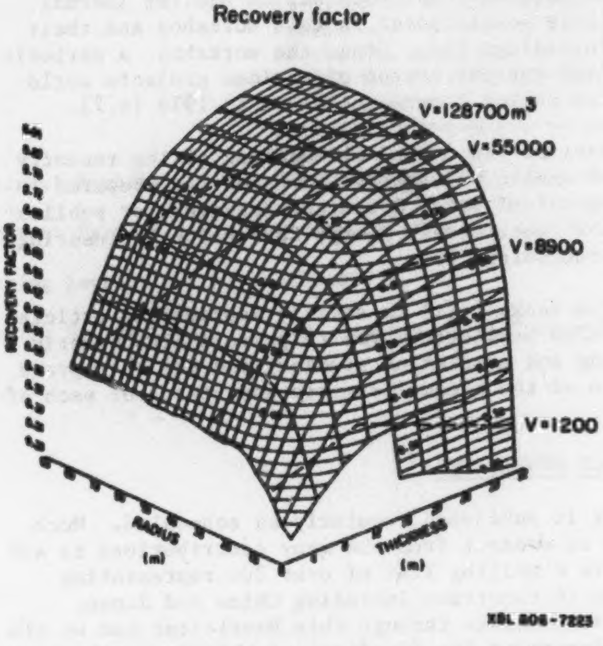

Fig. 1. The recovery factor as a function of aquifer thickness and storage radius The latter is defined as the radius reached by the storage temperature front at the end of injection period.

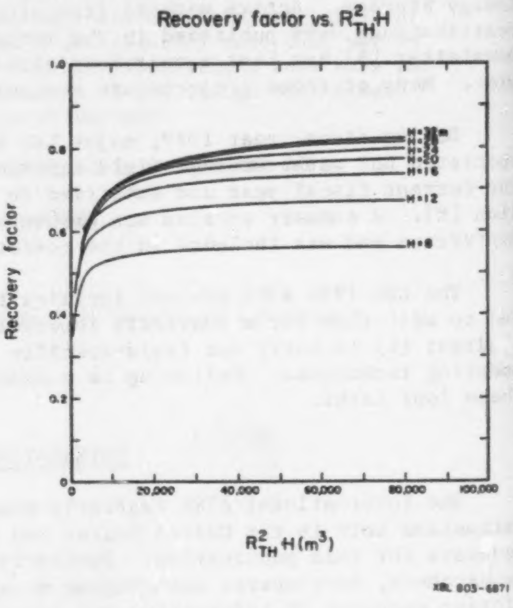

Fig. 2. The recovery factor as a function of storage volume, implicitly given by $R^2_{Th}H$.

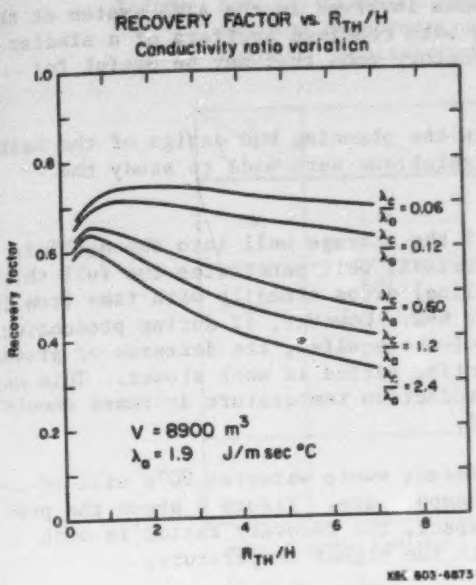

Fig. 3. The recovery factor as a function of aspect ratio, storage radius over aquifer thickness (R_{th}/H).

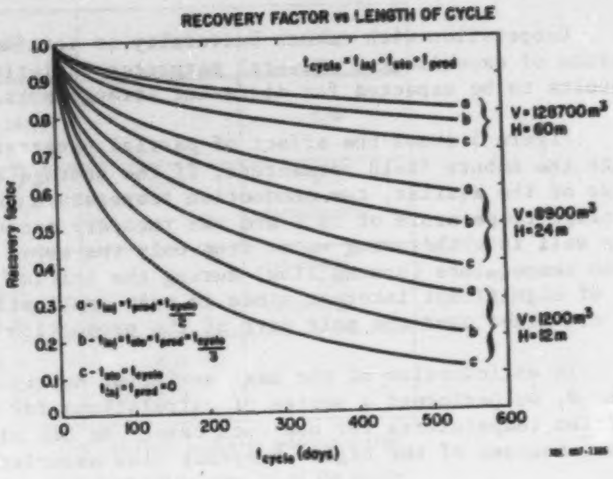

Fig. 4. The recovery factor as a function of cycle time periods, (t_{cycle}).

Figure 1 shows the energy recovery factor as a function of thermal radius, R_{th} and aquifer thickness, H. Each dashed line traces the recovery factor for a given fluid volume. There is an optimal value of R_{th}/H which yields the maximum recovery factor for each volume. Generally, the recovery factor is a much more sensitive function for small values of R_{th} and H than for large values. Figure 2 shows the recovery factor as a function of volume for a series of values of aquifer thickness, H. The recovery factor increases rapidly at first, then levels off. Figure 3 shows the recovery factor as a function of the aspect ratio, R_{th}/H, for a series of aquitard to aquifer thermal conductivity ratios. As this ratio decreases, the aspect ratio which yields the maximum recovery factor increases. Figure 4 shows energy recovery as a function of the time period of a single injection-storage-production cycle for several different injected volumes. The aquifer thickness for each volume is such that the aspect ratio is optimal. Lines "a" show the results for a cycle with no storage period, i.e., production begins as soon as injection ends. In this figure, injection and production periods are equal. We have found that varying the relative injection and production periods for a given storage period has only a minor effect on recovery factor. Lines labeled "b" show the results for a cycle with equal injection, storage, and production periods. Lines labeled "c" show the results for the hypothetical cycle that is all storage period, the hot water being instantly injected and later instantly produced. This represents the limit of very short injection and production periods.

A paper is being prepared (11) describing the detailed results of this work. Systematic graphs of the recovery factor as a function of key dimensionless parameters will be included and their use for practical field applications demonstrated. Plans for further calculations include the incorporation of gravity effects.

FIELD-SPECIFIC PLANNING AND SIMULATION STUDIES

During the early period of this fiscal year, the simulation of the two-cycle Auburn field experiments (1978-1979) with the LBL numerical model "CCC" was completed. Observed and calculated recovery factors are within two percent of each other and the production temperatures are reproduced within two degrees centigrade. No adjustable parameter was used. One may conclude that (a) we understand the physical processes involved in the ATES system at the Auburn field site, thus giving us confidence in dealing with confined aquifers of a similar type, and (b) the LBL numerical model "CCC" is a satisfactory code that may be useful for further applications.

Cooperation with Auburn University is continuing in the planning and design of the next series of experiments. Several parameter variation calculations were made to study the results to be expected for different arrangements.

Figure 5 shows the effect of partial penetration of the storage well into the aquifer. With the Auburn field parameters, if the storage and retrieval well penetrates the full thickness of the aquifer, the production temperature (solid line) drops steadily with time from the storage temperature of 55°C and the recovery factor, ε, is 69%. However, if during production the well is withdrawing water from only the upper half of the aquifer, the decrease of production temperature (broken line) during the initial production period is much slower. This may be of significant interest since in most applications production temperature decrease should be minimized over the main part of the production period.

In anticipation of the next series of Auburn experiments where water at 90°C will be stored, we performed a series of calculations for this temperature. Figure 6 shows the production temperatures for one such case. As one might expect, the recovery factor is much lower because of the higher buoyancy flow associated with the higher temperature.

Table 1 summarizes the recovery factors using the model "CCC" for four storage temperatures and three values of aquifer permeability. In all the cases, storage volume is assumed to be 55,000 m^3, thickness of the aquifer is 21 m, and permeability of the aquitard is 10^{-5} of that of the aquifer. The Auburn experiment corresponds to the 52 md permeability case. This table represents a substantial amount of computation, including different cycle periods and different penetration arrangements. The variations of the recovery factor is clearly seen. Details of these studies are presented and discussed in a paper under preparation [12].

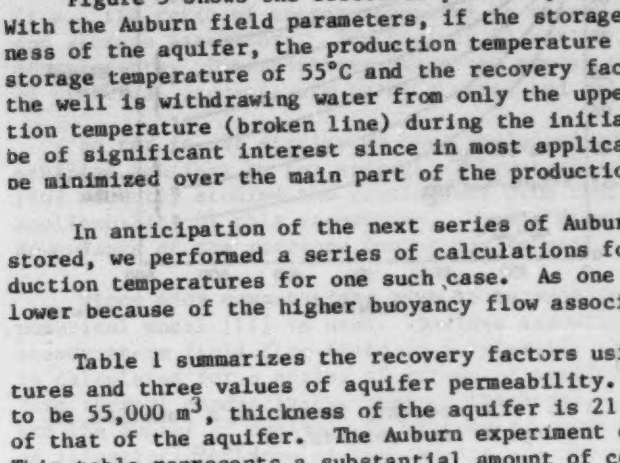

XBL 808-7252

Fig. 5. Production temperature versus time for the storage of 55°C water for two well penetration arrangements (ε is the energy storage-recovery factor).

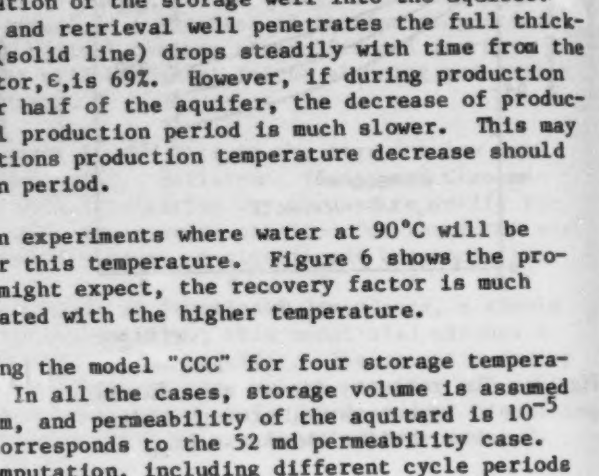

XBL 808-728

Fig. 6. Production temperature versus time for the storage of 90°C water for two well penetration arrangements. (ε is the energy storage-recovery factor).

TABLE. Summary table of energy recovery factors for different storage temperatures and different aquifer permeability values. (calculated with numerical model "CCC").

K_a \ T_{inj}	36^oC	55^oC	70^oC	90^oC
15d	0.69	0.68		0.58
52d	0.67	0.57 (1/2) 0.62	0.46	0.34 (1/2) 0.42 (1/3) 0.44
		(60-60-60) 0.65 (60-120-60) 0.57		(60-60-60) 0.42 (1/2) 0.51
175d		0.31 (1/2) 0.39 (1/3) 0.41	0.24 (1/2) 0.31 (1/3) 0.34	

Unless otherwise indicated:

$(t_{inj}, t_{store}, t_{prod})$ = (90-90-90) days

$T_o = 20^oC$

(1/2) or (1/3) indicates production from the upper 1/2 or upper 1/3 of the aquifer thickness respectively.

NUMERICAL MODEL IMPROVEMENTS

The LBL numerical model "CCC" (conduction-convection-consolidation) used over the years for aquifer thermal storage studies is one of the best validated and most realistic codes available. However it is specialized in the simulation of a water-saturated medium. Another LBL numerical model, TRUST (TRansient flow in Unsaturated and SaTurated porous media) is able to calculate saturated-unsaturated isothermal flows and is based on the same numerical scheme as "CCC". We have initiated work to combine the two codes and develop a numerical model that will simulate nonisothermal flows in unsaturated-saturated media. The resulting improved model will be useful in the study of the unsaturated storage systems that have been receiving much attention from the Europeans. Interest is increasing among U. S. researchers also. A careful modeling study is needed to show the feasibility of such a concept.

CONCLUSIONS

Substantial work has been done in 1980. The major conclusions are:

1. The quarterly Newsletter has proved to be an effective means of information exchange among workers in aquifer energy storage world-wide. We believe it has played a major part in promoting the development of this field both in the U. S. and other parts of the world.

2. A better understanding has resulted from the study of the energy recovery factor for various aquifer properties and storage conditions. We are developing several key parameter groups which may prove to be of great help in experimental design and industrial applications.

3. The success of the Auburn simulations has given us considerable confidence in numerical model "CCC". Further validation against an aquifer storage system of a different type will be useful in verifying the extent of its applicability. This model should be used to plan future experiments and to predict observations. Appropriate arrangements should be made for the industry to learn and use this model.

4. The improvements of the numerical model "CCC" to simulate nonisothermal unsaturated flow will result in a code that may prove to be very useful in the very near future.

ACKNOWLEDGEMENTS

Continued cooperation and assistance from my colleagues, T. Buscheck, C. Doughty, G. Hellstrom, D. Mangold, and J. Wang are much appreciated. Work done under the auspices of the Department of Energy, Division of Energy Storage, through the Pacific Northwest Laboratory.

REFERENCES

1. C. F. Tsang, M. J. Lippmann, and P. A. Witherspoon, Numerical Modeling of Cyclic Storage of Hot Water in Aquifers. Symposium on Use of Aquifer Systems for Cyclic Storage of Water. Fall Annual Meeting of the American Geophysical Union, San Francisco. 1976.

2. C. F. Tsang, M. J. Lippmann, and P. A. Witherspoon. Underground Aquifer Storage of Hot Water from Solar Energy Collectors. Proceedings of International Solar Energy Congress, New Delhi, India, January 16-21, 1978.

3. C. F. Tsang, T. Buscheck, D. Mangold, M. J. Lippmann. Mathematical Modeling of Thermal Energy Storage in Aquifers. Proceedings of Aquifer Thermal Energy Storage Workshop, Lawrence Berkeley Laboratory, Berkeley, California, May 10-12, 1978. LBL-8431.

4. Proceedings of Aquifer Thermal Energy Storage Workshop, Lawrence Berkeley Laboratory, Berkeley, California, May 10-12, 1978. LBL-8431.

5. ATES Newsletter, a quarterly review of aquifer thermal energy storage, Chin Fu Tsang, editor, published by Lawrence Berkeley Laboratory, Berkeley, California 94720.

6. C. F. Tsang. A Review of Current Aquifer Thermal Energy Storage Projects. Invited paper at the International Assembly on Energy Storage, Dubrovnik, Yugoslavia, May 27-June 1, 1979. LBL-9834.

7. C. F. Tsang and D. Hopkins. Aquifer Thermal Energy Storage—a Survey. Invited paper at Symposium on Recent Trends in Hydrogeology, Berkeley, California, February 8-9, 1979, to be published as a Special Paper of the Geological Society of America.

8. C. F. Tsang, T. Buscheck, C. Doughty. Aquifer Thermal Energy Storage—A Numerical Simulation of Auburn University Field Experiments. February 1980. Submitted to Journal of Water Resources Research.

9. C. F. Tsang, F. Molz, and D. Parr. Experimental and Theoretical Studies of Thermal Energy Storage in Aquifers. Proceedings of 15th Intersociety Energy Conversion Engineering Conference, Seattle, Washington, August 18-22, 1980, pp. 1244-1248.

10. G. Hellstrom, C. F. Tsang, and J. Claesson. Heat Storage in Aquifers: Buoyancy Flow and Thermal Stratification Problems. LBL-11059, to be submitted to Journal of Geophysical Research.

11. C. Doughty, G. Hellstrom, J. Claesson, and C. F. Tsang, paper in preparation.

12. T. Buscheck, C. Doughty, and C. F. Tsang, paper in preparation.

PROJECT SUMMARY

Project Title: Study of Coupled Energy and Mass Transport in Geologic Media

Principal Investigator: Stuart Childs

Organization:
Department of Soil Science
Oregon State University
Corvallis, Oregon 97331
(503) 754-2441

Project Goals: Examine the physical principles of energy and mass transport in geologic media, and identify soil and environmental conditions or parameters influencing the efficiency of aquifer thermal energy storage.

Project Status: A literature review on the subject of energy and mass flow through porous media has been completed. An annotated bibliography is being prepared and will contain key references identified in the literature review. A preliminary interpretive report containing information on important parameters involved in energy and mass transport in geologic media will be completed in September 1980.

Contract Number: DE-AC06-76RLO 1830, Subcontract B-97620-A-O

Contract Period: 1 July 1980 through 30 April 1981

Funding Level: $43,660

Funding Source: U.S. Department of Energy through Pacific Northwest Laboratory

PROJECT SUMMARY

Project Title: Hydrologic Studies Support

Principal Investigator: J. W. Crosby III, Vernon Ichimura

Organization:
Washington State University
Geological Engineering
Pullman, Washington 99164
(509) 335-8546

Project Goals: Alter the Intera Deep Well Disposal Model (DWDM) code to make it compatible with IBM computers without losing the accuracy apparent in runs made on CDC computers.

In addition to the basic comparison of old and new codes, an analysis will be made of the Mobile, Alabama test facility's two experiments performed between March 1978 and April 1979. Comparison of computed results will be made with data from the experiments.

Project Status: Of the two stated project goals, the first is nearing completion while the latter is in its infancy.

Truncation errors, resulting from the use of shorter word length processing, have been identified within the mass and energy balance algorithms of the Intera code. Increased precision in selected arrays and calculations have largely alleviated these difficulties. Published solutions have been employed to verify the altered algorithms. A fully double precision version of the Intera code is being developed for further comparisons. Test problems involving relatively large quantities of energy show much improved conservation via the budget algorithms.

A copy of the Auburn data has been received by Mr. Ichimura. He has completed transfer of the data to the WSU computer system. A graphics package has been developed for the expressed purpose of displaying not only the raw data but also the computed predictions of the Intera code. An ability to restart the code from previously stored information (from a preceeding simulation) has been developed. The additional flexibility which this option affords the code will be very useful in the forthcoming analysis of the Mobile, Alabama experiments.

Contract Number: DE-AC06-76RLO 1830, DE-AM06-76RL02221, Task Agreement No. AT06-79RL10119

Contract Period: 26 September 1979 through 31 December 1980

Funding Level: $30,000

Funding Source: U.S. Department of Energy, Richland Operations Office

PROJECT SUMMARY

Project Title: Non-Aquifer Seasonal Thermal Energy Storage Concepts

Principal Investigator: Donald E. Blahnik

Organization:
Pacific Northwest Laboratory
P.O. Box 999
Richland, Washington 99352
(509) 375-2954 (FTS: 444-7411 ext 2954)

Project Goals: Survey, evaluate and select non-aquifer thermal energy storage concepts for seasonal applications. If warranted, recommend further research and development that can lead to demonstration and commercialization of promising concepts.

Project Status: An initial survey, evaluation and selection of potential non-aquifer thermal energy concepts for seasonal use was completed in the first quarter of FY-1980. Results of the work were summarized in a draft report which is in process of being formalized for external distribution.

Literature was obtained and used to establish a non-aquifer STES library. The literature through September 1979 was reviewed and TES concepts were evaluated for their use in seasonal applications. The evaluation was not in depth but it covered the entire gamut of thermal energy storage concepts.

The brief evaluation indicated that sensible heat and cool concepts had the most near term promise because the state-of-the-art is more advanced. In general the best STES concepts appear to be using low temperatures (<95°C), low cost storage media (water and rock), construction with earth, good insulation, and economies of large scale.

In FY-1981 it is planned to update the literature survey and concept evaluations in the first quarter. The survey and evaluation of concepts in the literature will be kept current throughout the year along with the library. The most promising concepts will be evaluated more thoroughly, especially in the areas of cost and heat retention efficiency. A program plan will be established to develop promising concepts. A comprehensive formal report will be issued at the end of the year.

Contract Number: DE-AC06-76RLO 1830

Contract Period: Continuing

Funding Level: $78,000, FY-1980, B/O

Funding Source: U.S. Department of Energy, Office of Advanced Conservation Technologies

blank page

NONAQUIFER SEASONAL THERMAL ENERGY STORAGE

Donald E. Blahnik
Pacific Northwest Laboratory
P.O. Box 999
Richland, Washington 99352

ABSTRACT

An initial survey, evaluation, and selection of potential nonaquifer seasonal thermal energy storage (STES) concepts was completed, and the results were incorporated in a formal report. The preliminary evaluation indicated that sensible heating and cooling concepts had the most near-term promise because the state-of-the-art is the most advanced. In general, the best STES concepts use temperatures less than 95°C, low-cost storage media (water and rock), construction with earth, good insulation, and economies of large scale. The most promising concepts should be more thoroughly evaluated, especially for their cost and thermal effectiveness.

INTRODUCTION

Although the major thrust of the STES program is now in aquifer storage, preliminary investigations have been initiated to evaluate other thermal energy storage (TES) systems that might be proposed for STES. The main purpose of the nonaquifer STES task is to survey, evaluate, and select potential nonaquifer concepts for seasonal use.

A library for nonaquifer concepts has been established. TES literature is being obtained and reviewed to keep abreast of TES development worldwide. TES concepts that show STES potential are evaluated for the degree of technological development, for simplicity, reliability, and economy for likely time of implementation, and for safety considerations.

Concepts that pass the preliminary evaluation should be evaluated more thoroughly for thermodynamic and economic effectiveness before any detailed feasibility studies are made. Detailed feasibility studies should be made before large-scale demonstrations are undertaken.

This task has not proceeded beyond the preliminary evaluation of STES concepts. More thorough evaluation of the most promising concepts is planned for this fiscal year. If warranted, a program for further research and development of STES concepts will be initiated.

DISCUSSION

Most of the preliminary research for this task occurred in the first quarter of FY 1980. Literature was scanned up to September, 1979, to review nonaquifer thermal energy storage methods that might be used on a seasonal basis.

Since the oil embargo in 1973 many studies, laboratory work, and engineering tests have researched TES. Most of the research supported energy conservation and solar energy programs and applies to hourly and daily storage, rather than seasonal storage.

The most developed TES methods are also for hourly and daily storage. The only large-scale applied development for seasonal TES has been in the use of aquifers. Nonaquifer STES applied development has been mostly limited to small-scale solar ponds and earth storage.

For a coarse evaluation this study divided the concepts into sensible, latent, and thermochemical thermal energy storage categroies. Each category was subdivided into containment, storage media, insulation and heat exchanger components for the analysis.

SENSIBLE TES

Sensible TES is the most advanced technology because of its simplicity and relatively low cost. The most developed sensible concepts are used mainly for hourly and daily storage. In Europe, daily storage with off-peak electrically powered MgO, Al_2O_3, and cast iron TES furnaces is a well-developed concept. Hot water tank TES is an old and well-developed method that only applies to daily or weekly storage.

Hourly and daily storage with high-temperature pressurized water (>100°C) is also well-developed, but the high cost of pressure vessels makes longer storage unlikely. This concept is used mainly to supply peaking steam and to heat boiler feedwater.

Daily and weekly storage systems using water and/or rocks are used extensively in solar home heating applications. Earth and wet earth (mud) storage have been used in agriculture and home heating.

Large insulated pond TES with water appears to be one of the most promising methods for STES. Large volumes of low-temperature heat can be stored at a relatively low cost. This would be attractive for district water heating and agricultural uses. Coupled with heat pumps in buildings, this method can be used for both heating and cooling when two ponds are used. This method provides a viable alternative to aquifer TES where aquifer storage is not practical. Ponds can also be covered with solar heat collectors to provide a heat source for the pond.

Wet earth TES, which has promise for home, farm, and other small-scale STES systems, would be studied further.

Other storage concepts that may be used for STES include natural lakes and ponds, solar ponds, mine open pits, caverns, and rock. Abandoned underground mines or natural caverns that can be easily sealed and are not too deep would be good candidates. However, these concepts are very site specific. Lacking a source and use for the heat nearby can be a problem.

The use of large insulated tanks should also be explored because they are the least site specific. The apparently higher cost of tanks may be offset by better storage efficiencies.

LATENT TES

Overall, latent TES is not a well-developed method. It is usually more complex and costly than sensible heat concepts.

Researchers are experimenting with Geauber's salt and paraffin for daily low-temperature TES. Salts and eutectics are being developed for daily TES high-temperature applications such as power generation, boiler feed water preheating, and industrial process heating.

Use of latent heat in seasonal applications will probably be limited to ice cooling of building and refrigeration facilities in the near-term. Compacted winter snow and ice can be harvested and placed in an insulated reservoir for summer cooling of buildings or refrigeration of crops. Sites for use of this concept are limited, however, and and ice harvesting methods and economics must be studied further.

Practically all other latent heat TES concepts will be limited to hourly, daily, and perhaps weekly applications. This is due to the high cost of materials, heat exchangaers, and containment. A hybrid concept of water and encapsulated phase change material may provide a daily fixed-temperature buffer storage for a STES system.

THERMOCHEMICAL TES

Thermochemical TES is even less developed and more complex than latent TES. The development work in this area has been primarily limited to paper studies and laboratory scale tests. The only concept advanced enough to be considered for seasonal use is the sulphuric acid/water heat pump.

Reports disagree about the potential of thermochemical TES for STES applications. Engineering and full-scale tests must be performed to determine the actual potential of thermochemical STES.

COMPARISON OF TECHNOLOGIES

Table 1 shows a rough comparison of the technologies. Sensible TES is currently the most attractive technology for seasonal storage. The only possible exceptions are ice for latent TES and sulphuric acid/water reactions in thermochemical TES. Developments in all three technologies should be continually reviewed and evaluated in case achievements and improvements are made.

RECOMMENDATIONS AND CONCLUSIONS

Based on a quick literature review and preliminary evaluations the currently most promising nonaqufier STES concepts for more detailed evaluation are:

Sensible STES Heating(a)

- Large engineered inslulated-pond TES with < 95°C water

(a) Also cooling with heat pumps.

- Wet earth TES with <95°C water

- Natural lakes and ponds, solar ponds, rocks, and water in mines, caverns and large tanks.

Latent STES Cooling

- Ice and compacted snow TES.

Thermochemical STES Heating and Cooling

- Sulphuric acid/water heat pump at 66-200°C.

These recommended concepts should be considered for use in conjunction with heat pump systems, for use with each other and perhaps for coupling with aquifers.

It is important to make thorough cost, thermal, environmental, and other analyses before initiating large-scale project work on the recommended concepts.

A more in-depth review may reveal that some concepts were overlooked or underevaluated in this broad but shallow review. Research and development may improve other concepts to where they should be considered for STES. Because of the need for large thermal energy inventories and low inventory turnover rates for STES, the principal criterion will be the low-cost of construction, storage media, and operation.

The brief evaluation indicated that sensible heat and cool concepts had the most promise because the state-of-the-art is the most advanced. In general the best STES concepts use low temperatures (<95°C) low-cost storage media (water and rock), construction with earth, good insulation, and economies of large scale.

REFERENCES

1. Blahnik, D.E., 1980. "Preliminary Survey and Evaluation of Nonaquifer Thermal Energy Storage Concepts for Seasonal Storage," PNL-3625, Pacific Northwest Laboratory, October, 1980.

2. Baylin, Frank, 1979. "Low Temperature Thermal Energy Storage: A State-of-the-Art Survey," SERI/RR-54-164, Solar Energy Research Institute, July, 1979.

blank page

Table 1. Generalized Relative Comparison of TES Technologies

Subject of Comparison	Sensible TES	Latent TES	Thermochemical TES
• State of Technology Development	1	2	3
• Simplicity	1	2	3
• Reliability	1	2	3
• Economy	1	?	?
• Near-Term Implementation (<5 yrs)	1	2	3
• Safety and Environmental Considerations	1	2	3
• Potential TES Time Applications			
Hourly Storage	1	2	3
Daily Storage	1	2	3
Weekly Storage	1	3	3
Seasonal or Annual Storage	2	X	3
Multi-Year Storage	X	X	3
• Advantages	1. Most well developed and used TES technology 2. Simplest and most reliable 3. Low cost material and container 4. No phase change to contend with 5. Materials are readily available 6. Simple heat exchangers used	1. Energy stored and recovered at a nearly constant temperature 2. Continued development may verify lower cost and higher performance of PCM for energy storage 3. Smaller volume required if temperature swing is small 4. Usually less site specific than the other technologies 5. Some sensible heat is also stored	1. Permits indefinite storage at ambient temperature with essentially no time-dependent heat losses; has potential for multi-year storage if inventory cost is justified 2. Energy storage density is high (7-15 times sensible heat storage) 3. Energy can be released to meet variable demands 4. Has potentially large internal heat fluxes 5. Stores high temperature heat for the longest time period.
• Disadvantages	1. Energy returned at an ever-decreasing temperature; May require booster heat. 2. Must be well insulated.	1. Technology not well developed 2. Volume increases 5-40% during melting 3. Corrosion uncertainties. 4. Must be well insulated. 5. Material breakdown due to cycling and leaks. 6. Temperature governs material selection.	1. Technology not developed; many technical problems; complex. 2. Safety problems due to to reactions and leaks. 3. Material handling problems. 4. Uncertain reliability and lifetimes. 5. High cost until breakthroughs are made. 6. For the high temperature reactions more sophisticated materials, catalysts, and safety designs are required. 7. High temperature reaction material will also react with water and carbon dioxide. Therefore system must be well sealed.

Ratings:
1 = Predictable, good, or developed
2 = Moderately predictable, fair, or partially developed
3 = Unpredictable, poor, or undeveloped
X = Not feasible

Note: Development advancements can change the ratings. There are two specific exceptions; ice in latent TES and sulfuric acid/water reactions in thermochemical TES.

blank page

COMPRESSED AIR

ENERGY STORAGE PROGRAM

blank page

PROJECT SUMMARY

Program Title: Compressed Air Energy Storage Technology Program

Program Manager: W. V. Loscutoff

Organization: Pacific Northwest Laboratory
Richland, Washington 99352
Telephone: (509) 375-2768

Program Goals: Develop design and stability criteria for long-term operation of underground reservoirs used for CAES in order to accelerate the commercialization of the concept. Develop and assess second-generation technologies for CAES that require little or no supplementary firing by petroleum fuels in order to eliminate the dependence of CAES on these fuels.

Program Status: The reservoir stability criteria studies are progressing satisfactorily. Preliminary stability criteria for the three major types of storage reservoirs have been formulated. Generic numerical studies are complete. Most generic laboratory studies are complete. Field studies project plans have been prepared and studies are scheduled for start-up in FY-1981.

In second-generation technologies, studies have been directed at screening the major advanced technologies: thermal energy storage, fluidized bed combustion, and coal gasification. The screening is scheduled for completion in FY-1981. Decisions on more comprehensive studies and development of one or more advanced concepts are planned for FY-1981. Evaluation of equipment for advanced CAES concepts and study of new CAES concepts are continuing.

Contract Number: DE-AC06-76RLO 1830

Contract Period: FY-1980

Funding Level: $3,160K

Funding Source: U.S. Department of Energy

COMPRESSED AIR ENERGY STORAGE TECHNOLOGY PROGRAM OVERVIEW

W. V. Loscutoff and L. D. Kannberg
Pacific Northwest Laboratory
Richland, Washington 99352

ABSTRACT

Energy storage is a key element in the electric utility industry strategy for shifting energy consumption from oil to coal, nuclear and renewable energy sources. The DOE Compressed Air Energy Storage (CAES) Technology Program is directed at developing a new technology designed to reduce the consumption of oil in the generation of electric power. The program has two major elements: Reservoir Stability Studies and Second-Generation Concepts Studies. The Reservoir Stability Studies are aimed at developing stability criteria for long-term operation of large underground reservoirs used for compressed air storage. The Second-Generation Concepts Studies are aimed at developing new concepts that will require little or no petroleum fuels for operation.

In this overview, we outline the program efforts during FY-1980, identify the major accomplishments and propose future activities that are required to meet the objectives of the program.

INTRODUCTION

Compressed air energy storage (CAES) is a technique for supplying electric power to meet peak load requirements of electric utility systems. It incorporates a modified state-of-the-art gas turbine and an underground reservoir---an aquifer, a salt cavity or a mined hardrock cavern. The compressor and turbine sections of the gas turbine are alternately coupled to a motor/generator. During nighttime and weekend off-peak periods, low-cost power from base load plants using coal or nuclear fuels, would be used to drive motors to compress air which would be stored in the underground cavern. During the subsequent daytime peak-load periods the compressed air would be withdrawn from storage, mixed with fuel, burned and expanded through the turbines to generate peak power. This concept reduces the consumption of premium fuels by more than 60 percent for conventional CAES systems. Some advanced CAES concepts would not require petroleum fuels at all.

Studies have shown that the CAES concept is technically feasible and, for utilities with a proper power generation mix, economically viable. CAES systems offer several advantages over conventional systems used by utilities for meeting peak load requirements. Replacement of current gas turbines by CAES plants could result in annual savings of more than 100,000,000 barrels of oil. The net annual oil saving would be greater in the future with CAES plants that do not require petroleum fuels for operation. CAES plants are not limited to the same degree of siting difficulties faced by conventional pumped hydro plants. Finally, a well designed CAES plant should have a smaller adverse impact on the environment than either a conventional peaking plant or a pumped hydroelectric storage facility.

In view of the potential benefits that the concept offers, the Department of Energy (DOE) has undertaken a comprehensive program in order to accelerate commercialization of the technology. The Pacific Northwest Laboratory (PNL) was selected by DOE as the lead laboratory for the CAES Technology Program. As such, PNL is responsible for assisting the DOE in program responsibilities for planning, budgeting, contracting, managing, reporting and disseminating information. Under subcontract to PNL are a number of companies, universities and consultants that are responsible for various research tasks within the program. This report presents an overview of the CAES program activities by PNL and its subcontractors during FY-1980.

PROGRAM OBJECTIVES

The CAES Technology Program has evolved into two basic research and development elements and a supporting effort on environmental concerns. Recognizing that long term reservoir stability is a key issue to successful commercialization of CAES technology, the Reservoir Stability Studies element has had the major emphasis in the early phases of the program, and will have during FY-1981. Recognizing also that the petroleum fuel requirements of conventional CAES systems may be an obstacle to large scale acceptance of the concept, the Second-Generation Concepts Studies element has been established and will dominate the research and development activity during the latter phases of the program.

The objectives of the program are as follows:

- Reservoir Stability Studies - Establish stability criteria for large underground air reservoirs (in salt domes, hard rock, and porous rock formations) that may be used for air storage in utility applications.
- Second-Generation Concepts Studies - Develop advanced CAES technologies that would eliminate the dependence of CAES systems on petroleum fuels.

PROGRAM STRUCTURE

The structure of the CAES Technology Program represents continuation of tasks initiated during FY-1977, FY-1978 and FY-1979. It also includes several major new items initiated during FY-1980. The latter includes activities in field studies and screening studies of second-generation concepts.

In the Reservoir Stability Studies, four phases of activity for each of the three major types of storage reservoirs (aquifers, salt cavities, and hard rock caverns) have been either completed or are in effect. These phases are as follows:

- Phase 1 - State-of-the-art surveys (Preliminary stability criteria)
- Phase 2 - Numerical studies (Interim stability criteria)
- Phase 3 - Laboratory studies (Interim stability criteria)
- Phase 4 - Field studies (Final stability criteria)

This approach was dictated by the need to make optimal use of knowledge available from related disciplines and to provide the technical information to the DOE/EPRI Demonstration Program in a rapid manner. Phase 1 has been completed in FY-1979. Phases 2 and 3 are planned for completion during FY-1981. Phase 4 activities for aquifer reservoirs were initiated during FY-1980.

In the Second-Generation Concepts studies, three concepts have been or are in the process of being evaluated:

- CAES/FBC - Coal-fired fluidized bed combustion integrated with CAES
- CAES/TES - Thermal energy storage integrated with CAES
- CAES/CG - Coal gasifiers integrated with CAES

The feasibility of the three concepts are being compared with conventional CAES plants and with other types of energy storage for electric utilities in a comprehensive screening study. In addition, there is a task within the program to evaluate component and system requirements for second-generation CAES concepts. This task will identify any equipment development that may be required to promote the feasible advanced CAES concepts to demonstration.

The CAES Technology Program is also committed to identifying the impacts that this new technology may have on the environment. A program element on environmental concerns is an integral part of the overall program. However, it is funded by the Division of Environmental Control Technologies and, therefore, will not be covered in this report.

A work structure outline for the CAES Technology Program is shown in Figure 1.

FUNCTIONAL ORGANIZATION

The Pacific Northwest Laboratory (PNL) leads this program and is performing the required program management, planning and research support in the area of porous rock studies. Under subcontract to PNL, in Reservoir Stability Studies, Re/Spec provides support in the numerical and experimental studies of the behavior of hard rock caverns; Louisiana State University (LSU) supplies experimental support in the study of the behavior of salt cavities; Serata Geomechanics supplies numerical support in the study of the behavior of salt cavities; Terra Tek and Los Alamos Scientific Laboratory are supporting studies of porous rock reservoirs; Rowe and Associates have been developing a numerical model to study the "Champagne Effect". Major support in the Second-Generation Concepts Studies is provided by two subcontractors. The United Technologies Research Center is responsible for evaluating the feasibility of integrating coal-fired fluidized bed combustors with CAES and Acres American Incorporated is establishing the feasibility of integrating thermal energy storage with CAES. The program organization is shown in Figure 2. Major accomplishments reached by PNL and its subcontractors during FY-1980 are described in the next section.

PROGRAM ACCOMPLISHMENTS

The accomplishments of FY-1980 were highlighted by the initiation of the porous rock field studies, completion of the generic numerical studies and completion of several studies on selected advanced CAES concepts. There were also several setbacks in the program. Field studies using salt cavities and an experimental thermal energy storage test facility had to be postponed indefinitely because of budget limitations. In general, the progress within the program was consistent with the long-term planning.

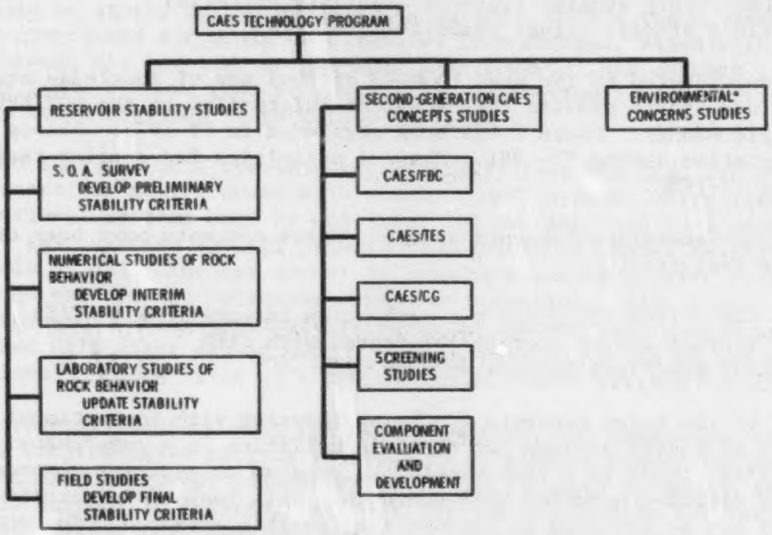
CAES TECHNOLOGY PROGRAM
RESERVOIR STABILITY STUDIES
SECOND-GENERATION CAES CONCEPTS STUDIES
ENVIRONMENTAL* CONCERNS STUDIES
S.O.A. SURVEY DEVELOP PRELIMINARY STABILITY CRITERIA
NUMERICAL STUDIES OF ROCK BEHAVIOR DEVELOP INTERIM STABILITY CRITERIA
LABORATORY STUDIES OF ROCK BEHAVIOR UPDATE STABILITY CRITERIA
FIELD STUDIES DEVELOP FINAL STABILITY CRITERIA
CAES/FBC
CAES/TES
CAES/CG
SCREENING STUDIES
COMPONENT EVALUATION AND DEVELOPMENT

*FUNDED BY THE DIVISION OF ENVIRONMENTAL CONTROL TECHNOLOGIES

Fig. 1. Compressed Air Energy Storage Technology Program Outline

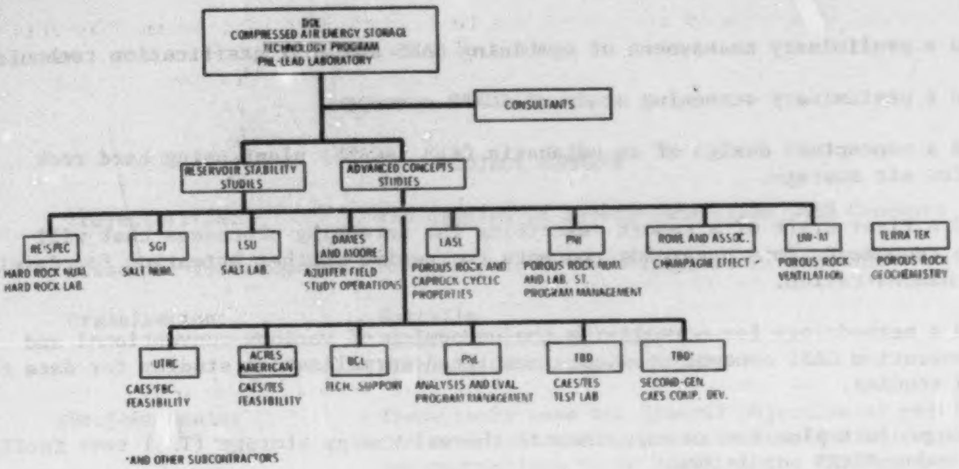
DOE
COMPRESSED AIR ENERGY STORAGE
TECHNOLOGY PROGRAM
PNL-LEAD LABORATORY
CONSULTANTS
RESERVOIR STABILITY STUDIES
ADVANCED CONCEPTS STUDIES
RE/SPEC
HARD ROCK NUM.
HARD ROCK LAB
SGI
SALT NUM.
LSU
SALT LAB.
DAMES AND MOORE
AQUIFER FIELD STUDY OPERATIONS
LASL
POROUS ROCK AND CAPROCK CYCLIC PROPERTIES
PNL
POROUS ROCK NUM. AND LAB. ST.
PROGRAM MANAGEMENT
ROWE AND ASSOC.
CHAMPAGNE EFFECT
UM-M
POROUS ROCK VENTILATION
TERRA TEK
POROUS ROCK GEOCHEMISTRY
UTRC
CAES/FBC FEASIBILITY
ACRES AMERICAN
CAES/TES FEASIBILITY
BCL
TECH. SUPPORT
PNL
ANALYSIS AND EVAL.
PROGRAM MANAGEMENT
TBD
CAES/TES TEST LAB
TBD*
SECOND-GEN. CAES COMP. DEV.
*AND OTHER SUBCONTRACTORS

Fig. 2. CAES Technology Program Functional Organization

RESERVOIR STABILITY STUDIES

During FY-1980, efforts concentrated on completion of numerical modeling studies, continuation of laboratory studies and initiation of field studies through site exploration and confirmation. Accomplishments during FY-1980 include the following:

- Completed all generic structural and fluid flow numerical studies of porous media, hard rock and salt reservoirs.
- Expanded in-mine CAES tests for salt in Louisiana and completed substantial cyclic thermal and mechanical laboratory testing of salt.
- Completed all generic laboratory studies of hard rock subject to CAES cyclic mechanical, thermal and chemical loading.
- Completed supporting laboratory studies of structural behavior for porous rock response to cyclic ventilation and geochemical alteration and response.
- Identified, leased, explored and confirmed a site near Pittsfield, IL, for the aquifer field studies.
- Released a RFP and reviewed proposals for construction and operation of the aquifer field test.
- Completed construction of the porous media flow facility to test and evaluate the affects of combined mechanical, thermal, and chemical conditions associated with CAES operation.
- Completed site evaluation for CAES field studies in salt and porous rock reservoirs.

SECOND-GENERATION CONCEPTS STUDIES

The major milestones, accomplishments and activities in the Second-Generation Concepts Studies during FY-1980 were as follows:

- Completed a conceptual design and cost estimate for a CAES/FBC plant.

- Performed a preliminary assessment of combining CAES and coal gasification technologies.
- Completed a preliminary screening study of ACAES concepts.
- Completed a conceptual design of an adiabatic CAES (ACAES) plant using hard rock caverns for air storage.
- Completed a first draft of a report describing the screening processes that will result in recommendations regarding concepts to receive further attention for development and demonstration.
- Developed a methodology for normalizing the economics of various conventional and second-generation CAES concept studies; completed normalization studies for data from completed studies.
- Prepared a project plan for an experimental thermal energy storage (TES) test facility operated under ACAES conditions.

More detailed descriptions of the activities and accomplishments are given in the papers presented on the specific task in the CAES program.

REPORTS PUBLISHED DURING FY-1980

Incremental Cost Analysis of Advanced Concept CAES Systems, C. A. Knutsen, Knutsen Research Services, Bothell, WA, PNL-3118, September 1979.

Numerical Analysis of Temperature and Flow Effects in a Dry, Two-Dimensional, Porous-Media Reservoir Used fof Compressed Air Energy Storage, L. E. Wiles, PNL-3047, October 1979.

Potential Petrophysical and Chemical Property Alterations in a Compressed Air Energy Storage Porous Rock Reservoir, J. A. Stottlemyre, R. L. Erikson and R. P. Smith, PNL-2974, October 1979.

The Economics of Compressed Air Energy Storage Employing Thermal Energy Storage, S. C. Schulte and R. W. Reilly, PNL-3191, November 1979.

Structural Analysis of Porous Rock Reservoirs Subjected to Conditions of Compressed Air Energy Storage, J. R. Friley, PNL-3231, January 1980.

Compressed Air Energy Storage Technology Program Annual Report for 1979, W. V. Loscutoff, Staff Members and Subcontractors of Pacific Northwest Laboratory, PNL-3395, June 1980.

Porous Media Experience Applicable to Field Evaluation for Compressed Air Energy Storage, R. D. Allen and P. J. Gutknecht, PNL-3294, June 1980.

An Experimental Study of the Response of the Galesville Sandstone to Simulated CAES Conditions, R. L. Erikson, J. A. Stottlemyre and R. P. Smith, PNL-3399, July 1980.

PROJECT SUMMARY

Project Title: PNL Studies of Second-Generation CAES Concepts

Principal Investigator: M. K. Drost, R. W. Reilly, F. R. Zaloudek

Organization:
Battelle
Pacific Northwest Laboratory
Richland, Washington 99352

Project Goals: These tasks have the general objective of providing the technical and economic information to support recommendations to DOE/STOR on the development of advanced CAES plants.

Project Status: This summary covers the three major tasks performed at PNL.

Feasibility of CAES/CG - An assessment was made of the technical and economic viability of a CAES plant based on a cycling gasifier in an utility peaking application. The results indicated that this CAES concept may not be as technically and economically viable as other concepts under consideration in this program.

Advanced Concepts Technical Analysis and Support - Preliminary technical and economic assessments were completed for several candidate CAES concepts including 1) a combined CAES and steam plant, 2) ACAES using an aquifer for the combined storage of heat and compressed air and 3) an integrated CAES/solar plant.

Comparative Economics of Advanced Concepts - A methodology was developed to place the various CAES and advanced concepts CAES studies on the same economic bases to allow direct comparisons of capital and power costs. This methodology was applied to data from engineering and economic studies already completed and preliminary comparisons made. The study will be completed in FY-1981.

Contract Number: DE-AC06-76RLO 1830

Contract Period: October 1979 through September 1980

Funding Level: $83K

Funding Source: U.S. Department of Energy

PNL SECOND-GENERATION CONCEPTS STUDIES

M. K. Drost, R. W. Reilly, J. K. Young and F. R. Zaloudek
Pacific Northwest Laboratory
PO Box 999
Richland, Washington 99352

ABSTRACT

Levelized power costs were estimated for three CAES concepts that do not require petroleum-derived fuels for operation. These concepts include: 1) adiabatic CAES (ACAES) with aquifer air and heat storage, 2) direct coupled steam (DCS)/CAES and 3) solar/CAES utilizing a high temperature central receiver. The results indicated that both the ACAES/aquifer and DCS/CAES concepts may be economically competitive with the ACAES/hard rock concept presently being studied by Acres American, Inc. (AAI). They both show substantial economic advantages over a present technology cycling coal-fired steam plant. The solar/CAES plant was found to have significantly lower power costs than a large central receiver, Rankine cycle solar power station. It also shows surprising competitiveness with the other advanced concepts CAES systems considered in this paper.

INTRODUCTION

This paper summarizes several preliminary technical and economic evaluations performed as part of FY-1980 CAES Program, Task SG-6, "Technical Analysis and Support". These evaluations were undertaken to determine if specific proposed concepts warranted sufficient merit to justify additional engineering and economic attention. The results have and will be used to formulate recommendations to DOE on future program directions. The concepts considered included:

- Adiabatic CAES (ACAES) with aquifer heat and air storage
- Direct coupled steam (DCS)/CAES cycle
- Solar/CAES

CONCEPT DESCRIPTIONS

ACAES/AQUIFER CONCEPT

In this concept, a geological aquifer is used to store both compressed air and a portion of the heat of compression. Since it is probable that temperatures in aquifer structures will have to be limited to 290°C or less, only a limited amount of heat can be stored in the aquifer. To store and effectively utilize all of the heat developed during compression, auxiliary thermal energy storage provisions must be included in the system. Six different cycle arrangements were considered. One of the three more promising systems is illustrated in Figure 1. In this system, a regenerative air heater stores the heat of compression from the low pressure (LP) compressor during the charging cycle; the heat of compression from the high pressure (HP) compressor is stored in the aquifer. A trim aftercooler is used to limit the temperature of the air entering the aquifer. During the recovery cycle, the hot air from the aquifer is expanded in the HP turbine and reheated in the regenerative air heater before final expansion in the LP turbine.

Two types of regenerative air heaters were considered, direct and indirect contact types. The direct contact type consists of an above ground vessel filled with a thermal storage media such as small pebbles or spheres of other dense media such as white cast iron. During charging, hot air is blown through the media; during discharge, cool air is blown through the hot media and is heated. The indirect type consists of a molten salt which is stored in an unpressurized tank. This tank is arranged to form a thermocline to separate the hot and cold molten salts. The heat is transferred between the air and molten salt by means of heat exchangers. This is a sensible heat storage device and no phase change occurs during operation. Preliminary cost comparisons indicated that this direct type to be less costly than indirect types. Therefore, subsequent considerations were limited to only direct air heaters.

DCS/CAES CYCLE

In FY-1979, several direct coupled steam/CAES cycle plant designs were briefly studied.(1) The results indicated that this concept may have some promise. One cycle arrangement, shown in Figure 2, was singled out for a more detailed consideration during FY-1980. In this cycle arrangement, a coal-fired steam generator provides steam to a turbine which drives the CAES compressor. It also directly heats a molten salt stored in an unpressurized vessel. During discharge, the energy in the molten salt is used to heat the compressed air being withdrawn from storage.

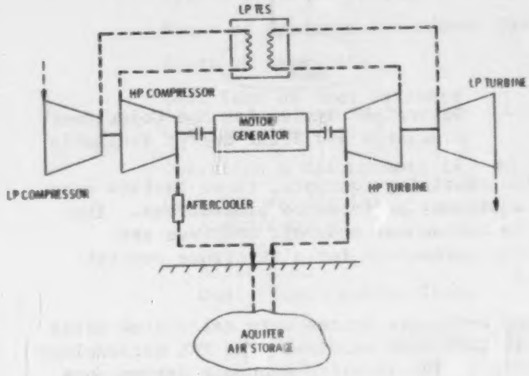

Fig. 1. ACAES/Aquifer Cycle Arrangement

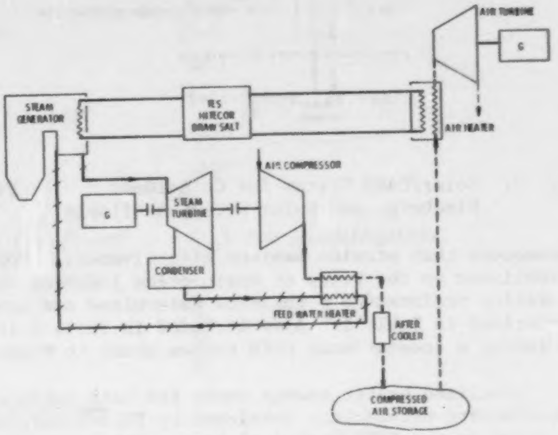

Fig. 2. DCS/CAES Cycle Arrangement

SOLAR/CAES

Earlier studies have shown that solar-assisted CAES is not competitive with conventional or adiabatic CAES. However, when compared to other solar energy conversion schemes, this concept may represent a very efficient and economic use of the solar resource. To further explore this possibility, a very preliminary evaluation of this concept was undertaken. Two cycle arrangements were considered. The first, shown in Figure 3 is applicable to situations where the energy withdrawal period corresponds to the availability of solar energy. The second, in Figure 4, is applicable when solar availability is non-coincident with withdrawal. Both cycles are essentially ACAES types utilizing a high temperature central receiver to enhance the operation of the regenerative air heaters. In the absence of solar insolation, either cycle will function as a conventional ACAES plant at somewhat reduced efficiency.

METHOD OF ANALYSIS

The extent of the analytic development of the concepts varied somewhat because of the different intended use of the results of each analysis. In the ACAES/aquifer analysis, parametric studies were performed using the CYCLOPS code to identify cycle arrangements and operating

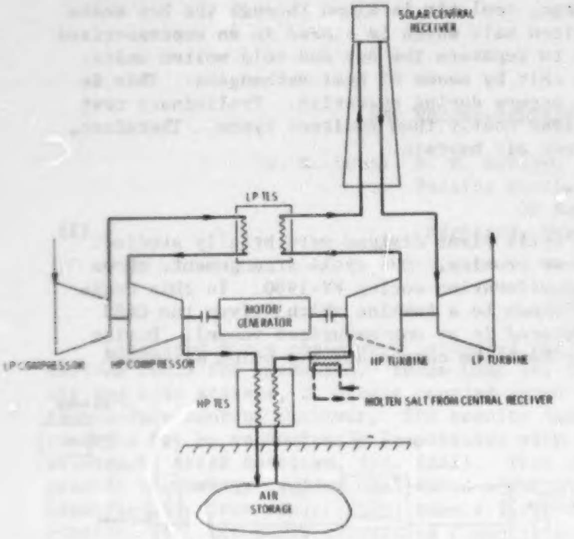
SOLAR CENTRAL RECEIVER
LP TES
LP COMPRESSOR
HP COMPRESSOR
MOTOR/ GENERATOR
HP TURBINE
LP TURBINE
HP TES
MOLTEN SALT FROM CENTRAL RECEIVER
AIR STORAGE

Fig. 3. Solar/CAES System for Coincident Discharge and Solar Energy Available

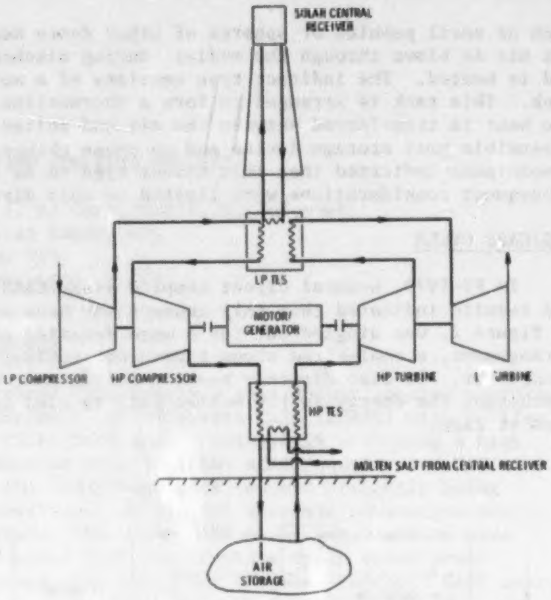
SOLAR CENTRAL RECEIVER
LP TES
LP COMPRESSOR
HP COMPRESSOR
MOTOR/ GENERATOR
HP TURBINE
LP TURBINE
HP TES
MOLTEN SALT FROM CENTRAL RECEIVER
AIR STORAGE

Fig. 4. Solar/CAES System for Non-Coincident Discharge and Solar Energy Available

parameters that provide maximum effectiveness. For the remaining concepts, these factors were established on the basis of engineering judgment and equipment performance limitations. The operating performance parameters determined and used in subsequent economic analyses are summarized in Table 1. Also included in Table 1 are the parameters for a reference concept including a conventional CAES system shown in Figure 5.

Levelized busbar energy costs for each subject and reference system were calculated using the standard methodology developed by PNL$^{(2)}$ for use in CAES cost studies. The PNL methodology is based on the EPRI Technical Assessment Guide$^{(3)}$ (1976). The specific economic assumptions are summarized in Table 2. Capital costs of major plant components, air storage system balance of plant, engineering and related costs for the ACAES/aquifer concept were derived from Reference (4). The costs for the high temperature solar receiver and associated equipment were obtained from reference (5).

TABLE 1. PERFORMANCE PARAMETER

	ACAES/Aquifer	DCS/CAES	Solar/CAES	Conv. CAES
Overall Pressure Ratio	46	68	46	46
Heat Rate (Btu/kWhr)	14,500	11,900	11,400	11,300
LP Compressor Exit Temp. (°C)	405	65	450	65
HP Compressor Exit Temp. (°C)	290	65	450	65
Air Storage Temp. (°C)	290	65	65	65
HP Turbine Inlet Temp. (°C)	290	550	550	550
LP Turbine Inlet Temp.	390	550	900	1,010

TABLE 2. ECONOMIC AND RELATED ASSUMPTIONS

Fixed Charge Rate (%/Year)	18
Discount Rate (%/Year)	10
Inflation Rate (%/Year)	6
Escalation Rates	
Petroleum Fuels (%/Year)	8
Coal (%/Year)	7
Baseload Electricity (%/Year)	7
Capital Equipment/Const. (%/Year)	6
Operations/Maintenance (%/Year)	6
Energy Prices	
Distillate #2 ($/$10^6$ Btu)	5.24
Residual Oil ($/$10^6$ Btu)	4.33
Coal ($/$10^6$ Btu)	1.34
Baseload Electricity (mill/kWhr)	11.4
System Lifetime (Years)	30
Shape of Construction Payout Curve	Bell-Shape, Rt. Skew
Start of Operation	1990
Base Year of Cost Estimate	1980
Construction Period	5
Operation & Maintenance (% Capital Cost/Year)	2 (1 for ACAES/Aquifer)
Capacity Factor (%)	
ACAES/Aquifer	25
DCS/CAES	30
Solar CAES	30
Coal-Fired Cycling Steam	30

RESULTS AND CONCLUSIONS

The calculated levelized busbar costs for the three concepts considered in this report are summarized in Figure 6. Also shown in Figure 6 are several alternate intermediate load concepts which are included for reference purposes. The sources of the economic data for these reference concepts are indicated in Figure 6. These data have been manipulated to place them on the same economic bases as previously described.

It should be noted that the concepts considered were analyzed in somewhat differing detail and some of the plant and economic factors used in the analyses may have differed slightly. Therefore, the results should not be used to define future power costs. Instead, they should be used on the comparitive bases as indicators of potential economic competitiveness.

From examination of Figure 6, it can be seen that both ACAES/aquifer and DCS/ACAES concepts show definite prospects of economic advantage over present technology cycling coal plants and conventional CAES. They will probably also be competitive with the ACAES/hard rock concept being pursued by Acres American, Inc. (AAI). The original intent of the cost study of the solar/CAES concept was to compare it with a solar central receiver, Rankine cycle power station. Figure 6 indicates that Solar/CAES does show a substantial power cost advantage over the solar plant as anticipated. However, its apparent competitiveness with the ACAES/aquifer, DCS/CAES and ACAES/hard rock concepts was somewhat surprising. Because of the preliminary nature of the Solar/CAES evaluation, this comparison must be considered as tentative. Final conclusion regarding its competitiveness must await a more detailed analysis planned for FY-1981.

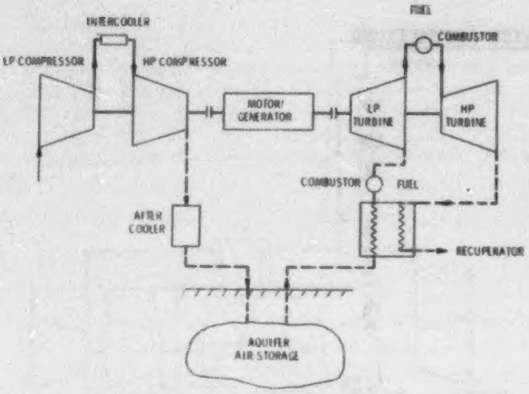

Fig. 5. Conventional CAES Reference System

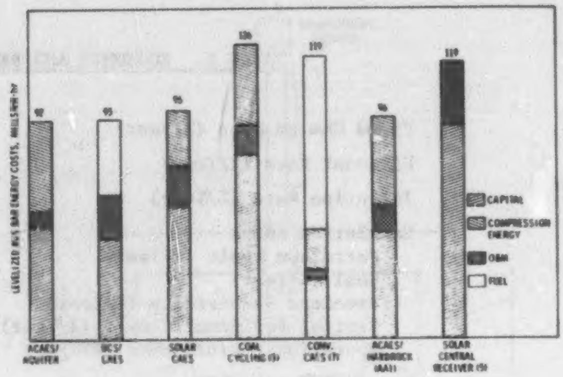

Fig. 6. Levelized Busbar Energy Costs for CAES Systems Studied

According to present CAES program plans, AAI will perform a more detailed engineering and economic analysis of the ACAES/aquifer concept in FY-1981. The solar/CAES concept will be examined further to refine the preliminary cost figures presented in this paper. Further activities concerning the DCS/CAES concept are not currently included in the FY-1981 CAES Program Plan, but may be undertaken later pending availability of funding.

ACKNOWLEDGMENT

This work was sponsored by the U.S. Department of Energy, Divisions of Thermal and Mechanical Energy Storage and Energy Systems under the Compressed Air Energy Storage Program.

REFERENCES

1. Allemann, R. T., and M. K. Drost, Advanced Concepts Studies, Proceedings of the 1979 Mechanical and Magnetic Energy Storage Contractors' Review Meeting, December 1979.

2. Reilly, R. W., The Economics of Compressed Air Energy Storage with Thermal Energy Storage, presented at the 15th Intersociety Energy Conversion Engineering Conference, Seattle, WA, August 1980.

3. EPRI Technical Assessment Guide. EPRI PS-866-SR, Electric Power Research Institute, Palo Alto, CA, June 1978.

4. Hobson, J. J., et al, Feasibility of the Compressed Air Storage as a Peak Shaving Technique in California, Prepared for the California Energy Commission by Acres American, Inc., Buffalo, NY, 1978.

5. Apley, W. J. et al, Assessment of Generic Solar Thermal Systems for Large Power Applications, Volume I: Analysis of Electric Power Generating Costs for Systems Larger than Ten Mwe, PNL-3533, Richland, WA, October 1980.

6. Preliminary Engineering Study and Conceptual Design of Adiabatic Compressed Air Energy Storage Plant with Aquifer Storage - Progress Review, Prepared by Acres American, Inc. for PNL, July 1980.

7. Drost, M. K., F. R. Zaloudek and W. V. Loscutoff, A Preliminary Study of Adiabatic Compressed Air Energy Storage in Aquifers, prepared for presentation at the 1980 ASME Annual Meeting, Chicago, IL, November 1980.

PROJECT SUMMARY

Project Title: Technical and Economic Assessment of Fluidized Bed Augmented Compressed Air Energy Storage System

Principal Investigator: Robert D. Lessard

Organization: United Technologies Research Center
Silver Lane
East Hartford, Connecticut 06108

Project Goals: (1) Assess fluid bed combustor (FBC) and turbomachinery technology relative to their integration potential in compressed air energy storage (CAES) applications; (2) Identify a preferred CAES/FBC power plant system configuration; (3) Transform the selected CAES/FBC system configuration into a preconceptual power plant design; and (4) Evaluate the part-load and load-following capabilities of the selected CAES/FBC power plant.

Project Status: The efforts related to achieving the first three of the four goals mentioned above have been completed and documented in United Technologies Report No. R80-954490-20. The analysis and initial documentation for the fourth goal, evaluation of part-load capability, have been completed.

The major conclusions of the study are as follows: (1) coal-fired CAES/FBC systems should be technically feasible in the near future, (2) a CAES/open-bed PFBC configuration would provide the best candidate for early commercialization; (3) a CAES/PFBC power plant could be designed and built by utilizing many standard equipment items and modifying existing equipment designs; (4) the economic competitiveness of the CAES/PFBC is attractive for peak- to mid-load power generation; and (5) preliminary indications are that a CAES open-bed PFBC should have good part-load and load following capabilities.

Contract Number: EY-76-C-06-1830, Subcontract B-51299-A-L

Contract Period: 1 November 1978 through 31 December 1980

Funding Level: $355,994 (through 30 September 1980)

Funding Source: U. S. Department of Energy through Pacific Northwest Laboratory operated by Battelle Memoiral Institute

CAES/FBC STUDIES

Robert D. Lessard
William A. Blecher
United Technologies Research Center
Silver Lane
East Hartford, Connecticut 06108

ABSTRACT

This paper presents the highlights of a recently completed program to assess the technical and economic feasibility of advanced concepts for generating peak-load electric power from a compressed air energy storage (CAES) power plant incorporating a coal-fired fluid bed combustor (FBC). Specifically, it reviews the progress made in the study program since the Reference 1 presentation, and includes: a preconceptual design of a CAES power plant utilizing a pressurized fluid bed combustor (PFBC); an economic analysis based upon the PFBC/CAES power plant preconceptual design; and an investigation of the part-load transient capabilities of the power plant. In addition, the paper presents the conclusions, derived from these phases of the study program, which indicate that a PFBC/CAES power plant could produce competitive peak- and mid-range electrical energy, and that a CAES power plant with an open-bed PFBC appears to have no equipment-related constraints which would prevent the power plant from being responsive to utility requirements for a peak- or mid-range power plant.

INTRODUCTION

The initial phase of this multi-year program dealt with an assessment of the fluid bed combustor and turbomachinery technologies and how they might be applied to CAES applications (Ref. 2). This was followed by a comprehensive systems analysis to select a preferred FBC/CAES configuration (Refs. 1 and 3). The conclusions derived from these two phases indicated that: 1) although there are still several obstacles to overcome, there is strong evidence an FBC could be successfully coupled with the turbomachinery of a CAES power plant; and 2) the utilization of an open-bed PFBC would provide the most attractive and logical near-term application of an FBC in a CAES power plant system.

Having assessed the feasibility of the technology and identified the most promising FBC/CAES system configuration, it became appropriate to perform a preconceptual design study. The results of this preconceptual design were used to provide a basis for developing realistic equipment cost estimates which were then employed in an economic comparison between the PFBC/CAES power plant and competing alternative power plants. In addition, the physical characteristics of the major equipment items defined for the PFBC/CAES power plant during the preconceptual design effort were used to provide a basis for estimating the part-load and transient response behavior which was then compared to the behavior desired by electric utilities for peak-load power plants. The purpose of this paper is to present the highlights of the preconceptual design, economic analysis, and part-load and transient capability evaluation. Highlights of the preconceptual design and economic analysis have also been presented in greater detail in previous papers (Refs. 4 and 5).

This program has been supported by the U.S. Department of Energy under Subcontract No. B-51299-A-L, Prime Contract DE-AC06-76RLO 1830 with Pacific Northwest Laboratory operated by Battelle Memorial Institute. In the performance of this contract, United Technologies Research Center (UTRC) was assisted by Coal Processing Consultants Limited of the United Kingdom and Acres American Incorporated.

POWER PLANT PRECONCEPTUAL DESIGN

A design approach philosophy was adopted which mandated the maximum utilization of existing CAES components and plant design (i.e., Refs. 6 and 7). It also included modification, where necessary, to the operating requirements and/or existing designs to assure compatibility between them. For the purposes of this preconceptual design, a four-unit plant was selected. The key design point operating characteristics of the plant are summarized in Table 1.

The site arrangement of the complete four-unit FBC/CAES plant is shown in Fig. 1. The underground cavern is positioned on the upper border of the site. No plant components are positioned above the cavern structure. The compensating reservoir is located adjacent to the underground cavern, in the upper-right corner of the site. The power block (one quadrant of which is shown in Fig. 2) is located toward the center of the site and contains the turbomachinery buildings, fluidized bed combustors, coal and dolomite processors, and the central control and administration building. Within the power block, the four turbomachinery systems are arranged to minimize piping and electrical system complexity and achieve optimum coal combustion systems control through close grouping of the processing and combustion systems. The electrical switchyard and forced draft wet cooling towers are located adjacent to the power block.

The fluid bed combustor system encompasses the equipment for: coal and dolomite handling, coal and dolomite preparation, coal and dolomite feeding, fluid bed combustion and particulate cleanup, ash and spent dolomite removal, and controls and instrumentation. The coal and dolomite are unloaded into underrail recovery hoppers and conveyed to stockpiles. Separate mills for the coal and dolomite dry and crush the material to the required top size of 3 mm (1/8 in) for feeding to the combustor. The coal and dolomite, in correct proportion, are fed in batches to a storage/primary injector system. Fuel from the primary injector is continuously fed to the combustor via twenty-four feed lines. The fluid bed combustor pressure vessel (Fig. 3) contains the bed and the three-stage cyclone gas cleanup system. It has a length of 38.4 m (126 ft) and a diameter of 11.6 m (38 ft). It operates at 850 C (1562 F) and 15.2 bar (15 atm) with a fluidizing velocity of 0.9 m/s (3 ft/sec). The coal-dolomite mixture is injected pneumatically through feed points immediately above the distribution plate, while the combustion air passes upward through the distributor plate. After combustion in the bed, the combustion gases and entrained particles enter the freeboard where most of the particles are deposited out of the gas stream. The remainder of the harmful particles are removed in three high-efficiency cyclones used for gas cleanup. Ash and spent dolomite are released through a bed level control system into a pneumatic conveying system. After cooling, the solids are discharged through pressure locks, then conveyed to storage.

The power generation system includes: low-pressure and booster compressors, low-pressure and expansion turbines, clutches, a motor/generator, and heat exchangers. The turbomachinery has been placed on a common centerline (Fig. 4) and rotate at 3600 rpm. The compressors and turbines are on opposite ends of the motor/generator and are connected by clutches so that they can alternately drive, or be driven by, the motor/generator during compression or generation periods. The total length of the turbomachinery train is 38.4 m (126 ft), excluding the recuperator duct. During the off-peak compression mode, an axial-flow, seventeen-stage, low-pressure compressor pressurizes ambient air to 16.8 bar (atm) with one intercooling stage. The air is again intercooled prior to compression to storage pressure in the booster compressor. The booster compressor is a seven-stage, heavy-duty, centrifugal compressor with intercooling after the fourth stage. The air is after-cooled to 49 C (120 F) and put into storage. During the power generation mode, air from storage is heated in the recuperator and expanded through a two-stage turbine to about 15 bar (atm). After leaving the expansion turbine, the air travels to and from the PFBC via a co-axial inlet/outlet duct (refer to Fig. 3) with the cooler, expansion turbine exit air on the outside and the hotter products of combustion on the inside. The hot gas is expanded through a four-stage, low-pressure turbine which produces most of the output power. Heat in the turbine exhaust is recovered in the recuperator.

The balance of plant includes those components and systems required to support the operation of the turbomachinery and PFBC systems. Most of these components and systems are common in both function and size to commercially available facilities. The balance of plant can be separated into three distinct sections: 1) the energy storage system including those items in the PFBC/CAES plant required to deliver, store, and regulate the pressure of the air; 2) the plant mechanical system including the mechanical equipment and systems required to support the CAES turbomachinery and PFBC plant; and 3) the plant electrical system including the electrical equipment and systems required to effect a workable PFBC/CAES power plant.

ECONOMIC ANALYSIS

The plant direct costs were developed using realistic equipment cost estimates for the major components. Of the $458.9 million (July '79 $) total direct cost, the PFBC system, including all coal handling and processing, is the most expensive item accounting for about 43 percent of the total direct cost. The turbomachinery and compressed air storage systems account for about 25 percent and 13 percent, respectively, of the cost. The power plant total capital investment (assuming a January 1990 commercial operation date) was obtained by accounting for escalation prior to construction, a contingency allowance, an engineering and management fee, escalation during construction, and interest during construction. The values of these parameters were prescribed by DOE. The January 1990 dollar estimate was then deflated to January 1980 dollars. The resulting capital investment is $706.7 million (January '80 $).

Power plant operating costs were estimated for fuel, compression energy, and operating labor plus maintenance. These operating costs were calculated on a levelized basis using an EPRI/DOE costing procedure and combined with the annual capital cost estimate to produce a levelized annual cost estimate and a levelized busbar electric cost estimate. The resulting levelized annual costs are depicted in Fig. 5 for a range of capacity factors. The levelized busbar cost corresponding to an annual utilization of 2190 hr/yr is 117.9 mills/kWh. Preliminary cost comparisons were made with a select group of competing oil-fired power plants. This comparison was made on a levelized annual cost basis and is included in Fig. 5. It appears from this illustration that the coal-fired PFBC/CAES system emerges as the lowest cost alternative of those considered for annual utilization above 1925 hrs/yr.

PART-LOAD OPERATION

The performance characteristics of the open-bed PFBC/CAES power plant used for the preconceptual design were based on steady-state operation at full-load design point. All power plants, but especially peak-load power plants, must have some degree of load-following capability. This implies the ability to operate in steady-state, part-load conditions. In order to simulate this operation, it was necessary to first identify the effect of steady-state, part-load operation on the major components, the most important being the PFBC.

The open-bed PFBC/CAES power plant system would achieve part-load operation by concurrently and proportionately varying the mass flow of both the air and coal to the PFBC to produce a varying thermal output. Operation in this manner will also: 1) produce a constant bed temperature, and therefore, a constant low-pressure turbine inlet temperature because the air and fuel flows remain proportional; 2) provide a bed pressure that is directly proportional to the flow through the bed because the low-pressure turbine nozzle area is fixed resulting in choked flow; and 3) yield a constant superficial velocity in the bed over the entire load range because the flow rates are proportional to pressure and the bed temperature remains constant.

Despite this recognized procedure for operating an open-bed PFBC, there were some reservations about the part-load capabilities of the PFBC system. Consequently, an investigation was initiated to address these reservations by examining key PFBC operating parameters, including combustion efficiency, freeboard and cyclone combustion, sulfur retention, fluidization, elutriation, and solids handling all at 100-percent, 50-percent, and 25-percent design load.

The combustion efficiency is expected to be at least 98.5 percent over the operational range of 25-percent to 100-percent load at the design bed temperature and fluidizing velocity. Higher efficiencies could be achieved by increasing the number of solids feed points. Because of the high combustion efficiency, little combustion is expected in the freeboard or cyclones. Combustion conditions do not, therefore, represent a limitation to steady-state, part-load operation. No experimental data on sulfur retention directly related to the expected conditions in the combustor exist, and model predictions differ significantly. However, no difficulties are envisioned in designing a solids injection system capable of supplying the range of dolomite required (Ca/S ratio of 1.5 at 100-percent to possibly 2.8 at 25-percent load) to meet the specified goal of 85-percent sulfur retention.

An analysis of fluidization conditions expected throughout the 25-percent to 100 percent load range indicates that satisfactory fluidization could be maintained for both steady-state and transient operation. An estimate of the solids loading of the combustion gas at the cyclone entry revealed an increase from 4075 ppm at steady-state, 25-percent load to 5033 ppm at steady-state, 100-percent load. This increase results partly from the increased solids fuel rate and partly because of the higher proportion of fuel material due to the denser fluidizing gas. However, because the gas velocities in the cyclones remain nearly constant over the load range, resulting in nearly constant efficiency, and because the dust elutriated at high loads is coarser than at low loads, the increase in dust loading in the cleansed gas will be less than at the cyclone inlet. Consequently, elutriation should not pose a problem as long as the detailed design of the solids handling equipment takes into account the momentary high particulate loadings in the combustion gas expected on turnup after prolonged part-load, steady-state operation.

TRANSIENT OPERATION

The ability of a generating unit to respond to load changes is an important factor affecting its desirability to a utility system. While interconnecting tie-lines lessen the effect of load disturbances, it is generally required that these disturbances be corrected by either increasing or decreasing output in less than 10 minutes. While there is no fixed requirement for response time, a typical utility guideline would require a load change capability of between 3 and 5 percent of design load per minute. These rates will vary depending on the size and characteristics of other units in the utility. For example, if a utility uses a large percentage of base-load power from units with limited response capability, the remaining units must make up for this by having a proportionately greater capability. This is especially true of a peaking unit such as the CAES system.

To determine the ability of the system to respond to load changes, transient simulations were made using a UTRC computational model. However, it was first necessary to prepare a dynamic representation of the PFBC to use in that model. The PFBC model is a linearized representation of the equations shown in Fig. 6. It assumes that the heat of combustion is the sum of the heat from the volatile matter which burns instantaneously plus the heat from carbon burn-up which is a direct function of the mass of carbon in the bed. The latter assumption arises from the fact that there is approximately 300 percent of theoretical air in the bed and, therefore, the rate of carbon burn-up is governed primarily by the amount of carbon exposed to the air. As a result, when the coal feed rate is increased, heat release is initially increased only by the volatile matter (approximately 35 percent). The remaining increase occurs as carbon inventory builds up over a time constant of approximately 250 seconds. Because of the good heat transfer between the gases in the bed and bed material, the entire bed temperature must change with combustor outlet temperature. This results in a time constant between a change in heat release and bed temperature and between air flow and bed temperature of approximately 335 seconds. Because of the time lag between fuel rate and heat release, when both fuel rate and air flow are changed together to produce the same steady-state bed temperature, bed temperature does not remain constant but is temporarily disturbed before returning to its initial value. This is shown in Fig. 7 for a 10-percent change in both fuel and air flow rate. If bed temperature were to remain constant, fuel flow would have to be changed initially by more than the corresponding fractional air flow change.

To determine the effect of other parts of the CAES system on combustor response, the dynamic combustor model was incorporated into the overall CAES system simulation model. Other than the PFBC, the major factors affecting CAES system response are the heat exchanger thermal mass and the volumetric lag associated with changing pressure in the PFBC containment vessel. The effect of these factors on the bed temperature response to a 10-percent change in both air flow and fuel rate is shown in Fig. 8. When compared with Fig. 7, it can be seen that the magnitude of the temperature disturbance is decreased and the time to reach the peak disturbance is lengthened from 5 to 8 minutes.

Because it is necessary to hold bed temperature relatively constant to avoid damage to the refractory material in the bed, it appears that coordination of fuel rate and air flow will be an important factor in system design. To identify the required response of the fuel feed mechanism, a number of different rates of change of air flow (which approximates power level change) were examined. At a 15-percent-per-minute change in throttle valve restriction, the required rate of change in fuel flow is slightly greater than 18 percent per minute. This is shown in Fig. 9 which presents the fuel rate required to maintain constant bed temperature as the throttle valve restriction is changed from

25-percent to 100-percent load in 5 minutes. While commercial equipment can respond at 18 percent per minute or slightly faster, it is generally not sized for much more than 10 percent over the design feed rate. As shown in Fig. 9, a feed rate of 20 percent in excess of design will be needed to maintain constant bed temperature for the specified transient. Assuming that fuel rate can respond as shown in Fig. 9, Fig. 10 shows the resultant change in output power. Because of volumetric and thermal lags, it takes slightly more than 5 minutes to reach 100 percent. The change in air temperature out of the cold side of the heat exchanger is shown in Fig. 11. Because of the high cold-side film coefficient, heat exchanger metal temperature will closely follow this profile. Thus, the heat exchanger will have to be designed to withstand a 250R (140K) temperature change in approximately 7 minutes.

It is apparent that output changes on the order of 15 percent per minute over a large range are feasible with current state-of-the-art equipment. For smaller excursions (on the order of 25 percent) rates of change of 25 percent per minute may be feasible. Because of these rapid response rates, the desirability of the system should be greatly enhanced.

CONCLUSIONS

The conclusions derived during these phases of the study program indicate:

1. A PFBC/CAES power plant could be designed and built by utilizing many standard equipment items.

2. The economic competitiveness of the PFBC/CAES is such that above an annual utilization of about 1925 hrs/yr, it could produce lower cost power than oil-fired CAES plants.

3. There do not appear to be any equipment limitations which would constrain the PFBC/CAES power plant from being responsive to utility part-load or transient requirements.

ACKNOWLEDGMENT

Special recognition should be given to A. J. Giramonti of UTRC, D. Merrick of Coal Processing Consultants, and M. J. Hobson of Acres American for their contributions during the study program.

REFERENCES

1. Giramonti, A. J.: "Preliminary Evaluation of Coal-Fired Fluid Bed Combustion-Augmented Compressed Air Energy Storage Power Plants," Proceedings of the 1979 Mechanical and Magnetic Energy Storage Contractors' Review Meeting, August 1979.

2. Lessard, R. D., A. J. Giramonti, and R. L. Sadala: "Coal-Fired Fluid Bed Compressed Air Energy Storage Power Plants - A Preliminary Technical Assessment," Proceedings of the 14th IECEC, Vol. 1, August 1979.

3. Lessard, R. D., A. J. Giramonti, and D. Merrick: "Preliminary Evaluation of Coal-Fired Fluid Bed Combustion-Augmented Compressed Air Energy Storage Power Plants," 25th ASME Gas Turbine Conference, ASME Paper 80-GT-160, March 1980.

4. Lessard, R. D., A. J. Giramonti, and D. Merrick: "Coal-Fired Fluid Bed Combustion Augmented Compressed Air Energy Storage Systems," Proceedings of the 15th IECEC, Vol. 1, August 1980.

5. Lessard, R. D., A. J. Giramonti: "Coal-Fired Fluid Bed Combustion-Augmented Compressed Air Energy Storage Power Plants: A Technical and Economic Assessment," Joint Power Generation Conference, ASME Paper 80-JPGC/GT-1, September, 1980.

6. Giramonti, A. J., et al.: "Preliminary Feasibility Evaluation of Compressed Air Storage Power Systems," United Technologies Research Center Report R76-952161-5, NTIS PB 259-281/4G1, December 1976.

7. "Preliminary Design Study of Underground Pumped Hydro and Compressed Air Energy Storage in Hard Rock." Potomac Electric Power Company Contract EC-77-C-01-5047 with Department of Energy and Electric Power Research Institute.

Table 1 - Key PFBC/CAES Power Plant Operating Characteristics

Power, MW - 4 units		
Turbine	876.4	
Compressor	799.6	
Heat Rate, kJ/kWh (Btu/kWh)		
Generation	4788	(4538)
Compression	9595	(9095)
Round trip	14383	(13633)
Storage pressure, bar (atm)	72.1	(71.2)
PFBC bed temperature, C (F)	850	(1562)
PFBC bed pressure, bar (atm)	15.2	(15.0)
ET inlet temperature, C (F)	264.2	(507.5)
LT inlet temperature, C (F)	850	(1562)
Annual utilization, hr/yr	2190	
Capacity factor	0.25	

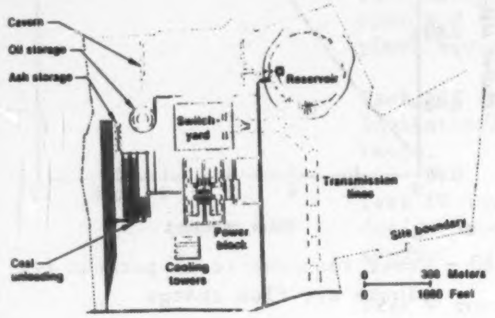
Cavern
Oil storage
Ash storage
Switch-yard
Reservoir
Transmission lines
Site boundary
Power block
Cooling towers
Coal unloading
0
300 Meters
0
1000 Feet

Fig. 1 - Site arrangement plan

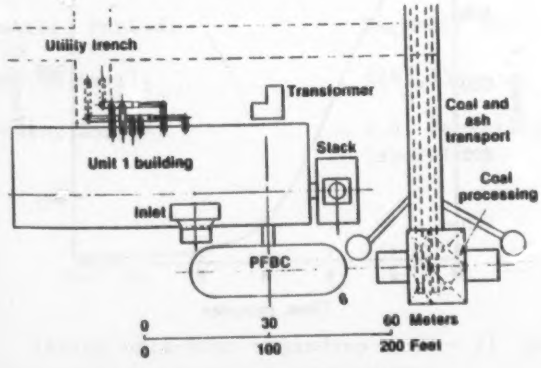
Utility trench
Transformer
Unit 1 building
Stack
Coal and ash transport
Coal processing
Inlet
PFBC
0
30
60 Meters
0
100
200 Feet

Fig. 2 - Power block arrangement

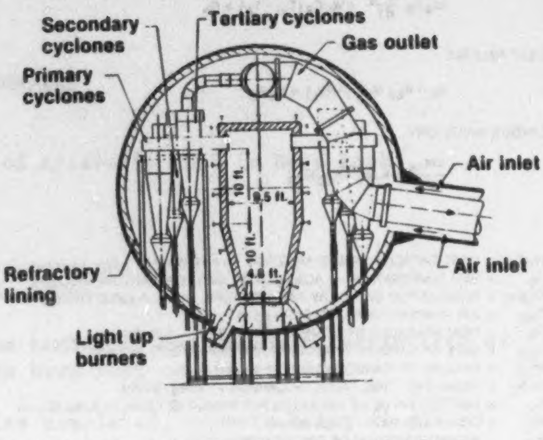
Secondary cyclones
Tertiary cyclones
Gas outlet
Primary cyclones
Air inlet
10 ft.
9.5 ft.
10 ft.
4.6 ft.
Air inlet
Refractory lining
Light up burners

Fig. 3 - Fluid bed combustor end view

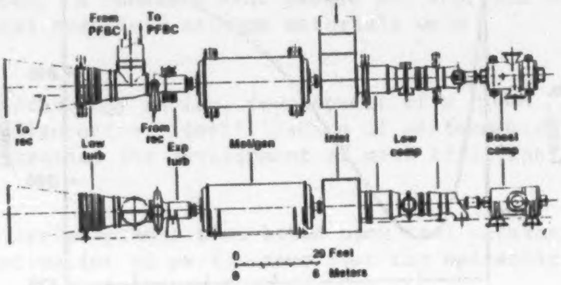
Air
From PFBC
To PFBC
To rec
Low turb
From rec
Exp turb
Motgen
Inlet
Low comp
Boost comp
0
20 Feet
0
6 Meters

Fig. 4 - Turbomachinery train

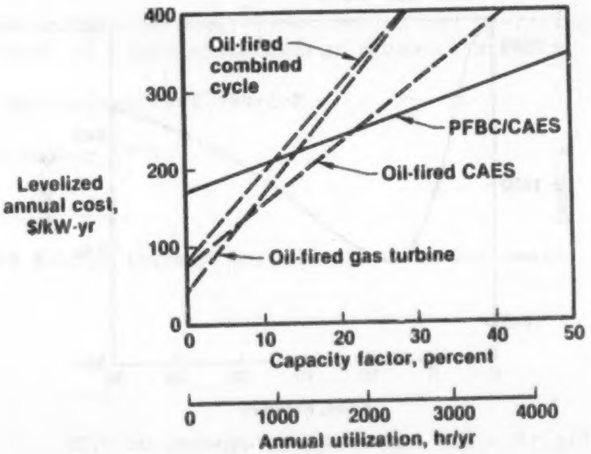

Fig. 5 - Cost comparison

HEAT BALANCE

$$M_B C_B \frac{dT_B}{dt} = W_G C_G (T_{IN} - T_B) + Q_C$$

HEAT RELEASE

$$Q_C = K_{CB} M_{CB} (HHV_C) + K_V W_C$$

CARBON INVENTORY

$$\frac{dM_{CB}}{dt} = K_C W_C - K_{CB} M_{CB}$$

$M_B C_B$ = HEAT CAPACITY OF BED MATERIAL — kJ/C (Btu/F)
T_B = BED TEMPERATURE — ALSO OUTLET GAS TEMPERATURE — C (F)
$W_G C_G$ = COMBUSTION GAS FLOW TIMES SPECIFIC HEAT — kJ/s-C (Btu/sec-F)
T_{IN} = AIR TEMPERATURE INTO BED — C (F)
Q_C = HEAT RELEASED BY COMBUSTION IN BED — kJ/s (Btu/sec)
K_{CB} = RATE OF CARBON COMBUSTION/CARBON IN BED — 1/sec
M_{CB} = AMOUNT OF CARBON IN BED — kg (lb)
HHV_C = HIGHER HEATING VALUE OF CARBON — kJ/kg (Btu/lb)
K_V = HEATING VALUE OF VOLATILES PER POUND OF COAL — kJ/kg (Btu/lb)
W_C = COAL FEED RATE — kg/s (lb/sec)
K_C = WEIGHT FRACTION OF FIXED CARBON IN COAL

Fig. 6 - Combustor equations

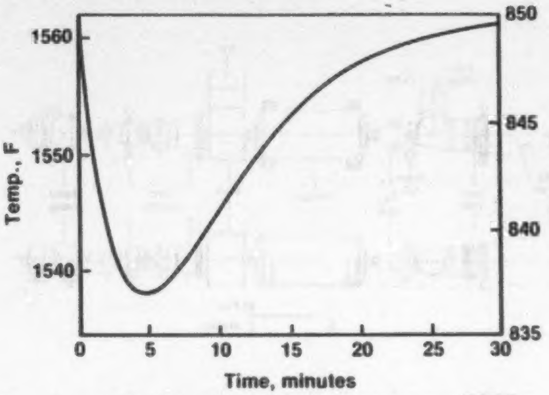

Fig. 7 - Bed temperature response at PFBC; 10-percent increase in fuel rate and air flow

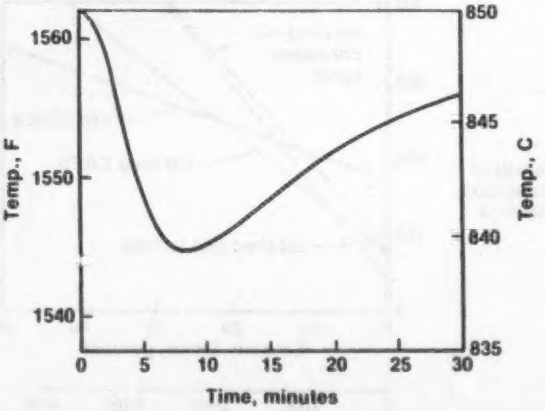

Fig. 8 - Bed temperature response of PFBC integrated into PFBC/CAES power plant; 10-percent increase in fuel rate and air flow

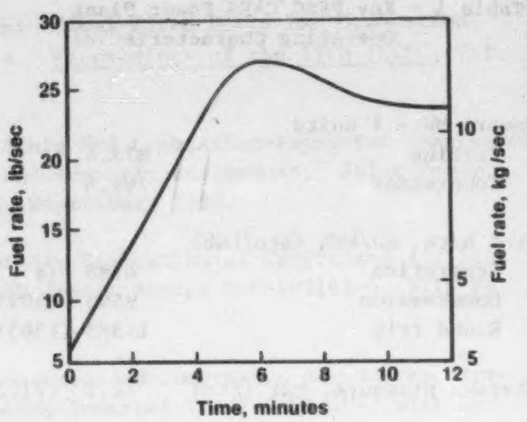

Fig. 9 - Required fuel rate for 15-percent per minute air flow change

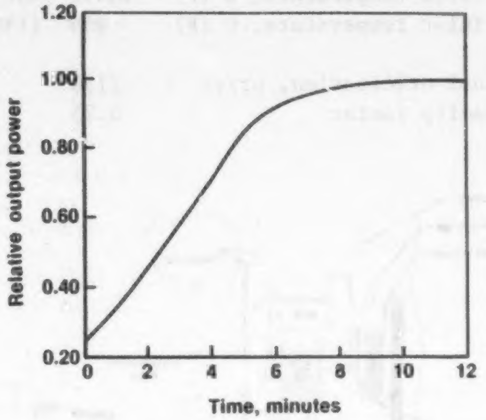

Fig. 10 - Power response to 15-percent per minute air flow change

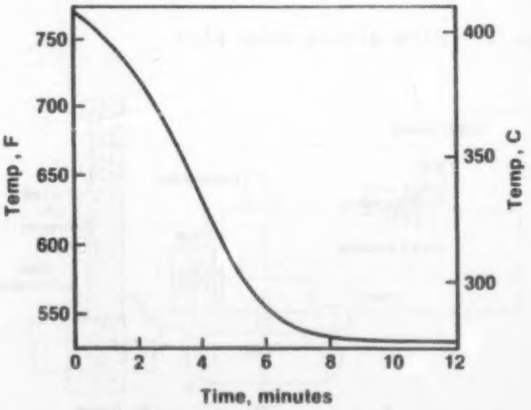

Fig. 11 - Heat exchanger cold-side outlet temperature response to 15-percent per minute air flow change

PROJECT SUMMARY

Project Title: Conceptual Design of Adiabatic CAES in Hard Rock

Principal Investigator: M.J. Hobson

Organization: Acres American Incorporated
Columbia, Maryland 21044

Project Goals: Determine near-term technical and economic feasibility of adiabatic CAES with hard rock cavern storage.

Project Status: Technical activities completed, reports being finalized covering the five project tasks.

Task I involved technology review, storage material cost/performance assessment and analysis of the Thermal Energy Storage (TES) system. A sensible heat pebble bed approach was selected and several candidate storage materials were identified.

Task II involved technology review, development of a turbomachinery configuration, identification of performance, cost and future potential for development of more efficient plant equipment.

Task III involved cycle optimization based upon real machinery limitations and estimation of performance over the operating range.

Task IV involved development of a 4-unit conceptual plant design based upon the site used for the recent PEPCO CAES/UPH study.

Task V involved estimation of plant construction and operating costs and development of comparative energy production costs.

Contract Number: EY-76-C-06-1830, Subcontract B-82284-A-E

Contract Period: December 1979 - December 1980

Funding Level: $249,353

Funding Source: U.S. Department of Energy through Battelle-Pacific Northwest Laboratory

DOE Thermal-Mechanical Energy Storage
Annual Contractors Review Meeting

ADIABATIC COMPRESSED AIR ENERGY STORAGE IN HARD ROCK

C. L. Driggs, Project Coordinating Engineer
Acres American Incorporated
The Clark Building
Columbia, Maryland 21044

INTRODUCTION

The construction and operation of the Huntorf CAES plant was a milestone achievement which demonstrated the commercial availability of compressed air storage. The Huntorf equipment design, which operates on natural gas, has since been modified for application to the 60 Hertz systems of U.S. utilities and has been the cornerstone of both the MSS and the PEPCO CAES engineering studies.

The Huntorf plant was ordered in 1972, before the rise of the OPEC cartel, the U.S. natural gas shortages of the mid-seventies, the Fuel Use Act of 1978, deregulation of oil and gas, and the present instability of the Middle East. Although the BBC CAES design promises dramatic reductions in the usage of liquid or gas fuels to produce peaking power compared to combustion turbines, there has been no dramatic rush to install these plants in the U.S. Part of this hesitancy may be attributed to utility overcapacity in many regions and a traditionally cautious attitude. However, concerns regarding price and availability of gas or oil throughout the lifetime of a CAES plant are often quietly expressed.

The goal of indigenous fuels substitution within the CAES cycle has been the driving force behind studies of fluidized bed and coal gasification CAES variants. Adiabatic CAES is a different approach which eliminates all fuel input within the CAES plant. Instead, the heat of compression is reused in the CAES expansion cycle through the use of thermal storage. This approach was first patented in 1972 and studied in some depth in an EPRI funded effort performed by the Central Electricity Generating Board (U.K.) in 1978. The study concluded that high temperature (1200 to 1500°F) adiabatic CAES cycles should only be considered as long term developments, and recommended further study of hybrid cycles which incorporated fuel topping.

This paper discusses the findings of a conceptual design study performed during 1980 which examined pure adiabatic CAES cycles operating in the temperature range of 700 to 900°F. The project involved an investigation of the technical and economic feasibility of using commercially available technology to construct a plant based on the PEPCO study site and plant design requirements. This work was supported by the U.S. Department of Energy under Subcontract No. B-82284-A-E, Prime Contract DE-AC06-76RLO 1830 with Pacific Northwest Laboratory (PNL) operated by Battelle Memorial Institute. The project is now complete, and a final report will be available from PNL shortly.

THE ADIABATIC CAES CYCLE

Comparison of the basic adiabatic CAES concept (Figure 1) to the oil-fired plant design reveals several changes. There are no fuel supply and combustion systems, which are replaced by one or more thermal energy storage (TES) systems, and no compressor intercooling system. Allowable compressor exit temperature dictates the cycle operating pressure, and exit temperature and pressure are a function of compressor efficiency. As no fuel is used, high efficiency combustion cannot be employed to make up for compressor losses as is the case with combustion turbines. As a result, the use of a relatively inefficient compressor leads to lower operating pressure, but substantially reduces cycle

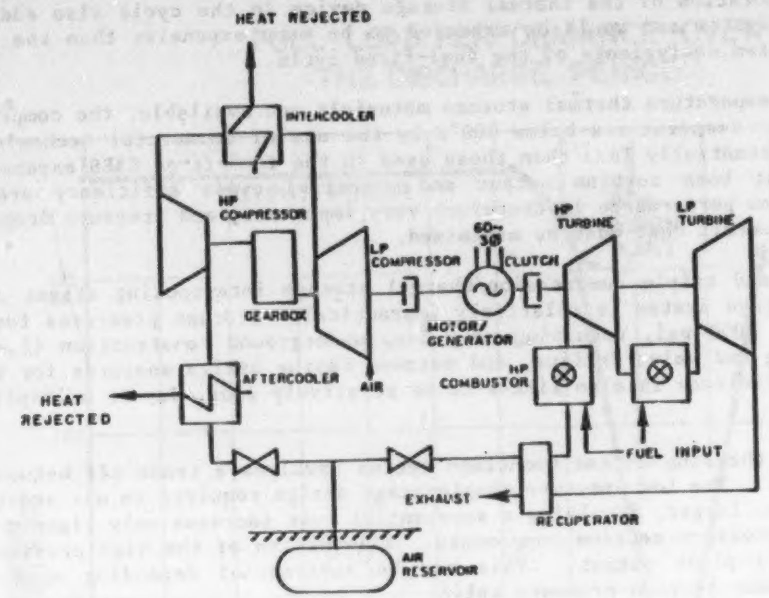
HEAT REJECTED
INTERCOOLER
HP COMPRESSOR
GEARBOX
LP COMPRESSOR
60–3Ø
CLUTCH
MOTOR/GENERATOR
HP TURBINE
LP TURBINE
AIR
AFTERCOOLER
HEAT REJECTED
HP COMBUSTOR
FUEL INPUT
EXHAUST
RECUPERATOR
AIR RESERVOIR

A. CONVENTIONAL CAES

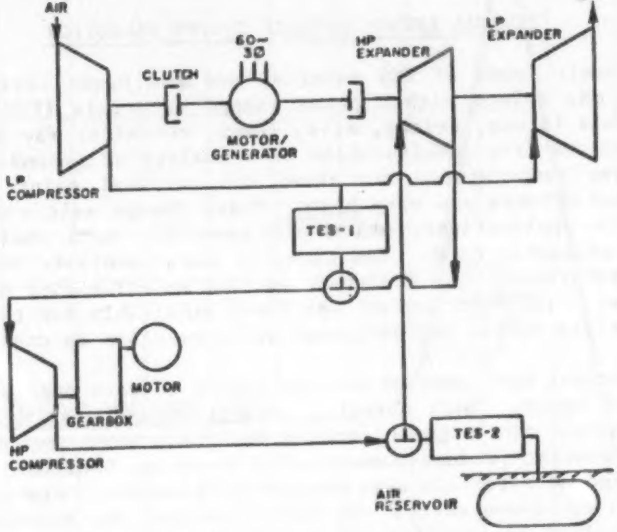
AIR
CLUTCH
60–3Ø
MOTOR/GENERATOR
HP EXPANDER
LP EXPANDER
EXH
LP COMPRESSOR
TES-1
MOTOR
GEARBOX
HP COMPRESSOR
TES-2
AIR RESERVOIR

B. ADIABATIC CAES

CAES CONFIGURATIONS

ACRES

BATTELLE PACIFIC NORTHWEST LABORATORY

CONCEPTUAL DESIGN AND ENGINEERING STUDIES—ADIABATIC CAES

FIGURE 1

ACRES AMERICAN INCORPORATED

performance. Incorporation of the thermal storage device in the cycle also adds unavoidable losses to the system and would be expected to be more expensive than the combustion and intercooling system equivalents of the fuel-fired cycle.

Although high temperature thermal storage materials are available, the compressor heat source was limited to temperatures below 900°F by the use of commercial technology. Such temperatures are substantially less than those used in the fuel-fired CAES expansion cycle, with the result that both turbine output and potential cycle efficiency are reduced. Thermal storage system performance is therefore very important, and pressure drop, temperature variation and overall cost must be minimized.

Single, double and triple compression/thermal storage intercooling stages are possible, but the three stage system is relatively impractical. Storage pressures for a three-stage cycle approach 5000 psi, requiring very deep underground construction (i.e., 12,000 feet), unusual piping and valve designs, and extreme casing design measures for the turbomachinery. Plant efficiency is also likely to be relatively poor, due to multiplication of efficiencies.

A comparison of the single- and two-stage cycles involves a trade off between capital cost and plant output. The low pressure single-stage design requires an air storage system volume some five times larger, involving a substantial cost increase only lightly offset by elimination of high pressure section components. Elimination of the high pressure turbine will cause a loss in plant output. This may be substantial depending upon operating temperatures and turbine section pressure split.

Selection of plant design pressure in the PEPCO CAES study was based upon a PEPCO criterion of lowest capital cost, as levelized cost differences between pressures were negligible. This approach reflected the difficulty in obtaining construction funds now experienced (and likely to continue) by private utilities. The minimum capital cost approach was also used in this study to select the two-stage arrangement as the design cycle.

THERMAL ENERGY STORAGE SYSTEM SELECTION

There are two basic types of TES material and two basic categories of TES system. First, the designer may select either phase change materials (PCM's, such as water) or sensible heat materials (stone, bricks, oils, water, ceramics) may be used. Phase change materials were eliminated from consideration on a variety of grounds. Water could not be used as the operating temperatures are above the critical point, and thus containment pressures and required volumes are very high. Phase change salt systems are unproven for most commercial scale applications, which are generally much smaller than the size of facility needed for adiabatic CAES. Additionally some candidate PCM's were dangerous to handle at normal temperatures. The designer may also select either a direct or an indirect contact heat exchanger. Indirect contact was found unsuitable for this plant design as the temperature differentials across the exchanger walls resulted in unacceptably high losses.

Extensive evaluations were carried out for direct contact sensible heat systems of the pebble or checker bed types. Both material properties and cost were used to select the most promising materials. The highest ranking materials were crushed rock, sintered iron ore pellets, and a fireclay product commercially known as Denstone (Norton Company trade name) (Table 1). Selected materials were modeled to simulate performance in various pebble bed arrangements, using computerized routines provided by Massachusetts Institute of Technology and the Central Electricity Generating Board. The computer simulation activities allowed development of a TES system configuration with acceptable performance.

FULL LOAD PERFORMANCE OVER THE DISCHARGE PERIOD

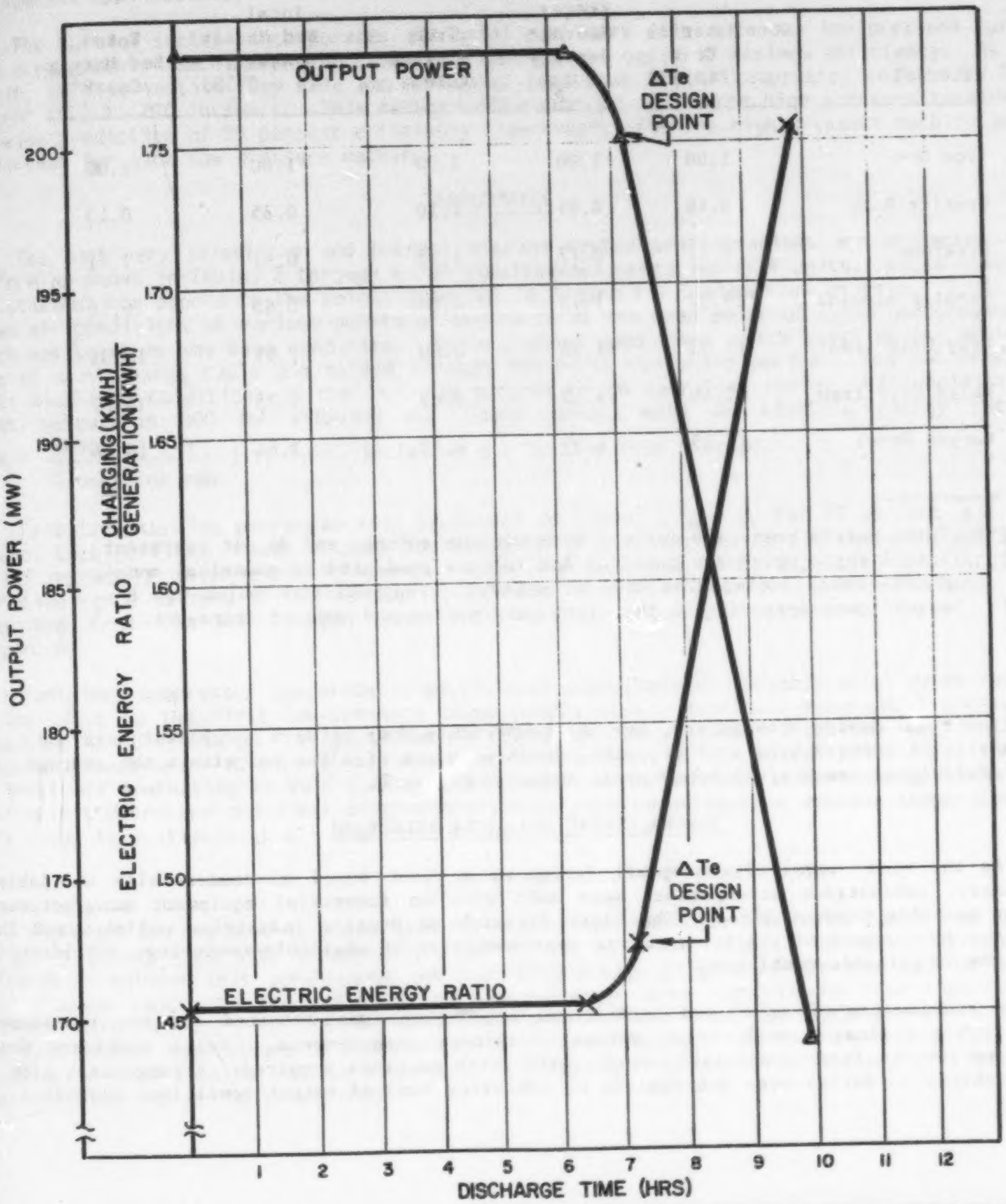

BATTELLE PACIFIC NORTHWEST LABORATORY

CONCEPTUAL DESIGN AND ENGINEERING STUDIES—ADIABATIC CAES

ACRES

ACRES AMERICAN INCORPORATED

FIGURE 2

Table 1

Preliminary Ranking of Selected Potential Heat Storage Materials

Material	Material Cost (F.O.B.)	Energy Storage Density (C_p)	True Minimum Volume	Total Bed Matrix Mass (e = 0.38)	Total Bed Matrix Cost**
Iron Ore	1.00	1.00	1.00	1.00	1.00
Granite Rock	0.16	0.91	1.10	0.85	0.13
Denstone	8.67	0.77	1.33	0.91	7.91
Tabular Alumina	18.22	1.13	0.89	0.88	16.14
Gray Cast Iron	11.33	1.26	0.80	1.61	18.31
White Cast Iron	12.44	1.62	0.62	1.35	16.87
Forged Steel	11.29	1.39	0.72	1.61	18.24

** Total matrix costs are derived from minimum volumes and do not represent actual costs which are based on bed volumes predicted by numerical models. Matrix costs exclude the cost of material transportation which can be significant depending on the distance traveled and mode of transport.

With the final design arrangement, average temperature drop between compressor exit and turbine inlet temperatures is 25°F, with pressure losses of a few psi within the storage beds. Full cycle temperature behavior is shown in Figure 2.

TURBOMACHINERY AND CYCLE SELECTION

As the study involved conceptual design of a plant based on commercially available machinery, subcontract arrangements were made with an industrial equipment manufacturer having suitable product lines. The Clark Division of Dresser Industries collaborated in both the development of cycle parameters representative of available technology and identification of suitable machinery.

A combination of axial and centrifugal compressors was selected for the two-stage study cycle following analysis of several machinery arrangements. Axial machinery was selected for the first compression stage, with three machines required. Arrangements with two machines in series were not capable of achieving desired output conditions whereas a two-into-one arrangement was found to achieve desired efficiency and exit conditions. Barrel type centrifugals were selected for the second stage of compression. Casing and rotor material modifications are required for the high-temperature machines, but these are considered well within the limits of present commercial technology and typical of orders for special applications.

The turbine section incorporates all axial machinery with a tandem low pressure turbine arrangement. Machinery selections were made on the basis of maximum efficiency. As a result, turbine section flow rate was increased over that of the compressor section by 20 percent (650 to 780 lbs/sec). This reduced clearance losses in the high pressure turbine, allowing prediction of 85 percent efficiency (isentropic) for the high pressure machine and 88 percent for each low pressure machine.

PERFORMANCE

The machinery selections and thermal storage system configurations are projected to perform as shown in Tables 2 through 4 for simultaneous operation of 4 units. Cycle analysis stations correspond to the points labelled in Figure 3 - System Flow Diagram. Table 2 shows air conditions at various points of the cycle at the mean point of cycle performance, which was taken as the base condition. Table 3 shows conditions which exist at the beginning of a discharge cycle and extend through the early operating period. Table 4 represents discharge conditions in the last few minutes of an operating cycle. Base condition plant output is 800 MW allowing for house loads, with an electric energy ratio $(\text{EER} = \frac{\text{Charging kWh}}{\text{Generation kWh}})$ of 1.48, including air leakage from storage.

Part-load turbine performance is projected in Tables 5 and 6, for 75 percent and 50 percent turbine flow. Power outputs for these conditions are 570 MW (72 percent) and 343 MW (43 percent), while electric energy ratios are 1.54 and 1.72 respectively. Turbine operating range is zero to 100 percent at rated conditions. Nearly linear performance is projected from the zero output flow condition of about 20 percent of rated flow (Figure 4).

Part-load compressor operation is possible by adjustment of variable inlet guide vanes at the inlet to the first low-pressure stage compressors. Available range at the design condition of 90°F ambient is approximately 63 to 104 percent of design flow (Figure 5). Compressor section efficiency at minimum flow is 91 percent of the design point efficiency. As inlet air preheating to 90°F (using a section of the trim cooler) is required to maintain exit temperature and limit discharge pressure with reductions in ambient temperature, this range is available at all times of the year.

PLANT LAYOUT

The plant arrangement is based upon the layout developed for the PEPCO fuel-fired CAES study. Figure 6 is a site arrangement plan for the adiabatic plant. The most noticeable differences between this arrangement and the PEPCO design (Figure 7) are the lack of both fuel storage tanks and the large air-cooled exchanger area required for the fuel-fired design. Turbomachinery hall arrangement (Figure 8) differs from the PEPCO design in that the centrifugal compressors are driven by a separate motor. As the centrifugal train occupies an area used to enclose compressor intercoolers in the fired design, no significant building changes were required.

Table 2

CAES PLANT THERMODYNAMIC ANALYSIS
ACAES STUDY - PNL
ACAES DESIGN POINT

COMPRESSION

COMPONENT NO.	1	2	3	4	5	6	7	8	9	10	11
COMP. NAME	INLET	COMPR	PIPE	COMPR	PIPE	VALVE	PIPE	HEATX	PIPE	VALVE	PIPE
FLOW, LB/S	2600.0	2600.0	2600.0	2600.0	2600.0	2600.0	2600.0	2600.0	2600.0	2600.0	2600.0
TEMP, F	90.0	494.6	494.6	877.9	877.9	877.9	877.9	455.0	455.0	455.0	455.0
PRES, PSIA	14.2	78.0	77.8	221.3	220.7	220.7	221.2	216.2	214.1	214.1	213.7
H, BTU/LB	131.5	229.5	229.8	327.5	327.5	327.5	327.5	219.6	219.6	219.6	219.6

COMPONENT NO.	12	13	14	15	16	17	18	19	20	21
COMP. NAME	PIPE	HEATX	COMPR	PIPE	COMPR	PIPE	VALVE	PIPE	HEATX	PIPE
FLOW, LB/S	2600.0	2600.0	2600.0	2600.0	2600.0	2600.0	2600.0	2600.0	2600.0	2600.0
TEMP, F	455.0	236.0	461.4	461.4	830.0	830.0	830.0	830.0	125.0	125.0
PRES, PSIA	210.2	206.2	453.5	452.5	1216.3	1201.3	1201.2	1201.5	1209.5	1263.0
H, BTU/LB	219.6	165.6	220.9	220.9	315.4	315.4	315.4	315.4	133.7	133.5

GENERATION

COMPONENT NO.	22	23	24	25	26	27	28	29	30	31	32
COMP. NAME	CAVRN	HEATX	PIPE	HEATX	PIPE	VALVE	PIPE	PIPE	VALVE	TURBN	PIPE
FLOW, LB/S	3120.0	3120.0	3120.0	3120.0	3120.0	3120.0	3120.0	3120.0	3120.0	3120.0	3120.0
TEMP, F	125.0	100.0	100.0	805.0	805.0	805.0	805.0	805.0	805.0	437.9	437.9
PRES, PSIA	1263.0	1263.0	1188.4	1184.4	1148.4	1148.3	1125.7	1125.2	1110.6	237.9	237.5
H, BTU/LB	133.5	126.9	127.3	308.8	308.8	308.8	308.9	308.9	308.9	215.3	215.3

COMPONENT NO.	33	34	35	36	37	38	39	40	41
COMP. NAME	VALVE	PIPE	HEATX	PIPE	VALVE	PIPE	PIPE	VALVE	TURBN
FLOW, LB/S	3120.0	3120.0	3120.0	3120.0	3120.0	3120.0	3120.0	3120.0	3120.0
TEMP, F	437.9	437.9	862.0	862.0	862.0	862.0	862.0	860.0	237.6
PRES, PSIA	237.5	238.5	233.5	232.3	232.3	231.5	231.0	229.0	15.2
H, BTU/LB	215.3	215.3	323.3	323.3	323.3	323.3	323.3	323.3	166.9

COMPRESSOR POWER,	MW
1	276.61
2	274.76
3	156.07
4	266.36
TOTAL	973.79

MOISTURE REMOVED,	LB/S
1	0.00
2	0.00
3	0.00
4	0.00
TOTAL	0.00

TURBINE POWER,	MW
1	300.26
2	501.93
3	0.00
4	0.00
TOTAL	802.20

FUEL CONSUMPTION,	LB/S
1	0.00
2	0.00
3	0.00
4	0.00
TOTAL	0.00

SUMMARY: DAILY STORAGE CYCLE

ELECTRIC ENERGY RATIO (KWHR IN/KWHR OUT) = 1.477
SPECIFIC FUEL CONSUMPTION, BTU/KWHR = 0.0
"ROUNDTRIP" HEAT RATE, BTU/KWHR = 14773.7
HEATING VALUE OF FUEL, BTU/LB = 0.0
AIR STORED, M LB/DAY = 93,600
AIR LEAKAGE, MM LB/DAY = 1.310

COMPRESSION TIME/GENERATION TIME = 1.22
AIR FLOW TO STORAGE CAVERN, LB/S = 2600.0
AIR FLOW FROM STORAGE CAVERN, LB/S = 3120.0
STORAGE PRESSURE, PSIA = 1263.0
COMPRESSION TIME, HRS = 10.00

Table 3

CAES PLANT THERMODYNAMIC ANALYSIS
ACAES STUDY - PNL
DISCHARGE BEGINNING

COMPRESSION

COMPONENT NO.	1	2	3	4	5	6	7	8	9	10	11
COMP. NAME	INLET	COMPR	PIPE	COMPR	PIPE	VALVE	PIPE	HEATX	PIPE	VALVE	PIPE
FLOW, LB/S	2600.0	2600.0	2600.0	2600.0	2600.0	2600.0	2600.0	2600.0	2600.0	2600.0	2600.0
TEMP, F	90.0	494.6	494.6	877.9	877.9	877.9	877.9	455.0	455.0	455.0	455.0
PRES, PSIA	14.2	78.0	77.8	221.3	220.7	220.7	221.2	216.2	214.1	214.1	213.7
H, BTU/LB	131.5	229.5	229.8	327.5	327.5	327.5	327.5	219.6	219.6	219.6	219.6

COMPONENT NO.	12	13	14	15	16	17	18	19	20	21
COMP. NAME	PIPE	HEATX	COMPR	PIPE	COMPR	PIPE	VALVE	PIPE	HEATX	PIPE
FLOW, LB/S	2600.0	2600.0	2600.0	2600.0	2600.0	2600.0	2600.0	2600.0	2600.0	2600.0
TEMP, F	455.0	236.0	461.4	461.4	830.0	830.0	830.0	830.0	125.0	125.0
PRES, PSIA	210.2	206.2	453.5	452.5	1216.3	1201.3	1201.2	1213.5	1209.5	1263.0
H, BTU/LB	219.6	165.6	220.9	220.9	315.4	315.4	315.4	315.4	133.7	133.5

GENERATION

COMPONENT NO.	22	23	24	25	26	27	28	29	30	31	32
COMP. NAME	CAVRN	HEATX	PIPE	HEATX	PIPE	VALVE	PIPE	PIPE	VALVE	TURBN	PIPE
FLOW, LB/S	3120.0	3120.0	3120.0	3120.0	3120.0	3120.0	3120.0	3120.0	3120.0	3120.0	3120.0
TEMP, F	125.0	100.0	100.0	830.0	830.0	830.0	830.0	830.0	830.0	456.3	456.3
PRES, PSIA	1263.0	1263.0	1188.4	1184.4	1148.6	1148.4	1125.4	1124.9	1110.1	237.8	237.4
H, BTU/LB	133.5	126.9	127.3	315.4	315.4	315.4	315.4	315.4	315.4	219.9	219.9

COMPONENT NO.	33	34	35	36	37	38	39	40	41
COMP. NAME	VALVE	PIPE	HEATX	PIPE	VALVE	PIPE	PIPE	VALVE	TURBN
FLOW, LB/S	3120.0	3120.0	3120.0	3120.0	3120.0	3120.0	3120.0	3120.0	3120.0
TEMP, F	456.3	456.3	877.0	877.0	877.0	877.0	877.0	877.0	246.1
PRES, PSIA	237.5	238.3	233.3	232.1	232.1	231.3	230.8	228.8	15.2
H, BTU/LB	219.9	219.9	327.2	327.2	327.2	327.2	327.2	327.2	168.9

COMPRESSOR POWER, MW	
1	276.61
2	274.76
3	156.07
4	266.36
TOTAL	973.79

MOISTURE REMOVED, LB/S	
1	0.00
2	0.00
3	0.00
4	0.00
TOTAL	0.00

TURBINE POWER, MW	
1	306.45
2	507.83
3	0.00
4	0.00
TOTAL	814.28

FUEL CONSUMPTION, LB/S	
1	0.00
2	0.00
3	0.00
4	0.00
TOTAL	0.00

SUMMARY: DAILY STORAGE CYCLE

ELECTRIC ENERGY RATIO (KWHR IN/KWHR OUT) = 1.455
SPECIFIC FUEL CONSUMPTION, BTU/KWHR = 0.0
"ROUNDTRIP" HEAT RATE, BTU/KWHR = 14554.5
HEATING VALUE OF FUEL, BTU/LB = 0.0
AIR STORED, M LB/DAY = 93,600
AIR LEAKAGE, MM LB/DAY = 1.310

COMPRESSION TIME/GENERATION TIME = 1.22
AIR FLOW TO STORAGE CAVERN, LB/S = 2600.0
AIR FLOW FROM STORAGE CAVERN, LB/S = 3120.0
STORAGE PRESSURE, PSIA = 1263.0
COMPRESSION TIME, HRS = 10.00

Table 4

CAES PLANT THERMODYNAMIC ANALYSIS
ACAES STUDY - PNL
DISCHARGE ENDING

COMPRESSION

COMPONENT NO.	1	2	3	4	5	6	7	8	9	10	11
COMP. NAME	INLET	COMPR	PIPE	COMPR	PIPE	VALVE	PIPE	HEATX	PIPE	VALVE	PIPE
FLOW, LB/S	2600.0	2600.0	2600.0	2600.0	2600.0	2600.0	2600.0	2600.0	2600.0	2600.0	2600.0
TEMP, F	90.0	494.6	494.6	877.9	877.9	877.9	877.9	455.0	455.0	455.0	455.0
PRES, PSIA	14.2	78.0	77.8	221.3	220.7	220.7	221.2	216.2	214.1	214.1	213.7
H, BTU/LB	131.5	229.8	229.8	327.5	327.5	327.5	327.5	219.6	219.6	219.6	219.6

COMPONENT NO.	12	13	14	15	16	17	18	19	20	21
COMP. NAME	PIPE	HEATX	COMPR	PIPE	COMPR	PIPE	VALVE	PIPE	HEATX	PIPE
FLOW, LB/S	2600.0	2600.0	2600.0	2600.0	2600.0	2600.0	2600.0	2600.0	2600.0	2600.0
TEMP, F	455.0	236.0	461.4	461.4	830.0	830.0	830.0	830.0	125.0	125.0
PRES, PSIA	210.2	206.2	453.5	452.5	1216.3	1201.3	1201.2	1213.5	1209.5	1263.0
H, BTU/LB	219.6	165.6	220.9	220.9	315.4	315.4	315.4	315.4	133.7	133.5

GENERATION

COMPONENT NO.	22	23	24	25	26	27	28	29	30	31	32
COMP. NAME	CAVRN	HEATX	PIPE	HEATX	PIPE	VALVE	PIPE	PIPE	VALVE	TURBN	PIPE
FLOW, LB/S	3120.0	3120.0	3120.0	3120.0	3120.0	3120.0	3120.0	3120.0	3120.0	3120.0	3120.0
TEMP, F	125.0	100.0	100.0	548.0	548.0	548.0	548.0	548.0	548.0	250.7	250.7
PRES, PSIA	1263.0	1263.0	1188.4	1184.4	1145.5	1145.4	1127.4	1126.9	1115.3	238.9	238.6
H, BTU/LB	133.5	126.9	127.3	242.6	242.6	242.6	242.6	242.6	242.6	169.1	169.1

COMPONENT NO.	33	34	35	36	37	38	39	40	41
COMP. NAME	VALVE	PIPE	HEATX	PIPE	VALVE	PIPE	PIPE	VALVE	TURBN
FLOW, LB/S	3120.0	3120.0	3120.0	3120.0	3120.0	3120.0	3120.0	3120.0	3120.0
TEMP, F	250.7	250.7	708.0	708.0	708.0	708.0	708.0	708.0	151.1
PRES, PSIA	238.6	240.2	235.2	233.9	233.9	233.2	232.7	230.7	15.2
H, BTU/LB	169.1	169.1	283.6	283.6	283.6	283.6	283.6	283.6	146.1

COMPRESSOR POWER, MW		MOISTURE REMOVED, LB/S		TURBINE POWER, MW		FUEL CONSUMPTION, LB/S	
1	276.61	1	0.00	1	235.73	1	0.00
2	274.76	2	0.00	2	441.23	2	0.00
3	156.07	3	0.00	3	0.00	3	0.00
4	266.36	4	0.00	4	0.00	4	0.00
TOTAL	973.79	TOTAL	0.00	TOTAL	676.95	TOTAL	0.00

SUMMARY: DAILY STORAGE CYCLE

ELECTRIC ENERGY RATIO (KWHR IN/KWHR OUT) = 1.751
SPECIFIC FUEL CONSUMPTION, BTU/KWHR = 0.0
"ROUNDTRIP" HEAT RATE, BTU/KWHR = 17507.0
HEATING VALUE OF FUEL, BTU/LB = 0.0
AIR STORED, M LB/DAY = 93,600
AIR LEAKAGE, MM LB/DAY = 1.310

COMPRESSION TIME/GENERATION TIME = 1.22
AIR FLOW TO STORAGE CAVERN, LB/S = 2600.0
AIR FLOW FROM STORAGE CAVERN, LB/S = 3120.0
STORAGE PRESSURE, PSIA = 1263.0
COMPRESSION TIME, HRS = 10.00

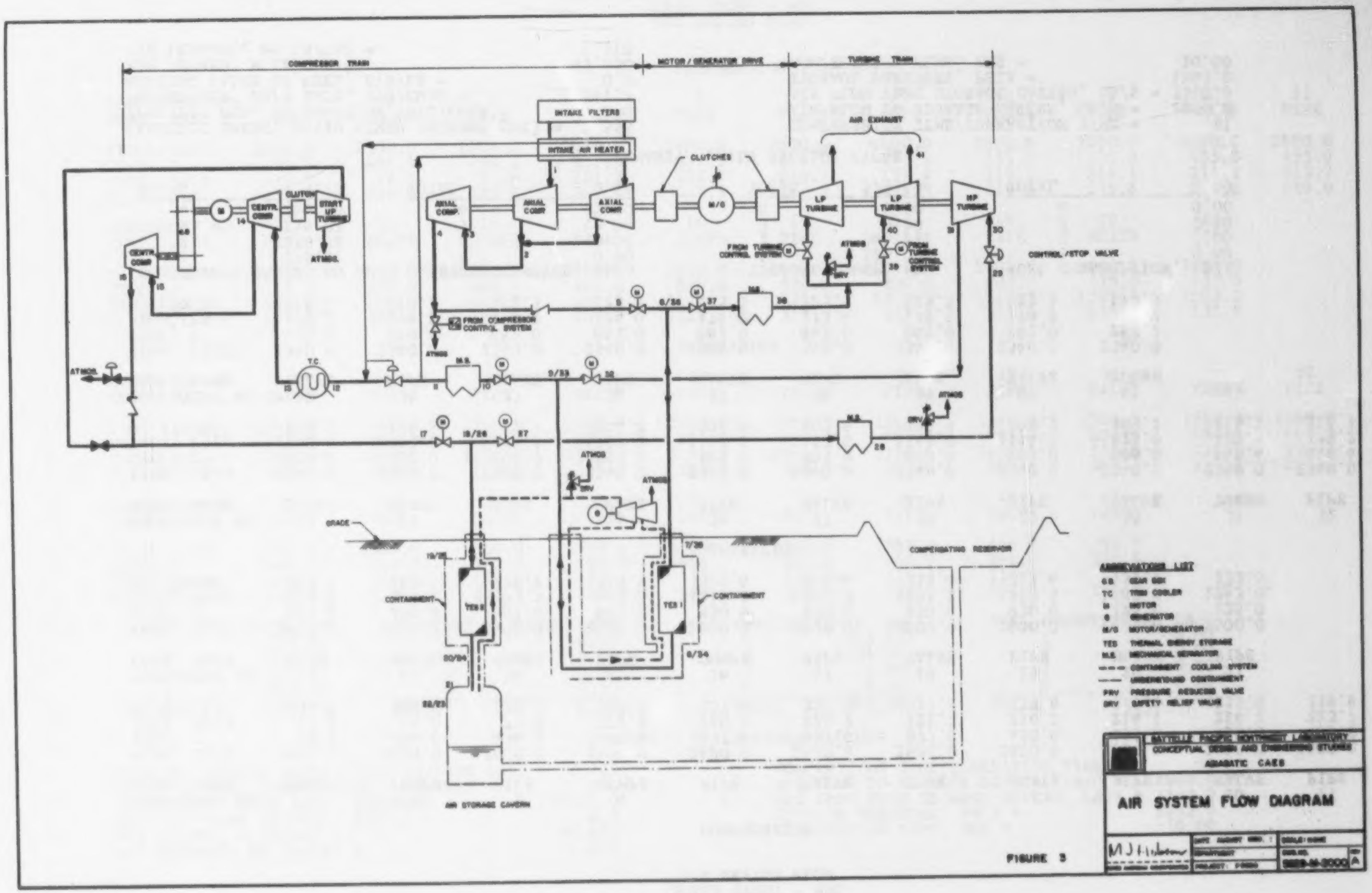
COMPRESSOR TRAIN
MOTOR / GENERATOR DRIVE
TURBINE TRAIN
INTAKE FILTERS
INTAKE AIR HEATER
CLUTCHES
AIR EXHAUST
CENTR. COMP
G.B.
M
CENTR. COMP
CLUTCH
START UP TURBINE
ATMOS.
AXIAL COMP.
AXIAL COMP
AXIAL COMP
M/G
LP TURBINE
LP TURBINE
HP TURBINE
FROM TURBINE CONTROL SYSTEM
FROM TURBINE CONTROL SYSTEM
FROM COMPRESSOR CONTROL SYSTEM
CONTROL / STOP VALVE
SRV
ATMOS
T.C.
M.S.
GRADE
COMPENSATING RESERVOIR
CONTAINMENT
TES 2
TES 1
AIR STORAGE CAVERN
1
2
3
4
5
6/36
37
38
39
40
41
31
30
29
28
9/33
32
10
11
12
13
14
15
16
17
19/26
27
19/25
20/24
21
22/23
7/35
8/34
ABBREVIATIONS LIST
G.B. GEAR BOX
TC TRIM COOLER
M MOTOR
G GENERATOR
M/G MOTOR/GENERATOR
TES THERMAL ENERGY STORAGE
M.S. MECHANICAL SEPARATOR
CONTAINMENT COOLING SYSTEM
UNDERGROUND CONTAINMENT
PRV PRESSURE REDUCING VALVE
SRV SAFETY RELIEF VALVE
BATTELLE PACIFIC NORTHWEST LABORATORY
CONCEPTUAL DESIGN AND ENGINEERING STUDIES
ADIABATIC CAES
AIR SYSTEM FLOW DIAGRAM
MJ Hiblum
DATE AUGUST
DEPARTMENT
PROJECT
SCALE: NONE
DWG. NO.
REV
A

FIGURE 3

Table 5

CAES PLANT THERMODYNAMIC ANALYSIS
ACAES STUDY - PNL
75% DESIGN FLOW

```
                                             COMPRESSION

COMPONENT NO.      1        2        3        4        5        6        7        8        9       10       11
COMP. NAME       INLET    COMPR    PIPE     COMPR    PIPE     VALVE    PIPE     HEATX    PIPE     VALVE    PIPE

FLOW, LB/S      2600.0   2600.0   2600.0   2600.0   2600.0   2600.0   2600.0   2600.0   2600.0   2600.0   2600.0
TEMP, F           90.0    494.6    494.6    877.9    877.9    877.9    877.9    455.0    455.0    455.0    455.0
PRES, PSIA        14.2     78.0     77.8    221.3    220.7    220.7    221.2    216.2    214.1    214.1    213.7
H, BTU/LB        131.5    229.8    229.8    327.5    327.5    327.5    327.5    219.6    219.6    219.6    219.6

COMPONENT NO.     12       13       14       15       16       17       18       19       20       21
COMP. NAME       PIPE     HEATX    COMPR    PIPE     COMPR    PIPE     VALVE    PIPE     HEATX    PIPE

FLOW, LB/S      2600.0   2600.0   2600.0   2600.0   2600.0   2600.0   2600.0   2600.0   2600.0   2600.0
TEMP, F          455.0    236.0    461.4    461.4    830.0    830.0'   830.0    830.0    125.0    125.0
PRES, PSIA       210.2    206.2    453.5    452.5   1216.3   1201.3   1201.2   1213.5   1209.5   1263.0
H, BTU/LB        219.6    165.6    220.9    220.9    315.4    315.4    315.4    315.4    133.7    133.5

                                             GENERATION

COMPONENT NO.     22       23       24       25       26       27       28       29       30       31       32
COMP. NAME       CAVRN    HEATX    PIPE     HEATX    PIPE     VALVE    PIPE     PIPE     VALVE    TURBN    PIPE

FLOW, LB/S      2340.0   2340.0   2340.0   2340.0   2340.0   2340.0   2340.0   2340.0   2340.0   2340.0   2340.0
TEMP, F          125.0    100.0    100.0    805.0    805.0    805.0    805.0    805.0    805.0    440.4    440.4
PRES, PSIA      1263.0   1263.0   1191.6   1187.6   1157.6   1157.6   1145.0   1144.5    825.0    179.5    179.2
H, BTU/LB        133.5    126.9    127.2    308.8    308.8    308.8    308.9    308.9    309.2    216.1    216.1

COMPONENT NO.     33       34       35       36       37       38       39       40       41
COMP. NAME       VALVE    PIPE     HEATX    PIPE     VALVE    PIPE     PIPE     VALVE    TURBN

FLOW, LB/S      2340.0   2340.0   2340.0   2340.0   2340.0   2340.0   3340.0   2340.0   2340.0
TEMP, F          440.4    440.4    862.0    862.0    862.0    862.0    862.0    862.0    288.7
PRES, PSIA       179.2    179.9    174.9    174.0    174.0    173.4    172.9    170.9     15.2
H, BTU/LB        216.1    216.1    323.3    323.3    323.3    323.3    323.3    323.3    179.3

 COMPRESSOR POWER, MW    MOISTURE REMOVED, LB/S          TURBINE POWER, MW      FUEL CONSUMPTION, LB/S
     1          276.61          1            0.00          1         224.09          1              0.00
     2          274.76          2            0.00          2         346.51          2              0.00
     3          156.07          3            0.00          3           0.00          3              0.00
     4          266.36          4            0.00          4           0.00          4              0.00
 ----------------------  -------------------------       ------------------     ------------------------
 TOTAL          973.79   TOTAL               0.00        TOTAL       570.60     TOTAL               0.00

                                   SUMMARY:  DAILY STORAGE CYCLE

ELECTRIC ENERGY RATIO (KWHR IN/KWHR OUT) =  1.558       COMPRESSION TIME/GENERATION TIME =       .91
SPECIFIC FUEL CONSUMPTION, BTU/KWHR =         0.0       AIR FLOW TO STORAGE CAVERN, LB/S =    2600.0
"ROUNDTRIP" HEAT RATE, BTU/KWHR =         15577.7       AIR FLOW FROM STORAGE CAVERN, LB/S =  2340.0
HEATING VALUE OF FUEL, BTU/LB =               0.0       STORAGE PRESSURE, PSIA =              1263.0
AIR STORED, M LB/DAY =                     93,600       COMPRESSION TIME, HRS =                10.00
AIR LEAKAGE, MM LB/DAY =                    1.310
```

Table 6

CAES PLANT THERMODYNAMIC ANALYSIS
ACAES STUDY - PNL
50% DESIGN FLOW

COMPRESSION

COMPONENT NO.	1	2	3	4	5	6	7	8	9	10	11
COMP. NAME	INLET	COMPR	PIPE	COMPR	PIPE	VALVE	PIPE	HEATX	PIPE	VALVE	PIPE
FLOW, LB/S	2600.0	2600.0	2600.0	2600.0	2600.0	2600.0	2600.0	2600.0	2600.0	2600.0	2600.0
TEMP, F	90.0	494.6	494.6	877.9	877.9	877.9	877.9	455.0	455.0	455.0	455.0
PRES, PSIA	14.2	78.0	77.8	221.3	220.7	220.7	221.2	216.2	214.1	214.1	213.7
H, BTU/LB	131.5	229.8	229.8	327.5	327.5	327.5	327.5	219.6	219.6	219.6	219.6

COMPONENT NO.	12	13	14	15	16	17	18	19	20	21
COMP. NAME	PIPE	HEATX	COMPR	PIPE	COMPR	PIPE	VALVE	PIPE	HEATX	PIPE
FLOW, LB/S	2600.0	2600.0	2600.0	2600.0	2600.0	2600.0	2600.0	2600.0	2600.0	2600.0
TEMP, F	455.0	236.0	461.4	461.4	830.0	830.0	830.0	830.0	125.0	125.0
PRES, PSIA	210.2	206.2	453.5	452.5	1216.3	1201.3	1201.2	1213.5	1209.5	1263.0
H, BTU/LB	219.6	165.6	220.9	220.9	315.4	315.4	315.4	315.4	133.7	133.5

GENERATION

COMPONENT NO.	22	23	24	25	26	27	28	29	30	31	32
COMP. NAME	CAVRN	HEATX	PIPE	HEATX	PIPE	VALVE	PIPE	PIPE	VALVE	TURBN	PIPE
FLOW, LB/S	1560.0	1560.0	1560.0	1560.0	1560.0	1560.0	1560.0	1560.0	1560.0	1560.0	1560.0
TEMP, F	125.0	100.0	100.0	805.0	805.0	805.0	805.0	805.0	805.0	444.0	444.0
PRES, PSIA	1263.0	1263.0	1193.9	1189.9	1164.2	1164.2	1158.6	1158.1	550.0	122.3	122.1
H, BTU/LB	133.5	126.9	127.2	308.8	308.8	308.8	308.8	308.8	308.7	217.1	217.1

COMPONENT NO.	33	34	35	36	37	38	39	40	41
COMP. NAME	VALVE	PIPE	HEATX	PIPE	VALVE	PIPE	PIPE	VALVE	TURBN
FLOW, LB/S	1560.0	1560.0	1560.0	1560.0	1560.0	1560.0	1560.0	1560.0	1560.0
TEMP, F	444.0	444.0	862.0	862.0	862.0	862.0	862.0	862.0	375.4
PRES, PSIA	122.1	122.6	117.6	117.0	117.0	116.6	116.1	114.1	15.2
H, BTU/LB	217.1	217.1	323.2	323.2	323.2	323.2	323.2	323.2	200.5

COMPRESSOR POWER, MW	
1	276.61
2	274.76
3	156.07
4	266.36
TOTAL	973.79

MOISTURE REMOVED, LB/S	
1	0.00
2	0.00
3	0.00
4	0.00
TOTAL	0.00

TURBINE POWER, MW	
1	146.93
2	196.93
3	0.00
4	0.00
TOTAL	343.86

FUEL CONSUMPTION, LB/S	
1	0.00
2	0.00
3	0.00
4	0.00
TOTAL	0.00

SUMMARY: DAILY STORAGE CYCLE

ELECTRIC ENERGY RATIO (KWHR IN/KWHR OUT) = 1.723
SPECIFIC FUEL CONSUMPTION, BTU/KWHR = 0.0
"ROUNDTRIP" HEAT RATE, BTU/KWHR = 17233.0
HEATING VALUE OF FUEL, BTU/LB = 0.0
AIR STORED, M LB/DAY = 93,600
AIR LEAKAGE, MM LB/DAY = 1.310

COMPRESSION TIME/GENERATION TIME = .61
AIR FLOW TO STORAGE CAVERN, LB/S = 2600.0
AIR FLOW FROM STORAGE CAVERN, LB/S = 1560.0
STORAGE PRESSURE, PSIA = 1263.0
COMPRESSION TIME, HRS = 10.00

PART LOAD TURBINE SYSTEM OUTPUT

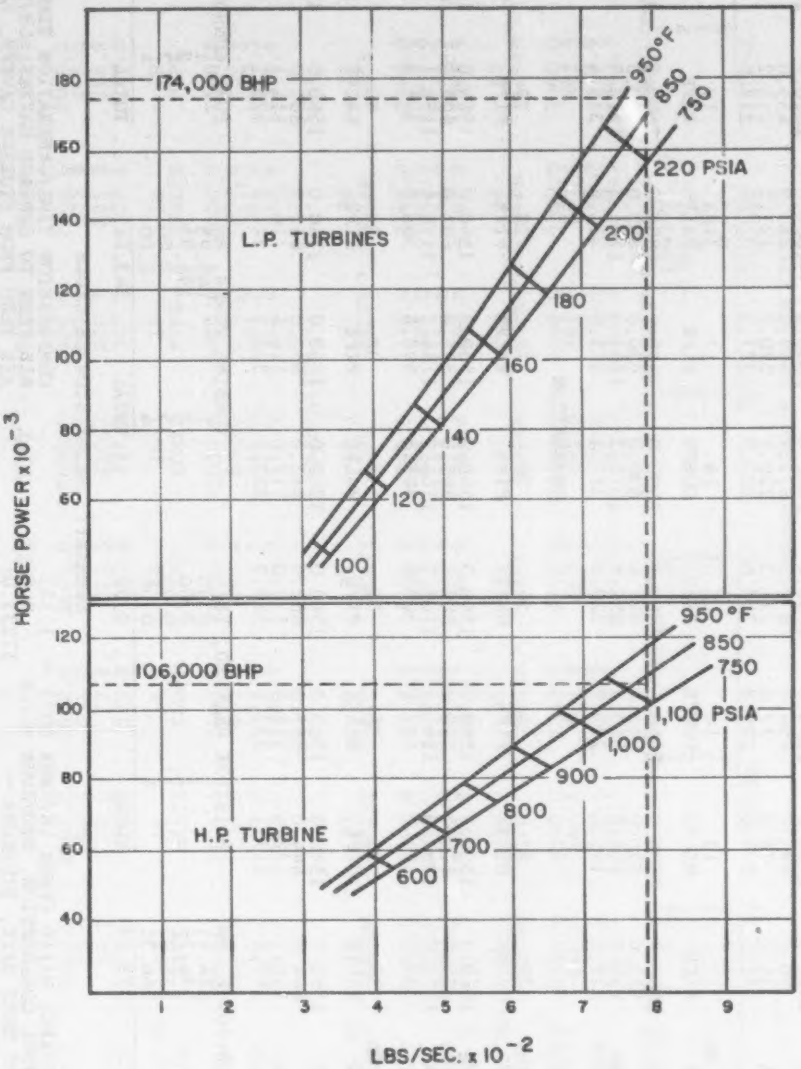

ACRES

BATTELLE PACIFIC NORTHWEST LABORATORY

CONCEPTUAL DESIGN AND
ENGINEERING STUDIES—ADIABATIC CAES

ACRES AMERICAN INCORPORATED

FIGURE 4

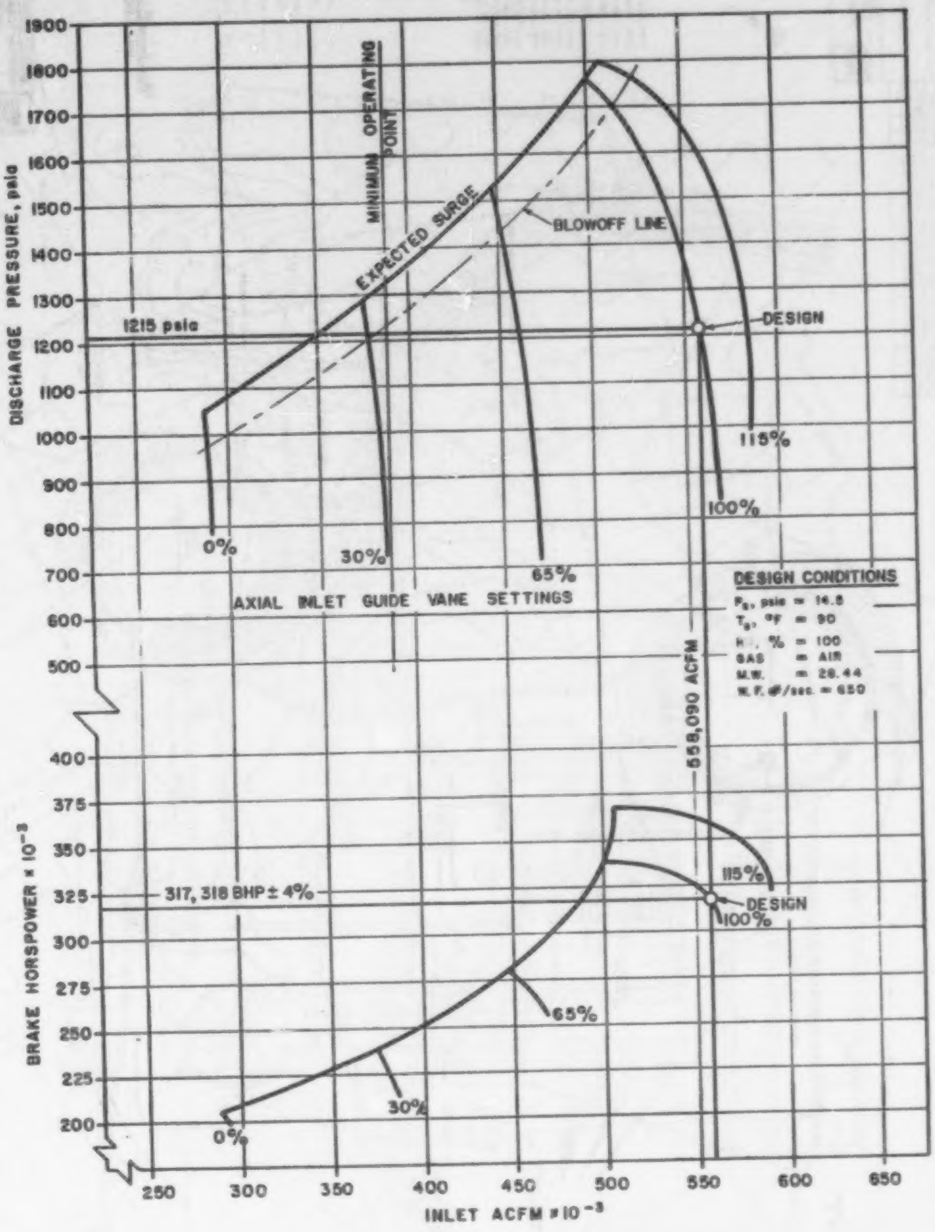

OVERALL COMPRESSOR SYSTEM PERFORMANCE CURVE

ACRES

BATTELLE PACIFIC NORTHWEST LABORATORY

CONCEPTUAL DESIGN AND ENGINEERING STUDIES—ADIABATIC CAES

FIGURE 5

ACRES AMERICAN INCORPORATED

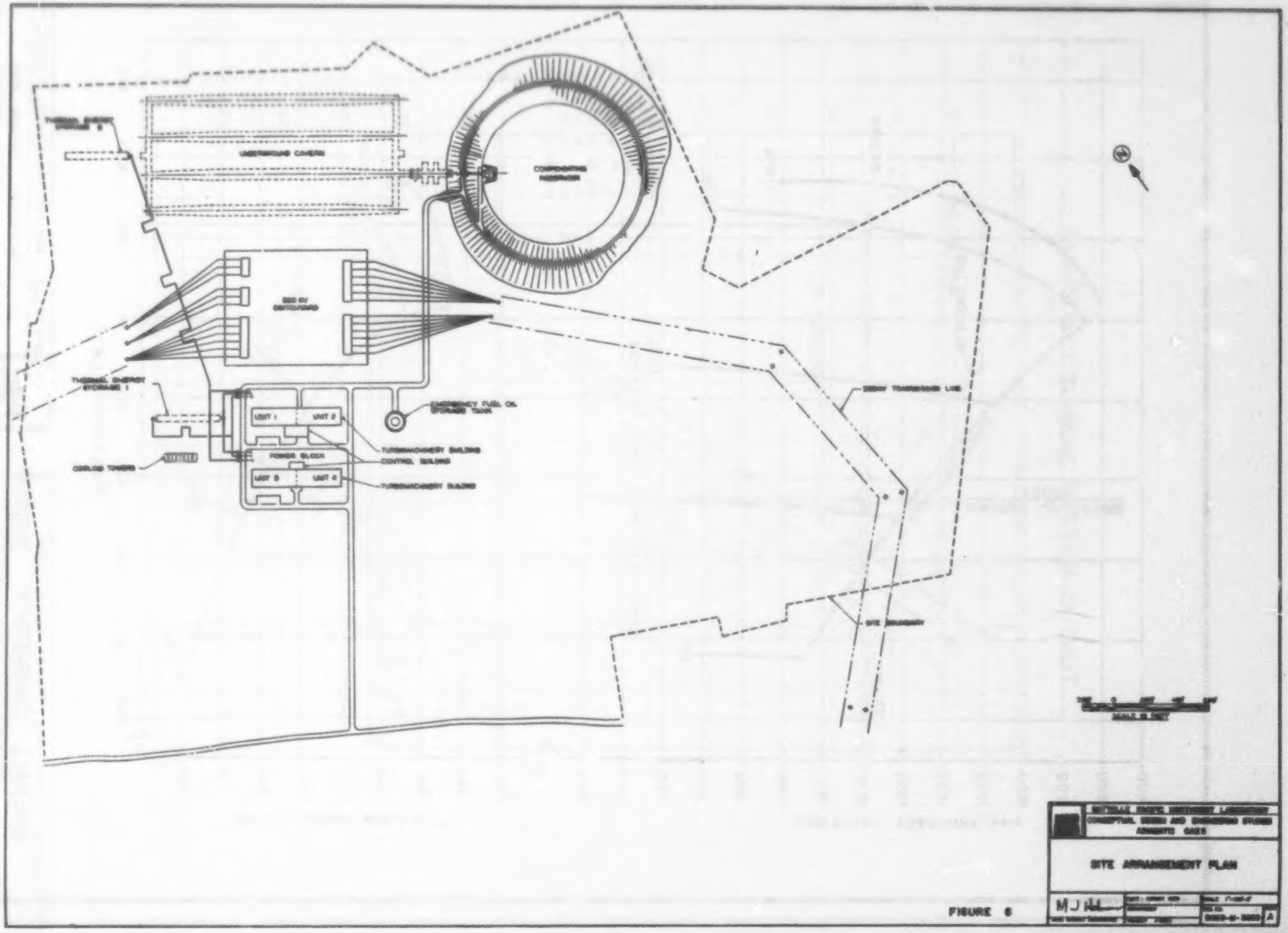
THERMAL ENERGY STORAGE 2
UNDERGROUND CAVERN
COMPENSATING RESERVOIR
500 KV SWITCHYARD
THERMAL ENERGY STORAGE 1
COOLING TOWERS
UNIT 1
UNIT 2
POWER BLOCK
UNIT 3
UNIT 4
TURBOMACHINERY BUILDING
CONTROL BUILDING
TURBOMACHINERY BUILDING
EMERGENCY FUEL OIL STORAGE TANK
500KV TRANSMISSION LINE
SITE BOUNDARY
SCALE IN FEET
BATTELLE PACIFIC NORTHWEST LABORATORY
CONCEPTUAL DESIGN AND ENGINEERING STUDIES
ADIABATIC CAES
SITE ARRANGEMENT PLAN

FIGURE 8

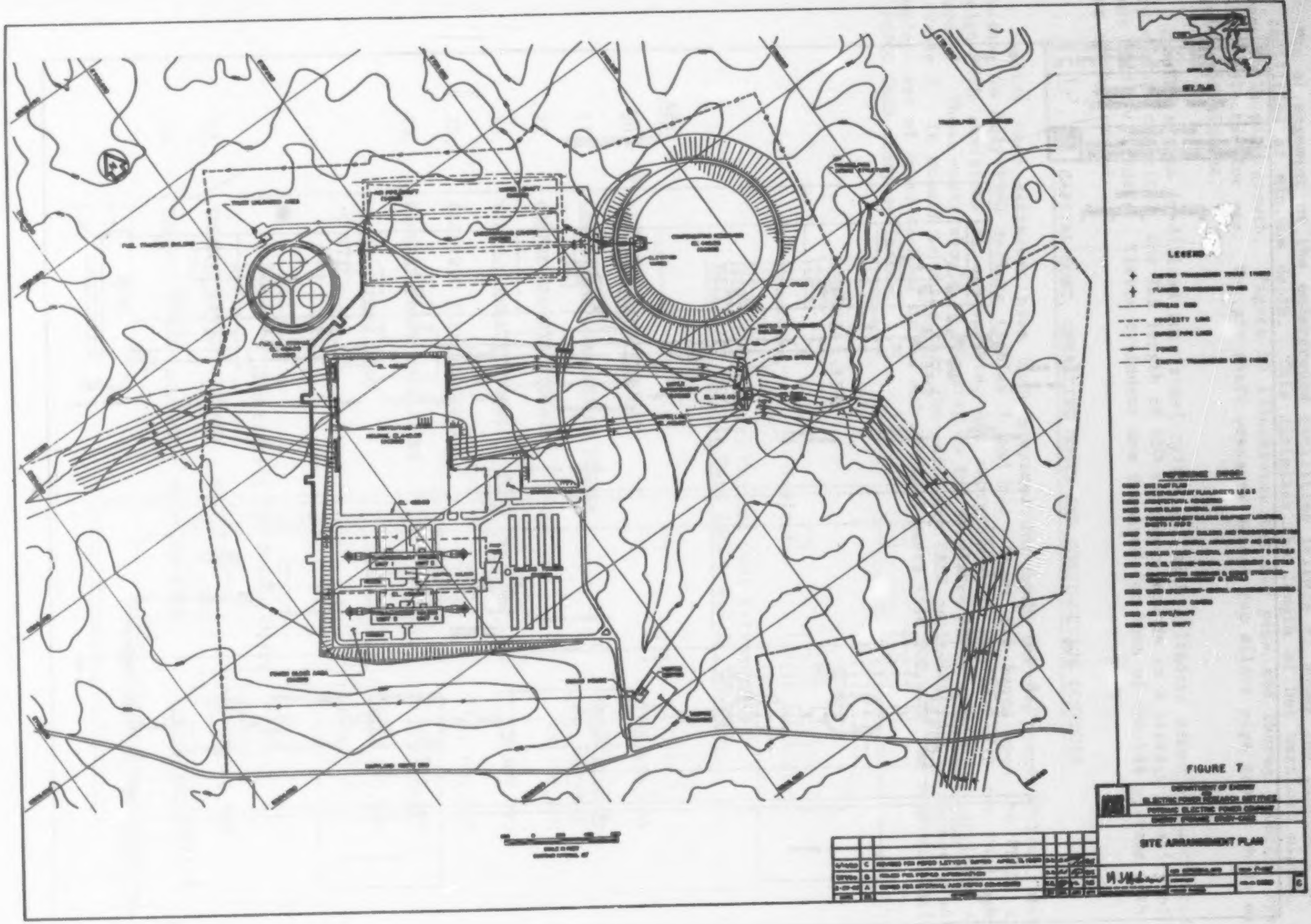
LEGEND
FIGURE 7
DEPARTMENT OF ENERGY
AND
ELECTRIC POWER RESEARCH INSTITUTE
POTOMAC ELECTRIC POWER COMPANY
SITE ARRANGEMENT PLAN

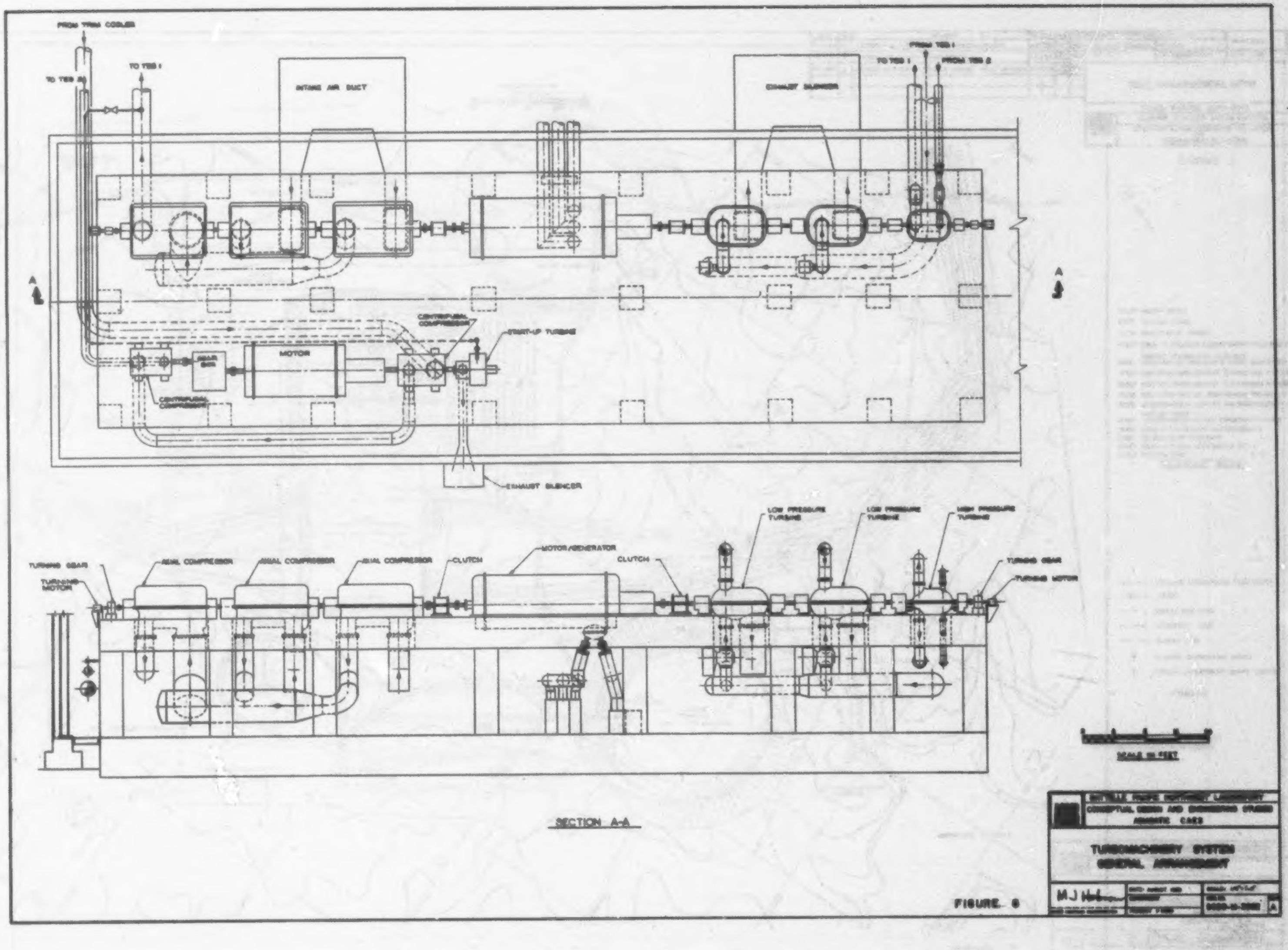
FROM TRIM COOLER
TO TES 2
TO TES 1
INTAKE AIR DUCT
EXHAUST SILENCER
TO TES 1
FROM TES 1
FROM TES 2
A
A
CENTRIFUGAL COMPRESSOR
START-UP TURBINE
MOTOR
CENTRIFUGAL COMPRESSOR
EXHAUST SILENCER
LOW PRESSURE TURBINE
LOW PRESSURE TURBINE
HIGH PRESSURE TURBINE
MOTOR/GENERATOR
TURNING GEAR
TURNING MOTOR
AXIAL COMPRESSOR
AXIAL COMPRESSOR
AXIAL COMPRESSOR
CLUTCH
CLUTCH
TURNING GEAR
TURNING MOTOR
SCALE IN FEET
SECTION A-A
BATTELLE PACIFIC NORTHWEST LABORATORY
CONCEPTUAL DESIGN AND ENGINEERING STUDIES
ADIABATIC CAES
TURBOMACHINERY SYSTEM
GENERAL ARRANGEMENT
M J H
A

FIGURE 8

The arrangement of the underground facilities (Figure 9) shows the placement of the TES facilities at minimum depth. This minimizes the length of hot vertical piping, and consequently pipe growth. Figure 10 illustrates the air pipe and thermal storage system designs selected for use. The air shaft pressure vessel cap allows pipe growth while maintaining containment.

The TES system is divided into steel cylinders, with cylinders added or subtracted to vary storage capacity. The TES length of 420 feet corresponds to a storage capacity of 8.3 hours with 9 cylinders. Eleven cylinders are required for both of the TES systems with 10-hour storage capacity.

CAPITAL COST, OPERATING COSTS AND CONSTRUCTION SCHEDULE

Capital cost estimates have been prepared for both the 8.3- and 10-hour storage designs, in July 1980 dollars (Tables 7 and 8). These are based upon the PEPCO study design with revisions as appropriate, and reorganized to conform with the PNL code of accounts. These costs should be compared to the escalated PEPCO preliminary estimate shown in Table 9. It should be noted that the adiabatic CAES estimates include the cost of one complete set of spare machine rotors and overhaul parts ($14,000,000), an item not included in PEPCO CAES study estimates.

Table 7

Conceptual Capital Cost Estimate
Adiabatic CAES In Hard Rock - 8.3 Hr. Storage

Acct		
20.	LAND AND LAND RIGHTS	$ 16,496,000
21.	GENERATION/COMPRESSION SYSTEM	230,249,000
22.	COMPRESSED AIR STORAGE	55,120,000
23.	THERMAL ENERGY STORAGE - IRON ORE FILL	58,099,000
25.	ELECTRIC PLANT EQUIPMENT	67,094,000
26.	GENERAL PLANT FACILITIES	10,572,000
	DIRECT COST 7/80 COST/KW	$437,630,000 $547

Alternative TES Design Costs

23.	THERMAL ENERGY STORAGE - ROCK FILL	55,590,000
23.	THERMAL ENERGY STORAGE - DENSTONE FILL	110,786,000

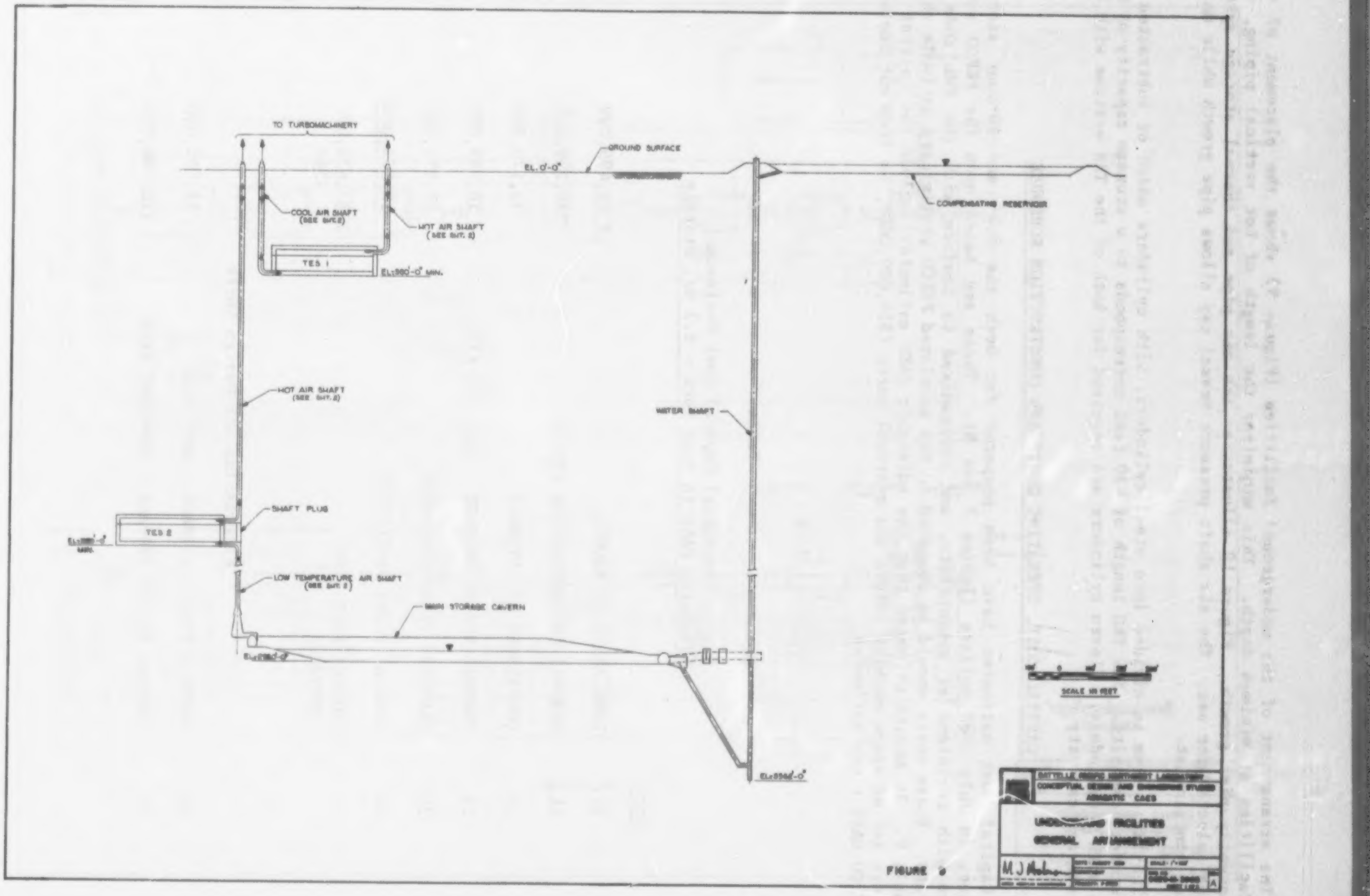
TO TURBOMACHINERY
GROUND SURFACE
EL. 0'-0"
COMPENSATING RESERVOIR
COOL AIR SHAFT (SEE SHT. 2)
HOT AIR SHAFT (SEE SHT. 2)
TES 1
HOT AIR SHAFT (SEE SHT. 2)
WATER SHAFT
SHAFT PLUG
TES 2
MIN.
LOW TEMPERATURE AIR SHAFT (SEE SHT. 2)
MAIN STORAGE CAVERN
SCALE IN FEET
BATTELLE PACIFIC NORTHWEST LABORATORY
CONCEPTUAL DESIGN AND ENGINEERING STUDIES
ADIABATIC CAES
UNDERGROUND FACILITIES
GENERAL ARRANGEMENT
M J Malone
A

FIGURE 9

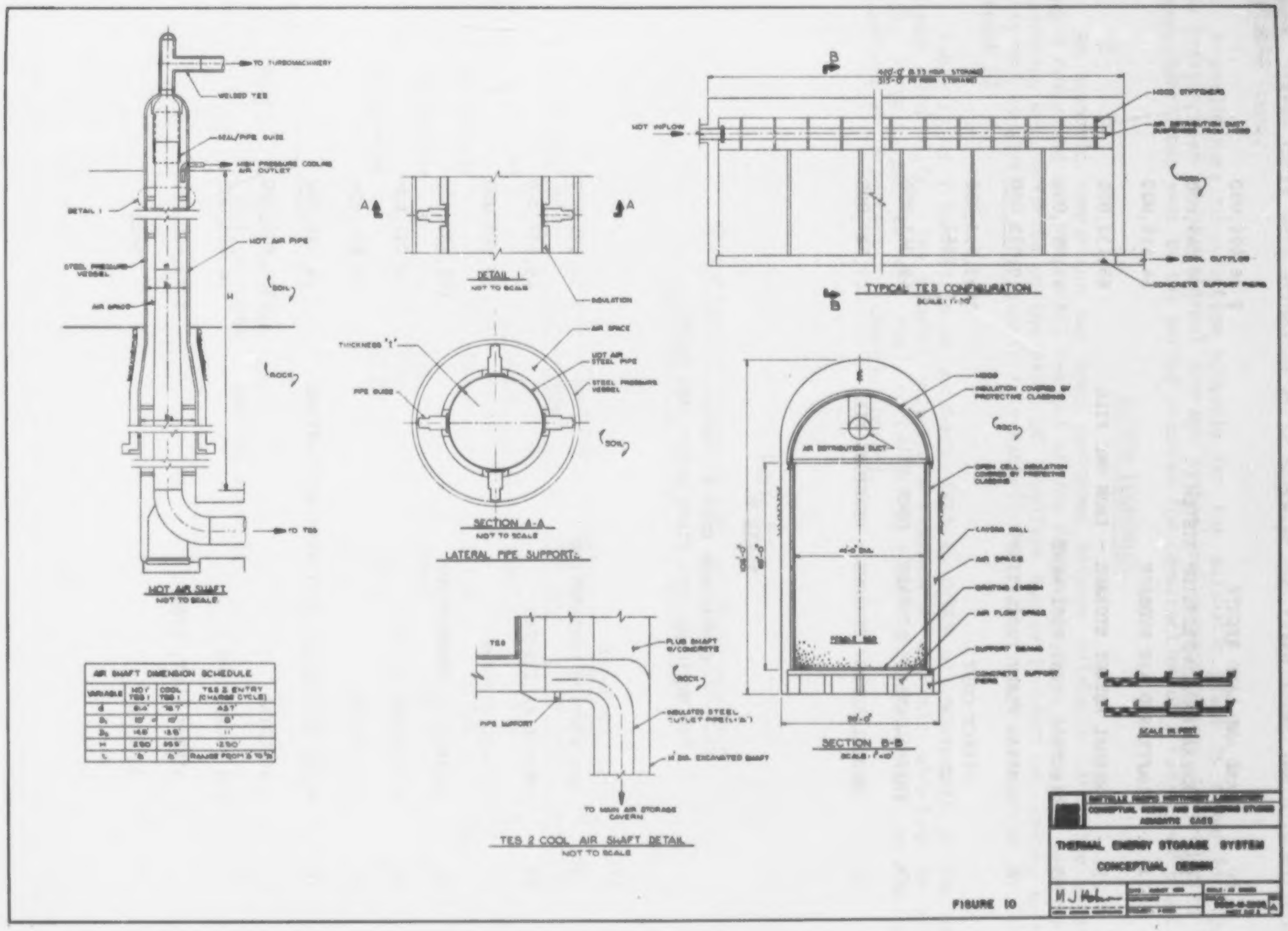
TO TURBOMACHINERY
WELDED TEE
SEAL/PIPE GUIDE
HIGH PRESSURE COOLING AIR OUTLET
DETAIL 1
HOT AIR PIPE
STEEL PRESSURE VESSEL
AIR SPACE
H
SOIL
ROCK
TO TES
HOT AIR SHAFT
NOT TO SCALE
AIR SHAFT DIMENSION SCHEDULE
VARIABLE
HOT TES 1
COOL TES 1
TES 2 ENTRY (CHARGE CYCLE)
d
D1
D2
H
t
RANGE FROM
DETAIL 1
NOT TO SCALE
INSULATION
A
A
THICKNESS 't'
PIPE GUIDE
AIR SPACE
HOT AIR STEEL PIPE
STEEL PRESSURE VESSEL
SOIL
SECTION A-A
NOT TO SCALE
LATERAL PIPE SUPPORT
TES
PLUG SHAFT W/CONCRETE
ROCK
PIPE SUPPORT
INSULATED STEEL OUTLET PIPE
EXCAVATED SHAFT
TO MAIN AIR STORAGE CAVERN
TES 2 COOL AIR SHAFT DETAIL
NOT TO SCALE
B
B
HOT INFLOW
HOOD STIFFENERS
AIR DISTRIBUTION DUCT SUSPENDED FROM HOOD
ROCK
COOL OUTFLOW
CONCRETE SUPPORT PIERS
TYPICAL TES CONFIGURATION
HOOD
INSULATION COVERED BY PROTECTIVE CLADDING
ROCK
AIR DISTRIBUTION DUCT
OPEN CELL INSULATION COVERED BY PROTECTIVE CLADDING
CAVERN WALL
AIR SPACE
GRATING
AIR FLOW SPACE
SUPPORT BEAMS
CONCRETE SUPPORT PIERS
PEBBLE BED
SECTION B-B
SCALE IN FEET
BATTELLE PACIFIC NORTHWEST LABORATORY
CONCEPTUAL DESIGN AND ENGINEERING STUDIES
ADIABATIC CAES
THERMAL ENERGY STORAGE SYSTEM
CONCEPTUAL DESIGN
M J

FIGURE 10

Table 8

BATTELLE - PNL
Adiabatic-CAES in Hard Rock - 10 Hr. Storage

20.	LAND AND LAND RIGHTS	$ 16,496,000
21.	GENERATION/COMPRESSION SYSTEM	230,249,000
22.	COMPRESSED AIR STORAGE	64,410,000
23.	THERMAL ENERGY STORAGE - IRON ORE FILL	65,132,000
25.	ELECTRIC PLANT EQUIPMENT	67,094,000
26.	GENERAL PLANT FACILITIES	10,572,000
	DIRECT COST COST/KW	$453,953,000 $567
23.	THERMAL ENERGY STORAGE - ROCK FILL	62,065,000
23.	THERMAL ENERGY STORAGE - DENSTONE FILL	129,527,000

Table 9

COMPARISON COST ESTIMATE
900 MW/10 HR FUEL FIRED PEPCO CAES PLANT

Acct		
10.	CONSTRUCTION PREPARATION	$ 14,996,000
20.	SURFACE FACILITIES	16,007,000
30.	STORAGE SYSTEMS	58,263,000
40.	GENERATION/COMPRESSION	172,580,000
50.	MECHANICAL B.O.P.	30,751,000
60.	SWITCHYARD	37,814,000
70.	PLANT ELECTRICAL EQUIPMENT AND SYSTEMS	14,498,000
	SUBTOTAL	$344,909,000
	10% ESCALATION	34,491,000
	DIRECT COST, 7/80	$379,400,000
	COST/KW	$422

Operating costs were developed based upon an estimated plant staff of 68 men (fully manned station), maintenance requirements for the turbomachinery and general plant maintenance. These costs were estimated at $2.64/kW-yr for fixed items and 0.19 mills/kWh for variable items.

A preliminary construction schedule for the adiabatic plant is shown in Figure 11. The construction of the thermal storage system and deeper caverns is projected to add approximately one year to the period required for construction of a fuel-fired plant.

SYSTEM ECONOMICS

An economic comparison has been performed between adiabatic CAES, the underground pumped hydro and oil-fired CAES designs of the PEPCO Study and combustion turbines. The evaluation was performed on the basis of levelized energy (production) costs, using fuel costs and escalation rates supplied by Battelle-PNL. The results are shown in Tables 10 through 12.

Table 10 is a comparison of adiabatic CAES to PEPCO oil-fired CAES on the basis of 30-year plant life. The results indicate a substantial economic advantage to adiabatic CAES, largely due to oil fuel cost (at $5.50/10^6 Btu, 1980) and escalation rate (8 percent vs. 7 percent for charging power).

Table 10

Comparison of Adiabatic CAES vs. Oil-Fired CAES

1980 Levelized Busbar Cost (mills/kWh)

		Adiabatic CAES		
Capacity Factor	Oil-Fired CAES 10 hour	10 hour Iron Ore	8.3 hour Iron Ore	10 hour Denstone
10 percent	167.6	160.7	156.6	175.0
15 percent	136.4	123.6	120.9	132.6
20 percent	120.3	104.9	102.5	111.6
25 percent	111.1	87.5	---	92.9

NOTES: 30-year life assumed.
Escalation rates as per PNL directive.

PRELIMINARY ACAES CONSTRUCTION SCHEDULE

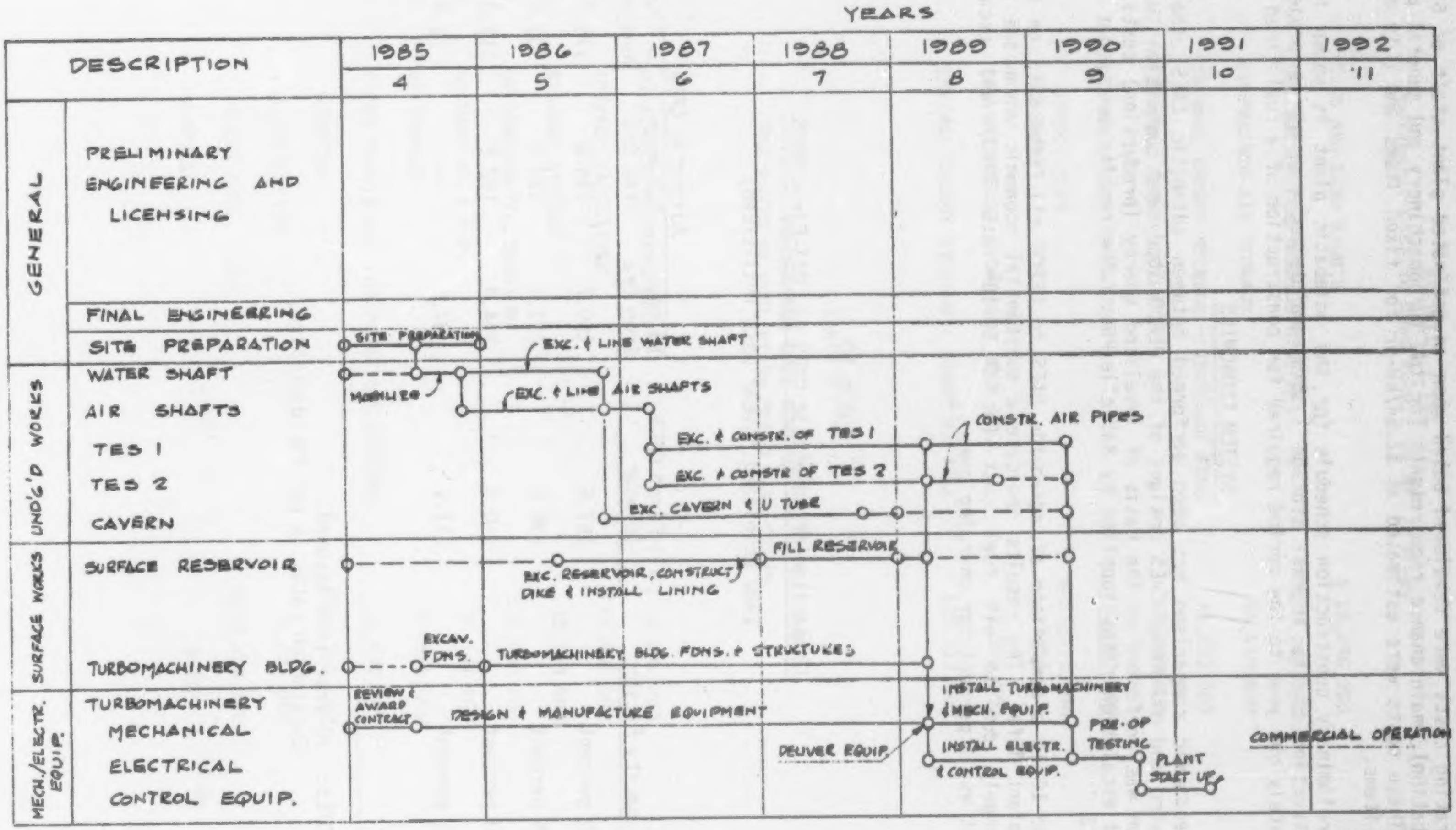

FIGURE 11

Table 11 is a comparison of adiabatic CAES to the PEPCO UPH design on the basis of 50-year plant life. The economy of scale and slightly better efficiency of the UPH design results in a lower production cost throughout the operating range.

Table 11

Comparison of Adiabatic CAES vs. UPH
1980 Levelized Busbar Cost (mills/kWh)

	UPH - 10 Hour		800 MW Adiabatic CAES	
Capacity Factor	2000 MW	1000 MW	10 Hour	8.3 Hour
10 percent	139.7	168.4	170.2	167.7
15 percent	107.6	126.8	130.5	127.8
20 percent	91.0	105.3	109.7	107.5
25 percent	81.6	93.1	97.2	---

NOTES: 50-year life assumed for adiabatic CAES and UPH.
Escalation rates as per PNL directive.

Table 12 shows a comparison of UPH, oil-fired CAES, adiabatic CAES and combustion turbines. The analysis covered a period of 150 years to provide a common basis for plants of differing lives, and included periodic replacement of components as required. The results indicate that adiabatic CAES is substantially more economic than combustion turbines, and significantly lower in cost than oil-fired CAES, regardless of plant life. UPH again exhibits lower levelized costs.

Table 12

150 Year Comparison of UPH, Oil-Fired CAES,
Adiabatic CAES and Combustion Turbines
1980 Levelized Busbar Cost (mills/kWh)

	UPH - 10 Hour		Oil-Fired CAES	Adiabatic CAES - 10-Hour 800 MW		CT*
Capacity Factor	2000 MW	1000 MW	10-Hour 900 MW	30-Yr Life	50-Yr Li	50 MW
10 percent	169.6	203.6	254.2	242.1	212.5	431.0
15 percent	131.7	154.4	230.3	184.2	159.8	400.6
20 percent	112.1	129.0	206.6	152.5	135.5	384.9
25 percent	101.0	114.6	193.0	134.6	121.1	376.0

---

* 300 $/kW capital cost, 2.0 mill/kWh var. O&M, 140 mill/kW-yr fixed O&M, 12,000 Btu/kWh and 30-year life assumed for combustion turbines.

Escalation factors and fuel costs as per PNL directive.

SENSITIVITY ANALYSIS

A number of sensitivity tests have been performed for such factors as plant life, TES fill material selection, storage capacity, charging energy cost, and cycle arrangement.

PLANT LIFE

At this stage, the actual life of an adiabatic CAES plant is difficult to project. The underground facilities (excluding TES) should certainly outlast the surface equipment. The cyclic life of the thermal storage fill material is uncertain, and for this reason is due for testing in future programs. The life of the TES containment and underground piping will depend upon TES material behavior. The mean time between overhauls of the turbomachinery, as no combustion is involved, is expected to be much longer than for combustion turbines based upon thermal cycling and gas path corrosion factors. Erosion life of the blades will depend primarily upon the range of particulate size generated by TES materials and particle separator efficiency. It is reasonable to suppose, therefore, that if particulate erosion can be eliminated by high efficiency separation, and cyclic fatigue is reduced by low temperature operation of rotational equipment, the life of the adiabatic CAES plant can be considerably extended beyond conventional CAES assumptions. Use of a 50-year life indicates a better than 5 percent improvement on 30 year calculations of the levelized energy cost of the plant (Table 12).

An analysis was also performed to assess the impact of replacing TES fill materials every ten years. The results show an increase in the levelized cost of the 30 year, ten hour iron ore fill plant (Table 10) of 0.3 mills at 20 percent annual capacity factor. The calculation includes the cost of materials and an estimate of access, fill removal and replacement, and return to service costs. The results suggest fill degeneration will have a negligible effect on plant economics.

FILL MATERIAL AND PLANT STORAGE CAPACITY

The selection of fill material affects the size of TES containment required as different materials exhibit different performance characteristics. Accounting for these changes, the effect of material selection is shown in Table 10 for Denstone. The use of rock rather than iron ore produced cost differences of approximately 0.1 mills for 8.3 hours and 0.5 mills for 10 hours of storage. These results indicate the relative insensitivity of the levelized costs to changes in TES fill materials in particular and capital cost variation in general.

The effect of storage capacity is shown in Tables 10 and 11 for 30- and 50-year plant lives.

CHARGING ENERGY COST

The adiabatic plant electric energy ratio (EER) is somewhat higher at 1.48 than the PEPCO UPH plant design EER of 1.32. Using the 150-year plant life for comparison, an increase in charging power cost to the level used in the PEPCO study for UPH (1980 equivalent of 20.9 mills/kWh) increases UPH levelized cost by 42.2 mills (64 percent) and adiabatic CAES by 47.2 mills (53 percent) for 20 percent capacity factor. Adiabatic CAES is therefore more adversely affected than UPH by charging power cost increases. Fuel fired CAES, as would be expected from its lower EER, is less sensitive with a levelized cost increase of 31 mills (20 percent), but at a levelized cost of 184.3 mills is still not competitive.

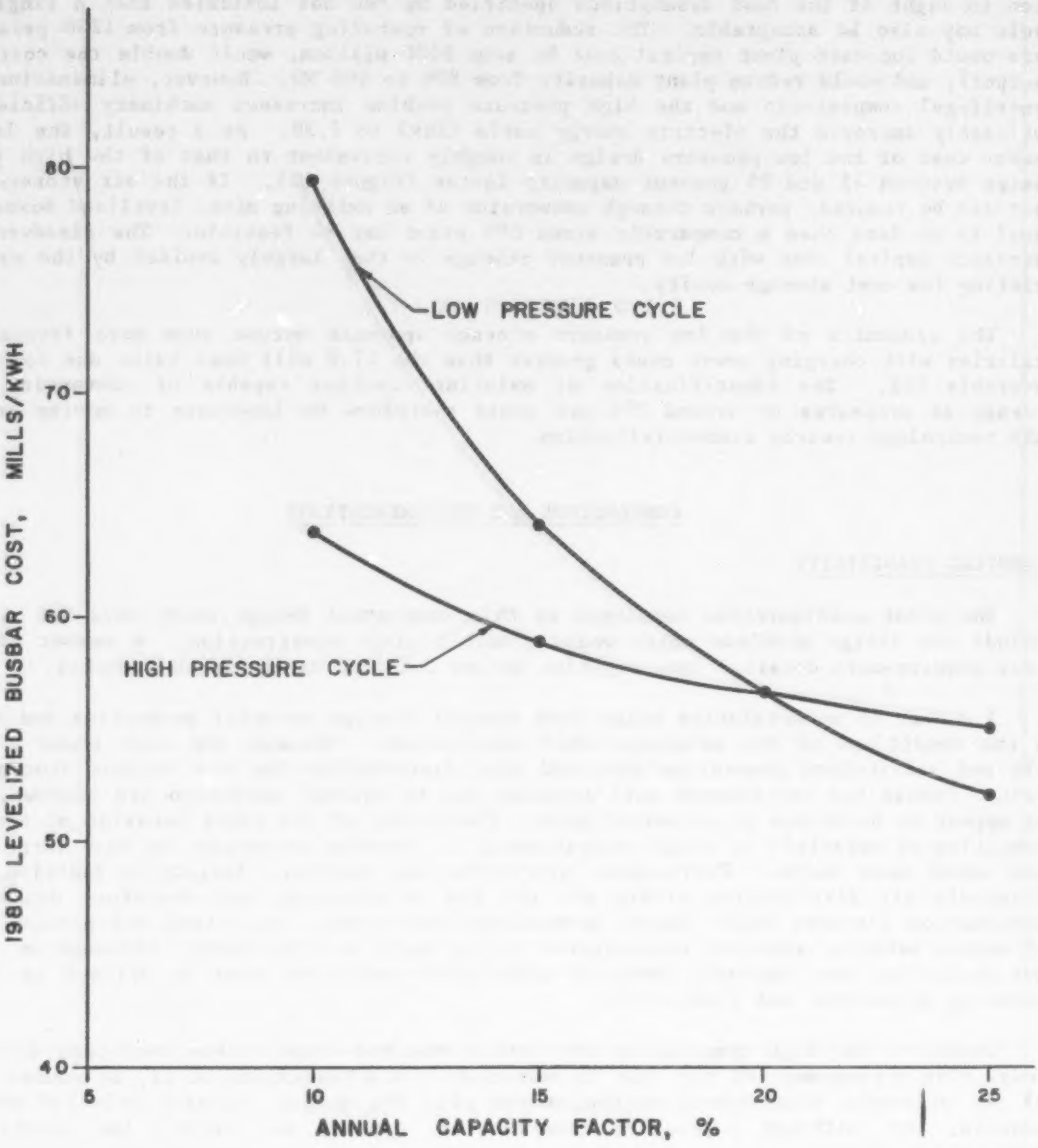

COMPARISON OF
LOW AND HIGH PRESSURE CYCLES

ACRES

BATTELLE PACIFIC NORTHWEST LABORATORY
CONCEPTUAL DESIGN AND
ENGINEERING STUDIES—ADIABATIC CAES

ACRES AMERICAN INCORPORATED

FIGURE 12

CYCLE OPTIMIZATION

Adiabatic CAES cycle optimization studies incorporated a rough cost tradeoff analysis which identified the two-stage cycle as the most desirable. Re-examination of this selection in light of the cost assumptions specified by PNL has indicated that a single stage cycle may also be acceptable. The reduction of operating pressure from 1200 psia to 240 psia would increase plant capital cost by some $100 million, would double the cost per kW (output), and would reduce plant capacity from 800 to 500 MW. However, elimination of the centrifugal compressors and the high pressure turbine increases machinery efficiency and noticeably improves the electric energy ratio (EER) to 1.38. As a result, the levelized busbar cost of the low pressure design is roughly equivalent to that of the high pressure design between 15 and 25 percent capacity factor (Figure 12). If the air storage system cost can be reduced, perhaps through conversion of an existing mine, levelized busbar costs equal to or less than a comparably sized UPH plant may be feasible. The disadvantage of increased capital cost with low pressure storage is thus largely avoided by the use of an existing low cost storage cavity.

The economics of the low pressure storage approach become even more favorable for utilities with charging power costs greater than the 11.8 mill base value due to the more favorable EER. The identification of existing cavities capable of conversion to air storage at pressures of around 250 psi could therefore be important to moving adiabatic CAES technology towards commercialization.

CONCLUSIONS AND RECOMMENDATIONS

TECHNICAL FEASIBILITY

The plant configuration developed in this conceptual design study does not appear to include any design problems which would prohibit plant construction. A number of design areas require more detailed investigation before detailed design could progress.

A number of uncertainties exist with thermal storage material properties and behavior in the conditions of the adiabatic CAES application. Unknown are such items as cyclic life and particulate generation rate and size distribution for the various storage materials. Pebble bed containment wall stresses due to thermal expansion are unknown, but do not appear to be severe or uncontrollable. Prediction of the exact behavior of such large quantities of materials in single containments is somewhat uncertain, as such large systems have never been built. Performance prediction is, however, largely a function of how accurately air distribution within the bed can be achieved, and therefore depends upon construction features which ensure as-designed conditions. Part-load and partial cycling TES system behavior were not investigated to any depth in this study. Although no significant deviations are expected, behavior under such conditions must be defined to identify operating procedures and limitations.

Design of the high temperature air shafts received considerable attention during this study. The arrangement of the pipe to accommodate startup expansion is, of course, critical to successful containment of the stored air. The design approach selected should be adequate, and, although unusual in construction, appears well within the capability of construction technology.

The availability of suitable valves was investigated by both Acres and Dresser-Clark and does not appear to be a problem at this stage. The large piping required in the low pressure plant sections will involve custom fabrication, but adequate facilities are available.

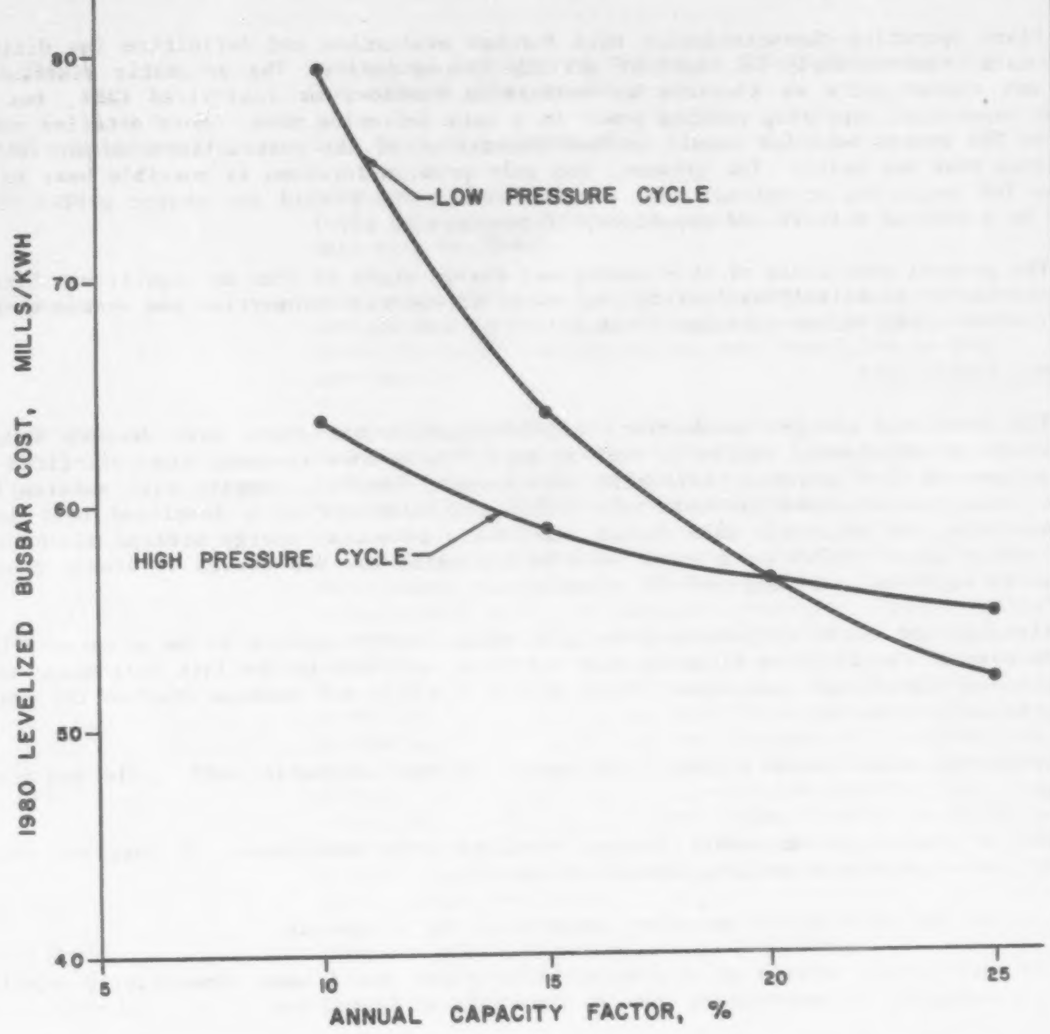

COMPARISON OF
LOW AND HIGH PRESSURE CYCLES

ACRES

BATTELLE PACIFIC NORTHWEST LABORATORY

CONCEPTUAL DESIGN AND
ENGINEERING STUDIES—ADIABATIC CAES

FIGURE 12

ACRES AMERICAN INCORPORATED

The availability of turbomachinery based upon commercially offered designs appears good. Some modification to standard product designs would be required to achieve the temperature limits proposed in this study (870°F max), but no insuperable problems are anticipated. The use of temperatures above those proposed will, however, require extensive compressor redesign or development of new designs. The design configuration does include a high horsepower gearbox in the centrifugal compressor train, which is a state-of-the-art component and requires design evaluation. Other compressor arrangements are possible which could eliminate this gearbox.

Plant operating characteristics need further evaluation and definition (as discussed previously), particularly in light of utility system needs. The adiabatic plant design does not appear quite as flexible as combustion turbines or fuel-fired CAES, but does appear capable of supplying peaking power in a load following mode. More detailed evaluation of TES system behavior should include definition of any restrictions on partial load operation that may exist. (At present, the only problem foreseen is possible heat buildup in the TES requiring occasional heat purging with a short cold air charge period. This could be a weekend maintenance procedure, if required at all.)

The general conclusion of this conceptual design study is that no significant barriers are foreseen to technical feasibility, but that TES material properties and system behavior need further study before technical feasibility is certain.

ECONOMIC FEASIBILITY

The levelized energy (production) cost evaluation has shown that despite somewhat poorer system efficiency, adiabatic CAES is very likely more economic than oil-fired CAES even at present fuel prices. Adiabatic CAES cannot, however, compete with substantially larger underground pumped hydroelectric (UPH) installations on a levelized cost basis. Alternatively, the adiabatic CAES design provides a potential energy storage plant option for the size range of 200 to perhaps 1000 MW for which the UPH design is likely unsuited because of high cost and long overall construction period.

Although not directly addressed in this study, there appears to be a potential for shorter overall construction schedule than oil-fired CAES due to the lack fuel usage in the cycle and no significant emissions. This should simplify and perhaps shorten the permitting process considerably.

Acres recommends that further development of the adiabatic CAES cycle be pursued through:

(1) a program of materials testing combined with development of improved thermal storage system modeling/design routines and,

If the above proves materials properties are acceptable:

(2) preliminary design of a demonstration plant based upon commercially available equipment in association with an interested utility, and

(3) development of more advanced high efficiency axial compressors capable of discharge temperatures in the range of 1000 to 1200°F.

PROJECT SUMMARY

Project Title: Analytical Modeling of Champagne Effect Hydraulically Compensated CAES Reservoir

Principal Investigator: D.S. Rowe, C.A. McMonagle

Organization:
Rowe & Associates
14400 Bellevue-Redmond Road, Suite 208
Bellevue, WA 98007

Project Goals: Develop an analytical model to determine if blowout is a problem in Compressed Air Energy Storage (CAES) systems and to determine which parameters are most sensitive to that assessment.

Project Status: An analytical model has been developed and a variety of conservatively oriented calculations have been performed which indicate that the Champagne Effect is unlikely to cause blowout for a properly designed CAES system.

A one-dimensional analytical model is used to represent the entire system consisting of the air-pipe, storage cavern, compensation pipe, and surface reservoir. Thermo-hydraulic aspects of air, water, and dissolved air are modeled using the two-fluid approach and conservative constitutive relationships are utilized in system calculations. Variations in design and constitutive relationships have been studied to show that a reduction of dissolved air, an increase of friction, and a deep compensation reservoir would mitigate the Champagne Effect. Most conservative results are obtained for homogeneous flow and for equilibrium deaeration of the water. Best estimate calulations of CAES operation could be done through a refinement of constitutive relations and validation with experimental data.

Contract Number: DE-AC06-76RLO 1830; Subcontract B-43388-A-L

Contract Period: Fiscal Year 1980

Funding Level: $37,000

Funding Source: U.S. Department of Energy through Pacific Northwest Laboratories

ANALYTICAL MODELING OF THE CHAMPAGNE EFFECT IN HYDRAULICALLY COMPENSATED CAES RESERVOIRS

D. S. Rowe and C. A. McMonagle
Rowe & Associates
14400 Bellevue-Redmond Road
Suite 208
Bellevue, WA 98007

ABSTRACT

An analytical model has been developed and a variety of preliminary, conservatively oriented calculations have been performed which indicate the Champagne Effect is unlikely to cause blow-out for a properly designed CAES system.

A one-dimensional analytical model is used to represent the entire system consisting of the air-pipe, storage cavern, compensation pipe and surface reservoir. Thermo-hydraulic aspects of air, water and dissolved air are modeled using the two-fluid approach. Variations in design and constitutive relationships have been studied to show that a reduction of dissolved air, an increase of friction and a deep compensation reservoir mitigate the Champagne Effect. The most conservative results are obtained when homogeneous flow and equilibrium deaeration of the water are assumed. Best estimate calculations of CAES operation could be done through a refinement of constitutive relations and validation with experimental data.

INTRODUCTION

The purpose of this paper is to present an analytical model which can calculate the dynamic behavior of a hydraulically compensated compressed air energy storage (CAES) system. In the CAES concept, high pressure air is stored in a deep mined cavern where the pressure is maintained by the hydrostatic head from a surface reservoir during periods of energy storage as shown in Figure 1. The purpose of the hydrostatic head, maintained by the water-filled compensation pipe, is to maintain nearly constant pressure in the cavern.

During the air storage period, air dissolves in the water by diffusion through the air-water interface. While this process is slow, there is concern about the impact of fully air-saturated water as a limiting condition at the start of air charging. As air-saturated water flows up the compensation pipe to the reservoir, the decreasing pressure field causes supersaturation and air may come out of solution to form bubbles (Champagne Effect). This two-phase, air-water mixture would flow to the surface with an increasing air volume fraction due to continued deaeration and decompression of the air in the decreasing pressure field. The net result would be a reduced hydrostatic head on the cavern which could drive the flow even faster. There is some concern that this could be an unstable flow resulting in loss of cavern pressure and eventual blowout. This would not be an acceptable situation since it could lead to loss of substantial energy and possibly cause property damage and personal injury.

Previous discussions and analyses have identified the nature of the problem and have pointed out that the Champagne Effect discharge would be self limiting due to fluid friction in the compensation pipe(1,2,3). The analytical methods of these previous studies were limited to a consideration of separate effects or used rather simplified models for two-phase flow. While they provided important insight, they did not include the dynamic behavior of the two-phase flow as completely as the model presented here. Cavern operation

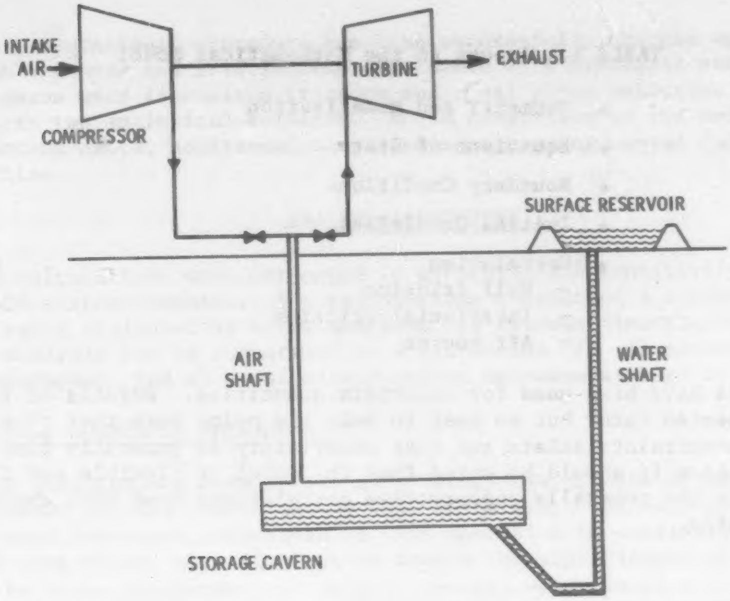

Fig. 1. Schematic Description of the Compressed Air Energy Storage Concept

could be expected to have oscillatory behavior; thus, there is a need to include the space and time distribution of air-saturation, void fraction, pressure and fluid velocity. The effects of relative phase motion are also important since there are regions where the air and water move at different velocities and even in opposite directions.

ANALYTICAL MODEL AND SOLUTION METHOD

The analytical model has been adapted from the two-fluid modeling philosophy which has emerged as current state-of-the-art approach for considering two-phase flow(4,5). The basic approach is to write the conservation equations for each phase and then to couple them by interface conditions. This general methodology has had considerable success for complex two-phase flow in nuclear reactor safety applications(4).

ANALYTICAL MODEL

Equations describing conservation of mass and momentum for the air, liquid and dissolved air are used to calculate the thermo-hydraulic response of the CAES system as a function of time. One-dimensional flow at constant temperature, dissolved air velocity equal to the liquid velocity and uniform phase and velocity distributions across the pipe cross-section are assumed. The model allows unequal air and water velocities, and nonequilibrium dissolved air concentrations.

Model inputs required for closure are summarized in Table 1. The geometry, equations of state, boundary conditions and initial conditions are generally well defined or easily established. There is some uncertainty however, in the phenomenological relationships for the wall and interfacial friction, and air source. Experimentally determined relationships would be most useful for best estimate calculations. Unfortunately, there is little experimental data available for CAES systems. Even though the most correct relationships may not be available, natural limits are available for these quantities which can be used for bounding calculations. For example, the air source can be no greater than that following equilibrium.

The calculations performed to date have focused on bounding calculations in an effort to present a conservative estimate of the thermo-hydraulic response in CAES. Therefore,

TABLE 1. Inputs to the Mathematical Model

- Geometry and Nodalization
- Equations of State
- Boundary Conditions
- Initial Conditions
- Correlation
  - Wall friction
  - Interfacial friction
  - Air source

conservative estimates have been used for uncertain quantities. Details of the selected correlations are presented later but we want to make the point here that physical bounds are available where uncertainty exists and that uncertainty is generally limited to friction and the air source. Also it should be noted that the model is flexible and it would be a simple task to replace the generally conservative correlations used with experimentally determined relationships.

SOLUTION METHOD

The conservation equations are solved numerically with a semi-implicit finite difference method similar to the ICE[(6)] algorithm. Time step size is limited by a Courant condition because the momentum flux terms are treated explicitly. The solution algorithm is iterative.

Conservation equations are written for a number of connected control volumes that represent the system as illustrated in Figure 2. Each control volume simulates part of the system and all thermo-hydraulic quantities are solved for each volume at incremental

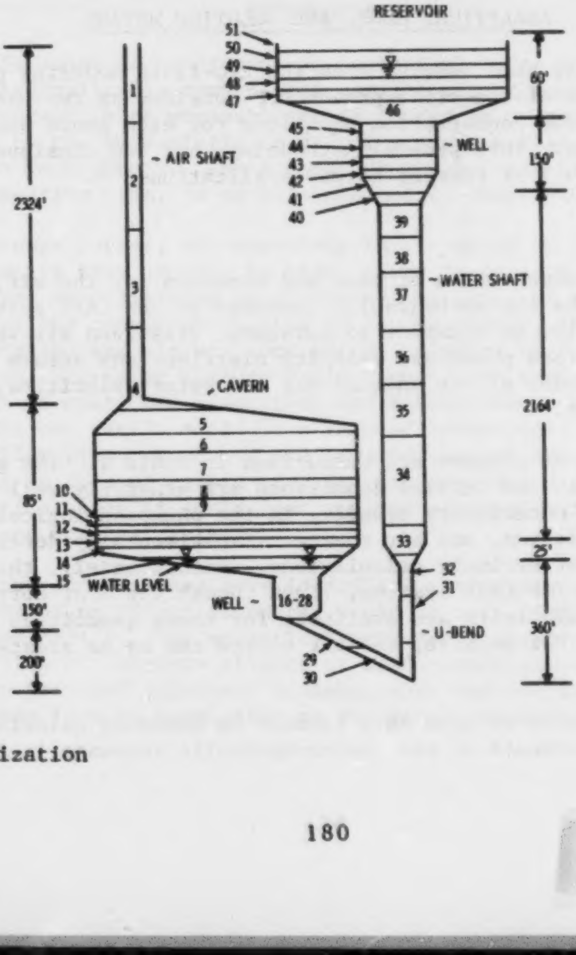
RESERVOIR
51
50
49
48
47
46
45
44
43
42
41
40
~ WELL
~ AIR SHAFT
1
2
3
4
2324'
60'
150'
39
38
37
36
35
34
33
~ WATER SHAFT
2164'
, CAVERN
5
6
7
8
9
10
11
12
13
14
15
85'
WATER LEVEL
WELL ~
16-28
32
31
~ U-BEND
25'
360'
29
30
150'
200'

Fig. 2. System Nodalization

best copy available

time steps. The computational procedure has been successfully checked against an analytical solution for both a damped and frictionless air cavern with hydraulic pressurization. The analytical test cases used linearized friction and equal phase velocity. The air sources were set to zero in the analytical solution. While comparison to the analytical solution provides an important check, additional comparisons with experimental data would provide further verification.

ANALYTICAL RESULTS

A series of calculations were performed to determine the sensitivity of various parameters on CAES system dynamics. The calculations considered a system with dimensions typical of that being evaluated by Acres American for Potomac Electric Power Company. The results of that analysis can be summarized by a discussion of: 1) parameters which affect the Champagne phenomena; and 2) a calculated cavern response typical of a worst case.

PARAMETERS AFFECTING CHAMPAGNE PHENOMENA

A variety of calculations were performed to study the effects of varying model input parameters and cavern initial conditions on CAES operation. The objective of these studies was to find the most important parameters to CAES operation in consideration of the Champagne Effect. Table 2 summarizes those items which reduce the significance of the Champagne Effect. As can be seen, the parameters include design, operational and physical quantities. These trends were determined by comparing the results from a standard case to the results from a case where only a single parameter was changed. For example, a decrease in the deaeration rate reduced the cavern oscillations. Those results were the basis from which we selected criteria for a worst case type analysis.

TABLE 2. Parameter Variations Reducing the Champagne Effect

- Design Parameters
  - Include deep surface reservoir
  - Provide cavern bottom contouring
  - Modify design (not yet considered)
    - U-bend
    - Flow restricting orifice
    - Pipe diameter
- Operational Parameters
  - Reduce compressor start-up rate
  - Reduce compressor flow rate
  - Impede air dissolution rate
  - Charge from high water level
- Correlation Parameters
  - Increased wall friction
  - Reduced interfacial friction
  - Model nonequilibrium air source

SAMPLE CALCULATIONS

It is desirable to have conservatively oriented calculations to assess the impact of the Champagne Effect on CAES operations because uncertainty exists in some parameters. This is done by bounding model input rather than changing the analytical model. The analytical model is quite general and dictates the phenomena that can be modeled. For example, inertial effects and relative phase motion are determined directly from the model. We do not obtain conservatism by altering this mathematical representation.

In an attempt to be conservative for this particular calculation, we accentuated the Champagne Effect by selecting inputs opposite to the results in Table 2. Specifically, the parameters adding to the conservatism in this calculation are: 1) a low water level, 2) full charging rate, 3) maximum initial dissolved air, 4) approximately homogeneous wall friction, 5) interfacial friction for small diameter bubbles, and 6) equilibrium deaeration without dissolution. The nodalization and initial water level position is shown in Figure 2. While we believe these specifications make the calculation highly conservative, we did not attempt to find "the" worst case.

The boundary conditions for this case are atmospheric pressure at the reservoir and a sequential startup of the four compressors at five minute intervals with a 15 second startup ramp between initiation and full flow for each compressor. A maximum air flow of 2640 lbm/sec is obtained at 915 seconds and is maintained at that value for the remainder of the calculation.

Figure 3 shows the liquid velocity at Node 39, the highest velocity region in the system. An oscillatory characteristic is shown with a maximum velocity of approximately 18 feet/second. The velocity is significantly reduced beyond 4000 seconds because the liquid level in the cavern has entered the well and the cavern begins pressurizing as the liquid level drops and the hydrostatic head correspondingly increases. This hydrostatic pressurization is a most important damping feature of CAES design. Figure 4 shows the air source at Node 39. The air source is positive during upflow as water containing a high concentration of dissolved air enters this region. During flow reversal, the air source is zero because liquid with a low air concentration from the reservoir flows into the higher pressure compensation pipe. The flow reversal also causes a reduction in the dissolved air concentration throughout the compensation pipe. Figure 5 shows the cavern pressure at Node 6. Pressure decreases are consistent with the air release and associated reduction in hydrostatic head in the compensation pipe. The pressure increase starting at approximately 4000 seconds is caused by an increasing hydrostatic head as the liquid level drops from the large area cavern to the relatively small area well.

As a contrast to the full charging illustration at low water level, another calculation was run utilizing all features of the previous example except the initial cavern water level was raised to Node 6 of Figure 2. This case represents a more typical condition from which full charging would be applied. This calculation is also conservative with respect to the Champagne Effect because bounding initial conditions and constitutive relationships were used. Figure 6 shows the resulting liquid and air velocities at Node 39. This result shows only modest oscillatory behavior and a quasi-steady condition is reached by 2000 seconds.

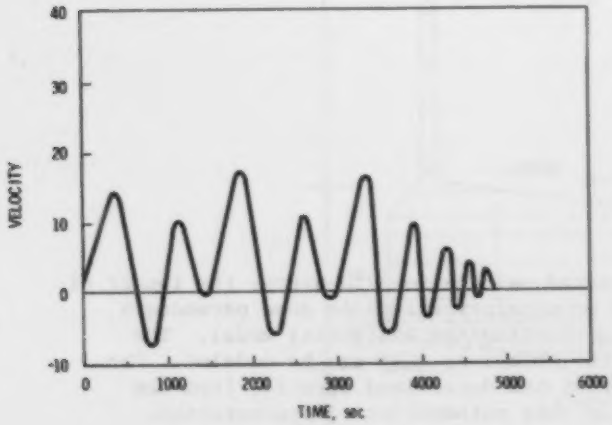

Fig. 3. Liquid Velocity at Node 39

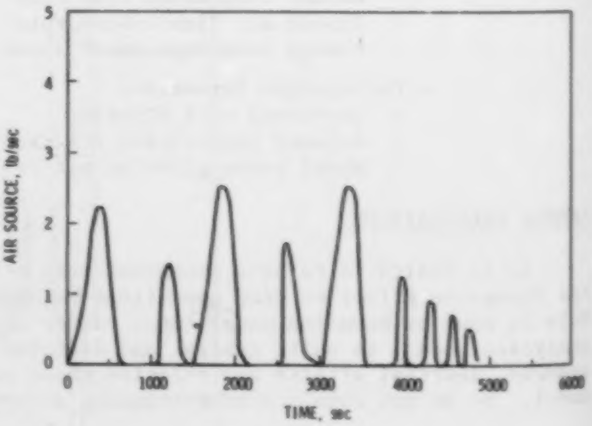

Fig. 4. Air Source at Node 39

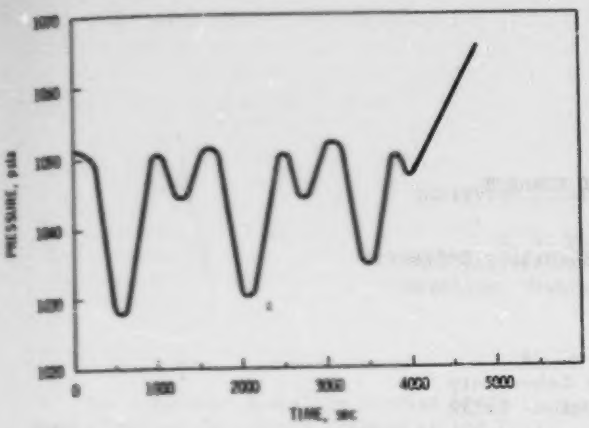

Fig. 5. Cavern Pressure at Node 6

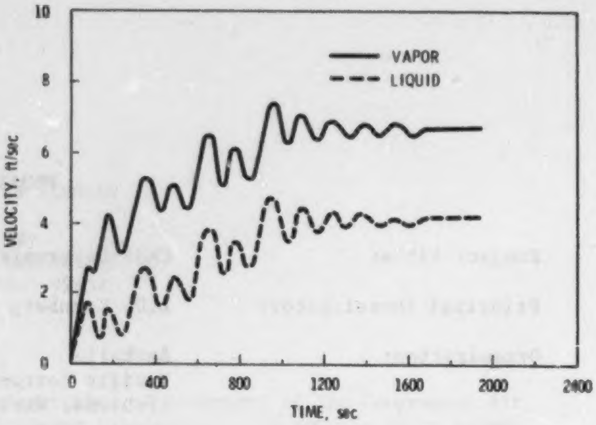

Fig. 6. Liquid and Vapor Velocity at Node 39

CONCLUSIONS

An analytical model has been developed and a variety of conservatively oriented calculations have been performed which indicate that the Champagne Effect is unlikely to cause blowout for a properly designed CAES system.

Results have shown that the Champagne Effect can produce flow oscillations during the charging phase of operation and that those oscillations can be reduced by appropriate design and/or operational considerations. A conservative analysis shows that blowout is unlikely for a design similar to that being considered by Acres American for the Potomac Electric Power Company.

ACKNOWLEDGEMENTS

This work was supported by the U.S. Department of Energy under Subcontract No. B-43388-A-L, Prime Contract DE-AC06-76RLO 1830 with Pacific Northwest Laboratory operated by Battelle Memorial Institute. We would like to acknowledge the inputs of W. V. Loscutoff (PNL), E. D. Shippey (Acres American), and Potomac Electric Power Company.

REFERENCES

1. J. C. Mollendorf, "Champagne Effect Phenomena in Hydraulically-Compensated Compressed-Air Energy Storage Systems," (Report to Acres American).

2. W. A. Blecher, A. J. Giramonti, and E. B. Smith, "The Champagne Effect in Hydraulically Compensated Compressed Air Energy Storage Systems," United Technologies Research Center, East Hartford, CT.

3. J. Pellin, (SEO, Luxembourg), Presentation at DOE/EPRI Meeting, Washington, D.C. (December 14, 1979).

4. Transient Reactor Analysis Code (TRAC-PIA), Los Alamos Scientific Laboratory, Los Alamos, NM.

5. M. Ishii, Thermo-Fluid Dynamic Theory of Two-Phase Flow, Eyrolles, Paris, (1975).

6. F. H. Harlow and A. A. Amsden, "A Numerical Fluid Dynamic Method for All Flow Speeds," Journal of Computational Physics, Vol. 8, (1971) pp. 197-213.

PROJECT SUMMARY

Project Title: CAES Reservoir Stability Criteria

Principal Investigator: L.D. Kannberg

Organization: Battelle
Pacific Nortwest Laboratory
Richland, Washington 99352

Project Goals: Develop design and stability criteria for CAES underground reservoirs.

Project Status: Preliminary stability criteria have been completed for candidate rock types (salt, porous rock, hard rock). Research needs were identified and were pursued by numerical modeling and laboratory studies. A site has been identified and confirmed for testing of CAES in porous rock.

Numerical modeling of porous rock reservoirs concentrated on well coning and on air bubble development. Laboratory work addressed porous rock structural and hydraulic response to cyclic flow of various fluids at elevated pressures and temperatures. A site was identified in west-central Illinois for small-scale field testing.

Numerical modeling of salt proceeded with analysis of cavern response to thermal and cyclic thermal and mechanical loads. Laboratory and in-mine work concentrated on determining basic strength characteristics of salt from various sites, permeability of salt in mines, and strain and acoustic emission from cyclically loaded salt specimens. A field site was selected for testing. However, activity has been postponesd indefinitely.

Numerical modeling of hard rock caverns continued to develop basic design nomograms and address CAES specific cavern stability concerns (cyclic thermal and mechanical loading). Laboratory efforts concentrated on response of typical hard rocks to cyclic loads at elevated temperatures and strength reduction due to enhanced weathering. No field studies are planned in hard rock.

Contract Number: DE-AC06-76RLO 1830

Contract Period: October 1979 to September 1980

Funding Level: $2,070,000

Funding Source: U.S. Department of Energy

RESERVOIR STABILITY STUDIES

T. J. Doherty
Pacific Northwest Laboratory
Richland, Washington 99352

ABSTRACT

The Reservoir Stability Studies project is the geotechnical component of the Compressed Air Energy Storage Technology Program at the Pacific Northwest Laboratory. Its purpose is to establish stability criteria for underground air storage reservoirs for CAES application in salt, hard rock and porous media geologies through applied research studies. This paper provides the overview and structure of that project and indicates 1980 progress with respect to program goals. Included is summary reporting on fluid thermal and thermomechanical modeling of porous media reservoirs.

INTRODUCTION

The Reservoir Stability Studies project, within the Compressed Air Energy Storage Program at Pacific Northwest Laboratory (PNL) is sponsored by the Thermal and Mechanical Energy Storage Division of the Department of Energy. The goal of these studies is to reduce or eliminate geotechnical uncertainties associated with CAES in underground reservoirs. The specific objective of this project is to establish stability criteria for large underground air reservoirs that may be used for utility applications.

Three major reservoir types are being examined within the project: solution mined domal salt caverns, hard rock excavations with constant pressure water compensation, and anticlinal structural traps of porous media. Three separate stability criteria result from a series of phased studies, initiated by a survey of the state-of-the-art. This has been completed. This survey led to recommendation of nearly concurrent numerical evaluations and laboratory studies of the geotechnical stability concerns in operational CAES reservoirs. The final step in the Reservoir Stability Studies project is validation of results through field studies or site specific applications (Figure 1).

Responsiveness to the joint DOE-EPRI Demonstration programs and interested utility needs required that the stability criteria resulting from these studies be available as soon as possible. Preliminary criteria for the three reservoir types were made available in 1979 reflecting the state-of-the-art. Interim criteria are under final review by program participants with the completion of baseline model development. Refinement and validation of these criteria through continued experimental studies, field studies, and site specific application is presently underway.

PROJECT STRUCTURE

The Reservoir Stability Studies project is separated into three study areas defined by the reservoir type (Figure 2). Responsibility for carrying out the specific tasks within each area have been divided between selected subcontractors or handled by the internal resources of PNL. Tasks within the project are outlined below:

1. Interim Reservoir Stability Criteria - PNL, Central Washington University
2a. Numerical Studies of Porous Media - PNL
    i. Thermal-Flow Analysis
    ii. Thermomechanical Modeling

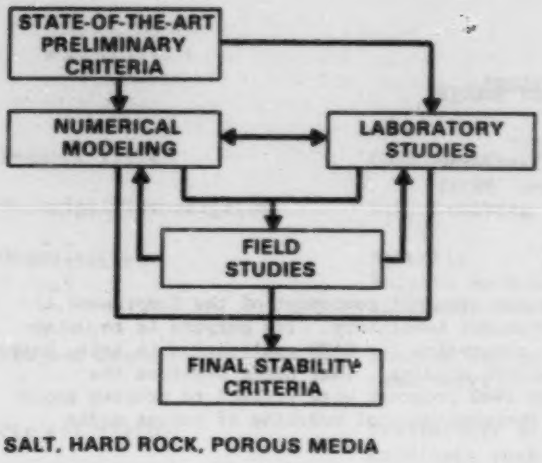
STATE-OF-THE-ART PRELIMINARY CRITERIA
NUMERICAL MODELING
LABORATORY STUDIES
FIELD STUDIES
FINAL STABILITY CRITERIA
SALT, HARD ROCK, POROUS MEDIA

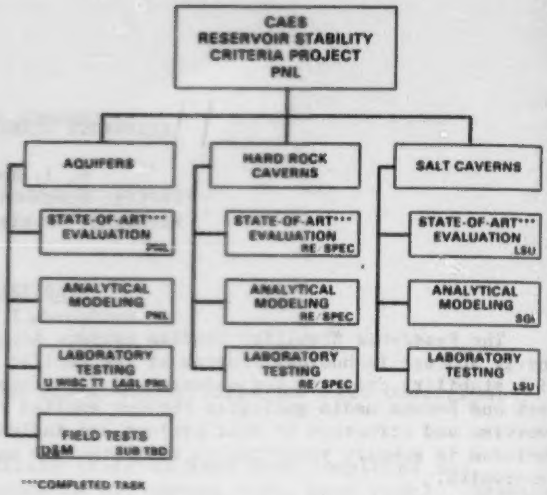
CAES RESERVOIR STABILITY CRITERIA PROJECT PNL
AQUIFERS
HARD ROCK CAVERNS
SALT CAVERNS
STATE-OF-ART*** EVALUATION PNL
ANALYTICAL MODELING PNL
LABORATORY TESTING U WISC TT LASL PNL
FIELD TESTS D&M SUB TBD
STATE-OF-ART*** EVALUATION RE/SPEC
ANALYTICAL MODELING RE/SPEC
LABORATORY TESTING RE/SPEC
STATE-OF-ART*** EVALUATION LSU
ANALYTICAL MODELING SGI
LABORATORY TESTING LSU
***COMPLETED TASK

Fig. 1. CAES Reservoir Stability Plan of Action Fig. 2. CAES Reservoir Stability Studies Outline

2b. Numerical Studies of Salt Cavities - Serata Geomechanics
2c. Numerical Studies of Hard Rock Caverns - Re/Spec Inc.
3a. Laboratory Studies of Porous Media - PNL
  i. Air-Water-Rock Interaction - PNL
  ii. Porous Media Flow Facility - PNL
  iii. Air Ventilation Study - University of Wisconsin at Milwaukee
  iv. Thermomechanical Properties - Los Alamos Scientific Laboratory
  v. Moist Air Flow Tests - Terra Tek Inc.
3b. Experimental Studies of Domal Rock Salt - Louisiana State University
3c. Laboratory Studies of Hard Rock Caverns - Re/Spec Inc.
4. Porous Media Field Studies - PNL
  i. Exploration - Dames & Moore
  ii. Operation - To be decided

PROJECT STATUS

All contract and control milestones were met on or ahead on schedule. Development of numerical models to predict reservoir response to CAES operations has been completed. Drilling, seismic, land leasing and exploration contracts were let in the final quarter of FY-1980, initiating brisk activity in the exploration phase of the Porous Media Field Study. The operational phase of the field study will be initiated with the award of a major subcontract from proposals now under evaluation. Experimental studies are well underway and most generic evaluations are complete. Continued refinement of methods and specific studies will be continued in support of field studies and site specific studies carried out by interested utilities.

Included within this review are papers by project participants in the areas of salt and hard rock studies, and on the experimental and field study aspects of the porous media studies. The remainder of this paper will summarize FY-1980 activities in fluid thermal and thermomechanical modeling of porous media reservoirs.

FLUID THERMAL MODELING

Fluid thermal modeling for FY-1980 concentrated on development of a two-dimensional bubble development models for two-phase flow in porous media.

OVERVIEW

The initial charging of the reservoir will involve the displacement of water from the air storage zone which requires a two-phase, multi-dimensional model. With some modification, the numerical model developed for the analysis of water coning was adapted to the prediction of bubble development. In the modified model the pressures and fluid distributions in the reservoir are predicted from a solution of the combined continuity and momentum equations for each phase. Capillary pressure and relative permeability are also included in the model. The solution is achieved by finite difference techniques in a simultaneous, implicit fashion.

Two notable modifications have been made to the water coning model. The wellbore, having a porosity of unity and essentially no flow resistance was removed to enhance the computational speed of the code. Prediction of near-wellbore bubble growth is not of significant interest given scale and time considerations. A second modification involves the air and water boundary conditions. A method was developed for injecting air into the reservoir and to allow water to escape the computational zone. This method was based on the idea that the growth of the bubble is pressure limited rather than flow limited. Water extraction wells can be simulated as though the water were escaping to a hydrostatic sink (or some other pressure) and at some distance from the air storage zone, the aquifer will exist at its undisturbed hydrostatic pressure. This new approach allows both air and water to cross any boundaries based on some specified pressure. This allows the flexibility of including multiple sources and sinks.

Initial indications are that the model in its present state may be expensive to exercise in comparison to previous codes developed under fluid thermal numerical studies. This model should be competitive with any other available codes with similar capability because the algorithms are based on state of the art technology. Full three-dimensional models, which would be considerably more costly to operate are being avoided. In two dimensions we have developed both an R-Z (cylindrical) and an X-Y (rectangular) model. The R-Z model provides for single well evaluations. The X-Y model used vertically can model the vertical dimension and can provide for multiple wells, but lacks an expanding flow area. The horizontal rectangular model; i.e., the areal model, can model multiple wells and has the effective flow area domain of the R-Z model, without vertical distinction. The inherent limitations in two dimensions are compensated for by cost effectiveness and some flexibility.

ANALYSIS AND RESULTS

Three problems have been addressed. These were:

1. Establish reasonable agreement with the Katz and Coats model.
2. Demonstrate capability to evaluate enhanced bubble growth rates using water extraction wells.
3. Compare the R-Z model with the areal model for single well air injection and determine the validity of the vertical equilibrium assumption.

Each of these areas is discussed below.

The Katz and Coats Model

Katz and Coats(1) have provided a method for analytically calculating bubble growth rates for one-dimensional (radial) flow of water in porous media. A bulk compressibility of the rock and water is included. The method does not account for capillary pressure or relative permeabilities. The bubble is assumed to exist at uniform pressure inside a sharp displacement front. Although the applicability of the model is limited, its accuracy has not, to our knowledge, been criticized.

The X-Y areal model was used to develop two bubble growth solutions which were compared with results obtained for the same conditions using the Katz and Coats model. In both comparisons the bubble pressure or source pressure was 90 atm and the hydrostatic pressure was 50 atm. The first case was run for about 60 hours of air injection. The Katz and Coats model displaced about 5.83 m^3 of water from a unit thickness chosen. The code predicted a displacement of 5.25 m^3 of water. For a second case, the relative permeabilities of both the air and water were set to unity and the air was considered to be immobile until the liquid saturation essentially equaled the residual value of 20% of pore volume. This modeled the sharp displacement front of the Katz and Coats model. In less than two hours of simulated air injection the source cell was void, effecting a water displacement of 0.20 m^3. The Katz and Coats model was used to determine a water displacement of 0.15 m^3.

For these two cases the computer code bounds the predictions of the Katz and Coats model. General agreement was achieved. The hydrostatic boundary pressure used in the code enhances the comparative bubble growth rate. However, in the first case the fluid mobilities (reduced by relative permeability effects) apparently have a greater influence, thereby resulting in a predicted bubble growth rate that was lower than that for the Katz and Coats model. In the second case the difference in fluid mobilities has been effectively eliminated, showing the response to the hydrostatic boundary condition.

Water Extraction Wells

A very obvious limitation of the Katz and Coats model is the inability to simulate more than one well. Bubble growth rate could be considerably enhanced by extracting water from wells outside the air bubble. An analysis to demonstrate this ability and to suggest the benefit to bubble growth was performed (Figure 3). Forty hours of air injection were simulated. Without the benefit of water extraction wells the code predicted that the mass of water displaced was less than half the amount of extraction modeling. Obviously, the presence of the water extraction wells enhances the bubble growth rate.

R-Z Modelling

The R-Z analysis provides a comparison between the vertically averaged saturations and the saturation distributions as predicted by the X-Y areal model. This comparison displays the importance of modelling the gravitational term.

A comparison of solutions from the X-Y areal model and the R-Z model requires some compromise due to the fundamental geometric difference. The solution used to represent the areal model was that generated for and discussed as the first case in the comparison with the Katz and Coats model. To the extent possible the R-Z model was subjected to the same conditions without sacrificing its additional capabilities. For example, the radial node points coincided with the node points along the boundary of the rectangular grid. Model air injection required a vertical permeability in the wellbore cell to represent a wellbore through the top 20 m of a 30-m-thick reservoir.

Reasonable agreement between the X-Y areal model and the R-Z model has been achieved. With the results of the X-Y model scaled to reflect the volumes of the R-Z model, the displacement figures of Table 1 are provided for comparison. This scaling accounts for vertical thickness and the fact that the X-Y model includes a quadrant while the R-Z model spans one radian. The scaling is intended to equalize flow areas at the inlet and outflow boundaries.

The agreement between the air injection numbers is better than that for displaced water. This is due to differing compressible volumes in the two models.

The important point at issue beyond this comparison is the significance of the vertical effects. In Figure 4 the vertically averaged saturation from the R-Z model are compared to results from the X-Y areal model. These results suggest that, at least during the initial stages, gross bubble development can be reasonably modelled without consideration of the vertical fluid distributions. This may not be true either later in the development process or for anisotropic conditions.

The vertical saturation profiles given in Figure 5 suggest that vertical equilibrium would require three zones; a fully saturated zone at the bottom, a region containing only residual water (in this case a saturation of 0.20) at the top, and a transition zone (in this case

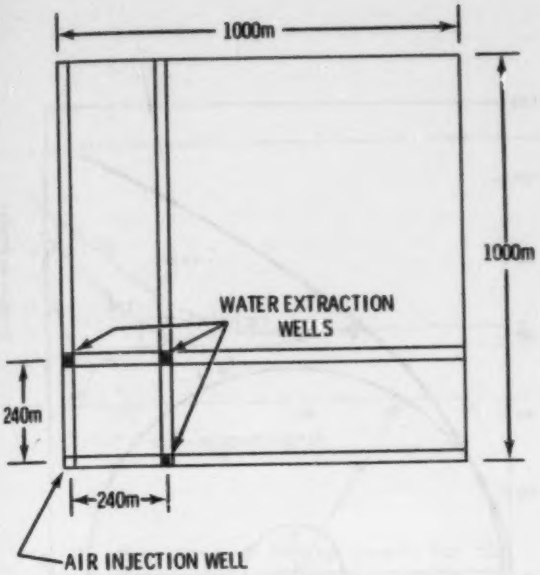

Fig. 3. Definition of Well Grid

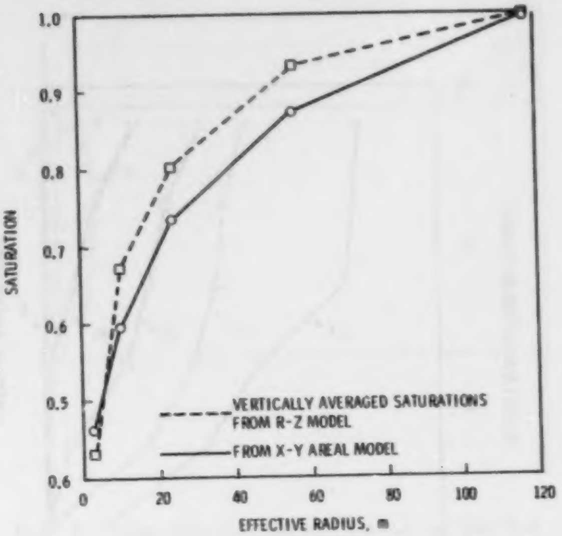

Fig. 4. Saturation Profiles After 35 Hours of Air Injection

TABLE 1. Air Injection and Water Displacement After 35 Hours of Simulated Bubble Growth Using Different Model Geometries

Model Geometry	Injected Air (gm)	Displaced Water (gm)
R-Z	$1.94 \cdot 10^8$	$1.58 \cdot 10^9$
X-Y areal	$1.81 \cdot 10^8$	$1.30 \cdot 10^9$

approximately 10 m) separating the two. The transition zone is defined by the capillary pressure function. This distribution is not manifested here, but for lower flow rates and conditions of greater vertical mobility, the VE assumption may be acceptable. Given the possibility that the vertical behavior of the reservoir is eventually to be in question, we are working on methods that will allow its consideration without using fully 3-D modelling.

THERMOMECHANICAL ANALYSIS

Structural investigations conducted during FY-1980 were an extension of efforts conducted during FY-1979 and described in Reference 2. Efforts focused upon extending the analysis capability to treat the effects of well casing/rock interaction and upon utilitizing more refined porous rock response data (as reported in Reference 4) in assessing rock behavior in the porous zone.

Thermo elastic and failure characteristics of Galesville sandstone were determined experimentally for temperatures, load conditions and stress levels thought to exist at a porous CAES site.(4) A parabolic Mohr coulomb failure was constructed by performing at least squares fit of this data corresponding to 120°C temperature. This data is shown in Figure 6.

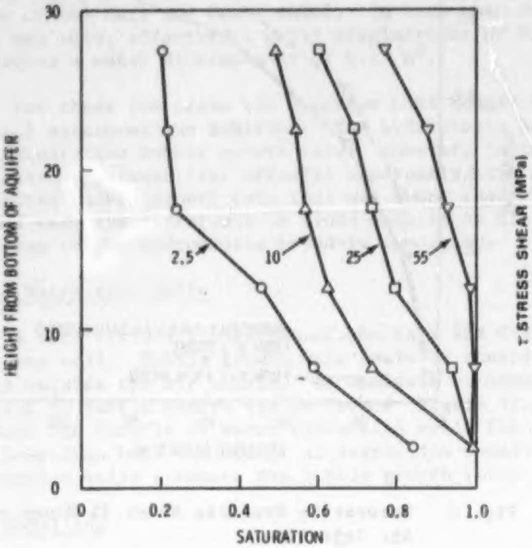

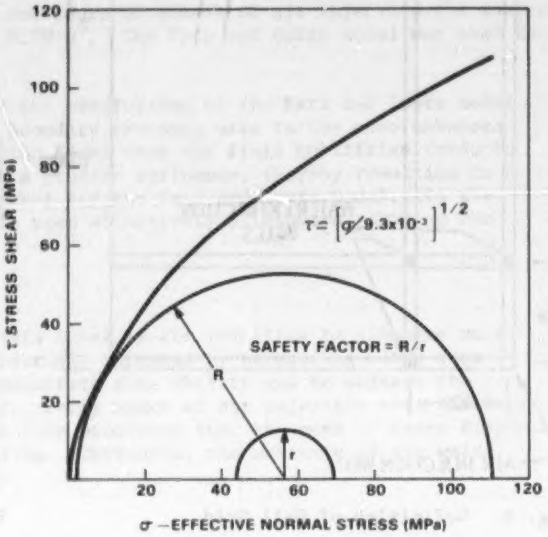

Fig. 5. Saturation Profiles from R-Z Model for Various Radial Nodes (m)

Fig. 6. Mohr Coulomb Failure Envelope for Galesville Sandstone (120°C)

A finite element model was constructed and loaded with in-situ conditions, thermal conditions, and pore pressure thought to be typical of porous CAES operations. A more detailed discussion of these conditions is given in References (3) and (4).

A measure of response severity in the porous zone can be described by a factor of safety which indicates the closeness with which a stress state comes to the failure envelope. If the stress state is represented by the smaller of the two circles of Figure 7, and if the larger of the two circles is both concentric with the smaller circle and tangent to the envelope, then the radius ratio R/r quantifies the factor of safety. Failure is assumed not to occur as long as this factor of safety is greater than unity. A factor of safety plot for the mid-plane of the porous zone at various times is shown in Figure 2. Figure 8 is a contour plot of the region in week one with factor of safety below one. Observation of this plot reveals that the severest condition of stress for the porous zone (based upon the assumptions inherent in the analyses) would occur at the outer periphery of the heated control zone during site start up. A closer look at the stress distribution causing this low factor of safety (slightly below unity inside the one contour) is a hoop "tensile effect" caused by a thermal radial expansion of central cylindrical body of heated rock. This transient phenomena may not be harmful to the reservoir and in fact could enhance permeability by generating radial cracks.

These analyses do indicate the need for careful evaluation of start up procedures and analysis of the development of thermal storage regions within porous media. Hot air injection into a porous media reservoir would not result in serious structural damage to the reservoir from heating if reasonable control, careful completion methods and responsible operating procedures are used.

ACKNOWLEDGMENT

This work was supported by the U.S. Department of Energy under prime contract DE-AC06-76RLO 1830 with Pacific Northwest Laboratory operated by Battelle Memorial Institute. Numerical modeling was performed by Larry Wiles, Dick McCann, and John Friley of PNL, and their assistance in assembling this note is acknowledged.

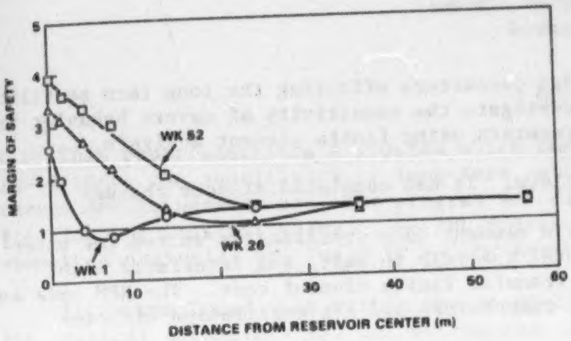

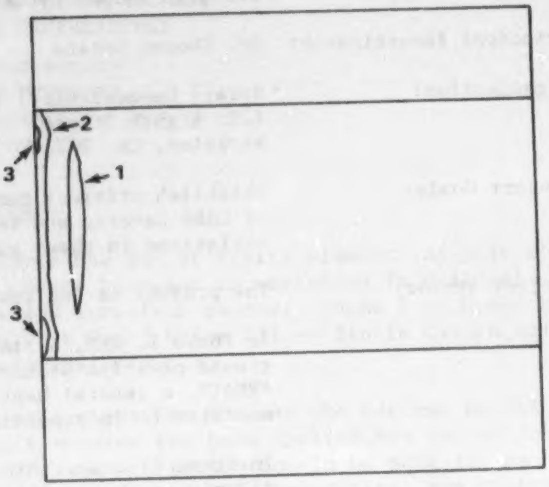

Fig. 7. Mohr Coulomb Safety Factor for the Porous Zone (120°C Experimental Data)

Fig. 9. Mohr Coulomb Safety Factor at the End of Week One

REFERENCES

1. D. L. Katz and K. H. Coats, Underground Storage of Fluids, Ulrich's Books, Inc., Ann Arbor, MI, 1968.

2. J. R. Friley, "Structural Response of a Generic Porous Site," Proceedings of the 1979 Mechanical and Magnetic Energy Storage Contractor's Review Meeting, CONF 790854, August 1979.

3. L. E. Wiles, "Two-Dimensional Fluid and Thermal Analysis of Dry Porous Rock Reservoirs for CAES," Proceedings of the 1979 Mechanical and Magnetic Energy Storage Contractor's Review Meeting, CONF 790854, August 1979.

4. J. D. Blacic, P. H. Halleck, and P. 'Onfro, "Thermo-Mechanical Properties of Galesville Sandstone," Proceedings of the 1979 Mechanical and Magnetic Energy Storage Contractor's Review Meeting, CONF 790854, August 1979.

PROJECT SUMMARY

Project Title: Numerical Modeling of Behavior of Caverns in Salt for CAES with Elevated Temperatures

Principal Investigator: Dr. Shosei Serata

Organization:

Serata Geomechanics, Inc.
1229 Eighth Street
Berkeley, CA 94710

Project Goals: Establish critical design parameters affecting the long term stability of CAES caverns and investigate the sensitivity of cavern behavior to variations in these parameters using finite element analysis.

Project Status: The project is 90% complete. It has consisted of four phases:

In Phase I, REM, a finite element code specifically suited for underground cavities structural analysis in salt, was interfaced with *HEAT*, a general heat transfer finite element code. The REM code was modified to incorporate temperature and air penetration effects.

In Phase II a specific structural analysis problem given by PNL to illuminate the capabilities of REM and *HEAT*, primarily with respect to cyclic analysis, was completed.

Phase III, a single cavern parametric analysis of a prospective CAES site, was completed. It consisted of two parts. First, a preliminary pie-slice analysis, to determine the ranges of the critical parameters, was made. Second, a full cavern axisymmetric analysis, to focus on specific ranges shown to be of importance, was made.

In Phase IV an analysis of a particular test borehole in the Jefferson Island mine being monitored by LSU was undertaken. It is 75% complete.

Major conclusions are as follows: 1) In situ lateral stress is the most dominant parameter governing long term cavern behavior. Stability is greatly reduced as the in situ lateral stress approaches the theoretical limit. 2) Given that other critical parameters maintain moderate values, CAES caverns are structurally very stable in the long term for temperatures to 200°F. 3) Air penetration and boundary deterioration primarily affect the local stability of CAES caverns and have relatively minor significance in determining the global stability. 4) At cavern length to width ratios of less than 8, the supporting effect of the roof and floor greatly reduces radial strain. 5) Cycling of pressure and temperature has only a minor effect on long term cavern behavior.

The results of this study indicate that the most important aspect of further work will be determining the quantitative aspects of material deterioration by brittle creep due to air penetration into granular salt interstitial space under CAES operating conditions.

Contract Number: DE-AC06-76RLO 1830, Subcontract B-82290-A-P

Contract Period: January 22, 1980 through September 30, 1980

Funding Level: $70,792

Funding Source: Department of Energy through Pacific Northwest Laboratory

NUMERICAL MODELLING OF BEHAVIOR OF CAVERNS IN SALT FOR COMPRESSED AIR ENERGY STORAGE WITH ELEVATED TEMPERATURES

Dr. Shosei Serata
James F. McNamara
Serata Geomechanics, Inc.
Berkeley, CA

ABSTRACT

This paper describes a program which employed the use of finite element analysis to investigate the sensitivity of long-term salt cavern behavior to variation in critical cavern design parameters. The program was divided into four phases: Phase I -- Model Modification and Testing; Phase II -- PNL Selected Test Case; Phase III -- Single Cavern Axisymmetric Analysis; and Phase IV -- LSU Borehole Analysis.

It is concluded that within the scope of this study, as long as the extreme values of the critical parameters are not approached, salt caverns for CAES application can be considered stable for at least thirty years. Further investigation should be made in the areas of in situ stress determination, laboratory testing of salt properties, and comprehensive accumulation of existing field data to better correlate the REM finite element program to empirical data.

INTRODUCTION

Use of solutioned salt cavities as a possible means of storage for compressed air has been under investigation by the Department of Energy (DOE) for a number of years. In connection with this, Serata Geomechanics, Inc., has been conducting numerical stability studies of caverns in salt using the finite element program, REM. These analyses have been primarily involved with determining the values of the critical design parameters that will ensure long-term cavern stability.

In the studies previously conducted(1) the critical design parameters considered in the numerical studies were cavern depth, cavern air pressure, in situ stress condition, salt strength, cavern separation and cavern length to diameter ratio. The results of these previous analyses indicated the following: (1) Cavern depths to 4000 feet are considered safe under most normal operating circumstances; caverns should be no deeper than 2500 feet if depressurization is a frequent likelihood, if cavern separation is less than four times the cavern diameter, or if excess in situ lateral stress is 100% of the theoretical maximum; (2) Depressurization of a CAES cavern should only be allowed in a period of emergency; (3) Sharp increase in boundary strain is anticipated for caverns in domes in which the excess in situ lateral stress approaches 100% of the theoretical maximu; (4) As other parameters take on extreme values, salt strength becomes more critical; (5) Increases in cavern length beyond five times the diameter have only a small effect on the boundary strain; and (6) The minimum cavern separation of four times the diameter for a two-cavern system with both caverns operated at the same pressure.

To continue and expand this previous work, two other critical parameters affecting the long-term stability of CAES operating facilities were added to the current program of parametric study: (a) elevated temperature and (b) boundary deterioration due to air penetration.

BACKGROUND ON ANALYSIS METHOD

The program used for all the structural analysis in this project was REM. It is a finite element code capable of computing displacements, strains, and stresses in two-dimensional axisymmetric, plane strain and generalized plane strain problems. The constitutive model contains elastic, viscoelastic, and viscoplastic components, making it ideally suited to stability analysis of underground cavities in salt. A detailed description of the model and the special functions it employs can be found in (1).

PROJECT DESCRIPTION

The project was divided into the four following phases:

PHASE I — MODEL MODIFICATION AND TESTING

In order to quantitatively evaluate the effects of elevated temperature in a CAES environment, several programming modifications had to be made. The basic changes were made in the following areas:

(1) REM was interfaced with a heat transfer code, *HEAT*, whose output can be used as thermal input to REM; (2) A linear thermal expansion term was included in the volumetric part of the constitutive model in REM; (3) An experimentally determined temperature factor was included in the viscoplastic creep rate formula and (4) Octahedral shear strength was modified to include temperature dependence.

After these modifications were made, they were tested extensively and were verified as correct.

PHASE II — PNL SELECTED TEST CASE

Phase II work consisted of a specified benchmark type problem suggested by PNL, designed to provide baseline checking of *HEAT* and REM. A single "pie-slice" of elements was used, simulating a horizontal section of an infinitely long single vertical cavern with circular cross-section. The analysis was done plane strain, and since symmetry was assumed in the radial direction, only a single "slice" was needed. The simulations made were:

(1) A two-year solutioning simulation using REM; (2) Temperature analysis using *HEAT* for short-term cyclic loading and long-term constant loading; (3) Thermomechanical analysis using REM for short-term cyclic loading and long-term constant loading.

PHASE III — SINGLE CAVERN AXISYMMETRIC ANALYSIS

The single cavern axisymmetric analysis consisted of two parts: a preliminary pie-slice analysis designed to examine the full range of values of the critical parameters, and the full axisummetric analysis designed to concentrate on smaller variations. The basic parametric approach was to establish base conditions, or reference conditions, reflecting what is expected to be a moderate CAES operating environment and vary the values of the critical parameters with respect to these conditions. For the preliminary analysis, two sets of base conditions were used, reflecting moderate to moderately extreme CAES circumstances. The values and ranges of the critical parameters were:

Variable Condition	γ_c	ΔP_L	T_c^o	H
Base Condition I	3.3%	0	130°F	2500'
Base Condition II	1. %	.5max	200°F	3000'

Ranges:

γ_c: critical strain .1,.33,1.,3.3 (%)

ΔP_L: in situ lateral stress -.5,0.,5.,1. (*max)
T_c: cavern temperature 115,130,165,200,250,300 (F^o)
H: cavern depth 2500,3000 (feet)

For the full cavern axisymmetric analysis, one set of base conditions were used:

Condition \ Variable	γ_c	ΔP_L	T_c	P_i	L/D
Base Condition	.1	.5	175°	500 psi	4

Ranges:
γ_c: critical strain .1,1 (%)
ΔP_L: in situ lateral stress .5,.75,1. (*max)
T_c: cavern temperature 150,175,200 (F^o)
P_i: cavern pressure 500,1000 (psi)
L/D: cavern length to diameter ratio 2,4,8

In all of the above analyses, the salt material properties were assumed to be of medium strength. In the preliminary analysis, the cavern pressure was maintained at 735 psi and in the full cavern analysis the cavern depth was maintained at 3000 feet. In order to quantify the temperature and boundary deterioration effects, a control case was run for each set of base conditions in which no thermal input was used.

PHASE IV — LSU BOREHOLE ANALYSIS

In order to provide a more realistic link between the computer simulation results and actual CAES conditions, computer evaluation of test boreholes being monitored in the Jefferson Island Mine by Professor Robert Thoms at LSU was undertaken. The work done in this phase is expected to be the beginning of an extensive calibration of the REM projections to actual test data gathered from field conditions emulating CAES operating environments.

RESULTS

Phase I work in conjunction with Phase II work indicated that the REM and *HEAT* codes were well suited to a wide variety of thermomechanical analysis, including both thermal conduction and convection, cyclic temperature and pressure thermomechanical loading, sequential excavation simulation, and non-linear temperature dependent viscoplastic analysis. The Phase II work itself specifically indicated that thermal cycling will only occur within the first ten feet of CAES cavern boundaries and will primarily affect the tangential and vertical stress patterns there, while the pressure cycling will affect the stress condition into the dome as far as 1-2 cavern diameters away for a 300-foot diameter cavern. An attempt was made to quantify the purely cyclic effects and indicated in a preliminary way that cycling of cavern temperature and pressure has only a minor influence on cavern stability.

In Phase III, the amount of parametric analysis conducted led to a large base of results, and hence only the highlights will be mentioned here. The values in Figures 1-3 that will be referenced here are taken from the full cavern axisymmetric analysis and indicate the maximum strain and strain rates attained on the cavern boundary.

Increased plasticity extension surrounding a CAES facility is expected for elevated cavern temperatures. In comparing the control case and the cases in which the cavern temperatures ranged from 150°-200°F, increases in plasticity of 1 - 1 1/2 cavern diameters were in evidence. For cavern temperatures to 200°, CAES facilities are expected to be very stable given that other parameters maintain moderate values, and if other parameters are actually favorable, cavern temperatures to 300°F could possibly be maintained.

In the preliminary analysis, variations in γ_c, the critical parameter governing boundary deterioration due to air penetration, produced only minor differences in overall cavern stresses and strains. In going to the full cavern axisymmetric analysis, effective mean stress was used to calculate the octahedral shear strength of the salt and more of an effect was realized. This can be seen in the decrease in max radial strain in going from the base conditions to γ_c=1% in Figure 1. Another indication of the effect of boundary deterioration can be seen by examining Figures 1,2,&3 for P_i=1000psi. Increased cavern pressure is expected to increase long-term cavern stability unless it simultaneously causes increased air penetration and hence boundary deterioration. Even though the max radial strain on the boundary for the P_i=1000psi case is less at 10^4 days than the base condition case, the max radial strain rate has been increasing through time and by 10^4 days is in fact slightly higher for the P_i=1000psi case. This indicates that the competence of the boundary salt is being slowly undermined by high cavern pressure.

The single most critical factor to determine for CAES facilities is the in situ stress condition as can be seen in Figures 1-3. As ΔP_L approaches the theoretical maximum, large increases in boundary strain and strain rate occur.

The maximum cavern boundary strain at 10^4 days is reduced a factor of 2 in going from L/D=8 to L/D=2 (Fig.). This is due to the increased support given by the roof and floor and is consistent with the preliminary pie-slice results which compared quite closely with the L/D=8 results, indicating that for L/D=8 the center cavern is already behaving like an infinitely long cylinder. Finally, cyclic analysis of 100-days was made to compare with the L/D=2 case and indicated only slight differences in the boundary creep rate due to the cyclic loading.

In Phase IV, the primary interest was in borehole closure and the results indicate that in the first year of atmospheric loading the borehole diameters should decrease an average of about $5x10^{-3}$ ins and should subsequently expand upon the cyclic loading projected to begin February 1981. The expansion should amount to about $4x10^{-4}$ ins average over the first 20 days.

CONCLUSIONS

This program has indicated that given moderate values for the critical design parameters discussed, CAES facilities in salt can be considered structurally stable for at least 30 years with elevated temperatures. Since there is little actual data available from operating CAES sites, these analyses should be considered as establishing the relative importance of the parameters involved. Because of the importance of determining realistic stress and strain values through computer simulation, it is recommended that future work be concentrated on establishing with greater accuracy the quantitative aspects of salt deterioration due to air penetration and salt expansion due to elevated temperature.

REFERENCES

1. "Numerical Modelling of Behavior of Caverns in Salt for Compressed Air Energy Storage (CAES)," Contract EY-76-C-06-1830, Serata Geomechanics, Inc., May 22, 1979.

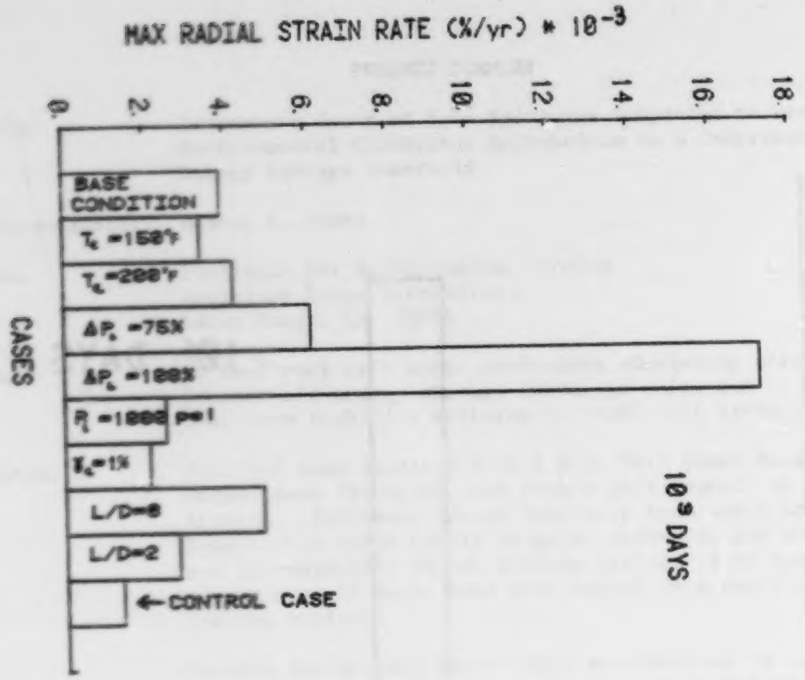

FIGURE 1

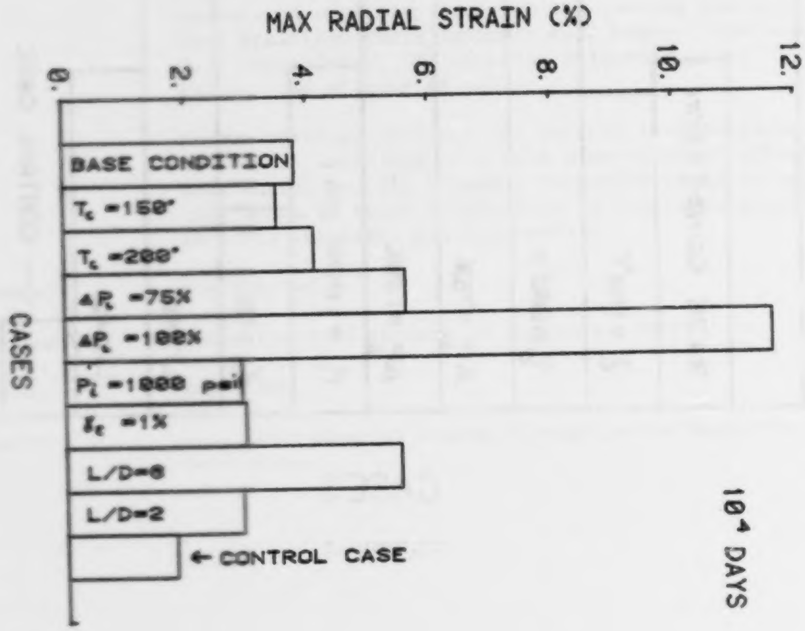

FIGURE 2

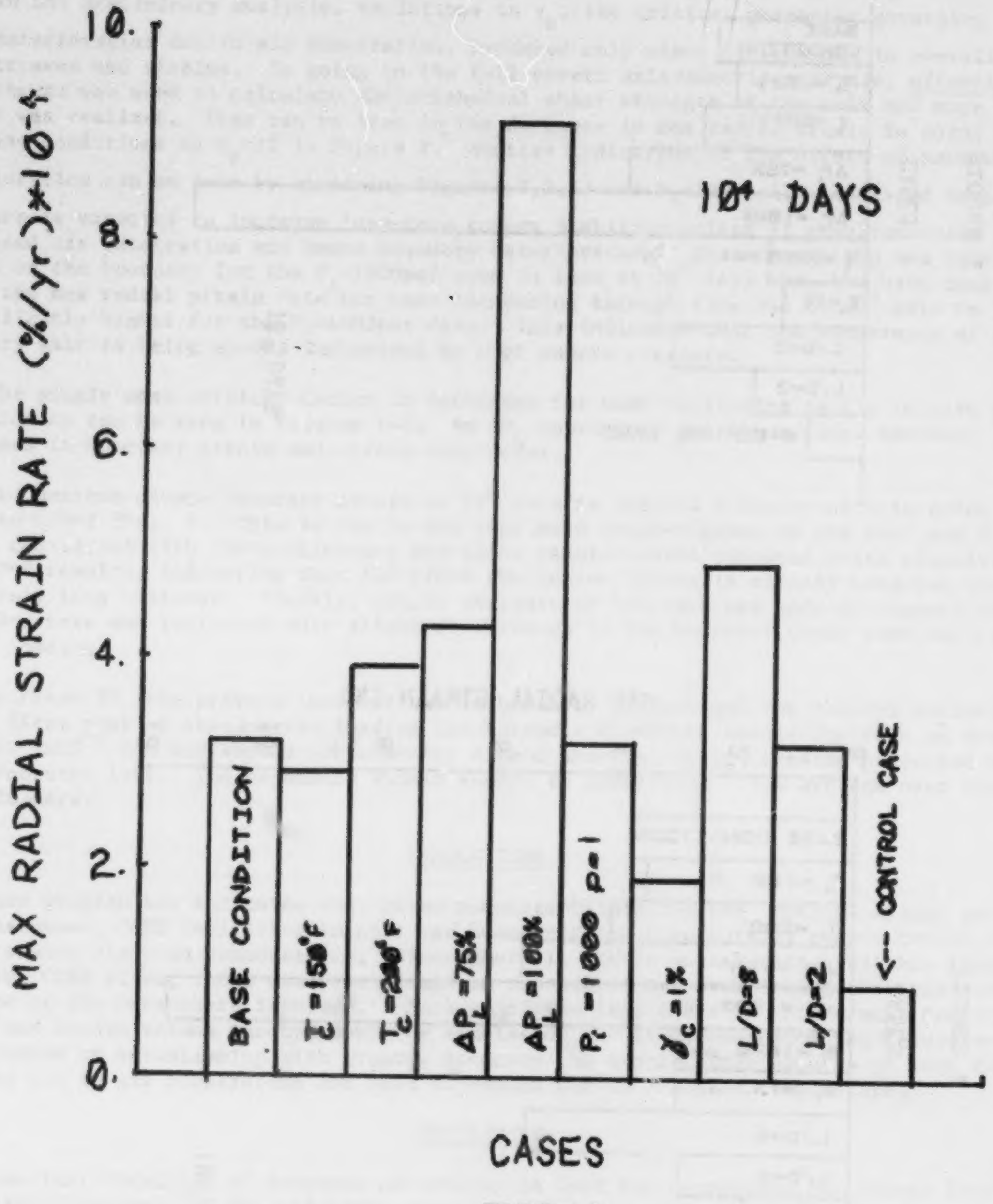
MAX RADIAL STRAIN RATE (%/yr)*10-4
10.
8.
6.
4.
2.
0.
10⁴ DAYS
BASE CONDITION
T_c =150°F
T_c =200°F
ΔP_L =75%
ΔP_L =100%
P_i =1000 psi
γ_c =1%
L/D=8
L/D=2
<-- CONTROL CASE
CASES

FIGURE 3

PROJECT SUMMARY

Project Title: Laboratory Tests of Salt Specimens Subjected to Loadings and Environmental Conditions Appropriate to a Compressed Air Energy Storage Reservoir.

Principal Investigator: Robert L. Thoms

Organization:
Institute for Environmental Studies
Louisiana State University
Baton Rouge, LA 70803

Project Goals: To test rock salt under conditions simulating effects of compressed air energy storage (CAES) in salt, and to formulate long-term stability criteria for CAES salt caverns.

Project Status: Salt has been obtained from 7 U.S. Gulf Coast domes and one West German dome (Huntorf), and from a salt deposit in northwest Arizona. Jefferson Island dome salt from south Louisiana has been tested under cyclic triaxial extension for over 2000 hours and approximately 84,000 loading cycles. Salt specimens from six sources (3 each) have been tested in a Brazilian "index" testing series.

In-situ bench-scale experiemnts are underway in two south Louisiana salt mines, i.e., Cote Blanche and Jefferson Island. Qualitative gas permeability tests have been performed by injecting Freon 12 into one hole and checking nearby holes for cross-borehole flow. Further, preliminary cyclic pressurization borehole tests have been performed.

Major conclusions to date are: (a) permeability of rock salt depends on confining pressure and loading history, (b) results from Brazilian tests indicate salt behaves similarly from U.S. Gulf Coast domes, (c) acoustic emissions permit monitoring of cyclic load effects on salt.

Recommendations include: (a) perform in-situ permeability tests at several locations in a salt mine to check effects of varying salt character, (b) continue long-term tests on salt in laboratory so as to build a data base to formulate quantitative criteria for CAES salt reservoirs.

Contract Number: B-67966-A-H

Contract Period: 1 October 1978 through 30 September 1980

Funding Level: $324,166

Funding Source: U.S. Department of Energy through Battelle-Pacific Northwest Laboratory

LABORATORY TESTS OF ROCK SALT

R. L. Thoms
Louisiana State University

ABSTRACT

Tests of rock salt are described for applications relative to long-term compressed air energy storage (CAES) in salt reservoirs. Effects of cyclic loads on strength (and stability) and permeability of rock salt are investigated through an integrated study including laboratory and in situ tests and limited complementary numerical modeling.

INTRODUCTION AND OVERVIEW

The objectives of this study are to perform tests on rock salt that simulate compressed air energy storage (CAES) effects around salt caverns; and to formulate relevant long-term stability criteria. Currently no significant amounts of data exist on long-term cyclic load effects on rock salt, and such data are necessary as a bases for CAES cavern stability criteria.

Implementation of CAES cavern stability criteria will permit designers and operators to select ranges of pressures and temperatures suitable for site specific salt reservoirs and also consistant with lifetimes planned for the associated surface peaking-power generating facility. That is, CAES reservoir capacity should be maintained at an acceptable volume, without unusual maintenance, over the design lifetime of the facility.

The general methodology of this study, from the earliest planning stage, has encompassed testing performed both in the LSU laboratory and in situ in salt mines, along with limited numerical modeling for interpreting resulting data.

FINDINGS AND RECOMMENDATIONS

From laboratory tests: (1) rock salt apparently has good endurance to cyclic load effects within the modest ranges used to date. (2) Under cyclic loads, rock salt exhibits short term response (displacement) that is approximately linear with varying loads; however, the accumulated short term responses generate an envelope which trends along typical time dependent salt displacement behavior, i.e., rapid movement following initial load application and then decreasing (rate) with time. (3) Monitoring acoustic emissions (AE) is a viable apparently, the only current practical means of continuously tracking behavior of salt caverns subjected to cyclic loadings. (4) Results from Brazilian tests are relatively closely grouped from 6 sources including: 4 U.S. domes, an Arizona deposit, and the Huntorf dome of West Germany.

From in situ mine tests: (1) permeability is "induced" in relatively unconfined salt around openings mined in salt. However, if salt is continuously confined and relatively undisturbed, its permeability apparently remains small. (2) Behavior of salt around cyclically pressurized test holes indicates close correlation between AE and applied loads.

Recommendations based on objectives of this study and findings to date include: (1) Continue in situ permeability tests in the mine and extend them to several locations so as to span a variety of salt. (2) Continue long-term laboratory tests on salt so as to extend data base on salt behavior under simulated CAES environments. The additional data obtained should furnish an adequate data base for formulation of long-term stability criteria for CAES caverns.

WORK ACCOMPLISHED

Since the last annual review in the Fall of 1979 this study has steadily progressed, both in the LSU CAES laboratory and in the in situ tests currently being carried out in the two salt mines of south Louisiana. Accomplishments will be described briefly here in three main categories, i.e., relative to: (1) the LSU laboratories, (2) the in situ mine tests, and (3) complementary modeling and analysis.

Laboratory Tests

Within the LSU laboratory test category, a variety of salt has been obtained for testing. Salt from the following U.S. Gulf Coast domes has been obtained in amounts adequate for at least index (Brazilian) tests: Avery Island, Jefferson Island, Choctaw, West Hackberry, Bryan's Mound, Rayburn's and Vacherie. In addition, salt from the Red Lake deposit of Arizona, and from the Huntorf dome of West Germany is on hand at LSU. Most of this salt was kindly donated to the LSU CAES program as indicated in the Acknowledgements Section of this report. Salt from other sources also is tentatively available for this study, however recent efforts have been spent more on accumulating test results rather than additional salt.

Laboratory results include data from quick index tests and long-term tests. The Brazilian (or indirect tension) test was selected for index purposes because it is a relatively well known test and because it can be quickly performed on specimens requiring modest preparation time and a small quantity of cylindrical salt core.

A small test machine was selected and modified to carry out Brazilian tests on rock salt (manufactured by Geotest, Inc.). Applied loads and acoustic emissions were monitored and recorded for each test. The ultimate load was transformed into a measure of tensile "strength" by conventional linear elasticity formulae. It should be noted here that the authors are aware that these values do not represent the "true" tensile strength of salt, since salt is a time dependent, nonlinear material for which linear elasticity does not apply.

Figure 1 is a display of Brazilian test results for salt from the sources indicated. The results are relatively closely grouped together, with the largest variation in fact occurring within data associated with one U.S. dome (West Hackberry).

Six test machines have been developed for long-term triaxial cyclic tests. The machines are capable of applying coupled lateral and axial stresses up to 5000 psi (34.5 mPa) and 11,250 psi (77.6 mPa), respectively. Data recorded include applied pressures, specimen displacements (axial), and acoustic emissions. Pressure and displacements data are recorded on a data "logger", and acoustic emissions are displayed on a screen and periodically photographed for "hard copy" records.

As of September 25, 1980 a Jefferson Island salt specimen had undergone 2340 hours and 102,140 cycles of load under triaxial extension conditions. The lateral stresses varied between approximately 2550-2700 psi (17.6-18.6 mPa), and the longitudinal stresses between 300-550 psi (1.0-3.8 mPa) during a typical cycle. Approximately 3.7% extensional strain had been accumulated over this test period. Other long-term tests are in progress under conditions selected to simulate loading environments around CAES caverns.

Apparatus has been developed to perform laboratory controlled permeability tests of salt under confining cyclic stress conditions. A pressure gradient can be applied along the length of a 4-in. (100 mm) diameter cylindrical salt specimen confined within a pressure jacket and loaded axially. Various combinations of pressure or/and flow (inlet and outlet) can be monitored (and pressures recorded) to obtain laboratory measures of salt permeability. Salt generally will be tested under confining pressures similar in magnitude to that anticipated around CAES reservoirs. Some permeability tests will be carried out under atmospheric pressure levels; but then, mainly for index purposes.

In Situ Tests in Salt Mines

Considerable effort within this category of the study has been spent developing representative in situ tests for CAES caverns. Test sites have been developed for this study in the Jefferson Island (JI) and Cote Blanche (CB) salt mines in south Louisiana. This has been carried out with the generous concurrence and assistance of the mine owners and operators (please note Acknowledgements Section).

Initially, relatively shallow, vertical 4-in. (100 mm) diameter test holes were drilled in the JI mine within a protective shed. A limited number of cyclic air pressure loadings were applied to one vertical hole to develop associated instrumentation. However, safety considerations caused the use of these holes to be terminated when it became known that horizontal partings were present in the mine floor in the general area (encountered later in drilling). Such partings, when filled with relatively high pressure air, conceivably could cause floor upheaval. Thus, a different configuration of hole was sought for CAES tests.

Test holes were subsequently drilled beneath mine pillars to depths of around 20 ft. (6.1 m) at angles of approximately 45-60°. A series of 2-in. (50 mm) diameter parallel holes were drilled in the JI and CB mines by mine personnel. This work was delayed for about 6 months (Sept. 79-Feb. 80) because of the classification of most of the south Louisiana salt mines as "gassy" by the Mining Safety Health Administration (MSHA). Four holes at JI and two at CB were prepared for testing by epoxying aluminum pipe into the first 10 ft. (3 m) of the hole. This insured that relatively undisturbed and strongly confined salt in the lower 10 ft. (3 m) of the hole would be utilized for in situ testing. Figure 2 displays a test hole being prepared for emplacement of the aluminum pipe.

For the in situ cyclic pressurization tests, an "instrumentation head" was developed that threaded onto the pipe and permitted electrical conductor leads to be passed through to a precision borehole caliper within the pressurized borehole. The borehole caliper was also developed for this study, and consisted of an assembly of LVDT and mechanical linkages. A control unit also was developed for cyclic air pressure applications to the test holes.

Two "check-out" trials of the in situ test instrumentation were carried out in the JI mine in late August, 1980. Figure 3 is an overview photograph of the test set-up. Air pressure was furnished by a "bottle" and data were collected for approximately 4 hours on the second trial. Input pressure, borehole diametrical displacements, and acoustic emissions were monitored and recorded. Over the last 2 hours, input pressures were cycled between 125-175 psi (862-1206 kPa).

The data recorded were still being analyzed as of mid-September, 1980; however, there appear to be definite correlations (as anticipated) between the recorded parameters. Of particular note was the apparently strong correlation between levels of acoustic emissions (monitored via a sensor on the aluminum pipe "head") and magnitude of applied pressures.

In situ gas permeability tests of qualitative character also were carried out. In situ tests by previous workers (Aufricht and Howard, Journal of Petroleum Technology, Aug., 1961) were modified and adapted for the current CAES study at LSU. In these tests, Freon-12 (F-12) gas was injected into a test hole, and an electronic halogen-gas detector was used to sample neighboring holes for possible flow of gas through the surrounding salt. No gas flow was detected between the slant test holes; however, for horizontal holes in pillars, a high level of "induced permeability" generally was present at shallow depths. This is due to fissuring of salt when unconfined and subjected to large extensional strains typical of "free" salt faces in mines. For example, in Figure 3, fissures can be seen in the pillar face above the downward slanting test holes. However, no cross-borehole gas flow could be detected between the holes in the confined and relatively undisturbed salt beneath the same pillar.

Complementary Modeling and Analysis

Limited complementary modeling was performed at LSU to aid in selecting test parameters and configurations of in situ test holes, and generally for planning and data analysis. A nonlinear time dependent finite element computer program, initiated through LSU prior to the current CAES study, was utilized by R. M. Gehle for this purpose. Cases analyzed included: a "typical" CAES cavern (for test parameters), in situ slant test boreholes and typical Brazilian test specimen. Mr. G. S. Gipson also obtained solutions for time dependent temperatures in triaxial test specimens and pressure distributions around the early vertical shallow test boreholes.

An "exact" analytical solution was obtained by G. S. Gipson for flow through permeable media between two approximately parallel boreholes. This solution, employing bipolar coordinates and classic potential theory, can be used for analysis of in situ permeability tests involving gas flow between boreholes.

FUTURE WORK

Long-term laboratory tests on salt obviously require considerable amounts of time. Cyclic coupled stress and thermal loadings under triaxial extension conditions are the most time consuming and difficult tests to perform; and to date, such a test has not been initiated. Thus "conventional" laboratory tests are planned for more complicated loading conditions. In addition, correlation studies are planned for Brazilian tests and triaxial tests to insure that the Brazilian test is sufficiently sensitive for general index testing of salt for CAES applications.

Permeability testing of salt will continue in the laboratory to determine effects of cyclic loadings simulating CAES conditions around reservoirs.

Plans for in situ tests include continued cyclic pressure testing with monitoring of possible salt degradation, displacements, and acoustic emissions. Monitoring also will include possible changes in induced permeability between the holes. Further, if access is permitted, in situ permeability tests will be performed in different types of salt (different in color, crystal size, and amount of impurities) within a mine.

Finally, quantitative stability criteria will be formulated on the data base accumulated from the testing described in the preceding text.

ACKNOWLEDGEMENTS

The assistance and generous cooperation of the following companies and laboratories are gratefully acknowledged: Diamond Crystal, Inc.; PB/KBB; Domtar, Lt.; Sandia Corporation; International Salt, Inc.; and Morton-Norwich, Inc.

This study was supported by the U.S. Department of Energy through Pacific Northwest Laboratory operated by Battelle Memorial Institute; Subcontract No. B-67966-A-H, Prime Contract No. DE-AC06-76RLO-1830.

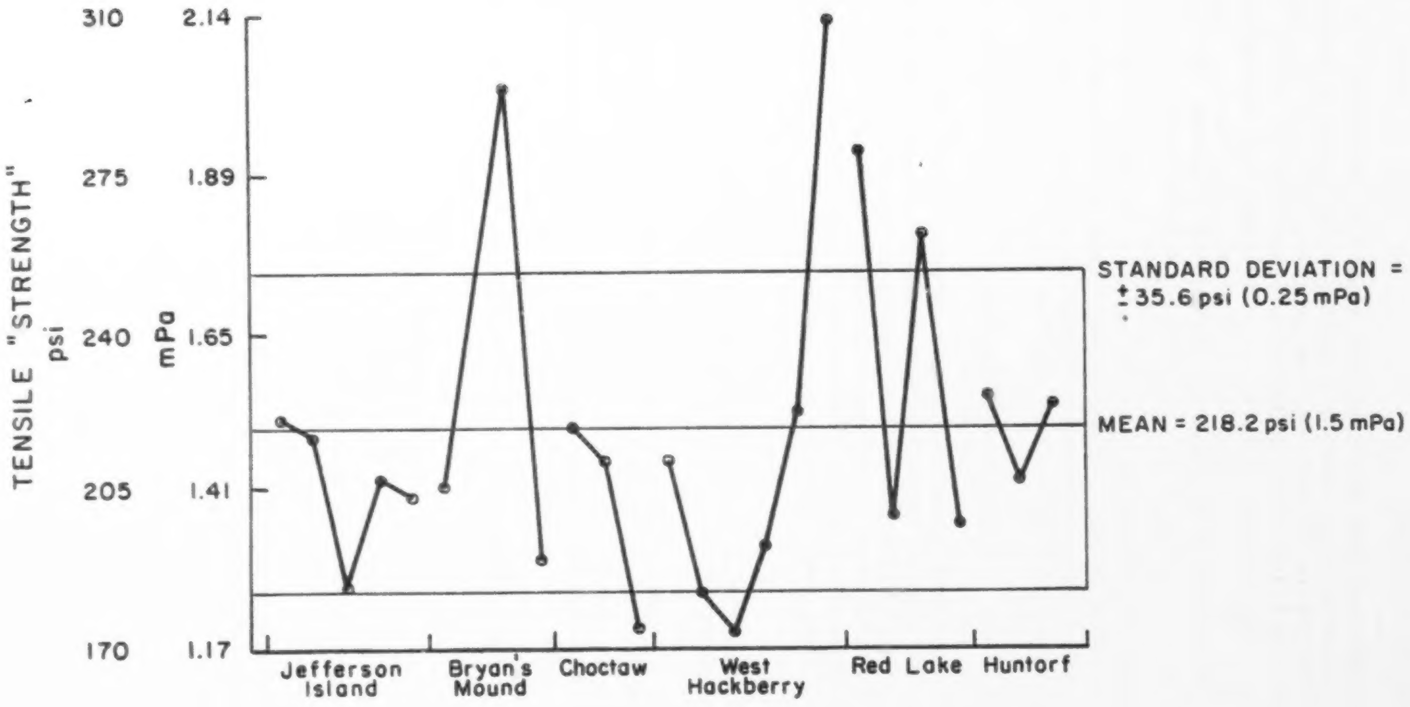

FIG. 1. **BRAZILIAN TEST RESULTS FOR SALT FROM DIFFERENT SOURCES**

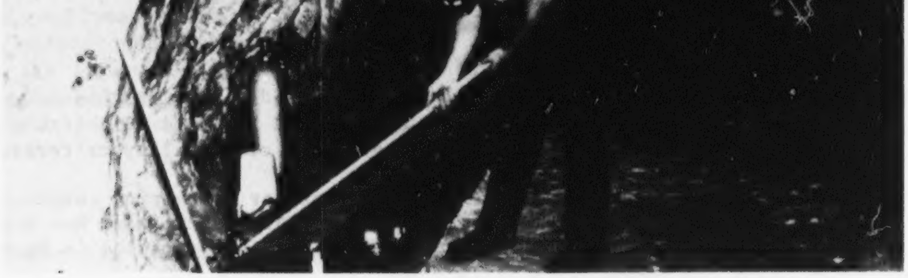

Figure 2. Test Hole Preparation in Mine

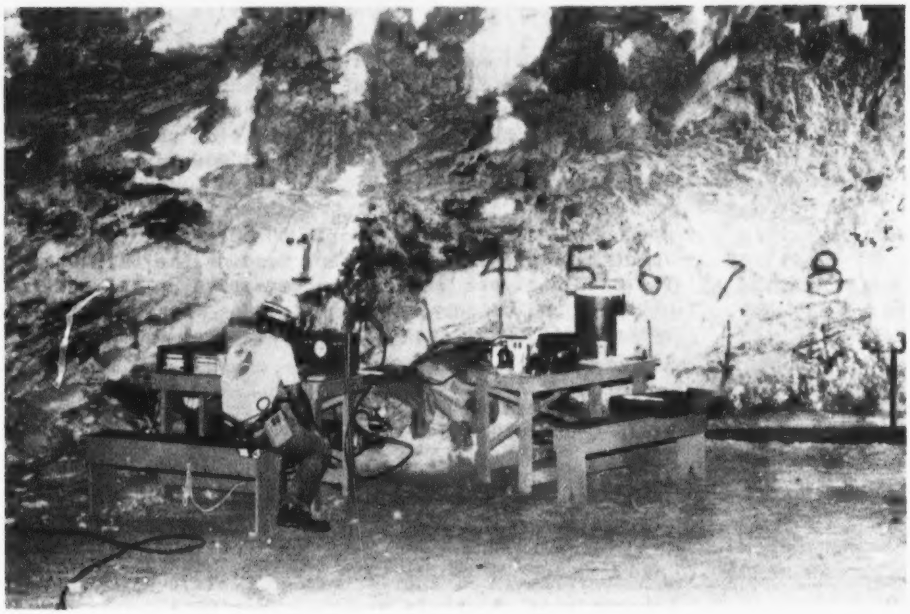

Figure 3. In Situ Test Site

PROJECT SUMMARY

Project Title: Numerical Modeling to Predict Behavior of Underground Hard Rock Caverns Used for Compressed Air Energy Storage

Principal Investigator: Arlo F. Fossum

Organization:
RE/SPEC Inc.
P.O. Box 725
Rapid City, SD 57709
(605)-343-7868

Project Goals: Develop and use numerical models to evaluate the behavior of compensated CAES caverns in hard rock and establish a methodology for the development of stability criteria.

Project Status: The generic portion of the project is nearing completion. It consists of two major phases. The first phase has been completed. The second phase will be completed in September, 1980.

In Phase 1 the major generic rock property characteristics were established, a conceptual numerical CAES simulation model was formulated, and modeling procedures were established for the construction and operational stages of a CAES cavern.

In Phase 2 parametric analyses were made of the excavation and operation of a CAES cavern, precedent information was gathered for underground storage caverns in Scandinavia, and studies were made of the influence of joints on the potential for rock failure around a cavern. Numerical modeling of remedial action is in progress.

Upon completion of the generic phase of the project, a site specific analysis will be performed on the PEPCO CAES site. The CAES analysis methodology developed in the generic phase will be used to design stable caverns for the PEPCO operating cycle and to evaluate the Acres American design of the PEPCO caverns.

Contract Number: Special Agreement No. B-49407-A-H/Prime Contract EY-76-C-06-1830

Contract Period: August 31, 1978 through September 30, 1980

Funding Level: $276,431

Funding Source: U.S. Department of Energy through Pacific Northwest Laboratories, Battelle Memorial Institute

NUMERICAL STUDIES OF CAES CAVERNS IN HARD ROCK

Terje Brandshaug
Arlo F. Fossum
RE/SPEC Inc.
P.O. Box 725
Rapid City, SD 57709

ABSTRACT

This paper summarizes a program to develop and use numerical models to evaluate the behavior of compensated CAES caverns in hard rock and establish a methodology for the development of stability criteria.

It is concluded that there is adequate information available to enable a designer to design an underground opening with the size, shape, and depth required of a CAES cavern with regard to its excavation and construction, based on a combination of numerical modeling and precedent considerations. It is recommended that numerical methods be used in combination with in situ tests to permit the development of a design methodology for the operation of a CAES cavern.

INTRODUCTION

Compressed air energy storage (CAES) has been identified as one means of bulk energy storage with near-term possibilities. Figure 1 illustrates the basic features of a compensated CAES system. A collection of parallel storage caverns is envisioned with each cavern connected at either end by entries to common air and water crosscut tunnels. The crosscut tunnels are connected to the surface compression/generation equipment by an air shaft. The crosscut water tunnels are connected to a surface reservoir by a water inlet/outlet shaft. The surface reservoir provides the compensating head for maintaining constant air pressure in the storage caverns. The operating conditions in a CAES cavern will likely include maximum air pressures of 7 to 7.5 MPa, air temperatures on the order of 40°C to 100°C, and water temperatures from near freezing 0°C to 20°C.

The technical and economic feasibility of CAES is affected by unknowns related to the response of underground caverns to pressure, temperature, and moisture fluctuations that will be encountered in the daily charge and discharge operations of the plant. The temperature fluctuations may generate thermomechanical stresses that could conceivably cause chemical and mechanical damage to cavern walls. Dilatency and/or fracturing could occur in caverns leading to leakage or other damage. Spalling and further disintegration of the walls could lead to successive caving, blowouts, and eventually, to total collapse and surface subsidence. The possibility of these and other potential problems have been alluded to in the literature but little or no data have been available to predict the conditions for which problems might be expected, actions required to prevent their occurrence, or the consequences of failures that might occur.

This program was established to develop and use numerical models to evaluate the behavior of compensated CAES caverns in hard rock and establish a methodology for the development of stability criteria.

BACKGROUND OF NUMERICAL MODELING IN ROCK MECHANICS

Rock mechanics numerical models have been used in the design of underground openings for simulation of thermal, thermomechanical, and hydrological behavior. Depending upon the level of detail required, these models can be used for scoping calculations for pre-

---

RSI PUBL. No. 80-18

conceptual designs, sensitivity calculations for conceptual designs, or for detailed modeling for final designs. These models however are hampered by the difficulty of characterizing or defining adequately the rock mass material properties and other geotechnical features. Thus it must be acknowledged that numerical modeling will not in itself provide answers to all of the questions relating to the unknowns that may affect the technical and economic feasibility of CAES. In recognition of this fact, Pacific Northwest Laboratories (PNL) has sponsored companion programs including a state-of-the-art survey and a rock mechanics laboratory scale testing program.

The state-of-the-art survey has revealed that because there are so many variables that could be important in design in rock, and because it is nearly impossible to evaluate the impact of all these variables on design, a number of empirical approaches have evolved that incorporate those variables that are known to be important from past experience and from reviews of case histories. Although generally conservative these empirical approaches have not been consistent.

One of the goals of this program was to fit, when possible, the results of numerical modeling into a framework of accumulated knowledge and precedent experience, recognizing that a CAES cavern will be subjected to conditions never before encountered by large rock masses.

PROGRAM DESCRIPTION

The program consisted of the following two major phases:

PHASE I. Numerical CAES Simulation Model

A numerical CAES simulation model was developed that is capable of modeling (1) the material characterization of the rock, including the intact and jointed rock mass behavior within both the elastic and inelastic regimes; (2) the geometric construction sequence of the CAES cavern; (3) the cyclic variation in temperature and pressure within the cavern and the associated rock response; and (4) the motion of air or water within the rock mass. This model consists of discrete, but quasistatically coupled, submodels of particular phenomenological events.

PHASE II. Numerical Modeling and Parametric Analyses

A literature survey was made to accumulate knowledge that is currently available in underground excavation practice including a bulk of detailed precedent information, case history results, rock mass quality considerations, and support requirements based on precedent experience. In addition attempts were made to gather as much information as possible on underground air storage caverns in Scandinavia including the world's first two air surge chambers. This information included methods for site selection and characterization, including geological data, selection of depth, orientation and cross section of caverns, methods and details of excavation and rock reinforcement, operating conditions, and testing procedures for liquid or gas leakage.

Numerical simulations and parametric analyses were conducted for the construction and operation of hypothetical CAES caverns with the use of the numerical procedures developed in PHASE I. Excavation stress modeling results were incorporated into empirical guides for excavation stability that take into account rock classifications based on rock mass strength, in situ stress, and maximum compressive stress concentrations along a cavern periphery. See References 1 and 2. Transient and quasi-steady heat transfer simulations were made for the cyclic heating and cooling of CAES caverns corresponding to the emptying and filling of hot air and cold water during the daily charge and discharge operations. Thermoelastic and failure analyses of intact and jointed rock were made making use of the temperature fields calculated in the heat transfer simulations. Simulations were also made of the operational behavior as the strength degraded from fatigue and/or thermal shock. Special topics included the modeling of artificial support and air leakage.

RESULTS

Parametric analyses of the excavation phase of CAES caverns resulted in a catalogue of stress concentration factors for single and multiple caverns with different shapes and extraction ratios under a range of initial in situ stress states. This information was related to case history data for determination of artificial support requirements for caverns situated at a depth of 750 m in igneous rock. An example of such a guide is given in Figure 2. Quantitatively it was found that the rock around a single cavern experiences higher stresses than those induced in the rock around parallel caverns until the extraction ratio is less than 20 percent. For extraction ratios less than 20 percent a multiple cavern array behaves as a single cavern.

The air and water temperatures assumed in the thermal analyses were 40°C and 10°C respectively. It was found that after 50 operational cycles, the rock temperatures approached a steady oscillatory behavior within the first meter into the cavern walls. Since both the roof and the floor were maintained at constant temperatures of 40°C and 10°C respectively, the temperature gradient extended much farther into the rock at these two locations than into the walls. Figure 3 shows the temperature isotherms around a CAES cavern for different operational cycles. Relatively high thermal gradients exist in the rock all around the cavern. The thermal gradients in the roof and the floor diminish as operation continues; however, the gradient in the walls does not change substantially from the initial stage of operation.

The oscillatory behavior of the temperatures in the cavern walls leads to oscillatory behavior of the stresses as well. Figure 4 shows three types of cyclic behavior that can result, namely tension-tension, tension-compression, and compression-compression cycling. It was found that for multiple caverns, extraction ratios could be found for which the tension-tension, and tension-compression cycling could be eliminated.

In the failure analyses performed for the excavation phase, it was found that caverns could be located in a competent igneous rock at 750 m without failure for a wide range of initial in situ stress ratios and cavern height-to-width ratios. However, when two sets of joints were introduced situated at $\pm$ 45 degrees to the horizontal, joint failure could occur as shown by the shaded regions in Figure 5. Decreasing the depth to 500 m decreased the failure zone to that shown in Figure 6. When the cavern of Figure 5 was pressurized, corresponding to a static head of water of 750 m, joint failure was limited to the zones shown in Figure 7. Thus the pressurization of the cavern is an unloading process.

In the failure analyses performed for the operation phase, it was found that multiple caverns could be located in a competent igneous rock at 750 m without failure even after substantial strength reductions caused by fatigue or thermal shock were simulated. However for the cases considered, no tensile stresses had developed.

It was found in the simulations of reinforcement measures that artificial support such as rock bolts provided little or no increase in structural stiffness or strength. This is not to say that rock bolting does not provide suport. However the nature of the support is different than implied above. Rock bolts are used primarily to support blocks or pieces of rock occuring from intersecting joints etc.

Air leakage simulations made with the use of stress-dependent permeability relationships, showed that the coefficient of lateral earth stress had only minor influence on the volume of air leakage. However, the location of leakage in the cavern is strongly dependent on the in situ stress ratio, with the higher value giving rise to a greater loss of air through the cavern walls.

CONCLUSIONS AND RECOMMENDATIONS

Generally speaking, there is adequate information available to enable a designer to design an underground opening with the size, shape, and depth required of a CAES cavern with regard to its excavation and construction, based on a combination of numerical modeling and precedent considerations. The design methodology used in this study for the excavation phase of a CAES cavern can provide a guide in the evaluation of support requirements for caverns of different shapes when excavated in a rock mass with relatively well quantified rock properties and geotechnical characteristics. However, since the empirical information used in this design methodology often includes different types of rock masses in the same classification, different support could be called for in a site specific situation. Thus results obtained by this method thermal/mechanical cycling of rock masses. Scoping calculations similar to those of this program are necessary to identify regions of high stress or zones of potential failure. Designs can then be modified to reduce potential problems. For example, the results of this program indicate that induced cyclic tensile stresses can be eliminated by choosing an adequate extraction ratio.

Since experience is non-existent or limited on the behavior of large rock masses subjected to the operating conditions of CAES caverns, it is recommended that numerical methods be used in combination with in situ tests to permit the development of a design methodology.

This brings to an end the generic portion of the hard rock numerical studies. A site specific study has been recommended and will begin with an investigation of a proposed CAES demonstration project to be located in a foliated metamorphic rock type.

ACKNOWLEDGMENT

This work was supported by the U.S. Department of Energy under Subcontract No. B-49407-A-H Prime Contract DE-AC06-76RLO-1830 with Pacific Northwest Laboratory operated by Battelle Memorial Institute.

REFERENCES

1. Hoek, E.: "The Role of Modeling in the Design of Nuclear Waste Repositories—The Designer's Viewpoint," Proc. Workshop on Thermomechanical Modeling for a Hardrock Waste Repository, Lawrence Livermore Laboratory (UCAR-10043)/Battelle-ONWI, Berkeley, (1979).

2. Gnirk, P. F. and Fossum, A. F.: "A Synopsis of Stability and Design Criteria for CAES and UPHS in Hard Rock Caverns," Proc. Int. Symp. on Subsurface Space (Rockstore 80), Stockholm, v. 2, pp. 615-622, (1980).

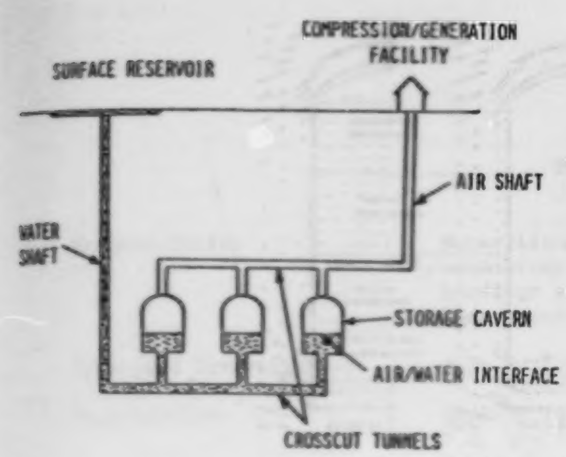
COMPRESSION/GENERATION FACILITY
SURFACE RESERVOIR
AIR SHAFT
WATER SHAFT
STORAGE CAVERN
AIR/WATER INTERFACE
CROSSCUT TUNNELS

FIGURE 1. Underground Layout of CAES Caverns.

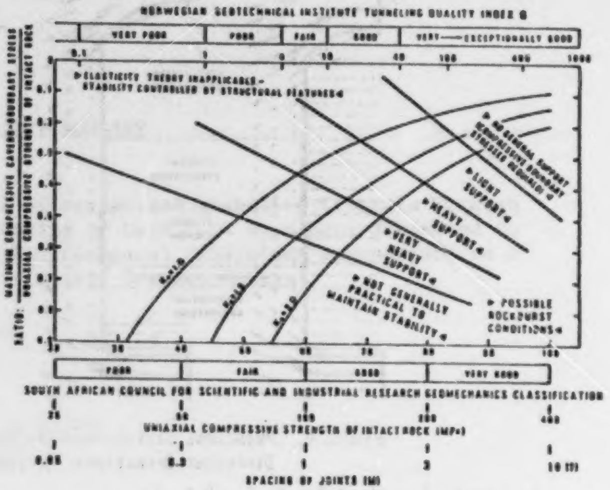

FIGURE 2. Stability Guide for Artificial Support of the Crown of the Central Cavern of a Three-Cavern Array with H/W = 2.0 and an Extraction Ratio of 40% for a Depth of 750 m in Igneous Rock.

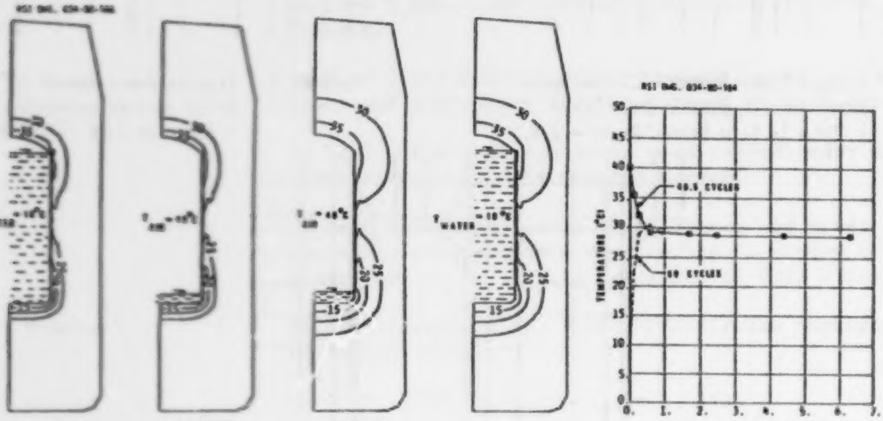

FIGURE 3. Temperature Isotherms (^{o}C) Around a CAES Cavern for Different Operational Cycles.

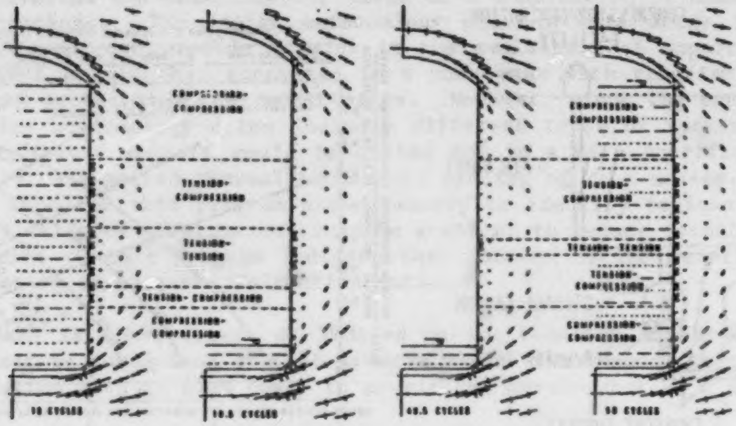
COMPRESSION-
COMPRESSION
TENSION-
COMPRESSION
TENSION-
TENSION
TENSION- COMPRESSION
COMPRESSION-
COMPRESSION
COMPRESSION-
COMPRESSION
TENSION-
COMPRESSION
TENSION- TENSION
TENSION-
COMPRESSION
COMPRESSION-
COMPRESSION
10 CYCLES
10.5 CYCLES
40.5 CYCLES
50 CYCLES

FIGURE 4. PRINCIPAL STRESS TRAJECTORIES AROUND A CAES CAVERN FOR DIFFERENT OPERATIONAL CYCLES.

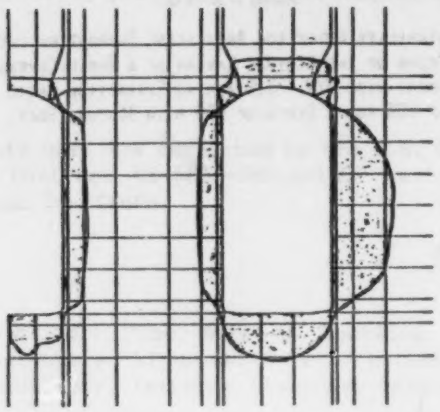

FIGURE 5. FAILURE ZONES AROUND CAES CAVERNS AFTER INITIAL EXCAVATION. DEPTH = 750 M IN SITU STRESS RATIO = 1.5.

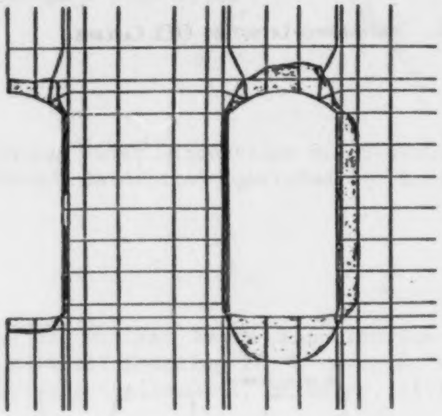

FIGURE 6. FAILURE ZONES AROUND CAES CAVERNS AFTER INITIAL EXCAVATION. DEPTH = 500 M IN SITU STRESS RATIO = 1.5.

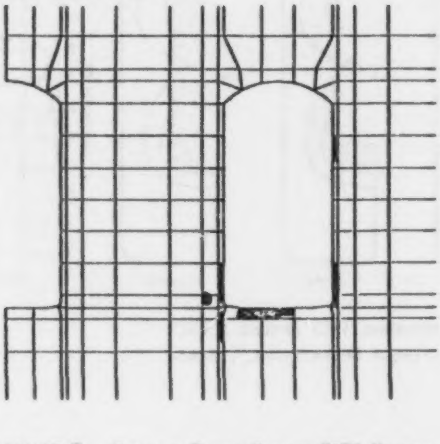

FIGURE 7. FAILURE ZONES AROUND CAES CAVERNS DURING OPERATION. DEPTH = 750 M IN SITU STRESS RATIO = 1.5.

PROJECT SUMMARY

Project Title: Establishment of Design and Stability Criteria Through Laboratory Testing of Hard Rock Specimens Subjected to Loadings and Environmental Conditions Appropriate to a Compressed Air Energy Storage Cavern

Principal Investigator: Arlo F. Fossum

Organization:
RE/SPEC Inc.
P.O. Box 725
Rapid City, SD 57709
(605)-343-7868

Project Goals: Investigate the properties of hard rock specimens, from formations suitable for CAES under the cyclic conditions imposed by a CAES installation, by means of laboratory scale testing; and to formulate preliminary design and stability criteria for CAES caverns.

Project Status: The generic portion of the project has been completed. It consisted of five main tasks.

In Task 1 the rock properties important to CAES were determined. A literature survey was completed to assess areas where data were lacking. Representations were established between a rock's thermal properties and its petrography.

In Task 2 hard rock specimens were procured and prepared for testing.

In Task 3 the mineralogical composition of all selected rock types was determined for the purpose of rock characterization.

In Task 4 the rock specimens were tested under conditions appropriate to a CAES storage cavern.

In Task 5 the results of this program and other previously PNL sponsored programs were scrutinized to arrive at a set of guidelines to be used by designers of CAES caverns.

Contract Number: Special Agreement No. B-512958-A-E/Prime Contract EY-76-C-06-1830.

Contract Period: March 2, 1979, through August 5, 1980

Funding Level: $205,925

Funding Source: U.S. Department of Energy through Pacific Northwest Laboratories, Battelle Memorial Institute

LABORATORY STUDIES OF HARD ROCK FOR CAES

Arlo F. Fossum
RE/SPEC Inc.
P. O. Box 725
Rapid City, SD 57709

ABSTRACT

This paper summarizes a program to investigate the properties of hard rock specimens, from formations suitable for CAES that are subject to the conditions envisioned for a CAES cavern by means of laboratory scale testing.

It is concluded that although the compressive and tensile strengths are adversely influenced by a Compressed Air Energy Storage Cavern environment, the reduced failure strength of hard rocks is sufficiently high to indicate that a CAES plant could be operated satisfactorily.

INTRODUCTION

The energy shortage that became evident during the last decade demonstrated the need for energy conservation. Of special importance is the need to conserve premium fuels. Electric utilities can help by meeting peak power demands without the use of premium fuel burning peaking plants. The dependence on these peaking plants could be reduced or even eliminated if the surplus capacity of base plants during off-peak periods, nighttime, and weekends could be used to supply daytime excess peak demand. All that is needed is a means to store the surplus energy efficiently.

Energy storage has been used by a number of utilities over the past 15 years in the USA, and for more than 40 years in Europe. Some attempts have been made to use storage devices such as lead-acid batteries, but the only effective device for the bulk storage of energy has been the hydroelectric pumped storage facility. This system uses water as the working fluid, storing energy by increasing the potential energy of the water by pumping it to a high level reservoir, and releasing energy through the kinetic energy of the stored water passing through a turbine. Currently the installed capacity of conventional pumped storage in the USA is roughly 10,000 MW. However, conventional pumped storage suffers from some significant disadvantages. Suitable sites are usually remote from load centers. In addition these sites are often the subject of considerable opposition from environmentalists. Therefore, attention has been focused in recent years on the development of alternative means of bulk energy storage. These alternatives include underground pumped hydro (UPH), compressed air energy storage (CAES), various types of batteries, heat storage, and magnetic energy storage. Of these, compressed air energy storage has been identified as one with near-term possibilities.

The technical and economic feasibility of CAES is affected by unknowns related to the response of underground caverns to pressure, temperature, and moisture fluctuations that will be encountered in the daily charge and discharge operations of the plant. The temperature fluctuations will generate thermomechanical stresses that could conceivably cause chemical and mechanical damage to cavern walls. Dilatency and/or fracturing could occur in caverns leading to leakage or other damage. Spalling and further disintegration of the walls could lead to successive caving, blowouts and eventually, to total collapse and surface subsidence. The possibility of these and other potential problems have been alluded to in the literature but little or no data have been available to predict the conditions for which problems might be expected, actions required to prevent their occurrence, or the consequences of failures that might occur.

This program was established to investigate the properties of hard rock specimens, from formations suitable for CAES that are subjected to the conditions envisioned for a CAES cavern by means of laboratory scale testing.

RSI-PUBL. No. 80-17

BACKGROUND OF ROCK MECHANICS LABORATORY SCALE TESTING

Laboratory scale testing of rock specimens will not in itself provide answers to all of the questions relating to the unknowns that may affect the technical and economic feasibility of CAES. Historically laboratory testing has played a relatively minor role compared with the other factors considered in arriving at solutions to practical engineering problems encountered during the rock mechanics analyses of conventional underground openings. In recognition of these facts, Pacific Northwest Laboratories has sponsored companion programs including a state-of-the-art survey and a numerical modeling program.

The most often quoted rock property is the uniaxial compressive strength. This property has been used as an indicator for many different purposes. Rock mechanics engineers have related uniaxial compressive strength to pillar strength, rippability of a rock mass, strength of joints, support requirements of excavations, and to appropriate mining methods. For these purposes rough estimates of uniaxial compressive strength and tensile strength from point load tests generally suffice. However, a CAES cavern is a major underground structure that will be subjected to conditions never before encountered by large rock masses. The response of the rock mass to the associated induced stresses is of utmost concern and an accurate assessment is required of not only the uniaxial compressive strength but also of the triaxial strength under the pertaining conditions. In addition, the elastic properties under known applied stress conditions are required as input for numerical stress analyses. One of the purposes of this program is to determine which properties are significant, what tests should and can be performed, and what kind of results can be expected.

PROGRAM DESCRIPTION

The program was divided into the following five tasks:

TASK 1. Determination of Significant Rock Properties

Information was gathered regarding the proposed operating condition for CAES installations and for existing caverns of similar size and shape to permit an assessment of what rock properties were important and over what range of temperature and pressure they needed to be known. A literature check was made to determine the availability of the requisite rock properties at the appropriate environmental conditions. An evaluation was made of techniques available from composite material mechanics for evaluating thermal properties from a knowledge of the thermal properties of a rock's constituent minerals and their volume percent.

TASK 2. Procurement of Specimens

Rock specimens of several typical CAES host rock types were selected and acquired for testing. These included two granites, a gneiss, a quartzite, and a dolomite.

TASK 3. Selection of Specific Procedures for Rock Characterization

A geological description including the mineralogical composition of all selected rock types was made. Magnifications of 35 and 200X were used with an optical microscope and 250 to 1000X magnifications were used on a scanning electron microscope.

TASK 4. Laboratory Testing

Tests were conducted on rock specimens at room and elevated temperatures with dry and saturated moisture conditions. These tests included indirect tension tests, unconfined compression tests, triaxial compression tests, anisotropic triaxial compression tests, mechanically cycled fatigue tests, thermally cycled fatigue tests and thermal conductivity tests. The tests were designed 1) to determine the amount of strength and stiffness reduction caused by the non-ambient conditions associated with CAES, 2) to determine if the methods for estimating the shear strength-normal strength relationship are adequate over pressure ranges appropriate to CAES, 3) to determine if the methods for estimating thermal conductivity are adequate, and 4) to establish the amount and type of testing needed to define the properties of the rock adequately for CAES application.

TASK 5. Establish Stability and Design Criteria

The results of this program and other PNL sponsored programs were scrutinized to arrive at a set of guidelines to be used by designers of CAES caverns.

RESULTS

Information collected in TASK 1 revealed that the operating conditions in a CAES cavern will likely include maximum air pressures of 7 to 7.5 MPa, requiring a facility depth of 715 to 765 m, air temperatures on the order of 40°C to 100°C, and water temperatures from near freezing $0°C^+$ to 20°C. The significant rock properties include physical, hydrological, and thermomechanical properties. Generally speaking, the greatest inadequacies in physical, hydrological, and mechanical properties data exist in the areas of laboratory and in-situ values for non-intact rock testing at non-ambient conditions. Some types of data for intact rock at ambient and non-ambient conditions are also marginal to somewhat inadequate.

It was found that satisfactory results could be obtained from composite material mechanics for estimates of upper and lower bounds of thermal conductivity but that less satisfactory results could be expected for prediction of thermal expansion coefficients.

The testing program revealed that, for all rock types tested, the unconfined compressive strength decreased with water saturation. Uniaxial compressive strength reductions of 12 to 25% were observed after the rock specimens were saturated with water. This strength degradation can be attributed to a weakening of bonding strength of the rock structure and occurs regardless of the initial degree of saturation or pore-water pressure.

Temperatures of the order of 50-150°C had negligible affect on the strength properties of all rocks tested. However it was found that when a rock was heated and then quenched in water, a significant reduction was observed in the compressive strength. Most of the damage occurs in the first cycle. No discernable difference existed between the compressive strength of rock specimens cycled between 10°C and 50°C and those cycled between 10°C and 150°C. After the first cycle in which the compressive strength dropped an average of 18% for all rock types tested, no subsequent damage was noticeable upon further cycling. The friction angle, as determined from a Mohr's diagram, was unaffected by this thermal cycling. Figure 1 shows the Mohr failure envelope for Redfield Granite after one thermal cycle between 10°C and 50°C together with the failure envelope obtained at ambient conditions. Figure 2 shows similar results for Kasota Dolomite. Note that because the friction angle is unaffected by this cycling, the actual percentage of shear strength reduction decreases with increasing confining pressure.

Mechanical fatigue testing showed that, for loading that alternates between tension and compression, over 50 percent of the tensile strength could be lost within 10,000 cycles corresponding to a CAES cavern life of approximately 30 years. The damage occurs in the tensile portion of the cycle. Figure 3 shows cyclic stress-strain curves for Redfield Granite cycled between ± 62 percent of its tensile strength. Damage from micro-cracking can be seen by the change in modulus in the tensile region of the stress-strain plot of cycle 2500. Figure 4 shows how the modulus decays with cycles, and Figure 5 is an S (strength) -N (cycles) plot for Redfield Granite cycled in the tension-compression mode. Fatigue strengths were much higher in the tension-tension and compression-compression modes for all rock types tested.

Planes of foliation in a rock mass have a pronounced affect on ultimate strength reminiscent of jointed rock behavior as shown in Figure 6. When the direction of the major principal stress is oriented at 30 to 50° from the foliation plane, the strength can be reduced by as much as 50% as compared to that for orientation of 0 and 90°.

CONCLUSIONS AND RECOMMENDATIONS

Strength reductions can be expected in the tensile and compressive strength of rock masses subjected to a CAES cavern environment. The loss of tensile strength is not a major concern since this strength is generally quite low to begin with. The loss of compressive strength caused by the presence of moisture and thermal shock, although of the order of 20%, is tempered by the fact that the frictional coefficient remains relatively constant. Thus the percentage loss of failure strength of the rock decreases with increasing mean stress. Most of the damage will be caused in the first few cycles.

Over the confining pressure and temperature ranges of interest to CAES application, the failure envelopes were linear for the stronger hard rocks and parabolic for dolomite. Because the friction coefficient was not influenced by the non-ambient conditions, reasonable estimates could be made in the future of the failure envelopes with relatively easy to obtain indirect tension and unconfined uniaxial compression tests. Strength reduction factors could be obtained routinely for site specific rocks from these tests. A reasonable assumption to make after the failure envelope has been established is to truncate the tensile portion of the envelope to zero. This is advisable since an already low tensile strength will be reduced by mechanical fatigue and thermal shock.

This program has demonstrated that although the compressive and tensile strengths are adversely influenced by a CAES cavern environment, the reduced failure strength of initially intact hard rocks is sufficiently high to indicate that a CAES plant could be operated satisfactorily. It has also been demonstrated that foliated and/or jointed rock masses require special attention and assessment of strength requirements and strength values become quite site specific.

This brings to an end the generic portion of the hard rock laboratory studies. Site specific studies have been recommended and will begin with an investigation of Sykesville gneiss, a foliated metamorphic rock that will be the host for a CAES demonstration project.

ACKNOWLEDGMENT

This work was supported by the U.S. Department of Energy under Subcontact No. B-51295-A-E/Prime Contract DE-AC06-76RLO-1830 with Pacific Northwest Laboratory operated by Battelle Memorial Institute.

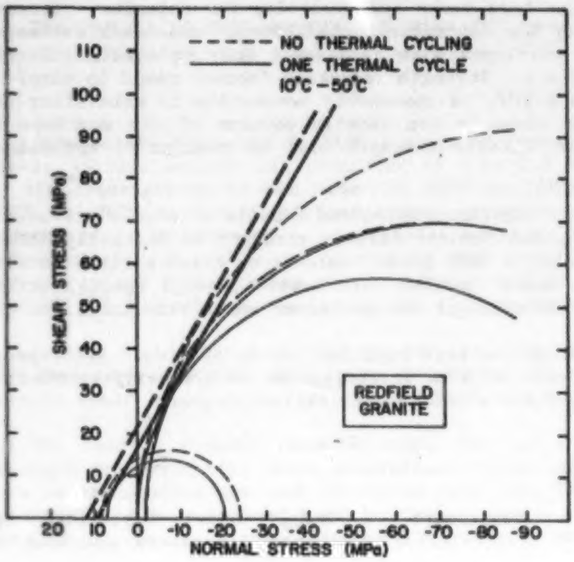

Figure 1. Mohr Failure Envelopes for Redfield Granite.

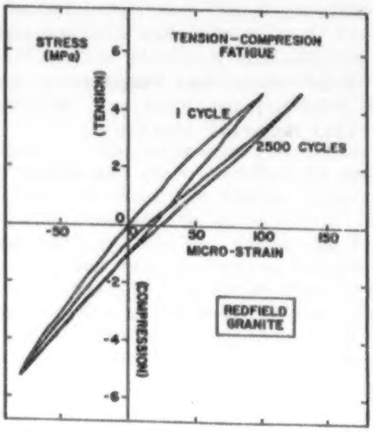

Figure 3. Cyclic Stress-Strain Curves for Redfield Granite.

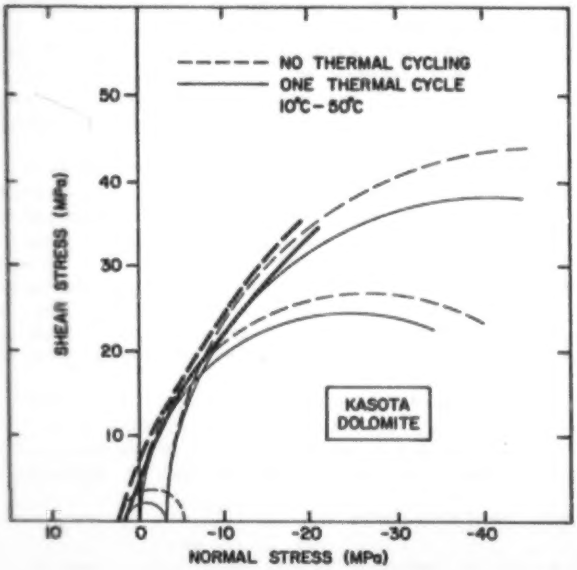

Figure 2. Mohr Failure Envelopes for Kasota Dolomite.

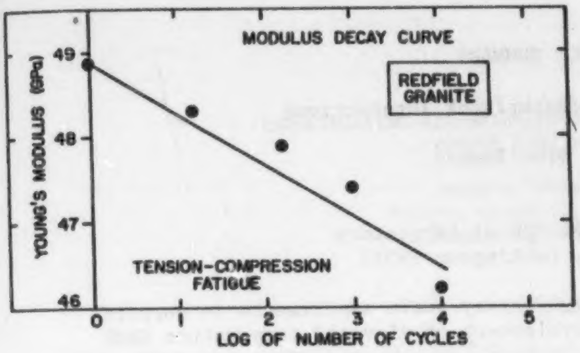

Figure 4. Modulus Decay Curve for Redfield Granite.

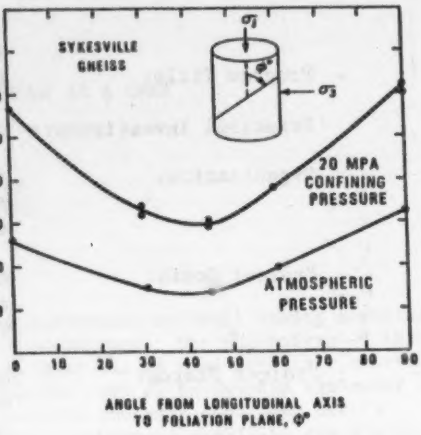

Figure 6. Variation of Compressive Strength of Sykesville Gneiss with Foliation Angle.

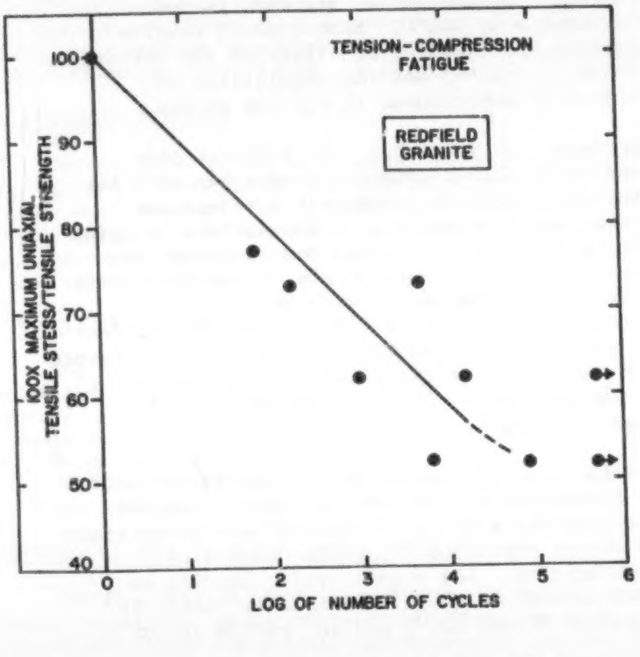

Figure 5. Tension-Compression S-N Curve for Redfield Granite.

PROJECT SUMMARY

Program Title: CAES Air/Water/Rock Interactions

Principal Investigator: James A. Stottlemyre

Organization:
Battelle
Pacific Northwest Laboratory
Richland, Washington 99352

Project Goals: Conduct laboratory-scale experiments in support of the development of elevated temperature CAES reservoir design and operating criteria.

Project Status: Results from PNL autoclave investigations of Galesville sandstone indicate good porosity and permeability stability at temperatures of up to 300°C for a dry air environment. However, in a humid air or liquid water environment, some sandstone disaggregation was observed at temperatures greater than 150°C.

Results from PNL corrosion tests of three carbon steel well casing materials indicate an acceptably low corrosion rate even in humid air environments at 300°C. Some concern remains regarding the physical stability of the corrosion product (hematite) and the possibility of particulate entrainment in the air stream.

Experiments at Terra Tek Inc. indicate that flooding of silica-cemented sandstones with hot water may result in permeability reductions without sample compaction. Particulate plugging appears to be the cause and the magnitude may be rock-type dependent. Tests at the University of Wisconsin-Milwaukee reveal that cyclic ventilation of sandstones with warm dry air does not significantly degrade rock properties. Future work will focus on the effects of hot humid air to span the gap between dry air and liquid water results.

Results from experiments at Los Alamos Scientific Laboratory reveal that for carbonate cemented sandstone the elastic "constants" are temperature and stress dependent apparently caused by densification. Low stress cyclic loading has little effect on elastic "constants" until 10^3 cycles at 50 and 120°C and 10^4 cycles at 200°C.

Contract Number: DE-AC06-76RLO 1830

Contract Period: October 1979 to September 1980

Funding Level: $299K

Funding Source: U.S. Department of Energy

INVESTIGATING AIR/WATER/ROCK INTERACTIONS IN A CAES POROUS ROCK RESERVOIR

James A. Stottlemyre
Pacific Northwest Laboratory
Richland, Washington 99352

ABSTRACT

This paper is a summary of FY-1980 laboratory tests on sandstones and well casing materials subjected to simulated Compressed Air Energy Storage (CAES) conditions. The objectives of this experimental program are: 1) to generate and interpret data that can be used to select reservoirs and develop operating criteria, and assess environmental issues; and 2) to develop equipment and procedures for site-specific field project support. Specific subtasks described herein cover well casing corrosion tests; sandstone permeability and mechanical stability tests with elevated-temperature dry air; similar tests with groundwater; and the development of strategy for future experiments in the porous-media flow facility currently undergoing acceptance testing.

INTRODUCTION AND SUBTASK DESCRIPTIONS

This paper is a summary of FY-1980 results from the following subtasks: 1) well casing corrosion, 2) dry air ventilation of sandstones, 3) thermomechanical stability of sandstones, 4) permeability stability of sandstones, and 5) experimental strategy development for FY-1981. The results described herein represent efforts from a variety of organizations and individuals which are mentioned throughout the text. All tests were, to the extent possible, conducted under simulated reservoir conditions, e.g., elevated temperatures, pressures, and flow rates.

WELL CASING CORROSION

The objective of the well-casing corrosion study being conducted at Pacific Northwest Laboratory is to determine how compressed air energy storage environments affect standard carbon steel casings. Unstressed, electrically isolated samples of three carbon steel casings (A120, H40, and A53B) were autoclaved at various humidities, temperatures, and exposure durations. All tests were run at 12.1 MPa and at temperatures between 50°C and 300°C. Humidity was varied from zero to 100 percent. The effects of salt in the humidified air were also analyzed.

DRY AIR VENTILATION OF SANDSTONES

The objective of a laboratory study at the University of Wisconsin at Milwaukee under the direction of Professor Howard J. Pincus is to determine the physical stability of sandstones exposed to the cyclic ventilation of dry air at temperatures up to 300°C. Variables of primary interest are permeability, porosity, fabric, elastic moduli, and strength properties. This study was designed as a prelude to humid air investigations and has provided baseline (dry air) data on a variety of potential reservoir materials. The primary independent variables analyzed were temperature, air pressure, flow velocity, and the number of ventilation cycles.

THERMOMECHANICAL STABILITY OF SANDSTONES

Thermomechanical stability tests for Galesville sandstone have been completed at Los Alamos Scientific Laboratory under the direction of Dr. James Blacic. The tests focused on how temperature, effective stress, and mechanical stress cycling affect elastic constants and strength properties of Upper Cambrian Galesville sandstone cores taken from a field site in Warren County, Illinois. Test samples, which were right circular cylinders 2.5 cm in diameter by 6.3 cm long, were jacketed and tested in a triaxial, externally-heated pressure vessel. Axial load was applied at a constant displacement rate. Sample strains were determined with three axial and three radial LVDT displacement gages. Confining pressures varied from 0.5 to 41.4 MPa, pore fluid pressures from zero to 10.4 MPa, temperatures from 37 to 204°C, cyclic stress from 5.2 to 10.4 MPa, and the number of axial load cycles from one to 10,000. Dependent variables of primary interest were Young's modulus, Poisson's ratio, inelastic volume strain (difference between total and elastic deformation) at ultimate stress, and ultimate shear strength.

PERMEABILITY STABILITY OF SANDSTONES

Permeability and creep compaction tests for consolidated sandstones under simulated CAES operating reservoir conditions were conducted at Pacific Northwest Laboratory and at Terra Tek, Inc. These tests were motivated by previous studies at Stanford, Texas A&M, and the University of California at Berkeley, where researchers have observed that the permeability of sandstones subjected to distilled water can decrease by 60 percent or more over the temperature range of 25 to 150°C.(1,2,3) However, no systematic change in permeability has been observed for sandstones when dry gas is used as the working fluid. No data exist for humidified air, however, and it is uncertain whether the sandstone response to humidified air would mirror liquid-water or dry-gas results. Since the CAES porous-media flow facility (offering controlled humidity, temperature, stress, and flow conditions) was not as yet available, it was decided to investigate the cause(s) of permeability degradation in a liquid-water environment.

The objectives of the permeability/compressibility tests are: 1) to separate the effects of temperature and time (fluid volume handled), and 2) to quantify the relative importance of thermal expansion of sand grains into pore throats, sample compaction (pore volume reduction) with or without geochemical weakening, anomalous fluid viscosities, pre-existing fines (loose particles), water sensitivity, temperature-induced sandstone disaggregation (cement dissolution and/or sand grain microcracking), mineral scaling, and particles introduced with the inlet fluid (apparatus corrosion products or other contaminants).

All tests were conducted under a confining pressure of 14.8 MPa; a pore fluid pressure of 5.9 MPa; temperatures of 25, 75, 110, 150°C; a flow rate of 8 to 16 ml/min; with samples 5.40 cm x 10.16 cm; and with fluid types such as distilled water, and a 2-percent $CaCl_2$ solution. Permeabilities were computed using Darcy's law corrected for fluid density and viscosity variations; strains were measured with linear variable differential transducers (LVDTs); and temperatures were measured with thermocouples.

EXPERIMENTAL PLANNING FOR FY-1981

The final subtask involved designing experimental strategy for FY-1981 activities in the CAES porous-media flow facility. Briefly, these future experiments will focus on permeability to humidified air, creep compaction, particle carryover, thermal fatigue, and porous-media desaturation. Another important area of research involves trying to resolve the differences in stability among silica-cemented sandstones, carbonate-cemented sandstones, and carbonates.

RESULTS AND CONCLUSIONS

WELL CASING CORROSION

Results of the corrosion study are given in Table 1 and Figure 1. The only significant corrosion product identified was hematite, an iron oxide. As expected, corrosion rates increased with temperature and decreased with time due to the formation of a protective scale. The rates appear to be acceptable with respect to well casing longevity. Only general corrosion was observed, even in a chloride environment. However, the samples were not exposed to artificial stress conditions in these screening experiments. The question of corrosion scale stability, especially in a cyclical temperature environment, is still unresolved. Based on preliminary evidence, it appears that corrosion products, especially at the lower temperatures, may be susceptible to cracking and sloughing under casing expansion/contraction cycles. It is possible that particles will be entrained in the air stream if corrosion products are not strongly adhered to the metal.

DRY AIR VENTILATION OF SANDSTONES

Based on the dry air ventilation test at the University of Wisconsin, it appears that even under the worst combination of temperature (50 to 200°C), axial pressure drop (0.5, 1.0

TABLE 1. Corrosion Rates (mm/yr)*

Pipe Casing	Temperature 175°C	 300°C
A120	0.036 ± 0.009	0.070 ± 0.022
H40	0.056 ± 0.013	0.078 ± 0.015
H53B	0.064 ± 0.008	0.063 ± 0.001

*Test Conditions: 100% Humid Air (Salt Solution Reservoir), 12.1 MPa (120 Atm) 336 Hr.

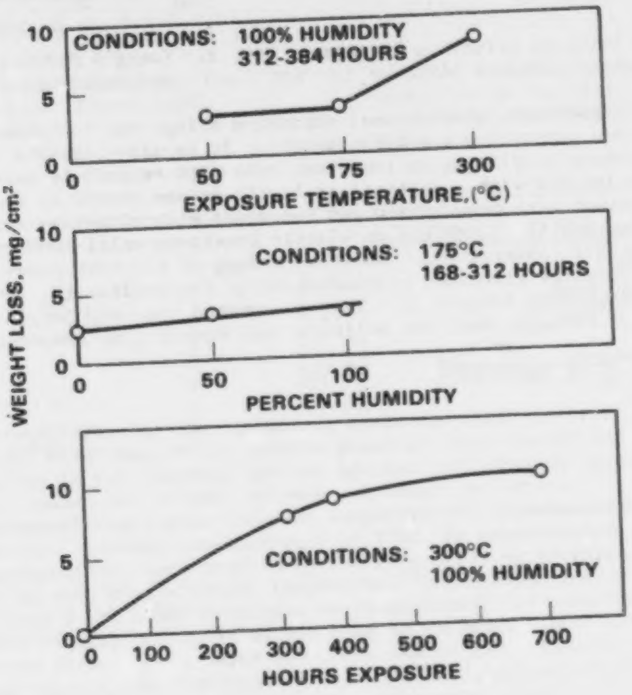

Fig. 1. Corrosion Data for Carbon Steel A120 Well Casing Material

MPa), and number of ventilation cycles (500, 1500, 2500) the permeability of Mt. Simon sandstone decreases by no more than 2.0 percent and that the porosity is totally unaffected. Furthermore, the ventilation with dry air has no effect on specific heat capacity, thermal expansion coefficients, or thermal conductivity. At temperatures of up to 95°C cyclical exposure to air and water has no measurable effect on room-temperature compressive strength, Young's modulus, permeability, porosity, and fabric for St. Peters sandstone.

THERMOMECHANICAL STABILITY OF SANDSTONES

Based on the thermomechanical property tests at LASL, it appears that, at least for carbonate-cemented Galesville sandstone, elastic constants are temperature and stress dependent over the range of 37 to 204°C and 0.5 to 41.4 MPa. Generally, Young's modulus increases and Poisson's ratio decreases with increasing temperature and pressure (Figures 2 and 3). It is

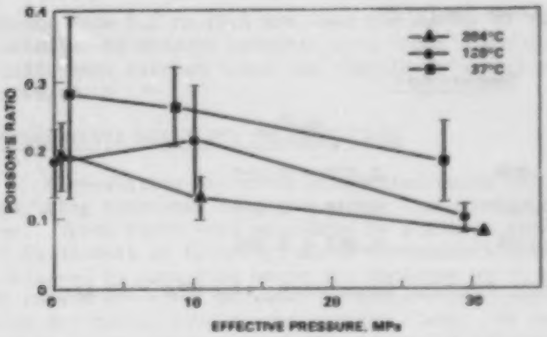

Fig. 2. Poisson's Ratio vs Effective Pressure and Temperature (Blacic LASL)

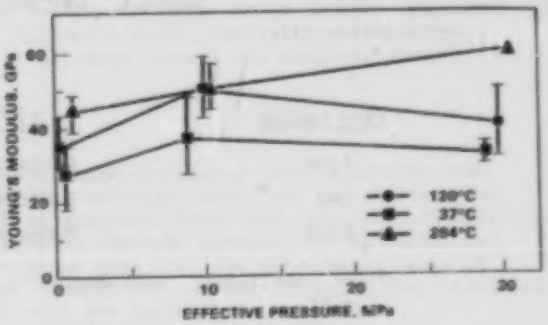

Fig. 3. Young's Modulus vs Effective Pressure and Temperature (Blacic LASL)

speculated, but not confirmed, that thermal expansion brings the individual grains into more intimate contact, thus supporting a stiffer matrix. It is also possible that the dolomitic content of the sandstone is playing an important role with respect to pore volume reduction. Brittle failure was induced with a critical inelastic volume strain of about $4.5 \pm 2 \times 10^{-3}$, which decreases somewhat with temperature and increases with effective stress. Low mechanical-stress cyclic loading has little effect on elastic constants until 1000 cycles at 37 and 120°C and 10,000 cycles at all temperatures. Another finding of the LASL study is that the coefficient of thermal expansion in the direction perpendicular to the bedding is significantly larger than that parallel to the bedding (Figure 4). This phenomenon can have important implications for incremental confining stresses near the wellbore that result from temperature gradients.

PERMEABILITY STABILITY OF SANDSTONES

The compressibility, particle carryover potential, and permeability to liquid water of Massillon sandstone and Ottawa sand are being studied at PNL and Terra Tek. The ratio K_f/K_i of the final (steady state) permeability and the initial permeability at any given temperature for Massillon sandstone is reported in Figure 5. Similar results for Ottawa sand are shown in Figure 6. Although the permeability decreases somewhat with time (fluid volume handled), and at room temperature, the decrease at 150°C is significantly greater. Although the cause of this temperature sensitivity is still unknown, some theoretical explanations have been eliminated thus far as not applicable. Incremental volume strain data as a function of temperature are plotted in Figure 7. Comparing these data with those for a zero porosity quartz aggregate yields a reasonable estimate of pore volume reduction (sample compaction plus expansion of grains into pore throats). For Ottawa sand, the total reduction in pore space between 25°C and 150°C was about 0.8%, roughly half of which is attributable to grain expansion, and the remainder of which reflect bulk compaction. For Massillon sandstone, total pore volume loss was approximately 0.4%. This loss was caused by individual grain expansion into pore throats, since bulk compaction was negligible.

The Kozeny-Carman Equation was used to approximate reductions in permeability. Table 2 shows the results of such a comparison between calculated and measured permeability reductions, where the calculated value is based on pore volume reductions alone, but the measured value includes all potential damage mechanisms. It appears that pore volume reduction due to bulk compaction and/or expansion of matrix constituents into pore throats is not a significant factor in explaining observed permeability decreases with time and temperature.

Although the data collected are not comprehensive enough to generate definitive conclusions, preliminary observations appear to support the following: 1) increases in the total dissolved solids concentration have no measurable effect on viscosity; 2) sample compaction and thermal

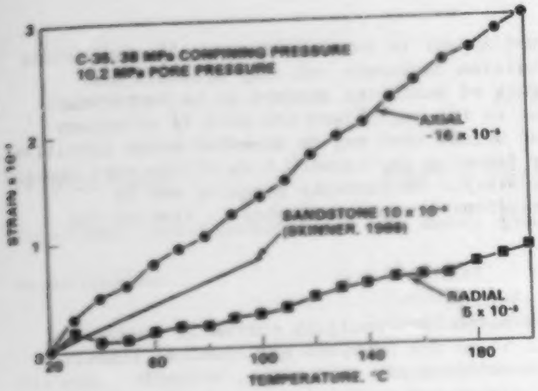

Fig. 4. Thermal Expansion vs Temperature for Galesville Sandstone (Blacic LASL)

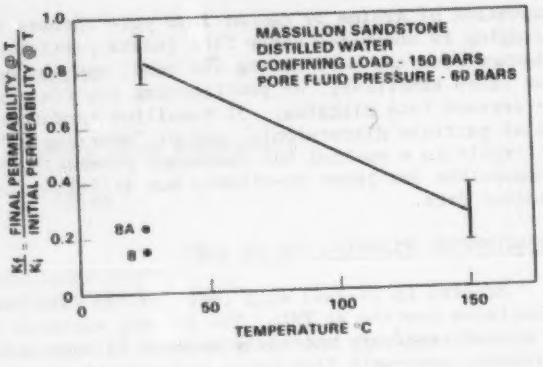

Fig. 5. Ratio of the Final (Steady State) Permeability to the Initial Permeability at a Given Temperature for Massillon Sandstone

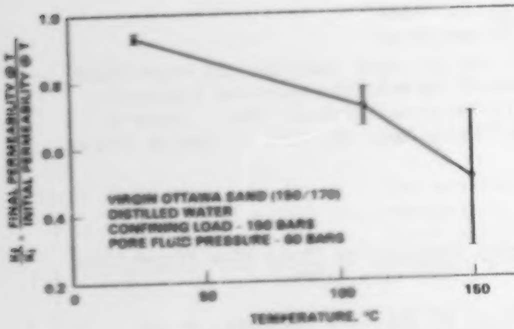

Fig. 6. Ratio of the Final (Steady State) Permeability to the Initial Permeability at a Given Temperature for Ottawa Sand

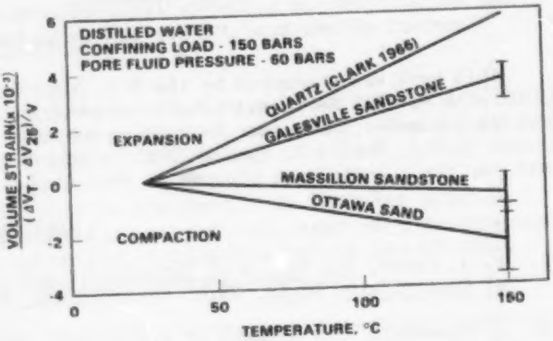

Fig. 7. Incremental Volume Strain vs Temperature

TABLE 2. Results of Pore-Volume-Reduction Analyses*

Sample Type	Incremental Volume Strain (10^{-3})	Porosity Change Measured (%)	Permeability Ratio (K_f/K_i) Calculated**	Measured***
Quartz	5.50	-	-	-
Ottawa Sand	-2.10 ± 1.30	0.80 ± 0.10	0.91 ± 0.04	0.49 ± 0.19
Massillon Sandstone	-0.5 ± 0.2	0.40 ± 0.03	0.95 ± 0.02	0.26 ± 0.11

*Temperature 150°C, Confining Load 150 Bars, Pore Fluid Pressure 60 Bars, Distilled, Deaerated Water

**Calculation: Modified Kozeny Carman Equation for pore volume reduction only.

***Measured: Includes all potential damage mechanisms.

expansion of grains or cement into pore throats do not appear to be significant; 3) particulate plugging is suspected since fine quartz particles, calcium carbonate and clay minerals are flushed from the core during the test, and the quantity of particles appears to be temperature and fluid sensitive; 4) prefiltering the fluid prior to its entry into the core is necessary to prevent face plugging; 5) Massillon sandstone and Ottawa sand may be somewhat water sensitive (clay particle dispersion); and 6) "shutting in" or removing the front 0.5 cm of the core appears to result in a partial but temporary permeability recovery. Particulate plugging may be responsible for these reactions, but definitive conclusions are not warranted in view of the limited data.

EXPERIMENTAL PLANNING FOR FY-1981

Efforts in FY-1981 will focus on the CAES porous-media flow facility currently undergoing acceptance testing at PNL. The primary emphasis will be on the physical and chemical stability of porous reservoir materials exposed to controlled humidified air conditions, effective stresses, near-well flow rates and directions, and elevated and cyclical temperatures. Initial investigations will be made about permeability/compressibility changes, particle carryover, desaturation, and thermal fatigue. Evidence collected to date indicates that reservoir stability under elevated-temperature, CAES operating conditions is good for dry sands and sandstones, but is still questionable under liquid-water and humid air conditions. Therefore, FY-1981 investigations will focus on the effects of humidified air and on identifying the apparent damage mechanism(s) in liquid-water environments.

ACKNOWLEDGEMENT

This work was sponsored by the U.S. Department of Energy under contract (DE-AC06-76RLO 1830) with Pacific Northwest Laboratory, which is operated by Battelle Memorial Institute. Special acknowledgement goes to Rebecca P. Smith (PNL), Robert L. Erikson (PNL), James D. Blacic (LASL), Howard J. Pincus (UWM), Craig H. Cooley (Terra Tek) and Gary J. Banick (Terra Tek) for their individual efforts in this study.

REFERENCES

1. F. J. Casse, The Effect of Temperature and Confining Pressure on Fluid Flow Properties of Consolidated Rocks, Ph.D. dissertation, Stanford University, 1974.

2. A. Muhammadu, The Effects of Temperature and Pressure on Absolute Permeability of Sandstones, Ph.D. dissertation, Stanford University, 1976.

3. A. H. Danesh, J. Ramey, "The Effect of Temperature Level on Absolute Permeability of Unconsolidated Silica and Stainless Steel," Transactions, Geothermal Resources Council, Vol. 2, 1978.

4. R. D. Sydansk, "Discussion of the Effect of Temperature and Confining Pressure on Single-Phase Flow in Consolidated Rocks," Soc. Pet. Engrs. J, August 1980.

PROJECT SUMMARY

Project Title:	Field Studies of Porous Rock Reservoirs
Principal Investigators:	N. Rudd, Robert D. Allen
Organization:	Battelle Pacific Northwest Laboratory Richland, Washington 99352
Project Goals:	Demonstrate the feasibility of storage and cycling of warm compressed air in an aquifer. Investigate physical, chemical, mineralogical, and biological effects of CAES on reservoir rock and caprock and compare with laboratory results. Verify and evaluate numerical modeling of dehydration and water displacement, thermal growth, and cyclic thermal performance. Evaluate system performance with respect to bubble growth rate, mass transfer rates, thermal recovery, water production, and entrainment of mineral particles.
Project Status:	The aquifer field plan is complete. It includes program management, site-selection procedures, test plan development, field setup and operation, activity schedule for FY-1980 through 1982, and projected expenditures. A doubly plunging anticline situated in Pike County west of Pittsfield, Illinois, has been identified. It is characterized by substructural domes, some of which are believed suitable for small scale CAES and testing. The detailed structure and lithology, based upon high resolution shallow seismic surveying, borehole drilling, geophysical logging, and core examination and physical analysis show at least one promising dome. An RFP has been issued to solicit proposals for air injection/withdrawal tests at the site.
Contract Number:	DE-AC06-76RLO 1830
Contract Period:	October 1979 to September 1980
Funding Level:	$548,000
Funding Source:	U.S. Department of Energy

FIELD STUDIES OF POROUS ROCK RESERVOIRS

Neilson Rudd
Dames & Moore

and

Robert D. Allen
Pacific Northwest Laboratory

ABSTRACT

A small-scale field experiment is planned to test compressed air energy storage (CAES) in porous rock reservoirs (aquifers). The proposed site is located west of the town of Pittsfield in Pike County, Illinois. In this project, warm compressed air will be injected into a shallow aquifer and air migration, water displacement, and temperature change will be monitored within a radial array of instrumented, small-diameter boreholes. Changes in chemical and physical properties of reservoir and caprock will be evaluated by analysis of cores obtained before and after injection and air cycling.

The project is divided into three phases: I. Development of the field test plan and preliminary site selection; II. Exploration and confirmation of specific site and site acquisition; and III. Site development, surface plant installation, field testing, and laboratory examination. Phase I is complete, and Phase II is expected to be completed in 1980.

INTRODUCTION

Compressed air energy storage (CAES) is a concept in which electrical energy generated during periods of off-peak demand is used to compress air; the stored air is then used to produce electricity during periods of peak demand. To achieve air containment economically, the compressed air is stored below ground within solution-mined salt cavities, excavated hard rock caverns, or the space made by displacing water from porous and permeable sandstones or carbonates. For storage in porous media or aquifers, the compressed air must be further confined by structural or stratigraphic entrapment to prevent its dispersal.

Structural entrapment is usually created by a convex cap of impermeable rock overlying a porous and permeable reservoir as illustrated in Figure 1. Stratigraphic entrapment results from variations in porosity and permeability within a single stratum, for example, a permeable sand lens confined within a stratum of impermeable shale. Structural entrapment with its more readily defined boundaries and more uniform reservoir development is preferred for storage purposes.

The storage of natural gas(1,2) within Paleozoic anticlinal aquifers has been generally successful in the upper Midwest where caprock permeabilities are low, less than 1×10^{-4} md, and threshold or displacement pressures are high, 2 MPa (300 psi) or higher.

The clear parallel between storage of natural gas and the storage of compressed air led to the aquifer concept for CAES; however, significant differences require evaluation. In CAES the cycling period is daily or weekly compared to seasonal cycling in natural gas storage. Reservoir temperatures are higher in CAES than in natural gas storage both because of the more frequent cycling and because it is advantageous in terms of efficiency and reduced fuel consumption to store and recover the heat of compression. Compressed air is an oxidizing medium as opposed to natural gas, which tends to be a reducing medium. The viscosity and humidity of compressed air exceed those encountered in normal gas storage operations.

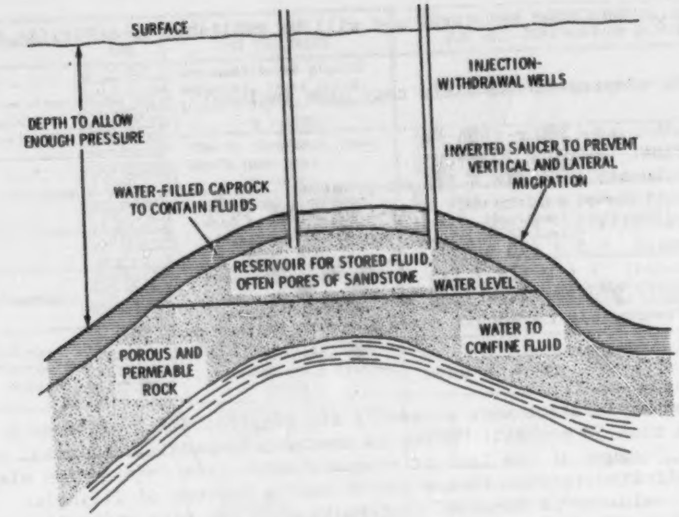
SURFACE
INJECTION-WITHDRAWAL WELLS
DEPTH TO ALLOW ENOUGH PRESSURE
INVERTED SAUCER, TO PREVENT VERTICAL AND LATERAL MIGRATION
WATER-FILLED CAPROCK TO CONTAIN FLUIDS
RESERVOIR FOR STORED FLUID, OFTEN PORES OF SANDSTONE
WATER LEVEL
WATER TO CONFINE FLUID
POROUS AND PERMEABLE ROCK

Fig. 1. Structural Trap Composed of an Aquifer and Caprock

The Pacific Northwest Laboratory under contract with the Department of Energy is evaluating CAES in aquifers and preparing for a small-scale field test. The characteristics of CAES in aquifers have been numerically modeled with respect to temperature distribution, water displacement, dehydration, time, and thermal recovery.(3) Laboratory experiments have simulated CAES conditions of pressure, temperature, chemistry, and flow rate.(3) The field test is now needed to validate both numerical and laboratory conclusions; to demonstrate injection, storage and recovery of air; and to evaluate preliminary reservoir stability criteria.

The field test requires injection of compressed air into a shallow confined aquifer over a period of several months to establish a bubble. This will be followed by cyclical injection and withdrawal of air at ambient and elevated temperatures. The reservoir will be monitored for temperature, pressure, water content and air content during the test. Geochemical, mineralogical, mechanical, and physical property measurements will be made on pre-test and post-test specimens cored at various radii and depths.

This project was planned to transpire in three phases. Phase I consisted of the field test plan and preliminary site screening. Phase II involves site acquisition, seismic exploration, and confirmation by drilling, logging, and core analysis. Phase III will include all aspects of site development, field testing of aquifer and caprock, and laboratory examination.

PHASE I

FIELD TEST PLAN

This task constitutes preparation of the field test plan. The elements of the field test plan include:

- Project management, schedule and budget
- Identification of necessary site characteristics
- Regional site screening
- Selection of candidate sites
- Acquisition of testing and development rights
- Qualification of candidate site
- Development of field experimental plan
- Conduct of field tests
- Pre- and post-test coring and analysis
- Integration of field, laboratory, and numerical modeling results
- Restoration of field site.

The field test plan has been completed and will be published as a Pacific Northwest Laboratory topical report.

The site criteria adopted in the field test plan include:

- Reservoir depth: ca. 200 m (656 ft)
- Reservoir radius: > 100 m (328 ft)
- Reservoir thickness: 5 m (16.4 ft) or greater
- Reservoir pore volume: up to 10^6 m^3 (1.307×10^6 yd^3)
- Reservoir permeability: > 300 md
- Vertical closure: > 5 m (16.4 ft)
- Caprock thickness: > 6 m (19.7 ft)
- Caprock threshold pressure: > 1380 kPa (200 psi)
- Lithology: impermeable carbonate or shale over pure sandstone

SITE SELECTION

Site selection and exploration were primarily the responsibility of Dames & Moore, Park Ridge, Illinois. More than 50 potential sites in southern Wisconsin, Illinois, and Indiana were initially considered. Because of the lack of adequate subsurface information elsewhere, the search was ultimately limited to the oil and gas producing regions of Illinois. Ten sites there were more intensively evaluated in terms of conformity with the site criteria, confidence in structural interpretation, adequacy of reservoir and caprock, potential conflict with recovery of other mineral resources, and general environmental suitability.

The site considered most favorable is located west-northwest of the community of Pittsfield in Pike County, Illinois. A simplified stratigraphic column for the area is shown in Figure 2. The specific structure considered is a doubly plunging anticline, that is, a fold with strata sloping downward on all sides from a common crest. This shape, when reflected by underlying impermeable strata, creates areas of structural entrapment or closure. The anticline is elongated, approximately 25 km (17 mi) long and 10 km (6 mi) wide. The height of the structural closure (called vertical closure) on top of the Silurian formation at this site is at least 75 m (250 ft), and there are indications of smaller, localized areas of closure along the crest of the anticline. It is expected that one of these small areas of structural closure would be suitable for the field test while the large size of the Pittsfield dome as a whole would ensure containment of the compressed air if any air were to escape from the immediate test area. The projected storage reservoir is the St. Peter sandstone formation, and it is expected that the Platteville and Joachim formations would provide an adequate composite caprock. A structure contour map of the uppermost Silurian stratum is shown in Figure 3.

PHASE II

SITE ACQUISITION

An option and air storage easement and lease was developed through the cooperative efforts of Campbell, Furnall, Moore & Jacobsen, Attorneys at Law, Mt. Vernon, Illinois; Pacific Northwest Laboratory; and Coates Field Service, Oklahoma City, Oklahoma. This instrument provides exploration rights with options for drilling of test holes and finally an option to lease the required surface and subsurface rights for development of the field test. Access to 5,946 acres has been obtained to date and is concentrated over the more favorable small areas of local closure.

EXPLORATION

Exploration for the specific field study site has incorporated high-resolution seismic surveying and a number of exploratory wells. The objective has been to define a specific area of local closure small enough for this project, approximately 4.05 ha (10 acres) with a vertical closure of 5 m (16 ft) or more.

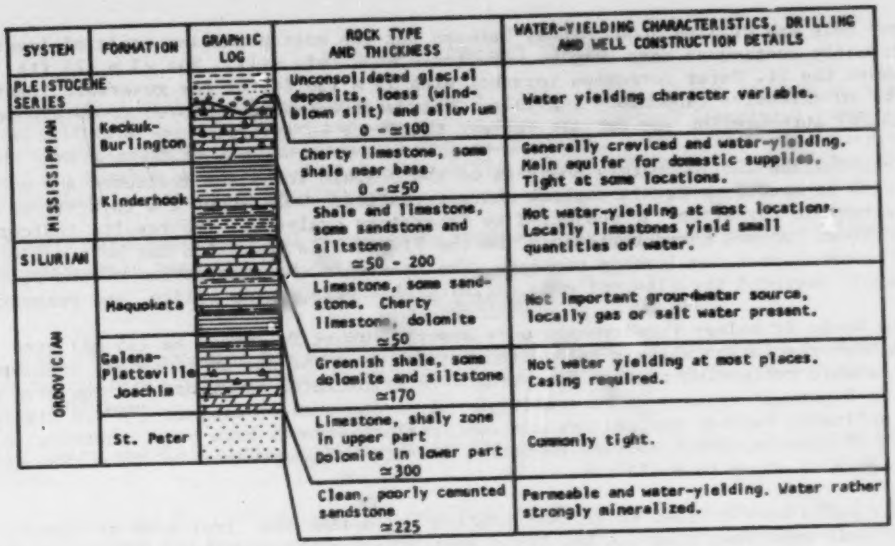

SYSTEM	FORMATION	GRAPHIC LOG	ROCK TYPE AND THICKNESS	WATER-YIELDING CHARACTERISTICS, DRILLING AND WELL CONSTRUCTION DETAILS
PLEISTOCENE SERIES			Unconsolidated glacial deposits, loess (wind-blown silt) and alluvium 0 - ≃100	Water yielding character variable.
MISSISSIPPIAN	Keokuk-Burlington		Cherty limestone, some shale near base 0 - ≃50	Generally creviced and water-yielding. Main aquifer for domestic supplies. Tight at some locations.
	Kinderhook		Shale and limestone, some sandstone and siltstone ≃50 - 200	Not water-yielding at most locations. Locally limestones yield small quantities of water.
SILURIAN			Limestone, some sandstone. Cherty limestone, dolomite ≃50	Not important groundwater source, locally gas or salt water present.
ORDOVICIAN	Maquoketa		Greenish shale, some dolomite and siltstone ≃170	Not water yielding at most places. Casing required.
	Galena-Platteville Joachim		Limestone, shaly zone in upper part Dolomite in lower part ≃300	Commonly tight.
	St. Peter		Clean, poorly cemented sandstone ≃225	Permeable and water-yielding. Water rather strongly mineralized.

Fig. 2. Generalized Column of Rock Formations in Study Area

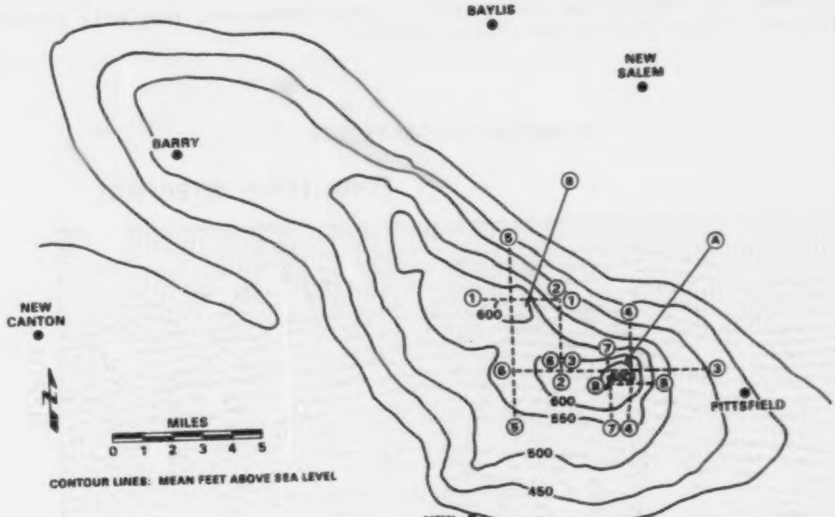
BAYLIS
NEW SALEM
BARRY
NEW CANTON
PITTSFIELD
NEW HARTFORD
MILES
0 1 2 3 4 5
CONTOUR LINES: MEAN FEET ABOVE SEA LEVEL
600
600
550
500
450
400
Ⓐ
①
②
③
④
⑤
⑥
⑦
⑧

Fig. 3. Structure Contours of the Uppermost Silurian Stratum.

The first hole was drilled about midway between the two most promising areas of local closure. Virtually continuous core samples were taken from this well. The 23 m (75 ft) of caprock above the St. Peter formation together with 15 m (50 ft) of the reservoir itself were subjected to extensive laboratory analysis. This well was also employed to obtain seismic velocity data for interpreting the seismic surveys that were to follow.

Visual examination and laboratory analysis of the Joachim formation indicated a 4 m (13 ft) thick layer with apparently adequate caprock characteristics. Only about 2 m (6.6 ft) of the lowermost Platteville formation was subjected to laboratory analysis. The results indicated generally excellent caprock characteristics; so the Platteville formation can be considered a "reinforcing" caprock over the Joachim caprock. The reservoir characteristics of the St. Peter formation greatly exceeded the site criteria defining thickness, permeability, and porosity.

After the basic lithology requirements were assured, about 24 linear km (15 mi) were surveyed with high-resolution seismic reflection techniques. The survey lines are indicated in Figure 3. A seismic reflection section from line 4 is illustrated in Figure 4. One area of closure ("A" in Figure 3) appears to be confirmed. A second area of closure ("B" in Figure 3) is less well defined. Further exploratory and confirmatory efforts have been concentrated on the first area of closure, which appears to have a diameter of approximately 300 m (984 ft) and a vertical closure of about 10 m (33 ft).

Additional wells were drilled to further confirm and define the first area of closure. The first such well went down into the St. Peter formation. Eighteen meters (60 ft) of the Platteville-Joachim caprock were cored for analysis, and additional samples of the St. Peter reservoir were cored for air-water-rock compatibility and other testing required by the Illinois Environmental Protection Agency. A piezometer tube was designed to measure reservoir pressure and to permit sampling of reservoir fluids. Analyses were performed for all items under Title 40, Federal Regulations Parts 141 and 143, and all items under EPA Proposed Water Quality Criteria. Gamma ray emission, spontaneous potential resistivity, and uphole (sound) velocity logs were also recorded for this well.

Subsequent boreholes may be limited to a depth of about 107 m (350 ft) to the top of the Galena formation. Since both drilling and seismic data indicate that the structure on the Galena conforms closely to that at the top of the St. Peter formation, this will permit further structural definition without penetration of the caprock.

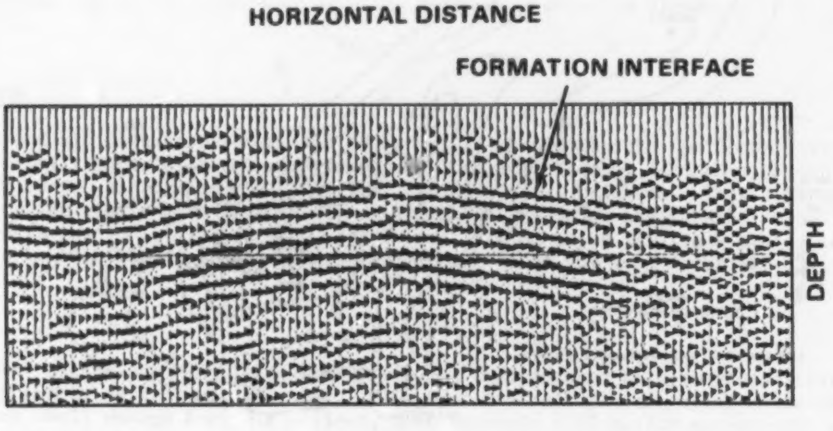

Fig. 4. Seismic Reflection Section of Anticlinal Structure.

SUMMARY OF PROJECT STATUS

At the end of FY-1980, Phase I was completed. A local structural closure at the top of the Pittsfield dome was identified and appears to have the desired structural, caprock, and reservoir characteristics for the proposed CAES test project. Field and laboratory testing are continuing to further document and characterize this site, and it is expected that this work will be concluded in the fall of 1980.

A Source Selection Panel was convened in September to evaluate proposals addressing Phase III, the CAES field test itself.

REFERENCES

1. N. Rudd, "Evaluation of Cap Rock for Underground Compressed Air Energy Storage," Compressed Air Energy Storage Symposium, Pacific Grove, CA, May 15-18, 1978, Proceedings, pp. 243-278, (Jan. 1979).
2. D. L. Katz and E. R. Lady, Compressed Air Storage, Ulrich's Books, Inc., Ann Arbor, MI, (1976).
3. R. D. Allen and P. J. Gutknecht, "Porous Media Experience Applicable to Field Evaluation for Compressed Air Energy Storage," PNL-3294, Pacific Northwest Laboratory, (June 1980).

blank page

MAGNETIC ENERGY STORAGE PROGRAM

blank page

PROJECT SUMMARY

Project Title: Magnetic Energy Storage Program Overview

Principal Investigator: Mitchell O. Hoenig

Organization:
Francis Bitter National Magnet Laboratory
Massachusetts Institute of Technology
150 Albany Street
Cambridge, Massachusetts 02139

Due to large variations in demand, electrical utilities must produce a large fraction of their power output using premium fuels such as oil and gas. The use of diurnal energy storage would reduce power generating fuel costs, as well as reduce our reliance on imported oil, a national goal.

Superconducting Magnetic Energy Storage (SMES) does not require the conversion of electrical energy for the sake of storage. It is potentially more than 90 percent efficient. On the other hand, it represents the most advanced technology and is capital-intensive.

DOE has been supporting SMES, as well as alternate methods of energy storage for a number of years. Currently a small (8 KWH) SMES system is being built by Los Alamos Scientific Laboratory (LASL). It will be installed and operated at the Bonneville Power Administration (BPA) within a few years. Ultimately, a demonstration plant (0.5 to 50 MWH) will have to be built in order to qualify SMES for full scale (1000 to 10,000 MWH) operation. A decision to proceed with a demonstration plant will have to be made by DOE. Innovative programs, as well as technological breakthroughs, are needed in order to qualify SMES for demonstration plant funding.

Contract Number: DE-AC02-80ET26502

Contract Period: 1 September 1980 through 31 August 1981

Funding Level: $80,000

Funding Source: U.S. Department of Energy, Division of Energy Storage

MAGNETIC ENERGY STORAGE PROGRAM OVERVIEW*

Mitchell O. Hoenig
Franics Bitter National Magnet Laboratory**
Massachusetts Institute of Technology
150 Albany Street
Cambridge, Massachusetts 02139

INTRODUCTION

Prime contractors of the Superconducting Magnetic Energy Storage (SMES) Program of the Department of Energy (DOE) are the University of Wisconsin (U of W), the Los Alamos Scientific Laboratory (LASL) and MIT. Our eminent colleagues from LASL and the University of Wisconsin, together with their subcontractors, are responsible for technology development. They will cover their progress in subsequent papers. MIT's role is that of a technical monitor and advisor to DOE. The purpose of this Overview is to focus on overall objectives of the program.

SUMMARY

Due to large variations in demand, electrical utilities must produce a large fraction of their peak power output using premium fuels such as oil and gas. The use of diurnal energy storage would reduce power generating fuel costs, as well as reduce our reliance on imported oil, a national goal.

Superconducting Magnetic Energy Storage (SMES) does not require the conversion of electrical to and from non-electrical forms. It is potentially more than 90 percent efficient. On the other hand, it represents the most advanced and capital intensive technology of any of the storage alternates.

DOE has been supporting SMES, as well as alternate methods of energy storage for a number of years. Currently a small (8 KWH) SMES system is being built by Los Alamos Scientific Laboratory (LASL)! It will be installed and operated at the Bonneville Power Administration (BPA) within a few years. Ultimately, a demonstration plant (0.5 to 50 MWH) will have to be built in order to qualify SMES for a full scale (1000 to 10,000 MWH) operation. A decision whether or not to build a demonstration plant will have to be made as early as 1983 by DOE! Innovative programs utilizing technological breakthroughs are needed in order to qualify SMES for demonstration plant funding.

ENERGY STORAGE

(1) Cyclic variations: (a) second by second
(b) diurnal

Diurnal variations are seasonal, varying between 35 and 85% of summer peak load, and 44 and 90% of winter peak load.

(2) Present pattern of electrical power generation:
- (a) Baseload - large capital-intensive plants, steam, coal and nuclear.
- (b) Intermediate demand - (10 to 14 hrs./day) - older, less efficient equipment.
- (c) Short-term peak demand - (3 hrs./day), fast starting, low-capital-cost equipment, expensive fuel. Oil-fired turbines are typical. Cost of electrical power for the short term is 5 to 10 times more costly than baseload power.

---

*Supported by the Department of Energy, Division of Energy Storage Systems.

**Supported by the National Science Foundation.

(3) If energy storage were available, essentially only base load generators would be used. They would operate at constant power.

Overall energy production costs would stabilize at reduced levels. Use of premium fuels would be minimized, thus satisfying a federal concern and our primary task.

Use of premium fuels by electric utilities:
(a) Oil....... 1.74 MBD** .... in 1978
a peak consumption level
(b) Gas....... 4 TCF*** .... in 1972
3.2 TCF .... in 1978

SMES

(1) Energy stored is proportional to (a) number of turns,
(b) current level,
(c) the enclosed volume.

(2) Must use superconductors. Normal conductors are resistive and rapidly convert stored energy to thermal energy.

(3) Major problems facing a SMES system, in addition to cost, are:
- (a) electrical stability,
- (b) protection in case of quench,
- (c) structural integrity.

(4) Design options:
- (a) Cooling techniques available are:
  - (i) Pool boiling helium at 4.2 K and 1 atm,
  - (ii) Superfluid helium at approx. 1.8 K and 1 atm, or at 1.8 K and approx. 40 torr,
  - (iii) Supercritical (single phase) helium at or above 2.5 atm and temperatures between 4.2 K and 8 or 9 K.
- (b) Refrigeration is costly. The compressor energy requirement is approximately 400 and 1000 times the energy input at the 4.2 K and 1.8 K temp. levels (resp.).
- (c) Choice of superconductor:
  - (i) NbTi is most developed. To be economical it requires operation at 1.8 K in spite of the higher refrigeration costs.
  - (ii) Nb_3Sn is less developed. Equivalent current levels (compared to NbTi at 1.8 K) could be obtained at 4.2 K.
- (d) Choice of structure:
  - (i) Large magnetic fields associated with high currents produce very large mechanical forces on the current conductor.
  - (ii) The conductor must be properly restrained with axial and radial supports.
  - (iii) Where supports rest on external, room temperature structure, the supports must also act as thermal insulators.
  - (iv) Major designs to date, by the University of Wisconsin (U of W)[1] and the Los Alamos Scientific Laboratory (LASL)[2], have assumed the use of radial, insulating struts resting on bedrock.

---

*Million barrels per day
**Trillion cubic feet

(5) Size and Scope of SMES:

SMES has the potential to be competitive with alternate energy storage concepts on a large scale.

- (a) Current SMES concept (U of W):
  - (i) Energy
    - Energy stored: 10,000 MWH ($3.6.10^{13}$ J)
    - 10 HR power rate: 1,000 MW
  - (ii) Geometry
    - Simple solenoid coil
    - Coil diameter: 280 m
    - Coil height: 150 m
    - Coil depth: 300 to 400 m below surface
    - Coil would be segmented and located in a number of concentric horizontal tunnels, but with slightly different tunnel diameters.
  - (iii) Superconductor
    - Superconductor: M.F. NbTi in copper
    - Stabilizer: High (though not exotic) purity aluminum
    - The conductor: Approx. 8 cm diameter solid with superconductor and stabilizer integrated in a hub-and-spoke, high-strength aluminum spine, filled in with additional aluminum stabilizer.
    - Current level: 100,000 (plus) amps
    - Field: 2 to 3 Tesla
  - (iv) Stability: Inherent in use of Superfluid helium (HeII) coolant and high stabilizer content.
  - (v) Protection: Segmentation of coil and HeII dewars, using helium enthalpy to slow down quench.
  - (vi) Structure: Use of high strength aluminum spine. Support of conductor against bedrock by means of radial, A-frame, insulating struts.
  - (vii) Bedrock load: 300 to 400 psi
- (b) An alternate U of W Concept:[3] "Low-aspect ratio design"
  - (i) Energy: Same
  - (ii) Geometry: Simple Solenoid
    - Coil diameter: 1100 m (or larger)
    - Coil height: approx. 11 m
    - Coil depth: 10 m below surface
  - (iii) Bedrock load: Reduced from 300 to 30 psi
- (c) Other alternatives:
  - (i) All alternatives to the simple solenoid would require an increase in quantity of materials.
  - (ii) A toroidal coil configuration would provide self shielding.
  - (iii) LASL has been looking at the possible use of cabled conductors.
  - (iv) MIT has been looking into the use of alternatives to helium enthalpy as a means of slowing down temperature rise in the event of quench, as well as reducing helium inventory.

ECONOMICS OF SMES

The conclusion must be reached that the economics of a large (10,000 MWH) SMES system are uncertain. An independent study by J. Nicol and B. Winer, Arthur D. Little, Inc.,[4] (ADL) has shown that SMES, with its high energy-conservation efficiency, could be economically very attractive in comparison to alternate energy storage methods. ADL cautions, however, that the technological base for an accurate evaluation is not available at this time. A more conservative review of SMES by Battelle[5] is in agreement with this view. They suggest, moreover, that the economic impact of some key technical problems could preclude the use of SMES under economically competitive circumstances.

DOE POSITION ON SMES

(1) SMES has to compete with pumped underground hydro (UPH) and underground compressed air storage (CAES).

(2) Decision point on SMES is likely to come towards the end of (CY) 1983. At that time DOE will have to decide to either:
   (a) Build a first generation "non-oil-fired CAES", or
   (b) Proceed to build a 0.5 to 50 MWH demonstration SMES.

(3) SMES concepts have a potential 90% (plus) overall, efficiency, 20% higher than competing concepts.
   (a) SMES represents the highest technology requirements and is capital intensive.
   (b) Present SMES concepts compete marginally.
   (c) Innovative programs are needed. Only a new approach or technological breakthrough will give SMES a clear competitive advantage.

(4) DOE is committed to construct and operate LASL's 30 MJ (8 KWH) SMES demonstration system at Bonneville Power Administration (BPA). For details see subsequent LASL papers.

(5) DOE is committed to support SMES Programs at U of W and LASL (see subsequent papers).

MIT POSITION

As technical monitors and consultants to DOE, we at MIT are committed to:

(1) Encourage and support both LASL and Wisconsin in their SMES programs.

(2) Compare existing technological concepts in terms of feasibility, protection, long term maintenance, repairability, as well as cost.

(3) Search for new and innovative concepts, materials and fabrication techniques in order to make SMES more competitive.

(4) Generate uniform costing standards based on a consensus between research laboratories and participating industry.

(5) Examine existing as well as proposed tasks in terms of cost-effective utilization of limited resources presently available. Establish a list of priorities.

(6) Resolve the question of environmental magnetic shielding and evaluate its effect on cost and space constraints.

(7) Bring industry into the SMES planning process.

(8) Help bring SMES to its 1983 decision point.

REFERENCES

(1) Review of Diurnal Superconducting Energy Storage at the University of Wisconsin, R. W. Boom; Paper I-1, Proceedings of the International Symposium on Superconductive Energy Storage, Osaka, Japan, 1979. Status of Superconductive Energy Storage Project at the University of Wisconsin, S. W. Van Sciver; Paper II-2, same proceedings.

(2) 1-GWH Diurnal Load-Leveling Superconductive Magnetic Energy Storage System Reference Design, W. V. Hassenzall and J. D. Rogers; Paper II-5, Proceedings of the International Symposium on Superconductive Energy Storage, Osaka, Japan, 1979.

(3) "Low Aspect Ratio Solenoids", R. W. Boom, et al; DOE Review June 25, 1980, unpublished memorandum. Diurnal Energy Storage Systems Design, R. W. Boom, to be presented November 11, 1980 as part of "Magnetic Energy Storage Program", this conference.

(4) "An Evaluation of Superconducting Energy Storage"; Arthur D. Little, Inc. to DOE, Div. of Energy Storage, 1979.

(5) "Superconducting Magnetic Energy Storage - A Review of Technical, Economic and Marketing Factors", Battelle, Columbus Laboratories to DOE, Div. of Energy Storage, January 1980.

PROJECT SUMMARY

Project Title:	Superconducting Magnetic Energy Storage (SMES)
Principal Investigator:	John D. Rogers
Organization:	University of California Los Alamos Scientific Laboratory Los Alamos, New Mexico 87545 (505)-667-5427; FTS 843-5427
Project Goals:	The goals of the SMES program are two-fold. These are to design, fabricate, and place into operation a 30-MJ, 10-MW SMES unit for electric utility transmission line stabilization on the Bonneville Power Administration (BPA) system by 1982-83. The second goal is to design and have constructed a SMES unit up to 10 MWh size. This unit will be for a completely detailed engineering prototype demonstration of an electric utility diurnal load-leveling system.
Project Status:	The engineering design of the BPS SMES transmission line stabilization system is in an advanced state. Many large hardware items are specified and on order. The refrigerator was installed in a trailer with controls added for remote operation. Acceptance tests were performed at the factory and the unit has been delivered to the Los Alamos Scientific Laboratory (LASL). The design of the 30 MJ superconducting coil was completed by General Atomic Company (GA) with the exception of the coil top interface for dewar mounting. GA is now fabricating the coil. An engineering design of the seismic load coil support was completed. All copper and additional superconducting wire were obtained for the 5 kA cable. Development of the 5 kA cable is complete and New England Electric Wire is making the cable. The heat rejection unit has been trailer mounted and is ready for operation. Trailer installation is now contracted for the helium gas recovery system. The converter manufacture is complete and factory testing for acceptance was successfully conducted. The converter power transformers are built and undergoing factory tests. The auxiliary power transformers were obtained. The BPA site installation layout has been devised. Detailed controls design and operating logic for remote microwave link operation of the SMES unit in the BPA system are well established, and many electronic components are on order. The LASL, BPA, DOE interface working agreement was completed. The work done on the large diurnal load leveling SMES was a preliminary 50 kA wire rope superconducting cable design and a study of SMES units on power system stability.
Contract Number:	W-7405-ENG-36
Contract Period:	Continuing
Funding Level:	$1,580,000 FY1980
Funding Source:	Department of Energy, Division of Energy Storage Systems and Division of Electrical Energy Systems.

WIRE ROPE SUPERCONDUCTING CABLE FOR DIURNAL LOAD LEVELING SMES

G. A. Costello
Department of Theoretical and Applied Mechanics
University of Illinois at Urbana-Champaign
Urbana, Illinois 61801

ABSTRACT

This paper is concerned with the design of a wire rope cable for a superconducting magnetic energy storage (SMES) unit. The superconducting wires in the rope permit the passage of large currents in the relatively small conductors of the windings and hence cause large electromagnetic forces to act on the rope. The diameter of the rope, from a strength point of view, can be considerably reduced by supporting the rope at various points along its length.

INTRODUCTION AND SUMMARY

The high magnetic fields of large SMES devices produce very large outward forces on the superconducting wires. One such design to resist these forces would be to support the superconducting wires with a wire rope. The superconducting wires could be wrapped helically around the outside of a stainless steel wire rope.

Figure 1 shows a schematic drawing of a rope loaded with a force per unit length, p. The force, p, per unit length acts normal to the deformed centerline of the rope. The arc

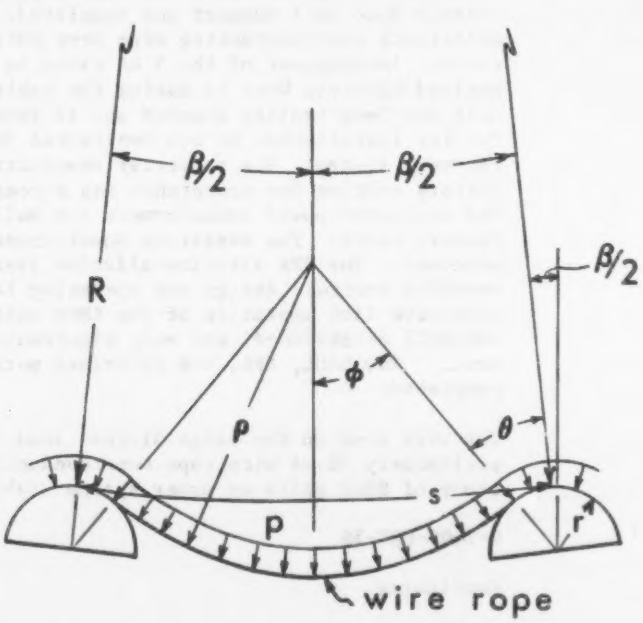

Fig. 1. Superconducting cable wire rope schematic with uniform force loading.

length spacing, s, of the support points is determined by the radius, R, to the support points and the number of supports, n. Hence

$$s = \frac{2\pi R}{n}, \text{ and} \tag{1}$$

$$\beta = \frac{s}{R} \tag{2}$$

An examination of Fig. 1 yields the following equations

$$\phi = \Theta + \frac{\beta}{2}, \tag{3}$$

$$\rho\phi + r\Theta = \frac{L^*}{2}, \text{ and} \tag{4}$$

$$(\rho + r) \sin \phi = (R + r) \sin \frac{\beta}{2}, \tag{5}$$

where L^* is the final stretched length of the rope between supports. The above relations were determined by neglecting the bending stiffness of the wire rope and thus allowing each section of the rope to deform into a segment of a circle.

Figure 2 shows the general loading system acting on a wire rope which is deformed into a circular segment of radius, ρ. F and M_T are the axial force and axial twisting moment, respectively, and M_B is the bending moment applied to the rope. The twisting moment, q, per unit length must be applied to keep the rope in equilibrium. In general, q is small and will be neglected in this analysis.

The component parts of a wire rope are shown in Fig. 3. The core of the rope will be, in our present design, another wire rope strand. Additional strands will be wrapped helically around the core to provide the required strength.

The axial force, F, in the rope is given by the equilibrium equation

$$p\rho = F \tag{6}$$

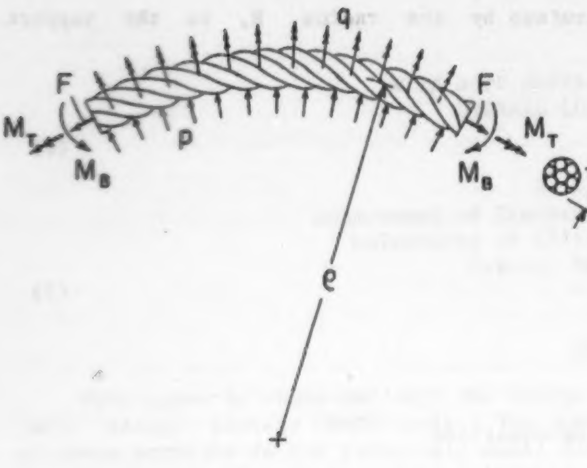

Fig. 2. Wire rope loading system.

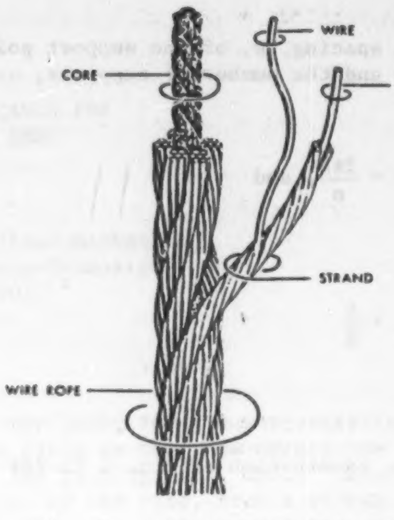

Fig. 3. Wire rope components.

The axial force is also given by the expression[1]

$$F = A\bar{E}\frac{(L^* - L_o)}{L_o} = A\bar{E}\varepsilon \ , \qquad (7)$$

where A is the metallic area of the rope, $\bar{E}$ is the modulus of elasticity of the rope, L_o is the unstretched length of the rope between supports, and ε is the axial strain in the rope.

Recent investigations[2,3,4,5] have shown that the largest tensile stresses occur in the center wire if the residual stresses are neglected. The axial straight wire in the center of the rope will receive the largest axial stress and the largest stress due to bending. The stresses in the nearby wires are close to the stresses in the center wire, and, hence, the center wire stresses will be used as a basis for design. The maximum tensile stresses in the center wire are given by the expression

$$\sigma_{max} = E\frac{(L^* - L_o)}{L_o} + \frac{Ec}{\bar{r}} \ , \qquad (8)$$

where E is the modulus of elasticity of the material in the rope, c is the center wire radius, and $\bar{r}$ is the radius, of curvature of the center wire. For the curvatures under consideration the stresses due to bending will be rather large unless the wire radius, c, is very small.

Consider, for example, a wire rope consisting of a 7 x 19 wire rope core around which will be wrapped helically six strands consisting of 7 x 19 wire rope. This process can be continued until the required area is formed. The next layer would contain twelve strands, etc. Let, for example, the total number of wires in the rope be given by

$$133 + 6(133) + 12(133) + 18(133) = 4921$$

Assuming the same wire radius, the area is given by the expression,

$$A = 4921 \times \pi c^2 . \tag{9}$$

Values for the wire rope superconducting cable representative of a typical 1 to 10 GWh diurnal load leveling SMES coil[6] have been chosen to demonstrate the practical nature of a wire rope cable. The example presented is not an optimized design. Let $R = 2598.43$ in. and $s = 78.74$ in. The angle β is then equal to 1.735°. Let the load per unit length p equal 1341.67 lb/in., the value of $r\theta$ equal 15 in., and $\phi = 50^\circ$. Equation 3 determines θ and Eq. 5 determines ρ. Hence $\theta = 49.132^\circ$ and $\rho = 34.245$ in. Let the metallic area equal 1.15 in.^{2} and $E = 13{,}000{,}000$ psi. A very safe working stress limit of 100,000 psi was chosen for the wire in the rope. The yield stress for three-quarter hard 304 stainless steel is 170,000 psi at liquid helium temperature. The 0.00862 in. radius wire will more nearly be full hard with >50% cold reduction with a yield stress near 220,000 psi. Equations 6 and 7 yield a strain ε equal to 0.00307. Since the area is 1.15 in.^{2}, Eq. 9 yields $c = 0.00862$ in. The maximum tensile stress is then given by Eq. 8 and hence

$$\sigma_{max} = 30{,}000{,}000\ (0.00307) + \frac{30{,}000{,}000 \times 0.00862}{17.49}$$

$$= 92{,}100 = 14{,}785 = 106{,}800 \text{ psi} < 110{,}000 \text{ psi}$$

The final length of the rope between supports is given by Eq. 4; hence,

$$L^* = 2\left[34.245\ (0.8726) + 15\right] = 89.764 \text{ in.};$$

and the original length of the rope between supports is

$$L_o = 89.489 \text{ in.}$$

The diameter of the rope is 1.81 in., and the bearing stresses on the support is

$$\sigma_{bearing} = \frac{3968.63}{1.0 \times 1.81} = 2{,}192.6 \text{ psi.}$$

CONCLUSION

A method of design has been developed which will determine the necessary dimensions of a wire rope used as a support structure for superconducting wires. The design takes advantage of the properties of a wire rope, that is, the ability to resist large tensile forces with relatively small bending stiffness. A superconducting cable based upon a wire rope for use in a diurnal load leveling SMES unit provides a simple means of fabrication at the SMES site. Inherent in a wire rope is that continuous lengths of cable can be made by very conventional means at low costs without concern for making joints in either the superconducting strands or the wires of the rope.

REFERENCES

1. Wire Rope Handbook, Leschen Wire Rope Company, Saint Joseph, Mo., 1971.

2. Costello, G. A., and Phillips, J. W., "Effective Modulus of Twisted Wire Cables," Journal of the Engineering Mechanics Division, ASCE, Vol. 102, No. EMI, Proc. Paper 11944, Feb., 1976, pp. 171-181.

3. Costello, G. A., "Large Deflections of Helical Spring Due to Bending," Journal of the Engineering Mechanics Division, ASCE, Vol. 103, No. EM3, Proc. Paper 12964, June 1977, pp. 479-487.

4. Costello, G. A., "Analytical Investigation of Wire Rope," Applied Mechanics Reviews, Vol. 31, No. 7, July 1978.

5. Costello, G. A., and Butson, G. J., "A Simplified Bending Theory for Wire Rope," submitted for publication to ASCE.

6. Rogers, J. D., Hassenzahl, W. V., and Schermer, R. I., "1-GWh Diurnal Load-Leveling Superconducting Magnetic Energy Storage System Reference Design," Los Alamos Scientific Laboratory report LA-7885-MS, Vol. I through Vol. VIII (September 1979).

PROJECT SUMMARY

Project Title: A Study of the Effects of Energy Storage Inductor-Converter Units on Power System Stability

Principal Investigator: Richard T. Byerly

Organization:
Westinghouse Electric Corporation
Advanced Systems Technology
East Pittsburgh, Pennsylvania 15112

Project Goals: Develop a mathematical model suitable for representing SMES units in power system stability studies. Incorporate that model into a large-scale stability program. Perform demonstration studies to illustrate the effects of SMES units on power system stability.

Project Status: The project has been completed, and the final report is in preparation.

The SMES unit model encompasses the converter and converter transformer, the converter control system, and the storage inductor. Documentation of the model is specifically intended to facilitate computer programming and includes flowcharts as well as equations and block diagrams.

The Westinghouse 2000 bus stability program has been modified to accommodate the model. Detailed instructions for data preparation for the SMES unit model have been written, including SMES unit data forms.

Demonstration studies based on two hypothetical systems have been performed, emphasizing the potential for improved damping of oscillations associated with synchronizing power flow.

The influence of an SMES unit on power system dynamic behavior depends on its storage capacity, the rating of conversion equipment, the location of the unit, its control system, and operating circumstances. These factors can be investigated in the context of large-system stability studies.

Contract Number: LASL 4-L69-6553L-1

Contract Period: September 17, 1979 through September 1, 1980

Funding Level: $37,921

Funding Source: U.S. Department of Energy through Los Alamos Scientific Laboratory

EFFECTS OF SMES UNITS ON POWER SYSTEM STABILITY

Richard T. Byerly Jose A. Juves
Westinghouse Electric Corporation
Advanced Systems Technology
East Pittsburgh, Pennsylvania

ABSTRACT

A mathematical model suitable for representing SMES units in power system stability studies has been developed and incorporated into an existing large-scale stability program. Demonstration studies have been performed which emphasize the use of SMES units to improve the damping of oscillations associated with synchronizing power flow among generators. The capability exists to conduct stability studies of large systems which include SMES units.

INTRODUCTION

Normal operation of electric power systems involves generator speed variations which are characterized, in part, by oscillations. Such oscillations usually decay with time but, in some circumstances, may persist or increase in magnitude. Unstable oscillations may represent interactions among a few generators and have primarily local effects, or they may involve large groups of generators and have widespread effects.

Small SMES units, such as the one discussed in reference 1, have the potential to improve the damping of one or more modes of oscillation. The influence of an SMES unit depends on its storage capacity, the rating of conversion equipment, the location of the unit, its control system, and operating circumstances. Investigation of these factors in the context of large-system studies is desirable, especially for modes of oscillation involving large groups of generators. This development project has been motivated by that need.

SMES MODEL DESCRIPTION

The SMES unit model encompasses the converter and the converter transformer, the converter control system, and the storage inductor. Detailed discussion of the model, including equations, block diagrams, and flowcharts to facilitate computer programming, is contained in reference 2. It is sufficient here to describe the general features of this model.

The converter and converter transformer equations relate the positive-sequence fundamental-frequency alternating voltage and current of the transformer primary to the direct voltage and current of the storage inductor. The model accounts for the effects of delayed ignition and commutation and the constraints imposed by minimum ignition and extinction angles. The inductor current bypasses the converter during intervals of low commutation voltage.

The conversion equations are combined with the usual ac network equations and solved iteratively. The solution process determines correct and compatible values of voltage and current on both sides of the converter.

The primary objective of converter control in the SMES model is to obtain a desired power flow to or from storage. The desired power will generally be derived from one or more ac system variable such as frequency, machine speed, or transmission line power. The model provides as many as three parallel dynamic control channels whose input signals may be independently selected from a list of ac system functions. The output signals from these channels are summed to obtain a variable component of desired power to storage.

Momentary values of desired power and inductor current determine a corresponding desired value of converter terminal voltage. Ignoring secondary control objectives, the converter ignition angle is adjusted, within limits, to establish the desired terminal voltage.

The model of the converter control system also has provision for gradual correction of inductor current drift, but this function is not likely to be significant in the short time interval of most stability studies.

Inductor current is calculated from its initial value and the integral of converter terminal voltage with respect to time. The control objectives related to power and drift correction are set aside if the resulting terminal voltage would cause inductor current limits to be violated.

The Westinghouse 2000 Bus Stability Program has been modified to accommodate this SMES unit model. The demonstration study results described in the following paragraphs were obtained with that program.

HYPOTHETICAL SYSTEM WITH A DC LINE

The diagram of Fig. 1 shows a dc line transmitting power from the generator at bus 1 to an ac network. The machine at bus 5 is a condenser connected to the tertiary of the inverter transformer. The primary terminal of the inverter transformer is bus 6.

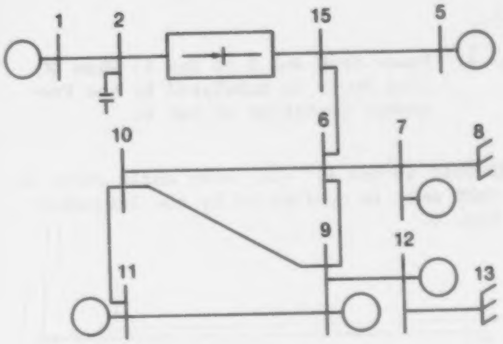

Fig. 1. Single-line Diagram for Hypothetical System with a DC Line.

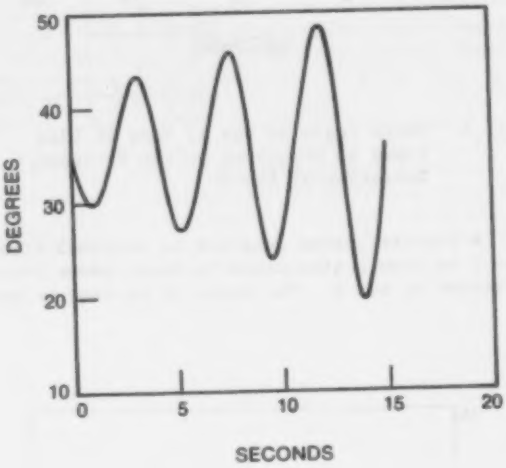

Fig. 2. Rotor Angle at Bus 12 for Unstable System Oscillation in the Absence of Either DC Line or SMES Unit Damping.

There are five modes of oscillation associated with synchronizing power flow between the infinite buses and the machines at buses 5, 7, 9, 11, and 12. An eigenvalue analysis of these modes of oscillation is contained in Appendix E of reference 3. One mode, in which the five synchronized machines oscillate coherently relative to the infinite buses, is unstable. The rotor angle of the generator at bus 12, shown in Fig. 2, is taken from a simulation of this unstable mode. The motions of the other four synchronized machines are similar.

Positive damping for this mode can be obtained by modulating the dc line power. The rotor angle in Fig. 3 is from a simulation in which the dc line power is modulated by the frequency deviation at its inverter transformer primary, bus 6. The power from bus 6 to bus 15 is shown in Fig. 4. These relatively short-term power variations change the speed and kinetic energy of the generator at bus 1, which acts as a flywheel. The period of the oscillation is too short for significant turbine speed-governing system response.

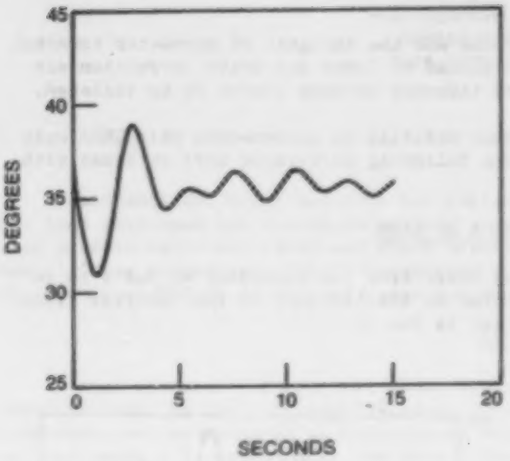

Fig. 3. Rotor Angle at Bus 12 When DC Line Power Is Modulated by the Frequency Deviation at Bus 6.

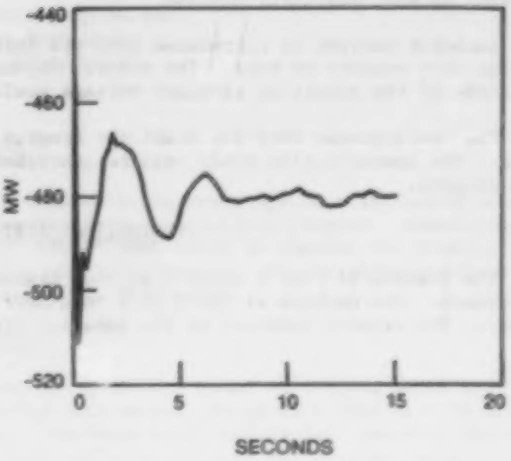

Fig. 4. Power from Bus 6 to Bus 15 When DC Line Power Is Modulated by the Frequency Deviation at Bus 6.

A similar system behavior is obtained with an SMES unit at bus 6. The rotor angle curve in Fig. 5 is from a simulation in which power flow to an SMES unit is controlled by the frequency deviation at bus 6. The power to storage is shown in Fig. 6.

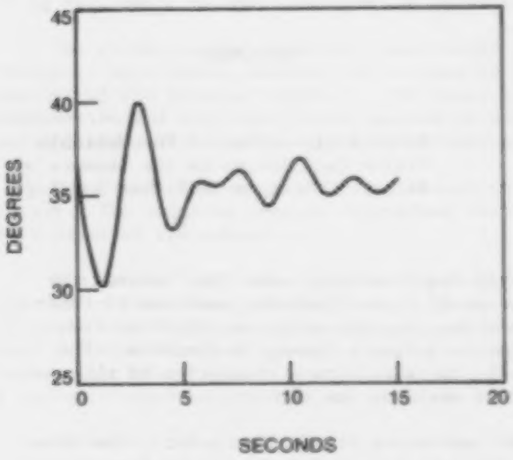

Fig. 5. Rotor Angle at Bus 12 When Power Flow to SMES Unit at Bus 6 Is Controlled by Frequency Deviation at Bus 6.

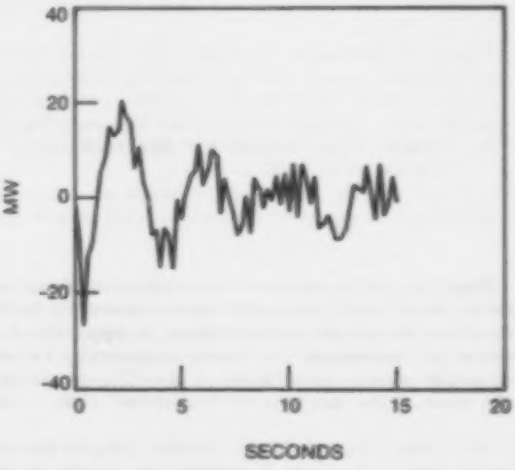

Fig. 6. Power to SMES Unit at Bus 6 Controlled by Frequency Deviation at Bus 6.

FAULT SIMULATION

The simulations to be described were made to test the SMES unit model in the presence of nearby ac system faults. The system of Fig. 7 has an unstable mode of oscillation that is damped by an SMES unit at bus 5 controlled by the speed deviation of the generator at bus 6.

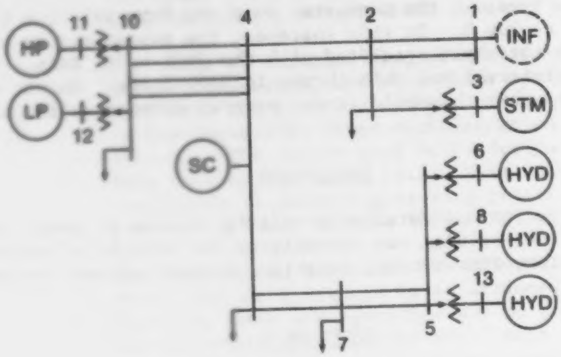

Figure 7. Hypothetical System Diagram.

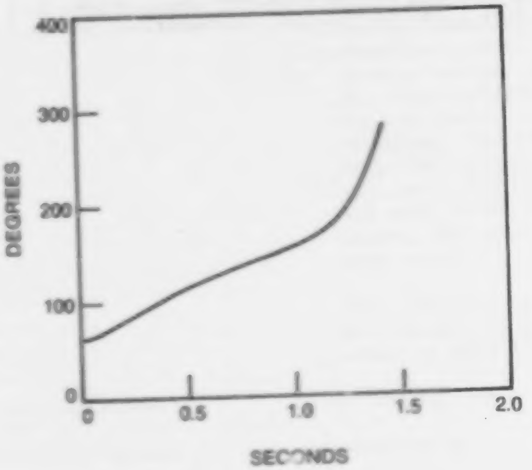

Fig. 8. Rotor Angles for Generators at Buses 6, 8, and 13 Following Fault at Bus 5.

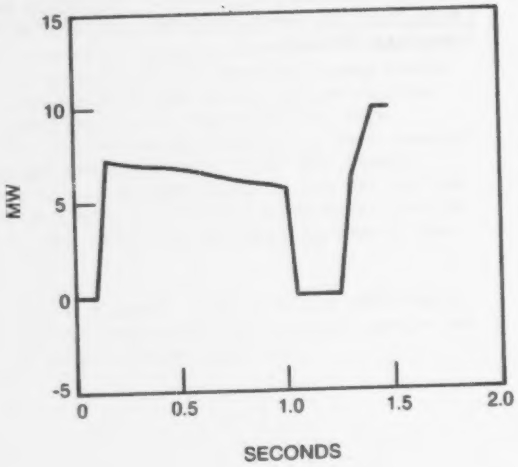

Fig. 9. Power to SMES Unit at Bus 5 Following Fault at Bus 5.

A fault at bus 5 on one of the lines to bus 7 is cleared by tripping both ends of the faulted line after six cycles. The generators at buses 6, 8, and 13 rapidly lose synchronism with the rest of the system as shown by the rotor angle curve of Fig. 8. Power to the SMES unit is shown in Fig. 9. During the fault, inductor current bypasses the converter because the commutation voltage is zero. The voltage across the inductor is zero, and there is no current in the converter transformer primary. When the fault is cleared, converter operation recovers, and power flows to storage because the speed deviation of the generator at bus 6, which controls converter power, is positive. Power is limited by the relatively low voltage at bus 5 following the fault. The converter is operating at the minimum ignition angle, and the gradual decline in power is associated with a gradual drop in voltage at bus 5 as the generators pull out of step.

Inductor current again bypasses the converter over the interval from 1.05 seconds to 1.25 seconds due to low voltage at bus 5. In this instance, the bypass occurs because the voltage at bus 5 falls below 0.7 pu, a threshold specified with the SMES model data. The converter might have operated through this interval had this threshold been lower. On the other hand, bypass will occur without regard to this threshold if the program detects an inability to commutate due to low voltage.

CONCLUSION

The capability exists to conduct detailed stability studies of large electric power systems which include SMES units. Such studies can investigate the effects of various factors, including SMES storage capacity, converter rating, location, control system design, and system operating conditions.

REFERENCES

1. R. I. Schermer, 30MJ Superconducting Magnetic Energy Storage for BPA Transmission Line Stabilizer. Mechanical, Magnetic, and Underground Energy Storage 1980 Annual Contractors' Review, Washington, D.C., November 10-13, 1980. U.S. Department of Energy.

2. R. T. Byerly, R. J. Bennon, D. E. Sherman. A Study of the Effects of Energy Storage Inductor-Converter Units on Power System Stability. Final Report, Contract LASL 4-L69-6553L-1, Funded by U.S. Department of Energy through Los Alamos Scientific Laboratory. Westinghouse Electric Corporation, Contractor.

3. EPRI EL-727, Contract 744-1. Frequency Domain Analysis of Low-Frequency Oscillations in Large Electric Power Systems. Final Report, Part 1--Basic Concepts, Mathematical Models, and Computing Methods.

PROJECT SUMMARY

Project Title: Superconducting Magnetic Energy Storage (SMES)

Principal Investigator: John D. Rogers

Organization:
University of California
Los Alamos Scientific Laboratory
Los Alamos, New Mexico 87545
(505)-667-5427; FTS 843-5427

Project Goals: The goals of the SMES program are two-fold. These are to design, fabricate, and place into operation a 30-MJ, 10-MW SMES unit for electric utility transmission line stabilization on the Bonneville Power Administration (BPA) system by 1982-83. The second goal is to design and have constructed a SMES unit up to 10 MWh size. This unit will be for a completely detailed engineering prototype demonstration of an electric utility diurnal load-leveling system.

Project Status: The engineering design of the BPS SMES transmission line stabilization system is in an advanced state. Many large hardware items are specified and on order. The refrigerator was installed in a trailer with controls added for remote operation. Acceptance tests were performed at the factory and the unit has been delivered to the Los Alamos Scientific Laboratory (LASL). The design of the 30 MJ superconducting coil was completed by General Atomic Company (GA) with the exception of the coil top interface for dewar mounting. GA is now fabricating the coil. An engineering design of the seismic load coil support was completed. All copper and additional superconducting wire were obtained for the 5 kA cable. Development of the 5 kA cable is complete and New England Electric Wire is making the cable. The heat rejection unit has been trailer mounted and is ready for operation. Trailer installation is now contracted for the helium gas recovery system. The converter manufacture is complete and factory testing for acceptance was successfully conducted. The converter power transformers are built and undergoing factory tests. The auxiliary power transformers were obtained. The BPA site installation layout has been devised. Detailed controls design and operating logic for remote microwave link operation of the SMES unit in the BPA system are well established, and many electronic components are on order. The LASL, BPA, DOE interface working agreement was completed.

The work done on the large diurnal load leveling SMES was a preliminary 50 kA wire rope superconducting cable design and a study of SMES units on power system stability.

Contract Number: W-7405-ENG-36

Contract Period: Continuing

Funding Level: $1,580,000 FY1980

Funding Source: Department of Energy, Division of Energy Storage Systems and Division of Electrical Energy Systems.

30-MJ SUPERCONDUCTING MAGNETIC ENERGY STORAGE
FOR BPA TRANSMISSION LINE STABILIZER

R. I. Schermer
Los Alamos Scientific Laboratory of the
University of California
Los Alamos, New Mexico 87545

ABSTRACT

The Bonneville Power Administration operates the transmission system that joins the Pacific Northwest and southern California. A 30-MJ (8.4-kWh) Superconducting Magnet Energy Storage (SMES) unit with a 10-MW converter can provide system damping for low frequency oscillations. The unit is scheduled to operate in 1982. Progress during FY 80 is described. The conductor has been fully tested both electrically and mechanically, all of the necessary copper and superconductor has been purchased, and the first production lengths of cable have been fabricated. All major components of the electrical and cryogenic systems except the gas recovery unit have been received, but the refrigerator, converter, and one transformer were damaged during shipment. The dewar is being procured, and the coil support system has been designed. Support work at LASL to prepare for subsystem testing is nearly complete.

INTRODUCTION AND SUMMARY

The Pacific Northwest and southern California are part of the Western U.S. Power System and are connected by two 500-kV, ac-power transmission lines, collectively referred to as the Pacific AC Intertie, and one ± 400 kV dc-transmission line, the Pacific HVDC Intertie. These transmission lines are operated by the Bonneville Power Administration (BPA).

The stability of the Western Power System is affected by relative weakness of the tie provided by the 905-mile-long Pacific AC Intertie. Studies made before energization of the Pacific AC Intertie showed that negatively damped oscillations with a frequency of about 20 cpm were likely to occur, and in 1974 negatively damped oscillations with a frequency of 21 cpm (0.35 Hz) were observed. Subsequent to these instabilities, BPA installed equipment on the HVDC Intertie to modulate power flow between the interties, damping the oscillations, and increasing the stability limit of the Pacific AC Intertie from about 2100 MW to 2500 MW, whenever the HVDC Intertie is operating. However, the availability of the HVDC Intertie is 89.5%, and the southern terminal was down for six months at one time as a result of earthquake damage. A back up stabilizing system could be used. Late in 1975, representatives of BPA and the Los Alamos Scientific Laboratory (LASL) developed the concept of installing a small SMES unit for the purpose of providing system damping similar to that now available through modulation of the interties. The design parameters of the unit to be installed at the Fite Substation near Tacoma are summarized in Table 1.

Several descriptions of the project have appeared previously,[1,2,3] and should be consulted for details. This report will concentrate principally on the work done in FY 80.

Figure 1 is an isometric view of the 30 MJ system components in their planned arrangement. At the upper left of the figure is the ac-dc converter flanked by two, 6-MVA, transformers. The right half of the figure is occupied by the cryogenic system -- refrigerator, heat rejection subsystem, gas recovery subsystem, liquid nitrogen supply, and gaseous helium supply with each subsystem housed in its own trailer. Not shown is the control trailer, located immediately behind the cryogenic system trailers, that houses the mini-computers which permit the system to run unattended. All of the above subsystems are being assembled at LASL for test under computer control prior to final assembly at Tacoma. The coil and nonconducting dewar will be shipped directly to Tacoma without a test at LASL.

TABLE 1

DESIGN PARAMETERS OF THE 30-MJ SYSTEM STABILIZING SMES UNIT

Maximum power capability, MW	10
Operating frequency, Hz	0.35
Energy interchange, MJ	9.1
Maximum stored energy, MJ	30.0
Coil current at full charge, kA	5
Maximum coil terminal voltage, kV	2.18
Coil operating temperature, K	4.5
Coil lifetime, cycles	$>10^7$
Heat load at 4.5 K, W	<150
Coil diameter, m	3.0

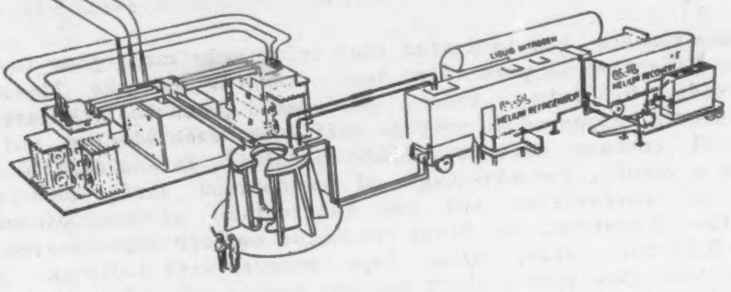

Fig. 1. Isometric view of 30-MJ system layout.

In the center of Fig. 1 is the coil, contained within its nonconducting liquid helium vessel. The 5-kA superconducting cable for the coil is being fabricated on schedule with the first lengths already produced and completion set for January 1981. Coil fabrication has begun and is on schedule. Dewar design was delayed pending completion of a detailed engineering of coil support under seismic loads, so that dewar procurement is behind schedule and the dewar has become the critical path item.

SITE PREPARATION

The test area at LASL has been provided with all necessary utilities. All the cryogenic and control trailers have been properly located as in Fig. 1 - with the exception of the gas recovery trailer - and all plumbing interconnections have been made, electrical interconnections have been fabricated and installation is proceeding.

An Interface Working Agreement, signed by LASL, BPA, and DOE, provides an understanding of work to be done at the Fite Substation, Tacoma, WA. A meeting was held between the LASL SMES staff and three engineers from BPA in early June. The meeting resulted in task assignments for the two parties. LASL and BPA have continued to interchange technical information as detailed at this meeting. One hundred thousand dollars was transferred to BPA to initiate work at the Fite Substation and acquisition of electrical hardware. The BPA tasks consist primarily of items with short lead times. Buswork design will begin early in FY 81, but active site preparation need not proceed until late FY 81 or early FY 82.

CONDUCTOR DEVELOPMENT

The final cable design for the 30-MJ coil is shown in Fig. 2 and specified in Table 2. This design, which differs slightly from previous descriptions, has passed all planned mechnical and electrical tests and meets or exceeds all specifications. Details of conductor development and testing have been reported elsewhere.^{4,5,6} A stability test was run on a 7-m length of pre-production finished conductor. The sample was wound in a single layer on a special toothed form using chip-on-a-strip and support slats to simulate actual coil geometry as closely as possible. From the results, the finished New England Electric Wire (NEEW) conductor is expected to carry up to 8200 A at 2.8 T and recover if only one second cable goes normal and 7900 A at 2.8 T if all the second cables go normal, that is, lose their superconductivity from a perturbation.

A compacted first subcable requires 5.04 times as much copper as composite core. Accordingly, we purchased 3.5×10^6 m of 0.511 mm PDOF copper wire. The copper wire as re-annealed had a ratio of electrical resistance at 300 K to resistance at 4.0 K of 321 ± 25, as measured on 21 samples. Conductor design was based on a ratio of 150, so the copper is much better than actually required. After compaction, the first subcable must be annealed at 325° C for 2 hr.

Preliminary experiments had indicated that relatively small gaps in an insulating wrap on a cable were very effective in permitting heat transfer to the liquid helium. Mylar strip, 0.25-in. wide, 0.005-in. thick, perforated with two staggered rows of 1/16-in. holes on 1/8-in. centers, appeared to provide sufficient ventilation while simultaneously preventing accidental contact between second subcables. Recent experiments were done with such insulation. As a result, the advantage of perforated strip does not overcome the additional expense of perforation and the fabrication problems produced by the lack of adhesive on the strip. Therefore, the final conductor employs unperforated, adhesive backed, 0.005-in. thick, 0.25-in. wide, Mylar tape wrapped with 0.040-in. gaps. Alternating current loss calculations show that a short between second subcables can be tolerated at an approximate rate of one short per one-hundred conductor twist pitches or about one short

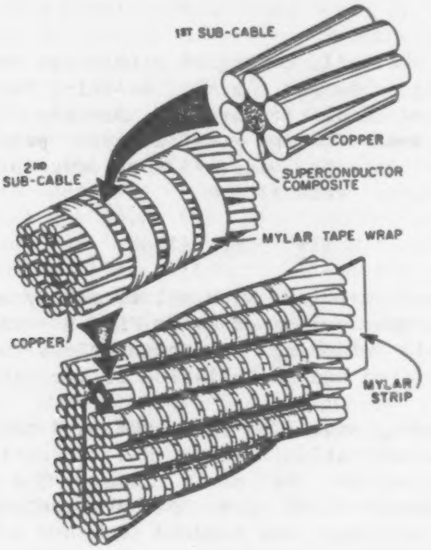

Fig. 2. Low-Loss cryostable cable for 30-MJ coil.

TABLE [illegible]

CABLE SPECIFICATIONS FOR 30-MJ COIL

A. Superconductor Composite Core	
Area of NbTi, mm^2	4.85×10^{-2}
Filament diameter, μm	6.5
Number of filaments	1464
Strand diameter, mm	0.511
Cu to NbTi ratio	2.94:1
Twist pitch, mm	5.0
B. First Subcable: Six copper wires cabled about one core	
Uncompacted diameter, mm	1.52
Compacted diameter, mm	1.37
Overall Cu to NbTi ratio	26.7:1
Twist pitch, mm, and direction	13.5; L.H.
C. Second Subcable: Six first subcables around a stranded, insulated copper core	
Diameter, mm	4.11
Twist pitch, mm, and direction	34.9; R.H.
Insulation type	Mylar, adhesive
Insulation size, mm	0.15 × 6.4
Insulation pitch, mm, and direction	8.64; L.H.
D. Finished Cable: Ten second subcables around a Mylar strip	
Strip dimension, mm	15 × 0.25
Conductor dimension, mm	23.6 × 7.6
Twist pitch, mm, and direction	200; L.H.

every 60 ft. The first production run at NEEW clearly shows that shorts do occur but less frequently than this limit. At present there is no way to measure quantitatively the frequency of inter-cable shorts. To control ac losses, it is important that shorts not develop between second subcables during the coil lifetime.

The only significant cyclic load applied to the conductor is radial compression, that is, pressure normal to the wide face. Calculated maximum stress values range from 200 psi if $E = 1.3 \times 10^4$ psi to 420 psi if $E = 2 \times 10^5$ psi. Preliminary measurements made on actual 5 kA cable indicate a value of $E = 2 \times 10^4$ psi, so that a test based on $E = 2 \times 10^5$ psi should be conservative. Cyclic loading at 4 K can be conducted at a rate of ~500,000 cycles per day, and a larger load must be used at 10^6 cycles to simulate the effect of 10^8 cycles. A study of existing data between 10^5 and 10^6 cycles for steel, copper, cloth-based-phenolic, and glass-based-epoxy indicates that a stress multiplier of 1.5 should conservatively cover the worst case. Therefore, the test sample was cycled between a maximum stress of $1.5 \times 420 = 630$ psi and a minimum stress of 2/3 this value.

The sample was a full-scale coil section, 4 turns high in the axial direction, 2 turns thick in the radial direction, and 4 in. long. All of the second subcables in seven out of eight conductors, were continuously monitored for inter-cable shorts. No shorts developed and no damage occurred for 1.1×10^6 cycles in liquid helium.

COIL DESIGN AND CONSTRUCTION

A contract for coil design (Phase I - \$288,000) and construction (Phase II - \$1,130,000) was placed with General Atomic Company. Phase I has been completed, resulting in the design presented by J. Purcell in the following paper of this meeting. The coil consists of 20 double pancakes. NEEW has produced sufficient conductor for three additional double pancakes. This part of the project is on schedule. Completion dates are January 1981 to complete conductor fabrication, April 1981 to complete coil winding, and August 1981 to complete the coil assembly, provided funds are available.

COIL SUPPORT

At Tacoma, the 30-MJ system will be installed in a Zone C seismic region, with design accelerations of 0.24 g horizontal and 0.16 g vertical, based on a 135 yr earthquake. Because support of a superconducting coil against seismic loads had never been addressed previously, there are no existing conceptual guidelines and a significant engineering effort was required. Other large magnets are usually supported against the walls of a metal dewar, which is constructed piece-by-piece about the coils and welded closed. This approach is not suitable for a plastic dewar, which should be constructed completely without seals or joints to be free of helium leaks. The design of a stiff support system was necessary to suspend the coil freely within a separately constructed, open-mouth helium vessel. Numerical computations were performed based on the response spectrum technique and finite element codes and analysis rules developed for seismic studies on nuclear reactor systems. Coordination with General Atomic on the seismic design resulted in the pinning together of the coil inner support rings to increase the inter-pancake shear capability. The coil is suspended from the dewar lid by a system of six shear panels and six vertical struts. The shear panel system has been designed to withstand a lateral load of 22,000 lbs per panel. Each vertical load strut has been designed to withstand from 22,000 lb tension to 9000 lb compression. Vertical and lateral loads are transmitted through the dewar lid to six external transverse beams, which in turn rest upon six pairs of concrete pillars. The outer pillars are visible in Fig. 1. The entire support system has a lowest resonant frequency of 7.0 Hz, above the 3 to 4 Hz maximum in the seismic spectrum. Coil motion within the helium vessel is less than 1/4 in. in any direction, considerably less than the 1-in. minimum design clearances.

DEWAR VESSEL

Because the dewar design could not proceed until the support design was fixed, procurement was delayed until the dewar has become the critical path item for the project.

Because the coil cycles continuously at a frequency of 0.35 Hz the liquid helium vessel must be made of glass reinforced epoxy to avoid eddy current heating which would occur in a metal walled dewar. The room temperature vessel can be constructed either of a suitable plastic or of 300 series stainless steel. The cover plate can be constructed either of glass reinforced epoxy, fabric reinforced phenolic, or 300 series stainless steel. Further, the vessels can be assembled with either demountable or permanent seals. RFQs have been issued covering various combinations of these options for the vessels with bid responses expected in late November. The lid, which is the complex interface between the coil electric and support systems, cryogenic system, and vacuum system, is still under detailed design. Lid fabrication is not expected to be a critical path procurement item.

ELECTRICAL SYSTEM

The 10-MW converter was completed by Robicon Corporation at a cost of $190,000 plus $50,000 for the SCRs. After tests at the Robicon plant the converter was accepted and shipped to Los Alamos in September 1980. The unit has been set up and will be connected to an existing 3.25 MVA transformer unit. The converter was dropped during unloading at LASL causing damage to the cabinet. Damage to the electrical circuit must be determined by electrical tests. Two 6-MVA transformers were built by the Niagara Transformer Company at a cost of $122,300. The transformers were accepted by LASL personnel after witness tests. The two transformers were to have been shipped directly to Tacoma, WA in late September for installation at the substation. The first transformer was damaged during shipment and has been returned to the supplier for inspection and repair.

Considerable work has been done on the design of the control, instrumentation, and data acquisition system (CIDA), to allow the BPA installation to operate under remote control. A microcomputer system, using principally Digital Equipment Corporation components, was designed, purchased, is being installed in a control trailer. About 350 digital and 200 analog signals, originating in the electrical and cryogenic subsystems are being fed through optical couplers into the microprocessor system for control and data acquisition functions. Most of the hardware of the CIDA system, such as instrumentation cables between subcomponents and the control trailer, and a junction box with signal decouplers for all channels, has been designed and built. Measuring current sharing among second subcables and potential differences for quench protection of the coil requires circuits to operate in a high magnetic field. Special instrumentation is being developed to meet this requirement.

The electrical system, except for the transformers, will be tested with a resistive load under computer control at LASL, disassembled, shipped to Tacoma, WA, and re-assembled. All electrical interconnections have been designed with this requirement in mind. Manual tests at full current should be performed by December 1980 with all tests scheduled for completion by August 1981.

GENIC SYSTEMS

All the components of the cryogenic system are mounted on trailers, as seen in Fig. 1, to be portable. In particular, the system will be assembled at LASL during FY 81, which will permit an extensive test of the system under computer controlled operation and will limit the amount of plumbing and electrical work at Tacoma. All LASL tests are scheduled for completion by August 1981. A discussion of the status of the cryogenic system components follows.

The installation of the CTI Cryogenics Model 2800 helium liquifier/refrigerator into its trailer was completed. Tests at the vendor's plant demonstrated a liquefaction rate of 80 ℓ/hr, limited by pressure drop in the vendor's gaseous helium system external to the trailer. The refrigerator is expected to supply approximately 90 ℓ/hr in operation. The trailer was then delivered, by truck, to LASL where initial pressure tests revealed that several serious leaks had developed inside the refrigerator cold box during shipment as the result of insufficient bracing. The cold box, exclusive of the vacuum shell, has been returned to the manufacturer for repair. The gas recovery system was designed by LASL and will be constructed by the Meyer-Hinds Co. of Santa Fe, NM at a cost of $45,000. Meyer-Hinds is awaiting delivery of high pressure plumbing supplies and has already received the re-conditioned trailer needed to house the system. Two Corblin compressors, obtained as excess property, have been rebuilt and successfully operated at LASL. They have not been shipped, however, pending test of a mounting system intended to isolate compressor vibration from the trailer. A 1000 kW cooling tower has been installed on a flat bed trailer and fitted with all necessary electrical and mechanical components by Western States Mechanical Contractors, Albuquerque, NM, at a cost of $50,000. All subsystem functions have been successfully verified. The system can be tested under its specified 300 kW cooling load with the refrigerator compressors even if the cold box is not operable. The liquid nitrogen trailer has been put in place. Minor rework will be performed after refrigerator tests determine the time variation of the required liquid nitrogen flow. Liquid nitrogen transfer lines, located as excess property, have been installed. Gaseous helium requirements during LASL tests will be considerably less than for BPA operation. At LASL, a borrowed tube trailer will suffice; at Tacoma, a railroad car will most likely be used because it appears more economical. The LASL test will employ a pair of existing liquid helium transfer lines. A new pair of lines with liquid nitrogen shielding, having lower losses, are the last remaining major item of cryogenic equipment to be purchased for operation at Tacoma.

An existing 4-ft diameter metal dewar has been outfitted for testing the refrigeration system. The assembly contains approximately 1000 lbs of phenolic discs to act as a thermal load during cooldown, 300 W of electrical heaters, fluid distribution piping, and an array of thermometers and level sensors. A manifold system that permits cooldown of the transfer lines prior to introducing coolant to the dewar will also be used on the 30-MJ dewar. Besides testing the refrigerator, the experiment is designed to investigate fluid flow patterns during cooldown.

REFERENCES

1. H. J. Boenig,J. C. Bronson, D. B. Colyer, W. V. Hassenzahl, J. D. Rogers, and R. I. Schermer, June 1978, "A Proposed 30-MJ Superconducing Magnetic Energy Storage Unit for Stabilizing an Electric Transmission System," Los Alamos Scientific Laboratory report LA-7312P.

2. J. D. Rogers, H. J. Boenig, J. C. Bronson, D. B. Colyer, W. V. Hassenzahl, R. D. Turner and R. I. Schermer, Jan. 1979, "30-MJ SMES Unit for Stabilizing an Electric Transmission System," IEEE Trans. on Magnetics, Vol. MAG-15, Jan. 1979, pp. 820-823.

3. R. I. Schermer, Dec. 1979, "The Stabilization Unit for Bonneville Power Administration," Proc. 1979 Mech. and Magnetic Energy Storage Contractors' Review Meeting, CONF-790854, pp. 10-19.

4. M. D. Henke and R. I. Schermer, Nov. 1979, "Fabrication of Built-Up Conductors for Large Pulsed Coils," Proc. Eighth Symp. Eng. Prob. Fusion Res. IV, IEEE Service Center, Piscataway, NJ, pp. 1743-1746.

5. J. D. Thompson, J. J. Wollan, B. Turck, and R. I. Schermer, ibid., pp. 1739-1742.

6. R. I. Schermer, H. J. Boenig, M. Henke, R. D. Turner, and R. Schramm, "Conductor Qualification Tests for the 30-MJ Bonneville Power Administration SMES Coil," 1980 Applied Superconductivity Conference, Santa fe, NM, Sept. 29-Oct. 2, 1980.

PROJECT SUMMARY

Project Title: Superconducting Magnetic Energy Storage (SMES)

Principal Investigator: John D. Rogers

Organization:
University of California
Los Alamos Scientific Laboratory
Los Alamos, New Mexico 87545
(505)-667-5427; FTS 843-5427

Project Goals: The goals of the SMES program are two-fold. These are to design, fabricate, and place into operation a 30-MJ, 10-MW SMES unit for electric utility transmission line stabilization on the Bonneville Power Administration (BPA) system by 1982-83. The second goal is to design and have constructed a SMES unit up to 10 MWh size. This unit will be for a completely detailed engineering prototype demonstration of an electric utility diurnal load-leveling system.

Project Status: The engineering design of the BPS SMES transmission line stabilization system is in an advanced state. Many large hardware items are specified and on order. The refrigerator was installed in a trailer with controls added for remote operation. Acceptance tests were performed at the factory and the unit has been delivered to the Los Alamos Scientific Laboratory (LASL). The design of the 30 MJ superconducting coil was completed by General Atomic Company (GA) with the exception of the coil top interface for dewar mounting. GA is now fabricating the coil. An engineering design of the seismic load coil support was completed. All copper and additional superconducting wire were obtained for the 5 kA cable. Development of the 5 kA cable is complete and New England Electric Wire is making the cable. The heat rejection unit has been trailer mounted and is ready for operation. Trailer installation is now contracted for the helium gas recovery system. The converter manufacture is complete and factory testing for acceptance was successfully conducted. The converter power transformers are built and undergoing factory tests. The auxiliary power transformers were obtained. The BPA site installation layout has been devised. Detailed controls design and operating logic for remote microwave link operation of the SMES unit in the BPA system are well established, and many electronic components are on order. The LASL, BPA, DOE interface working agreement was completed.

The work done on the large diurnal load leveling SMES was a preliminary 50 kA wire rope superconducting cable design and a study of SMES units on power system stability.

Contract Number: W-7405-ENG-36

Contract Period: Continuing

Funding Level: $1,580,000 FY1980

Funding Source: Department of Energy, Division of Energy Storage Systems and Division of Electrical Energy Systems.

30 MJ SUPERCONDUCTING COIL DESIGN AND FABRICATION*

John R. Purcell
General Atomic Company
San Diego, California 92138

ABSTRACT

The Bonneville 30 MJ superconducting stabilizing coil is being constructed by General Atomic under contract to LASL. Upon completion of the design, General Atomic began the procurement of materials and is now ready to start coil winding.

INTRODUCTION

The 30 MJ coil is a solenoid with a winding bore of 107 in. It will be 48 in. tall and have an outside diameter of 134 inches. Peak field on the conductor will be about 2.8 T at full current of 4900 A, and the stored energy will be 32 MJ. The total weight of the finished coil will be 37,800 pounds. Construction is proceeding somewhat ahead of schedule. Most of the materials are in hand and coil winding should start in November of 1980.

DESIGN FEATURES

The magnet is a superconducting solenoid consisting of 20 individual coils, each wound in the double pancake fashion, stacked on top of each other and held together by 48 aluminum tie rods.

The basic dimensions are shown in Fig. 1 and the basic design parameters in Table 1. Each of the 20 coils consists of an inner support ring (a filament wound fiberglass-epoxy composite), the conductor, a stainless steel support strap, interturn insulator, and interlayer spacer plates.

The conductor configuration is shown in Fig. 2. One composite niobium-titanium/copper superconductor strand is surrounded by six copper wires to form an 81.7 A subcable. Six of these first-level subcables are twisted around one insulated copper cable to form the second-level cable. Ten second-level cables are twisted into the final conductor.

The stainless steel support strap is anchored to the inner support ring with several fasteners and interwound with the conductor to carry the hoop stresses and axial loads. Strap tension during coil winding is held to 1100 lb. This tension will give a preload sufficient to prevent the coil from lifting off the coil form during energization. An insulator strip, also providing coolant passages, is wound into the coil on both sides of the conductor (see Fig. 3).

A plastic ramp inserted at the circumference guides the conductor to the outside coil. The stainless steel strip is tied to itself and winding tension is maintained by an adjusting screw. There is plastic insulation between the two parts of the tensioning clamp to avoid a closed loop; the peak voltage across this connection is 8.75 V.

Each double pancake is wound from one length of conductor. A perforated and grooved interlayer spacer plate is inserted between the top and bottom layer of each coil and also in between the coils.

---

*Work supported by LASL Agreement X-49-6722H-1, under Department of Energy sponsorship.

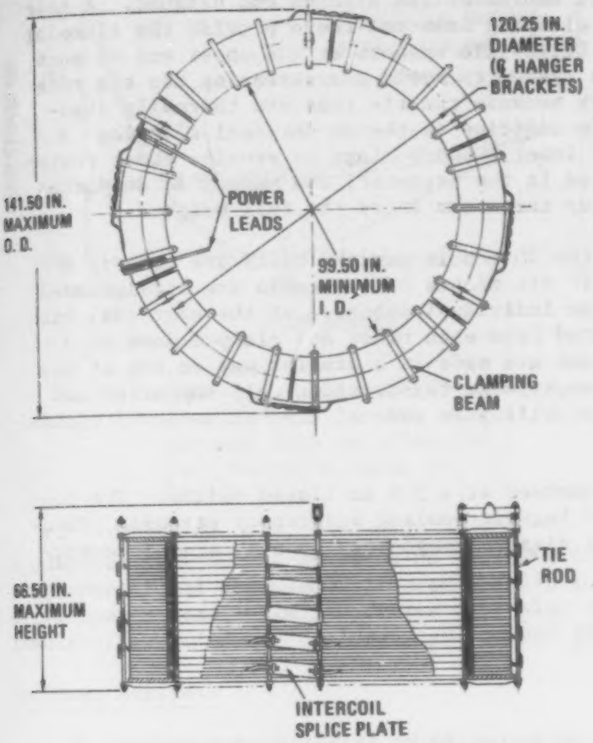
120.25 IN.
DIAMETER
(℄ HANGER
BRACKETS)
141.50 IN.
MAXIMUM
O. D.
POWER
LEADS
99.50 IN.
MINIMUM
I. D.
CLAMPING
BEAM
66.50 IN.
MAXIMUM
HEIGHT
TIE
ROD
INTERCOIL
SPLICE PLATE

Fig. 1. Magnet assembly.

TABLE 1
30 MJ COIL – BASIC PARAMETERS

STORED ENERGY, PEAK	30 MJ
PEAK CURRENT	4900 A
PEAK MAGNETIC FIELD	2.05 TESLA
PULSE FREQUENCY	0.35 HERTZ
PULSE AMPLITUDE	4000 A to 4900 A (20–30 MJ)
DESIGN OPERATING LIFE	10 YEARS
PEAK POWER TRANSFER	10 MW
AMPERE-TURNS	4.51×10^6
COOLING	LIQUID HELIUM BATH, 4.5 K
CONDUCTOR MATERIAL	NbTi/COPPER
NUMBER OF LAYERS	40
WINDING I.D.	107.4 in.
WINDING O.D.	133.1 in.
COIL HEIGHT	47.7 in.
TOTAL WEIGHT	37,800 lb

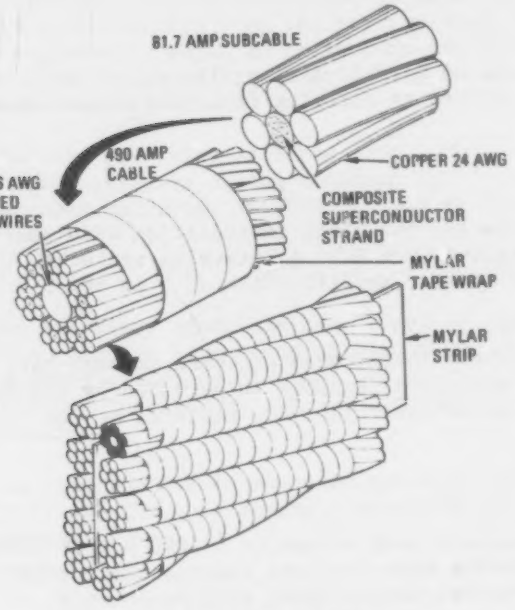
81.7 AMP SUBCABLE
490 AMP
CABLE
SEVEN 26 AWG
INSULATED
COPPER WIRES
COPPER 24 AWG
COMPOSITE
SUPERCONDUCTOR
STRAND
MYLAR
TAPE WRAP
MYLAR
STRIP

Fig. 2. LASL 30 MJ coil
4.90 kA conductor.

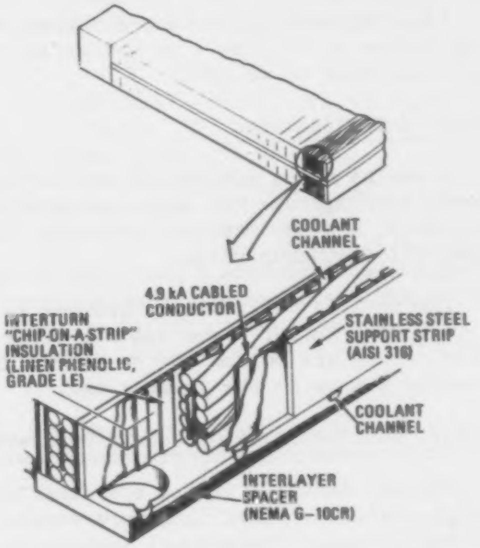
COOLANT
CHANNEL
4.9 kA CABLED
CONDUCTOR
INTERTURN
"CHIP-ON-A-STRIP"
INSULATION
(LINEN PHENOLIC,
GRADE LE)
STAINLESS STEEL
SUPPORT STRIP
(AISI 316)
COOLANT
CHANNEL
INTERLAYER
SPACER
(NEMA G–10CR)

Fig. 3. Single coil assembly,
isometric view.

The magnet is assembled using 20 double-coil subassemblies stacked and aligned. A pair of tie rods connects an upper and lower plastic clamping beam and these provide the clamping forces to hold the magnet together. A stack of Belleville washers at the upper end of each tie rod provides the necessary elasticity of the system to avoid overstressing the tie rods during cooldown and operation. This is necessary because the tie rods are thermally insulated from the coil and will cool down first. In addition to the 24 vertical clamping devices, spiral pins are driven through adjacent inner support rings to provide shear resistance during the design base earthquake. Installed in the cryostat, the magnet is supported by six hanger beam assemblies designed so that any three can carry the full weight.

The electrical connections between each of the 20 double pancake coils are made in a staggered pattern around the outside of the coil. Six inches of the cable are straightened out and each individual subcable is soldered to an individual subcable of the next coil with a 3 in. overlap. All ten connections are insulated from each other and clamped down on a splice plate. The lead-in and lead-out connections are made in a similar way on top of the magnet. The lead entering the bottom coil is brought down the outside, well supported and clamped with an extra copper bar for additional stability in case of low helium level within the dewar.

The coil is cooled by natural convection, immersed at 4.5 K in liquid helium. The conductor is designed to facilitate intimate contact between coolant and copper strands. Channels, grooves, and vent holes are provided in all plastic components to aid natural convection and removal of gases from inside the coil.

ANALYSIS

Pulsing Losses

The operational pulsing loss in the coil is estimated to be 48 W. Superconductor hysteresis loss is the major loss component (37 W), while the eddy current coupling loss is estimated to be 9 W. The remaining 2 W of the pulsing loss arises from eddy current heating in the cable splices and other metallic components.

Fatigue Life Considerations

All components have been designed and analyzed to fulfill the requirement of 10^8 operating cycles at 0.35 Hz. An operating cycle is defined as changing from 100% stored energy to 67% and back up to 100%.

Seismic Considerations

A design basis earthquake was defined, considering the final installation site near Tacoma, Washington. The expected seismic accelerations are 0.24 g laterally and 0.16, vertically, and the response spectrum indicates a maximum amplification of 6 in the 3 Hz structural frequency range.

The coil is vertically supported by six stainless steel tubes attached through ball joints to the hanger beams and the dewar cover. Horizontal support is provided by six shear panels, which are bolted to the top of the coil; the shear forces are resisted by two kinematic joints on the dewar cover.

Winding, Cooldown, and Operating Stresses

Two key design criteria are limiting the conductor hoop stress to 15,000 psi or less through stainless steel interturn support and assuring that the coil remains under radial compression under operational loading to avoid relative motion among coil components.

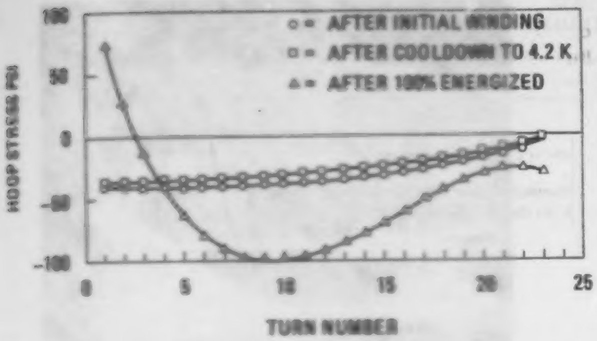

Fig. 4. Conductor hoop stress versus turn numbers for the central pancake with an effective coil radial modulus of 20,600 psi.

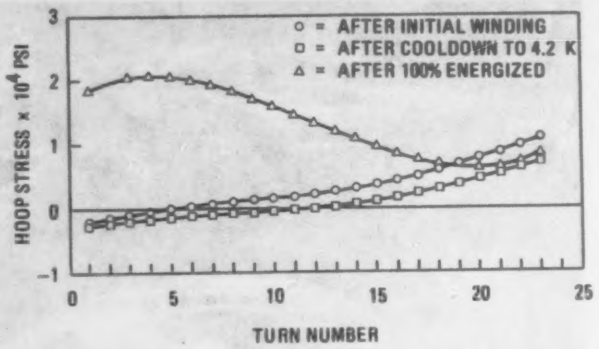

Fig. 5. Stainless steel hoop stress versus turn numbers for the central pancake with an effective coil radial modulus of 20,600 psi.

A computer program was prepared to evaluate the conductor, support strap, and inner support ring operational stresses. Figures 4 and 5 show examples of conductor and stainless steel strap hoop stress. Similar curves were plotted for the inner support ring and conductor insulator for winding, cooldown, and operating stresses.

Cooldown Analysis

The cooldown temperature profiles across the coil were calculated using the two-dimensional General Atomic transient thermal analysis code TAC2D.

For the high-temperature portion of the cooldown (300 K to 140 K) helium gas cooled by liquid nitrogen will be circulated through the coil. The cooldown will then proceed using the cold gas available from the refrigerator turbine expanders. As the coil nears 4 K, liquid helium will begin to collect in the dewar and the process will be continued until the operating level of liquid helium is reached. No external liquid helium storage will be used in this system.

The cold gas inlet manifold, the outlet manifold, and the baffle system are arranged so that thermal stresses during cooldown are within acceptable limits. For the tie bolts, the maximum cooldown stress is 7000 psi and for the stainless steel strap, 14,000 psi.

CONSTRUCTION

The stainless steel has been received and a length is shown being started into a winding in Fig. 6. In the background of Fig. 6 the epoxy glass coil bobbins can be seen. Figure 7 shows a spool of conductor ready for winding, and Fig. 8 is a closeup of the conductor and the interturn insulation. The winding line is now operational (Fig. 9) and the coil winding is proceeding.

The construction schedule is shown in Fig. 10. We are ahead of schedule and should be able to finish the coil assembly by mid-FY-81 if funding constraints do not force a delay in the program.

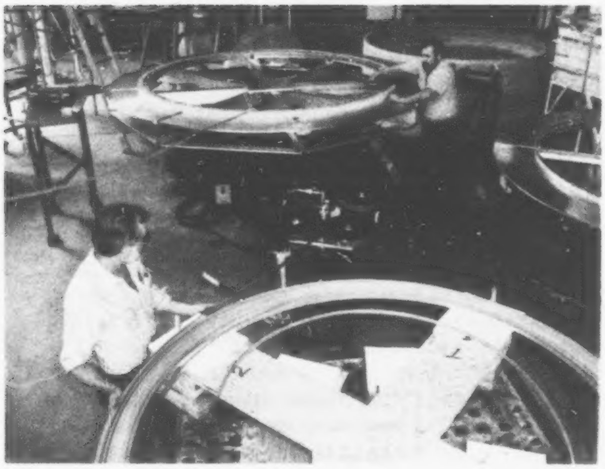

Fig. 6. Photo of stainless steel being started into the winding. In the background the fiberglass-epoxy bobbins can be seen.

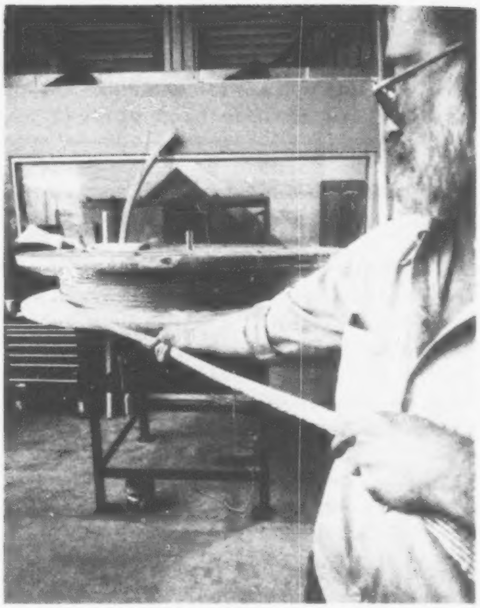

Fig. 7. Photo of a spool of conductor ready for winding.

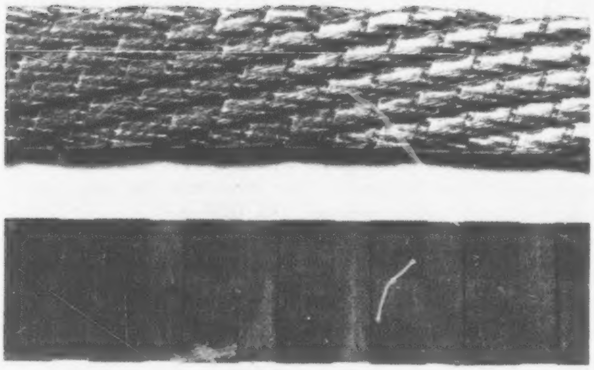

Fig. 8. Closeup of conductor and interturn insulation.

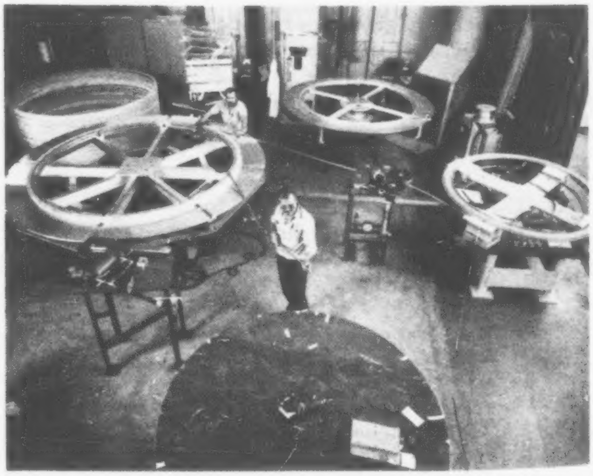

Fig. 9. Winding line.

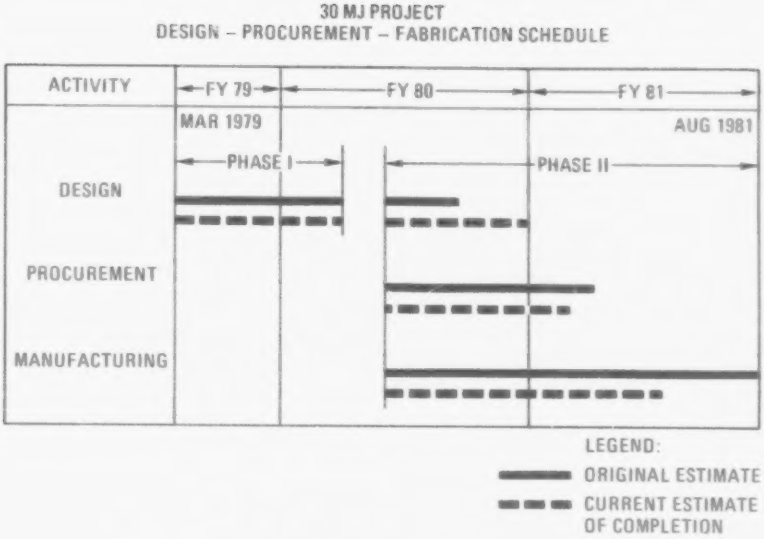

Fig. 10. Construction schedule.

PROJECT SUMMARY

Project Title:	Superconductive Energy Storage
Principal Investigator:	R.W. Boom
Organziation:	531 Engineering Research Building University of Wisconsin Madison, Wisconsin 33706 (608) 263-5026
Project Goals:	To develop hardware components, produce engineering system designs, procure manufacturing and assembly equipment designs, revise cost estimates, and assess operational efficiencies for large underground superconductive storage systems.
Project Status:	Component development in three areas: cryogenics, conductor and structures is under way. Rock mechanics design and experimentation is under way. Parallel efforts supported by the Wisconsin Utilities are under way on the same schedule in five other areas: magnetics, environmental studies, system design, electrical, and safety. Two new designs have been studied: a low aspect ratio single solenoid and a 15 tunnel circular pattern of coils. These new designs may provide significant technical and economic advantages.
Contract Number:	DE-AC02-76ET-26602
Contract Period:	FY-80
Funding Level:	$400,000
Funding Source:	U.S. Department of Energy Division of Energy Storage

DIURNAL SUPERCONDUCTIVE ENERGY STORAGE SYSTEM DESIGN

Y.M. Eyssa and R.W. Boom
University of Wisconsin
Madison, Wisconsin 53706

ABSTRACT

A summary report of our FY-80 study of superconductive energy storage for electric utility systems is presented. Conceptual designs have all been for one layer solenoids of aluminum-NbTi composite conductors cooled to 1.8 K in superfluid helium. The solenoids are mounted underground in bedrock in one or more tunnels. The two preferred designs in 1980 are: a 15 tunnel solenoid arranged in a circular pattern and a large radius single tunnel solenoid. The electrical energy storage efficiency in all cases is 95 to 96%. Much of this design work was presented at the 1980 Applied Superconductivity Conference [1].

INTRODUCTION

Superconductive energy storage studies at Wisconsin have been underway since 1970. By 1974 we had settled on composite conductors of NbTi plus aluminum, 1.8 K pool cooling, single layer high current solenoids and structure provided by in-situ bedrock. Three phase Graetz bridge circuits were designed for the ac-dc conversion interface between dc current in a storage magnet and three phase ac current in the electric utility network.

A solid monolithic conductor and its dewar were rippled along the circumference to reduce cooldown motion in the radial direction from about 20 cm unrippled to 0.4 cm rippled. The ripple radius was typically 1 meter. Struts of fiberglass epoxy were optimized as to length and cooling stations in order to best transfer forces from the low temperature turns to the room temperature rock face. Scaling laws were developed to extrapolate similar aspect ratio magnets to other sizes for different stored energies, magnetic fields and heat leak through the struts.

Over the years better design, component improvements and engineering optimization have led to the series of storage cost estimates shown in Table 1 for three tunnel units.

Table 1. Storage Costs for 10^4 MWh Discharged Daily, Including Amortized Capital and Operating and Maintenance Costs

Year	Costs* mills/kWh	Comments
1970	117.0	steel structure, copper conductor
1974	31.4	rock structure, aluminum conductor
1976	21.7	optimized design, rectangular conductor
1978	22.3	round conductor, fiberglass polyester struts

*Cost estimates have been extrapolated to 1978 dollars

The cost of energy from superconducting magnetic energy storage consists of the amortized storage unit capital cost and O & M costs (Table 1) plus the purchase cost of energy to place into storage. Since I-C unit storage efficiencies are about 96%, the incremental value of energy delivered from storage is only 4% higher than the incremental cost of buying energy to charge an I-C unit. Usually there is considerable available charging capacity in the incremental cost range of 15-30 mills/kWh. Thus I-C storage is a competitor to the more expensive intermediate generators by providing power in the 30-50mills/kWh range.

In comparison to other storage units only I-C superconductive storage is 96% efficient. Compressed air storage burning fuel is the lowest in efficiency at 50% while advanced batteries may become the best of the rest at 70-80% efficiency. Pumped hydrostorage is traditionally 66% efficient. Not only does efficiency affect the cost of delivered energy but also the size of a storage unit. One of the main points in the A.D. Little study of SMES by B.M. Winer and J. Nicol is that less efficient storage units need to be much larger in order to provide energy without premature depletion[2].

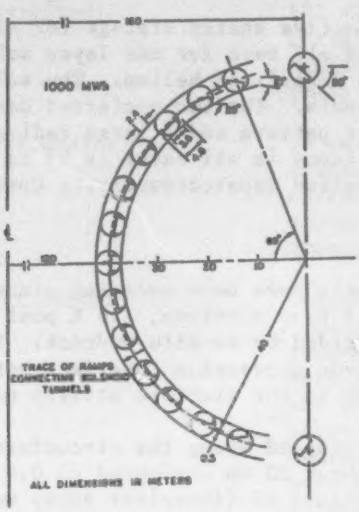

Fig. 1 Cross Section of 15 Tunnel 1000 MWh Energy Storage Solenoid. Dimensions in meters.

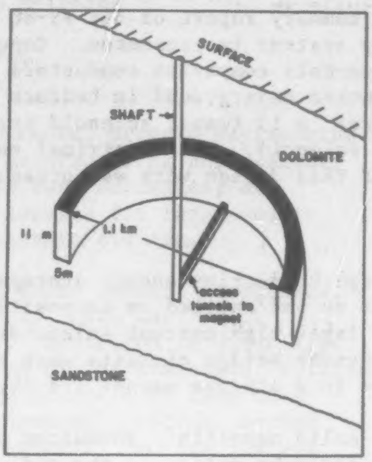

Fig. 2 Three-dimensional view of the Low Aspect Ratio 1,000 MWh cavern system for a dolomite site in Wisconsin. The cavern system was modeled at a mean depth of 30 m.

DESIGN

A design which reduces the need for cold axial structure in the unit was reported on in 1979[3,4,5]. A sketch of this design is shown in Fig. 1. There are 15 tunnels arranged in a circular pattern. The resultant forces are primarily radially directed outward along the 40 m radii. The orientation of the forces normal to the rock structure greatly reduces the shear loading and the need for axial structure. Specifications are listed in Table 2. The use of many tunnels reduces the accumulation of axial forces by transferring these forces more frequently. For more details about the 15 tunnel design see last year's report[3].

The second design currently under consideration is a single solenoid of aspect ratio $\beta=0.01$, where $\beta=\text{height} \div \text{diameter}$. The sketch in Fig. 2 is for a 1000 MWh unit mounted in a tunnel very near the surface. Specifications are listed in Table 3. It need not be very deep because the radial pressure on the rock is only about 30 psi as compared to 300 psi for the 15 tunnel unit. Thus simple surface trenching may be used to form the tunnel. Conductor installation, dewar assembly and eventual repair should all be easier for an open top tunnel.

Another bonus for a low aspect ratio coil is the short axial height. Axial forces can be balanced internally by cold structure without connection (and heat leak) to the rock surfaces. This option is possible for any solenoid but becomes too expensive for longer coils.

Table 2 Fifteen Tunnel Solenoid

Energy Stored	1186 MWh
Major Radius	120 m
Minor Radius	40 m
Total Turns	554
Turns per Central Tunnel	36
Turns per End Tunnel	43
Current per Turn	300,000 A
Central Average Field	2.5 T
Maximum Field	4.2 T
Total Normal Force	8.8×10^{10} N
Total Tangential Force	1.7×10^{9} N
Normal Strut Material*	0.79×10^{6} Kg
Tangential Cold Structure*	1.2×10^{6} Kg
Tangential Strut Material*	0.03×10^{6} Kg
Extra Safety Structure*	2.0×10^{6} Kg

*Material is polyester fiberglass used at 1.9×10^{8} N/m^2 (27,000 psi)

Table 3. Single Segment Low Aspect Ratio Design $\beta = 0.01$

Energy Stored	1030 MWh
Radius	360 m
Height	11.2 m
Total Turns	112
Current per Turn	400,000 A
Maximum Midplane Field	2.5 T
Maximum End Field	5.2 T
Total Radial Force	8.0×10^{9} N
Radial Strut Material*	0.8×10^{5} Kg
Cold Axial Structure*	6.75×10^{6} Kg

*Material is polyester fiberglass used at 1.9×10^{8} N/m^2 (27,000 psi)

The heat leak through the radial struts is very small for low aspect ratio coils since the total radial force is small, F_r (β=0.01)=1/10 F_r(β=0.3). The heat leak refrigeration for a β=0.01 coil is about 1% E per day. Thus the total efficiency is the electrical storage efficiency of 96% (charge and discharge) with a constant cooling power requirement of less than 2%.

The radial force and axial structure dependence on β used in the above discussion are shown in Fig. 3[1,5]. The quality factors Q_c and Q_{fr} plotted in Fig. 3 are defined in the following equations:

$$M_{axial} = Q_c \frac{\rho}{\sigma} E \qquad (1)$$

$$F_{radial} = Q_{fr} E^{2/3} B_M^{2/3}, \qquad (2)$$

where M_{axial} is the internal cold axial structure, ρ is the axial structure density, σ is the average stress, E is the stored energy and B_M is the maximum field on the median plane.

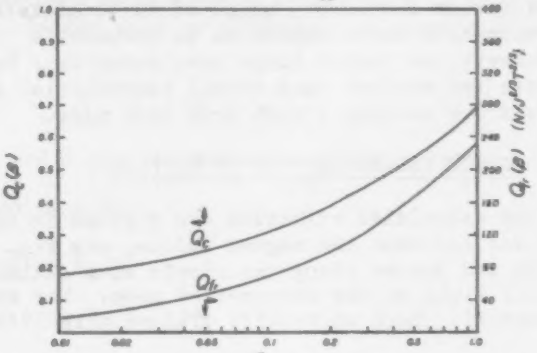

Fig. 3 Comparison of structure quality factor Q_c and radial force quality factor Q_{fr} vs. aspect ratio β for thin wall solenoids.

A comparison of the two designs is presented in Table 4. The differences in forces and refrigeration favor the low aspect ratio system. The amount of fiberglass structure favors the 15 tunnel design. Conductor amounts favor the 15 tunnel unit slightly. Total efficiency is best for the low aspect ratio coil, although electrical storage efficiency is identical since storage efficiency depends only on the ac-dc bridge circuitry. The electrical storage efficiency refers to the fraction of energy stored which is available for discharge. Total efficiency includes power to run the cooling system even though refrigeration power does not deplete stored energy.

Table 4 Design Comparisons

Areas of Change	One Tunnel Low Aspect Ratio		Fifteen Tunnel Segmented Solenoid
Radius	560 m		120 m
Height	12 m		36 m
No. of Tunnels	1		15
Depth of Tunnels	D > 10 m		D > 100 m
Total Radial and Axial Force Carried to the Rock	1/20	:	1
Strut Refrigeration	1/20	:	1
Structure (warm and cold) (lbs)*	17×10^6		10×10^6
NbTi (lbs)	330,000		280,000
High Purity Aluminum (lbs)	5.10×10^6		4.2×10^6
Helium (liters)	1×10^6		1×10^6
Efficiency	94%		85%
Safety Scheme	Dump Helium		Coupled Discharge One Coil
Radial Pressure	~30 psi		~300 psi
Areas of Similarities			
Storage Efficiency	~96%		~ 96%
Median Plane Field	2.5T		2.5T
Strut Length	1m		1m

*Material is polyester fiberglass used at 1.9×10^8 N/m^2 (27,000 psi)

Table 5. Comparison of Cost Factors for Different Design

	Dewar wt.	Conductor wt.	Radial Strut wt.	Axial Cold Structure % of $\frac{\ell}{g}$ E
Five Segments Hourglass	1.0	1.0	1.0*	16%*
15 Tunnel Design	0.97	1.01	.78*	3.23%*
Single Segment Design (β = .01)	.82	1.2	0.08	18%

*Excluding extra structure required for safety

Table 5 is a list of comparative cost factors. Since a proper design and cost estimate for the low aspect ratio system has not been made the factors given can be used only to identify cost trends. Preliminary cost estimates for the older 5 tunnel hourglass design and for the newer 15 tunnel design are in the range of 18-40 mills/kWh which is acceptable[6]. The low aspect ratio coil would appear to be comparable in cost according to the factors in Table 5. However, we expect large cost reductions because of less expensive surface rock excavation costs and surface open tunnel construction and repairs. No estimate of the excavation costs for an open trench have been made.

FORCE VARIATIONS DUE TO RIPPLES

The conductor, dewar and associated structure are rippled in the radial direction at a radius of curvature much smaller than the magnet radius, see Fig. 4. The presence of ripples changes local fields and forces along the ripple with minimum axial field at the strut mount and maximum axial field at the unsupported node. The details of the method of calculation will be published[7]. Here we briefly discuss this effect and its impact on magnet design.

Assuming a uniform current distribution of J per meter, the axial fields at the inner and outer walls of a thin wall solenoid are:

$$B_{i,o} = \pm 1/2\ \mu_o J + \mu_o K\ J \qquad (3)$$

where the positive sign is for the inner wall field and the negative sign is for the outer wall field, and K(β) is a shape factor which varies between 0.0 and 0.5. For an unrippled solenoid the K(β) factor is:

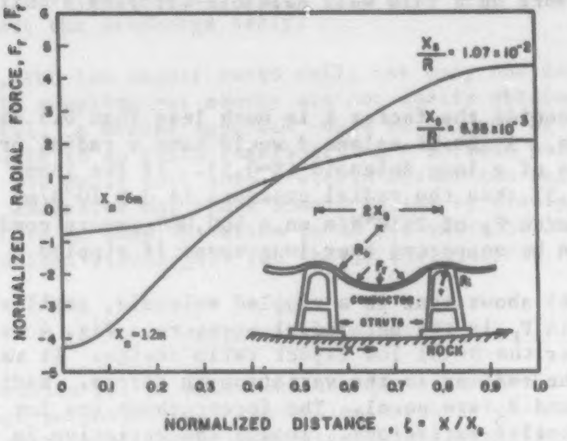

Fig. 4 Radial force variations in a rippled β=.01, 1000 MWhr, 2.5T solenoid that has a major radius 560 m, height = 11m, r_o=10m and R_i=2m. The average force F_r on a 400,000 ampere conductor is 2×10^4 N/m. The maximum variation in case of a 12 m span between struts is ± 450% of the average force F_r. For 6 m span the variation varies between -100% and +210% of the average force, $\overline{F}_r$.

$$K_o(\beta,\beta_Z) = \frac{1}{4\pi}\int_o^{\pi} d\theta \qquad \frac{\beta-\beta_Z}{[(\beta-\beta_Z)^2 + 4\sin^2(\theta/2)]^{1/2}} + \frac{\beta+\beta_Z}{[(\beta+\beta_Z)^2 + 4\sin^2(\theta/2)]^{1/2}} , \quad (4)$$

where β is the aspect ratio and β_Z is defined as the axial distance Z from midplane divided by the solenoid radius, R. For a very long solenoid K=0.5 which corresponds to zero field on the outer wall while for low aspect ratio solenoids K is << 1 and the difference between B_i and B_o is very small. In the case of a rippled solenoid the factor K varies along the ripple and is expressed as[7]:

$$K = K_o(\beta,\beta_Z) + G(\beta_Z, \alpha_i, \alpha_o, \eta_s, \xi) \qquad (5)$$

The parameters α_i,α_o, η_s and ξ are dimensionless lengths defined as:

α_i = inner ripple radius R_i/R,

α_o = outer ripple radius R_o/R,

η_s = half the ripple span X_s/R, and

ξ = coordinate X/X_s.

The axial field which is calculated numerically is found to change slightly for all designs considered. This can be understood by the fact that each ripple behaves as part of an auxilliary long solenoid which adds or subtracts some field to the main solenoid field. Negative curvature subtracts field while positive curvature adds field. We find that the 1000 MWh, 2.5T, β=.01 unit has variations in axial field along the ripples of about 10%. All thin wall solenoids have large radial end fields and large axial forces at the end turns. Since rippling has insignificant effect on these end fields and axial forces, we confine our calculations to radial forces.

The net radial pressure on a thin wall solenoid carrying a uniform current is

$$P_r = (B_i^2 - B_o^2)/2\mu_o. \tag{6}$$

For low aspect ratio solenoids the factor K is much less than 0.5 which results in $B_i \sim B_o$ and small radial pressure. A $\beta = .01$ solenoid would have a radial pressure equal to 8% of the radial pressure of a long solenoid (K=0.5). If the inner field at the midplane of a $\beta = .01$ solenoid is 2.5T then the radial pressure is 2×10^5 N/m^2 (30psi). This is equivalent to a radial force F_r of 2×10^4 N/m on a 400,000 ampere conductor. This force is very small and easily can be supported over long spans if rippled.

Inspection of Eq. (6) shows that in a rippled solenoid, small variations in B_i and B_o produce large variation in P_r in the net radial pressure. Fig. 4 is a sketch of the variation in radial forces for the $\beta = .01$ low aspect ratio design. It may be noticed that the shorter the span, $2X_s$, the smaller is the variation in forces. Radial forces can be zero at some points where B_i and B_o are equal. The forces shown are for the midplane turn. Other turns experience similar variations. Though the variation in the radial forces is high for low aspect ratio solenoids the maximum local forces are still smaller than for long solenoids by a factor of 3. It is worth mentioning that the total radial force in a rippled solenoid is equal to that of an unrippled solenoid. Hence the mass of radial struts required to carry radial forces to rock remains constant, independent of the magnet ripple.

The conclusion to draw from this analysis is that field and force variation are significant for rippled conductors, becoming 20∿30% for $\beta = 0.3$ solenoids and 100∿400% for $\beta = 0.01$ solenoids. If the conductor is to carry the full tensile load without other back-up structure then this variation in force will be an important factor in determining local radii of curvature, span distance between nodes and composite conductor size.

SAFETY

Quenches, normal region propagation and superconductive recovery are nonexistent problems with helium present. However, if helium is lost there is the problem of safely discharging the storage solenoid without damage. The problem is more severe than for smaller magnets because of the larger stored energy per gram of conductor, see Table 6.

Table 6. Energy Per Gram For Several Superconductive Systems

System	12 Ft. Buble Chamber	MHD Base Load	Tokamak Reactors	1000 MWh-SMES
Joules/gram (conductor)	2	7	66	429

We anticipate that a credible accident which might happen once in 10 to 20 years would be to lose vacuum or to lose capacity to refill helium with the solenoid fully charged. The catastrophic signal to take action would be that the helium level is dropping at an excessive rate. For the two designs different procedures would be followed.

The multi-tunnel case has been discussed by us previously [6]. In brief, ordinary copper switches could short out the good tunnels while the ac-dc bridge at full power rating could discharge the bad coil. Only 7% of the energy is associated with one tunnel and possibly one half is inductively coupled to nearby tunnels. The time for discharge would be 3% of 10 hours or 18 minutes. If part or all of the discharging coil became normal then some energy would be dissipated internally. However, no damage would result since the total energy, 429 joules/gram, would only raise the temperature to about 300 C. The key point is to start the discharge early.

The second design, the low aspect ratio coil, has only one dewar. The advantages of subdividing and mutually coupling out energy are not easily obtained, although switches per layer might be useful. A better approach would be to dump all of the helium quickly, possibly saving the liquid in an extra reservoir. A ± current pulse with eddy current heating should trigger the whole coil normal within one or two seconds, after which a safe discharge without excessive hot spots should follow by dissipating 429 J/g uniformly. An alternative to dumping helium is to add extra helium and increase the discharge voltage for a fast discharge. The choice would depend on the rate the helium level drops.

FORCE BALANCED COILS

In a recent publication [8] we addressed the question of the value of force balanced coils for energy storage purposes. Our conclusion is that force balanced coils have little to recommend them; in particular there is no structure saving in comparison to simple storage coils. This result is in direct contrast to the prediction of Mawardi[9] whose design for LASL was reported on at last year's storage contractor's meeting.

Our proof is outlined below. The reader is referred to Mawardi's paper [9] and our paper [8] for details. The force balanced suggestion can be understood by reference to Fig. 5. A dipole wound externally on the surface of a toroid will naturally squeeze in on the toroid which is naturally trying to expand. The opposing forces led to the idea that with proper current distributions it might be possible to cancel most of the forces resulting in a very small structure compared to $M=\rho E/\sigma$, where ρ is structure density, E is energy stored and σ is the average working stress. According to the Virial Theorem M is the minimum structure for any coil or system of coils. For those who might not believe in this use of the Virial Theorem we outline the following direct proof which does not rely on the Virial Theorem.

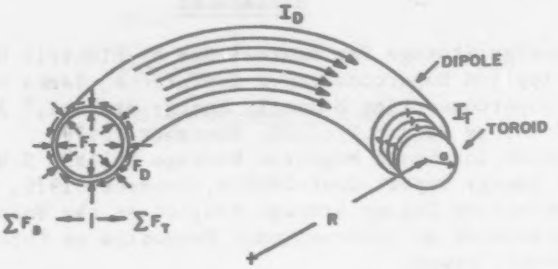

Fig. 5 Dipole and toroid energy storage coils. Expanding toroidal forces F_T are partially balanced by contracting dipole forces F_D. Even if net forces cancel the structural mass required is $\geq$ the Virial theorem mass.

METHOD

$E = 1/2\ LI^2$, (E=energy, L=inductance, I=current)

$L = \mu_o R f(\beta)$, (R=major radius, a=minor radius, $\beta = \frac{a}{R}$ aspect ratio)

$F = -\nabla E$, $(\frac{\partial}{\partial R}, \frac{\partial \beta}{\partial a} \frac{\partial}{\partial \beta})$

LEADS TO STRUCTURAL MASSES

$$M = \frac{\rho E}{\sigma} \left(\left|1 - \frac{\beta}{f} \frac{\partial f}{\partial \beta}\right| + \left|\frac{\beta}{f} \frac{\partial f}{\partial \beta}\right| \right) \qquad (7)$$

The first term is M_R, the structure needed around the major circumference. The second term is M_a, the structure needed around the minor circumference.

THREE CASES

$$1\text{- IF } 0 \le \frac{\beta}{f}\frac{\partial f}{\partial \beta} \le 1 \quad \text{THEN} \quad M = \frac{\rho E}{\sigma}$$

$$2\text{- IF } \frac{\beta}{f}\frac{\partial f}{\partial \beta} < 0 \quad \text{THEN} \quad M = \left(1 + 2\left|\frac{\beta}{f}\frac{\partial f}{\partial \beta}\right|\right)\frac{\rho E}{\sigma}$$

$$3\text{- IF } \frac{\beta}{f}\frac{\partial f}{\partial \beta} > 1 \quad \text{THEN} \quad M = \left(2\frac{\beta}{f}\frac{\partial f}{\partial \beta} - 1\right)\frac{\rho E}{\sigma}$$

$$\text{FOR ALL CASES } M \ge \frac{\rho E}{\sigma}$$

In case (1) both M_R and M_a are positive (in tension) which implies minimum structure. In case (2) M_R is positive (in tension) while M_a is negative (in compression) which is less efficient since then M_R must exceed M_a by at least $\rho E/\sigma$. In case (3) M_R is in compression and M_a is in tension which is likewise inefficient.

In conclusion note that structure for a force balanced systems is always at least the Virial Theorem amount. In the past we have recognized that accomodating even 1/3 of the Virial Theorem structure is too expensive to consider. The only qualification might be to recognize the possibility that some new, very inexpensive structural material may be invented which would cost only $0.10 per lb. installed. Therefore all designs should be in bedrock where structure to contain the energy is basically free rock except for excavation costs.

REFERENCES

1. "Superconductive Energy Storage for Diurnal Use by Electric Utilities", R.W. Boom, presented at 1980 Applied Superconductive Conference, Santa Fe, NM, Sept., 1980.
2. "An Evaluation of Superconducting Magnetic Energy Storage," J. Nicol and B.M. Winer, U.S. Department of Energy Report C-82820, November, 1979.
3. "Component Development for Large Magnetic Storage Units", S.W. Van Sciver and R.W. Boom, U.S. Department of Energy Report Conf-790854, December 1979, pp. 48-57.
4. "Status of Superconductive Energy Storage Project at the University of Wisconsin, S.W. Van Sciver, presented at International Symposium on Superconductive Energy Storage, Oct. 8-10, 1979, Osaka, Japan.
5. "Design Configurations for Large Superconductive Energy Storage Magnets," Y.M. Eyssa, A.S.M. Symposium on Superconducting Structures, Chicago, November, 1980.
6. Wisconsin Superconductive Energy Storage Project, Volume II, University of Wisconsin, January, 1976.
7. "Force and Magnetic Field Calaculations for Rippled Energy Storage Solenoids," Y.M. Eyssa and M.A. Hilal, to be presented at the 7th International Conference on Magnet Technology, March 30, 1981, Karlsruhe, Fed. Rep. of Germany.
8. "Considerations of a Large Force Balanced Magnetic Energy Storage Systems", Y.M. Eyssa and R.W. Boom, presented at the 1980 Applied Superconductivity Conference, Santa Fe, Sept. 1980.
9. "A Force Balanced Magnetic Energy Storage System", O.K. Mawardi, H. Nara and M. Grabnic, Proceedings of 1979 Mechanical and Magnetic Energy Storage Meeting, Conf-790854, p. 82.

best copy available

PROJECT SUMMARY

Project Title:	Superconductive Energy Storage
Principal Investigator:	R.W. Boom
Organization:	531 Engineering Research Building University of Wisconsin Madison, Wisconsin 53706 (608) 263-5026
Project Goals:	To develop hardware components, produce engineering system designs, procure manufacturing and assembly equipment designs, revise cost estimates, and assess operational efficiencies for large underground superconductive storage systems.
Project Status:	Component development in three areas: cryogenics, conductor and structures is under way. Rock mechanics design and experimentation is under way. Parallel efforts supported by the Wisconsin Utilities are under way on the same schedule in five other areas: magnetics, environmental studies, system design, electrical, and safety. Two new designs have been studied: a low aspect ratio single solenoid and a 15 tunnel circular pattern of coils. These new designs may provide significant technical and economic advantages.
Contract Number:	DE-AC02-76ET-26602
Contract Period:	FY-80
Funding Level:	$400,000
Funding Source:	U.S. Department of Energy Division of Energy Storage

CONDUCTOR AND STRUCTURAL COMPONENT STUDIES FOR DIURNAL ENERGY STORAGE

S.W. Van Sciver, K.S. Han, K.T. Hartwig, G.F. McIntosh and W.C. Young
University of Wisconsin
Madison, WI 53706

ABSTRACT

A summary of recent progress in the development of structural and conductor components for the Wisconsin diurnal energy storage project is presented. The present paper reviews the progress during the past year in structural design concepts and laboratory component development. Structural design concepts are presented which have been developed for the new low aspect ratio design for the energy storage coil. The major change in this area is cold structural support of axial forces with transmission of only radial forces to bedrock. The three areas in which laboratory studies have been carried out are: 1) insulating structural material testing; 2) cryogenic heat transfer studies and; 3) subcomponent testing of the composite conductor. The specific problems investigated within the past year are: fracture and strain release of bonded glass fiber reinforced polyester, heat transfer from cylindrical geometries in superfluid helium II and shear strength, and thermal and electrical conductivity of joints in Al-Al and Al-Cu composite specimens. Some discussion of future directions for this effort is included.

INTRODUCTION

Superconductive energy storage for utility load leveling has been under investigation at the University of Wisconsin for a number of years. The system design which has evolved consists of a large solenoid storing in the neighborhood of 1000 MWh and buried in bedrock. The bedrock structure is needed to economically carry the magnetic loads. The general details of the diurnal energy storage magnet are presented in a companion paper at this conference by R.W. Boom [1].

The Wisconsin energy storage magnet winding consists of a rippled single layer solenoid wound from an aluminum-NbTi composite conductor. The ripple allows the magnetic loads to be transmitted to the rock at discrete locations through thermally insulating struts. These struts have intermediate cooling stations to reduce overall refrigeration loads. The high current conductor is self supporting between struts and is housed in a dewar containing superfluid liquid helium at 1.8K.

The recent effort in the structural and conductor areas has been in two areas: First, with the evolution of the low aspect ratio design, new structural support concepts have evolved The principal change in this area being the cold structural support of axial force and transmission of only radial forces to the bedrock. Several laboratory studies structural, cryogenic and conductor components have continued. The present paper discusses progress in these two areas. Details of the effort in other phases of the Wisconsin energy storage project are given in the two companion papers at this conference [1,2].

AXIAL AND RADIAL SUPPORT CONCEPTS FOR LOW ASPECT RATIO MAGNETS

Radial forces are much smaller in low aspect ratio solenoids than in any previous designs. Axial forces are still substantial and are comparable to previous designs. However, because of the short height of a low aspect ratio coil, it is economically possible to carry all axial forces internally. The mass of the internal cold compressive structure for axial forces is tolerably small, see Fig. 3 of reference 1.

Analysis of the impact of these forces and constraints has led to an approach which separates the radial and axial supports. Conceptual designs for the two supports have been worked out so that all fabrication may be done in a factory with only hand tools required for assembly. This approach also simplifies installation of the dewar wall plates because the lateral rigidity of the axial supports is sufficient to permit mechanical attachment of the plates. Field welding will be primarily for vacuum sealing, not mechanical integrity.

The axial support concept is shown in Figure 1. High strength 7075-T6 aluminum forgings are constructed to match the thermal coefficient and modulus of elasticity of the conductor. A pinned and keyed design is used which permits all fabrication in the factory and assembly by stacking one element on top of another. Fiberglass-epoxy straps on top and bottom support and electrically insulate the conductor tieing the two forgings together to make a laterally rigid assembly. Longitudinal attachments provide stability to the entire axial assembly and close the electrical circuit to allow energy dumping by mutual inductance. Provision is made for mechanical attachment of the dewar walls so that no additional structure is needed. This method keeps the vertically flat surfaces from distorting due to internal pressure. The above design is based on closely spaced conductor support straps which hold the conductor essentially flat in the horizontal plane with very low stress in the axial direction. This method leaves nearly all of the allowable conductor (strain) for radial loads. In turn, the design can be simplified with a longer ripple and radial support points farther apart. As shown, the present design is based on a 10 m ripple with 2 m radius at the support points for a circumferential spacing of 12 m.

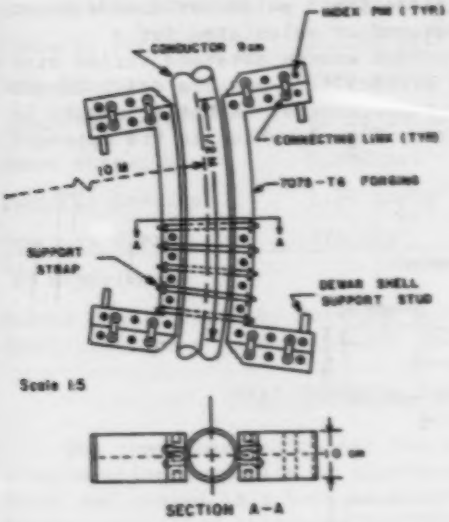

Fig. I
AXIAL SUPPORT CONCEPT

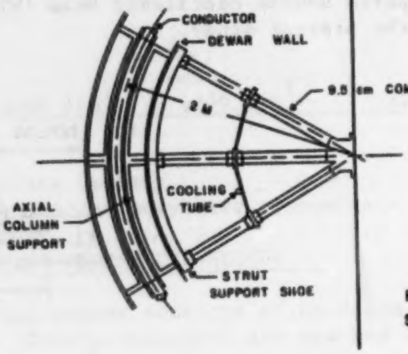

Fig 2.
STRUT ASSEMBLY

Fig. 1 Axial support concept for low aspect ratio design.

Fig. 2 Strut assembly for low aspect ratio design.

Separation of the axial and radial supports methods permits the radial struts to be designed for relatively small loads. This has an important bearing on the total magnet heat load since the struts react forces at 1.8 K to the tunnel wall at 300 K. Proposed design of a radial strut with one heat intercept is shown in Figure 2. The strut assembly is a modular design with one unit required for each turn of the magnet at each radial support point. The assembly will be completely shop fabricated and attached to the dewar wall and vacuum jacket by stud welded pins or bolts. Aside from the aluminum support shoe and support termination sockets, forces are reacted by 9.5 cm diameter polyester-fiberglass tubes which combine high strength, low thermal conductivity, and low cost.

For low aspect ratio magnets, future work is more in the direction of refinement than in basic concept. One outstanding task presently receiving attention is that of optimizing the number, temperature, and radial location of thermal shields. In this effort, emphasis is being placed on the efficiency and convenience of using boiling cryogenic liquids for heat intercepts. Liquid neon is being given serious consideration as the low temperature fluid in combination with liquid nitrogen for the high temperature shield.

INTERLAMINAR FRACTURE IN GLASS FIBER COMPOSITES

The superconductive energy storage magnet requires a large quantity of low-thermal-conductivity, high -load-carrying supporting structures to carry the radial and axial compressive loads from the 1.8 K magnet coils to room temperature bedrock. Engineering data is needed on low cost commercial composites for these struts. The main properties of concern are compressive strengths, delamination strengths, shear properties and compressive fatigue properties.

The present report deals with fracture energy of glass fiber polyester composite. Usually the fracture energy for an adhesive bond is measured or calculated for a rectangular cantilever beam specimen. However, the fracture energy obtained varies with a crack length which must be measured accurately. It is difficult to measure crack length at room temperature and almost impossible at cryogenic temperatures. A better sample is the width tapered double cantilever beam (WTDCB) specimen, Fig. 3, which is the approach employed in the present study.

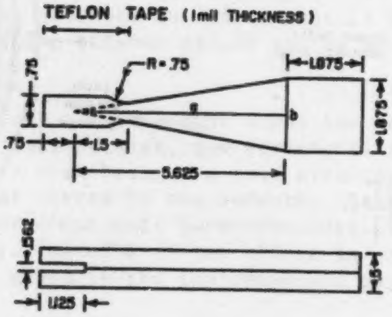

Fig. 3 Width tapered double cantilever beam (WTDCB) specimen. Two 1/4" samples bonded together.

Bond strength and fracture energy measurements of Extren*, a pultruded fiberglass polyester composite, are reported. This material is a candidate for construction of a component strut. The fracture behavior of the specimen as well as the effect of specimen geometry on fracture energy are studied at room temperature as well as 77 K. It is found that the fracture energy obtained decreases with increasing thickness of specimens, finally reaching a constant value. The minimum thickness requirement for the fracture test of Extren is one half inch. The fracture energy decreases with specimen width. A load-deflection hysteresis is observed to increase with specimen width. As the crack length increases hysteresis is dependent on the beam geometry, thickness, taper and crack length.

---

*Manufacturer: Morrison Molded Fiberglass Co.

The fracture energy at liquid nitrogen temperature (77K) is about 3 times as high as that at room temperature and the fracture energy transverse to the fiber direction is slightly higher than in the fiber direction. A summary of these results are listed in Table I along with other mechanical properties of Extren.

Table I

Properties of Extren at 300 and 77 K

	300 K		77 K	
Property	Longitudinal	Transverse	Longitudinal	Transverse
Tensile Strength	200,000 psi	10,000 psi		
Tensile Modulus	$2.0\text{x}10^6$ psi	$1.5\text{x}10^6$ psi	$2.4\text{x}10^6$ psi*	$1.8\text{x}10^6$ psi*
Compressive Strength	35,000 psi*	29,000 psi*	52,000 psi*	38,000 psi*
Flexural Strength	25,000 psi*	18,000 psi*		
Bond Strength	2380 psi*	2750 psi*		
Impact Strength	20 ft-lb/in	6 ft-lb/in		
Shear Strength	6,000 psi			
Specific Gravity	1.74 gm/cm^3			
Fracture Energy	774 J/m^2	1084 J/m^2	2200 J/m^2	3257 J/m^2

*UW Experiments

Extren Manufactured by Morrison Molded Fiber Glass Company
Unidirectional + random (44w/o) glass fiber reinforced polyester composite

HEAT TRANSFER FROM CYLINDERS IN SUPERFLUID HELIUM

The conductor design for the energy storage magnet consists of an 84 mm cylindrical cross-section composite of aluminum and NbTi. These conductors are stacked in a narrow dewar and cooled in a bath of superfluid helium at 1.8 K. In order to develop a reliable thermal stability criterion for the energy storage conductor, it is necessary to study the heat transfer in this configuration.

To model the conductor geometry, heat transfer studies have been carried out on right circular cylinders of 12.7 mm O.D. in both normal helium, 4.2K, and superfluid helium, $T<2.2$K. Results of steady state heat transfer measurements are shown in Fig. 4, which is a plot of the surface heat flux as a function of temperature difference between the bath and surface. These results are typical showing peak heat fluxes at 2.1 K about three times higher than occurs at 4.2 K. Recovery heat fluxes have even larger differences. A scaling model has been developed, which can successfully model steady state heat transfer in superfluid helium.

Measurements of transient heat transfer have also been carried out in the present geometry. It is found that very high heat fluxes can be transferred for short times.

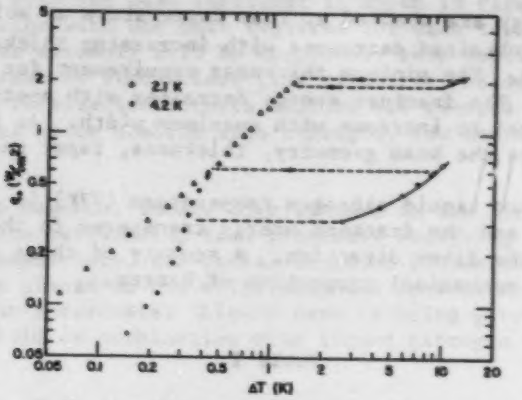

Fig. 4 Typical heat transfer curves for cylinders in normal and superfluid (T=2.1K) helium.

We have been able to transfer about 10 W/cm^2 for 200 msec with a bath temperature of 2.0K. These rates are very high and make the design criteria of 1 W/cm^2 for the full scale coil appear very conservative.

PROPERTIES OF JOINTS IN COMPOSITE SPECIMEN

The energy storage conductor contains four components. Current is carried by a composite of Cu:NbTi in an aluminum stabilizer. The conducting elements are supported by an internal structural member or cruciform made from strong aluminum alloy. To restrict the high purity aluminum from excessive plastic flow, the superconductor, stabilizer and cruciform are encased in an aluminum skin. The conductor is designed to be self supporting and have full cryogenic stability.

To insure stability the sectored conductors must have excellent thermal conductivity in the radial direction. The structural integrity of the bond between the stabilizer and the skin must be maintained for a low joint resistance. The method of joining the skin and stabilizer is thus of prime concern.

The work reported here includes results of preliminary bond studies on simple two component concentric cylindrical specimens joined by small amounts of cold work. The manufacturing concept envisioned for the Wisconsin conductor involves cold drawing together as a last fabrication step. It is necessary that this final draw adequately join all conductor components.

JOINT SHEAR STRENGTH

The shear strength of the joint between the tube and rod components of the composites was measured by loading 6.35 mm long cylindrical specimens in compression. All tests were performed at room temperature by monitoring the load-displacement behavior of samples held on a steel ring and loaded axially in the center. The compressive load was supported at one end of the specimen by the tube and balanced on the other end by an equal load applied evenly to the central rod. A shear stress was therefore generated in the joint region.

A summary of measurements of the joint shear stress at failure is presented in Table II. The failure stress uncertainties represent a scatter of one standard deviation and are noted to be in the range of 10-20% of failure stress for the codrawn samples. The uncertainty is less than 10% for the undrawn soldered samples. The strengths measured for the undrawn Cu-solder-Cu composites agree with previous work. The solder joints in the undrawn Al-Al samples had a strength above that of the pure Al core material and failure in the samples occurred by shear of the core Al.

Table II

The Shear Stress At Failure For Joints in Al-Al and Cu-Cu Composites Specimens

Sample	Core	Adhesive	Tube	Final OD (in)	Total Reduction in Area (%)	Joint Shear at Failure (psi)
D25b	Al^1	(none)	Al^2	0.365	36	4120 + 850
D33b	Al	solder^3	Al	0.365	36	3475 + 660
D34b	Al	solder	Al	0.462	0	(Al core failed)
D28b	Cu^4	(none)	Cu^4	0.410	36	4550 + 500
D30b	Cu	solder	Cu	0.410	36	7075 + 1030
D50a	Cu	solder	Cu	0.627	0	4475 + 385
D31b	Cu	Indium	Cu	0.410	36	8620 + 1990
D52a	Cu	Indium	Cu	0.627	0	1610 + 385

[1] 99.999 pure Al [2] Al alloy 8076 [3] 60% Sn-40% Pb [4] OFCH Cu

JOINT ELECTRICAL AND THERMAL RESISTANCE

Joint resistance was determined by applying a radially directed current to the center of a 3.2 mm thick cylindrical specimen and measuring the voltage drop across the bond region. Specimens were instrumented by mounting a current lead in the center, two potential difference taps on either side of the bond and a current lead clamped around the outside. Boundary resistivities were measured by the standard four point probe technique at room temperature 77K and 4.2K.

For measurements of the thermal resistance, each sample was instrumented to measure radial heat transfer with a heater, consisting of 80 Ω/m Evanohom wire wound on a copper post and varnished with GE 7031 into a central hole. The temperature difference measurements were made using Au 0.07 a/o % Fe to chromel thermocouples, one mounted in the core and another in the skin. The temperature profile in the core was assumed to be flat because of the high conductivity of the material. The samples were insulated on the ends with 20 to 30 mm of Stycase 2850 epoxy to insure only radial heat flow.

Displayed in Table III are electrical contact resistance values for different composites with varying reductions in area. Based on these data alone, there appears to be no clearly defined relationship between contact resistance and reduction.

Table III

Thermal and Electrical Contact Resistance of Various Composite Specimens

Sample	% Reduction	ρ_B(4.2 K)*	α_B*
Cu-Solder-Cu	36	0.06	-
Cu-Solder-Cu	66	0.15	-
Al-Al^1	22	0.14	1.4
Al-Al^2	22	0.35	7
Al-Al^2	50	0.69	>10
Cu-In-Cu	36	1.3	-
Cu-Cu	36	1.5	-

1. Part of a series with tube wall thickness 1.0 cm
2. Part of a series with tube wall thickness 2.4 cm

*ρ_B($\mu\Omega$-m^2), α_B(W/cm^{2}K^2)

Measurements of the thermal boundary conductance have been limited to the Al-Al composite specimens. For these data, we have assumed a metallic form for the contact conductance, and calculate a coefficient to the thermal contact conductance, α_B.

$$Q/A = \alpha_B T \quad \Delta T$$

where ΔT is the temperature difference across the boundary. Also listed in Table III are these values of the thermal contact conductance coefficient.

CONCLUSION

The following conclusions can be summarized from the studies reported in the present paper:

1) Conceptual design of the structural support for the low aspect ratio design presents a reasonable option which can be fabricated in a factory and assembled in the field.

2) Bonding studies of glass fiber polyester give engineering data for fracture energy of laminated bonds.

3) Heat transfer studies to HeII in cylindrical geometries give limiting values for the energy storage conductor.

4) Joint studies of cylindrical composite metal specimens indicate the need to have metallurgical bonds in the conductor.

Work is continuing in design and component development.

REFERENCES

1. R.W. Boom and Y.M. Eyssa, "Diurnal Energy Storage System Design", 1980 Annual Contractors Review Mechanical, Magnetic and Underground Energy Storage, Washington, DC, Nov. 10-13, 1980.
2. D.C. Larbalestier, K.T. Hartwig, A.W. West, D. Moffat, "Conductor Design and Development for Superconductive Magnetic Energy Storage Magnets", 1980 Annual Contractors Review Mechanical, Magnetic and Underground Energy Storage, Washington, DC, Nov. 10-13, 1980.
3. K.S. Han and J. Koutsky, "The Strain Energy Release Rate of Glass Fiber Reinforced Polyester Composite", ICMC Nonmetallic Materials at Low Temperatures-II, August 4-5, 1980, Cern Geneva, Switz.
4. S.W. Van Sciver and R.L. Lee, "Heat Transfer from Circular Cylinders in HeII," in Cryogenic Processes and Equipment in Energy Systems, ASME Century 2 publication, H00164, pp. 147-154.
5. K.T. Hartwig and S.W. Van Sciver, "Properties of Joints in Composite Specimens of Aluminum and Copper," Proceedings of 8th Symposium on Engineering Problems of Fusion Research, IEEE Publication No. CH1441-5/79, pp. 1794-6.

PROJECT SUMMARY

Project Title:	Superconductive Energy Storage
Principal Investigator:	R.W. Boom
Organziation:	531 Engineering Research Building University of Wisconsin Madison, Wisconsin 53706 (608) 263-5026
Project Goals:	To develop hardware components, produce engineering system designs, procure manufacturing and assembly equipment designs, revise cost estimates, and assess operational efficiencies for large underground superconductive storage systems.
Project Status:	Component development in three areas: cryogenics, conductor and structures is under way. Rock mechanics design and experimentation is under way. Parallel efforts supported by the Wisconsin Utilities are under way on the same schedule in five other areas: magnetics, environmental studies, system design, electrical, and safety. Two new designs have been studied: a low aspect ratio single solenoid and a 15 tunnel circular pattern of coils. These new designs may provide significant technical and economic advantages.
Contract Number:	DE-AC02-76ET-26602
Contract Period:	FY-80
Funding Level:	$400,000
Funding Source:	U.S. Department of Energy Division of Energy Storage

CONDUCTOR DESIGN AND DEVELOPMENT FOR SUPERCONDUCTING MAGNETIC ENERGY STORAGE MAGNETS

D.C. Larbalestier, K.T. Hartwig, A.W. West, and D.L. Moffat
University of Wisconsin
Madison, WI 53706

INTRODUCTION

The conductor of a superconducting magnetic energy storage (SMES) magnet designed for diurnal storage differs from conductors designed for other large superconducting magnets in a number of important respects. Since the purpose of a SMES magnet is to store electrical energy generated cheaply from base load capacity and then to supply it to the network at a later time when expensive peaking power would otherwise be used, the economic constraints are clear. Thus, the design of the SMES unit requires parallel attention to both the technical and economic feasibility of the solutions proposed. Such an analysis has led us to the choice of Nb-Ti of optimized and improved critical current density (J_c) as the superconductor, high purity aluminum (HPAl) as the normal metal stabilizer and an aluminum alloy as the structural material. The details of the arguments have been given previously: briefly they are that copper can never be affordable as a stabilizer since the weight required is too great and that Nb-Ti has increased so rapidly in price that a proper optimization for the desired field and temperature range is justified for a device where it forms about 15% of the total capital cost.

NIOBIUM-TITANIUM DEVELOPMENT

In our 1976 cost estimates Nb-Ti was costed at \$86/kg(1). It is now about \$200/kg, although it appears that the rate of increase in price should moderate to a rate approaching the normal inflation rate(2) by the introduction of pyrochlore Nb feedstock into the manufacturing process. Since Nb-Ti is required on an ampere-metre rather than a weight basis, the optimization of the superconductor in terms of the maximum available J_c at the desired field and temperature (compatible with reasonable manufacturing processes) is very important to the economics of a SMES unit.

Development of the J_c in Nb-Ti alloys has proceeded rather empirically.(3,4) Since the microstructures of optimized conductors are extremely complex and fine scale (see Fig. 1), it is difficult to relate the value of J_c obtained in commercial practice with the microstructure and the fabrication schedule which produced that microstructure. Generally the fabrication schedule is regarded as commercially secret and the exact alloy composition chosen varies from country to country.

The general aims of our effort have been the following:

1) To understand what is available from commercial Nb-Ti conductors world-wide (in general, foreign superconductors have higher J_c's but are more expensive).

2) To attempt to see if alternative optimizations of existing conductors will improve J_c at the low fields and low temperatures (3T, 2K) of SMES units.

3) To understand the relationship between processing, the microstructure developed by processing and the resulting superconducting properties so that commercially processed conductors will achieve significantly higher J_c.

4) To factor this understanding into the production of cheaper, higher J_c conductors. Significant raw material cost reductions may also be possible by using alloys of lower Nb content and by demonstrating that alloys of higher residual impurity can be used.

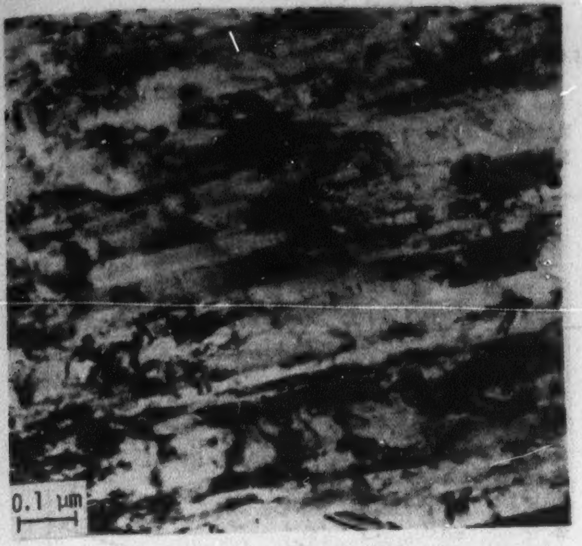

Fig. 1 Transmission electron micrograph of a commercial Nb 46.5w/o Ti alloy. Longitudinal section.

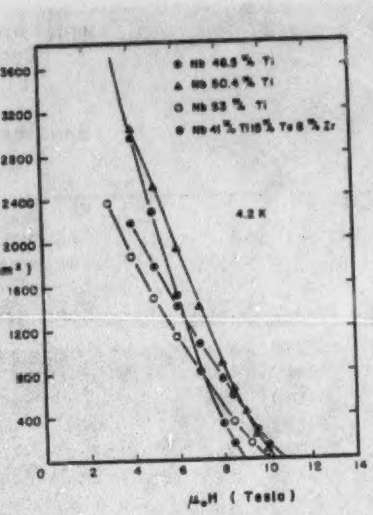

Fig. 2 Critical current density vs. field at 4.2 K for some commercial Nb-Ti alloys.

At this stage in our program we have made significant progress only on points 1 and 3 and we here report only on these two points.

CHARACTERIZATION OF COMMERICALLY AVAILABLE CONDUCTORS

Alloys of a number of different compositions are available around the world, individual manufacturers generally claiming that their particular alloy has optimum properties. Within the U.S., Nb 46.5w/o Ti is widely used but in Germany and Japan there is a greater preference for Nb 50w/o Ti. Other compositions favored by Japanese manufacturers are ternary and quaternary alloys containing Zr.

The range of J_c values found in these different materials is shown in Fig. 2 and the details of the composites are given in Table 1. These J_c values are genuine superconducting critical current densities taken at $\rho=10^{-14}$ Ωm. An important result of our investigation(5) is that, irrespective of country of origin, manufacturer or composition, the microstructure of all composites is qualitatively the same: all composites have a fine scale dislocation sub-band structure (diameter 30-50nm) produced by extensive cold-work together with α-Ti precipitates, presumably produced by heat-treatment at or near final size. Typical micrographs of these microstructures are shown in Figs. 1 and 3. This result is an important simplification of what still remains as a very complex problem - namely the "quantification" of microstructures such as those in Figs. 1 and 3 and their development during fabrication. Our studies(3-5,7) have clearly demonstrated that α-Ti precipitation is a common feature of all high J_c Nb-Ti base superconductors and that previous explanations based on sub-band diameter alone are inadequate. This point is demonstrated in Fig. 4.

Although the microstructures of the composites are qualitatively similar, the quantitative differences in the J_c values are large. At 5T and 4.2K, J_c ranges from 1600 to 2600 A/mm^2 and in the range of our SMES design (Fig. 5) the range in J_c is from 2800 to 4400 A/mm^2 (5T, 2K). It is particularly noticeable that the alloy containing Zr has the highest low field J_c. At present it is not clear whether this effect is intrinsic to Zr containing alloys or whether this is the result of superior optimization and this point is undergoing further study. The important point for SMES design is that the well-optimized conductor has a J_c 60% larger than the material routinely produced (Nb 46.5w/o Ti Fermilab

Table 1

Composite Details

Composition	Manufacturer	Number of Filaments	Filament Diameter (μm)	J_c 5T 4.2K Amm^{-2}	Sub-band Diameter (nm)
Nb 46.5w/o Ti	MCA	2100	10	1950	45.6
49.7	Vacuumschmelze	2000	9	1900	34.4
50.4	Vacuumschmelze	60	52	2610	39.8
52.7	Airco	180	38	1660	51.0
Nb 41w/o Ti 15w/o Ta 8w/o Zr	Kobe Steel	61	29	2230	41.4

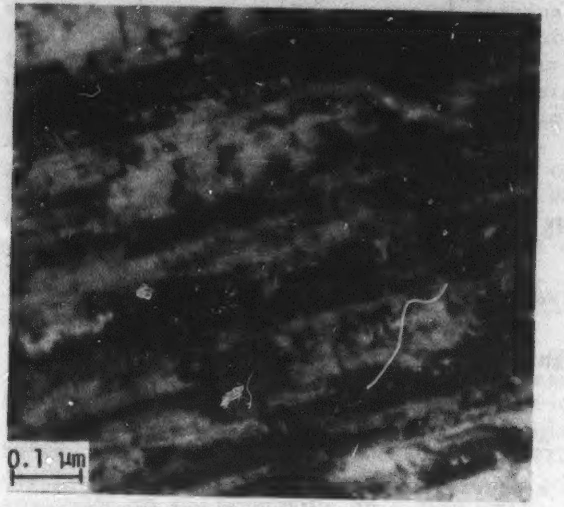

Fig. 3 Transmission electron micrograph of a commercial Nb 50.4w/o Ti alloy. Longitudinal section.

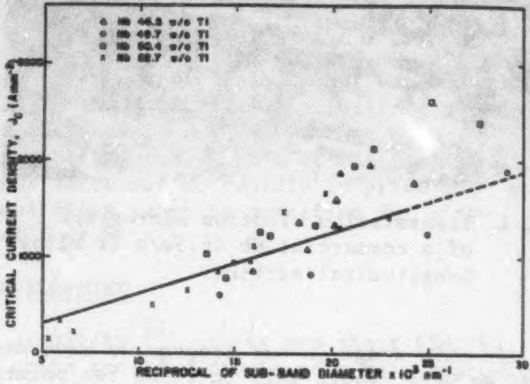

Fig. 4 Critical current density vs. the reciprocal of the sub-band diameter. The solid line is from the work of Neal et al[6] on alloys in which no α-Ti precipitation occurred. Values above the line show the beneficial effect of α-Ti precipitation in raising J_c.

conductor). Since we have certainly not yet reached the limits of J_c in Nb-Ti, these high J_c values translate into important reductions in the quality of material needed for a SMES unit.

MICROSTRUCTURE - PROCESSING RELATIONSHIPS

We initiated our studies of microstructure-processing-J_c relationships with a study$^{(7)}$ of a 2000-filament Fermilab Energy Saver conductor. This conductor was chosen since it is the most widely produced conductor and its properties, fabrication and costs are well established. Its superconducting properties are those shown in Figures 2 and 5 for Nb 46.5w/o Ti and are seen to be only moderate. It thus appears to be an excellent candidate for upgrading.

The sample of conductor used in this study had been taken from an intermediate stage in the manufacturing process. The conductor was 3.66mm in diameter and had already received an area reduction of ∿255:1 by cold-drawing after extrusion. Figure 6 shows a transmission electron micrograph of a transverse section of the conductor at this size. The microstructure consisted of irregular sub-bands with a wide range of sizes, (in a transverse section the sub-bands are viewed perpendicular to the drawing axis of the wire and appear as grains). The average sub-band size was 69nm. Electron diffraction analysis of the sample showed that it was single phase with no α-Ti present.

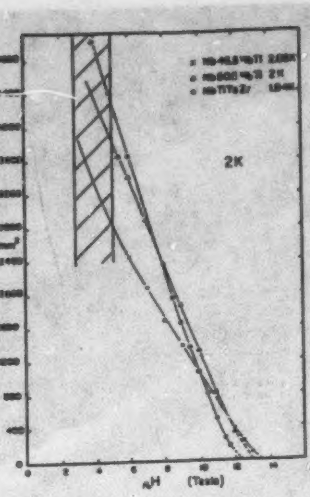

Fig. 5 Critical current density vs. field at 2K. Shaded area is region of SMES interest.

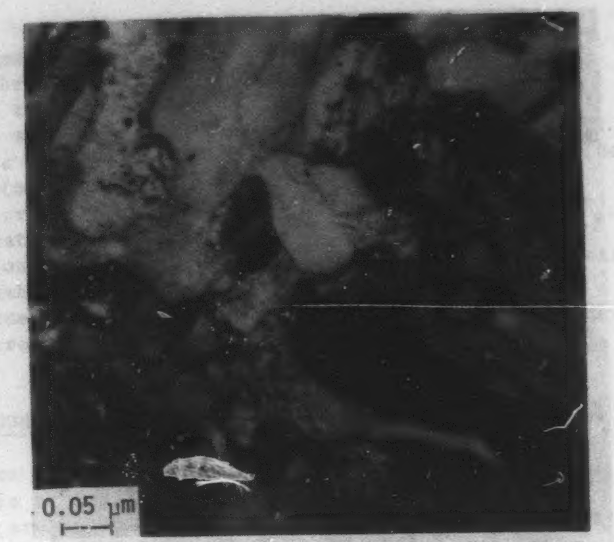

Fig. 6 Transmission electron micrograph of a Fermilab conductor, as-received. Transverse section, 3.66mm diameter.

Two samples of the conductor were heat-treated for 80 and 160 hours at 375°C. After these heat-treatments the average sub-band sizes increased to 116nm and 123nm respectively and both samples were found to contain α-Ti precipitates. The microstructures of the two samples were similar, consisting of more regular sub-bands containing dislocation arrays. A representative microstructure is shown in Fig. 7.

Lengths of the unheat-treated and heat-treated conductor were drawn down to a final diameter of 0.66mm with a 20% reduction in area at each pass. The sub-band diameter was measured after each reduction. The microstructure of the wire drawn from the unheat-treated sample is shown in Fig. 8. The sub-band boundaries are sharply defined and the interiors of the sub-bands do not appear to contain a high density of dislocations. In contrast, the wires drawn from the heat-treated samples had less well defined sub-band boundaries and the interior of the sub-bands appeared to contain a higher degree of deformation, Fig. 9.

A plot of sub-band diameter against area reduction is shown in Fig. 10 for all three samples. It can be clearly seen that, although the heat-treated samples had initially larger sub-band diameters than the unheat-treated sample, after drawing their sub-band sizes were smaller than the unheat-treated wire. The sub-band diameters are summarized in Table 2 together with the J_c values of the three samples at final wire size. The J_c values of the two heat-treated wires were from four to five times the J_c value of the unheat-treated wire.

Table 2

Sub-Band Diameters and J_c Values for Wire

Composite	Sub-Band Diameters nm 3.66mm	 0.66mm	J_c Amm^{-2} (5T, 4.2K)
Unheat-treated	69	51	366
80 hours at 375°C	116	37	1489
160 hours at 375°C	123	44	1541

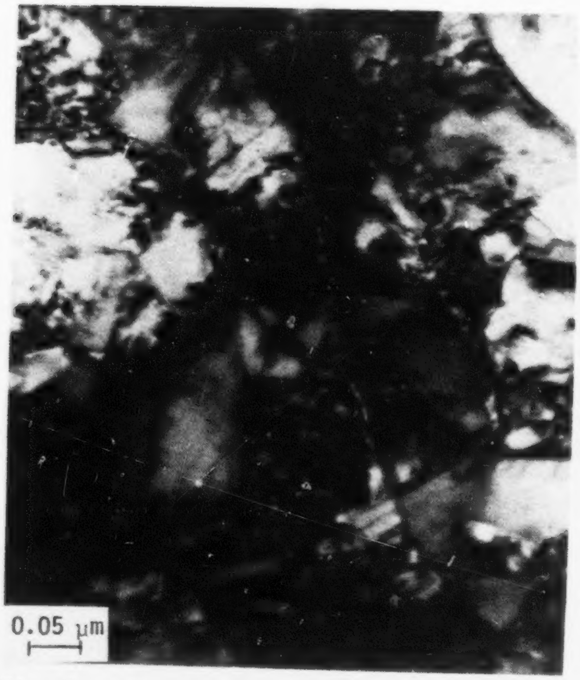

Fig. 7 Transmission electron micrograph of a Fermilab conductor, heat-treated for 80 hours at 375°C. Transverse section, 3.66mm diameter.

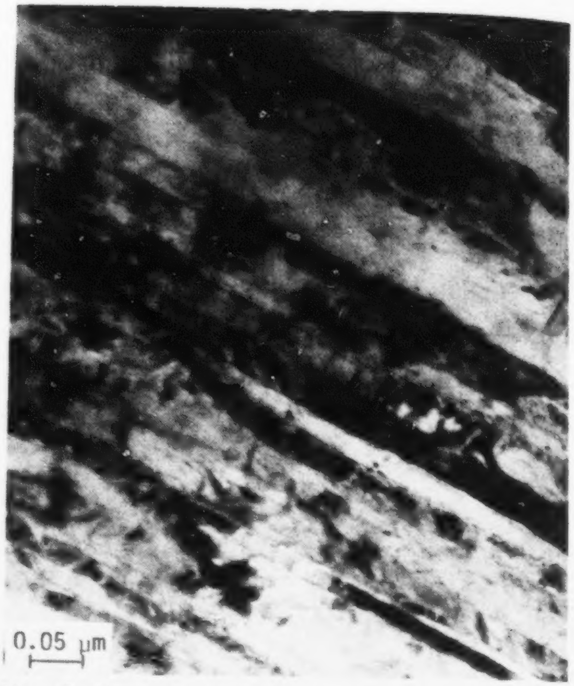

Fig. 8 Transmission electron micrography of Fermilab conductor after drawing to 0.66mm diameter, no heat-treatment. Longitudinal section.

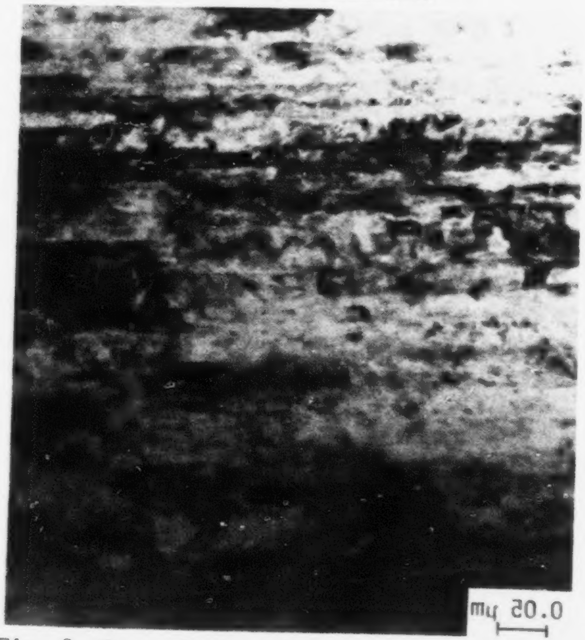

Fig. 9 Transmission electron micrograph of Fermilab conductor heat-treated for 160 hrs at 375°C and then drawn to 0.66mm diameter. Longitudinal section.

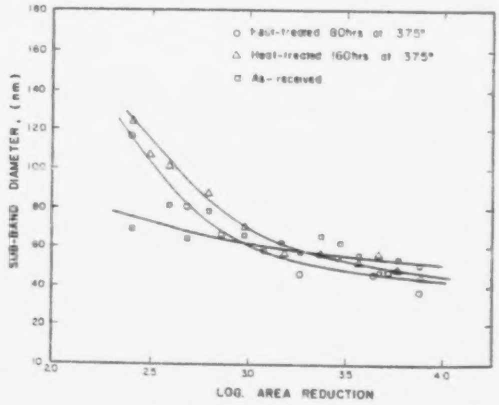

Fig. 10 Relationship between sub-band diameter and log area reduction for cold-worked Fermilab composites.

Microstructurally, the main differences between the heat-treated and unheat-treated wires were the appearance of the sub-bands and the fact that only the heat-treated samples contained α-Ti precipitates. These two features are interrelated in that the α-Ti precipitates formed during heat-treatment aided the refinement of the sub-band structure on subsequent drawing. An ill-defined sub-band structure and a small sub-band diameter appear to be necessary to attain high J_c values, but α-Ti precipitates are also required to provide maximum flux-pinning in the structure. The importance of α-Ti precipitates in obtaining high J_c in Nb 50 w/o Ti has been documented previously(8,9,10) together with the beneficial effects of two or more intermediate heat-treatments during drawing.(9) This work, however, provides the first microstructural information on the effect of intermediate heat treatments and demonstrates why it is physically reasonable for the J_c to be sensitive to the degree of cold work following the heat treatment. It is clearly to be expected that multiple heat treatments will allow further increase of J_c in this alloy and such experiments are now in progress.

ALUMINUM STABILIZED CONDUCTOR DEVELOPMENT

Recent work on conductor development has been in the areas of material characterization, joints and bonding. The objective is to develop a feasible composite conductor fabrication procedure Fabrication schemes are being tested in partial conductors and a reduced-scale model conductor. Present procedure calls for all components to be assembled during a final small reduction drawing step with solder bonding.

Residual resistivity ratios ($RRR_{300K}/R_{4.2K}$) and yield strengths have been measured for several commercial aluminum alloys and also for some special noncommercial alloys(11), see Tables 3 and 4. These alloys are under investigation for use as the conductor skin which must be moderately strong and have good thermal conductivity. As an example, Southwire Company's annealed Super T and annealed 1350(EC) have RRR's of 30-40 and yield strengths of about 100 MPa (14.5 Ksi). Either would be a good candidate for skin material.

Table 3

Residual Resistivity Ratios and Room Temperature Yield Strengths of Al Conductor Alloys

	Manufacturer	RRR ($\rho_{273K}/\rho_{4.2K}$)	Yield Strength* (psi)
1350 (EC) - H19	AEI	26	18,000
1350 (EC) - "Annealed"	Southwire	34	14,500
5005 - 0	Southwire	5.4	46,400
6201 - "Aged"	Southwire	7.1	50,400
8076 - H221	Alcoa	41	14,200
Triple E - "Annealed"	Southwire	35	14,400
NiCo - "Annealed"	Southwire	36	12,000
Stabiloy - 0	AEI	17	7,500
Super T - "Annealed"	Southwire	41	12,600

*Manufacturers value

Table 4

Residual Resistivity Ratios and Room Temperature Yield Strengths of Special Al Alloys

		RRR $\rho_{273}/\rho_{4.2}$	Yield Strength (psi)
Al-0.2 Au	peak-aged	146	6300
	over-aged	590	3850
Al-1.0 Co	as-extruded	180	7680
	annealed	325	4500
Al-1.0Ni_3Sb	as-extruded	180	6090
	over-aged	610	4060
Al-5.2 Ni	as-extruded	39	11900

Both the RRR and yield strength of a material change with cold work. Knowledge of these changes is needed to plan the proper manufacturing sequence from which a strong conductor with good thermal and electrical conductivities will result. Yield strengths and RRR's as a function of area reduction(12) by drawing have been measured for several alloys and are shown in Figures 11 and 12.

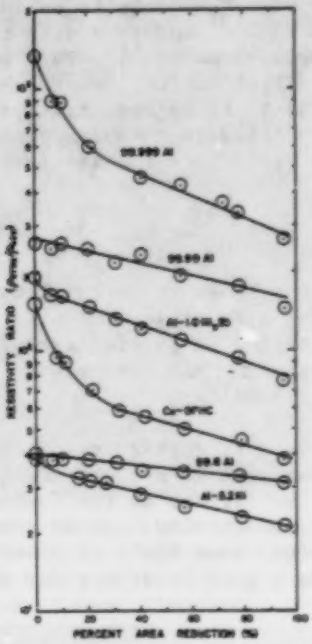

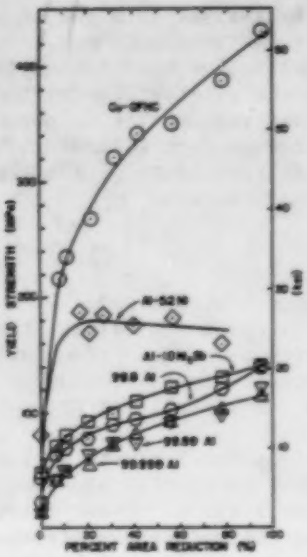

Fig. 11 Resistance ratio (RR) vs. percent area reduction (PAR) for high purity Al, Al conductor alloys and OFHC Cu.

Fig. 12 Yield strength ($\sigma_{0.2}$) vs. percent area reduction (PAR) for high purity Al, Al conductor alloys and OFCH Cu.

It is clear from the results that work hardening is very rapid at first and diminishes as the percent area reduction increases. The same trend is observed for changes in the resistivity with cold work. A conclusion of this study is that the final area reduction required for conductor fabrication will strengthen the conductor skin appreciably without severely degrading its conductivity.

Three properties that characterize metallurgical joints in the conductor are electrical resistivity, thermal resistivity, and shear strength. These properties have been measured on cylindrical samples of co-drawn or swaged Al-Al and Cu-Cu; tests were also made on joints that had been soldered prior to drawing or swaging. The results of this work are presented in a companion paper.

REFERENCES

1. UW Design, Wisconsin Superconductive Energy Storage Project Annual Report, Vol. II, January 1976.
2. W. McDonald, Wah Chang, private communication.
3. D.C. Larbalestier, Adv. in Cryogenic Eng., 1980 26 10.
4. D.C. Larbalestier, To appear in "Superconducting Materials", Ed. S. Foner and B.B. Schwartz, Plenum Press (1981).

5. A.W. West and D.C. Larbalestier, Adv. in Cryogenic Eng., 1980 26.
6. D.F. Neal, A.C. Barber, A. Woodcock and J. Gidley, Acta Met. 1971, 19 143.
7. A.W. West and D.C. Larbalestier, Applied Superconductivity Conference, Santa Fe, 1980. To appear in IEEE Trans. Mag.
8. I. Pfeiffer and H. Hillmann, Acta Met. 1968, 16 1429.
9. R. Arndt and R. Ebeling, Z. Metallk. 1974, 65 364.
10. J. Willbrand and W. Schlump, Z. Metallk. 1975, 66 714.
11. K.T. Hartwig and A.A. Saffari-Kermani, "Characterization of Several Al Alloys for Moderate Strength-High Conductivity Applications," Advances in Cryogenic Engineering Materials, Vol. 26, 1980, p. 621.
12. K.T. Hartwig and P.G. Appius, "Strength and Electrical Resistance of Cold-Drawn Al and Cu," Proceedings of the Eighth International Cryogenic Engineering Conference, C. Rizzuto, Editor, 1980, p. 720.

blank page

FLYWHEEL ENERGY STORAGE PROGRAM

blank page

PROJECT SUMMARY

Project Title: Mechanical Energy Storage Technology Project

Principal Investigator: Thomas M. Barlow

Organization:
Lawrence Livermore National Laboratory
P.O. Box 808, Mail Stop L-388
Livermore, CA 94550; Phone: (415)-422-8200

Project Goals: The goals of this project are to develop, demonstrate, and evaluate mechanical energy storage technology for vehicular and fixed-base applications and to carry out the R, D&D activities in a manner that maximizes the commercialization potential of the technology.

Project Status: The Lawrence Livermore National Laboratory's efforts were initiated in FY1975. Initially, these involved the development and characterization of fiber-composite materials for use in high performance flywheels. Late in FY1977 and FY1978, respectively, the project expanded to include development of MEST technology for application to electric and hybrid vehicles and evaluation of the laminated disc rotor concept. Funding in the former area was provided under the Electric and Hybrid Vehicle RD&D Act of 1976 (Public Law 94-413). In FY1980, the project was again expanded to include the technical management responsibility for flywheel rotor and mechanical component technology development as well as the evaluation of fixed-base applications of flywheel systems.

Milestones achieved in FY1980 included:

- Completion of tests of prototype flywheel units for electric vehicle application.
- Initiation of design for heat engine/flywheel vehicle.
- Completion of tests of advanced flywheel rotor concepts.
- Evaluation of flywheel rotor containment concepts.
- Qualification of an independent rotor test facility.
- Initiation of a multi-year planning effort for the project.

The project currently consists of six tasks, listed below. The estimated FY1980 expenditure level for each task is included; these do not include efforts directly funded by DOE.

• Transportation Applications	$ 97,000
• Fixed-Base Applications	250,000
• Fiber Composite Materials Characterization	370,000
• Flywheel Rotor Technology	1,250,000
• Advanced Component Technology	600,000
• Project Management and DOE Support	427,000

For the most part, the project's activities are carried out through subcontracts to private industry. In-house activities include technical management, material characterization, and tapered-thickness rotor concept evaluation.

Contract Number: W-7405-eng-48

Contract Period: Continuing

Funding Level:
$3,672,000 B/O - Energy Storage
$ 195,000 B/O - Distributed Solar Technology

AN OVERVIEW OF THE MECHANICAL ENERGY STORAGE TECHNOLOGY (MEST) PROJECT *

Thomas M. Barlow
Lawrence Livermore National Laboratory
7000 East Avenue
P.O. Box 808, L-388
Livermore, California 94550

ABSTRACT

This paper presents an overview of the Lawrence Livermore National Laboratory's Mechanical Energy Storage Technology Project, under which the field technical management of the DOE's flywheel technology program is exercised. The paper includes a summary of the project's objectives and approach, structure, and principal accomplishments in FY1980. The general trend in future plans is briefly described.

INTRODUCTION

Background

Flywheels have been used since ancient times; since the industrial revolution, their use in machinery has been commonplace. Their primary role has been that of mechanically correcting the timing mismatch that commonly occurs in most energy delivery systems, allowing energy sources to more effectively meet the requirements of energy uses.

The present-day and future requirements of energy storage technology are more rigorous than ever before. The continually increasing cost and shortage of petroleum-based fuels has become a serious problem for the Nation, and a broad base of new technologies is required to permit more effective utilization of these fuels and to allow substitution of other energy sources wherever practical.

Several characteristics of mechanical energy storage technology make it particularly attractive as an energy conservation concept. Specifically, the ability to accept and deliver energy at high rates is a vitally important attribute. Secondly, in contrast to a number of electrochemical energy storage methods, energy storage capacity is independent of delivery rate. These characteristics can be used to advantage to complement lower power-density energy storage devices, such as batteries in electric vehicles. In this application, several benefits may be realized:

- Extended battery life, by reducing the peak power demand on the battery.
- Impoved acceleration, by supplementing the power available from the battery.
- Increased range, by permitting the battery to operate in a more favorable load regime.

Significant benefits are also expected from the application of flywheel technology to heat-engine-powered vehicles. Improvements in fuel economy of 50% to 100% are forecast; the benefit in this case is achieved by recovering braking energy, using the flywheel to meet peak power demands, and permitting the engine to perform in its most favorable load/speed range.

With regard to photovoltaic and wind energy systems, the timing mismatch between energy supply and demand is readily apparent. While a variety of energy storage methods can be applied, certain operating characteristics of mechanical energy storage systems

---

*This work was performed under the auspices of the U. S. Department of Energy by Lawrence Livermore National Laboratory under contract No. W-7405-Eng-48.

are very promising. Among these are the all-mechanical nature of the system and the potential for simplified power-conversion hardware. Development of the technology for this application has only been recently initiated, and additional study is required to quantify the potential of the technology.

Through these applications, mechanical energy storage technology can provide significant savings in petroleum consumption. These savings will be realized by enabling and enhancing the market penetration of alternative energy sources; by allowing the more effective use of petroleum in conventional systems; and by facilitating increased utilization of non-petroleum-fueled systems, such as electric vehicles.

In order to realize the energy savings and substitution potential of flywheel technology, further development is required in several areas in order to improve its economic viability: fiber-composite materials and flywheel rotor design; energy conversion devices; and the associated components which affect the safety, reliability, and cost of the energy storage system.

Project History

The MEST Project was initiated early in calendar year 1979, when several independent, flywheel-related R&D efforts at the Lawrence Livermore National Laboratory (LLNL) were brought together. Subsequently, the Laboratory accepted the responsibility for the field technical management of the Department of Energy's flywheel technology efforts, and the work that had been directed by the Sandia Laboratory in Albuquerque, New Mexico, was transferred to LLNL. This transition was completed at the end of FY1979.

Acceptance of the field management role required an expansion of the Project's capability at LLNL. Additional staff members were added in order to carry out the necessary management activities--planning, preparing work package specifications, selecting and directing subcontractors, and maintaining accountability for the work. In addition, an expanded capability in critical path network analysis was acquired.

OBJECTIVES AND APPROACH

Objectives

The objectives of the MEST Project are to

- develop, demonstrate and evaluate mechanical energy storage technology for vehicular and fixed-base applications, and to
- carry out the R,D&D activities in a manner that maximizes the commercialization potential of the technology.

Approach

The management approach which is followed in the conduct of the MEST Project includes five principal actions:

- Identify technology areas and applications to be investigated.
- Provide an operating structure.
- Identify interrelationships, both within the project and with related work elsewhere.
- Develop and maintain a system of controls and accountability.
- Promote and develop participation by industry in all phases of the project.

The technical approach can be summarized in a similar manner:

- Identify R&D needs.
- Assess the applicability of MES technology.
- Carry out analytical and experimental efforts.
- Validate laboratory-scale results through proof-of-concept tests.
- Conduct limited-scale engineering demonstrations in cooperation with end-use organizations.
- Emphasize technology transfer by involving private industry in all phases of R&D.

STRUCTURE

Project Organization

The MEST Project consists of five technical tasks arranged into two primary areas--applications and technology base, as shown in Figure 1. Included in the applications area are the efforts to develop and evaluate MEST for transportation and fixed-base systems. Energy storage prototypes are developed and evaluated both, in the laboratory and as full-scale experimental prototypes. Analytical studies include design studies and evaluations of the technology's potential for energy savings and substitution.

The three "technology-base" tasks address (1) the development and characterization of fiber-composite materials for use in flywheel systems, (2) the advancement of flywheel rotor and containment technology, and (3) the development of specific component technology which is intimately associated with flywheel systems. Included in the latter task are energy conversion and transmission systems, test facilities and mechanical components.

Task Interactions

Figure 2 indicates the interactions and "products" of the technical tasks. Requirements, in terms of cost and performance, are developed through applications analysis; these requirements then became the criteria for technology development. The net results of the project are an evaluation of the technology on a system level and the establishments of a technology base for use by the private sector.

Subcontract Activities

The Project's activities are primarily carried out through subcontracts to private industries and universities. In-house activities at LLNL are limited to the areas of fiber composite materials and flywheel rotor technology.

Subcontracts are placed with the private sector on the basis of capability and project need. Many of the procurements are based on competitive proposals, with unsolicited proposals being evaluated on an individual basis.

In the 1980 fiscal year, 59 individual R&D activities were undertaken by the MEST Project, exclusive of the technical management function. Of these, 44 were subcontracted to private industry and 12 to universities or university-related laboratories; the remaining 3 were performed at LLNL. Twenty of these subcontracts will be described separately as a part of the 1980 Annual Contractors' Review; additional principal subcontractors and the respective areas of R&D are listed in Table I.

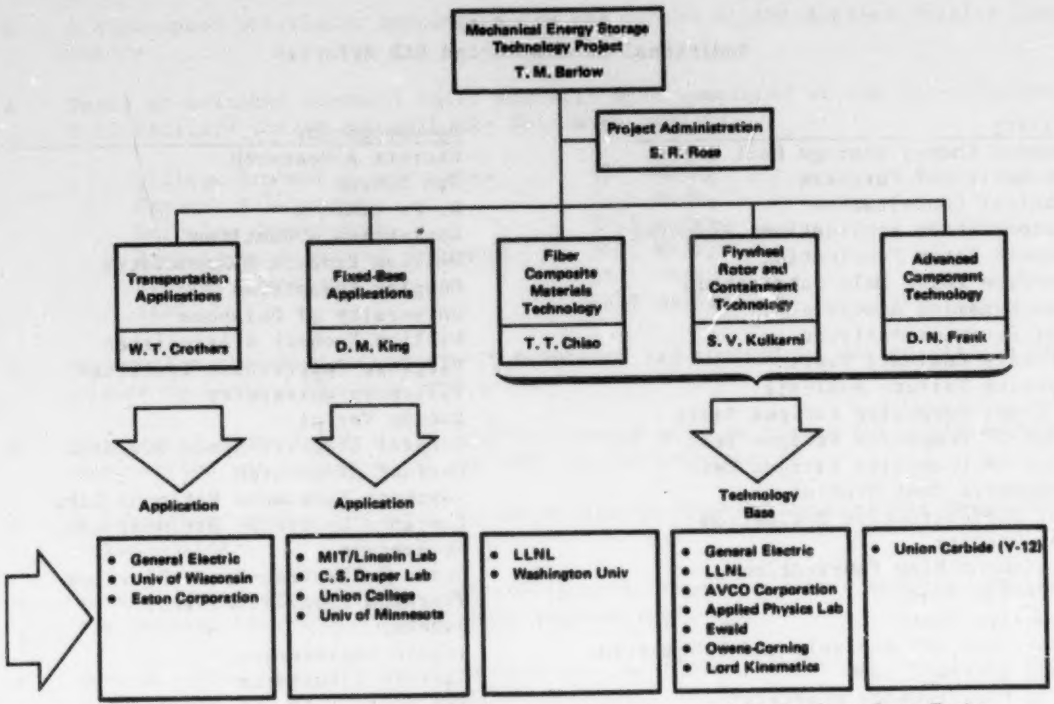
Mechanical Energy Storage Technology Project
T. M. Barlow
Project Administration
S. R. Rose
Transportation Applications
W. T. Crothers
Fixed-Base Applications
D. M. King
Fiber Composite Materials Technology
T. T. Chiao
Flywheel Rotor and Containment Technology
S. V. Kulkarni
Advanced Component Technology
D. N. Frank
Application
Application
Technology Base
• General Electric
• Univ of Wisconsin
• Eaton Corporation
• MIT/Lincoln Lab
• C.S. Draper Lab
• Union College
• Univ of Minnesota
• LLNL
• Washington Univ
• General Electric
• LLNL
• AVCO Corporation
• Applied Physics Lab
• Ewald
• Owens-Corning
• Lord Kinematics
• Union Carbide (Y-12)

Figure 1. The MEST Project Structure Consists of Applications and Technology Base Tasks. Subcontractors included in the 1980 Annual Contractors Review Are Indicated.

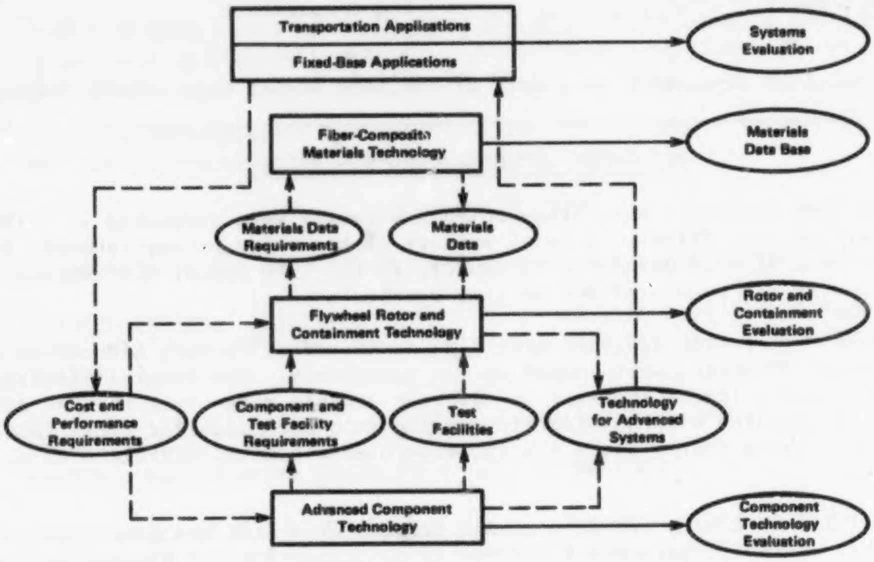
Transportation Applications
Fixed-Base Applications
Systems Evaluation
Fiber-Composite Materials Technology
Materials Data Base
Materials Data Requirements
Materials Data
Flywheel Rotor and Containment Technology
Rotor and Containment Evaluation
Cost and Performance Requirements
Component and Test Facility Requirements
Test Facilities
Technology for Advanced Systems
Advanced Component Technology
Component Technology Evaluation

Figure 2. Task Interactions Within the MEST Project

TABLE I
Additional Subcontracted R&D Efforts*

Activity	Subcontractor
Advanced Energy Storage Unit Tests	Garrett AiResearch
Transmatic CVT Purchase	Van Doorne
Technical Consultation	R. F. McAlevy
Transportation Applications Planning	Booz-Allen & Hamilton
Advanced Rotor Fabrication	William Brobeck & Associates
Disc-Type Rotor Mold Fabrication	Gougler Industries
Rotor Dynamics Analysis	University of Oklahoma
Rotor Dynamics Analysis	William Brobeck & Associates
Composite Laminate Tests	Virginia Polytechnic Institute
Composite Failure Analysis	Villanova University
S-2 Glass Composite Fatigue Tests	Boeing Vertol
Kevlar-29 Composite Fatigue Test	General Electric-Space Division
Kevlar-49 Composite Fatigue Test	Garrett AiResearch
Elastomeric Bond Studies	Lawrence Livermore National Lab.
Rotor Nondestructive Evaluation	Lawrence Livermore National Lab.
Rotor Testing	Rocketdyne
Containment Ring Fabrication	General Electric-Space Division
CVT Design Study	Traction Propulsion, Inc.
CVT Design Study	Vadetec
Hydrostatic CVT Analysis and Fabrication	Ifield Engineering
Vacuum System Study	Garrett AiResearch
Vacuum Requirements Analysis	SEN VAC
Pert Program Development	Shirley Software Systems
Applications Analysis	C. S. Draper Laboratory
1980 Flywheel Technology Symposium Support	La Posada Resort Hotel
Administrative Support	OAO Corporation

*Efforts not described separately as a part of the 1980 Annual Contractors' Review

PRINCIPAL ACCOMPLISHMENTS - FY1980

Many of the MEST Project's activities noted previously were completed in FY1980, and others will continue into FY1981. A brief summary of the major accomplishments follows, including both those efforts described separately in the 1980 Annual Contractors' Review and those which were not presented due to time constraints.

- Two prototype energy storage units, one developed by Garrett AiResearch and one by General Electric, were tested in the laboratory. The General Electric unit demonstrated a 15-20% increase in electric vehicle range over the SAE J227a-D cycle as compared with an electric vehicle incorporating electrical regeneration of braking energy and a 47% increase over a similar vehicle with no regeneration.

- An analysis of a heat-engine flywheel propulsion system was completed and critical operating parameters defined by the University of Wisconsin. Design efforts were initiated by the Eaton Corporation for a system to be incorporated in a Chevrolet Citation.

- The Union Carbide Corporation's Oak Ridge Flywheel Evaluation Laboratory was completed and qualified for operation by an independent review committee.

- A high-speed television imaging system was tested at the Applied Physics Laboratory.

- Tests of advanced flywheel rotor concepts were completed at the Union Carbide Y-12 facility and at APL with the following results:

William Brobeck & Associates	25 Wh/kg
Garrett AiResearch	74.4 Wh/kg
Hercules Corporation	37.5 Wh/kg
Rocketdyne Division, Rockwell	36.1 Wh/kg
General Electric	55 Wh/kg
LLNL	66.9 Wh/kg

- Flywheel containment studies were completed and conceptual design efforts initiated by General Electric and AVCO.

- Testing of a one-tenth scale flywheel energy storage system for a stationary application was completed at the MIT Lincoln Laboratory.

- A Laboratory evaluation of a variable-inertia flywheel concept was completed by Union College.

- Several CVT design concepts and configurations were reviewed and two obtained for testing (Van Doorne and Ifield Engineering).

- Several rotor design-related studies were completed, including dynamics (Univ. of Oklahoma and Wm. Brobeck), fatigue properties (Boeing Vertol, General Electric and Garrett AiResearch), manufacturing (Ewald Associates, Gougler Industries, Owens-Corning, and Lord Corporation), and failure analysis (Villanova University).

- A MEST Project multi-year planning effort was initiated; a network analysis program was purchased in order to allow fiscal year financial planning and analysis.

- Plans and arrangements were made for the 1980 Flywheel Technology Symposium, held in Scottsdale, Arizona, in October, 1980.

PLANNED EFFORTS

Planned efforts within the MEST Project currently include the following efforts:

- Transportation Applications - Electric/ and heat engine/flywheel vehicle systems work will continue, with increasing emphasis on the heat engine/flywheel system.

- Fixed Base Applications - Residential and small-scale industrial or commercial flywheel energy storage applications will be developed. Both applications analysis and hardware development will be included.

- Fiber Composite Materials Technology - A limited number of fiber and matrix material composites will be characterized; long-term behavior studies will continue.

- Flywheel Rotor and Containment Technology - Efforts on rotor development will be focused on a more limited number of configurations; cyclic behavior will be investigated, as will manufacturing and economic considerations. Effective containment concepts will be developed.
- Advanced Component Technology - Near-term efforts will include the development and operation of flywheel rotor test facilities and the investigation of appropriate CVT concepts. Other component technologies will be pursued as required in support of the applications tasks.

PROJECT SUMMARY

Project Title: Laboratory Development and Evaluation of a Regenerative Flywheel Energy Storage System

Principal Investigator: Edward P. Cornell

Organization: General Electric Company
Corporate Research and Development
Schenectady, New York 12301

Project Goals: Demonstrate new technology associated with a flywheel energy storage system comprised of a flywheel coupled directly to an a.c. synchronous motor/alternator and fed by a solid-state inverter/rectifier unit designed to provide the necessary frequency control from a constant d.c. voltage power supply. Determine electric vehicle range improvement that can be attributed to the use of a flywheel in combination with a lead-acid battery bank.

Project Status: The project has been completed.

A flywheel energy storage and recovery system for a battery/flywheel electric vehicle of the 3000-pound class was developed, fabricated, and laboratory tested. The vehicle propulsion system was simulated on a digital computer in order to determine the optimum system operating strategies and to establish a calculated range improvement over a non-regenerative, all electric vehicle. The flywheel energy storage system consists of a solid rotor, synchronous, inductor-type, flywheel drive machine electrically coupled to a d.c. battery electric propulsion system through a load commutated inverter. The motor/alternator unit is coupled mechanically to a small steel flywheel which provides a portion of the vehicle's accelerating energy and regenerates the vehicle's braking energy.

The energy recovery system operated successfully over the speed/torque/time profile of a 3000-pound vehicle operating repetitively on SAE J227a driving schedules. The maximum range obtained on the Schedule D cycle was 83.7 miles. This is estimated to be a 15% to 20% improvement in range over a regenerative, chopper-driver all-electric vehicle operating on the Schedule D driving cycle, and a 47% improvement over a non-regenerative all-electric vehicle on the same schedule.

Contract Number: W-7405-ENG-48, Subcontract 8990503

Contract Period: March 17, 1978, through June 30, 1980

Funding Level: $544,624

Funding Source: U.S. Department of Energy through the Lawrence Livermore National Laboratory

MECHANICAL ENERGY STORAGE TECHNOLOGY APPLICATION TO ELECTRIC VEHICLES

E.P. Cornell, F.G. Turnbull
Corporate Research and Development
General Electric Company
Schenectady, NY

ABSTRACT

The development, fabrication, and test of a regenerative flywheel energy storage system for a battery/flywheel electric vehicle for commuter application is reviewed. The system consists of a steel flywheel coupled to a high-speed inductor motor/alternator fed by a load-commutated inverter/rectifier which does not utilize a shaft position sensor for inverter control. Computer control is used to provide component as well as overall system control and data acquisition. This flywheel energy storage system was laboratory tested over the SAE J227a Schedules D, C, and B driving cycles, using a laboratory simulation of an electric vehicle drive. Results show that maximum benefit occurs on the Schedule D cycle for which the overall system was optimized. From these tests, recommendations for additional improvements to this propulsion system are made.

INTRODUCTION

A flywheel energy storage sytem was initially conceived in 1975 by the General Electric Company and proposed for demonstration to the U.S. Department of Energy, Division of Energy Storage Systems. The overall objective of the program was to demonstrate new technology associated with a flywheel energy storage system comprised of a flywheel coupled directly to an ac synchronous motor/alternator. The motor/alternator/flywheel unit would be hemetically sealed with the rotating assembly operating in a low-pressure helium atmosphere. The motor/alternator would receive power from a solid-state inverter/rectifier unit designed to provide the necessary frequency control from a constant dc voltage power supply.

A follow-on effort was initiated with the specific objective of laboratory testing an improved flywheel energy recovery system sized for a battery/flywheel electric vehicle weighing about 3500 pounds. Computer runs have been made to simulate an electric vehicle operating under the SAE J227a Schedule D driving cycle. The goal was to determine the performance improvement that can be attributed to the use of a small flywheel in combination with the battery bank. Analysis has indicated that the flywheel can isolate the battery from a portion of the acceleration power demands of the vehicle and can also recover a substantial portion of the braking energy.

OVERALL VEHICLE SYSTEM STUDIES

In analyzing the performance of a flywheel battery-powered vehicle operating on a duty cycle such as the SAE J227a Schedule D, many operating strategies were evaluated. This involved use of the flywheel energy and the battery energy, or both, to provide propulsion energy and to accept regenerative energy during various segments of the selected driving cycle. The selected cycle and the active subsystems are shown in Fig. 1.

The five segments of the SAE driving cylce are indicated at the top of Fig. 1. The accelerate portion is divided into two modes. In the first mode, from zero vehicle speed to the "motor cornering point," indicated by the circle, all of the power is supplied from the flywheel subsystem. At the "motor cornering point," the motor back EMF equals the battery voltage and the second mode commences. During Mode 2, both the battery and the flywheel subsystem share in supplying the accelerating power. Mode 3 begins when the vehicle has reached the desired steady speed. During this mode, all of the power is supplied from the battery. During Mode 4 (Coast) and Mode 5 (Brake), all of the recovered power is supplied to the flywheel subsystem. During Mode 6 (Idle) the flywheel subsystem is brought back to its initial speed with power from the battery. The shaded area in Fig. 1 is power supplied out of and into the flywheel subsystem to and from the propulsion motor. The cross-hatched area is the power supplied from the battery direct to the flywheel subsystem. The unshaded area represents the battery power supplied direct to the propulsion motor.

The overall system was modeled in a computer simulation. The energy storage package was considered as a single subsystem, containing the motor/alternator/flywheel and the power conditioning equipment. As such, only one parameter, the combined in/out energy efficiency, was required to define this subsystem. This value became an input to the computer program. It was assumed that the size and the speed range of the flywheel would be designed to be sufficient to store the braking energy and to provide the needed acceleration.

The battery/flywheel vehicle assumed for these simulation runs was taken as a modification of the all-battery electric vehicle that the General Electric Company has developed under separate DOE/JPL contract. The vehicle has an empty weight of 2,000 pounds, a battery weight of 1,100 pounds, and a passenger load of 600 pounds for a gross total weight of 3,700 pounds.

In assessing the results of the vehicle simulation runs, two criteria were used: first, the actual range for a repetitive J227a Schedule D cycle; and second, a comparison of this range with that computed for the pure battery electric vehicle. In the latter case, no regeneration into the battery was assumed for the reference vehicle since the amount of regeneration possible was not precisely known at that time.

Figure 2 shows the computer's predicted range of a non-regenerative all-electric vehicle and the predicted range of the battery/flywheel system operating in the modes shown on Fig. 1 as a function of flywheel in/out efficiency. The actual measured values of flywheel in/out efficiency (presented in Fig. 12) were less than the minimum value of 60% given on the curve. Extrapolation of the linear curve of range vs. in/out efficiency to a value of 50% gives the predicted increase in Schedule D driving cycle range using the flywheel package.

FLYWHEEL ENERGY STORAGE PACKAGE

INDUCTOR MOTOR

With respect to the flywheel drive machine the most difficult operating point of the J227a driving cycle occurs during vehicle braking and flywheel motoring. From an electrical point of view, the most severe machine load occurs at 145% of the base (or minimum operating) speed, where the commutation requirements are 230 amperes at 108 volts in the dc link. The electrical machine finally chosen from the trade-off study was a six-pole machine operating with a maximum speed of 20,000 r/min, with a rotor radius of 3.6 inches and a rotor length of 3.44 inches (active stator core length). A cross section of the machine is shown in Fig. 3.

FLYWHEEL

The energy stored in the inductor motor rotor is approximately 15 watthours over the speed range of 10,000 r/min to 20,000 r/min. An additional 90 watt-hours are stored in the steel flywheel. The flywheel operates at a moderate stress level in order to produce a factor of safety of 2.0 relative to the 10^7 cycle curve for alternating stress. Although a higher stress design is possible, it was not considered advantageous in this case; doubling the design stress would only remove aproximately 10% of the total package weight from the flywheel. The flywheel weight reduction may be counterbalanced by the need for a heavier containment ring. The higher stressed wheel would also be larger in diameter and occupy more vehicle space.

POWER CONDITIONER

The power conditioner is a load-commutated inverter utilizing only six power thyristors. Reversal of the power flow is provided by a hybrid reverser (two diodes and two contactors) rather than a second set of six thyristors.

Figure 4 shows the laboratory set-up with the inductor motor/flywheel package in the lower left of the photograph, the inverter/rectifier and its control located on the top of the right laboratory bench. The propulsion motor and road loss generator are located behind the bench.

SYSTEM TEST CONFIGURATION

A block diagram of the entire laboratory system is shown in Fig. 5. The major components (the battery, the dc propulsion motor, the hybrid reverser, the load-commutated inverter/rectifier, the inductor machine, and the energy storage flywheel together with the electromagnetic contactors) are shown. The elements of the inverter/rectifier and the system control are indicated. The simulated vehicle is comprised of a flywheel to simulate the vehicle inertia and a dc generator and a load resistor to simulate the road load (rolling and aerodynamic) losses.

A computer-based data acquisition system measured the various electrical and mechanical parameters and provided real time and summary performance data.

SYSTEM TEST RESULTS SUMMARY

The system tests were conducted using SAE J227a driving schedules. The flywheel/battery hybrid system divides the acceleration mode into two parts: the first using only the flywheel, and the second using both the battery and the flywheel to accelerate the vehicle.

SCHEDULE D DRIVING CYCLE

The Schedule D driving cycle tests were composed of two major parts: 1) with the cruise time set at 50 seconds and starting with a fully chaged battery, the system was continuously cycled until the battery was completely discharged in order to determine the range of the vehicle; and 2) the system was operated over a small number of repetitive cycles at 108 volts with the cruise time set at values both longer and shorter than the specified value of 50 seconds in order to show the effects of varying the stops per mile.

Three complete battery discharge tests were completed using the Schedule D parameters. The test was started with a fully charged battery and continued until either the battery or the flywheel were unable to meet the vehicle speed-time profile given in the Schedule D driving cycle. A summary of the range and battery data obtained during these three runs is given in Table 1. Data were taken from three runs in order to average out any variables associated with the battery charge at the beginning of the run.

The second series of tests, based on the Schedule D driving cycle, operated over a limited number of repetitive cycles, from a fixed value of d-c voltage, at an adjustable value of cruise time (both less than and greater than the 50-second cruise time specified in the Schedule D driving cycle). The system summary data were recorded; a representative sampling of the data is presented in Table 2.

The battery kWh/mile vs. stops/mile is plotted in Fig. 6. The curve is a straight line with a positive slope indicating that not all of the available kinetic energy is recovered and made available for acceleration. A 100% efficient energy recovery system would have a constant value of kWh/mile as a function of stops/mile. The zero stops/mile intercept is calculated based on the energy used during the cruise segment of the driving cycle. This would be the value of the battery energy for no stops per mile operation. The battery energy plotted in Fig. 6 does not include the field energy for the two electrical machines. It is estimated that the field requirements add approximately 3% to 4% to the average battery current.

In addition to the battery kWh/mile, three dimensionless ratios were calculated for each operation on the specified driving cycle. They are:

1. A Flywheel Effectiveness Factor. This is the ratio of traction motor energy in motoring to battery energy over one cycle. In an all-electric vehicle without regeneration, this ratio would be unity. Ratios greater than unity indicate that the flywheel energy storage package is supplying some net energy to the traction motor.
2. Range Improvement Factor. This is a calculated ratio based on the computer model of the lead-acid battery. The series resistor in the battery model is nonlinear and is a function of the peak battery current. In this system, the peak battery current is reduced from that in an all-electric vehicle; this should result in a greater energy storage capability of the battery, which could be indicated by a range improvement factor greater than unity.
3. Flywheel In/Out Efficiency. This ratio is a measure of the electrical energy into the flywheel energy storage package (power conditioner, inductor motor, and flywheel) divided by the output power from the same equipment operating with reverse power flow. The ratio includes the field energy losses of the inductor motor. The flywheel effectiveness and range improvement factors as a function of stops/mile on the Schedule D cycle are shown in Fig. 7.

These two curves are linear and show an increasing value for additional stops/mile where the flywheel energy storage system is used more frequently. These results provide quantitative data as to the greater advantage of the flywheel energy storage systems for multi-short-stop mission profiles.

The flywheel in/out efficiency is plotted vs. stops/mile in Fig. 8. For repetitive stops/mile greater than the value for Schedule D (approximately 1 stop/mile), the flywheel energy storage package maintains its energy efficiency at approximately 50% to 52%. At fewer stops/mile, the flywheel losses, and the fact that it is seldom used, result in a reduced in/out efficiency value.

Similar tests were conducted for the Schedule B and C driving cycles and are reported on in Reference 1.

During the Schedules B and C driving cycles, the vehicle cruise speed results in a greatly reduced amount of energy available for conversion from the vehicle inertia to the flywheel energy storage package for subsequent reuse during the next vehicle acceleration. This reduced amount of available energy reduces the in/out efficiency and the flywheel effectiveness and range improvement factors.

CONCLUSIONS AND RECOMMENDATIONS

The major conclusions resulting from the laboratory test of an improved flywheel energy recovery system sized for a battery/flywheel hybrid electric vehicle in the 3,500 pound class are:

1. The flywheel energy storage system performed as predicted in the mission for which it was designed and optimized.
2. The range of a 3,500 pound class electric vehicle with a flywheel energy storage package, operating on the SAE J227a Schedule D driving cycle, will be approximately 80 miles with presently available standard lead-acid electric vehicle batteries.
3. Performance of this flywheel energy storage system is highly dependent on the mission assigned to the electric vehicle.
4. The best performance was obtained for the SAE J227a Schedule D driving cycle (suburban cycle). The system as designed provides reduced improvement when operated on low maximum speed and low stops/mile missions.
5. Results indicate that continued effort on regenerative flywheel energy storage components and subsystems is warranted.
6. This system, implemented for laboratory evaluation of an electric vehicle flywheel energy storage system, does not represent a practical subsystem for vehicle implementation due to the following limitations:

   a. The vehicle cannot run indefinitely at constant speed below the cornering point speed.
   b. For low-speed operation, most, or all, of the vehicle acceleration energy must be supplied by the flywheel; whereas, during these conditions, extracting energy directly from the battery is desirable for efficiency reasons.
   c. During cruise conditions, flywheel energy cannot be used to supplement battery energy for passing or hill climbing.
   d. Regenerative energy cannot be converted to battery energy during prolonged negative grade operation.
   e. System components were not sized to provide performance of presently available electric vehicles; i.e., 0 mph to 30 mph in 9 seconds, 60 mph top speed, etc.

   Therefore, the system should be reconfigured with additional components to ensure that a vehicle implementation will result in highly competitive vehicular performance from operational, human factor, and safety viewpoints.

Based on the results of this laboratory test program, the following recommendations leading to improved performance are provided.

1. Extend the computer model of the flywheel energy storage package to include a more detailed calculation of the various subsystem energy losses (and therefore efficiency) as a function of operating conditions during the driving cycle rather than as a single, overall ("black box") efficiency value. This will aid in determining which subsystem is most appropriate for a particular vehicle mission. Various flywheel drive configurations should be included.
2. Evaluate advanced design synchronous motors with permanent magnet excitation in order to improve the system in/out efficiency.

3. Evaluate alternating current propulsion systems (induction motors and power conditioners) in order to improve the overall vehicle efficiency.
4. Evaluate continuously the variable transmission flywheel/propulsion systems in order to improve the overall vehicle efficiency.

ACKNOWLEDGEMENT

This work was sponsored by the U.S. Department of Energy under subcontract No. 8990503 from the Lawrence Livermore Laboratory of the University of California. Mr. Thomas Barlow of the Lawrence Livermore Laboratory was the Technical Monitor for the program.

REFERENCES

1. Cornell, E.P., Turnbull, F.G., Barlow, T.M., Evaluation of a Hybrid Flywheel/Battery Propulsion System for Electric Vehicles, paper presented at the 1980 Flywheel Technology Symposium, Scottsdale, Arizona, October 26-30, 1980.

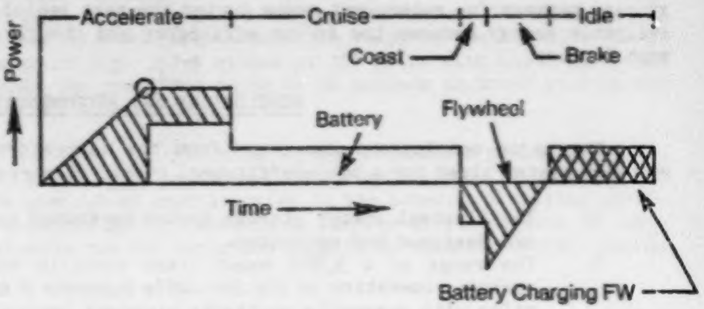
Accelerate
Cruise
Idle
Coast
Brake
Power
Battery
Flywheel
Time
Battery Charging FW

Fig. 1 Selected System Operating Strategy

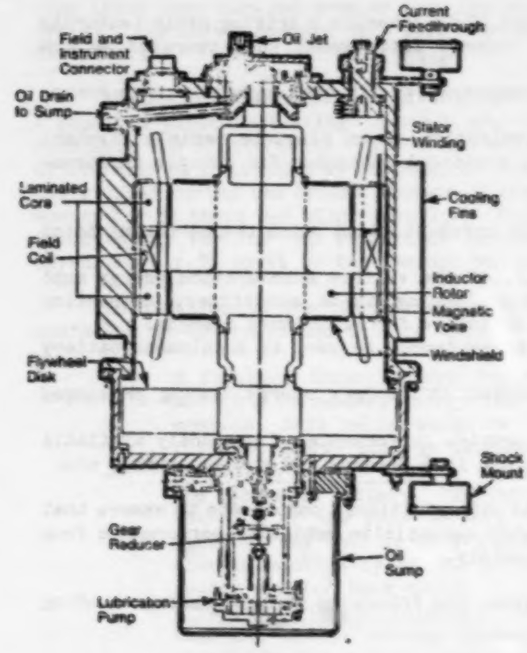
Current Feedthrough
Field and Instrument Connector
Oil Jet
Oil Drain to Sump
Stator Winding
Laminated Core
Cooling Fins
Field Coil
Inductor Rotor
Magnetic Yoke
Windshield
Flywheel Disk
Shock Mount
Gear Reducer
Oil Sump
Lubrication Pump

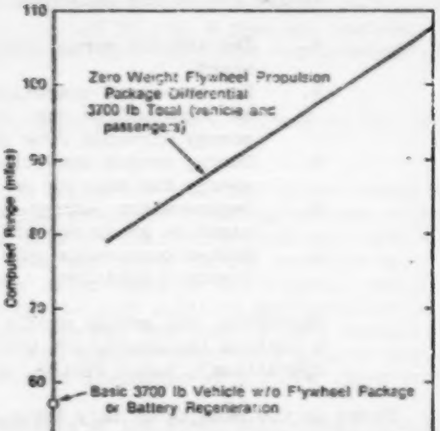

Fig. 2 Computed Range vs In/Out Efficiency on Schedule D Driving Cycle

Fig. 3 Detailed Layout of Flywheel Energy Recovery Unit

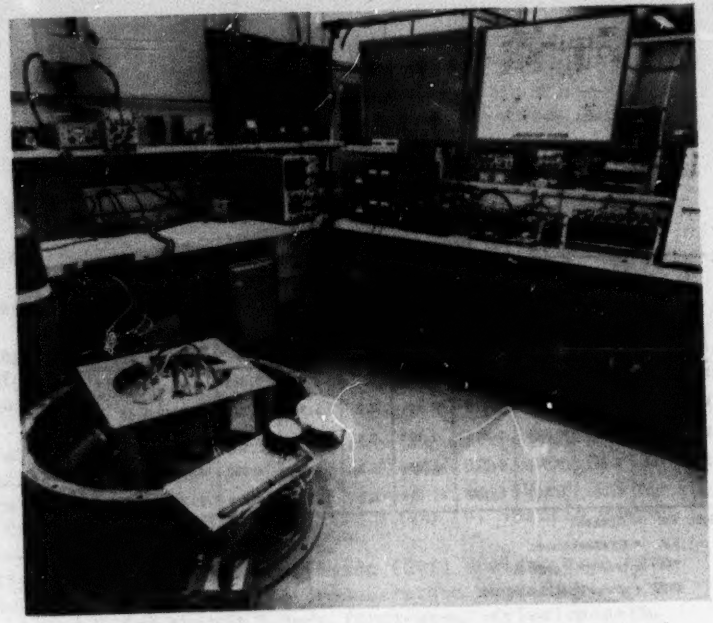

Fig. 4. Laboratory Set-Up of Inductor Motor/ Flywheel Package and Power Conditioner

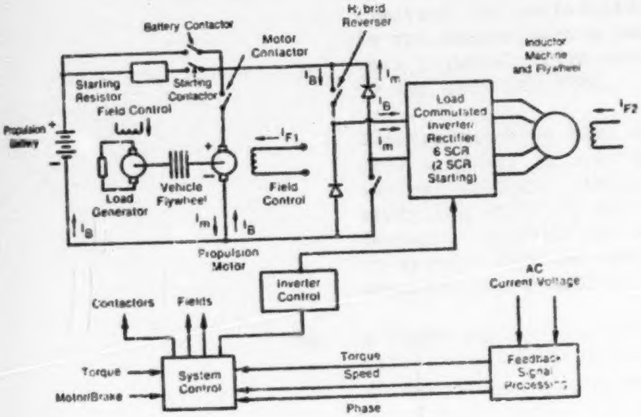
Battery Contactor
Hybrid Reverser
Motor Contactor
Inductor Machine and Flywheel
Starting Resistor
Starting Contactor
Field Control
Propulsion Battery
I_B
I_m
Load Commutated Inverter/ Rectifier 6 SCR (2 SCR Starting)
I_{F2}
I_{F1}
Load Generator
Vehicle Flywheel
Field Control
Propulsion Motor
Inverter Control
AC Current Voltage
Contactors
Fields
Torque
Motor/Brake
System Control
Torque
Speed
Phase
Feedback Signal Processing

Fig. 5. Schematic Diagram of Simulated Propulsion System

Table 1

SUMMARY DATA FROM OPERATION ON SCHEDULE D DRIVING CYCLE DURING A BATTERY DISCHARGE

Run	Total Number of Driving Cycles	Total Distance (miles)	Total Battery Energy (kWh)	Total Battery (Ah)	kWh/Mile	kWh/Cycle	Ah/Mile	Ah/Cycle	Stops/Mile
1	73	76.17	14.1	144	0.185	0.193	1.891	1.975	0.956
2	76	79.49	14.7	147	0.185	0.193	1.849	1.934	0.956
5	79	83.71	15.2	152	0.182	0.192	1.816	1.924	0.944

Table 2

SUMMARY DATA FROM SCHEDULE D DRIVING CYCLE WITH VARYING CRUISE TIMES

Run	Energy Efficiency FM	Energy Efficiency TM	Energy Efficiency PCU	In/Out Efficiency FW	Effectiveness Factor FW	Battery kWh	Total Distance (miles)	kWh/Mile	Range Improvement Factor	Stops/Mile	Cruise Time (s)
14	0.738	0.877	0.956	0.509	1.09	0.9	4.02	0.224	1.19	1.49	20
15	0.743	0.869	0.956	0.512	1.10	0.8	3.30	0.242	1.22	1.82	10
16	0.745	0.897	0.956	0.516	1.15	0.7	2.72	0.257	1.26	2.21	2
17	0.732	0.837	0.961	0.501	1.06	1.3	6.24	0.208	1.13	0.962	50
18	0.713	0.823	0.957	0.468	1.02	1.8	10.01	0.180	1.08	0.599	100

Note: FW = flywheel
FM = flywheel motor
TM = traction motor
PCU = power conditioning unit

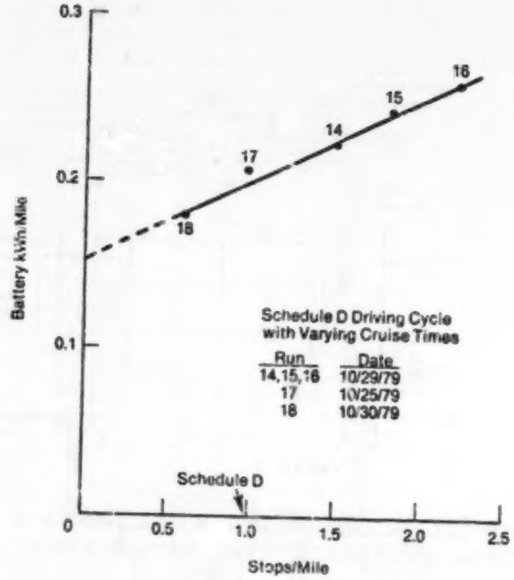

Fig. 6. Battery kWh/Mile vs Stops/Mile for Schedule D Driving Cycle with Varying Cruise Times

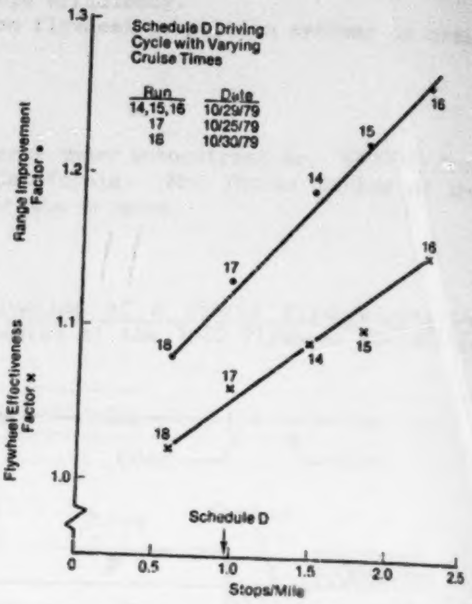

Fig. 7. Flywheel Effectiveness Factor and Range Improvement Factor vs Stops/Mile

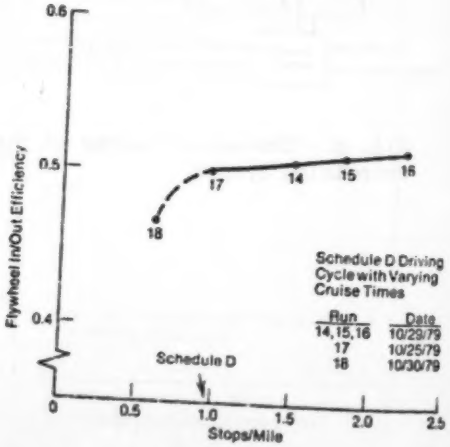

Fig. 8. Flywheel In/Out Efficiency vs Stops/Mile

PROJECT SUMMARY

Project Title: Flywheel-Engine Powerplant Research and Development Studies

Principal Investigators: Norman H. Beachley and Andrew A. Frank

Organization:
College of Engineering
University of Wisconsin
Madison, Wisconsin 53706

Project Goals: The overall objective is to provide engineering design and analysis services leading to the construction of a flywheel/heat engine demonstration vehicle with the goal of demonstrating 50 mpg over the Federal Urban Driving Cycle (FUDC) at 3,000 lb. inertia weight.

Project Status: Several continuously-variable transmission (CVT) designs have been developed that are suitable for the demonstration vehicle with packaging worked out for the GM X-body front-wheel-drive chassis. The Eaton Corporation now has a contract that will lead to system hardware, and we are working with them to give them the benefit of our previous work and experience.

Specifications have been developed for the CVT characteristics required for satisfactory installation, performance, and control in the demonstration vehicle. CVT efficiency characteristics for this flywheel drive vehicle have been specified that will provide 50 mpg over the FUDC.

Simulations have been made of mileage of the demonstration vehicle over a number of driving cycles. A real-time hybrid (digital-analog) computer simulation has also been developed and used to study the shifting and control problems of the alternative CVT designs. Studies are underway to determine optimal flywheel size. It appears that an energy storage capacity of about 0.3 hp-hr. is adequate for a 3000-lb. inertia weight vehicle.

A "four-square" dynamometer has been constructed for testing CVT efficiency characteristics and control concepts. Tests are being conducted on the van Doorne steel V-belt system at present.

Preliminary designs for "active" flywheel protection have been developed in order to stop the flywheel rotation when failure is impending without imparting angular momentum reaction to the vehicle, and to automatically disengage the flywheel from the vehicle's drive train.

Contract Number: W-7405-ENG-48, Subcontract 4492309, Amend. 2

Contract Period: 1 January 1980 through 30 September 1980

Funding Level: $90,000

Funding Source: U.S. Department of Energy through Lawrence Livermore National Laboratory

FLYWHEEL/HEAT ENGINE VEHICLE
DESIGN AND ANALYSIS

Norman H. Beachley and Andrew A. Frank
University of Wisconsin-Madison

ABSTRACT

This paper summarizes the research program at the University of Wisconsin which has been aimed at the design and construction of a second-generation flywheel automobile. One of the principal goals is to demonstrate 50 mpg over the Federal Urban Driving Cycle with a 3,000-lb car. Designs have been developed for several CVT's that would be suitable for the experimental car, including ways of packaging the various systems within the engine compartment of the X-body GM automobile. Specifications have been written for the required performance and efficiency characteristics of the CVT. Control-system principles have been developed with the aid of real-time hybrid computer simulations. A "four-square" dynamometer for testing CVT's has been designed and built. Tests are in progress for determining CVT efficiency and control characteristics. Safety flywheel concepts have been developed.

INTRODUCTION

The vehicle efficiency group at the University of Wisconsin has been involved in flywheel hybrid research over the past seven years. During that period we have performed many detailed system analyses and computer simulations to determine the fuel-saving potential of flywheel energy-storage vehicles and to develop practical designs for such vehicles. Our work has emphasized the required continuously-variable transmission and its control, since the CVT has been shown to be the most critical system component. In 1975-76 we designed and built an experimental flywheel vehicle based on a Pinto chassis and utilizing a slightly modified Pinto engine (1). This car demonstrated a fuel economy improvement of approximately 50% over the Federal Urban Driving Cycle, even though the powerplant system was constructed primarily of off-the-shelf components and contained many high loss elements.

The program with Lawrence Livermore Laboratory was initiated in February 1979. The basic goal of the program is to develop designs for and to coordinate the construction and testing of a second-generation experimental flywheel vehicle, a 3000-lb. inertia weight front-wheel-drive car capable of 50 mpg, or 100% improvement over the Federal Urban Driving Cycle (FUDC). The basic configuration of the vehicle is given by Fig. 1. One significant difference from the earlier Pinto flywheel car is the addition of a clutch within the flywheel package to allow the flywheel to be declutched when this would be advantageous in terms of either fuel economy or performance.

This paper is a report on the current status of the program. The work to date has produced several CVT designs suitable for the experimental vehicle, specifications for the CVT, simulations to demonstrate and study control aspects of various system designs, the design and construction of a transmission test facility, safety flywheel studies, and other work.

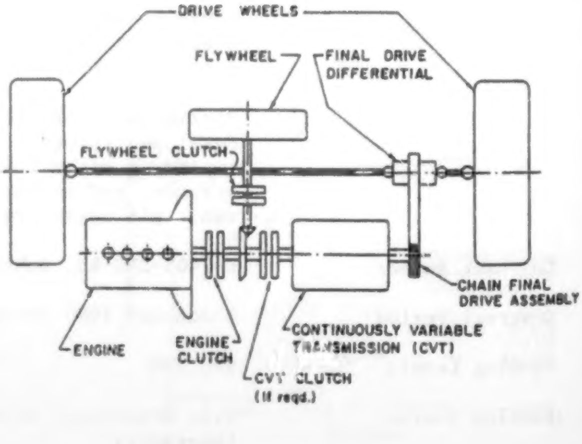

Fig. 1. Schematic diagram of a Flywheel Energy Management Powerplant (FEMP) system for a front-wheel drive vehicle.

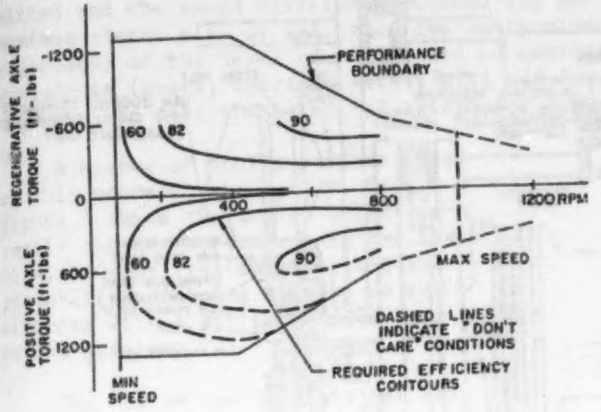

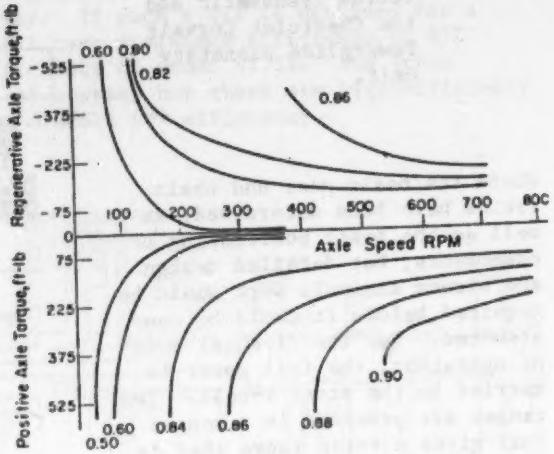

Fig. 2. Required efficiency characteristics of a CVT for an FEMP vehicle which will achieve 50 mpg over the FUDC at 3,000 lb inertia weight.

Fig. 3. The required CVT efficiency characteristics, as given in Fig. 2, for the most critical area of operation.

CONTINUOUSLY VARIABLE TRANSMISSION DESIGNS

Previous studies (1,2,3) have shown that the CVT is the most critical component of the system in terms of fuel economy. In order to assure that the experimental vehicle will be capable of 50 mpg over the FUDC, a specification for the CVT has been developed. The specification covers size, weight, torque capacity and other performance data, as well as efficiency requirements. The required efficiency characteristics are illustrated by Figs. 2, 3, and 4. The basic efficiency requirements (Figs. 2 and 3) show that, even though extremely high efficiency is not required under any conditions, efficiencies of about 80% are necessary when the power transmitted is as low as 5% of maximum. Analysis work has shown that these requirements, although not easy to achieve, are feasible. Figure 4 shows the maximum permissible no-load spin losses.

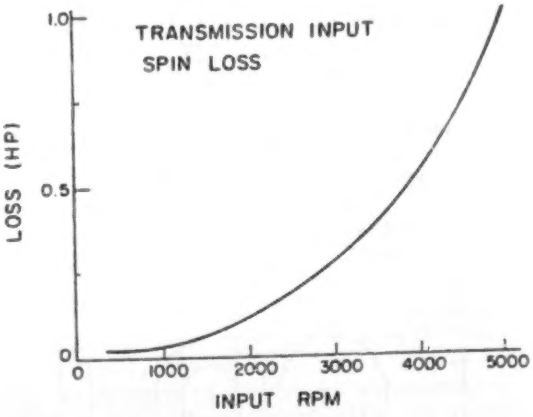

Fig. 4. Maximum allowable spin loss characteristics of a CVT for an FEMP vehicle which will achieve 50 mpg over the FUDC at 3,000 lb inertia weight.

Several CVT designs have been developed that appear capable of meeting the efficiency requirements and also being packaged in combination with a flywheel so as to fit within the space available under the hood of a GM X-body car.

STEEL V-BELT CVT

Figure 5 shows a CVT based on the van Doorne "Transmatic," a steel V-belt system (4). Figure 6 shows one way in which it could be packaged for the front-wheel-drive vehicle. The design has been developed to the point

Fig. 5. A CVT utilizing the van Doorne Transmatic and the Chevrolet Corvair Powerglide planetary unit.

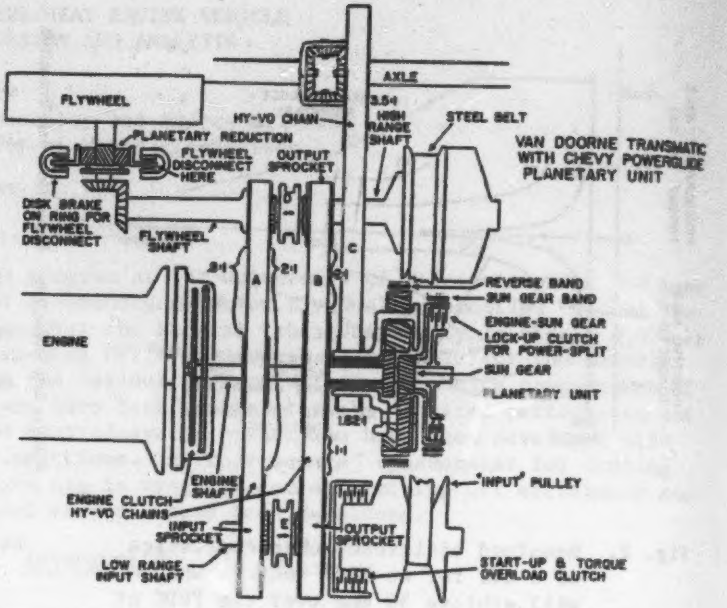
FLYWHEEL
AXLE
3.5:1
HY-VO CHAIN
HIGH RANGE SHAFT
STEEL BELT
VAN DOORNE TRANSMATIC WITH CHEVY POWERGLIDE PLANETARY UNIT
PLANETARY REDUCTION
FLYWHEEL DISCONNECT HERE
OUTPUT SPROCKET
DISK BRAKE ON RING FOR FLYWHEEL DISCONNECT
FLYWHEEL SHAFT
C
.8:1
A
2:1
B
2:1
REVERSE BAND
SUN GEAR BAND
ENGINE-SUN GEAR LOCK-UP CLUTCH FOR POWER-SPLIT
ENGINE
SUN GEAR
PLANETARY UNIT
1.82:1
1:1
ENGINE SHAFT
'INPUT' PULLEY
ENGINE CLUTCH
HY-VO CHAINS
INPUT SPROCKET
E
OUTPUT SPROCKET
LOW RANGE INPUT SHAFT
START-UP & TORQUE OVERLOAD CLUTCH

where the basic gear and chain ratios have been determined, as well as the basic positioning of components, but detailed design and stress analysis work would be required before it could be constructed. For the flywheel mode of operation, the full power is carried by the steel V-belt. Two ranges are provided in a manner that gives a ratio range that is the square of the basic V-belt value (e.g., a V-belt ratio range of 4 allows a system ratio range of 16). The mode change is accomplished by engaging one shifting dog while disengaging the other. This is to be done at approximately synchronous conditions, i.e., when there is little relative motion between the two halves of the dog to be engaged. After shifting, there will be little or no change of the V-belt ratio required, and the roles of the two sheaves (i.e., the direction of power flow) are reversed.

In direct engine drive when the flywheel is declutched, there are available not only the high and low range modes described above, but an additional cruise mode that uses power split, so that only part of the torque and power are carried by the Transmatic. The gearing is such that, with the continuously-variable capability of the V-belt, the engine can operate at optimal conditions during normal highway cruise.

Other CVT designs based on the van Doorne V-belt have been investigated, but the one illustrated in Fig. 5 appears at the present time to be the easiest to construct and install. It uses a stock Corvair Powerglide planetary gear set, which should reduce the construction costs considerably.

MULTI-SPEED GEARBOX/SLIPPING CLUTCH CVT

One approach that appears quite promising is to use a multi-speed close ratio gearbox in combination with a clutch that slips on a continual basis. The attractiveness of this concept lies

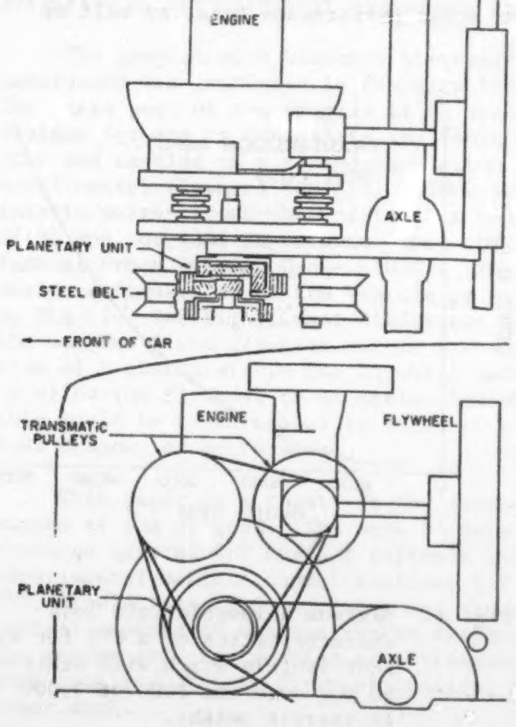
ENGINE
AXLE
PLANETARY UNIT
STEEL BELT
FRONT OF CAR
TRANSMATIC PULLEYS
ENGINE
FLYWHEEL
PLANETARY UNIT
AXLE

Fig. 6. Packaging of a flywheel system based on the CVT of Fig. 5 in a front wheel drive automobile.

in the fact that the losses in a slipping clutch are proportional to the power being transmitted and the speed difference between its two halves. If such a CVT is designed for a maximum clutch slip of 17%, then the basic clutch will have a minimum efficiency of 83% regardless of the level of power, and an average efficiency of about 91.5%. The other components (gears, bearings, etc.) will add losses, of course, but these are high-efficiency elements, so that the potential exists for very high overall CVT efficiency.

A number of configurations based on this concept have been studied. Figure 7 shows the design which currently appears best to us on the basis of efficiency, reliability, and the probability of being able to be constructed with a minimum of developmental problems (5).

The design can be described as basically a four-speed gear transmission in series with a three-speed one (with a common shaft), to produce twelve discrete speed ratios. At the output of the "twelve-speed" gearbox is a planetary reduction that can be shifted to provide a ratio of either 4:1 or 1:1 (direct drive). This arrangement theoretically provides 24 speed ratios, but in actuality only 18 are ever expected to be used. The twelve speeds with the 4:1 reduction are to be used with flywheel drive (up to about 45 mph), while gear ratios 3 through 8 are to be used for direct engine drive with the planetary locked up for a 1:1 ratio.

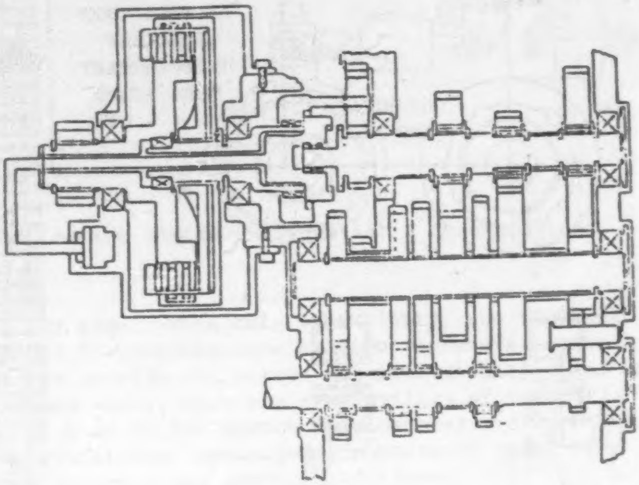

Fig. 7. A multi-speed gearbox with slipping clutch CVT (design by Michael Nohr).

The slipping clutch is a wet multi-plate disk clutch which is actuated hydraulically. When it is necessary to shift gears, the hydraulic pressure is reduced to zero, but the plates are not separated. If the driver is not using either the accelerator or brake pedal, the transmission is shifted into neutral, to avoid the friction of the clutch drag that occurs because the plates are not separated.

With twelve basic speeds for the flywheel drive mode, and the inflexibility of the flywheel, shifting sometimes must occur quite rapidly, several times per second in some extreme conditions. To accommodate this, the shifting dogs use no synchromesh, and have large spaces between the dog teeth (as used in motorcycle and racing-car transmissions). This will allow very quick shifts to be accomplished even if the clutch is not completely released. The shifting mechanism proposed (based on stock motorcycle components actuated by special hydraulic pistons) is illustrated in Fig. 8.

Although the basic concept and the mechanical design itself are relatively simple, the required controls are fairly sophisticated. It should be noted, for example, that a gear shift is immediately required when changing from driving with forward thrust to regenerative braking, since a slipping clutch can transmit torque only in the direction of slip. A real-time simulation of a flywheel car with this transmission is shown in Fig. 9 and discussed later in the paper.

HYDROSTATIC CVT

We have continued our studies on the concept of a hydrostatic or hydrostatic power-split CVT, the latter being the type of system used on the original University of Wisconsin

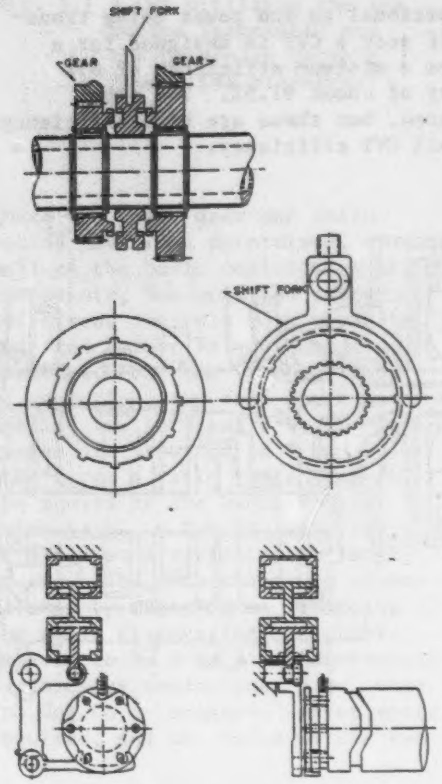

Fig. 8. Shift mechanism details, slipping clutch CVT.

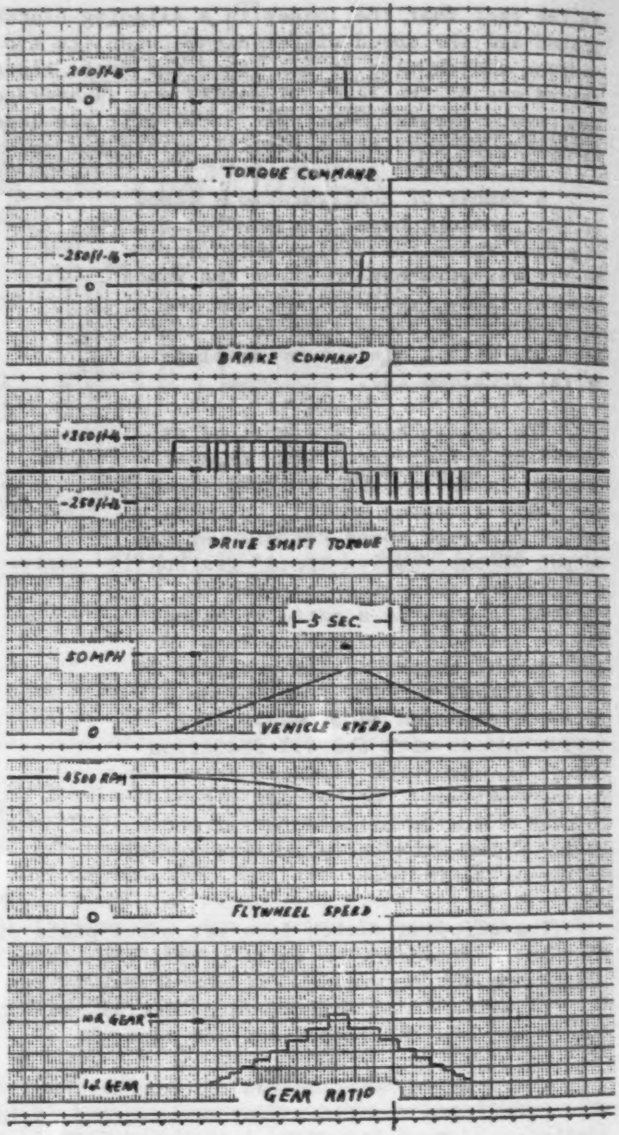

Fig. 9. Hard acceleration and deceleration--real-time hybrid (analog and digital) computer simulation of flywheel car with multi-speed gearbox with slipping clutch CVT.

flywheel Pinto car. The concept still appears very attractive, with efficiency and noise being the major problems. The problem of control is simplified by the use of hydraulics. We are currently collecting data and performing some experimental studies that will allow a better evaluation of the hydrostatic approach in the coming year.

ROLLING CONTACT TRACTION DRIVES

Although several types of rolling contact traction drives (e.g., the toroidal drive) appear quite attractive for use in a flywheel hybrid vehicle, we are not currently involved in this area of research.

SYSTEM STUDIES

The flywheel hybrid car concept on which our work is based, illustrated in Fig. 1, allows quite a wide variation in operational strategy. In particular, the inclusion of a clutch in the flywheel package makes it possible to switch from the flywheel drive mode to a

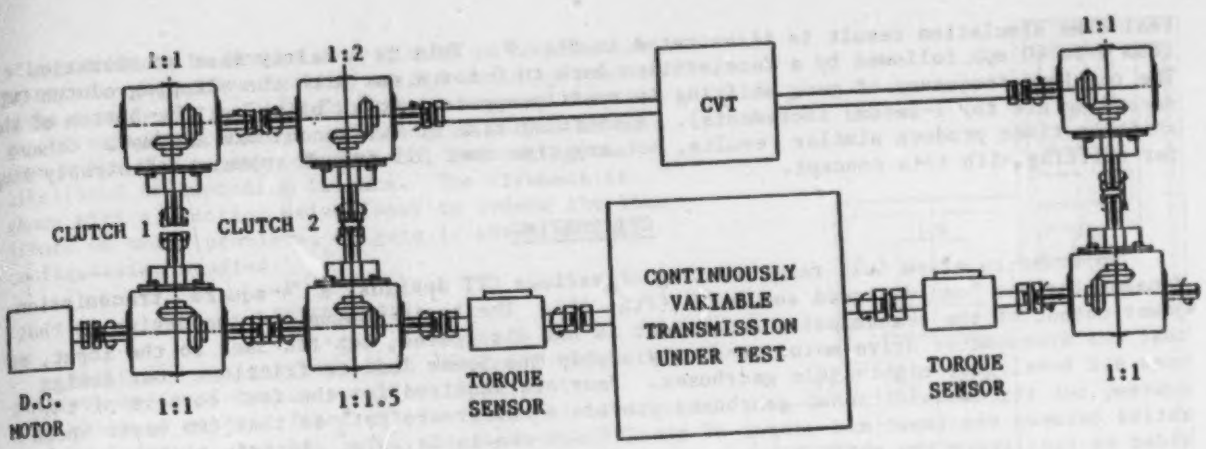

Fig. 10. The 4-square dynamometer system for testing continuously-variable transmissions.

direct engine drive mode, and vice-versa, at any time. With this versatility, the flywheel no longer needs to be large enough to handle all foreseeable acceleration maneuvers, as it can be readily declutched so that the engine can provide the torque required directly (and at maximum efficiency if power is above some minimum value, with the availability of the CVT). The minimum flywheel size is then determined so that it can absorb all, or nearly all, regenerative braking energy under expected driving conditions, and provide a means of using the engine at maximum efficiency in an on-off mode at low power demand conditions.

System studies are being conducted to determine the optimal flywheel size. Obviously, a small flywheel size is very attractive if it does not reduce the vehicle fuel mileage. The smaller the flywheel, the less its friction, weight, cost, and the more simple its installation. The smaller flywheel would necessitate more engine starts and stops, however, with attendant losses. The current study is an attempt to develop a control strategy (i.e., when the flywheel should be declutched, what its upper and lower speed limits should be under different driving conditions, etc.) that will result in a minimum flywheel size while still achieving the best possible fuel mileage.

The overall optimization problem is not simple, but preliminary work indicates that a flywheel energy storage capacity of about 0.15 kw-hr or less may be satisfactory (note that braking a 3,000-lb. vehicle from 60 mph to 0 mph would produce 0.136 kw-hr of regenerative braking energy if all the kinetic energy of the vehicle were recovered). If further studies verify that a flywheel no larger than this is required, then it would appear that either a composite or a simple steel flywheel design should be satisfactory.

REAL-TIME COMPUTER SIMULATIONS AND CONTROL STUDIES

In order to study control system requirements and operating strategies, a real-time hybrid (analog/digital) computer simulation program has been developed. With a car simulator (part of an actual car with front seat, brake and accelerator pedals and other driver controls), the simulation system allows a driver to "drive" the system over any chosen cycle. This approach allows the interactions between the driver and vehicle dynamics to be studied in detail, and has been found to provide information on idiosyncrasies of the various designs that are difficult to obtain by other analytical techniques. In general, the analog computer provides continual integration of the differential equations describing a vehicle system, while the digital computer provides the algebraic calculations required. Two slightly different versions of the program have been developed, one that represents a flywheel car with a general type of CVT, and one for such a car with a multi-speed gearbox/slipping clutch CVT. The latter is different mainly in that it keeps track of the shifting of the gearbox. The system operation during any run is recorded on an eight-channel strip chart recorder. One real-time simulation result is illustrated in Fig. 9. This is a fairly fast acceleration from 0 to 40 mph followed by a deceleration back to 0 for a car with the slipping-clutch CVT. The required frequency of gear shifting is readily apparent (the "blips" at the bottom of the recording are for 1-second increments). A shifting time of 0.1 second was assumed. Other shifting times produce similar results, but any time over 0.5 second appears undesirably long for shifting with this concept.

CVT TESTING

In order to allow full range testing of various CVT designs, a "4-square" transmission dynamometer has been designed and built (Fig. 10). The basic concept of the design is that power output of the transmission under test is not dissipated, but fed back to the input, so that the dynamometer drive motor need only supply the power lost to friction. Our design uses six bevel gear right-angle gearboxes. Four are required for the four corners of the system, but the two additional gearboxes provide an alternate path so that two basic speed ratios between the input and output of the CVT are available. Two electric clutches are provided to facilitate the shift between the two alternate ratios.

As shown in Fig. 10, a van Doorne Transmatic is being tested. Although this is an industrial unit, modifications will allow the efficiencies of the basic belt-sheave system to be determined, as well as the sheave loading required under all conditions of torque, speed, and speed ratio. Eventually a control system for the van Doorne CVT as designed for the flywheel car will be developed and tested on the dynamometer.

In order to provide the versatility necessary for full-range testing and testing under dynamic conditions, a second van Doorne Transmatic is included in the system in the power feedback loop between the output and input of the Transmatic under test. This will make it possible to see how a given control system will handle the various transient conditions of a driving cycle.

FLYWHEEL SAFETY STUDIES

It is important that there should be virtually no additional danger to vehicle occupants from the inclusion of an energy-storage flywheel. The two basic failure modes that could cause danger are: 1) a flywheel disk explosion, due to overstress, a material flaw, or an accident, 2) a sudden seizure of the disk due to a bearing or other mechanical failure, or due to an accident, in which the angular momentum of the disk would be almost instantaneously transferred to the vehicle. Studies of these problems have led to preliminary safety flywheel designs, one of which is illustrated in Fig. 11. The use of two counter-rotating disks

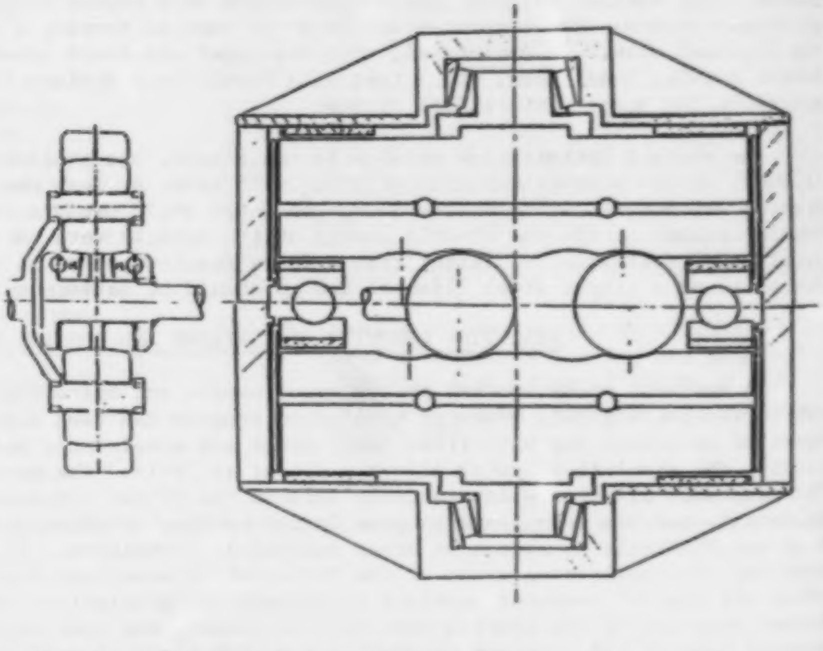

Fig. 11. Self-energizing flywheel braking and decoupling mechanism.

allows them to be braked with little or no momentum transfer. An active braking system would be used to brake the wheels quickly to a stop whenever they began to expand or produce an eccentric motion of more than a few thousandths of an inch, indicating the likelihood of impending failure. The flywheel is shown with a traction drive input to reduce the likelihood of noise problems. Figure 12 shows another configuration studied.

FUTURE WORK

Basic CVT designs have been developed under this program, and performance specifications written. With these as guides, final CVT designs will be developed by industry, and built for the second-generation flywheel car. This will involve a cooperative industry-university effort, with many conferences to insure that the CVT designers have the benefit of our many years of flywheel car experience and to provide us information on their new developments and innovations. The major goal is to construct a flywheel vehicle in the 3,000-lb. inertia weight class which will demonstrate fuel economy of 50 mpg over the FUDC, and 40 mpg over the highway cycle, with a control system such that the driver can drive it in essentially the same manner as a conventional automatic transmission vehicle, and a powerplant system that packages completely under the hood of a GM X-body car.

The work in progress is also expected to eventually lead to the design and construction of a 1500-lb flywheel vehicle that would be capable of 100 mpg over the FUDC and 80 mpg over the highway cycle.

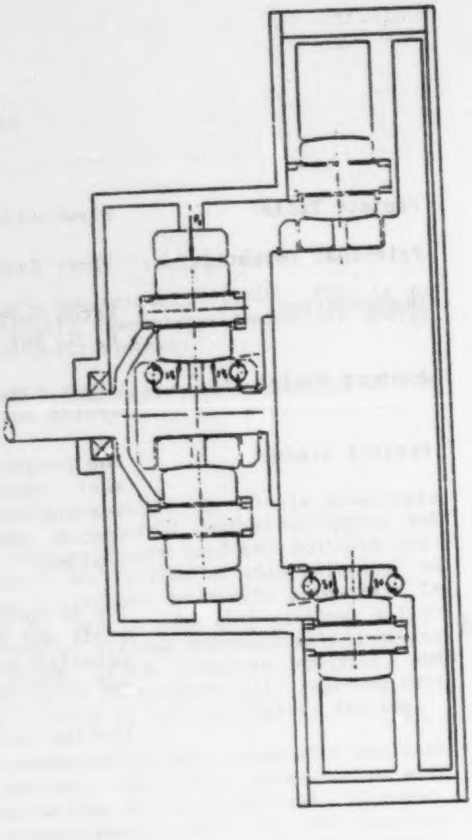

Fig. 12. A counter-rotating equal momentum concept which eliminates load support bearings.

REFERENCES

1. Beachley, N. H., and Frank, A. A., "Final Report--Flywheel Energy Management Systems for Improving the Fuel Economy of Motor Vehicles," Report DOT/RSPA/DPB-50/79/1, prepared for U. S. Dept. of Transportation, Aug. 1979.
2. Beachley, N. H., et al., "Experimental Evaluation of Flywheel Energy Management Automobile," Proc. 4th International Symposium on Automotive Propulsion Systems, April 1977.
3. Frank, A. A., and Beachley, N. H., "Design Considerations for Flywheel-Transmission Automobiles," SAE Paper 800886, 1980.
4. Scott, D., "Belt-Drive CVT for '82 Model Year," Automotive Engineering, Feb. 1980, pp. 136-140.
5. Mohr, M., "Slipping Clutch Continuously Variable Transmission Design Study," M. S. Thesis, University of Wisconsin, Madison, WI, 1980.

PROJECT SUMMARY

Project Title: Flywheel/Heat Engine Vehicle Design and Analysis

Principal Investigator: Ilmar Kalns

Organization: Eaton Corporation, Engineering & Research Center
P. O. Box 766, Southfield, MI 48037

Project Goals: Study concepts and design a Flywheel/Engine/CVT propulsion system suitable for installation in an X-body car.

Project Status: The project is about 1/3 completed. Its five principal tasks are: conceptualization of the system, definition of controls, testing and evaluation of a CVT, preliminary design of complete system, and simulation study of economy gains over conventional systems.

The selection of the system concept has been finalized through study and simulations of several potential schemes. The selected arrangement appears most likely to meet the economy and performance goals, as well as size and weight constraints.

Testing and evaluation of a potentially suitable CVT (Van Doorne's Transmatic) are in progress; initial indications are favorable. Prelimiminary layout of the propulsion system is expected to start shortly. Component size selection and packaging study of X-body car are nearing completion.

Simulation study of economy gains realized with the proposed system is to run concurrently with preliminary layout work.

Contract Number: Subcontract 9515409

Contract Period: 8/4/80 - 3/4/81

Funding Level: $276,059

Funding Source: University of California
Lawrence Livermore Labs

FLYWHEEL - HEAT ENGINE VEHICLE

Ilmar Kalns
Eaton Corporation

ABSTRACT

This paper summarizes work under Lawrence Livermore Labs Subcontract 9515409. This is an initial phase of a larger program whose goal is to successfully demonstrate Mechanical Energy Storage Technology (MEST) potential for energy savings in vehicular systems.

The initial phase comprises a study of promising system arrangements, the selection of one for further analysis, and its preliminary design.

INTRODUCTION

Research and development efforts on an international scale are exploring vehicle powertrain configurations incorporating a flywheel energy storage means, an internal combustion engine and a continuously variable transmission. Analytical studies and breadboard hardware indicate considerable potential for substantially improving fuel economy. Realization of this potential on a broader scale, however, is not likely until the concept is reduced to viable hardware. In order to successfully demonstrate MEST potential for energy savings in vehicular systems, a flywheel powertrain is to be designed to fit in a compact vehicle without substantially imparing its present safety, performance, ease of operation, handling, price, creature comforts, and noise and emissions levels. The fuel economy of the system is to be substantially improved over that of conventional powertrain systems in stop-and-go city driving as well as highway driving.

Eaton Corporation, a major manufacturer of vehicle powertrain systems, components and controls, has a natural interest in developments in this product area. This presentation will describe work in progress at Eaton's Engineering & Research Center in Southfield, Michigan, under Subcontract 9515409 from Lawrence Livermore Laboratories as part of DOE Contract W-7405-ENG-48. The subcontract covers only the initial phase, essentially a study and preliminary design phase, of the overall program.

Each task of this phase, along with its status, is described in the following, covering the first three months of work of a seven-month project.

DESCRIPTION OF TASKS

The work of this subcontract comprises the following five technical tasks:

1. System Concept Selection
2. Control System Design
3. Transmatic CVT Evaluation
4. Preliminary Propulsion System Design
5. Final System Performance Simulation

TASK 1 - SYSTEM CONCEPT SELECTION

This task consists of the following subtasks:

- Study functionality of systems
- Assess merits of each
- Propose and evaluate improvements
- Select most promising approach

Preparation for work under this task involved the study of pertinent references and reports in order to gain a better perspective of past efforts and current experience of others active in the flywheel-CVT area. Contact was also established with University of Wisconsin researchers, gaining valuable insights from their extensive efforts over the past several years.

With this background, complemented by Eaton's experience in vehicle powertrain product design and development, existing and proposed system concepts were surveyed. The attempt was to assess the capability to perform the intended function within the constraints of size, weight and cost commonly associated with passenger cars. Some of the less familiar system components, such as the flywheel and some types of CVT's, received particular attention since their proper integration into a smoothly functioning automatic system represents a major technical challenge of this program.

Over ten existing and proposed flywheel-CVT I. C. engine systems have been considered. At this time, it appears that a parallel engine-flywheel arrangement, in series with a Van-Doorne Transmatic and some ratio-extending gearing from a stock automatic, has the best chance of meeting program objectives. The scheme is presently being further refined prior to computer simulation and component size optimization.

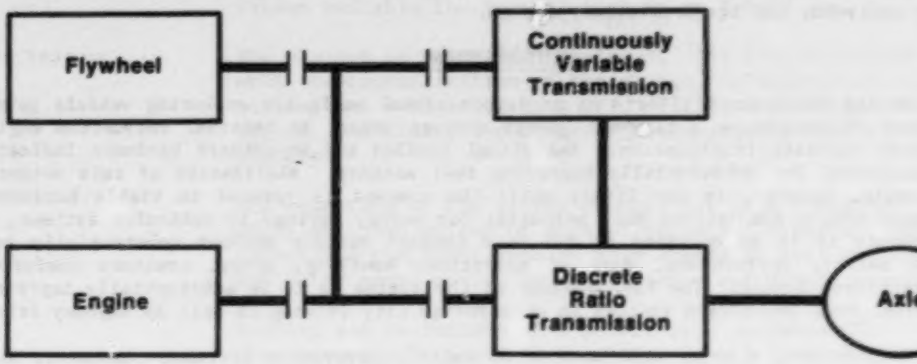
Flywheel
Continuously Variable Transmission
Engine
Discrete Ratio Transmission
Axle

Figure 1. Schematic of Preferred Powertrain Arrangement

TASK 2 - CONTROL SYSTEM DESIGN

This task consists of the following subtasks:

- Develop computerized model of propulsion system
- Define control strategy
- Conceptualize the control system
- Select component characteristics
- Optimize control strategy and components specs.

The propulsion system is to be modeled on the computer to simulate its function in various vehicle operational modes. The model will permit evaluation of alternative componentry and control strategies by subjecting the system to a prescribed load-speed spectrum, such as the Federal Urban Driving Cycle.

Vehicle performance and economy simulations have been completed for a stock Citation with both powertrain options, namely the 4-speed manual and the automatic transmission, obtaining close correlation with published data. Also, a 16-speed manual transmission was substituted for the 4-speed manual in order to approximately simulate a continuously variable transmission, obtaining a 25% fuel economy improvement. However, the program is not suited to simulation of unconventional drivetrain arrangements or components; hence, the aforementioned Citation simulations will be repeated on the more comprehensive Boeing's HEAVY program. The results will then serve as a basis of comparison for all future modifications of the basic powertrain. The HEAVY program, however, needs some minor additions of its own to simulate the more conventional drivetrain components. This work is expected to be completed shortly, and the modeling will begin immediately thereafter.

Definition of control strategy is broadly outlined in the CVT system specification formulated by Lawrence Livermore Labs. It represents a preferred schedule of propulsion system components utilization and interaction during three basic vehicle operating modes. The definition of operational modes has been recently revised to the following four: highway cruise with engine power, city driving with flywheel power, flywheel full mode, and flywheel emptying mode. All modes are to be driver-selected. The control process in each mode will be automated to a high degree in order to approach the ease of operation of conventional powertrains.

The completion of the remaining three subtasks of Task 2 is to be achieved through computer simulations of the propulsion system.

TASK 3 - TRANSMATIC CVT EVALUATION

This task comprises the following subtasks:

- Study the mechanical design and controls
- Adapt a test facility
- Design and build fixtures, install and instrument Transmatic
- Test efficiency across performance spectrum
- Test rate of ratio change
- Test sudden overload capability

The study of mechanical design and controls is continuing. Characteristics of the control system will be further explored during unit tests. Modifications of the controls will be attempted in order to improve part load efficiencies.

All test facility equipment has been received and installed. The system has been started up. Efficiency tests are in progress.

TASK 4 - PRELIMINARY PROPULSION SYSTEM DESIGN

This task comprises the following subtasks:

- Perform packaging study of the Citation
- Perform engineering analysis of propulsion
- Draw preliminary layout

The packaging study of the Citation is to examine component placement in the engine compartment with due consideration for safety, convenience and cost. Both the vehicle itself and a partial chassis layout have been received; the packaging study is underway.

Engineering analysis will determine the size of components for acceptable fatigue life and reliability. This subtask and the next one--preliminary layout--will run concurrently. Start of the work is anticipated this month.

TASK 5 - PERFORMANCE STUDY

This task comprises the following subtasks:

- Predict vehicle performance
- Estimate economy improvement

Basic performance of the finalized system will be determined with an updated system model. Simulated runs over prescribed driving cycle will indicate fuel economy gain likely to be realized by the flywheel-CVT system.

PROJECT SUMMARY

Project Title: Regenerative Braking Through Elastomeric Energy Storage

Principal Investigator: Lyle O. Hoppie

Organization:
Eaton Corporation
Engineering & Research Center
P. O. Box 766
26201 Northwestern Highway
Southfield, Michigan 48037

Project Goals: Determine the technical and economical feasibility of an elastomeric regenerative braking system (ERBS) for automotive applications.

Project Status: Phase II of this program was initiated in July 1979, and was subdivided into two major sections:

- Phase II-A was to cover the design, construction, laboratory testing and evaluation of full-size elastomeric energy storage units.
- Phase II-B was to cover the design, construction, laboratory testing and evaluation of a complete full-scale elastomeric regenerative braking system.

During Phase II-A, efforts were focused on multiple adjacent elastomeric rods stressed in torsion beyond the buckling limit such that "knots" were generated. The measured torque versus rotation characteristics were in good agreement with values predicted from empirical equations deduced during the Phase I testing of small-scale samples, and the measured round-trip efficiency of these full-size elastomeric energy storage units approached ninety percent. Due to the abrasion of adjacent elastomeric rods, however, the fatigue life of the full-size units was only a few thousand cycles, in general agreement with small-scale test results. The low fatigue life problem appears to have been solved by employing a different stressing scheme in which a single rod is axially preloaded prior to being placed in torsion; small-scale tests of this stressing scheme show fatigue lives in excess of 10^5 cycles.

The initial tasks of Phase II-B, initiated in June 1980, call for the evaluation of the new stressing scheme using molded full-size elastomeric energy storage units. If the test results are sufficiently encouraging, the balance of Phase II-B will be carried out.

Contract Number: University of California Subcontract 2617509

Contract Period: June 1980 - December 1980 for first part of Phase II-B

Funding Level: $272,000 for first part of Phase II-B

Funding Source: U. S. Department of Energy through Lawrence Livermore Laboratory

REGENERATIVE BRAKING THROUGH ELASTOMERIC ENERGY STORAGE

L. O. Hoppie, D. Speranza, and G. C. Nowell
Eaton Corporation

ABSTRACT

Results of tests on full-size elastomers designed around two different stressing schemes are presented. A fatigue life problem due to abrasion was uncovered while testing the first design, and tests are underway to determine whether or not the second scheme will exhibit a fatigue life problem. Also presented is the most promising torque control concept for a complete elastomeric regenerative braking system.

BACKGROUND

In the fall of 1978, Phase I of this project was initiated. The primary objectives were to theoretically compare various methods of stressing elastomers, to experimentally determine which commercially available elastomer is best suited for this application, to conceive of an efficient torque control concept, and to establish a criterion for the economic feasibility of an elastomeric regenerative braking system. Results of the studies on commercially available elastomers and on the economic feasibility were reported previously(1) and will not be repeated here. Since the termination of Phase I in the spring of 1979, however, the elastomer stressing scheme and the torque control concept have undergone significant revisions. An update of the progress in these areas is presented in this paper.

EVOLUTION OF THE STRESSING SCHEME

Figure 1 shows the various schemes which were compared in Phase I, during which it was concluded that the Torsionally Induced Tension scheme had the most promise of leading to a compact system of high efficiency. It was empirically deduced (1) that the torque-rotation characteristics for such a stressing scheme could be adequately described by the following relationship:

$$T(\theta) = \begin{cases} K_n \, \theta & \theta \leq \theta_{min} \\ T_{min} + \frac{1}{5} K_n \, (\theta - \theta_{min}) & \theta \geq \theta_{min} \end{cases} \qquad (1)$$

where

$$K_o = \frac{\pi}{2} GR^4/L \qquad (2)$$

$$K_n = \frac{2}{3} n^2 \, K_o \qquad (3)$$

$$\theta_{min} = \frac{L/R}{n+1} \text{ radians} \qquad (4)$$

$$T_{min} = K_n \, \theta_{min} \qquad (5)$$

and where n is the number of adjacent elastomeric rods each of radius R, length L, and shear modulus G.

Equation 1 is shown in Figure 2, where two distinct modes are evident. For $\theta \leq \theta_{min}$, the assembly of elastomeric rods behaves much like a conventional torsion bar having a rather unconventional cross section. For $\theta \geq \theta_{min}$, however, the stress distribution is such that

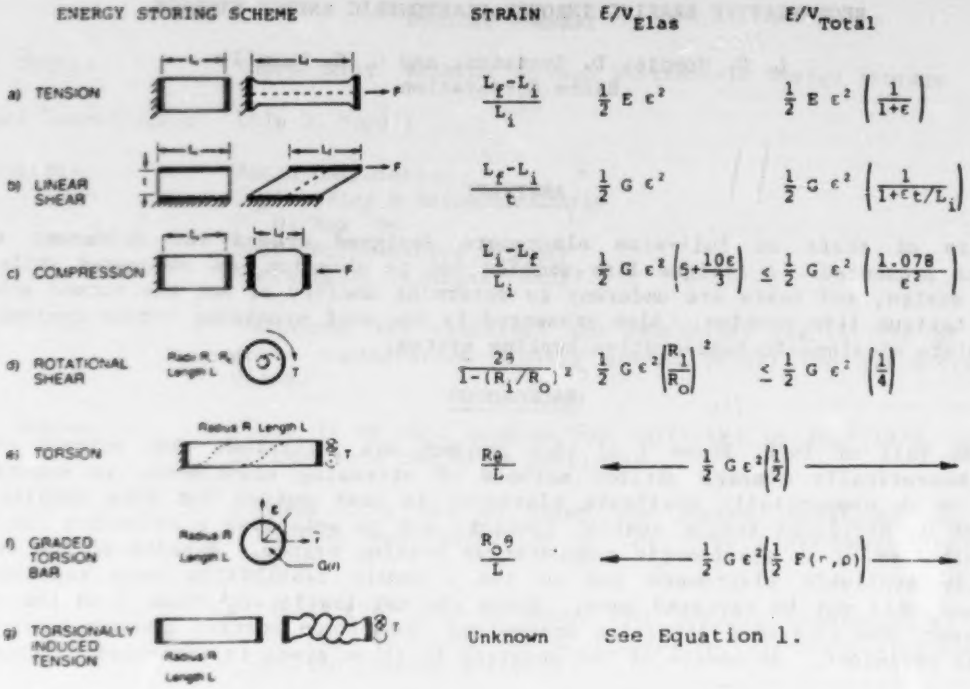
ENERGY STORING SCHEME
STRAIN
E/V_{Elas}
E/V_{Total}
a) TENSION
L_i
L_f
F
$\frac{L_f-L_i}{L_i}$
$\frac{1}{2}E\epsilon^2$
$\frac{1}{2}E\epsilon^2\left(\frac{1}{1+\epsilon}\right)$
b) LINEAR SHEAR
t
$\frac{L_f-L_i}{t}$
$\frac{1}{2}G\epsilon^2$
$\frac{1}{2}G\epsilon^2\left(\frac{1}{1+\epsilon t/L_i}\right)$
c) COMPRESSION
$\frac{L_i-L_f}{L_i}$
$\frac{1}{2}G\epsilon^2\left(5+\frac{10\epsilon}{3}\right)$
$\leq\frac{1}{2}G\epsilon^2\left(\frac{1.078}{\epsilon^2}\right)$
d) ROTATIONAL SHEAR
Radii R_i R_o
Length L
T
$\frac{2\theta}{1-(R_i/R_o)^2}$
$\frac{1}{2}G\epsilon^2\left(\frac{R_1}{R_o}\right)^2$
$\leq\frac{1}{2}G\epsilon^2\left(\frac{1}{4}\right)$
e) TORSION
Radius R Length L
T
$\frac{R\theta}{L}$
$\longleftarrow\frac{1}{2}G\epsilon^2\left(\frac{1}{2}\right)\longrightarrow$
f) GRADED TORSION BAR
Radius R
Length L
ϵ
T
$G(r)$
$\frac{R_o\theta}{L}$
$\longleftarrow\frac{1}{2}G\epsilon^2\left(\frac{1}{2}F(r,\rho)\right)\longrightarrow$
g) TORSIONALLY INDUCED TENSION
Radius R
Length L
T
Unknown
See Equation 1.

Figure 1. Comparison of Elastomeric Energy Storing Schemes

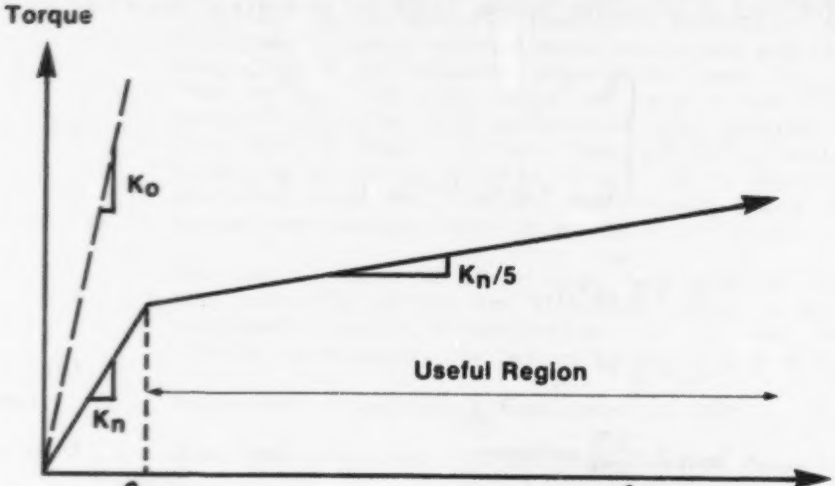

Figure 2. Empirical Torque-Rotation Characteristics of Elastomeric Torsion Bars

buckling of the rods results, leading to "knots." Figure 2 shows that the energy stored in a given volume of elastomer can be significantly increased if buckling is permitted. Consequently, one of the conclusions of the Phase I effort was that the Torsionally Induced Tension scheme should be pursued.

In the summer of 1979, Phase II-A was initiated, the primary objective being to evaluate full-scale elastomeric energy storage units in the Torsionally Induced Tension scheme. Figure 3 shows a photograph of such a unit mounted on a test fixture. In this case, a 2.87" diameter rubber extrusion was wrapped around and secured to pins having a 40" centerline spacing, in order to produce four rods which are nominally adjacent to each other. The unit is sized to store 10^5J, which is the kinetic energy of a 2,500 lb. vehicle traveling at approximately 30 mph.

Torque and axial load were measured by means of load cells attached to the stationary end (left end in Figure 3) of the test fixture, while rotational position is measured at the rotating end (right end of Figure 3). Rotation was achieved by means of a hydraulic motor, which in turn was controlled by rotational position feedback.

Figure 4 shows torque and axial force versus rotation data obtained during a test in which the unit was purposely wound until failure. The following data correspond to values pertinent to this test.

Revolutions at failure:	39 revolutions
Torque at failure:	1,020 ft-lb
Axial load at failure:	1,670 lb
Maximum axial load:	2,000 lb
Energy stored at failure:	1.35×10^5 ft-lb = 1.83×10^5 J
Volumetric energy density at failure:	177J/in^3 = 0.049W-hr/in^3
Gravimetric energy density at failure:	11.6J/g = 3,894 ft-lb/lb

Also shown in Figure 4 is the torque curve as predicted by the empirical equations deduced during the testing of small-scale samples.

The same test fixture and elastomer arrangement was used to investigate the round-trip energy transfer efficiency and fatigue life. During such tests, the elastomer was cycled between a lower limit of approximately three revolutions (the point beyond which the elastomer is in a buckling mode) to various upper limits on the order of twenty revolutions. Typically, nearly ninety percent of the energy delivered to the elastomer was subsequently redelivered by the elastomer, i.e., the total combined hysteresis and friction losses were only slightly in excess of ten percent of the energy delivered to the elastomer. With this elastomer arrangement, however, adjacent members abrade one another. The abrasion does not manifest itself as an excessive frictional loss, but does cause tears to develop, severely affecting fatigue life. For the tests which were performed on the full-scale unit shown in Figure 3, for example, the fatigue life was on the order of one thousand cycles, in agreement with values previously obtained from small-scale test results.

These test results demonstrated that large amounts of energy can be efficiently transferred to and from an elastomer at high power levels. Furthermore, the results showed that engineering information such as torque-rotation characteristics, hysteresis loss, etc., can be adequately scaled from small-scale test results. Consequently, small-scale tests were performed on stressing schemes different from the one described above in an attempt to find a stressing scheme with not only acceptable energy density and efficiency, but also with acceptable fatigue life and system adaptability.

The results of this effort led to isolated elastomeric rods initially stretched and then restrained from motion in the axial direction; energy is then delivered to or from the elastomer by rotating one end relative to the other. It was experimentally shown that by so prestressing a rod in the axial direction, significantly more rotational energy could be stored prior to buckling. In particular, small-scale tests of this stressing scheme, referred to as Axially-Loaded Torsion, showed that at an energy density equivalent to

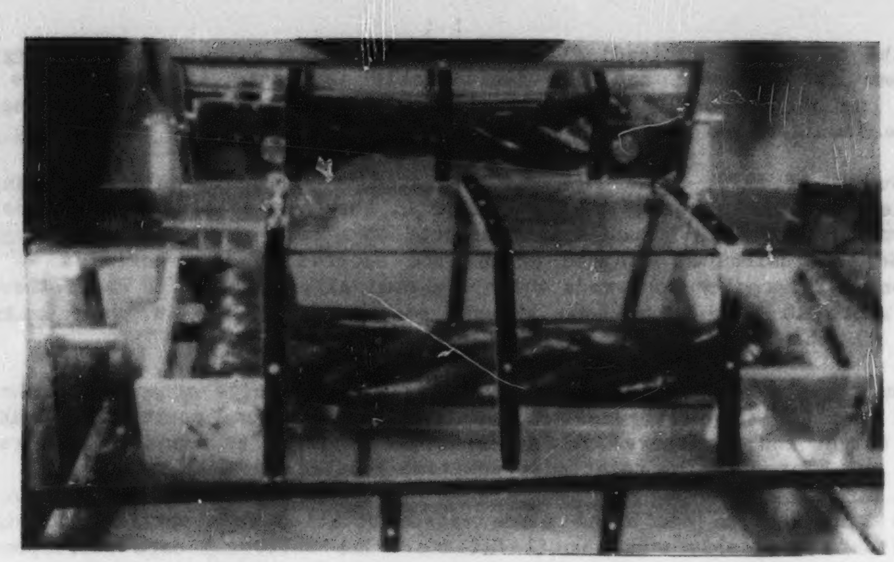

Figure 3. Full-Size Energy Storage Unit Under Test

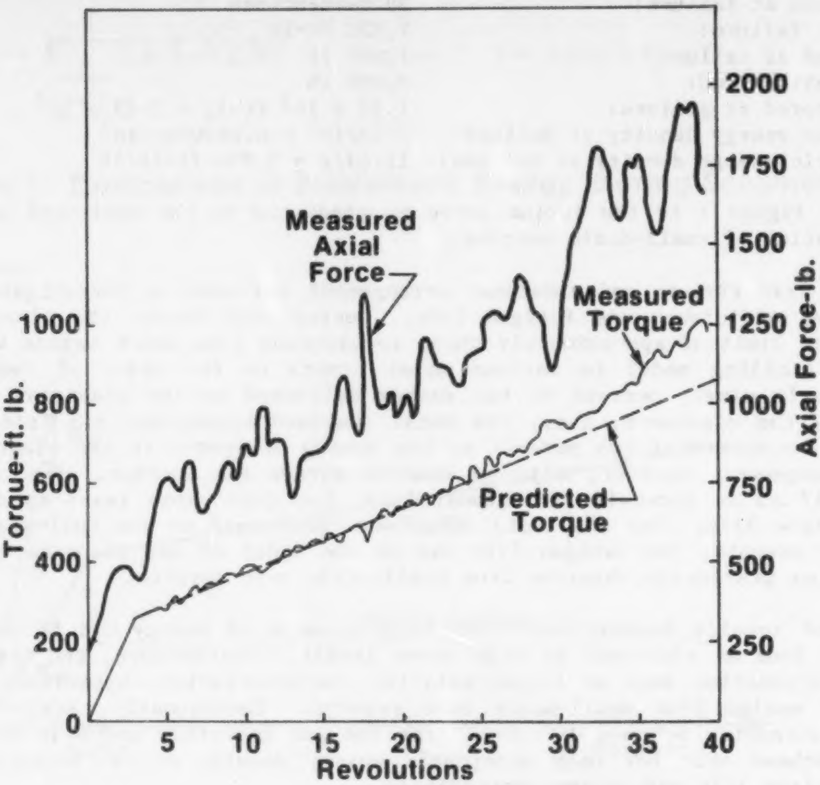

Figure 4. Torque and Axial Force Versus Revolutions on a Full-Size Elastomeric Energy Storage Unit

4 Rods Each 2.87 in. Dia. by 40 in. Length

approximately 10^5J per cubic foot, the round-trip efficiency was in excess of 90 percent, and the fatigue life was in excess of 10^5 cycles. The Torsionally Induced Tension scheme was thus abandoned and the Axially-Loaded Torsion scheme recommended for future work.

In the summer of 1980, the first part of Phase II-B was initiated, the primary objective being to evaluate full-scale moulded elastomers in the Axially-Loaded Torsion scheme. The tentative design for an automobile involves two units each initially 2' long by 7.5" diameter axially loaded such that the lengths and diameters become 8' and 3.75", respectively. Consequently, units such as shown in Figure 5 are now under test.

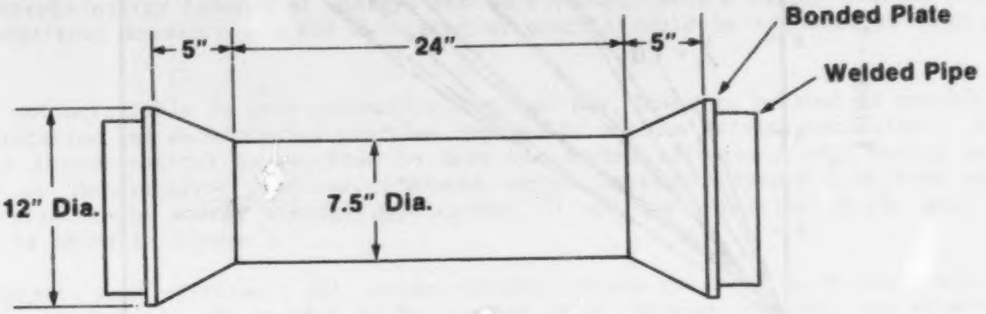

Figure 5. Dimensions of Elastomeric Energy Storage Units Being Tested

Note the uniform section of the elastomer has the dimensions indicated above, that the ends are flared to a 12" diameter, and that steel plates are bonded onto the elastomer as a straightforward method of attachment. This attachment method was chosen for the initial full-scale tests as it was felt that bonding to such a large plate would reduce the bond stress and present no unanticipated problems. This method is impractical in an automotive application, however, because of the excessive volume required by the ends. Another objective of the current effort, therefore, is to conceive of a compact method of attachment.

Some of the preliminary results obtained during the testing of a full-size unit are shown in Figure 6, where the effect of preloading the unit axially can be seen. Also indicated are the theoretical curves of Rivlin(2):

$$T = \pi r_i^4 M\theta/(\lambda l_i) \qquad (6)$$

$$F_Z = 2\pi r_i^2 M(\lambda - 1/\lambda^2) - \frac{\pi}{2} r_i^4 M(\theta/\lambda l_i)^2 \qquad (7)$$

In these expressions, l_i and r_i are the initial (unstretched) length and radius of the rod, M is a material property having units of a modulus, and λ is the elongation:

$$\lambda \equiv l_f/l_i = (r_i/r_f)^2 \qquad (8)$$

For each curve in Figure 6, the rotation is reversed at the point at which buckling is about to occur and then decreased to zero. Note that for the curves $\lambda = 2.0$, buckling did occur and the first "knot" was generated.

These and other data show that the energy which can be stored in a nonbuckling preloaded elastomeric torsion bar is given by

$$\text{Energy} \simeq \lambda^2, \qquad (9)$$

and, as indicated above, the tentative design calls for the value $\lambda = 4$.

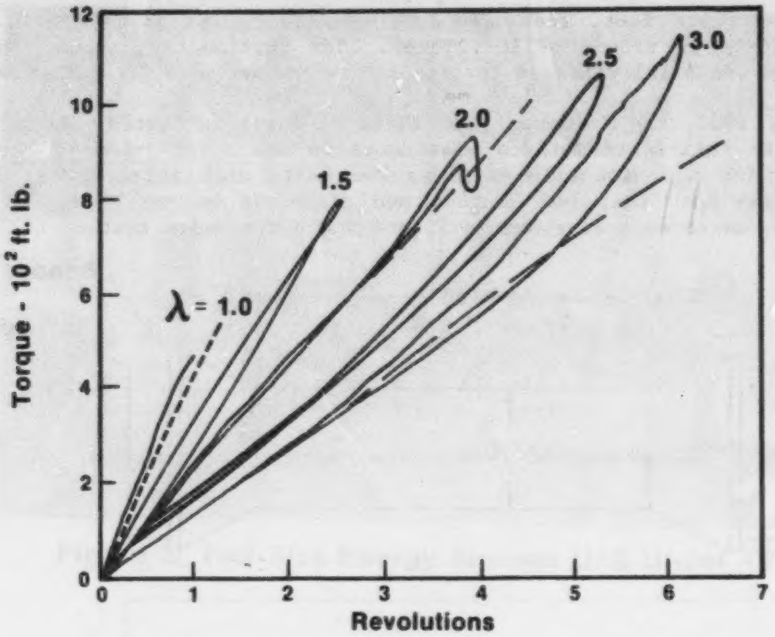

6(a). Torque versus Revolutions

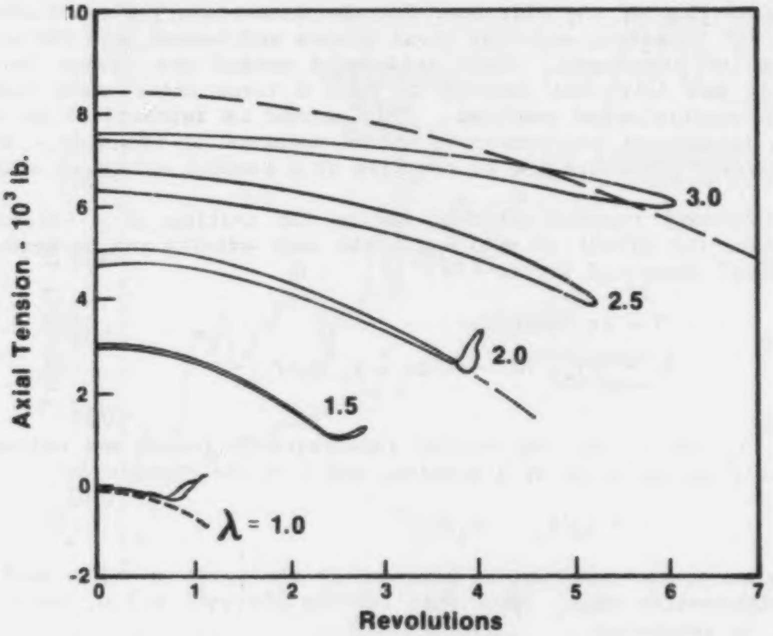

6(b). Axial Tension versus Revolutions

Figure 6. Torque and Axial Tension Characteristics of a Preliminary Full-Size Elastomeric Energy Storage Unit 24" Long by 7.5" Diameter

EVOLUTION OF THE TORQUE CONTROL SCHEME

The most important aspect of an elastomeric energy storage system is its inherent simplicity. The simplicity arises because the elastomer can be thought of as a spring, and consequently forms a naturally oscillating spring-mass combination when used in conjunction with, for example, an automobile. The implication is that, at least in principle, no transmission or power conversion equipment is required; one need only connect the elastomer to the driveline of a vehicle by a simple clutch in order to convert vehicular kinetic energy into stored strain energy (potential energy) and vice versa. With a simple clutch, however, only one predesigned acceleration and deceleration profile could be executed at high efficiency.

This is not acceptable in many automotive applications, however, because of nonuniformities in acceleration and deceleration profiles imposed by various driving conditions. Consequently, some torque control is required to keep the system efficiency high during various acceleration and deceleration profiles. Several torque control concepts have been considered for an elastomeric energy storage application,(3) and the evolution of the most promising scheme is shown in Figure 7.

The simplest, most efficient, but noncontrollable scheme is shown in Figure 7(a). Note that two elastomeric rods are assumed to be coupled by a chain at one end, and attached by way of two clutch/brake units to three gears at the other end: the middle gear of the set is coupled to the vehicle driveline by way of a main disconnect clutch. To decelerate the vehicle, the main and lower clutches are engaged while the upper unit is left in the brake position: the kinetic energy of the vehicle forces the elastomers to rotate such that initially straight lines on the elastomers become helical, as indicated by the dotted lines. Thinking of the elastomeric rods as torsional springs, it is clear that the device shown in Figure 7(a), when coupled to a vehicle, forms a simple spring-mass combination. Temporarily ignoring all losses and noting that the torque applied to the vehicle driveline is equal to the torque in the elastomer, the vehicle would thus be brought to rest with a velocity profile identical to the first quadrant of a cosine function plotted against time. To subsequently accelerate the vehicle, the main and upper clutches are engaged while the lower unit is left in the brake position: the stored potential energy would then be delivered to the vehicle in such a manner that the velocity profile is the first quadrant of a sine function plotted against time. The torque control scheme shown in Figure 7(a) thus has the following features:

- Very simple and compact.
- Inherently smooth but noncontrollable acceleration and deceleration profiles.

Thus, for the scheme in Figure 7(a), the torque on the vehicle shaft (normalized by the instantaneous torque in the elastomer) and the system efficiency are given by

$$T_{Vehicle}/T_{Elas} = 1 \qquad (10)$$

$$\eta = 1 \qquad (11)$$

Next consider the device shown in Figure 7(b), which is identical to the previous scheme except for the addition of a continuously adjustable device, shown as a variable sheave drive, linking the two elastomers at the left end. Operation is the same as in the previous scheme except energy is now permitted to circulate from the upper elastomeric unit to the lower through the variable sheave drive: this provides a means by which the torque applied to the vehicle shaft can be adjusted. In particular, if the efficiency of the variable sheave drive is η_{VSD}, and if all other losses are ignored, the following expressions for the normalized vehicle torque and the overall efficiency can readily be derived.

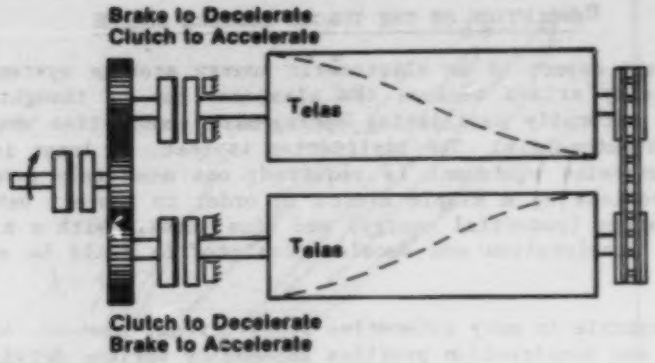
Brake to Decelerate
Clutch to Accelerate
Telas
Telas
Clutch to Decelerate
Brake to Accelerate

7(a). Basic Scheme with No Torque Control

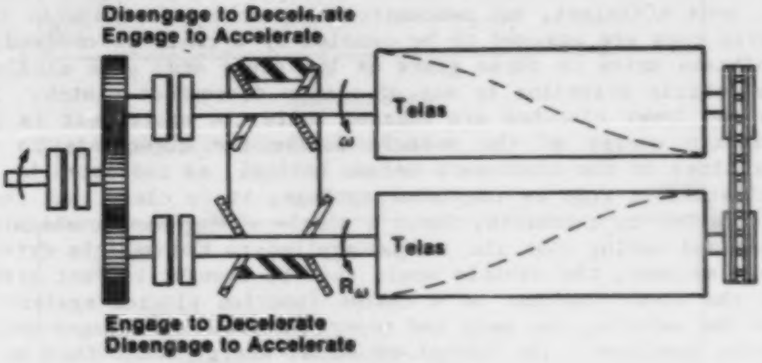
Disengage to Decelerate
Engage to Accelerate
Telas
ω
Telas
Rω
Engage to Decelerate
Disengage to Accelerate

7(b). Basic Scheme with Torque Control

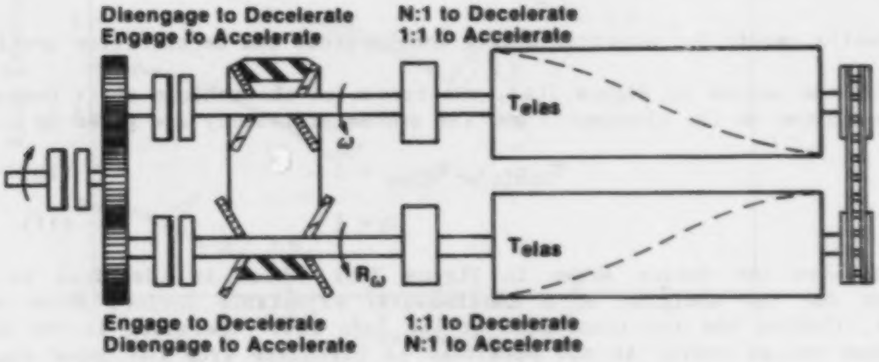
Disengage to Decelerate
Engage to Accelerate
N:1 to Decelerate
1:1 to Accelerate
Telas
ω
Telas
Rω
Engage to Decelerate
Disengage to Accelerate
1:1 to Decelerate
N:1 to Accelerate

7(c). Basic Scheme with Improved Torque Control

Figure 7. Evolution of a Promising Torque Control Scheme

For deceleration, $R \geq \eta_{VSD}$:

$$T_{Vehicle}/T_{Elas} = 1 - \eta_{VSD}/R \qquad (12)$$

$$\eta_{Decel} = \frac{R - 1}{R - \eta_{VSD}} \qquad (13)$$

For acceleration, $R \leq \eta_{VSD}$:

$$T_{Vehicle}/T_{Elas} = 1 - R/\eta_{VSD} \qquad (14)$$

$$\eta_{Accel} = \frac{1 - R/\eta_{VSD}}{1 - R} \qquad (15)$$

Equations 12 and 14 indicate that the torque applied to the vehicle can be adjusted, as desired, by changing the speed ratio, R, of the variable sheave drive. It is important to note, however, that adjustment of the speed ratio during acceleration or deceleration is not required: the vehicle would smoothly accelerate or decelerate with any fixed ratio. Changing the ratio changes the effective "spring constant" of the spring-mass combination, thus changing the natural frequency, permitting the acceleration and deceleration rates to be smoothly and continuously adjusted.

Finally, consider the scheme shown in Figure 7(c), in which the addition of two two-speed-ratio planetary gear sets is indicated. Again ignoring all but the losses in the variable sheave drive, the following relationships can readily be derived.

For deceleration, upper ratio N:1, lower ratio 1:1, $R \geq \eta_{VSD}/N$:

$$T_{Vehicle}/T_{Elas} = 1 - \eta_{VSD}/(NR) \qquad (16)$$

$$\eta_{Decel} = \frac{NR - 1}{NR - \eta_{VSD}} \qquad (17)$$

For acceleration, upper ratio 1:1, lower ratio N:1, $R \leq N\eta_{VSD}$:

$$T_{Vehicle}/T_{Elas} = 1 - R/(N\eta_{VSD}) \qquad (18)$$

$$\eta_{Accel} = \frac{1 - R/(N\eta_{VSD})}{1 - R/N} \qquad (19)$$

Comparison of Equations 16 and 17 with 12 and 13 shows that the effect of the upper ratio, N, during deceleration, is to effectively increase the variable sheave drive ratio, R, by a factor N. A similar comparison of Equations 18 and 19 with 14 and 15 shows that the effective ratio is reduced by a factor of N during deceleration.

Equations 10-19 are shown in Figure 8 for the specific example:

$$1/2 \leq R \leq 2 \text{ (Overall ratio 4:1)} \qquad (20)$$

$$N = 2 \qquad (21)$$

$$\eta_{VSD} = 0.8 \qquad (22)$$

Clearly the most efficient system is also the simplest, i.e., the first scheme. As has been pointed out, however, this scheme provides no adjustable vehicle torque. The second scheme does provide for smooth and continuous torque adjustment with a simple variable sheave drive having an overall ratio of only 4:1, but at a sacrifice of maximum torque and

$T_{vehicle}/T_{elas} = 1.0$

Efficiency = 1.0

8(a). Results for Scheme in 7(a)

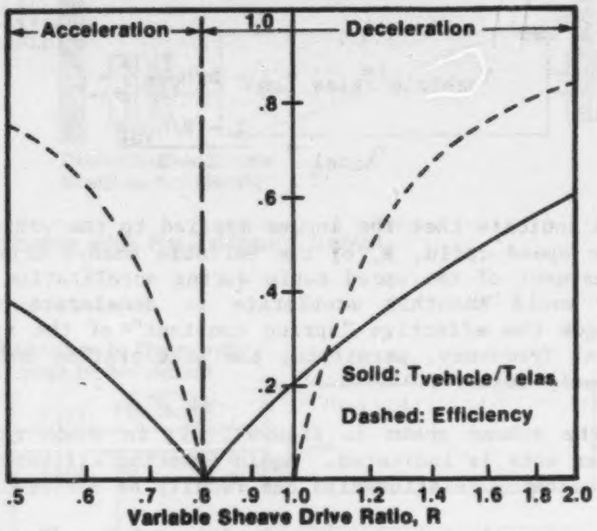

8(b). Results for Scheme in 7(b)

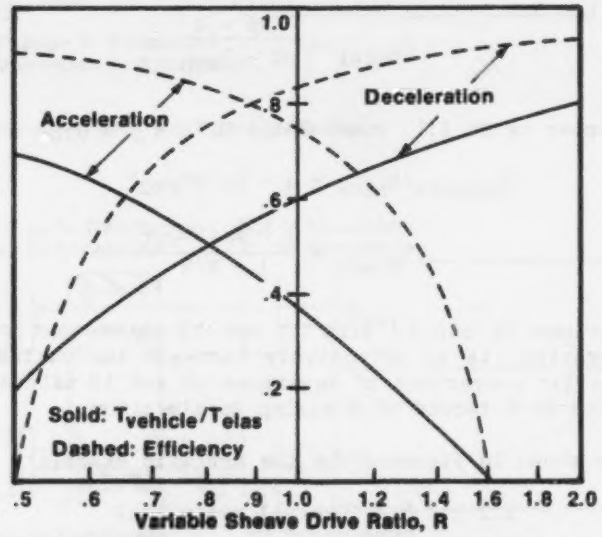

8(c). Results for Scheme in 7(c) with N = 2

Figure 8. Comparison of the Three Torque Control Schemes Shown in Figure 7. All Losses Except that of the Variable Sheave Drive are Neglected

overall efficiency, particularly at low torque levels. The addition of the two planetary gear sets in the third scheme does add complication, but enhances both the maximum torque and overall efficiency.

SUMMARY

Evaluation of full-size moulded elastomers stressed in the Axially-Loaded Torsion scheme is underway. Initial torque and axial load versus rotation test results agree well with theoretical predictions, and round-trip efficiencies of the elastomeric units are in the mid-ninety percent range. A torque control concept is being sought which will permit the torque to be continuously adjusted without a major sacrifice in either the simplicity or the efficiency.

REFERENCES

1. L. O. Hoppie, "Regenerative Braking Through Elastomeric Energy Storage," DOE, Division of Energy Storage Systems, Conf-790854, pp. 457-464.

2. R. S. Rivlin, "Large Elastic Deformations of Isotroipic Materials," Part VI, Phil. Trans. A, 242, pp. 173-195.

3. L. O. Hoppie et al., "The Feasibility of an Elastomeric Regenerative Braking System for Automotive Applications," University of California UCRL-15037, 1979.

PROJECT SUMMARY

Project Title:	"A Flywheel Energy Storage and Conversion System for Photovoltaic Applications."
Principal Investigator:	Philip O. Jarvinen
Organization:	Massachusetts Institute of Technology Lincoln Laboratory Energy System Engineering Group P.O. Box 73 Lexington, Massachusetts 02173 (617) 862-5500 ext. 213
Project Goals:	To develop a flywheel system to store electrical output from a solar photovoltaic array and convert it to regulated 60-Hz AC for use in residences or load centers, and to analyze its performance, worth, and cost.
Project Status:	A 1/10-scale model flywheel unit with a 400-pound rotor and storage capacity of 1 to 4 kWh has been built and tested over the full design speed range between 7500 to 15000 rpm. The unit consists of magnetic bearings, integrated motor-generator, motoring and power-conversion electronics, and vacuum and containment housing. Stand-alone cycloconverter and utility-interactive inverter power conditioners have been demonstrated experimentally which produce 120-V, 60-Hz AC with excellent power quality. Measured round-trip efficiencies of the stand-alone version of the flywheel storage system have exceeded 74 percent. Flywheel storage systems are the equal of or superior to battery systems for the same application. Manufacturing cost studies and user-worth analyses for flywheel systems of residential and load-center sizes have been completed. Residential flywheel systems have been found to be economically viable in stand-alone and utility-interactive applications.
Contract Number:	DE-AC02-76ET-20279
Contract Period:	FY-80
Funding Level:	$605K
Funding Source:	U.S. Department of Energy, jointly by Divisions of Energy Storage and Photovoltaic Energy Systems

PHOTOVOLTAIC ENERGY SYSTEM APPLICATIONS OF FLYWHEEL TECHNOLOGY* + ‡

Philip O. Jarvinen
MIT Lincoln Laboratory

ABSTRACT

Progress is reported on a project to develop a flywheel energy storage unit for use with photovoltaics in residential or load-center applications. The unit employs a high-efficiency, permanent-magnet motor-generator and uses either stand-alone cycloconverter or utility-interactive inverter power converters to convert DC input to regulated AC output. It also tracks the maximum-power-operating point of the solar array. Magnetic bearings are used to support the rotating element.

The project includes fabrication and test of a scale-model unit, measurement of round-trip storage efficiencies, demonstration of cycloconverter and utility-interactive inverter hardware and economic analyses of residential and intermediate load-center flywheel systems for manufacturing cost and user worth.

INTRODUCTION

Over the past year, MIT Lincoln Laboratory has been working on a flywheel storage project to develop a system with the following major components:

- Magnetic bearings
- Motor-generator
- Low-cost rotor (not part of the project)
- Power-conditioning electronics
- Vacuum housing.

This unit is intended to be a complete interface between a solar photovoltaic (PV) array and an AC load. Applications include a single-family residence and a 100-kW load center as point designs, with emphasis on the residence as the first and smallest use. The flywheel system being developed is also ideally suited to other storage applications for wind, load-leveling and peak-shifting systems. The project includes four major tasks: 1) to build and test a scale-model working system that is capable of operating in either a stand-alone or a utility-interactive mode and to evaluate experimentally its performance and efficiency; 2) to conduct system studies of a full-scale residential unit and develop scaling laws for flywheel storage systems for applications larger than residential; 3) to perform economic manufacturing cost studies and user-worth studies of residential and 100-kW flywheel systems; 4) to test the scale model over a range of residential loads and off-nominal conditions and modify the test set-up to include an advanced composite rotor.

The residential system concept is shown in the artist's sketch in Fig. 1, and its major components are depicted schematically in Fig. 2. Subscale, residential and 100-kW load-center flywheel system parameters are listed in Fig. 3. The 40-kWh, full-scale, residential unit, Fig. 4, is designed to supply 8-kW, steady-state, AC power and 10 kW peak. Scaling laws for flywheel systems were developed and are reported in Reference 1.

---

* This work was sponsored by the U.S. Department of Energy.

+ The U.S. Government assumes no responsibility for the work presented.

‡ Progress Report for the Mechanical, Magnetic, and Underground Energy Storage 1980 Annual Contractors' Review, Washington, DC, 10-13 November 1980.

C74-836

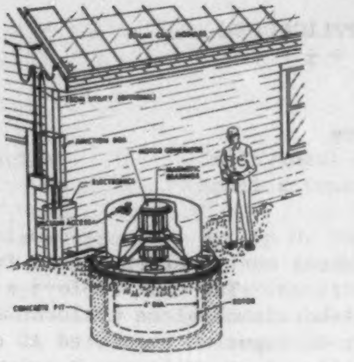
JUNCTION BOX
MOTOR GENERATOR
MAGNETIC BEARINGS
ELECTRONICS
CONCRETE PIT
ROTOR

Fig. 1. Residential photovoltaic storage concept.

C74-1060

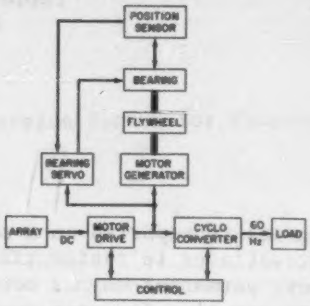
POSITION SENSOR
BEARING
FLYWHEEL
BEARING SERVO
MOTOR GENERATOR
ARRAY
DC
MOTOR DRIVE
CYCLO CONVERTER
60 Hz
LOAD
CONTROL

Fig. 2. Flywheel system concept.

C74-1062

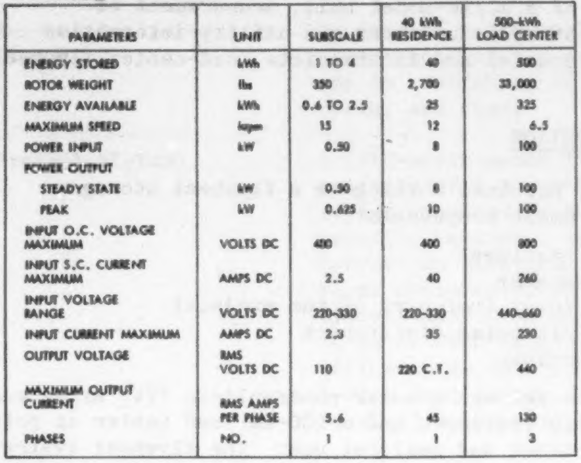

PARAMETERS	UNIT	SUBSCALE	40 kWh RESIDENCE	500-kWh LOAD CENTER
ENERGY STORED	kWh	1 TO 4	40	500
ROTOR WEIGHT	lbs	350	2,700	33,000
ENERGY AVAILABLE	kWh	0.6 TO 2.5	25	325
MAXIMUM SPEED	krpm	15	12	6.5
POWER INPUT	kW	0.50	8	100
POWER OUTPUT				
STEADY STATE	kW	0.50	8	100
PEAK	kW	0.625	10	100
INPUT O.C. VOLTAGE MAXIMUM	VOLTS DC	400	400	800
INPUT S.C. CURRENT MAXIMUM	AMPS DC	2.5	40	260
INPUT VOLTAGE RANGE	VOLTS DC	220-330	220-330	440-660
INPUT CURRENT MAXIMUM	AMPS DC	2.3	35	230
OUTPUT VOLTAGE	RMS VOLTS DC	110	220 C.T.	440
MAXIMUM OUTPUT CURRENT	RMS AMPS PER PHASE	5.6	45	130
PHASES	NO.	1	1	3

Fig. 3. Flywheel system design parameters.

C71-1055

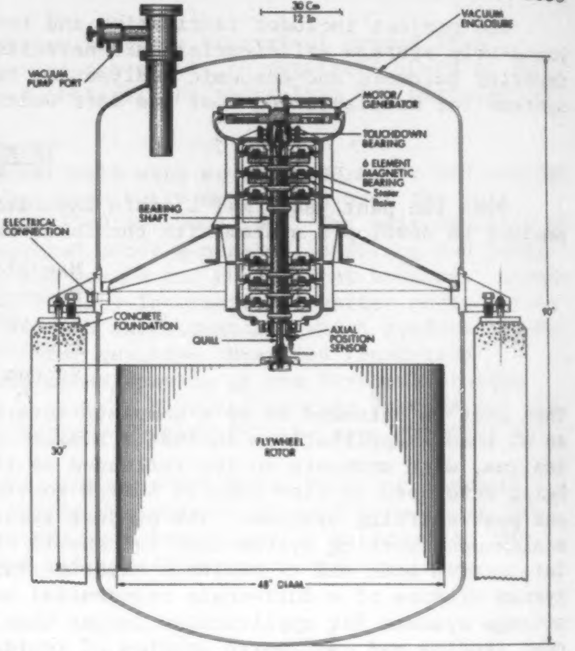
30 Cm
12 In
VACUUM ENCLOSURE
VACUUM PUMP PORT
MOTOR/ GENERATOR
TOUCHDOWN BEARING
6 ELEMENT MAGNETIC BEARING
Stator
Rotor
BEARING SHAFT
ELECTRICAL CONNECTION
CONCRETE FOUNDATION
QUILL
AXIAL POSITION SENSOR
FLYWHEEL ROTOR
90"
30"
48" DIAM.

Fig. 4. 40-kWh residential flywheel design.

C71-1020

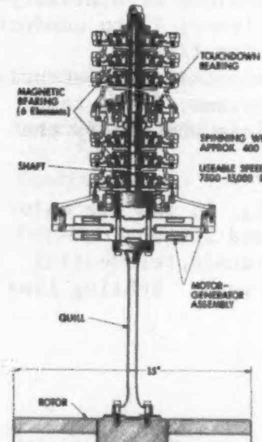
TOUCHDOWN BEARING
MAGNETIC BEARING (6 Elements)
SPINNING WEIGHT APPROX. 400 LBS.
USEABLE SPEED RANGE: 7500-15000 RPM
SHAFT
MOTOR-GENERATOR ASSEMBLY
QUILL
15"
ROTOR

Fig. 5. 1/10-scale experimental flywheel.

SUBSCALE FLYWHEEL UNIT

During FY-80, fabrication and assembly of a 1/10-scale unit, Fig. 5, were completed as were tests to verify the power electronics, the magnetic bearings and the motor generator. In one test, the flywheel unit was run continuously for over 2200 hours. The scale model which employs a 400-pound rotor is identical to the full-size unit except that to decrease the overall unit height, the quill hangs below the magnetic bearings rather than being telescoped internal to the bearings.

The subscale unit (shown in Fig. 6. being lowered into an existing vacuum tank) has been operated over its full design range between 7500 to 15000 rpm. In order to accomplish this, a solution had to be developed which eliminated the buildup of a low-frequency whirl mode which occurred at 11000 rpm due to internal flywheel hysteresis. A damper unit was developed which successfully eliminated all whirl effects. As part of this work, the flywheel unit was analyzed[2] for natural frequencies, whirl modes, dynamic response for given damping and flywheel imbalances, and self-excited instabilities due to internal damping. The effects of seismic forces and ground settlement on magnetically suspended energy storage wheels were also evaluated. It was determined that the flywheel and its suspension can safely withstand earthquakes of magnitude 4 on the Richter scale, that the flywheel will remain magnetically suspended during earthquakes of magnitude 4 or less, and that allowable differential settlement is greater than what can be expected to occur naturally during the life of a residential system.

The subscale flywheel test set-up is designed so that electrical power from the flywheel may be processed to 120 V, 60 Hz by either a cycloconverter or utility-interactive inverter system or be supplied directly to a resistor bank, Fig. 7. In an actual application, only one type of power-conversion equipment would be provided with the flywheel storage unit. The quality of the output power with cycloconverter or inverter has been measured and is excellent with total harmonic distortions of less than 5 percent and less than 2 percent, respectively, as shown in Fig. 8 and Fig. 9. The utility-interactive inverter is shown in Fig. 10.

P267-818

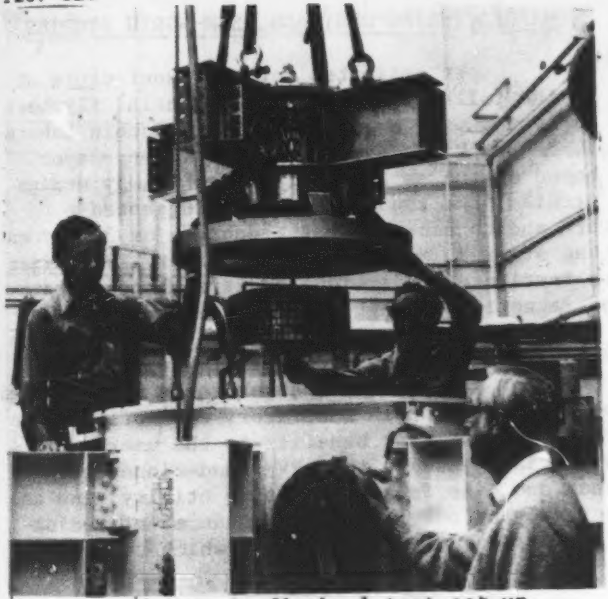

Fig. 6. 1/10-scale flywheel test set-up.

C74-1109

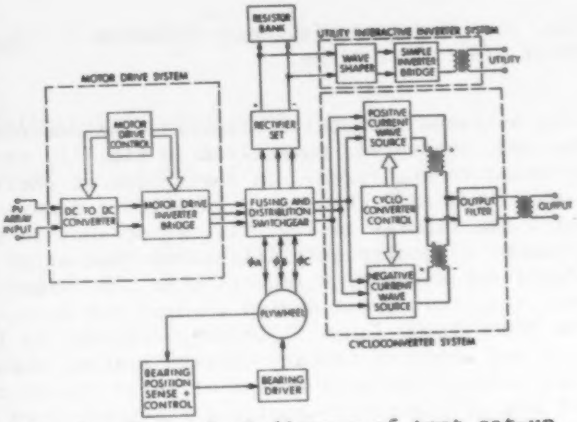
RESISTOR BANK
UTILITY INTERACTIVE INVERTER SYSTEM
WAVE SHAPER
SIMPLE INVERTER BRIDGE
UTILITY
MOTOR DRIVE SYSTEM
MOTOR DRIVE CONTROL
RECTIFIER SET
POSITIVE CURRENT WAVE SOURCE
PV ARRAY INPUT
DC TO DC CONVERTER
MOTOR DRIVE INVERTER BRIDGE
FUSING AND DISTRIBUTION SWITCHGEAR
CYCLO-CONVERTER CONTROL
OUTPUT FILTER
OUTPUT
ϕA
ϕB
ϕC
NEGATIVE CURRENT WAVE SOURCE
FLYWHEEL
CYCLOCONVERTER SYSTEM
BEARING POSITION SENSE + CONTROL
BEARING DRIVER

Fig. 7. Electrical diagram of test set-up

C74-967

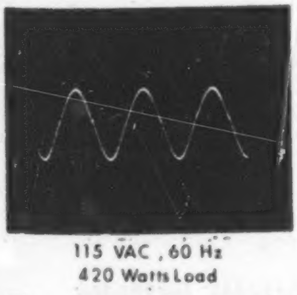

Fig. 8. Cycloconverter output waveform.

C74-1009

Fig. 9. Advanced utility-interactive inverter waveforms.

CP267-6117

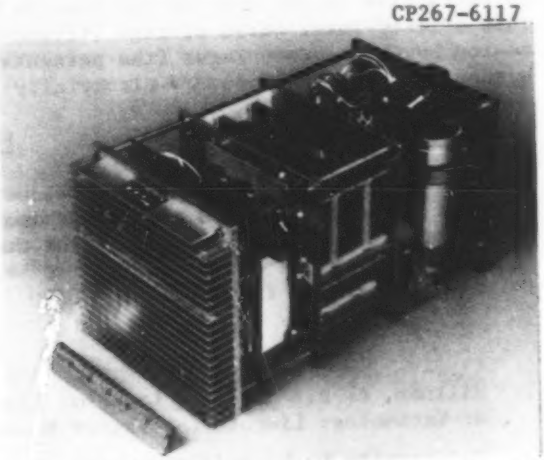

Fig. 10. Utility-interactive waveforms.

C74-1059

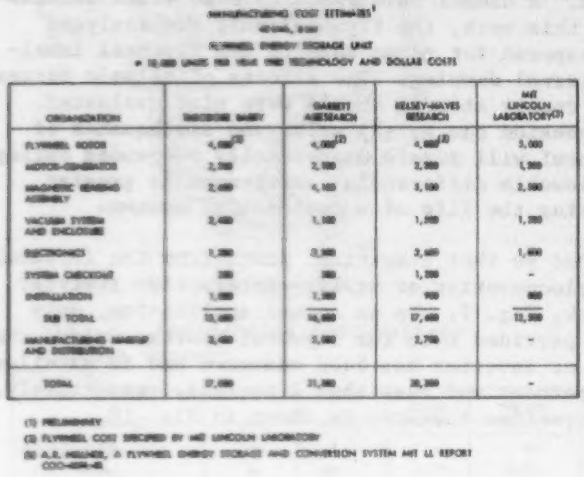

Fig. 11. Manufacturing cost estimates by three industrial firms.

Preliminary measurements of component and overall in-out flywheel power-transfer efficiencies have been taken on the subscale unit, Table I. With stand-alone cycloconverter power conversion, an in-out efficiency of 74 percent has been recorded. Efficiency tests with the utility-interactive inverter will be undertaken shortly and it is expected that an in-out efficiency of about 80 percent will be achieved. For purposes of comparison, the projected efficiency for a battery-inverter storage system is also listed in Table I. Flywheel efficiencies are seen to compare favorably with battery storage systems. A rigorous series of efficiency measurements are now underway to fully characterize the flywheel system over all expected operating conditions.

MANUFACTURING COST AND USER-WORTH STUDIES

Cost estimates for the manufacture of the full-size, 40-kWh, residential flywheel system were prepared for MIT Lincoln Laboratory by three industrial concerns: AiResearch, Theodore Barry Associates and Kelsey-Hayes. The cost estimates, summarized in Fig. 11, are based on the as given, 1980 technology design provided to the firms. In the course of their studies, the industrial firms suggested a number of design changes to facilitate manufacture and to achieve cost reduction of 30 percent below the figures in Fig. 11. Subsequent to those studies, MIT Lincoln Laboratory identified a number of design simplifications that might be instituted to achieve additional cost reductions; for example, a reduction in the number of magnetic bearings based on improved bearing test results. These design changes and design simplifications are expected to lower costs to the $8500-11000 range ($210/kWh-$275/kWh) by 1985. These costs are competitive with lead-acid and advanced battery storage systems when inverter and battery-charger costs are included with battery costs to arrive at total system cost. Under Lincoln Laboratory sponsorship, the MIT Energy Laboratory analyzed the break-even capital costs (net benefits to the user) for flywheel systems and concluded, for Phoenix residential systems, that PV stand-alone storage is attractive to the user if the home is more than one mile from an existing utility line and that utility-interactive storage (flywheel charging by PV only) value is enhanced at medium-to-low buy-back percentages (the percentage of the current electric rate at which the utility agrees to buy back excess PV electricity).

FUTURE PLANS

In the future, MIT Lincoln Laboratory will test the subscale flywheel system over a range of residential loads and off-nominal conditions; will modify the flywheel test set-up to include an advanced composite rotor and test for flywheel system performance; will investigate metallic-glass advanced-magnetic bearings; and will prepare cost analyses for the refined residential flywheel system.

REFERENCES

1. Millner, A. R.; "Scaling Laws for Flywheel System Components," Massachusetts Institute of Technology Lincoln Laboratory Report COO-4094-63, 15 November 1979.

2. Bucciarelli, L. L. and Rangarajan, A.; "Dynamic Analysis of a Magnetically Suspended Energy Storage Wheel," Massachusetts Institute of Technology Lincoln Laboratory Report DOE/ET/20279-102, August 1980.

3. Dinwoodie, T. L.; "Flywheel Storage for Photovoltaics - An Economic Evaluation of Two Applications," Massachusetts Institute of Technology Energy Laboratory, Report MIT-EL-80-002, February 1980.

TABLE I

COMPARISON OF EFFICIENCIES OF FLYWHEEL AND BATTERY STORAGE SYSTEMS

Measured Efficiency of Flywheel Energy Storage and Conversion System

DC-to-DC Down Converter	98%
Motor Electronics	96
Motor	98
Generator	91
Cycloconverter Electronics	89
Bearings and Tare	99 (0.8% of stored energy per hour)
TOTAL	74% (for one hour storage)

Projected Efficiency of Battery Inverter System

Maximum-Power-Point Tracker	98%
Battery	80
Inverter	85
TOTAL	67%

PROJECT SUMMARY

Project Title: Development and Assessment of Stationary Flywheel Storage Technologies

Principal Investigator: David B. Eisenhaure

Organization: The Charles Stark Draper Laboratory, Inc.
555 Technology Square
Cambridge, Massachusetts 02139

Project Goals: Assessment of flywheel storage technology and application coupled with developments in the bearing and power conditioning areas.

Project Status: The project is in progress and consists of the following elements:

a) Systems analysis directed toward assessing the status and worth of stationary flywheel storage.

b) Experimental investigation of magnetic bearing concepts and systems.

c) Development of a MOSFET based power conversion system for flywheel applications.

d) Investigation of field-modulated machines for flywheel applications.

e) Development of advanced hybrid ball/magnetic bearings and lubrication systems.

Work in the assessment area is currently directed toward assessing the worth of flywheels with current technology and with today's energy costs. Experimental investigations have indicated a number of areas where the performance of flywheel systems can be enhanced through technology improvements.

Contract Number: Subcontract 9385809

Contract Period: May 27, 1980, through September 30, 1980

Funding Level: $44,095

Funding Source: U.S. Department of Energy through Lawrence Livermore Laboratory, and Corporate Research Funds

DEVELOPMENT AND ASSESSMENT OF STATIONARY FLYWHEEL STORAGE TECHNOLOGIES

David B. Eisenhaure
The Charles Stark Draper Laboratory
555 Technology Square
Cambridge, Massachusetts 02139

ABSTRACT

The project for development and assessment of stationary flywheel storage technologies consists of the following elements: a) development of advanced hybrid ball/magnetic bearings and lubrication systems; b) experimental investigation of magnetic bearing concepts and systems; c) investigation of field-modulated machines for flywheel applications; d) development of a MOSFET based power conversion system for flywheel applications; e) systems analysis directed toward assessing the status and worth of stationary flywheel storage. Work in the assessment area is currently directed toward assessing the worth of flywheels with current technology and with today's energy costs. Experimental investigations have indicated a number of areas where the performance of flywheel systems can be enhanced through technology improvements.

INTRODUCTION

The Charles Stark Draper Laboratory (CSDL) is involved in the development of a number of flywheel related technologies. These developments include both technical and economic aspects and are aimed primarily at the development and commercialization of stationary flywheel storage systems. The technical systems work involves a detailed assessment of new or advanced technologies; it will determine subsystem and total system performance characteristics and will help in determining which subsystem areas would benefit from more R&D effort. This technical work is complemented by a number of component and system developments in process at Draper in both the bearing and power conversion areas.

The economic analysis involves modeling the system and performing a series of parametric studies to determine the overall worth of mechanical energy storage. To perform the analyses, available state-of-the-art systems codes, which combine technical and economic data, are employed.

The objectives of the economic analysis are to define and examine the role of advanced mechanical energy storage systems and subsystems in energy conservation when used in conjunction with solar and other power sources; define the developmental and functional requirements for these systems; provide technology development criteria as required.

One of CSDL's research goals is to develop a detailed understanding of how the performance characteristics of mechanical energy storage systems scale with increasing size. A preliminary understanding exists regarding the construction of small wheels and related system components; however, intermediate and large wheels are not well understood. Preliminary work will be initiated this year to identify component options and their characteristics. High priority would be given to determining the conversion efficiencies and steady-state losses associated with these systems. Further work could involve more detailed design trade-offs to identify areas for potential component R&D and to develop a data base to allow system procurement. This effort includes studying and evaluating various baseline implementation options including: electrical conversion systems, mechanical transmissions, and bearings.

CSDL feels that it is imperative to identify applications and corresponding requirements where mechanical energy storage has technical or economic advantages over other storage alternatives. Possible technical advantages of flywheel storage are in the areas of improved life, functioning, and efficiency. Three possible areas are solar voltaic well pumping, repeater stations, and subway systems. Assessment will be made in these areas and additional candidates will be identified during the fiscal year.

Development of an understanding of the value of storage to grid systems is in process. In mechanical energy storage applications in which energy can be obtained from the grid, analysis must consider both the storage and grid characteristics. In general, the grid will consist of a mix of base generating capacity (either nuclear, oil, or coal), gas turbine, peaking, storage and soft energy sources such as photovoltaic and wind. The analysis should consider the summation of amortized installation and generation costs. The addition of storage will affect the optimum mix as both capital cost of the grid and fuel cost must be considered in determining the worth of storage. During the coming fiscal year, conceptual models and strawman cases would be analyzed in order to develop an understanding of critical parameters. This effort would advance to more comprehensive studies as a series of reports updates our state of knowledge.

ADVANCED BALL BEARINGS FOR FLYWHEEL APPLICATIONS

The aerodynamic losses at high flywheel speeds require a relatively high vacuum, which in turn demands either a low-loss bearing that will operate in a vacuum environment, or rotating seals that characteristically have substantial associated losses (especially at high speeds).

The bearing requirements for a stationary energy-storage flywheel must include: stability; reliability; fail-safe operation; low loss at high speed; temperature insensitivity; and substantial capacity for combined loads at zero speed, at high speed, and in vacuum. Advanced retainerless ball bearings represent an ideal candidate for this application, particularly when combined with magnetic suspension of a major part of the flywheel weight. Such bearings are characterized by long life and minimum power dissipation, and are well suited for operation in a vacuum environment. These bearings consist of standard commercially available ball bearings, suitably modified for operation without the conventional ball retainer. In conventional ball bearings, the retainer is subject to violent instabilities of various types, which are particularly troublesome in vacuum operation, and typically treble the driving torque demand of the bearings. This problem is eliminated with retainerless operation as there is no possibility of retainer instability, and an optimum oil supply and scavenging system can be provided to ensure adequate elastrohydrodynamic (EHD) lubricant film thickness in all the ball race contacts, without introducing excess oil and unnecessary viscous drag.

The results are long reliable life and minimum friction loss. There are no known disadvantages resulting from retainerless operations. CSDL has produced prototype retainerless bearings which have successfully passed every performance test during their development. A pair is currently on life test at more than 13,000 hours in vacuum, without difficulty.

A typical retainerless bearing has an oil reservoir in its rotating inner race. During operation, oil is centrifugally pumped along the flow path and delivered to the bottom of the inner race groove. The lip of the inner race outer adaptor is shaped so that oil cannot flow uphill in the operating centrifugal field toward the stiffening ring, but must instead flow along the groove surface toward the ball inner-contact zone. It is then convected to the ball outer-contact on the ball surface. Thus, positive oil supply is assured at both races.

MAGNETIC BEARING RESEARCH

A topic of current research is the identification and solution of several unique control problems involved in the design of feedback compensation for the CSDL permanent magnet biased electromagnetic flywheel suspension system. This novel bearing system (Fig. 1) was developed as a part of an ongoing IR&D program to demonstrate the economic and engineering superiority of ultra-low-loss magnetic bearings through the analysis of a scale model flywheel energy storage module.

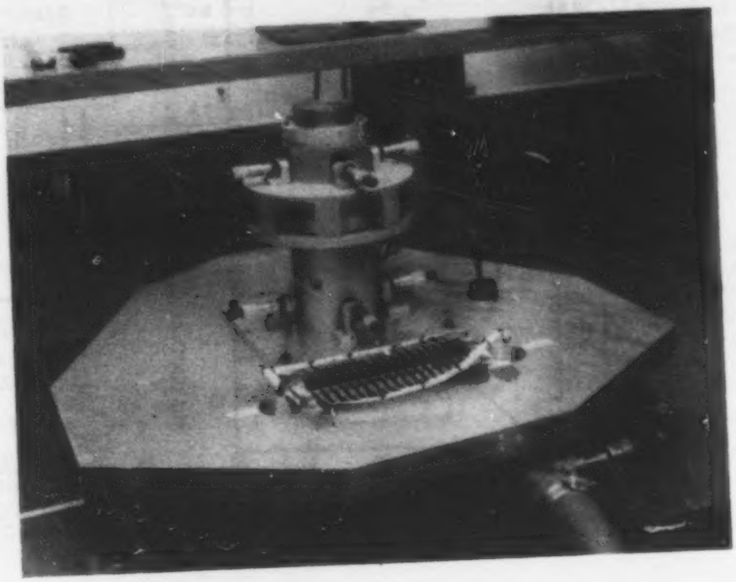

Fig. 1. Flywheel Magnetic Suspension System.

Permanent magnet biased electromagnetic bearings of this type have significant advantages over conventional suspension types. In terms of bearing power consumption (drag) alone, the advantage of utilizing this suspension type in large scale FESS applications is apparent (Fig. 2).

Compliance-induced housing resonance, the inherent instability of permanent-magnet suspensions, and magnetically induced dynamics are of particular concern to control engineers. Without proper control design, the existence of finite, lightly damped housing stiffness can cause oscillations in the independently controlled axial and radial suspension systems. Two alternatives for the suppression of these oscillations are notch filters in the compensation network and mechanical stiffening of the housing. The latter technique moves the oscillation frequency to a point far beyond the bandwidth of the system. These alternatives were implemented separately, and their results were compared. System performance was substantially improved through incorporation of either alternative. The final configuration, a combination of the two, allows extremely high bearing stiffness to be obtained without introducing undesirable oscillations.

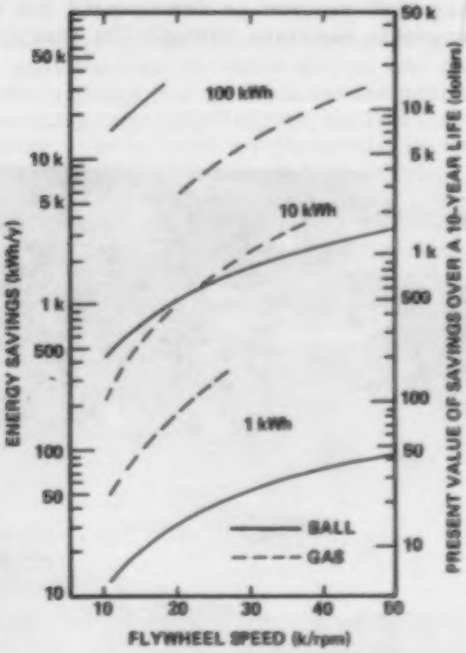

Fig. 2. Energy Savings Advantages of Magnetic Bearings Over Conventional Suspensions.

Eddy current damping in the suspension's magnetic circuit results in an increase in the order of the plant from second to third. Without proper consideration of these additional dynamics, the closed loop system would have insufficient phase margin to achieve stability. Compensation in the form of additional lead is readily incorporated into the control electronics.

FIELD-MODULATED MACHINE RESEARCH

Many stationary flywheel energy storage applications require some form of interface between the flywheel system and utility supplied electric power. The conventional approach to this problem is to generate variable frequency and transform this to 60-Hz power through the use of solid-state electronics. Historically, this approach has yielded acceptable performance, although it does not tend to be economically favorable for systems sized at the residential level. Field-modulated systems represent an alternative approach to flywheel power conversion which has been largely ignored despite significant advantages. Such a field-modulated approach requires ac rather than dc excitation of machine fields. This ac field excitation allows the output power to be converted to 60 Hz through the utilization of extremely inexpensive solid-state electronics without the use of brushes, commutators, etc.

CSDL has conducted several studies of approaches to field-modulated power conversion, and is at present engaged in a hardware development effort of such a system. Fig. 3 shows the system implementation for the dual-field dual-phase machine currently under test. This particular design has the advantage of requiring virtually no output filtering; both ripple and EMI are minimal with this configuration. The system is also capable of bidirectional power flow, which invites application to flywheel energy storage systems.

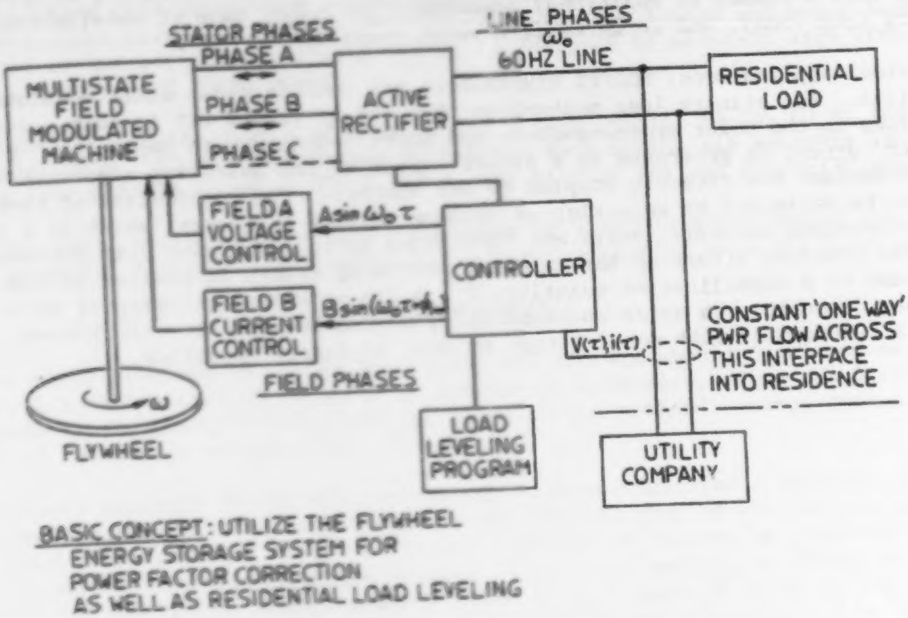
STATOR PHASES
PHASE A
PHASE B
PHASE C
LINE PHASES
ω_o
60HZ LINE
MULTISTATE FIELD MODULATED MACHINE
ACTIVE RECTIFIER
RESIDENTIAL LOAD
FIELD A VOLTAGE CONTROL
$A \sin \omega_o \tau$
FIELD B CURRENT CONTROL
$B \sin(\omega_o \tau + \phi)$
CONTROLLER
$V(\tau), i(\tau)$
CONSTANT 'ONE WAY' PWR FLOW ACROSS THIS INTERFACE INTO RESIDENCE
FIELD PHASES
ω
FLYWHEEL
LOAD LEVELING PROGRAM
UTILITY COMPANY
BASIC CONCEPT: UTILIZE THE FLYWHEEL
ENERGY STORAGE SYSTEM FOR
POWER FACTOR CORRECTION
AS WELL AS RESIDENTIAL LOAD LEVELING

Fig. 3. CSDL Frequency Conversion Concept.

Present hardware development is concentrated upon a 400-watt breadboard version of a bidirectional field modulated power converter. This technology, however, can readily be scaled up to the residential and commercial power levels, where it can provide an inexpensive, low maintenance interface between energy storage flywheels and the power grid.

HIGH EFFICIENCY PWM INVERTERS

Field-effect transistors have only recently become available as power devices, and are currently being produced with individual device ratings of 4.4 kW. At these power levels, FETs have become a serious competitor to bipolar transistors in medium power applications and, more specifically for flywheel applications, in pulse-width modulated inverters. These devices have a number of advantages compared to bipolar transistors, such as minimum drive requirements, low switching losses from extremely fast transition, and ease of paralleling. Newer devices with reduced on-resistance have eliminated the sole technical disadvantage. Current high prices are expected to be reduced as production increases.

The primary advantages of MOSFET transistors in flywheel applications are their extremely short switching times and minimal drive requirements. High device speeds are particularly advantageous when permanent magnet motors are utilized, for the combination of high drive frequency requirements for flywheel applications and low characteristic inductance of permanent magnet machines leads to extremely high modulation frequency requirements. High switching speeds reduce or eliminate filtering requirements while maintaining 60-Hz grid interface capability. The low drive requirements of these devices lead to substantial circuit simplification and contribute to high operating efficiencies. These devices have a number of additional advantages including ease of paralleling, extending Safe Operating Area (SOA), and an integral reverse rectifier.

For flywheel applications, MOSFET transistors are used in pulse width modulated (PWM) inverter designs. The primary loss mechanisms that can be traded off in such a design are switching losses in the power semiconductors and motor losses due to harmonics. Since the motor harmonic current is generated as a direct result of the switching algorithm selected, these loss mechanisms are directly coupled to one another. The combination of these loss mechanisms can be minimized by selecting an optimum carrier frequency, which is a trade-off between the decreasing harmonic losses and increasing switching losses with increased carrier frequency. The combined effect of harmonic and switching losses is plotted in Fig. 4 for differing values of a normalization quantity, N_m; a dimensionless grouping of motor operating parameters that determine the motor susceptibility to PWM-induced harmonic losses. This parameter is a function of both machine type as well as design specifics.

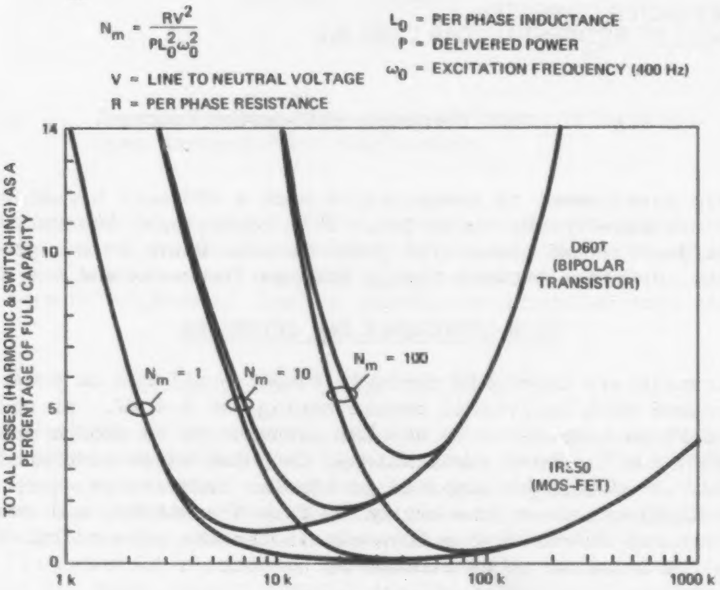

Fig. 4. Harmonic and Switching Losses.

Induction motors, because of relatively higher machine inductance, tend to have a lower N_m than an equivalently rated PM motor at the same excitation frequency. Similarly, an induction motor designed for higher starting torques will have a higher N_m than one designed for high efficiency. The curves span the range of practical motors for fly-wheel drive applications and demonstrate that FET devices are advantageous for all applications. They do, however, have particular advantages for high N_m and, therefore, PM motors.

CSDL is involved in the development of a microprocessor-controlled 15 kW, three-phase inverter utilizing this technology. This development involves the design, construction, and test of a prototype inverter. Trade-offs between switching losses and motor losses are computed, and optimized. The completed system is designed to maintain high efficiency throughout its power and speed range.

The inverter is being tested as a drive for both a 2-pole, 10-hp, 60-Hz induction motor and a 12-pole, 5-hp, 500-Hz PM brushless dc motor. Each of the six switches is formed by paralleling four HEXFETS rated at 400 V, 11 A, the highest ratings presently available.

The successful application of this technology to a PWM inverter suited for flywheel drive has potential for high efficiency and performance coupled with low costs.

ECONOMIC ANALYSIS

The economic problems of energy generation and storage should be viewed as a question of national policy rather than of consumer or industrial economics. Thus the first concept to be considered is the question: What is the value to the nation's energy system if we can store some of the energy we generate?

Preliminary analysis of the worth of energy storage indicates a value in utility-connected applications which is equivalent to the capital cost of the utility generating capacity which it eliminates. If a sufficient fraction of the energy generated by a power plant can be stored, the plant can be operated at constant output, as shown by the diagrams in Fig. 5(b), as contrasted to the varying output without storage shown in Fig. 5(a). Since the stored energy can be restored to the distribution system during peak demand periods, the plant can be sized to deliver constant full-load demand. The storage capacity thus replaces either an oversized power plant, or supplementary "peaking" plants.

Early studies of flywheel energy storage emphasized fuel savings and predicted savings of about $100 per kilowatt-hour. However, current studies take into consideration factors such as:

1) the greatly increased capital cost of power generation,
2) the fact that peaking plants use expensive and scarce fuels,
3) the greater efficiency obtainable from a plant operated at constant full load.

Application of these factors leads to much higher payoff than was predicted by the early studies.

As illustrated in Fig. 5(c), the storage need not be concentrated at the power plant, but can be distributed throughout the grid. This permits reduction in distribution costs, particularly if the storage elements are located close to centers of peaking load.

The aim of the economic study of utility grid-connected flywheel energy storage is to evaluate the factors involved in flywheel system costs and utility system savings, leading to the determination of the worth of the flywheel system.

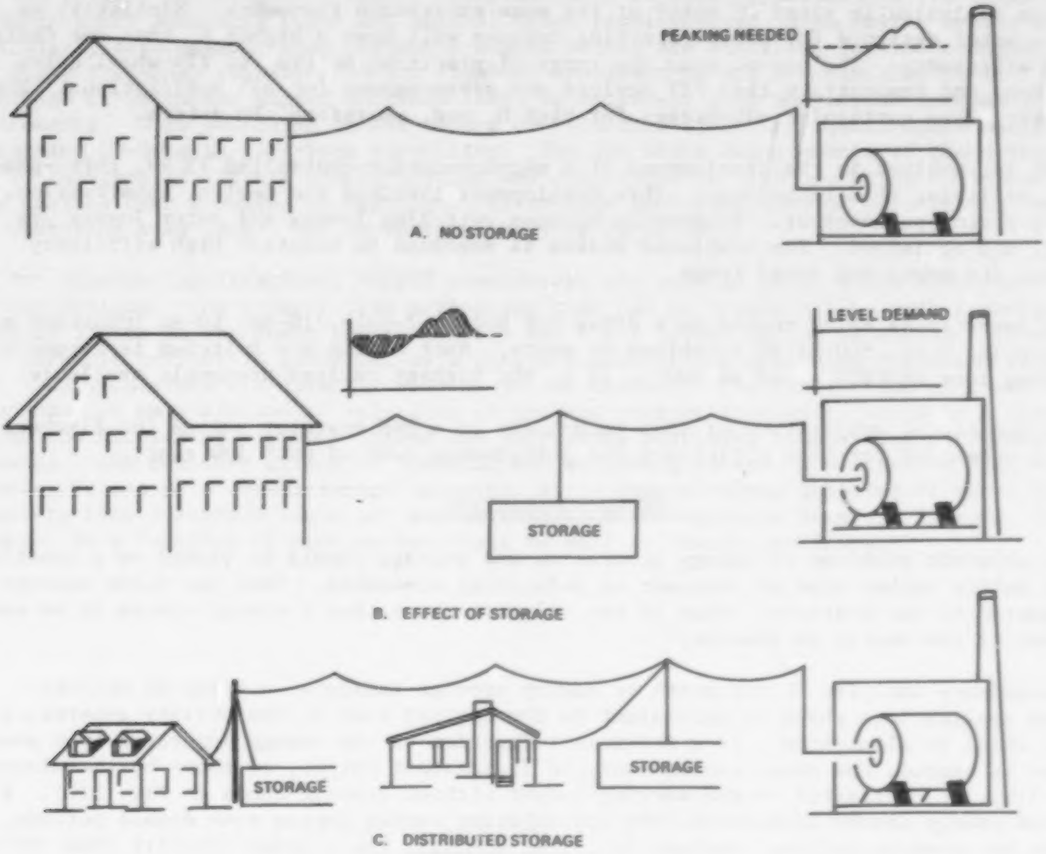
PEAKING NEEDED
A. NO STORAGE
LEVEL DEMAND
STORAGE
B. EFFECT OF STORAGE
STORAGE
STORAGE
C. DISTRIBUTED STORAGE

Fig. 5. Effect of Storage on a Utility System.

CONCLUSIONS

The successful development and commercialization of flywheel energy storage systems requires a thorough understanding of the economic and technical aspects of each application. There are currently a number of competing technologies that can be adapted to flywheel applications. The optimum choice between these technologies depends on the applications and is determined by both economic and technical issues. The most challenging problem facing the flywheel program is the successful integration of the appropriate component technology.

PROJECT SUMMARY

Project Title: Continued Development of the Band-Type Variable Inertia Flywheel

Principal Investigator: David G. Ullman

Organization: Union College
Department of Mechanical Engineering
Schenectady, N. Y. 12308

Project Goals: To determine whether or not the band-type variable inertia flywheel (BVIF) concept is a competitive energy storage and transmission device.

Project Status: The project has been completed. The following was shown:

1. The Band-Type Variable Inertia Flywheel (BVIF) is a system capable of storing and delivering energy in usable form. This is a single mechanism, which, unlike conventional flywheels, does not require any intermediate transmission equipment. A BVIF has been built and operated which is capable of smoothly accelerating a directly-connected inertial load from rest to a final speed without significant clutch-slipping losses or any additional transmission devices.

2. There are essentially three ways to attach loads to a BVIF. The first is an open-loop system with two degrees of freedom, referred to as the Type I. The second (Type II) is a single-degree-of-freedom unit with a fixed ratio between hub speed and casing speed. The third (Type III) has two degrees of freedom like Type I but includes power recirculation through a gear train like Type II. Of these, the Type III has been identified as the most promising configuration.

3. The Type III BVIF is capable of accelerating inertial loads smoothly and with stability to a terminal speed. That final speed can be greater than the initial flywheel speed, and both inner and outer elements of the BVIF slow down. The Type III BVIF is capable of yielding more than half of its stored energy to the load during such an operation.

4. Prototype testing in the Type III mode has produced real-world evidence of Type III BVIF capacity. Further work remains to be done to fully characterize the nature of such systems.

5. Subsequent efforts have shown that the Type III system can be built with energy densities greater than 10 watt hr/lb for both the energy storage and transmission systems.

Subcontract Number: 6186109

Contract Period: July 1, 1979 - July 1, 1980

Funding Level: $29,700.00

Funding Source: Lawrence Livermore Laboratories

CONTINUED DEVELOPMENT OF THE BAND-TYPE VARIABLE INERTIA FLYWHEEL

Dr. David G. Ullman
Department of Mechanical Engineering
Union College
Schenectady, New York 12308
Member, ASME

John Corey
Mechanical Technology Incorporated (MTI)
Latham, New York
(Formerly with Union College)
Member, ASME

INTRODUCTION

Many of the end uses of energy depend on its availability in mechanical form, usually as rotating shaft power. Consequently, great advantage would be had in terms of simplicity and overall system efficiencies if energy for such uses could be stored in a rotating mass. Such a device is by definition a flywheel, one of the oldest and most commonly used energy storage mechanisms.

Nonetheless, the uses of flywheels to date have been largely limited to reducing variations in the speeds of shafts driven by pulsed or irregular inputs or supplying peak forces in machine tools such as punch presses. The reason for this underutilization is an inherent difficulty in the power delivery capabilities of conventional flywheels. Specifically, the energy content, E, of a flywheel is a function of the polar moment of inertia, I, and the angular velocity, ω, ($E = \frac{1}{2} I\omega^2$), where the moment of inertia is a function of the mass and the effective radius of that mass from the axis of rotation ($I = \int_m r^2 dm$). For a fixed-inertia system such as the common rotating disk flywheel, then, the energy equation prescribes reduction in angular velocity as the only means of extracting energy. Most shaft loads, however, require a constant or increasing speed for their operation, so the only means of connecting a fixed-inertia flywheel to such loads is through some type of continuously variable transmission (CVT) or its electrical analog, a motor-generator system. The addition of such a unit to the system usually produces reduction in efficiency and increases in system complexity, weight, and cost. The design and development of effective flywheel energy transmission systems must precede any significant usage of flywheels as energy storage systems.

The flywheel described in this report releases energy in a manner intended to eliminate the need for a CVT or motor-generator by uncoupling the flywheel's energy content from its angular velocity. It is a variable-inertia flywheel (VIF), in which the moment of inertia term I, of the energy equation becomes a variable, allowing net energy release even if the speed term, ω, is constant or accelerating. For the flywheel under consideration here, the mechanism is a coiled thin band wound between an inner hub rotating with angular velocity ω_i and a concentric cylindrical outer casing rotating with angular velocity ω_o. Thus the BVIF is a two-degree-of-freedom device. The layout is much like the installation of a clockwork's mainspring except that no springiness is intended or assumed. As shown in Fig. 1 there are two inter-wound bands for balance but there could be more if desired. Variation in the moment of inertia is accomplished by relative rotation of hub and casing which winds the band material in onto the hub or out against the casing. This device is referred to as the Band-Type Variable Inertia Flywheel (BVIF). Figure 1 also defines the conventions used in all the ensuring discussion. The positive directions for all angular rates and torques are taken to be positive in the counter-clockwise direction shown. The subscripts used for these quantities are: "i" when referring to the inner hub, the inner rotating element, "o" when referring to the casing, the outer rotating element. The torques on hub and casing are due to the band segment between the tightly wound material about the inner hub and that pressed by centrifugal forces in the outer casing. This segment of the band is in tension. The bands exert a positive torque on the hub and a negative torque on the casing when wrapped in the direction shown. The band-wrap direction is defined to be positive when $\omega_o > \omega_i$ causes the bands to accumulate on the hub; negative if $\omega_o > \omega_i$ causes the bands to move out to the casing.

The development history of the BVIF leading to the research reported here is presented in References 1-5. Reference 1 presents an introduction to the variable inertia concept, discusses many potential configurations and studies one configured like a fly-ball governor. Reference 2 is a digested version of Reference 1. In Reference 3 the Band-Type Variable Inertia Flywheel is initially studied. Its equations of motion are derived and three potential ways of connecting it to external systems are developed. These three are the Type I, the inner hub connected to the load and the outer casing free; Type II, the inner and outer elements geared together, reducing the BVIF to a one-degree-of-freedom system; and Type III, the inner hub, outer casing and load are connected to the three elements of a planetary gear set as shown in Figure 2. In Reference 3 the Type II system was studied and found to be able to power a friction load at near constant speed but not have good inertia load powering capabilities.

This paper is a synopsis of research reported on in References 4 and 5 where the Type III BVIF, the configuration with the planetary gear set, has been more deeply studied. The operation of this system is explained and its operational potential discussed.

THE BVIF EQUATIONS OF MOTION

The equations of motion of the BVIF (regardless of which Type system) have been derived using Lagragian techniques in References 3 and 4. In Reference 4 the approach is made both through kinetic energy and separately through potential energy formulations. This dual approach is intended to gain insight into the complex variations of angular rate, band torque and moments of inertia which characterize the operation of a BVIF. Also in Reference 4, for completeness, the equations of motion have been derived using the standard Newtonian approach. The equations are highly nonlinear and unsolvable in closed form. However, computer solution of these equations has been made and insight gained through altering various geometric parameters, initial states and Type of configuration.

The Type III BVIF is by far the most complex dynamically of the BVIF configurations studied to date due to the inclusion of a planetary gear set. However, the complexity offers the most promise for versatility in operation. In this configuration, the two shafts of the BVIF (hub and casing) are connected to a load shaft via a planetary (epicyclic gear train) so that at any given time all three shafts can be rotating at different angular rates. The equations of motion are a set of 11 simultaneous nonlinear equations which can be solved for the torques and accelerations of hub, casing and load shafts.

BVIF PROTOTYPE TESTING

In order to verify the dynamic simulation results and gain knowledge of the BVIF's true potential, a prototype model was designed, constructed and tested. The design of the prototype model is based on the proof-of-concept model described in Reference 3. Like the previous version, this prototype is 10½" in diameter and 1 3/8" thick at the rim. The band material occupies a cavity 10" in diameter and 1.05" high. The maximum design rotational rate is 5000 rpm. The stresses resulting from this speed are quite conservative in keeping with the primary design objective of verifying the equations of motion not in producing a high energy density system.

To support the analysis the prototype model was used to accelerate an inertial load. The simulation was modified by the addition of bearing, gear, and windage friction (no vacuum was used). The gear and bearing friction values were measured (Reference 4) and the windage values were emphorical (Reference 3). A typical comparison of results is shown in Figure 3. Here the two measured values, the load shaft rpm and the inner hub shaft rpm are plotted with simulated values. Also plotted is the unmeasured outer casing rpm. As can be seen the simulation is always within 10% of the measured values.

In this experiment, the entire mechanism is initially rotating at 3500 rpm and the load is at rest. After an initial clutch slip the load shaft of the VIF, which has low moment of inertia, has slowed to the speed of the accelerating load. For the remainder of the simulation there is no more clutch slip. This slowing of the BVIF load shaft causes the inner hub shaft to slow relative to the outer casing. Thus the band starts to wind in with its tension trying to accelerate the inner hub and decelerate the outer casing. At about 10 sec all the elements of the BVIF are rotating at the same rpm. From this time on, the inner hub rotates faster than the outer casing and the band winds out. Were it not for the high frictions in this prototype model the acceleration of the load would continue. This is because the moment of inertia of the BVIF as seen by the load shaft is still decreasing even though the band is physically winding out (see References 3 and 4). The decay in rpm shown in Figure 3 is due to friction. Low friction simulations show the load accelerated and maintained at a constant rpm.

In operating the prototype speeds of up to 3500 rpm were run. At these speeds there was no problem with balancing. With the use of two bands, mass was always symetric about the axis. Potential problems which might be encountered in a moving base application are unknown, but the amount of material mass between the tight wound outer and inner sections of band are very small, and, thus, little problem is foreseen.

CONCLUSIONS AND RECOMMENDATIONS

1. The Band-Type Variable Inertia Flywheel (BVIF) is a system capable of storing and delivering energy in usable form. This is a single mechanism, which, unlike conventional flywheels does not require any intermediate transmission equipment. A BVIF has been built and operated which is capable of smoothly accelerating a directly-connected inertial load from rest to a final speed without significant clutch-slipping losses or any additional transmission devices.

2. There are essentially three ways to attach loads to a BVIF. The first is an open-loop system with two degrees of freedom, referred to as the Type I. The second (Type II) is a single-degree-of-freedom unit with a fixed ratio between hub speed and casing speed. Third (Type III) has two degrees of freedom like Type I but includes power recirculation through a gear train like Type II. Of these, the Type III has been identified as the most promising configuration.

3. The Type III BVIF is capable of accelerating inertial loads smoothly and with stability to a terminal speed. That final speed can be greater than the initial flywheel speed, and both inner and outer elements of the BVIF slow down. The Type III BVIF is ideally capable of yielding more than half of its stored energy to the load during such an operation.

4. Prototype testing in the Type III mode has produced real-world evidence of Type III BVIF capacity. Further work remains to be done to fully characterize the nature of such systems.

5. The next step in BVIF development is to integrate it into a system with a prime mover. The BVIF with its accelerating capability seems a good choice for hybridizing with a prime mover to add additional power during acceleration and absorbing power during braking.

REFERENCES

1. Ullman, D. G., "A Variable-Inertia Flywheel as an Energy Storage System," Ph.D. Dissertation, Ohio State University, March 1978.
2. Ullman, D. G. and Velkoff, H., "An Introduction to the Variable-Inertia Flywheel (VIF)," Journal of Applied Mechanics, Vol. 46, No. 1, March 1979.
3. Ullman, D. G., "Preliminary Development of the Band-Type Variable-Inertia Flywheel (BVIF)," Sandia Laboratories, Albequerque, N. M., (SAND 79-7089), November 1979.
4. Ullman, D. G., and Corey, J., "Second-Stage Development of the Band-Type Variable-Inertia Flywheel," to be published by Lawrence Livermore Laboratories, 1980.
5. Ullman, D. G. and Corey, J., "The Accelerating Flywheel," Presented at the 1980 Flywheel Energy Technology Symposium, October 26-30, Scottsdale, Arizona.

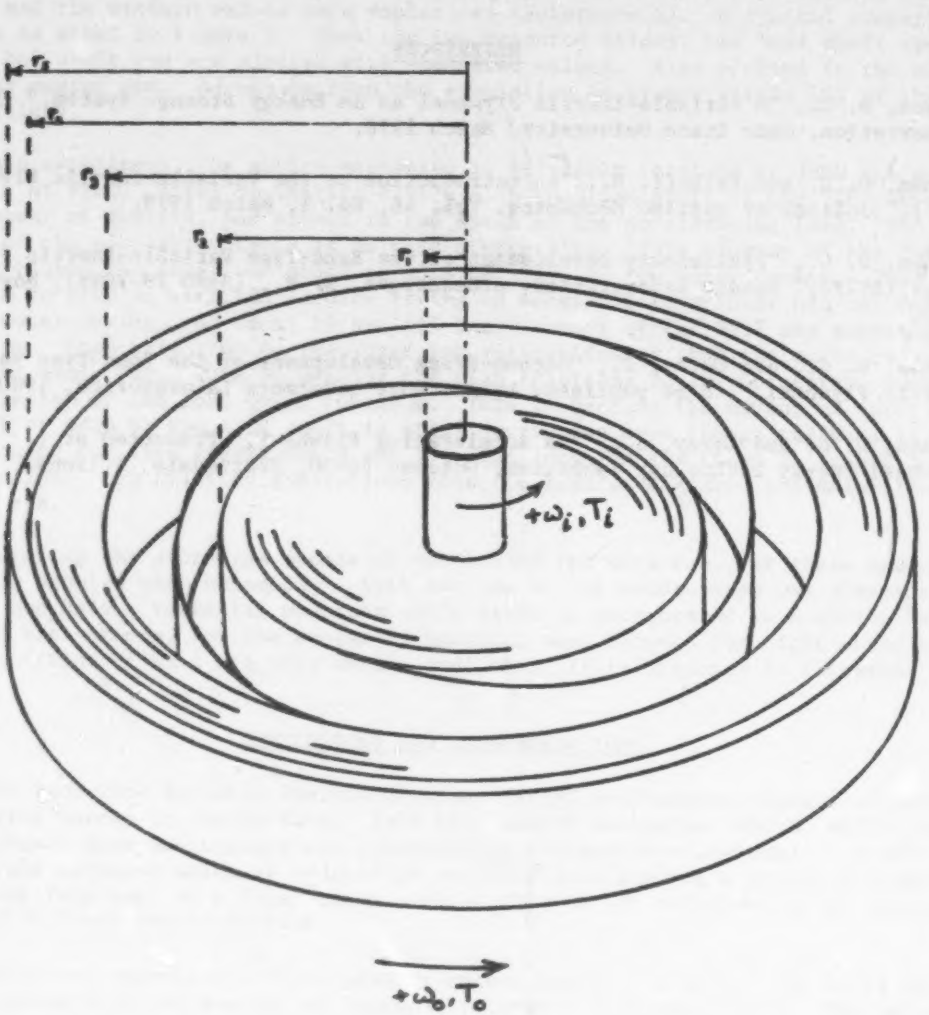
r_5
r_4
r_3
r_2
r_1
$+\omega_i, T_i$
$+\omega_o, T_o$

FIGURE 1. Basic BVIF Layout.

CUT AWAY VIEW OF THE VARIABLE INERTIA FLYWHEEL

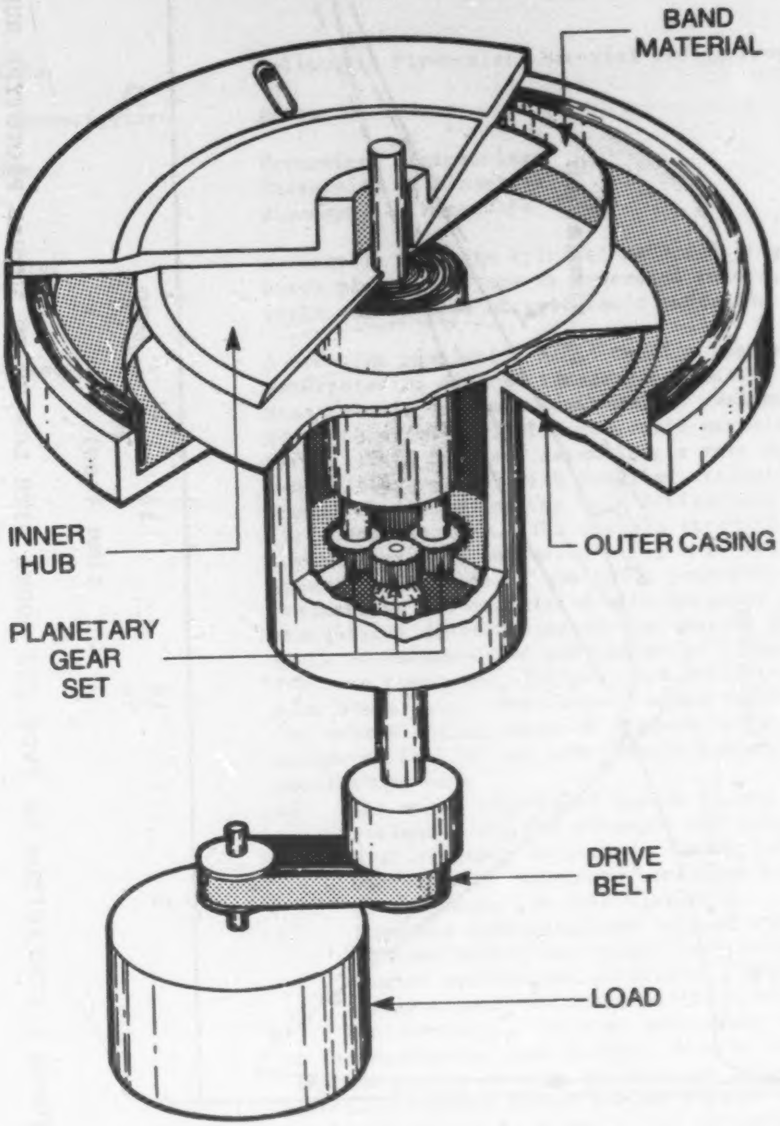
BAND MATERIAL
INNER HUB
OUTER CASING
PLANETARY GEAR SET
DRIVE BELT
LOAD

FIGURE 2.

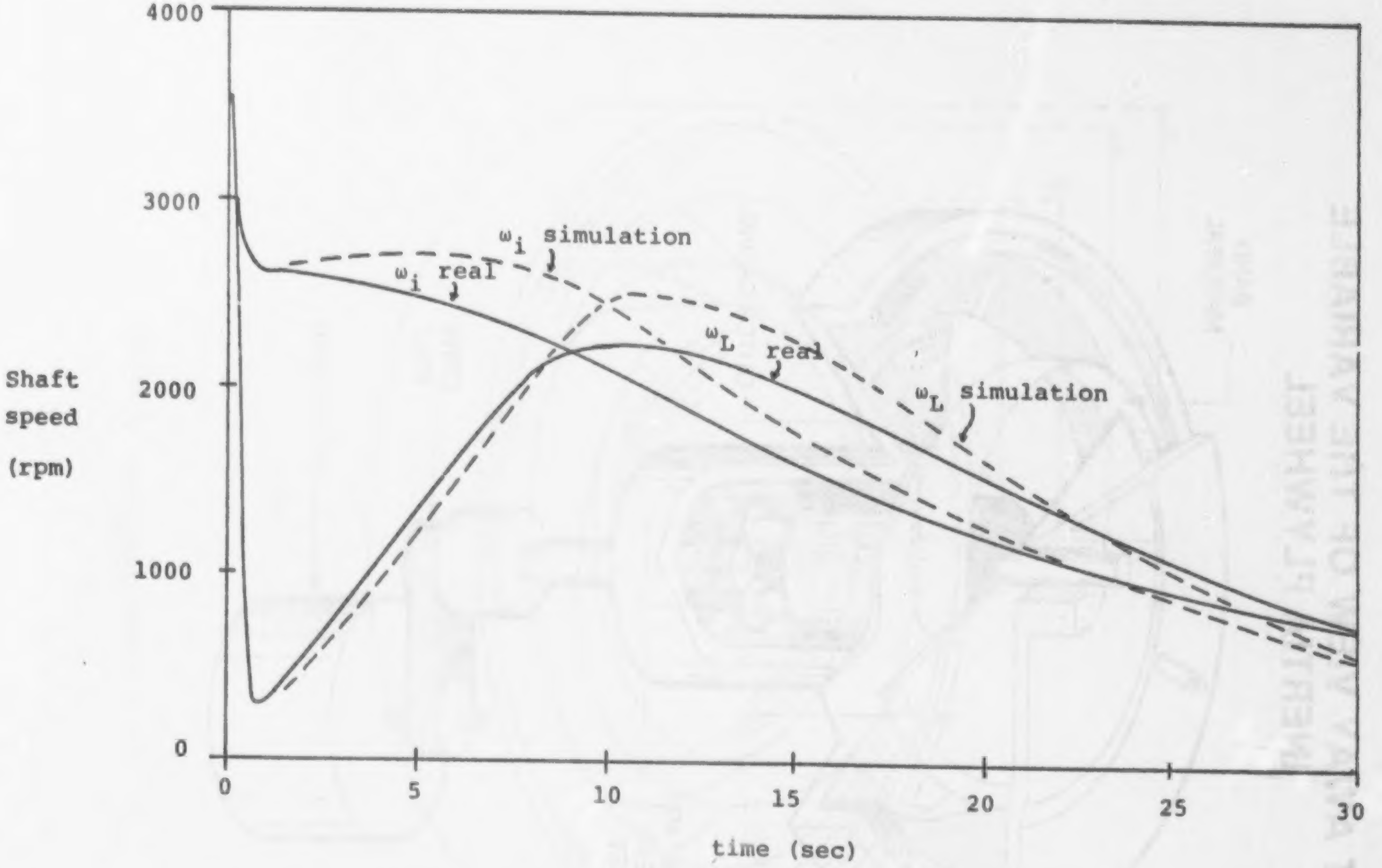

FIGURE 3. COMPARISON OF TYPE III MODEL WITH LOSSES TO ACTUAL PROTOTYPE RUN HISTORY

PROJECT SUMMARY

Project Title: Cellulosic Flywheels: Material Design Properties

Principal Investigator: Arthur G. Erdman

Organization:
Mechanical Engineering
University of Minnesota
Minneapolis, Minnesota 55455

Project Goals: Accurately evaluate critical material properties of hexagonal, birch plywood for use in evacuated rotors. Study further the costs and designs of cellulosic materials for rotors.

Project Status: A new high resolution rapid tensile testing method incorporating digital integrated acoustic emission measurements has been developed to evaluate the long term strength of viscoelastic composite materials using short term tests. This involved assembling a very precise, rapid data acquisition system, with detailed evaluation, analysis, and graphical display of the data derivatives and integrals and their correlations. The useable strength of hexagonal birch plywood has been estimated using this method which also appears applicable to synthetic composite materials. These evaluations are correlated with detailed measurements of the statistical distribution of the tensile strength to density ratio of vacuum-dried and 10% moist hexagonal birch plywood. Fracture toughness, fatigue, and duration of load tests are also being done. Preliminary measurements have been made of the vacuum drying rates of plywood disks and cylinders to evaluate the time and cost involved in this. The major conclusions are:

a) The major effects of vacuum drying plywood have been evaluated and its strength and density distribution statistically evaluated. Hexagonal birch plywood can therefore be reasonably designed in moderate performance, low cost flywheels.

b) Economic considerations suggest that hexagonal plywood is best suited for rotor cores around which to wrap higher performance materials. Highly oriented paper appears potentially competitive with other rotor materials for low cost stationary rotors.

It is recommended that further work be addressed to assembling compound rotors of high performance filament and ribbon materials wrapped around shaped plywood cores. Particular attention should be given to the potential of high performance paper.

Contract Number: W-705-ENG-48, Subcontract: 7551709

Contract Period: December 6, 1979, through December 5, 1980

Funding Level: $48,480

Funding Source: U.S. Department of Energy through Lawrence Livermore Laboratories

APPLICATIONS OF CELLULOSIC MATERIALS IN FLYWHEEL ROTORS

David L. Hagen, Arthur G. Erdman, Scott A. Gaff
Mechanical Engineering Department
University of Minnesota, Minneapolis, MN 55455

ABSTRACT

Preliminary studies of cellulosic rotors indicate that plywood cores in compound rotors and rotors wound with high performance paper appear promising. This paper reviews material properties that are critical in designing a plywood rotor core. Tensile tests of the distribution of strengths for vacuum dried hexagonal birch plywood show an approximately 10% decrease in performance upon drying from ambient conditions. High resolution tensile stress-strain tests coupled with precise digitally integrated acoustic emission measurements are proposed to estimate long term strength. Preliminary results are described. Measurements of the tensile fatigue of plywood samples are discussed. The hygroscopic nature of cellulose requires that consideration be given to careful drying of the material, and to the moisture release and outgassing rates in a vacuum. Similar phenomena are expected for other composite rotor materials.

INTRODUCTION

The rotor represents a major cost in flywheel energy storage systems. Efforts therefore have been directed towards finding materials with high performance per unit cost and with low assembly costs, especially for stationary applications. Cellulosic materials were suggested by D. W. Rabenhorst at the Applied Physics Lab, as potential candidates for low cost flywheel rotors. Tapered birch plywood disks were used by Rabenhorst as convenient cores around which higher performance materials such as Kevlar, fiberglass and steel hose wire were wound and spin tested (1). Further work was done testing plywood properties and developing plywood rotors at the University of Minnesota (2,3). Associated studies were also made of the rotors supports, system dynamics and controls, and a model demonstration system was built using a plywood rotor.

A detailed economic study of the costs of cellulosic materials and of assembling cellulosic rotors was then made for the Applied Plysics Laboratory (4). This indicated that plywood rotors were marginally competitive with E-glass or steel hose wire rotors, primarily due to comparitively higher container costs. However, wound rotors of so called "Superpaper" made of highly oriented fibers appear to provide potentially the lowest energy storage costs in a rotor of all the materials examined. Further studies of the sensitivity of flywheel system economics show a strong dependence on the rotor volume and container costs for cellulosic materials as compared with conventional high performance rotors (5,6). Plywood or similar pseudoisotropic materials defintely appear to be useful materials to make cores around which to wrap E-glass or steel hose wire while contributing to the energy storage potential of the rotor. Low container costs should make wound "Superpaper" rotors competitive with steel hose wire rotors.

The potential eonomic competitiveness of cellulosic rotors focuses attention on proving their technical feasibility. The strength distribution and toughness of materials under vacuum conditions control the energy storage capabilities and economics of rotors. These issues were therefore addressed (5-8). Several new methods of attaching hubs durably to cellulosic rotors were developed. Methods of balancing pseudoisotropic or wound rotors were designed using semi-automatic alignment methods which eliminate removing or adding material. Further design parameters were developed for use in preliminary design of the stiffness of rotor supports to accomodate material properties, dynamics and transmission limitations. Calculations and burst tests indicate that pseudoisotropic material made up of a 0 , 60 , -60 hexagonal configuration is considerably stronger than if made in the conventional 0 , 90 crossply configuration. The following discussion will concentrate on the results to date of the tensile testing program and how these pertain to the rotor design. Preliminary results will be given on the analyses of load deformation curves accompanied by acoustic emission measurements. These appear potentially useful for evaluating the damage rate and the long term strength. Drying rates and diffusion coefficients of plywood rotors have been measured as these affect the economics and feasibility of using cellulosic rotors in a vacuum.

TENSILE TESTS

The testing program was designed to evaluate the three major technical factors of intrinsic energy (tensile strength/density) distribution, moisture effects, and veneer orientation. The intinsic energy distribution was evaluated with 100 samples in each test series. Material that was vacuum dried was compared with material conditioned to 50% relative humidity (RH) to evaluate the effects of moisture loss. Finally tests would be run on plywood parallel to the grain and at the angle bisecting the grain angle in adjacent plies. The properties in this weakest direction are expected to correlate best with actual spin burst tests of disks of such pseudoisotropic material. Commercially available Finnish Birch plywood was tested and compared with specially made hexagonal birch plywood and the results were reported in references (5-8). (See Table 1 and Figure 1.) Commercially available birch plywood has a very broad distribution of strengths. The mean strength and intrinsic specific energy values of hexagonal plywood in the direction bisecting the grain direction in adjacent plies are 57% and 55% respectively of their corresponding values parallel to the grain (7,8). These represent a 92% improvement in performance compared to the conventional crossply configuration. As anticipated, tests of the hexagonal plywood show a drop in strength of about 10% when the material is vacuum dried. This loss is similar to that in conventional cross ply plywood. Some warping occurs in thin strips because hexagonal plywood has a helical geometry as compared to the crossply material which is symmetrically constructed. The plywood should be manufactured with the moisture content as close as possible to that of final use.

The standard deviations of the strengths of the custom made hexagonal birch plywood are considerably smaller than that of the commercially available conventional birch plywood. Furthermore, samples cut from the same board have strengths that are grouped much closer together. This may indicate that there are significant differences in the material used or in the procedures as to quantity of adhesive or its curing. Boards with very low strengths could probably be detected by use of non-destructive means such as ultrasonic or flexural modulus measurements. This would leave the remainder of the boards with a standard deviation of less than 5%. This data provides the fundamental information on the distribution of strengths of plywood necessary to to use plywood in high performance engineering aplications with a given confidence level. This is particularly important at low strengths where the design parameters are set. The broad distribution seen in conventional commercially available plywood was substantially reduced in custom-made clear hexagonal plywood. The strength of this hexagonal yellow birch plywood in the weakest region besecting adjacent plies was also double that of the conventional crossply imported birch.

HIGH RESOLUTION TENSILE AND ACOUSTIC EMISSION TESTS

The concept of a proportional limit is difficult to apply to wood since it exhibits considerable viscoelasticity. Thus any estimate of a proportional limit based on a given offset or visual estimation is dependent on the rate at which the test was conducted and is not an inherent absolute material property. Transitions in the curvature of the load deformation curve are not strikingly obvious, and may be hidden in the experimental error. Imaginative and painstaking tests have therefore been required to separate the effects of recoverable viscoelastic response in the wood from irrecoverable viscous permanent deformation or creep. There is some evidence in the literature which indicates that the rate of permanent deformation or damage increases rapidly when stressed above a given value which is approximately 50% of the short term strength (2,8). This is also the approximate constant stress level that is projected to be sustainable over 30 years or longer. If this level could be reliably measured in a short term test and be correlated with the long term strength, it would greatly simplify measuring the useable strength for new species or different moisture conditions.

Acoustic emissions occuring in the samples during tensile tests have been monitored, though very few such experiments have been made on wood. The rates of acoustic emissions show a rapid increase after the stress reaches a certain level. If the acoustic emissions are caused by failure of individual fibers, this presumably indicates damage to the material. Consequently the sample would become more flexible as well as weaker. The viscoelasticity would be expected to provide a stress dependent curvature to the graph. The load deformation graph would also presumably change slope at higher stresses as the modulus of the material was reduced. Accurate analysis of the slope of the load deformation curve was therefore expected to reveal a pronounced change in the rate of curvature above a certain stress region which should correlate with the acoustic emissions. Using a first order analysis, with fibers hypothesized to fail at equal strains, the acoustic energy released should be proportional to the change in stiffness or modulus of the tensile sample during the test. Both are expected to increase more rapidly with stress above a given stress region which could correlate with the long term strength. High resolution measurements of the load deformation curve coupled with the acoustic emissions were therefore conducted.

A micro-computer based data acquisition system was used to monitor and record the data, and to provide the preliminary data manipulation and reduc tion. Equipment with precision on the order of 0.01% was chosen. The stress and strain data were alternately taken and averaged over sixteen points with around 10,000 pairs of points taken per test. A least squares fit is then made every hundred points to calculate the slope. To monitor the acoustic energy released, a high speed digitizing, squaring and summing circuit with 12 bit resolution and 400 kHz throughput was designed and assembled. This suggests a 65 dB signal-to-noise ratio indicating that the limiting factor will be noise from the test equipment. Preliminary data was taken by monitoring the true rms of the acoustic emission signal, squaring and summing this to approximate the energy released. Preliminary results are shown in Fig. 2. The correlation between the slope of the load-deformation curve and the acoustic energy is shown in Fig. 3. Further data processing to remove numerical anomolies and avoid breaks in the curve due to fracture will improve the results significantly. A significant break in the curves is often seen and this point can presumably be taken as the stress or strain at which damage begins to rapidly increase.

TENSILE FATIGUE TESTS OF PLYWOOD

Conventional fatigue tests of wood on a rapid cyclic fatigue machine have been performed and show that wood is quite durable (2,8). Wood as a viscoelastic material exhibits a creep rate that is exponentially proportional to the absolute temperature. Constant stress has been shown to be more detrimental than daily applying and removing the stress up to several hundred cycles. This indicates that the duration under stress may be more significant than cyclic fatigue. Cyclic tensile fatigue and constant stress tests are being conducted on plywood along the weakest direction bisecting the grain direction in the adjacent plies. The fatigue test machine was designed for relatively stiff materials. Birch plywood has a much lower modulus, complicating the dynamic equations and stress applied. The flexibility of the wood required corrections for force transmissibility near resonance and resulting load applied. Other tests are also in progress to evaluate the fracture mechanics properties of birch plywood.

ROTOR DRYING RATES AND METHODS

Cellulose equilibrated at ambient conditions of 50% relative humidity will contain around 8% to 10% moisture. The time and effort required to dry the rotor and maintain vacuum are major factors in the overall economics of using cellulosic materials in flywheel rotors. Shrinkage or swelling with changes in moisture content can cause splitting of rotors. To solve the problems it is necessary to dry plywood disks before they are assembled into a rotor. Similarly the veneers must be dried as much as practical and adhesive chosen for minimum moisture content when the disks are assembled. Rotors must be kept in a carefully controlled environment and possibly coated with an hermetic epoxy coat such as has been developed by boat builders (7). Such a coat would probably be useful in reducing the rate of removal of moisture or volatile chemicals from a vacuum dried rotor while in a vacuum. This could minimize the pumping requirements and possibly permit periodic pumpdowns if an hermetic rotor pressure/burst container is used.

The rate at which moisture can be removed from a rotor or disk affects the pumping requirements and the drying costs. The moisture related properties of cellulose were reviewed and preliminary moisture loss data shown previously (7,8). The fractional moisture content remaining in a cylinder of finite length can be expressed as:

$$F(t)=0.562\exp(-2.47tr-5.78tp) \qquad t>0.2$$

where tr and tp are dimensionless time parameters proportional to diffusion coefficients and inversely proportional to the length and radius respectively. Preliminary measurements of the diffusion coefficients are shown in Fig. 4 (8). .Further tests are in progress.

CONCLUSIONS

The tensile strength and intrinsic energy distribution data obtained should enable serious evaluation of the technical and economic merits of plywood rotors. The shape of the strength distribution curve is significantly affected by material strengths and asembly methods which could be monitored through nondestructive methods and through careful quality control methods. The intrinsic energy distribution curve is not as variable as the strength. This should allow evaluation of the lower 10% of the distribution through proof testing fairly reasonably. The high resolution testing procedures coupled with monitoring the acoustic emissions appear to provide a new and useful approach to evaluating the performance of materials. Further analysis of this method coupled with fatigue tests would appear promising. The moisture loss tests suggest that the material must be dried as thoroughly as possible in thin sections. Epoxy coatings show some promise for maintaining the moisture status in a rotor and in minimizing vacuum pumping requirements. Epoxy coated rotors assembled and equilibrated under ambient conditions also appear to be suitable for low cost lower performance applications where evacuation and optimum performance are not required. Consideration should thus be given to plywood for rotor cores around which to wrap higher performance materials. Highly oriented "Superpaper" should also be considered in depth to evaluate its promise as a potentially competitive material to make low cost wound rotors.

ACKNOWLEDGEMENTS

Current support is from the Department of Energy administered by the Lawrence Livermore Laboratory. The Forestry Department of the University of Minnesota has kindly provided the tensile testing facilities and loan of the himidity conditioning equipment. Special thanks are due to Jon Blomgarden, Stuart Levy and Cathy Hagen for their invaluable assistance and encouragement.

Table 1. Tensile Strength & Intrinsic Energy of 16 Ply ½" Hexagonal Yellow Birch Plywood

Face Veneer Orientation	RH%	Number of Samples	Mean Strength MPa	Psi	Standard Deviations Psi	%	Drying Drop Δ%	Δ/S %
Parallel ≈ 0°	50	100	72.7	10,549	1,090			
	0	1	58.5		-	-	-22.0	
Mid Ply ≈ 90°	50	99	41.5	6,014	973	16.2		
	0	97	34.2	4,965	873	17.6	- 8.8	-0.76

Face Veneer Orientation	RH%	Number of Samples	Intrinsic Specific Energy KJ/KG	σ/ρ WH/LB	Standard Deviation KJ/KG	%
Parallel ≈ 0°	50	43	96.1	12.1	7.56	7.9
Perpendicular ≈ 0°	50	56	53.5	6.75	9.1	17.0

REFERENCES

1 D. W. Rabenhorst, "Composite Flywheel Development Program- Final Report." Johns Hopkins University, Applied Physics Laboratory: APL/JHU SDO-4616A NSF Grant No. AER 75-20607, May 1978.

2 D. L. Hagen, "The Properties of Natural Cellulosic Materials Pertaining to Flywheel Kinetic Energy Storage Applications." Proc. 1977 Flywheel Technology Symposium, October 5-7, 1977, San Francisco, pp409-428.

3 A. G. Erdman, D. A. Frohrib, W. L. Garrard, D. L. Hagen, T. P. Carlson, "The Development of a Cellulose Flywheel System for Rural Wind Energy Storage: Final Report." U. Minnesota for Minnesota Energy Agency, July 1978.

4 D. L. Hagen, A. G. Erdman, "Economics of Cellulosic Rotors." University of Minnesota, Final Report to the Applied Physics Laboratory, May 1979.

5 A. G. Erdman, D. A. Frohrib, W. L. Garrard, D. L. Hagen, T. P. Carlson, "The Development of a Cellulose Flywheel System for Rural Wind Energy Storage: Phase II. Final Report." University of Minnesota for the Minnesota Energy Agency, December, 1979.

6 D. L. Hagen, A. G. Erdman, D. A. Frohrib, "Design of Flywheel Rotors Utilizing Cellulosic Materials." Paper No. 799080, 14th Intersociety Energy Coversion Engineering Conference, Boston MA August 6, 1979.

7 Arthur G. Erdman, David L. Hagen, Darrell A. Frohrib, "Development of Cellulose Flywheel Rotors." University of Minnesota, Final Report UMN-ME-FL- 79-03 August 3, 1979 for Sandia Laboratory, Contract No. 07-9072. Sandia Report No 79-7099, February 1980, for DOE under contract DE-AC04-76DP00789.

8 David L. Hagen, Scott A. Gaff, Arthur G. Erdman, "Material Design Properties of Cellulosic Flywheel Rotor Cores." 1980 Flywheel Technology Symposium, Scottsdale AZ. October 26-30, 1980.

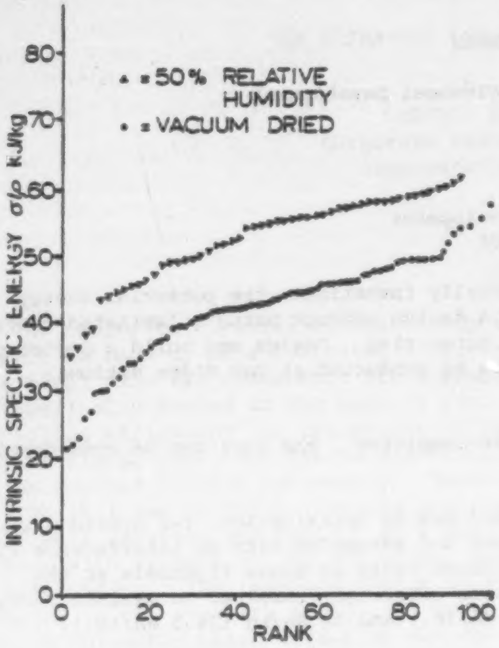

Fig. 1 Intrinsic Specific Energy Distribution of Hexagonal Yellow Birch Plywood Perpendicular to the Face Veneer.

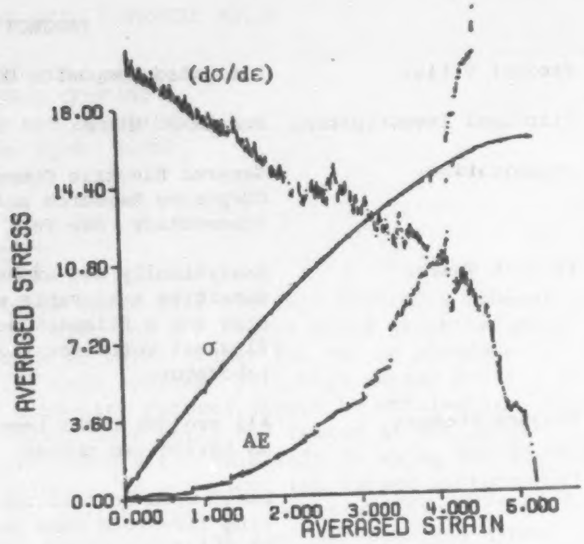

Fig. 2 Average stress (σ), stiffness (dσ/dε) and acoustic energy emitted (AE) vs. strain.

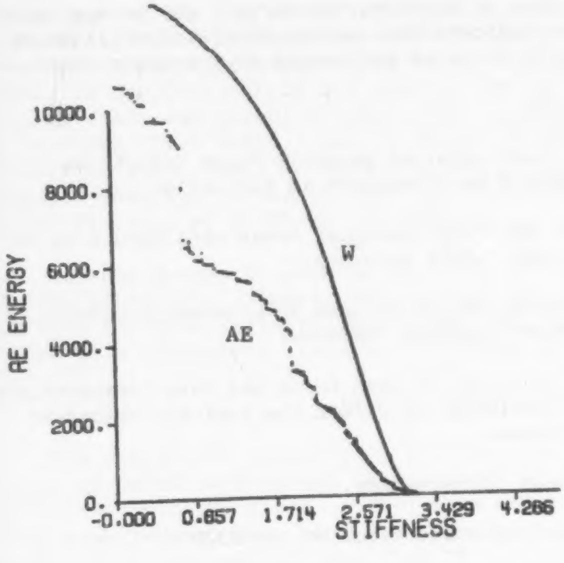

Fig. 3 Correlation of acoustic energy emitted (AE) and work (W) vs. stiffness (dσ/dε).

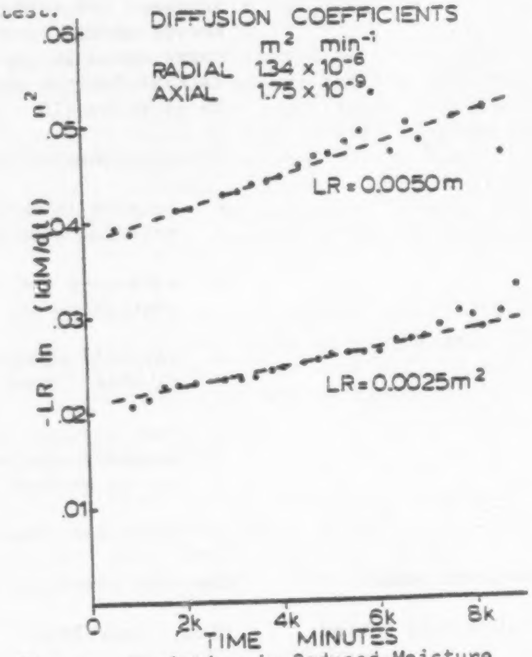

Fig. 4 Variation in Reduced Moisture Loss Rates with Time for Birch Plywood Disks during Vacuum Drying.

PROJECT SUMMARY

Project Title: **Laminated Composite Disc Flywheel Development**

Principal Investigator: **Ronald P. Nimmer**

Organization:
General Electric Company
Corporate Research and Development
Schenectady, New York 12301

Project Goals: **Analytically and experimentally investigate the potential energy densities achievable with a design concept using a laminated central disc and a filament wound outer ring. Design and build a prototype flywheel rotor for tests to be conducted at Oak Ridge National Laboratory.**

Project Status: **All project tasks have been completed. The work can be considered as having two phases.**

Based upon initial tests and design optimization, two hybrid disc-ring flywheels were designed and assembled with an interference fit in phase one. Subsequent burst tests of these flywheels at the Johns Hopkins Applied Physics Laboratory resulted in maximum energy densities of 57 Wh/kg (26 Wh/lb.) and 54 Wh/kg (24.5 Wh/lb.).

In phase two, two larger prototype flywheels were designed, fabricated and delivered for testing at Oak Ridge National Laboratory. Extensive supportive testing was conducted for effective design. These tests included ultrasonic modulus and damage definition, tensile tests, and fiber volume and void content measurements. Dynamic analyses and tests reflect a stiff flywheel rotor with little observed effect upon critical speeds due to the elastomeric bond. A burst speed in the vicinity of 66 Wh/kg (30 Wh/lb.) may be approached. Initial fatigue analyses indicate that energy densities of 33 Wh/kg to 44 Wh/kg (15 - 20 Wh/lb.) may be attainable at operating speeds.

Major recommendations are:

1. **Scatter in material test data and possible "size effect" on material strength should be considered in the design.**
2. **Alternate matrix for the graphite/epoxy outer ring should be investigated for improved radial strength.**
3. **Variable winding tension should be used in programmed winding of flywheel rings to avoid residual stresses.**
4. **Test results at one facility on both thick and thin laminates are needed to determine how large an effect the laminate thickness has on maximum performance**
5. **Additional fatigue work is necessary.**

Contract Number: Lawrence Livermore Laboratory Subcontract No. 2479309

Contracting Period: Fiscal year 1980

Funding Level: $127,881

Funding Source: U. S. Department of Energy/Lawrence Livermore Laboratory

THE ALPHA-PLY LAMINATED-DISC FLYWHEEL ROTOR

R. P. Nimmer
GENERAL ELECTRIC COMPANY
Corporate Research and Development
Schenectady, New York 12301

ABSTRACT

The composite flywheel concept being developed under this Lawrence Livermore Laboratory contract is made up of a laminated S2-glass/epoxy disc and a filament wound graphite/epoxy outer ring. The two components are assembled with an interference fit and an aluminum hub is elastomerically bonded to the central disc. With this approach both high energy density and high volume efficiency (in comparison to other composite rotors) should be attainable. During the past fiscal year, two hybrid disc/ring flywheels were built and tested at the Johns Hopkins Applied Physics Laboratory. These wheels reached approximately 54 Wh/kg and 57 Wh/kg (24.5 Wh/lb.) and 26 Wh/lb.) before ultimate failure. In addition, two larger prototype flywheels were designed and built. As a part of the design process, extensive information was gathered with respect to failure modes, material properties, residual stresses and dynamic characteristics. The improved design of these larger wheels should be reflected by energy densities in the vicinity of 60 - 66 Wh/kg (27 - 30 Wh/lb.). At writing, the first prototype wheel is currently being tested at the Oak Ridge National Laboratory.

INTRODUCTION

The concept of fabricating a composite flywheel using a laminated central disc and a thick, filament wound outer ring with an interference fit between the components was first suggested by Lustenader and Zorzi.(1) Extensive work with respect to the optimization, fabrication, and testing of such wheels has been reported by Nimmer, et al.(2,3,4,5) Prior to fiscal year 1980, fabrication and testing in this program had been limited to thick, flat, laminated S2-glass/epoxy discs without outside rings. The maximum energy density attained in these tests was approximately 40 Wh/kg (18 Wh/lb.). Work during the last fiscal year has resulted in the fabrication and test of two hybrid flywheels shown in Fig. 1 with S2-glass/epoxy central discs and graphite/epoxy outer rings. These two flywheels reached energy densities of 54 Wh/kg (24.5 Wh/lb.) and 57 Wh/kg (26 Wh/lb.) before ultimate failure. Based upon the results of these tests as well as other investigations which will be described herein, two larger, prototype flywheels have been fabricated which should be capable of energy densities in the vicinity of 60 Wh/kg (27 Wh/lb.).

It should also be pointed out that analyses related to the use of molded, short-fiber central discs with filament wound rings have also been carried out under this program. These analyses included optimization, creep, and fatigue investigations. This work will be documented in a subsequent Lawrence Livermore Laboratory report but will not be discussed herein.

INITIAL HYBRID DISC-RING FLYWHEEL TESTS

The design and assembly of the two 2.54 cm (1 inch) thick hybrid disc-ring flywheels tested at Johns Hopkins APL is discussed in detail in Ref. 4. The fiber volume content attained in laminated discs of this size was 48% while the void content averaged 1.8%. In addition, measurements made on typical graphite rings of this size show a fiber volume content of 60.9% and a void content less than 1%.

Both model wheels were tested at the Johns Hopkins Applied Physics Laboratory. In the case of wheel No. 1, the test proceeded uneventfully to a tip speed of 780 m/s (2550 f/s). In the vicinity of this tip speed, significant increases in the vacuum pressure of the spin pit were measured. In spite of this effect, acceleration of the wheel was still possible. As the wheel continued to accelerate above 780 m/s, increasing vertical vibration was measured reaching peaks of 8 g's. At 904 m/s (2970 f/s) the flywheel pulled loose from the air turbine shaft. The maximum energy density reached in this test was 54 Wh/kg (24.5 Wh/lb.). Post test examination revealed an intact flywheel. A circumferential crack was visible midway between the inside and outside radii of the graphite/epoxy ring.

Test results for flywheel No. 2 were very similar. In addition to the standard measurements collected in the first test, a high speed videotape record of the test was made during the second test. As in the previous test, the early stages of the test proceeded uneventfully. At a tip speed of 850 m/s (2785 f/s) the appearance of a circumferential crack in the graphite/epoxy ring was visible on the videotape. The appearance of this crack was accompanied by a rise in the vacuum pressure of the test facility. Vertical vibrations also increased in magnitude above the tip speed of 850 m/s. At a tip speed of 931 m/s (3055 f/s) the intact composite flywheel disc and ring separated from the aluminum hub at the elastomeric bond line. The maximum energy density reached in this test was 57 Wh/kg (26 Wh/lb.). Again both the disc and the ring were intact when examined after completion of the test except for the circumferential crack in the ring and outside diameter damage to the ring incurred after the wheel dropped from the shaft.

The results of these tests bear out a number of analytical predictions discussed in detail in Refs. 3, 5, and 6. Perhaps most important is the fact that the maximum energy density of a laminated flywheel can be substantially improved by the addition of a filament wound graphite ring. The highest energy density previously attained with 2.54 cm (1.0 in.) thick discs was improved 44% from 40 Wh/kg (18 Wh/lb.) to 57 Wh/kg (26 Wh/lb.) by the addition of a filament wound graphite ring. In addition, it is evident that with a proper interference fit, separation of the disc and ring can be precluded. Finally, the failure mode observed in the test (circumferentially cracked ring) coincides with one of the four predicted failures and, as will be subsequently seen, indicates that thinner outside rings should produce additional improvements in the maximum energy density.

PROTOTYPE FLYWHEEL DESIGN AND FABRICATION

The most important goal of the past fiscal year was the design and fabrication of two prototype flywheel rotors. In order to provide necessary insight into subsequent spin test results, a substantial foundation of data specifically related to the materials and processes used to fabricate these flywheels was accumulated. This data included fiber volume fractions, void content, moduli and strength. Damage analyses were carried out and corroborated with ultrasonic testing. Using this data as well as previous spin test results, the wheel design was optimized and the components manufactured and assembled. Some of the most important results will now be discussed.

LAMINATED DISC DAMAGE

Based upon classical laminated plate theory, an analysis of damage in a spinning, laminated disc was carried out and is discussed in detail in Ref. 7. The analysis accounts for accumulating damage in the disc which covers a progressively larger radius as the speed increases. Figure 2 describes the radial boundary of the damaged area (on the abscissa) predicted by the analysis as a function of the disc's tip speed (on the ordinate). The two curves are bounding analyses. Also indicated on the graph are three recorded tip speeds at failure of laminated discs made of S2-glass/epoxy. The lower two tests are associated with 2.54 cm (1 inch) thick discs built by the General Electric Company and are reported in Ref. 8 and the highest test speed is associated with a 1.00 cm (0.4 in.) thick disc built for the Lawrence Livermore Laboratory and recently tested at Johns Hopkins Applied Physics Laboratory. The most important result is that damage to the matrix of the disc will occur at low speeds in comparison to the ultimate disc failure. Comparing test results and predictions in Fig. 2 suggests that failure may occur before this damage covers the entire disc. Although there is not enough data to draw conclusions, it is interesting that the highest tip speed for an S2-glass/epoxy laminate is associated with a relatively thin disc in comparison to those tested by the General Electric Company. Although it would be expected that thinner discs may perform better, thick discs offer an advantage in fabrication by reducing the number of bonds necessary between individual discs to achieve required total energy levels. Additional testing should be carried out to explore the effect of thickness, since it may be a significant parameter.

Corroborating experimental evidence of the existence of this damage has also been discovered and presented in Ref. 7. Figure 3 illustrates the ultrasonic velocities measured through the thickness of a 1.0 cm (0.4 in.) thick S2-glass disc as a function of radial position after it was spun to a tip speed of 638 m/s (2090 f/s). These ultrasonic velocities are compared with velocities measured in a disc before spin testing. It should be noted that the wheel examined for damage in this test is the same wheel which was subsequently tested to 975 m/s (3200 f/s) at the Johns Hopkins Applied Physics Laboratory.

MATERIAL CHARACTERIZATION

Measurements for the fiber volume and void content of the prototype size laminated disc and filament wound ring are reported in Tables 1 and 2 and compared with smaller components. Experiments also indicate a residual moment in the ring resulting in a 48 MPa (7 ksi) tensile stress at the inside diameter of the ring. The existence of these stresses is consistent with the work of Knight(8) and Reuter(9) and should be eliminated with proper variation of winding tension.

Ultrasound techniques were also used to effectively determine the tangential and radial moduli of the ring as 127 GPa (18.3×10^6 psi) and 9.65 GPa (1.4×10^6 psi) respectively. Less success with these techniques was encountered in determining laminate stiffness, and as a result, results from thin-coupon, tensile tests(10) were relied upon for the modulus of the disc.

A significant difference in the radial strength of the graphite/epoxy rings with respect to initial expectation was discovered. Average strengths of 20 MPa (3 ksi) were found in filament wound panels instead of the expected 48 MPa (7.0) strength. In addition, tests on coupons cut directly from a filament wound ring show substantial scatter in results and thus suggest the possibility of a large "size effect"(11) which could further reduce expected strengths in the ring. Design optimization for the prototype was based on an estimated size effect. Substantially more data is required for accurate treatment of this effect.

All of the physical properties used to optimize the prototype flywheel design are summarized in Table 3. The strength associated with the laminated disc is an average of previous tests on 2.54 cm (1.0 thick) laminated discs. The circumferential strength of the graphite/epoxy ring is based upon data reported by Bullock(12) including an expected "size effect" upon strength as well as the measured residual stresses in the ring.

DESIGN OPTIMIZATION

Based upon the material properties shown in Table 3, the ratio of inside-to-outside diameters of the graphite ring was optimized for the prototype flywheels. Figure 4 is the resulting plot showing the ultimate energy densities expected for the governing failure modes as a function of the radius ratio β. The lowest $(\sigma_R)_{ULT}$ curve representing $(\sigma_R)_{ULT} = 12.4$ MPa (1.8 ksi) reflects the first approximation of expected average ring failure stress accounting for "size effect." The initial and ultimate failure points for the wheels tested at Johns Hopkins APL are also displayed. As can be seen, in one APL test the initial failure appears to have come at a radial stress of about 15 MPa (2.2 ksi) while the other appears to have reached 27 MPa (3.9 ksi). The design point for the two prototype flywheels is $\beta = 0.82$ and should change the ultimate failure mode of these flywheels to either a disc failure or fiber breakage in the ring. An energy density between 55 Wh/kg and 66 Wh/kg at failure may be attained since the disc failure line is based upon average, thick disc failures to date.

Also included in Fig. 4 are a set of curves describing expected average energy density for 10^6 cycle life. First order predictions indicate an energy density of about 32 Wh/kg (14.7 Wh/lb.) can currently be reached for 10^6 cycle life.

ASSEMBLY

The graphite/epoxy ring and the S2-glass/epoxy disc were assembled with an interference fit between the components. Prior to assembly the ring is placed over the disc as shown in Fig. 5. The tapered faces of the ring and disc allow the ring to slide down partially over the disc as shown in the figure. A combination of thermal contraction and force fit is used to complete the assembly. During this process, both the ring and disc are cooled to liquid nitrogen temperatures. In order to assess the effect of these temperatures upon the laminated disc, two tests were carried out. Neither ultrasonic examination reported in Ref. 4 nor more recent dye penetrant tests indicated any damage due to cryogenic temperatures. All assemblies were carried out without difficulty and a finished wheel is displayed in Fig. 6.

FLYWHEEL DYNAMICS

Several aspects of flywheel dynamic characteristics were also investigated. The rotor disc itself exhibits a first natural frequency measured at 830 Hz. Figure 7 illustrates the predicted whirl speed behavior of a three degree of freedom dynamic model of the rotor shaft system in a format similar to that used by Bert.(13) The intersection of the whirl speed curves (solid lines) with the dashed lines defined by

$$\omega = \Omega \tag{1}$$

$$\omega = 2\Omega \tag{2}$$

indicate the expected critical speeds at the Oak Ridge test facility. The effect of the elastomeric bond is reflected in the uppermost whirl speed plots. This natural frequency is associated with the hub vibrating with respect to the more massive flywheel. The frequency is sufficiently separated from the rotor shaft modes that no coupling is evident. The severity of this natural frequency will be established in subsequent tests.

POTENTIAL FOR ADDITIONAL IMPROVEMENT

With the materials and processes developed to date, a thick hybrid flywheel of the type described herein should reach an energy density in the vicinity of 55 Wh/kg to 60 Wh/kg (25 Wh/lb. to 28 Wh/lb.) at burst. Improvement of these energy densities can be achieved through improved material performance of the laminated disc as well as the circumferential strength of the wound outer ring. Based upon currently available data, such improvements could realistically lead to energy densities in the 66 Wh/kg to 77 Wh/kg (30 - 35 Wh/lb.) range at burst and a 44 Wh/kg (20 Wh/lb.) energy density at operating speed for 10^6 cycle life.

CONCLUSIONS AND RECOMMENDATIONS

The ability to enhance the energy density of a laminated S2-glass/epoxy disc with a filament wound ring has been established. Energy densities of 54 Wh/kg and 57 Wh/kg (24.5 and 26 Wh/lb.) at ultimate failure have been demonstrated. Improved design applied to the prototype wheels should eliminate failure of the graphite ring under radial stress and raise ultimate energy densities toward 60 Wh/kg (27.5 Wh/lb.). Additional improvement in laminated disc strength and circumferential strength of the graphite/epoxy ring could result in energy densities approaching 66 - 77 Wh/kg (30 - 35 Wh/lb.).

As part of any program to improve current performance levels, the following recommendations should be considered:

1. Scatter in material test data and possible "size effect" on material strength should be considered in the design.

2. An alternate matrix for the graphite/epoxy outer ring should be investigated for improved radial strength.
3. Variable winding tension should be used in programmed winding of flywheel rings to avoid residual stresses.
4. Test results at one facility on both thick and thin laminates are needed to determine how large an effect the laminate thickness has on maximum performance and appropriate processing parameters should be optimized.
5. Additional fatigue work is necessary.

ACKNOWLEDGMENTS

The disc-ring development program was funded by Lawrence Livermore National Laboratory under the project management of Dr. Satish Kulkarni. The process optimization, fabrication, and material characterization of the laminated discs was carried out under the direction of Kevorc Torossian at the General Electric Company's Large Steam Turbine Materials and Processes Laboratory. The filament wound graphite/epoxy rings were produced by Lord Kinematics, Inc., under the direction of Al Hannibal. Ultrasonic tests were conducted by Buzz Burnet and Bob Gilmore of the General Electric Company. The author would also like to acknowledge the extremely effective test techniques of David Rabenhorst and Bill Wilkinson at the Johns Hopkins Applied Physics Laboratory.

REFERENCES

1. Lustenader, E. L. and Zorzi, E. S., "A Status of the 'Alpha-Ply' Composite Flywheel Concept Development," presented at SAMPE Meeting, Anaheim, CA, May 3, 1978.
2. Nimmer, R. P., Torossian, K., Hickey, J., and Wilkinson, J. P. D., "Laminated Composite Disc Flywheel Development," First Interim Report, Subcontract No. 2479309, General Electric Co. Contractor's Report SRD-79-016 (also, Lawrence Livermore Laboratory Report UCRL-13973), January 1979.
3. Nimmer, R. P., Torossian, K. A., and Hickey, J. S., "Laminated Composite Disc Flywheel Development," Second Interim Report, Lawrence Livermore Laboratory Subcontract No. 2479309, General Electric Co. Contractor's Report SRD-79-114 (also, Lawrence Livermore Laboratory Report UCRL-15154), July 1979.
4. Nimmer, R. P., Torossian, K. A., and Hickey, J. S., "Laminated Composite Disc Flywheel Development," Third Interim Report, Lawrence Livermore Subcontract No. 2479309, General Electric Co. Contractor's Report SRD-80-091, February 1980.
5. Nimmer, R. P., "Laminated Flywheel Disc with Filament Wound Outer Ring," Proceedings of the 1979 Mechanical and Magnetic Energy Storage Contractors' Review Meeting, Washington, DC, August 1979.
6. Nimmer, R. P., "Parameter Design Analysis of a Hybrid Composite Flywheel Using a Laminated Central Disc and a Filament Wound Outer Ring," ASME paper 80-DET-97, presented at the Design Engineering Technical Conference, Beverly Hills, CA, Sept. 28 - October 1, 1980.
7. Nimmer, R. P., "Laminated Composite Flywheel Failure Analysis," Proceedings of the 1980 Symposium on Flywheel Energy Storage, Scottsdale, AZ, October 27-30, 1980.
8. Knight, C. E. and Pollard, R. E., "Prestressed Thick Flywheel Rims," Proceedings of the 1977 Flywheel Symposium, October 5-7, 1977, San Francisco, CA, Department of Energy Report CONF-77-063, March 1978.

9. Reuter, R. C., Jr., "Prediction and Control of Macroscopic Fabrication Stresses in Hoop Wound, Fiberglass Rings," Analysis and Test Methods for High Modulus Fiber Composites, ASTM STP 521, American Society of Testing and Materials, 1973, pp. 264-276.

10. Duke, J. C., Jr., "A Comparison of Quasi-Isotropic Fiber Reinforced Composite Laminates," Lawrence Livermore Report UCRL-15225, November 1979.

11. Jeryan, R. A., "Use of Statistics in Ceramic Design and Evaluation," Proceedings of the Fifth Army Materials Technology Conference, Newport, RI, March 21-25, 1977; Brook Hill Publishing Co., 1973, p. 42.

12. Bullock, R. E., "Strength Ratios of Composite Materials in Flexure and in Tension," Journal of Composite Materials, Vol. 8, April 1974.

13. Bert, C. W., Chen, T. L. C., and Kucay, C. A., "Critical Speeds and Natural Frequencies of Rim-Type Composite-Material Flywheels," Sandia Laboratory Report SAND78-7049, January 1979.

Table 1

TEST RESULTS OF ANALYZED SAMPLES

Wheel		% Glass by Height (Avg.)	% Glass by Volume (Avg.)	% Resin by Weight (Avg.)	Theoretical Density (Avg.)	Measured Density (Avg.)	% Voids (Avg.)	Glass Transition Temp. °C (Avg.)
No.	Dia.							
4	10"	66.55	NA	33.44	1.8529	1.8226	1.633	120
31	12"	66.33	48.39	33.66	1.849	1.812	1.97	117
33	15-1/2"	67.94	50.10	32.06	1.867	1.832	2.10	113.4

Table 2

RING CHARACTERISTICS

Ring Code No.	Mandrel Dia.	Winding Duration in Min.	Fiber	Density by Weight				Composite Density	By Volume	
				Fiber	Resin	% Fiber	% Resin		% Fiber	% Voids
749-7	7.88"	50	Graphite	1.73	1.161	72.5	27.5	1.510	63.24	0.95
TS-7	11.0"	50	Graphite	1.73	1.156	70.0	30.0	1.499	60.89	0.49
#25	14.5"	110	Graphite	1.73	1.156	68.26	31.73	1.468	58.75	1.75

best copy available

Table 3

Laminated S2-Glass/Epoxy Disc, α-9 Stacking Sequence	
Quasi-Isotropic Stiffness, E_{α}	20.0 GPa (2.9 × 10^6 psi)
Poisson Radius, ν_{α}	0.3
Stress at the Center of Disc at Failure, S_{α}	386 MPa (56 ksi)
Density, ρ_{α}	1.805 gm/cm^3 (0.065 lb./in.^{3})
Filament Wound Graphite/Epoxy Ring	
Circumferential Stiffness, E_L	126.2 GPa (18.3 × 10^6 psi)
Radial Stiffness E_T	9.58 GPA (1.39 × 10^6 psi)
Poisson Ratio, ν_{LT}	0.33
Ultimate Circumferential Stress, S_L	1296 MPa (188 ksi)
Ultimate Radial Stress, S_T	12.41 MPa (1.8 ksi)
Density, ρ_G	1.51 gm/cm^3 (0.0545 lb./in.^{3})

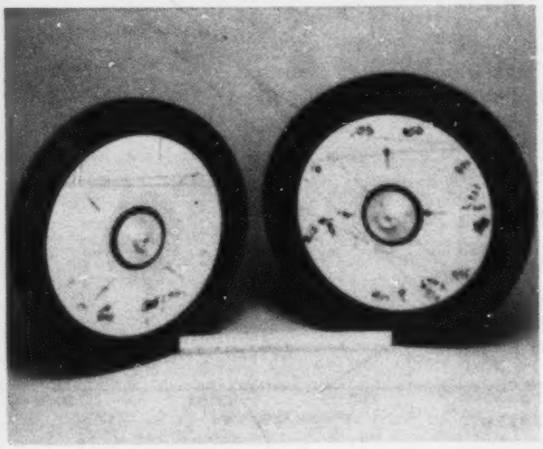

Fig. 1. Hybrid disc-ring flywheels tested at Johns Hopkins Applied Physics Laboratory.

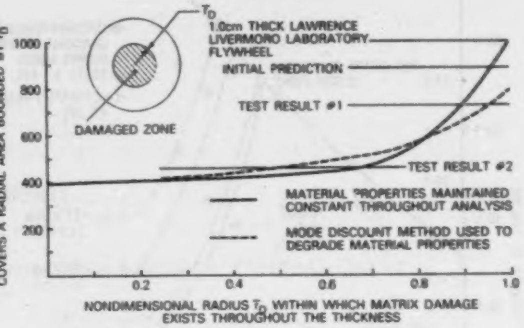

Fig. 2. Progressive matrix failure of a laminated S2-glass/epoxy disc with (0/-45°/45°/90°) stacking sequence.

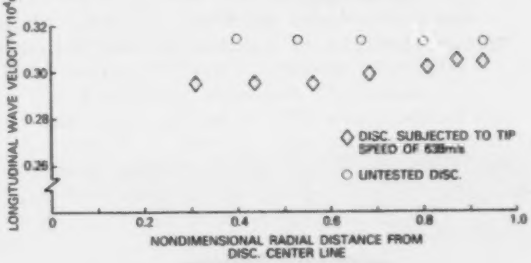

Fig. 3. Comparison of longitudinal wave speeds through the thickness of an S2-glass/epoxy disc before and after spin tests.

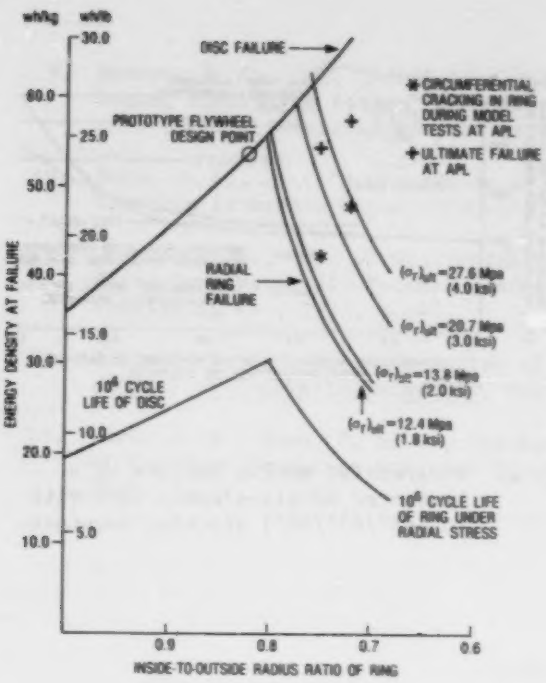

Fig. 4. Optimization curves for prototype flywheel.

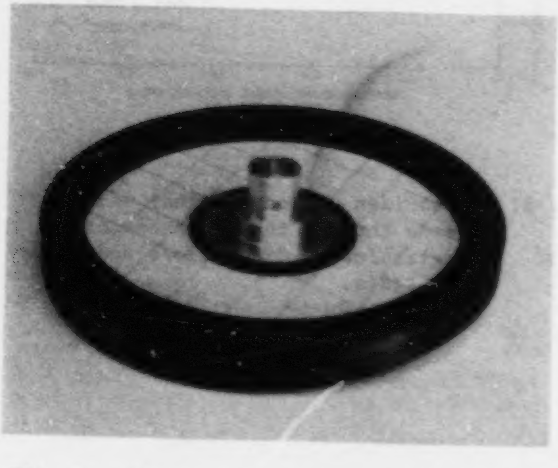

Fig. 5. Disc and ring components prior to assembly.

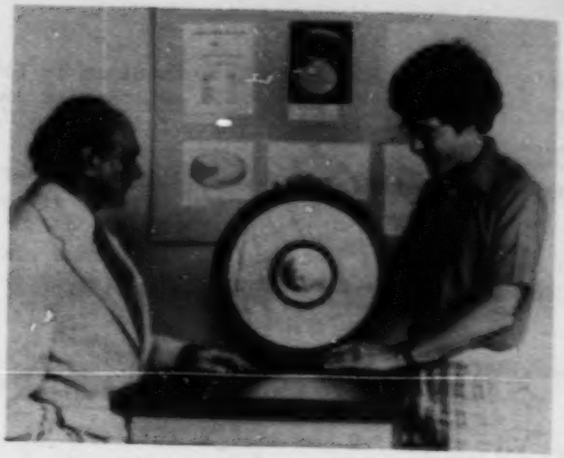

Fig. 6. Finished prototype flywheel.

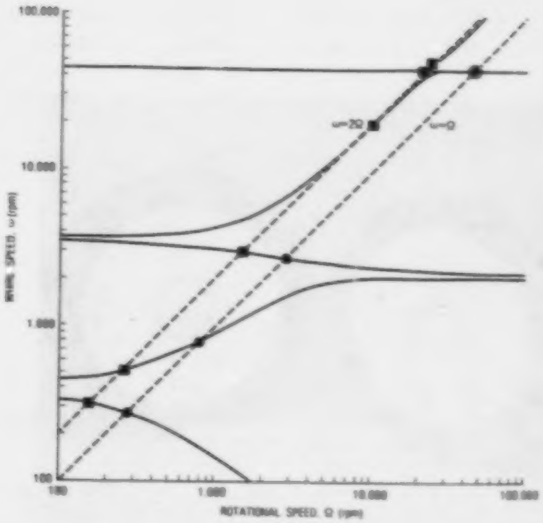

Fig. 7. Predicted whirl-speed curves for prototype flywheel in Oak Ridge test facility.

PROJECT SUMMARY

Project Title: Tapered Thickness Composite Laminate Flywheel Rotor Development Program

Principal Investigator: Satish V. Kulkarni

Organization:
Lawrence Livermore National Laboratory
P.O. Box 808, L-338,
Livermore, CA 94550
Telephone: (415)-422-7128; FTS 532-7128

Project Goals: 1) Prototype development of a tapered thickness composite laminate flywheel rotor; 2) Development of a bonded attachment technique for multiple discs and generation of design data for the rotor/hub elastomeric bond; and 3) Nondestructive inspection of various prototype composite rotors.

Project Status: Four 24 in. diameter, tapered thickness composite laminate rotors (two S2-glass/epoxy and two graphite/epoxy) were fabricated. These rotors utilized the matched metal die compression molding process for laminate fabrication and incorporated the edge thickening concept to increase energy density and a modified layup pattern to reduce strength anisotropy. One 15 in. diameter, constant thickness S2-glass/epoxy rotor was spin tested at APL and yielded an energy density of 30.4 wh/lb at burst. Finite element studies were conducted to optimize chopped fiber molded disc/filament wound rim hybrid rotor configurations. A biaxial stress test fixture was also designed and fabricated and is being assembled presently.

A rotor/hub bonding technique which employs polyurethane instead of natural rubber and adhesives has been developed. Static/fatigue design data for this elastomeric interlayer are being generated. Analytical and fabrication feasibility studies for the bonded attachment techniques for multiple discs have been initiated.

Nondestructive evaluation of the six prototype rotors (Garrett, Brobeck, Rocketdyne, Hercules, GE, and LLNL) was performed prior to spin testing at Y-12, Oak Ridge. Both ultrasonic and radiographic techniques were employed.

Contract Number: W-7405-ENG-48

Contract Period: October 1, 1979, through September 30, 1980

Funding Level: $318,000

Funding Source: U.S. Department of Energy

(Mr. Kulkarni's paper was not prepared for the proceedings.)

PROJECT SUMMARY

Project Title: Evaluation of Composite Flywheel Materials Construction

Principal Investigator: Alan D. Sapowith

Organization:
Avco Systems Division
201 Lowell Street
Wilmington, Massachusetts 01887

Project Goals: Evaluate the specific energy density capability of bi-directional woven flywheel materials.

Project Status: The initial evaluation effort has been completed. A follow-on effort to improve material performance has been initiated.

Bi-directional (radial and circumferential) woven flywheel materials (S Fiberglass) were fabricated and molded into thin discs. Tensile tests were run to determine stiffness and strength of the material as a function of radial location and orientation. These data were used with Avco's WHEEL code to compute the maximum specific energy capability of these materials and the failure mode and location.

Test data and analyses show that specific energy densities of 28 Wh/lb are representative of the materials fabricated. It is interesting to note that while measured hoop strengths were well above 100,000 psi and radial strengths approximately 20,000 psi, the mode of failure was in the hoop direction, primarily at the inside and outside radii. This is the result of the inertial loads in the system.

Contract Number: Subcontract 6692009

Contract Period: August 1979 through August 1980

Funding Level: $34,999

Funding Source: U.S. Department of Energy through Lawrence Livermore Laboratories

EVALUATION OF COMPOSITE FLYWHEEL MATERIALS CONSTRUCTION

Alan D. Sapowith
Avco Systems Division
201 Lowell Street
Wilmington, Massachusetts 01887

ABSTRACT

A preliminary effort was made to characterize the tensile properties of Avco's bi-directional hoop and radial flywheel weave. Initial designs were woven in S glass, molded and tested to determine tensile strengths and moduli in both the hoop and radial directions. These data were used with Avco's WHEEL code to produce estimates of specific energy capability at burst.

The energy estimate for these initial flywheel weaves was 28 W-hrs/lb. Follow-on work was proposed to improve projected performance and such efforts are underway.

INTRODUCTION AND BACKGROUND

Avco started development of its constant stress composite flywheel in 1975 under the U.S. Army MERDC Contract No. DAAG-53-75-0269. This contract culminated in an instrumented burst test which achieved a specific energy at burst of 32.3 watt-hrs/lb. The design results in a constant stress throughout the flywheel, but unlike familiar constant stress shapes, it takes the form of a right circular cylinder. Figure 1 shows the 19.5 inch diameter flywheel tested and its strain instrumentation. Figure 2 shows the constancy of strain (stress) over the wheel as a function of speed. The drop-off in radial strain near the rim is expected.

The design* employs composite fibres in the two principal flywheel directions: radial and circumferential (hoop). The radials tie the hoops together and balance the inertial load over the hoops. This is depicted in Figs. 3 and 4.

The present programs with D.O.E. are to evaluate materials that are woven to produce the desired radial and hoop combinations. An endless spiral bi-directional weave can be coiled to any thickness and molded to directly produce a near constant stress flywheel rotor. This is depicted in Fig. 5. Low costs in mass production are predicted for this design.

PROGRAM DESCRIPTION AND RESULTS

The objective of the initial efforts on the bi-directional weave is to mold flywheel disc materials, approximately 1/8 inch thick, and determine through tensile tests their radial and hoop properties. These in turn are used as inputs to Avco's finite element axisymmetric WHEEL code to estimate specific energy capability at burst of the discs.

Table 1 summarizes the general results of some 50 hoop and radial tensile tests. Figure 6 shows the goal and actual relationships between hoop and radial stiffness as a function of radial station. It is seen that this initial effort fell short of its goals.

The large difference between radial strength and hoop strength would seem to be unbalanced; however, these data, Table 1, when used with the WHEEL code, result in hoop rather than radial failures. This is shown in Table 2. The data here are shown for three choices of radial stiffness: 1) as caculated, 2) times 0.75, 3) times 0.50. Case 2 appears to match the measured data best. The data indicate for the initial material fabricated a specific energy at burst of 28 watt-hrs/lb.

---

* Patent Pending

CONCLUSIONS AND RECOMMENDATIONS

This initial evaluation of the bi-directional weave indicates that for the materials tested, the ratio of radial to hoop stiffness did not meet the optimum values. It is also concluded that for the materials evaluated, variation in radial stiffness has small effects on energy density. Further, it is concluded that both hoop and radial strengths must be improved if burst energies of 40 watt-hrs/lb. are to be achieved.

It has been recommended that these efforts be continued with a goal toward developing hoop and radial strengths compatible with achieving specific energy levels of 40 watt-hrs/lb. Follow-on efforts are in progress.

Table 1.

Summary of Tensile Values
Used in Burst Energy Estimates.

E_θ 10^6 psi	σ_θ 10^5 psi	E_r 10^6 psi	σ_r 10^4 psi
7.1-7.3	1.15-1.48	.42-.55	1.93-2.57

Table 2.
Critical Values of ω^2 and KE/W for $E_r(1)$, $E_r(2)$ and $E_r(3)$.

		Hoops				Radials		
E_r	R(in)	$\frac{\sigma_\theta}{\omega^2}$ (code) (psi)	σ_{crit} = $\sigma_{\theta_{fail}}$ (calc) (10^5 psi)	$\omega^2 = \frac{\sigma_{crit}}{(\sigma_\theta/\omega^2)}$ (10^7 sec^{-2})	$\frac{KE}{W}$ $\frac{\text{Watt hr}}{\text{lb}}$	σ_{crit}= $\sigma_{r_{fafl}}$ (meas) (10^4 psi)	$\omega^2 = \frac{\sigma_{crit}}{(\sigma_r/\omega^2)}$ (10^7 sec^{-2})	$\frac{KE}{W}$
(1)	5.25	0.00894	1.21	1.35		2.04	1.18	31.0
	6.75	0.00949	1.15	1.21		2.57	1.33	
	8.50	0.01052	1.23	1.17		2.25	1.56	
	9.375	0.01092	1.31	1.20		1.93	1.93	
	10.0	0.01311	1.48	1.13	29.7			
(2)	5.25	0.00844	1.21	1.43		2.04	1.42	37.3
	6.75	0.00948	1.15	1.21		2.57	1.55	
	8.50	0.01093	1.23	1.13		2.25	1.79	
	9.375	0.01151	1.31	1.14		1.93	2.18	
	10.0	0.01389	1.48	1.07	28.0			
(3)	5.25	0.00775	1.21	1.56		2.04	1.92	50.5
	6.75	0.00942	1.15	1.22		2.57	1.99	
	8.50	0.01147	1.23	1.07		2.25	2.21	
	9.375	0.01230	1.31	1.07		1.93	2.64	
	10.0	0.01497	1.48	9.89×10^6	26.0			

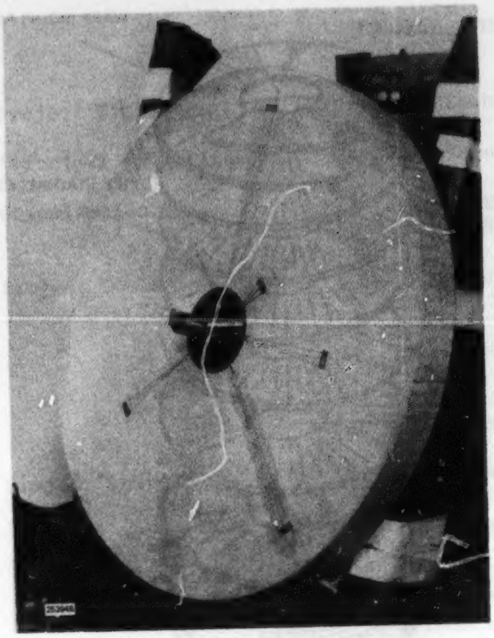

Fig. 1. Second Kevlar Flywheel.

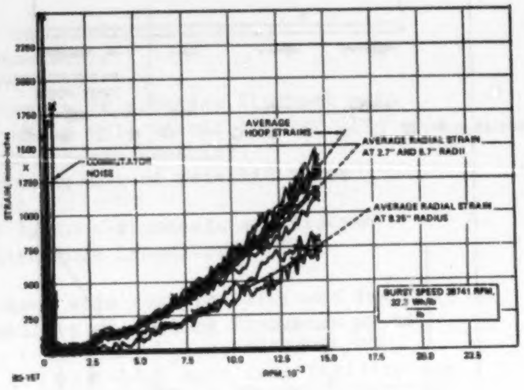

Fig. 2. Raw Strain Data.

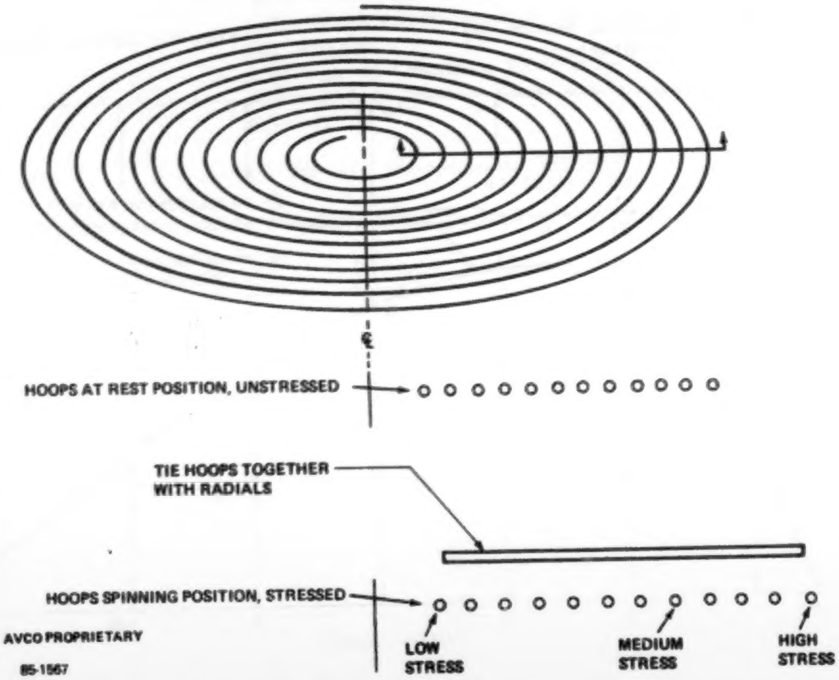
HOOPS AT REST POSITION, UNSTRESSED
TIE HOOPS TOGETHER WITH RADIALS
HOOPS SPINNING POSITION, STRESSED
LOW STRESS
MEDIUM STRESS
HIGH STRESS
AVCO PROPRIETARY
85-1567

Fig. 3. Avco's Flywheel Design (a).
(Patent Pending).

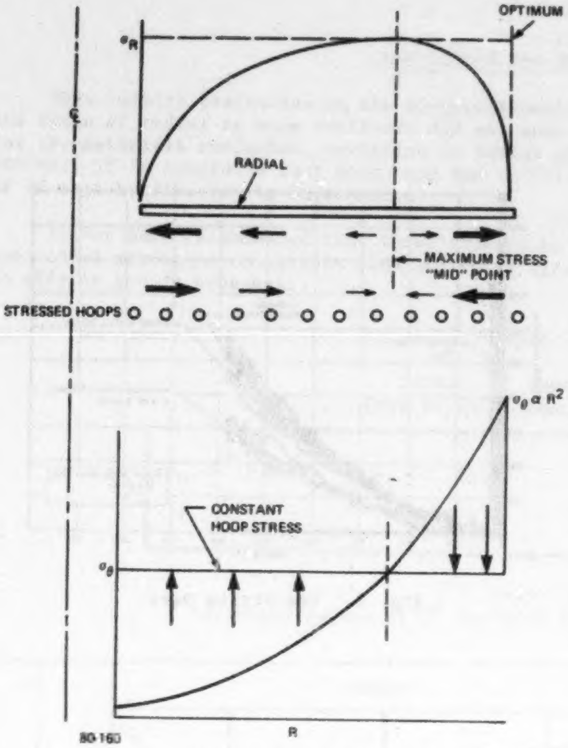
OPTIMUM
σR
σ
RADIAL
MAXIMUM STRESS
"MID" POINT
STRESSED HOOPS
σθ α R²
CONSTANT
HOOP STRESS
σθ
R
80-160

Fig. 4. Avco's Flywheel Design (b). (Patent Pending).

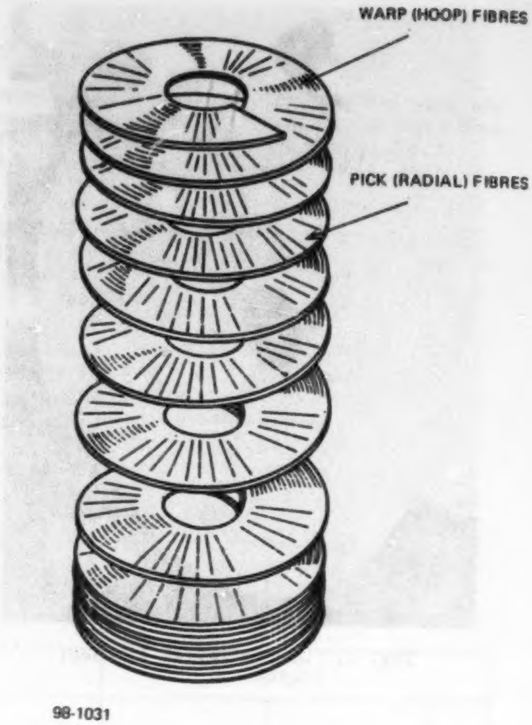
WARP (HOOP) FIBRES
PICK (RADIAL) FIBRES
98-1031

Fig. 5. Spiral Weave.

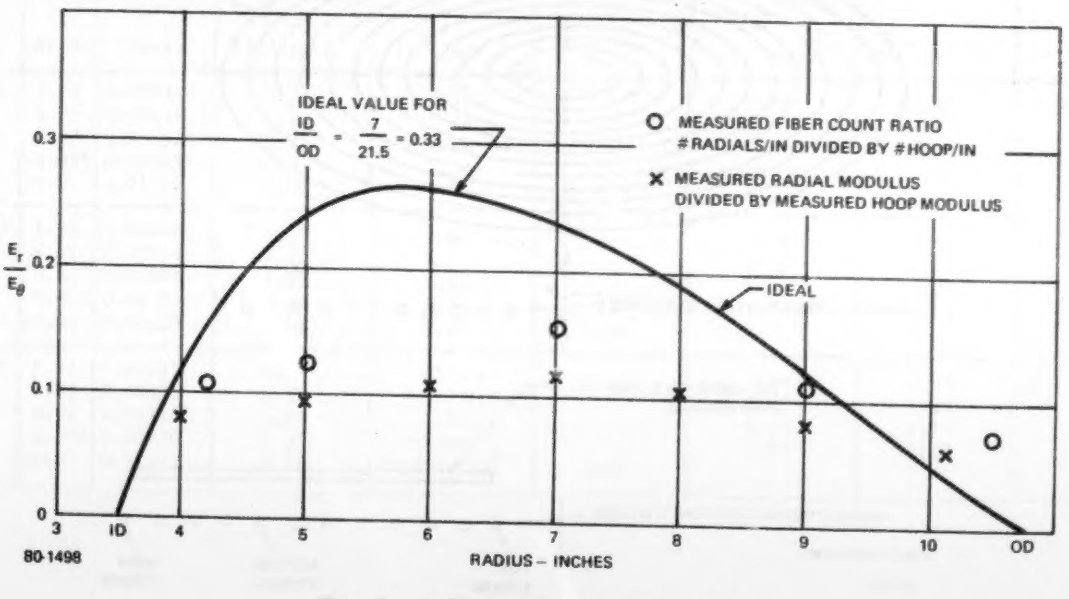

Fig. 6. E_r/E_θ vs. Radius for Typical Fiberglass Disc.

PROJECT SUMMARY

Project Title: Flywheel Technology Development at APL

Principal Investigator: David W. Rabenhorst

Organization: The Johns Hopkins University
Applied Physics Laboratory

Project Goals:

1. Define improvements to existing flywheel spin test facility which will permit testing flywheels up to 50 kilowatt-hours capacity.
2. Preliminary development of metallic glass ribbon flywheel.
3. Spin tests of various flywheels as directed by Lawrence Livermore Laboratory.

Project Status:

1. A 5 kilowatt-hour spin test facility was defined having a capability of testing flywheels up to 200 pounds at rotational speeds up to 60,000 rpm. A 50 kilowatt-hour spin test facility was defined having a capability of testing flywheels up to 4000 pounds at rotational speeds up to 18,000 rpm. Spin tests have demonstrated the feasibility of low cost metallic glass ribbon flywheels at energy densities of 12 to 24 wh/lb and 5000 to 10,000 wh/ft^3.
2. Feasibility has been demonstrated of recording television pictures at a rate up to 960 frames per second.
3. A number of Lawrence Livermore Laboratory furnished flywheels have been successfully spin tested.

Contract Number: W-7405-ENG-48, Subcontract 7825509

Contract Period: 21 March 1980 through 31 December 1980

Funding Level:

Section 1 - Flywheel Test Facility	$157,400
Section 2 - METGLAS Flywheel	$50,000
Section 3 - Flywheel Testing	$71,800

Funding Source: U.S. Department of Energy through the
Lawrence Livermore Laboratory

FLYWHEEL TECHNOLOGY DEVELOPMENT AT APL

D. W. Rabenhorst
The Johns Hopkins University
Applied Physics Laboratory

ABSTRACT

This paper summarizes a program which began on March 21, 1980 and is scheduled to end on December 31, 1980. It covers the Applied Physics Laboratory's flywheel technology efforts in three separate areas. The first area covers a rather extensive design study for an expansion of the Applied Physics Laboratory flywheel spin test facility to accommodate burst testing of flywheels up to 50 kw hours capacity. The second area covers the preliminary development of flywheels made from metallic glass ribbon. The third area concerns the spin testing of a variety of flywheels fabricated outside the Laboratory, and provided by the Lawrence Livermore Laboratory.

The conceptual design of the new flywheel spin test facility is complete, and the preparation of construction details, including cost and schedule items, is proceeding on schedule. The metallic glass flywheel spin testing to date has indicated that this configuration will be quite competitive in terms of energy per unit weight, energy per unit cost, and most especially in energy per unit volume. The outside flywheel spin testing program has included ten spin tests involving five different flywheel configurations. All were eventually spin tested to destruction, with complete video coverage.

INTRODUCTION

The work covered by this report was conducted under a single subcontract from the Lawrence Livermore Laboratory, which was divided into three sections. The first section was entitled FLYWHEEL SPIN TEST FACILITY: the second section was entitled METGLAS DEVELOPMENT: the third section was entitled FLYWHEEL SPIN TESTING. Although this work was initiated well into the fiscal 1980 year, it was substantially completed by the time of this report. Positive results were indicated in all three sections of the program, and recommendations are made for the continuation of the work in each of these three sections. In view of the diversity of technology in these three program sections, they will be reported in the following paragraphs as though they were separate programs.

Section I - Flywheel Spin Test Facility

As directed by the Lawrence Livermore Laboratory, the facility improvement design effort was divided into two distinct areas. The first of these involved the detail design, cost estimate, and projected schedule for improvements to the existing APL facility which would enable the spin testing of flywheels up to 50 kw hour capacity. While a new spin pit will be necessary, a substantial portion of the existing instrumentation, controls, video recording and operating equipment would be utilized. Also, an important factor in this spin test facility improvement program was the existence at APL of the engine-driven compressors which would be used to drive the air turbines in the new facility.

The second requirement stipulated by LLL was that an additional spin test facility to accommodate flywheels up to 5 kw hour capacity would be designed to be located within the 50 kw hour facility, in order to permit utilizing the essential elements of the drive train, the vacuum container and the vacuum equipment, as well as the instrumentation and controls of the larger facility for the 5 kw hour flywheel testing. The final design showed that significant savings would result from the combined 5 kw hour/50 kw hour spin test facility, with relatively few compromises in either case.

A substantial portion of the flywheel test facility effort involved a hardware feasibility demonstration of high speed television equipment, which was proposed to be utilized in the future large flywheel test facility described above.

The general characteristics of the 5 kw hour flywheel test facility are shown in Table 1. The performance characteristics represent the respective maximum conditions over a broad range of flywheel performance and a variety of flywheel configurations. The high rotational speed reflects the characteristics of a high performance flywheel with energy density of the order of 37 watt hours per pound, and also reflects a flywheel configuration having the highest intrinsic rotational speed for this energy density. This would be typical of the tapered solid disc flywheel, which, at an energy density of 37 watt hours per pound and a maximum diameter of 32 inches, could have a burst speed as high as 60,000 rpm. The high rotating mass of 1500 pounds represents the load capability of the turbine selected, and is well in excess of the maximum flywheel weight expected to be encountered.

TABLE 1

5 kwh Spin Test Facility Characteristics

Maximum Diameter = 32"; Maximum Axial Length = 31"

Performance Limits

Air Turbine	Maximum RPM	Maximum Weight	Nominal Horsepower
8" with 2:1 increaser	60,000	200 lb	20 - 30
14" with 2:1 increaser	36,000	200 lb	60 - 70
8" without increaser	30,000	1500 lb	20 - 30

The basic turbine for the 5 kw hour facility is the 8 inch Barbour Stockwell model with a nominal rating of 1500 pounds rotating mass at rotational speeds up to 30,000 rpm. A 2 to 1 speed increaser raises the maximum rotational speed to 60,000 rpm, but at a reduced rotating mass of 200 pounds. This is consistent with the energy density at this rotational speed at 5 kw hour total energy. For example, a 5 kw hour flywheel having an energy density of 37 watt-hours per pound will weigh 185 pounds.

Although the 8 inch turbine with a 2 to 1 speed increaser does provide adequate rotational speed range, it does not have sufficient horsepower to cover the life cycle requirements specified for the 5 kw hour test facility. For this reason a 14 inch Barbour Stockwell air turbine is also provided, which is also capable of being used with the same 2 to 1 speed increaser. This arrangement provides an average of 60 to 70 horsepower at rotational speeds up to 36,000 rpm. This is consistent with the life cycle requirements expected to be encountered.

The principal characteristics of the 50 kw hour flywheel spin test facility are shown in Table 2. The air turbines for this facility are the same as those specified for the 5 kw hour facility. However, they are used without the speed increaser to permit maximum rotational weight capability. The 50 kw hour flywheel would ordinarily require approximately 400 hp to give comparable life cycle testing times that the 50 hp turbine would provide for the 5 kw hour facility. However, the sponsor (LLL) recommended that, initially, the 50 hp air turbine be utilized in the large test facility, in order to minimize the time and funding required to make this facility initially available.

TABLE 2

50 kwh Spin Test Facility Characteristics

Maximum Diameter = 65"; Maximum Axial Length = 62"

	Performance Limits		
Air Turbine	Maximum RPM	Maximum Weight	Nominal Horsepower
8 inch	30,000	1500 lb	20 - 30
14 inch	18,000	4000 lb	60 - 70
14 inch[b]	10,000	5000 lb[a]	50 - 60[a,b]

[a] Projected value

[b] Temporary limit. Would eventually be ≈400 horsepower.

Also, a somewhat lesser compromise was made in limiting the maximum flywheel diameter to 65 inches; whereas, it is conceivable that some stationary flywheel applications could have as a design parameter the minimization of flywheel rotational speed, which could result in larger flywheel diameters. However, it is felt that the proposed facility design covers the most likely flywheel materials, configurations, performance levels and maximum sizes expected to be encountered in the foreseeable future.

It is also believed that this facility, as proposed, will cover not only the lower cost stationary flywheels, but also the higher performance vehicular flywheels which could be spin tested in this facility. This includes the capability on the low end of the performance spectrum of spin testing flywheels weighing as much as 5000 pounds at the lower rotational speed range, and flywheels weighing as much as 1500 pounds at the higher rotational speed range of 30,000 rpm.

The overall proposed APL spin test facility is shown in Figure 1. This three-level facility allows the complete spin chamber to be located below ground, while allowing adequate head room for the installation and removal of flywheels and the containment rings, as required. The third, or lower level, facilitates access to the bottom of the spin chamber for the installation and checkout of optical systems, as well as facility instrumentation and controls. Obviously, this access is also provided at the top end of the spin chamber.

As indicated in Figure 1, the engine-driven compressors, which provide the air at 90 to 120 psi to drive the turbines, are located immediately adjacent to the test facility. These existing compressors allow the use of the air turbines in lieu of the much more expensive electric drive systems, and eliminate the additional expense of providing electrical load banks for braking operations. The air turbines selected have reverse buckets for braking, and thus eliminate the need for a separate braking system.

The test facility control and instrumentation console is located in the building adjacent to the proposed facility. It is mostly comprised of existing equipment, thus minimizing the cost of the proposed facility.

The high speed television equipment, developed by the Video Logic Corporation of Sunnyvale, California, has demonstrated the feasibility of multiplexing two or more high-speed television cameras in a digitally synchronized format at a time interval between respective TV cameras equivalent to that required for a frame rate of 720 frames per second. The picture display from this TV equipment is a newly developed wide screen high fidelity format and the system demonstrated has an instant replay capability in either variable slow motion or still frame. The equipment also has the capability of immediately producing hard copy pictures printed directly from the video tape.

The high speed TV demonstration program involved the use of a two-camera system to demonstrate the foregoing capability. However, a considerable amount of work remains to be accomplished before a complete 960 frames per second television system can be put into operation in the proposed facility. This TV system may eventually consist of four multiplexed TV cameras operating in conjunction with a video recorder having a 10 megahertz band width. All principal elements of the proposed system exist at the present time.

According to the present schedule, a detailed installation design, as well as a cost and implementation plan will be completed by the end of the current calendar year.

Section II - METGLAS* Flywheel Development

The present METGLAS flywheel program involves the scale model testing as well as full-scale testing of flywheels up to a capacity of 200 watt-hours. It also includes the complete definition of a METGLAS ribbon flywheel having a one kilowatt hour capability. The 50 watt-hour sub-scale development program was successfully completed, leading to the satisfactory design for the full-scale 200 watt-hour flywheel. The typical flywheel in the series consisted of several hundred turns of METGLAS ribbon wound on a four-spoked intermediate aluminum hub and bonded only at the hub radial locations. Termination of the outer edge of the flywheel was achieved by bonding the complete final revolution to its substrate layer. The typical construction of the METGLAS amorphous metal ribbon flywheel is illustrated in Figure 2.

The results of the METGLAS ribbon flywheel program to date have been quite encouraging. However, a considerable amount of work needs to be done before flywheels of this configuration can be considered acceptable for commercial applications. The current program demonstrated that METGLAS flywheels can have an apparent useable energy density in excess of 12 watt-hours per pound and 4500 watt-hours per cubic foot. The studies in the program also indicated that METGLAS ribbon flywheels in a quasi-isotropic disc configuration may have twice this capacity. However, the present program does not include provision for long term testing to demonstrate this material under static fatigue and cyclic fatigue conditions. On the other hand, the encouraging results of the program to date appear to warrant support for follow-on programs which would investigate these areas. The current studies have shown that future METGLAS amorphous metal ribbon flywheels might have useable energy densities in the range of 20 to 30 watt hours per pound with useable energy per unit volume of about 10,000 watt-hours per cubic foot. These studies also indicated that if the METGLAS ribbon can be produced for $1 to $2 per pound, as predicted, then it can be reasonably expected that the resulting METGLAS ribbon flywheels can be made for less than $100 per kilowatt hour.

---

*Trademark of Allied Chemical Company, Morristown, New Jersey

Section III - Flywheel Testing

The APL/LLL contract provides for the spin testing of approximately ten flywheels fabricated by other agencies. By the time of this report, the Laboratory has conducted ten such spin tests involving five flywheels received from LLL. The typical program for the spin testing of each flywheel received is as follows: First, upon receipt at APL, the flywheel is carefully measured and weighed and its polar moment of inertia calculated. A preliminary spin test is then conducted using a dummy aluminum flywheel having approximately the same mass as the test flywheel. The dummy flywheel is spun over the entire rotational speed range expected to be encountered with the test flywheel, and notations are made of any system vibrational perturbances which are encountered. These include the various critical speeds of the system as well as an occasional minor vibration from causes other than critical speeds.

The second pre-test is conducted with a second dummy flywheel specifically designed to have a polar moment of inertia approximately the same as that of the test flywheel. This flywheel is then spin tested to a rotational speed up to at least the second critical speed of the system, in order to demonstrate that the first and second critical speeds, as well as any other perturbances encountered during the spin test, will not be damaging during the eventual test of the designated flywheel. The locations in the rotational speed range of the various types of disturbances vary from test to test depending upon the mass and moment of inertia of the flywheel being tested.

Each flywheel spin test includes a continuous video recording with phase locked Strobe lighting, such that the flywheel appears to be motionless on any given picture. Figure 3 illustrates a typical TV picture taken at a frame rate of 240 full pictures per second. In this picture it can be seen that a peripheral crack has developed in the outer windings of the flywheel, and that this crack has proceeded nearly all the way around the flywheel. In this particular instance the digital code of each television picture enabled the exact correlation of this crack initiation with a sudden increase in the vacuum pressure decay and corresponding axial vibration. Also, subsequent pictures, together with an examination of the flywheel debris, indicated that the bond between the aluminum hub and the fiberglass flywheel disc failed in shear, probably caused by the delaminated outer ring.

Table 3 is a summary of all the flywheels tested to date in the current program which began in March 21, 1980.

TABLE 3
Summary of Flywheel Testing through October 15, 1980

APL/LLL Subcontract No. 7825504

Test No.	Date	Test Designation	Other Designation	Type of Flywheel	RPM Reached
1 -	Prior to Contract	LLL 80-2SR	APL Sketch	rpm simulator	51,000
2 -	7/2/80	LLL 80-2SI	APL Sketch	Inertial simulator	8,000
3 -	8/1/80	LLL 80-2SI-2	APL Sketch	Inertia simulator	9,200
4 -	8/22/80	LLL 80-2	- -	Plain f.g. disc	49,050
5 -	9/3/80	LLL 80-2-2	- -	Plain f.g. disc	49,320
6 -	9/16/80	LLL 80-3SI	APL Sketch	Inertia simulator	8,300
7 -	9/18/80	LLL 80-3	GE Des. 3 #20	Ring and α ply	46,000
8 -	10/3/80	LLL 80-4	GE Des. 3 #23	Ring and α ply	46,060
9 -	10/15/80	LLL 80-5SI	APL Sketch	Inertia simulator	9,000
10 -	10/15/80	LLL 80-5	LLNL TT-1	Tapered fig. disc	NA

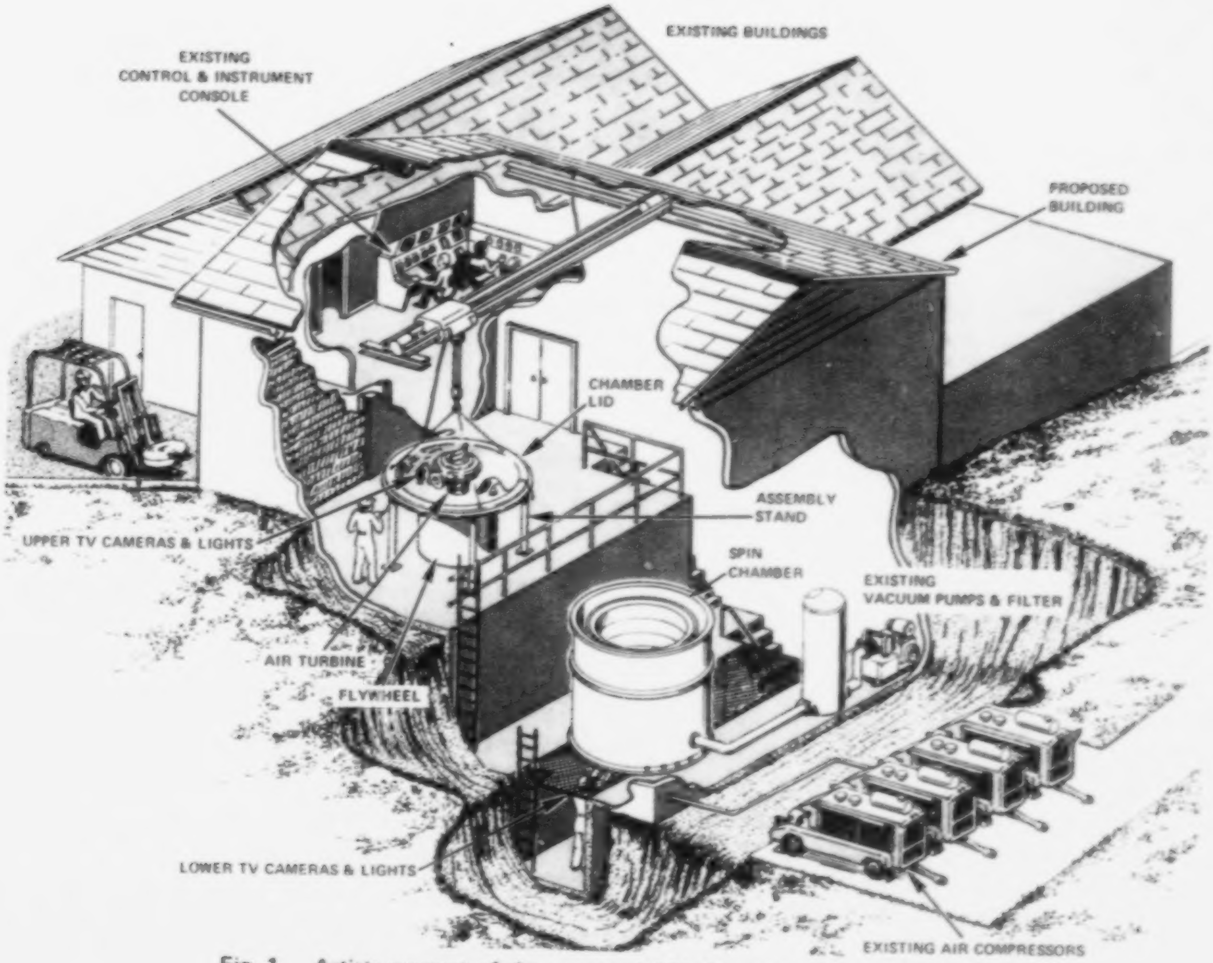
EXISTING BUILDINGS
EXISTING CONTROL & INSTRUMENT CONSOLE
PROPOSED BUILDING
CHAMBER LID
ASSEMBLY STAND
UPPER TV CAMERAS & LIGHTS
SPIN CHAMBER
EXISTING VACUUM PUMPS & FILTER
AIR TURBINE
FLYWHEEL
LOWER TV CAMERAS & LIGHTS
EXISTING AIR COMPRESSORS

Fig. 1 Artists concept of the proposed APL flywheel spin test facility.

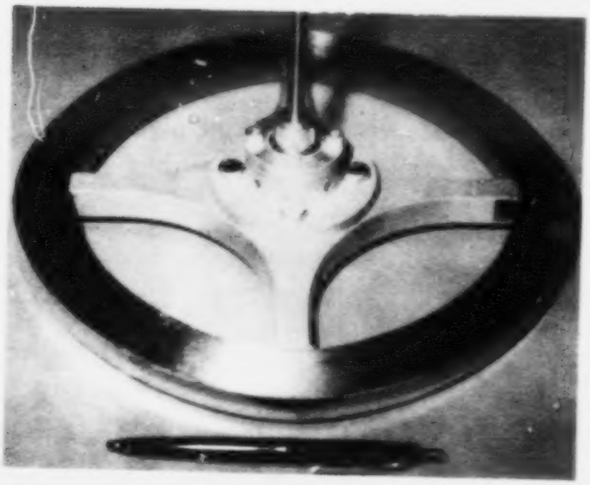

Fig. 2 APL experimental METGLAS ribbon flywheel.

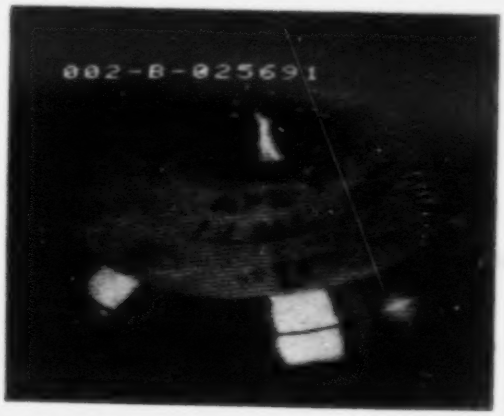
002-B-025691

Fig. 3 High speed TV picture.

PROJECT SUMMARY

Project Title: Low-Cost Compression Molded Fiber Reinforced Flywheels

Principal Investigator: Dr. John F. Kay

Organization:
Owens-Corning Fiberglas
Research and Development Division
Technical Center
Granville, Ohio 43023

Project Goals: To fabricate low-cost, medium-performance flywheel rotors using the compression molding process.

Project Status: Two rotor shapes are being considered: a constant one-inch thickness disc and a tapered Stodola profile. Two reinforcing glass fibers, E glass and S-2 Glass^{R}, are being employed in one- and two-inch chop length.

Preliminary work on constant thickness moldings indicates that compression molding is a viable process for producing flywheel rotors in a low-cost, high-throughput fashion suitable for automotive applications.

The variables to be addressed in future work are the SMC charge configuration, molding time, molding temperature, molding pressure, and flow control to maintain optimal reinforcement positioning. Molding of tapered thickness discs must also be addressed.

Contract Number: (P.O. #9093009)

Contract Period: June 24-September 30, 1980

Funding Level: $44,700

Funding Source: U.S. Department of Energy through Lawrence Livermore National Laboratories

LOW-COST COMPRESSION MOLDED FIBER REINFORCED FLYWHEELS

John F. Kay
Research and Development Division
Owens-Corning Fiberglas
Technical Center
Granville, Ohio 43023

ABSTRACT

Compression molded structural sheet molding compound (SMC) has been used to fabricate energy storage flywheel rotors. This technique has the potential of low-cost, high-throughput production of rotors for the automobile industry.

An isophthalic polyester resin and either E or S-2 Glass^R reinforcement were used for both constant and tapered molded rotors 21 inches in diameter. Materials characterizations have shown a tensile strength of 39 Ksi for the S-2 Glass^R reinforced rotors, which would allow the flywheel rotor to store approximately 44 watt hours per kilogram.

INTRODUCTION

Fiber reinforced plastic composites are attractive for energy storage flywheels since their high strengths and low densities provide high specific strengths when compared to metals.

For a filament-wound flywheel, the anisotropy of a composite allows the high-strength fibers to be aligned in the direction of the maximum stresses imposed by rotation. The filament wound rings are, however, utilized to their greatest energy storage potential when placed as far from the axis of rotation as possible. Among the methods to connect this filament wound ring to a central axis of rotation are spokes, machined hubs, other concentric rings, or solid disc-type cores.

Using unidirectional prepreg materials, several quasi-isotropic composite laminate rotor core designs were tested and were found to fail prematurely due to large directional strength variations in the laminated disc[1,2]. While each ply of unidirectional prepreg has very high strength when tested in the 0°, or fiber direction, this strength is compromised with the addition of other plies at angles up to 90° to its fiber axis. Interply shear also becomes a limiting design factor with the quasi-isotropic disc rotor.

In an attempt to provide a flywheel rotor that is isotropic within the plane orthogonal to the axis of rotation, a compression-molded disc made from structural sheet molding compound has been considered. While a randomly-oriented short fiber reinforced polyester-based composite does not possess the individual ply strength of unidirectional prepreg materials, it is hoped that a transversely isotropic disc can be made which will nearly possess the properties of the quasi-isotropic disc in its weakest direction. The problems of interply shearing effects would also be reduced. The cost of a compression molded flywheel core would be substantially less than that of a machined metal hub or series of concentrically wound inner core rings of filamentary composite material.

The radial expansion of the core material is contained with a filament-wound ring placed about its circumference. The high circumferential modulus of the continuous filament reinforced ring prevents radial expansion of the core as the wheel stores energy by rotation, results in higher operational speeds and, thus, enables storage of more kinetic energy.

The preliminary results described in this report describe efforts to investigate the feasibility of a compression molded flywheel core to be contained by a filament wound ring. The goal is a low-cost flywheel rotor system with an approximate energy storage density of 44 watt-hours per kilogram (20 watt-hours per pound) suitable for automobile applications.

MATERIAL

Compression molded sheet molding compound (SMC) provides a low-cost method of producing structural composites from glass reinforced plastic[3]. Structural sheet molding compounds are composed of 30-70 percent (by weight) fiber reinforcement and are designed to compete with and/or replace metal parts in load-bearing or structural applications. Figure 1 is a schematic diagram of the equipment used to make sheet molding compound, which is then compression molded to form the flywheel disc. The SMC-R process is attractive because of the material property adjustability that can be obtained by changing the resin, glass reinforcement type, length and relative volume fraction within the formulation.

The specific SMC formulation used in this study is listed in Table 1. The OCF E987 resin is a modified isophthalic polyester resin designed for use in structural sheet molding compound, chosen primarily for its low linear shrinkage and excellent dimensional stability. No filler was used because of the high-glass loading. R65 SMC material is composed of 35 percent (weight) resin paste and 65 percent chopped E or S-2 Glass^R roving. The high virgin fiber tensile strength of S-2 Glass^R (Table 2) results in increased tensile properties for the SMC composite and, thus, makes it attractive for the flywheel core material. The mechanical properties of R65, derived from flat laminate tests, are listed in Table 3 for one-inch and two-inch chopped reinforcements; the two-inch chopped fiber length results in slight increases in tensile properties.

Typical room temperature tensile stress-strain curves for R65 SMC materials are shown in Figure 2. Both E and S-2 Glass^R reinforced R65 exhibit two linear regions in the stress versus strain curve. The initial tangent modulus reported in Table 3 is the slope of the line to the proportional limit. The transition region between the initial slope and the lower secondary slope (higher strain rate) occurs at 0.5-0.7 percent strain. The transition region location depends both on the full-scale load used on the test instrument and on interpretation of the resultant curve. The initial slope of SMC reinforced with S-2 Glass^R roving is higher and displayed higher tensile strains to the proportional limit. The transition for both materials lasts for about 0.5 percent strain beyond the proportional limit where a secondary modulus 72 percent of the initial tangent modulus (79 percent for S-2 Glass^R) dictates the behavior to failure.

MOLD DESIGN

Two flywheel profiles were designed by LLL to the material properties of R65 SMC. The first is a constant thickness profile (Figure 3a) one-inch thick, 21 inches in diameter. The second design is a Stodola, tapered thickness profile (Figure 3b) one-inch thick at the center, 0.667 inches at the outermost edge.

The mold (Figure 4a) was machined at Gougler Industries*, and features an hydraulic ejector plate system (Figure 4b) to facilitate removal of the part from the mold. The tapered profile will be molded in the same mold base as the constant thickness disc by using a tapered thickness mold insert. This insert is approximately 23 inches in diameter and is interchangeable with the constant thickness insert within the same mold base. The mold is installed in a large hydraulic press (Figure 5) with steam

*Gougler Industries, Kent, Ohio

heated platens. By varying the steam pressure through the press platens and the mold base, the temperature of the molding surfaces can be controlled.

FLYWHEEL DISC MOLDING

Fifteen constant thickness discs have been molded to develop prototype parts. From the molded density of the flat laminates used for material property characterizations, a change of 22.5 pounds was determined to be adequate to test the concept.

Eighteen plies of R65 SMC were cut to 19.5 inch preform size, 88 percent coverage of the mold (Figure 6a). As each successive ply is added to the stack, the protective polyethylene film is removed (Figure 6b) and gross air pockets eliminated by rolling (Figure 7a), resulting in a stack of consolidated R65 SMC plies. The plies are placed in the mold (Figure 8a) and held at 270°F, 1000 psi, for 35 minutes. This long molding time is a result of the time-temperature relationship that depends on part thickness. Holding the part within the mold while exotherm heat is removed through the mold allows the curing reaction to proceed to completion and greatly reduces residual thermal stresses. The ejector system provides easy removal of the finished part (Figure 8b, 9). After the part has cooled, it is deflashed and is ready for installation of a filament wound containment ring.

CONCLUSIONS

Preliminary moldings have shown that fully-consolidated compression molded flywheel rotors can be made with R65 structural sheet molding compound. The interlaminar shear stresses that would be present using a quasi-isotropic lay-up of unidirectional prepreg are precluded with the transversely isotropic SMC rotor.

Although fully-consolidated constant-thickness rotor discs have been successfully molded, the problem of material flow at the mold edge, preform optimal size, and cure cycle optimization must still be addressed. Also, S-2 Glass^{R} reinforcement and the tapered profile discs have yet to be implemented.

Together with its filament-wound containment ring, it is hoped that this flywheel rotor concept can be made to store 44 watt-hours per kilogram and become part of an automobile flywheel energy storage system.

REFERENCES

1. Kulkarni, S. V., R. G. Stone, and R. H. Toland, "Prototype Development of an Optimized, Tapered-Thickness, Graphite/Epoxy Composite Flywheel," UCRL-52623, Lawrence Livermore Laboratory, November 1978.

2. Duke, J. C., "A Comparison of Quasi-Isotropic Fiber Reinforced Composite Laminates," UCRL-15225, Lawrence Livermore Laboratory, November 1979.

3. Jutte, R. B. "Structural SMC - Material, Process, and Performance Review," presented at SAE Congress and Exposition, Cobo Hall, Detroit, Michigan, February 27 - March 3, 1978.

Table 1
R65 SMC Resin Paste Formulation

	Component	Source/Trade Name	Weight (grams)
Resin	isophthalic polyester	OCF E987	12,000
Initiator	t-butyl perbenzoate	Lucidol	120
Thickener	magnesium oxide	Hatco Modifier M	600
Mold Release	zinc stearate	Tenneco DLG-10	480

Table 2
Glass Fiber Reinforcement Properties

	E Glass	S-2 Glass^R
Tensile strength Ksi (MPa)	500 (3445)	665 (4581)
Tensile modulus Msi (GPa)	10.5 (72.35)	12.6 (86.81)
Tensile elongation to failure (%)	4.8	5.4
Specific gravity lb/in^3 (g/cm^3)	0.094 (2.60)	0.090 (2.49)

Table 3
Structural SMC Data Summary - R65

	E Glass 1 Inch	E Glass 2 Inch	S-2 Glass^R 1 Inch	S-2 Glass^R 2 Inch
Tensile strength Ksi (MPa)	29.3 (202)	32.8 (225)	36.7 (253)	39.3 (271)
Tensile modulus Msi (GPa)	2.15 (14.8)	2.10 (14.5)	2.40 (16.5)	2.41 (16.6)
Tensile elongation to failure (%)	1.86	2.12	2.07	2.46
Poisson's Ratio	0.26	0.26	0.26	0.25
Density lb/in^3 (g/cm^3)	0.063 (1.738)	0.063 (1.752)	0.064 (1.770)	0.062 (1.721)

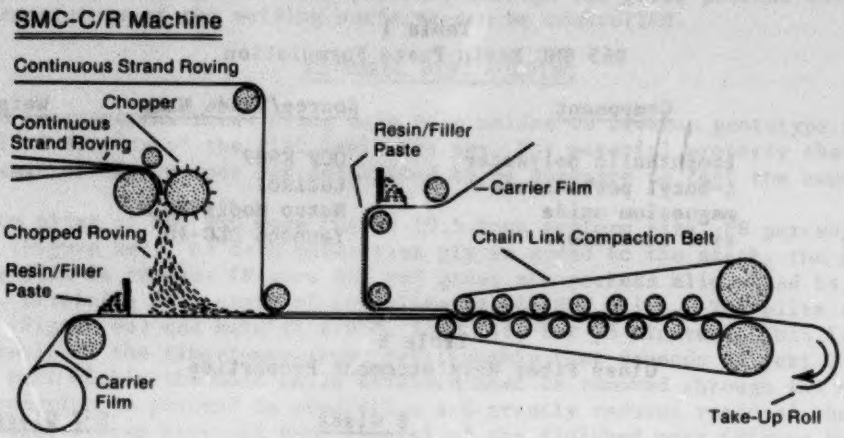
SMC-C/R Machine
Continuous Strand Roving
Chopper
Continuous Strand Roving
Resin/Filler Paste
Carrier Film
Chopped Roving
Chain Link Compaction Belt
Resin/Filler Paste
Carrier Film
Take-Up Roll

Figure 1- Schematic of SMC machine capable of producing SMC-R or SMC C/R. In making R65 SMC for a flywheel disc, a thin layer of polyester paste is deposited on the carrier film, onto which the one-inch or two-inch chopped glass roving is deposited. No continuous strands are added, but another layer of polyester paste is placed over the chopped glass. The "kneading" action of the offset chain-link compaction belt causes complete wetting of all fibers. The material is stored on a take-uproll until ready to use.

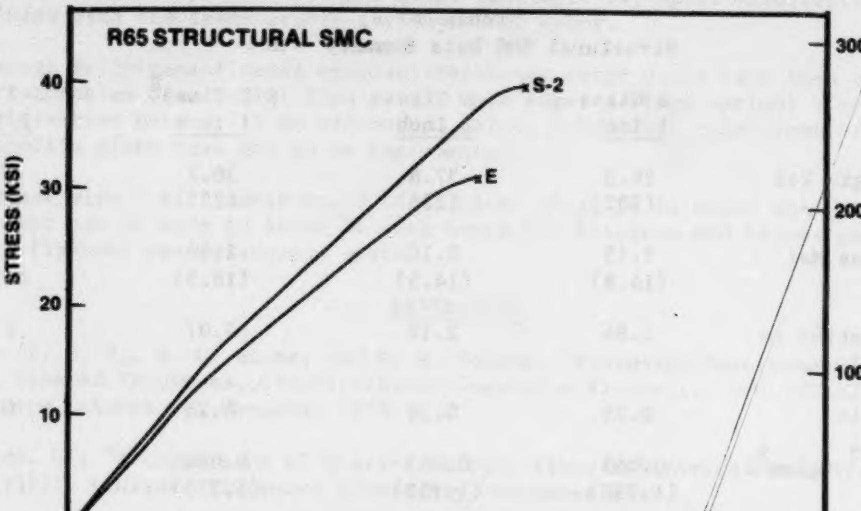

Figure 2 - Room temperature tensile behavior of R65 structural SMC. The transition between the initial tangent modulus to the proportional limit and the lower secondary modulus occurs at 0.5-0.7 percent strain. This transition is considered to be indicative of matrix damage. Increased strength and strain to failure are characteristic of SMC reinforced with S-2 Glass^{R} roving.

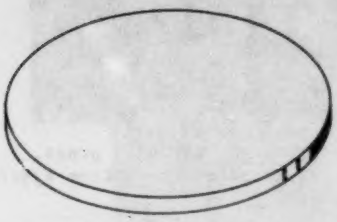

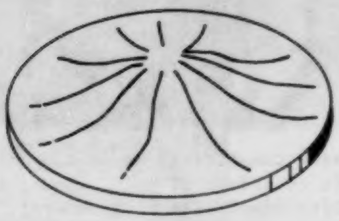

Figure 3a - Constant thickness profile rotor. The disc diameter is 21 inches at a constant one-inch thickness. Theoretical weight of the disc molded from R65 SMC is 22.5 pounds.

Figure 3b - Tapered thickness "Stodola" profile rotor. The disc diameter is 21 inches with a maximum thickness of one inch at the center and 0.0667 inches at the outermost edge. Theoretical weight of the disc molded from R65 SMC is 18.76 pounds.

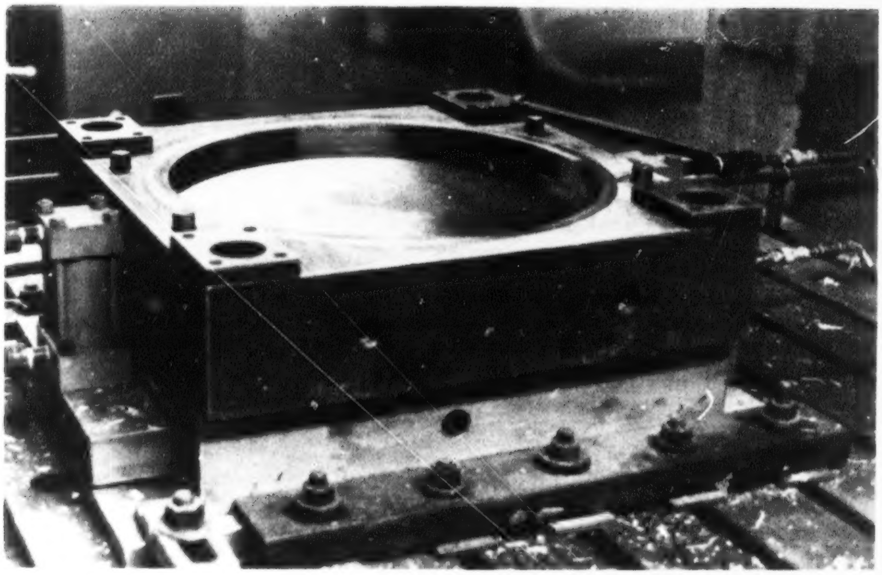

Figure 4a - Constant thickness mold installed in steam-heated hydraulic press. Hydraulic cylinders at each side of the mold base serve to raise the bottom ejector plate which simplifies part removal.

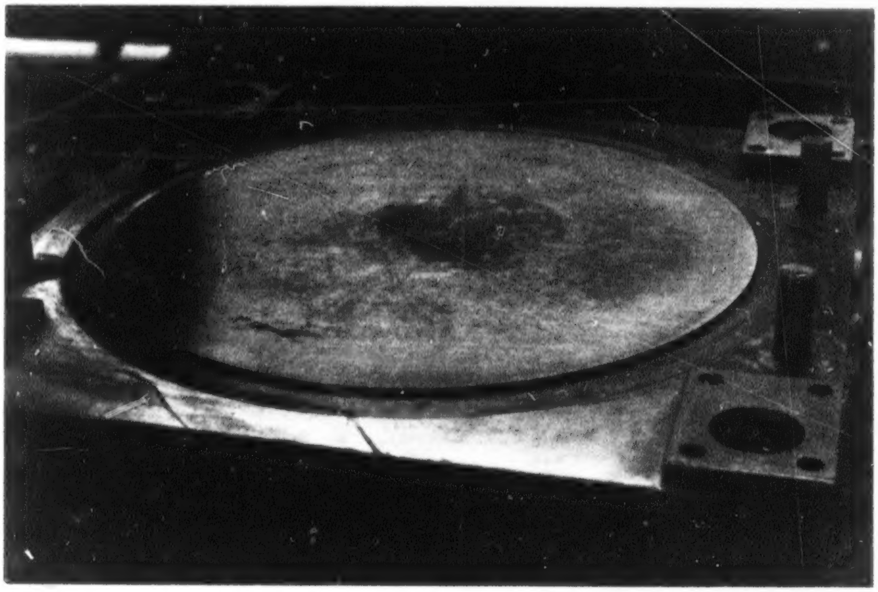

Figure 4b - Constant thickness mold with ejector plate in the "up" position. Part removal is made easier using this system, especially with a low-shrink polyester resin system.

Figure 5 - Constant thickness flywheel rotor mold installed in 860-ton hydraulic press. Both the press platens and the mold itself are steam heated to ensure constant molding temperature.

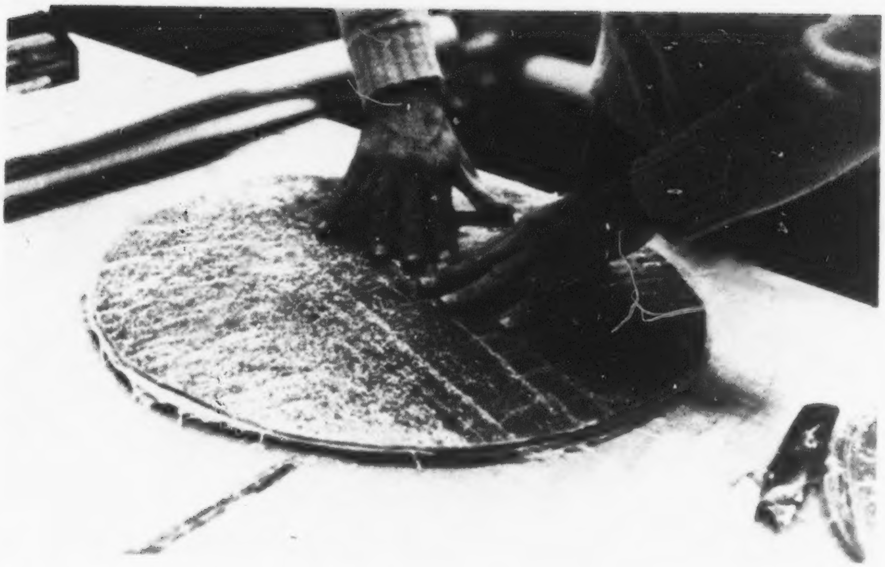

Figure 6a - Individual plies of R65 SMC are stacked together to form the charge for the flywheel.

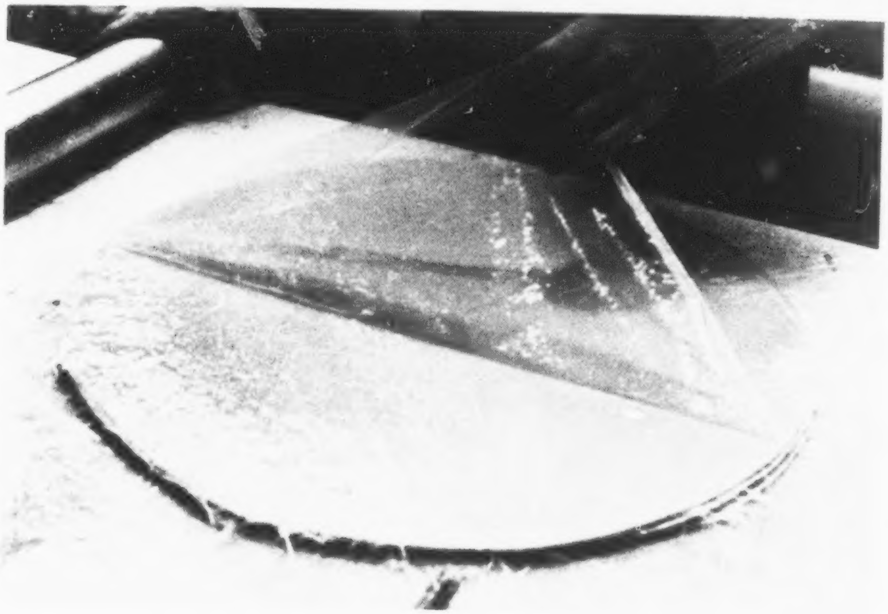

Figure 6b - The protective polyethylene carrier film is removed as each ply is positioned.

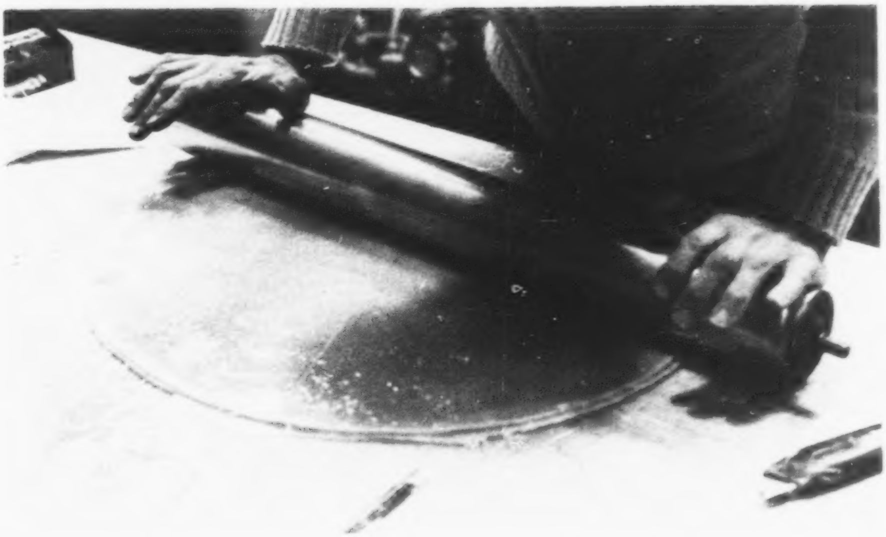

Figure 7a - As each SMC ply is placed on the stack, it is rolled to remove large air bubbles between the plies and consolidate, somewhat, the SMC charge.

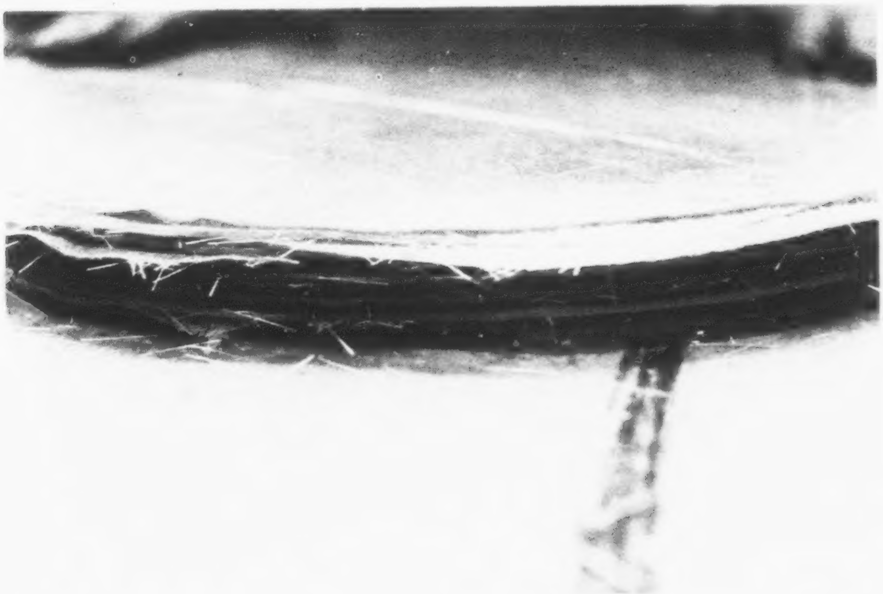

Figure 7b - The SMC charge for a constant thickness flywheel consists of 18 plies of R65 SMC. Mold coverage was approximately 88 percent.

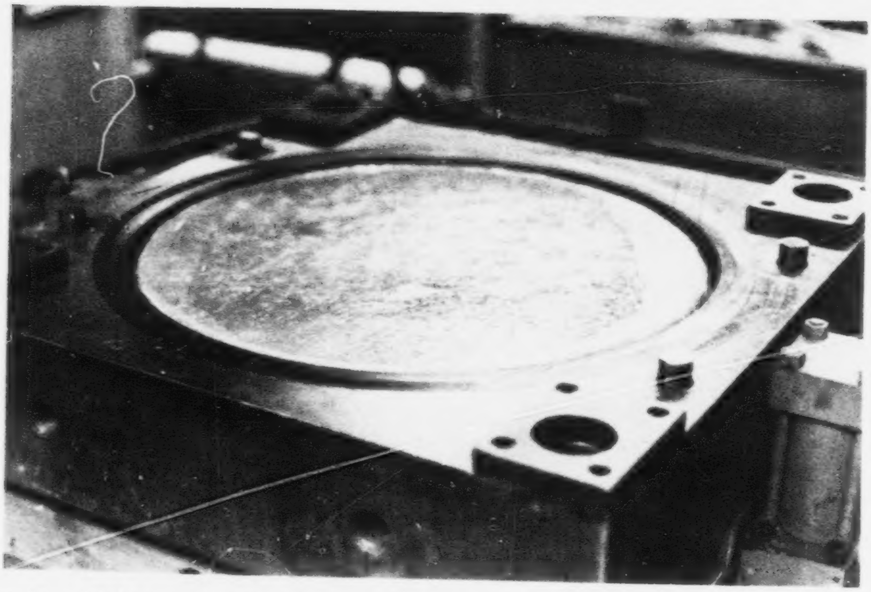

Figure 8a - Eighteen ply R65 SMC charge placed in the heated constant thickness mold immediately before mold closure. At 88 percent mold coverage flow of the material at the edges, a deleterious effect on mechanical properties, is minimized.

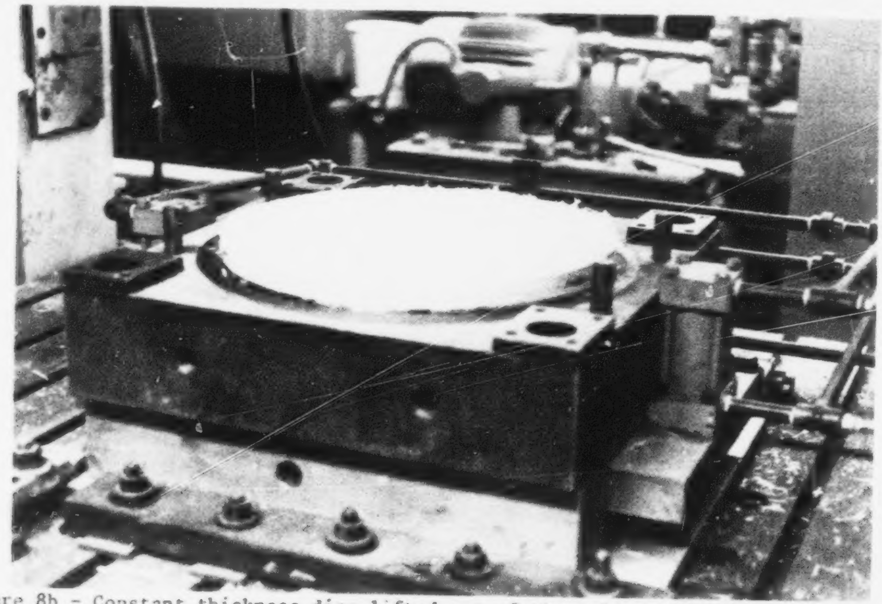

Figure 8b - Constant thickness disc lifted out of the mold by the bottom ejector plate. Removal of the part would be difficult without this system due to the low-shrink resin system.

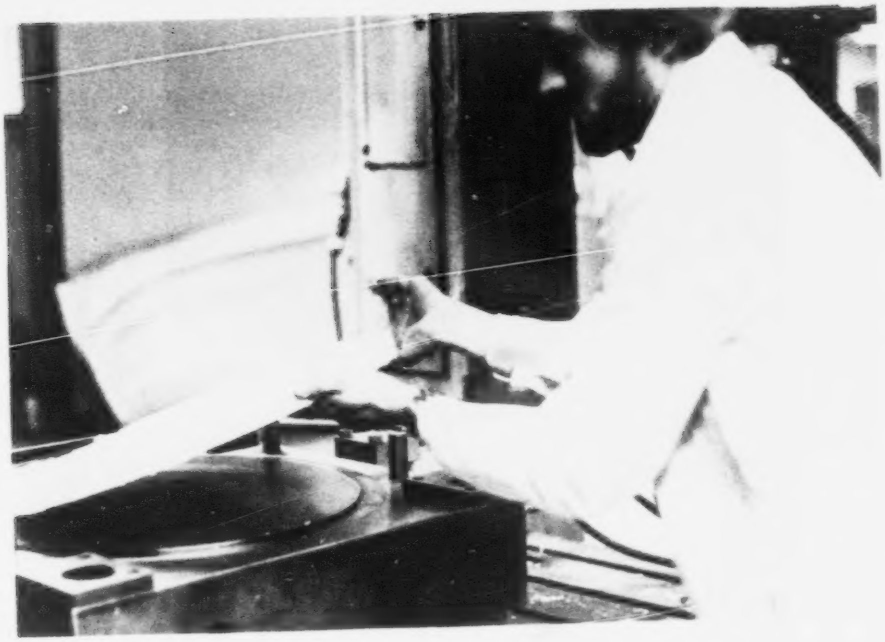

Figure 9a - Part removal from the mold. A small amount of edge flash is present and must be removed.

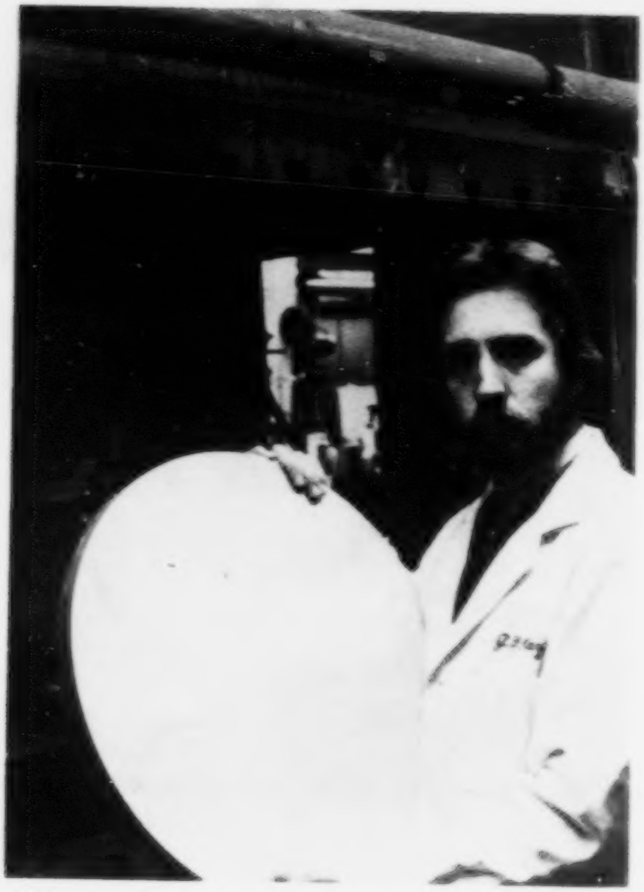

Figure 9b - The finished compression molded flywheel rotor weighs 22.5 pounds and is ready to be fitted with a filament wound containment ring.

PROJECT SUMMARY

Project Title: Fabrication of High Performance, Filament-Wound Fiber Composite Rings

Principal Investigator: Alan J. Hannibal

Organization:
Lord Kinematics
1635 West 12th Street
Erie, Pennsylvania 16512
(814) 456-8511

Project Goals: Fabricate circumferentially wound fiber composite rings for General Electric's laminated disk flywheel program.

Project Status: The project has been completed. In all, sixteen (16) composite rings were fabricated on a computer controlled filament winding machine. Eleven (11) of these rings were made of graphite/epoxy and the remainder were made of Kevlar 49/epoxy. The rings had either an 11.0 inch or 14.5 inch inside diameter. They were 1.0 inch in axial thickness and ranged in annular thickness from 0.5 to 2.5 inches. The fabrication method was basically a wet winding process using a circumferential wrap of a fiber tow under tension onto a mandrel. To assure satisfactory quality and appearance, several process issues were addressed, including fiber tie-off, accommodation of the mandrel taper and outside surface finish.

One ring was wound directly onto a laminated composite disk. Although its appearance was good, the difference in thermal expansion and contraction between the ring and the laminated disk caused them to separate after the cure cycle.

During the term of ths contract, several shortcomings in the composite rings were observed as a consequence of the winding process; namely, poor sidewall finish, the presence of residual stresses, nonuniform fiber fraction and void content in the radial direction, and relatively weak transverse strength. Most of these problems are being considered in an active subcontract with Lawrence Livermore Laboratories.

Contract Number: W-7405-ENG-48

Contract Period: 28 March 1979 through 11 July 1980

Funding Level: $26,650.00

Funding Source: U.S. Department of Energy through General Electric

FABRICATION OF HIGH PERFORMANCE, FILAMENT-WOUND FIBER COMPOSITE RINGS

Alan J. Hannibal
Lord Kinematics
1635 West 12th Street
Erie, Pennsylvania 16512

INTRODUCTION

Many different flywheel designs are presently being evaluated as potential candidates for commercial service in the future. Of these the "ring-on-disk" version, in which a circumferentially wound ring is mounted on an isotropic or quasi-isotropic composite disk, is straightforward in its construction and offers the advantage of lower cost over most of the other candidates. General Electric is the subcontractor to LLNL, having the development responsibility for the ring-on-laminated disk configuration.

Lord Kinematics entered into the flywheel energy storage program as a supplier of fiber composite flywheel rings to General Electric. Lord's participation was not a development effort per se, but was concerned with the application of standard wet filament winding techniques to fabricate composite rings of rectangular cross-section. For the most part, a specification was established jointly by General Electric and Lord early in the project in order to minimize the number of parameters that changed from ring to ring.

PROGRAM DESCRIPTION

The main thrust of Lord's effort was the fabrication of fiber composite rings and the bonding of aluminum hubs onto General Electric supplied laminated disks via elastomeric interlayers. The latter subject has been reported in the literature(Ref. 1) and will not be discussed in detail in this review.

In all, the contract called for the fabrication of sixteen fiber composite rings according to Table 1. Basically two fibers were used; Kevlar 49, 7100 denier, and 6000 filament Thornel 300 carbon fibers, WYP15 1/0. The Kevlar was dried prior to use. In all cases, the resin material was Shell's Epon 826 and the curative was Jeffamine D230 (100/34)--a room temperature curing epoxy system.

Before winding the rings a small development effort was undertaken to address several items of concern, specifically: 1) roving tie-off at the completion of the winding; 2) the removal of excess resin on the outer diameter before and during curing; 3) accommodation of the 0.025" taper on the inside diameter of the cutout in the mandrel.

Besides the separate rings listed in Table 1, one ring was wound directly onto a laminated disk with the hope of avoiding additional assembly steps.

DISCUSSION OF PROCESS

The rings were fabricated on a McLean-Anderson computer controlled filament winding machine as illustrated in Figure 1. The fiber tow was dispensed from a tension compensator which was set according to a measured tension of approximately three (3) pounds as the tow fed onto the mandrel, as shown in Figure 2. From the constant tensioning device, the fiber was fed through the impregnation bath. In the case of Kevlar 49, redirect bars were used and, in the case of carbon fibers, a roller drum was used. The impregnated fiber tow progressed through a feed eye attached to the carriage of the filament winding machine and onto the mandrel. A ceramic feed-eye was used with Kevlar 49 fibers and, alternately, a small roller was used for carbon fibers. The winding pattern was circumferential; that is, the fiber tow advanced one bandwidth longitudinally for each revolution of the mandrel.

TABLE 1: DESCRIPTION OF FIBER COMPOSITE RINGS WOUND FOR GENERAL ELECTRIC'S LAMINATED DISK FLYWHEEL PROGRAM

No.	Fiber/Epoxy	Inside Diameter (in)	Outside Diameter (in)	Annular Thickness (in)	Axial Thickness (in)
1	Kevlar 49	11.0	12.00	0.50	1.00
2	Kevlar 49	11.0	12.20	0.60	1.00
3	Kevlar 49	11.0	12.50	0.75	1.00
4	Kevlar 49	11.0	12.70	0.85	1.00
5	Kevlar 49	11.0	13.00	1.00	1.00
6	Thornel 300	11.0	13.40	1.20	1.00
7	Thornel 300	11.0	14.10	1.55	1.00
8	Thornel 300	11.0	14.80	1.90	1.00
9	Thornel 300	11.0	15.50	2.25	1.00
10	Thornel 300	11.0	16.20	2.60	1.00
11	Thornel 300	11.0	13.00	1.00	1.00
12	Thornel 300	11.0	13.80	1.40	1.00
13	Thornel 300	11.0	14.60	1.90	1.00
14	Thornel 300	14.5	17.70	1.60	1.40
15	Thornel 300	14.5	17.70	1.60	1.40
16	Thornel 300	14.5	17.70	1.60	1.40

The mandrel was comprised of three pieces which were bolted and pinned together as illustrated in Figure 3. The pieces were surface ground and assembled before machining the cut-out for the ring in order to assure perfect alignment when reassembled. The radius at the inside diameter of the cut-out eliminates sharp edges and, therefore, loose, resin-poor fibers.

After completion of the winding, the fiber tow was secured by stopping the winding approximately half-way through the last ply and placing a short, doubled-over fiber tow under the tow being wound. The loop end of the doubled-over fiber tow was oriented toward the edge of the mandrel on which the winding was to be completed. The winding was restarted, progressing slowly as the doubled-over fiber was wound under the ply. After the winding was finished, the fiber tow being wound onto the mandrel was cut and strung through the loop of the short fiber tow. The loop was then pulled under the final ply using the two loose ends. This procedure is illustrated in Figure 4.

To finish the outer surface, it was wrapped with a layer of porous release cloth, followed by a layer of bleeder cloth and held in place by a layer of teflon tape. The entire mandrel was then placed in a hot room (158°F) on a rotator for 1¼ hours (until gellation), and subsequently cured for two hours in an oven at 250°F. This approach provided a relatively smooth surface without excess resin.

Several attempts were made to compensate for the mandrel taper at the inside diameter of the cut-out using the programming feature of the filament winding machine. In all cases, the end result was a taper biassed in the opposite direction from the original taper. Happily, the most satisfactory solution was to ignore the taper by winding as though the mandrel were flat and letting the fibers level the winding naturally.

DIRECT OVERWRAP ONTO A LAMINATED COMPOSITE DISK

Filament winding a composite ring directly onto a solid disk creates a difficult problem because the two sides of the mandrel cannot be attached to one another in the usual fashion. Instead, each side must be held in place separately. To accomplish this end, both surfaces between the composite disk and the mandrel were covered with a 2-mil thick pressure sensitive adhesive film (Product No. 465, made by 3M). Also, a compressive force normal to the plane of winding was applied to the mandrel between the chuck and the floating center on the tailstock.

The assembled mandrel with composite disk is illustrated in Figure 5. At first, only the shaft plus Items 1 and 2 were used. In this configuration, the normal force was applied at the center of the mandrels causing them to deform conically and therefore separate slightly from the composite disk at the outside diameter. To correct this problem, Items 3 and 4 were constructed and positioned on the outside of Items 1 and 2 respectively. The normal force was then transferred to the outside diameter causing any gaps between the mandrel and the disk to close. Using this mandrel arrangement, a composite ring was successfully wound onto a composite disk.

The composite disk was prepared by first bonding a hub to it, then machining a flat outer surface concentric with the hub.

The process for winding the composite ring was exactly the same as for all the other rings. However, before the assembly could be removed from the filament winding machine, a series of four C-clamps was used to clamp the two sides of the mandrel together. The assembly was held in this fashion until after the ring was fully cured.

The flywheel assembly was cured at 158°F for sixteen hours rather than the usual 250°F in order to minimize the thermal expansion. Nevertheless, the differential expansion between the composite disk and the composite ring was such that at room temperature there was a gap between them, allowing for a little relative movement. The final product of a carbon/epoxy ring overwrapped onto a fiberglass laminated disk is illustrated in Figure 6.

DISCUSSION OF FUTURE WORK

During the term of this contract, several performance-related shortcomings were observed as a consequence of the winding process, namely, the presence of residual stresses, nonuniform fiber fraction and void content, and relatively weak transverse strength. These problems are presently being considered in an active contract with Lawrence Livermore Laboratories. What follows is a discussion of the measures which are being investigated to minimize their effects.

- The constant tension in the fiber tow as it is being wound produces residual stresses, as discussed in References 2, 3, and 4. For this program the equations derived by Reuter in Reference 4 are being applied to minimize the residual stresses as much as possible by varying the fiber tension.

- As the ring grows in annular thickness, the fiber fraction diminishes and the void content increases. This conclusion was demonstrated by General Electric. Reuter's work concludes that the fiber tension should increase with the number of plies to minimize residual stresses. By so doing, the fiber fraction near the outside will also be increased, and similarly one would expect the void content to decrease. Several other possible solutions, one or more of which will be investigated, are: 1) an overwrap of shrink tape; 2) an overwrap of dry Kevlar under high tension to squeeze out and absorb excess resin (the Kevlar is removed before curing); and 3) an overwrap of thermally expandable silicon rubber.

- The addition of a high strength silicon carbide whisker to the carbon fiber/epoxy system is being investigated in order to improve the transverse strength. The difficulty lies in the application of the SiC whiskers, which tend to clump. Several means for doing this are being considered. First, a double-impregnation bath system is being investigated. The first bath is pure resin, which impregnates the fiber tow. The second bath is a concentration of SiC whiskers in the same resin (typically 1% to 3%), which coats the fiber tow just prior to being wound onto the mandrel. A second approach involves a powder dispenser and an air supply which forces a metered amount of whiskers directly onto the winding. A third approach under consideration is a chamber of turbulent whiskers through which the impregnated fiber tow must pass before being wound onto the mandrel.

REFERENCES

1. McGuire, D.P. and Rabenhorst, D.W., "Composite Flywheel Rotor/Hub Attachment through Elastomeric Interlayers," 1977 Flywheel Technology Symposium Proceedings, held on Oct. 5-7, 1977 in San Francisco, California.

2. Chamis, C.C. and Liu, C.Y., "Residual Stresses in Filament Wound Laminates and Optimum Programmed Winding Tension," Proceedings of the 20th Annual Meeting of the Society of the Plastic Industry, Inc. (1965).

3. Knight, C.E. and Pollard, R.E., "Restressed Thick Flywheel Rims," 1977 Flywheel Technology Symposium Proceedings, held on Oct. 5-7, 1977 in San Francisco, California.

4. Reuter, R.C. Jr., "Prediction and Control of Macroscopic Fabrication Stresses in Hoop Wound, Fiberglass Rings," Analysis of the Test Methods for High Modulus Fibers and Composites, ASTM STP 521, American Society for Testing and Materials, 1973, pp. 264-276.

2799B/djr

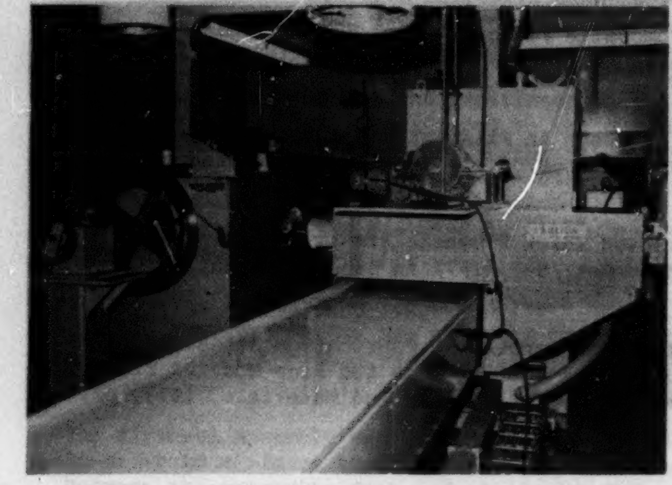

Fig. 1. McLean Anderson Computer Controlled Filament Winding Machine

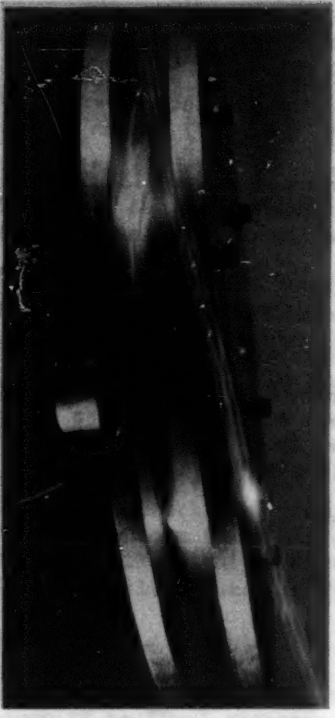

Fig. 3. Three-Piece Mandrel

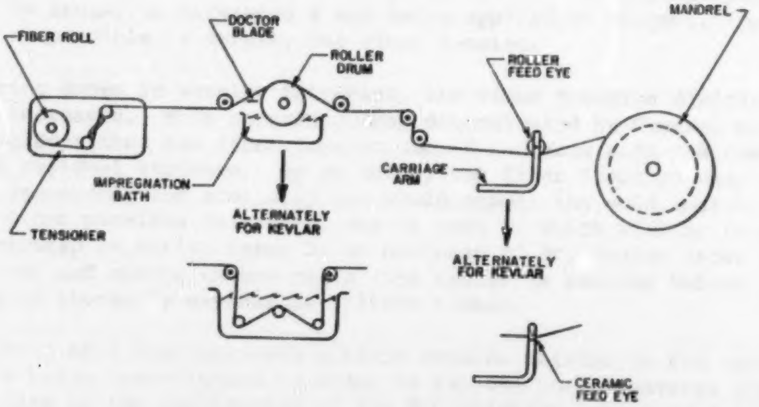
FIBER ROLL
DOCTOR BLADE
ROLLER DRUM
IMPREGNATION BATH
TENSIONER
ALTERNATELY FOR KEVLAR
ROLLER FEED EYE
CARRIAGE ARM
ALTERNATELY FOR KEVLAR
MANDREL
CERAMIC FEED EYE

Fig. 2. Process for Filament Winding a Fiber Composite Ring

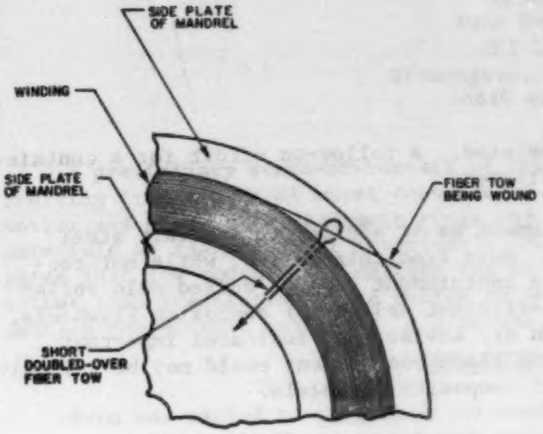
SIDE PLATE OF MANDREL
WINDING
SIDE PLATE OF MANDREL
FIBER TOW BEING WOUND
SHORT DOUBLED-OVER FIBER TOW

Fig. 4. Fiber Tow Tie-Off Procedure

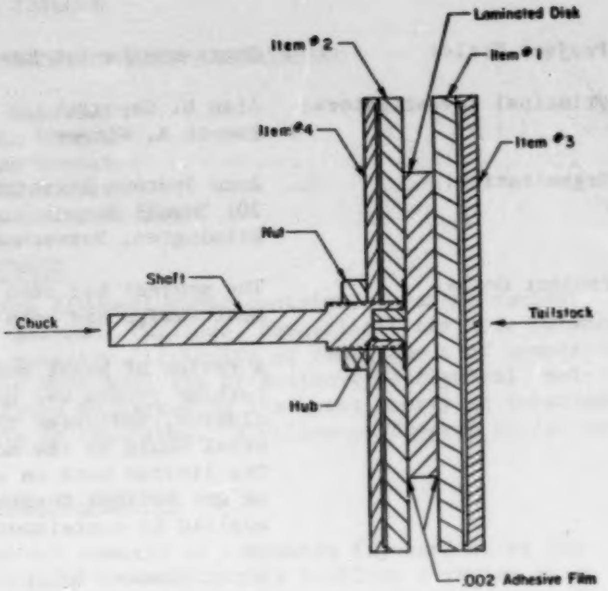
Laminated Disk
Item #2
Item #1
Item #4
Item #3
Nut
Shaft
Chuck
Tailstock
Hub
.002 Adhesive Film

Fig. 5. Mandrel for Direct Overwrap of a Composite Ring Onto A Composite Disk.

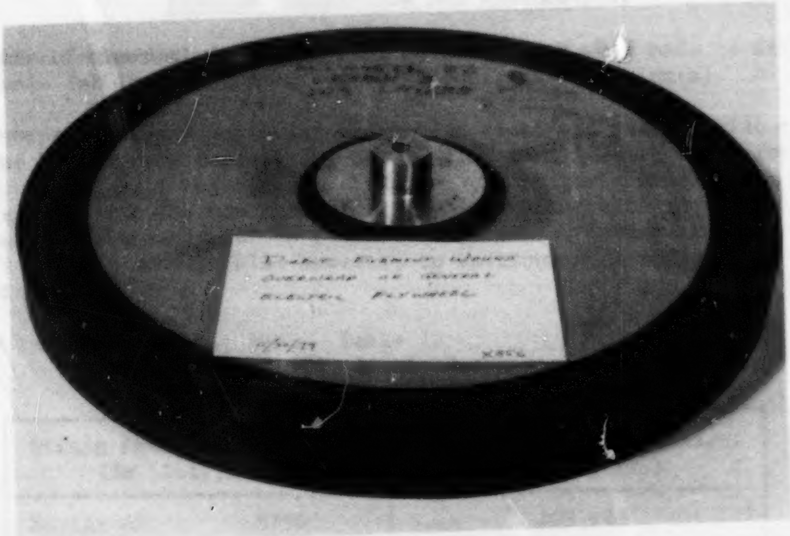

Fig. 6. Direct Overwrap of a Carbon/Epoxy Ring Onto A Fiberglass Laminated Disk With Hub.

PROJECT SUMMARY

Project Title: State-of-the-Art Review of Flywheel Burst Containment

Principal Investigators: Alan D. Sapowith
Emmett A. Witmer

Organization: Avco Systems Division
201 Lowell Street
Wilmington, Massachusetts 01887

Project Goals: The project has been completed. A follow-on effort for a containment design has been initiated.

A review of burst containment as it applied to aircraft steel turbine rotors was made. Data from this review, while not conclusive, indicated that a containment ring of coiled cold rolled steel would be the most efficient design for composite flywheels. The limited data on woven dry Kevlar that indicated important weight savings for turbine blade containment could not be directly applied to containment of composite flywheels.

A containment design concept for disc-type flywheels was generated. Very light containment weights were projected for this design which took advantage of the apparent slow growth of composite disc flywheels at failure (burst) initiation.

Contract Number: Subcontract 6692009
First Amendment

Contract Period: November 1979 through May 1980

Funding Level: $29,923

Funding Source: U.S. Department of Energy through Lawrence Livermore Laboratories

STATE-OF-THE-ART REVIEW OF FLYWHEEL BURST CONTAINMENT

Alan D. Sapowith
Emmett A. Witmer
Avco Systems Division
201 Lowell Street
Wilmington, Massachusetts 01887

ABSTRACT

A preliminary state-of-the-art of composite flywheel burst containment was conducted. Starting from a base of burst containment for aircraft turbines, comparisons are made between Kevlar and steel as containment rings and the relative difficulty of containment of composite materials as against steel (turbines). Failure mode analysis of a disc-type flywheel indicates that low containment weights can be achieved by capturing the burst energy as rotational rather than translational. A design to do this is described. A Follow-on Program to further develop containment design is in progress.

INTRODUCTION AND BACKGROUND

Avco was tasked to perform a state-of-the-art summary of composite flywheel burst containment. Since little previous data was available concerning this problem, a review of an analogous problem, burst containment of aircraft turbine blades, was made. This review was conducted by Dr. Emmett Witmer, M.I.T., as a consultant to Avco. It indicated that the lightest weight designs for turbines were those that used dry Kevlar weaves for the containment structure. The use of steel containment rings was decidedly heavier due to the high bending moments induced in the thick rings by local turbine blade impacts. Coiled cold rolled steel showed a marked improvement over cast steels due to their ability to withstand sharp bending radii. The objective of the balance of the program was to apply this background data to the containment of composite flywheels.

PROGRAM DESCRIPTION AND RESULTS

After the state-of-the-art search, several short studies were made to establish an approach or rationale for the development of burst containment design(s).

A first-cut comparison between Kevlar and coiled steel was made. While the Kevlar results for turbine blades were impressive, it was felt that local bending for composite flywheel bursts would not be a major factor and that the criteria should be a comparison of total strain energy (SE) for the containment ring vs the burst kinetic energy (KE) to be contained. When strain allowables of 10 percent are assumed, Kevlar is still the most efficient, Table 1. It is susceptible, however, to environmental effects and can be expected to be more expensive.

Table 1.
Specific Strain Energies.

Strain Energy Per Volume (In. lbs/in^3)		Strain Energy Per Weight (In. lbs/lb)
Kevlar 49	5750	109,943
Kevlar 29	3312	63,327
S-Glass	3125	34,722
Steel	4500	62,284

While local puncture of containment rings is an important consideration for turbine blades, it was believed to be less of a factor for composites. For preliminary evaluation of this factor, ballistic tests firing both steel and fiberglass pellets against steel plates were conducted. The two types of projectiles were launched into the target with a nominal impact energy of 1780 ft-lbs. This corresponds to an impact velocity of 2000 ft/sec for fiberglass and 1000 ft/sec for the steel projectiles. The test results, Tables 2 and 3, indicate that the confinement thickness for steel is approximately 2.5 times that required for fiberglass at the same energy level. It was also noted that the fiberglass broke up into smaller fragments upon impact whereas there was no breakup of the steel projectile.

Table 2.
Flywheel Fragmentation Impact Tests.

Test No.	Velocity (f/s)	Proj. Material	Proj. Wt. (gms)	Target[a] Thickness (inches)	Target Obliquity (Degrees)	Results
TS-1	1449	Fiberglass	13	0.035	40	Perf. target with significant residual energy. No impact on witness plate.
TS-2	1428	Fiberglass	13	0.105	40	Perf. target. Small dimple on witness plate.
TS-5[b]	1990	Fiberglass	13	0.280	40	No perf. witness plate dented.
TS-6[b]	2061	Fiberglass	13	0.210	40	No perf. Two dents in witness plate.
TS-7[b]	2000	Fiberglass	13	0.140	40	Perf. target. Two dents in witness plate.
TS-8[b]	1950	Fiberglass	13	0.175	40	No perf. One dent in witness plate.
TS-11[b]	1050	Steel	47.5	0.280	40	Perf. target.
TS-12[b]	1000	Steel	47.5	0.455	40	No perf.
TS-13[b]	1100	Steel	47.5	0.385	40	*Barely perf.* target.

(a)Target made up of 0.035 thick cold rolled steel plates.
(b)Nominal projectile KE 2000 ft-lbs.

Table 3.
Areal Density at Limit Perforation.

Projectile Material	Projectile Velocity (f/s)	Areal Density (gm/cm^2)	Target Thickness (cm)
Fiberglass	2000	0.36	4.10
Steel	1000	0.98	14.98

After several containment weight estimates were made using values of KE/SE extrapolated from turbine tests and steel for the containment ring, it was realized that containment weights could be markedly reduced if the burst energy could be captured as rotational rather than translational energy. A possible key to this was found in the failure mode of Avco's disc-type flywheel. This mode exhibited a slowdown at failure which was attributed to an initial growth of the flywheel prior to breaking in many fragments. This phenomena has been noted in other flywheel failures. Figure 1 shows the speed change at failure. The slowdown or increased moment of inertia represents a radial growth of 0.4 inch. By setting the gap between the rim of the flywheel and the containment ring to be less than the indicated 0.4 inch, essentially all of the burst energy could be contained as rotational. Figure 2 shows a suggested vacuum housing/containment ring design that successively allows capture of the rotational energy, spin up of the housing itself and subsequent stopping of the system. Component "5" in this figure acts as a bushing to allow the housing to spin. The radial stiffeners, "9", also act as aerodynamic fins which together with friction quickly slow down and stop the housing.

CONCLUSIONS AND RECOMMENDATIONS

1. Ballistic tests investigating local puncture show that glass composites are easier to contain than steel of equal kinetic energy by a factor of 2.5.
2. The ballistic tests conducted suggest low cost simulation methods for obtaining empirical data required to correctly implement simplified strain energy analyses for containment ring design.
3. Containment ring weight can be markedly reduced if flywheel burst energy is captured as rotational energy as against translational energy. This appears to be more easily accomplished for disc type flywheels than rim type.
4. Estimates show that for a reference 40 pound flywheel with a burst of energy of 0.8 kWh containment weights in steel are 105 pounds for rim type flywheels and 39 pounds for disc type flywheels. These weight estimates include the side walls of a vacuum housing.
5. While Kevlar is indicated to be the lightest weight material for containing aircraft turbine bursts it does not appear to offer substantial weight savings over steel for composite flywheel containment. For completeness (to fill in the apparent lack of data) Kevlar should be evaluated on a comparable basis with cold rolled coiled steel at representative strain rates.

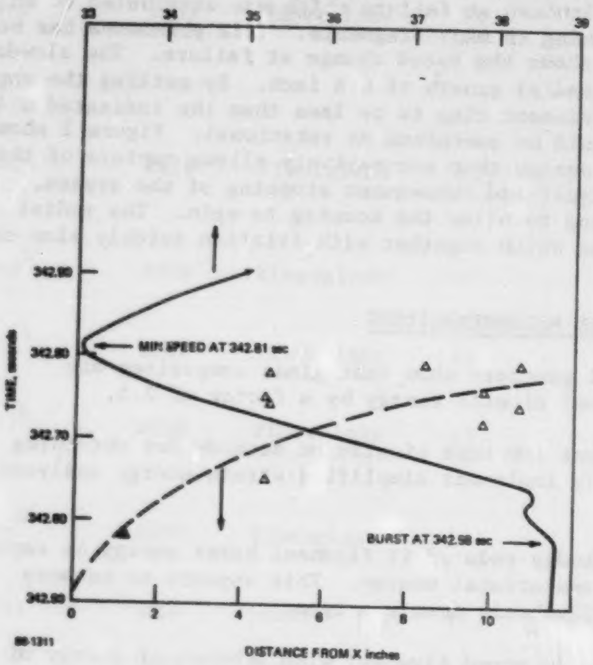

Fig. 1. Distance/Time Path from Suggested Failure Point X (X on ID at 90°).

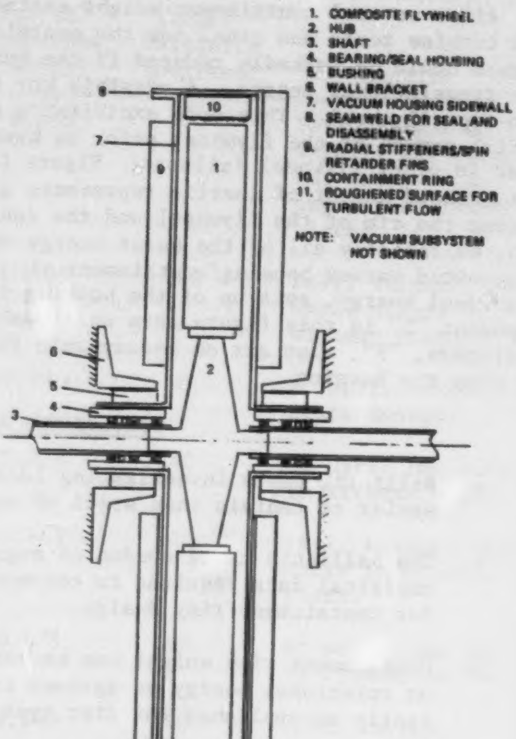
1. COMPOSITE FLYWHEEL
2. HUB
3. SHAFT
4. BEARING/SEAL HOUSING
5. BUSHING
6. WALL BRACKET
7. VACUUM HOUSING SIDEWALL
8. SEAM WELD FOR SEAL AND DISASSEMBLY
9. RADIAL STIFFENERS/SPIN RETARDER FINS
10. CONTAINMENT RING
11. ROUGHENED SURFACE FOR TURBULENT FLOW
NOTE: VACUUM SUBSYSTEM NOT SHOWN
8
10
7
9
1
6
5
4
3
2
11
80-1321

Fig. 2. Flywheel Module.

PROJECT SUMMARY

Project Title: Flywheel Containment Technology Assessment

Principal Investigators: Anthony P. Coppa, Carl H. Zweben

Organization: General Electric Company
Space Division
Box 8555, Philadelphia, Pa. 19101

Project Goals: Review and assess technology available for developing high performance, cost-effective containment housings for composite and metallic flywheels.

Project Status: The project has been completed and a report, entitled "Flywheel Containment Technology Assessment," has been issued. The major part of the assessment included the following topics: a) Physical features of the containment process; b) analytical methods; c) flywheel containment test methods and facilities; d) behavior of composite materials under impact loading; and e) composite flywheel failure behavior.

Metallic flywheels characteristically rupture in relatively large fragments which remain essentially intact during interaction with a containment housing. This results in relatively heavy containment requirements.

Composite rotors fail in a variety of modes depending on their detailed construction,and initial failure in some designs is accompanied by release of "hoop" type fragments which present lower damage hazards. Composite fragments, moreover tend to break up into smaller fragments during containment interaction and this transformation tends to reduce the damage potential. Hence, it appears that, in general, for an equal amount of stored energy, composite rotors require lighter containment

Design methods for reliably predicting initial and subsequent fragmentation for composite rotors and their effects on containment structures, however, do not exist at present. Efforts are now underway to develop such methods, as well as to gather together dynamic strength and other materials data that are required to implement them.

A significant conclusion resulting from the project is that the flywheel rotor and containment housing should be designed as a system in order to develop high performance systems.

Contract Number: W-7405-ENG-48, Subcontract 6624409

Contract Period: 21 August, 1979 through 20 November, 1979

Funding Level: $45,027

Funding Source: U.S. Department of Energy through Lawrence Livermore Laboratories.

FLYWHEEL CONTAINMENT TECHNOLOGY ASSESSMENT

Anthony P. Coppa
Carl H. Zweben
General Electric Company
Space Division, Box 8555
Philadelphia, Pa. 19101

ABSTRACT

This paper reports on particular aspects and results of a program to (a) assess containment technology that is currently available for the development of efficient flywheel systems and (b) design and fabricate preliminary containment structures for use in current prototype energy storage flywheel tests. The paper emphasizes the need to optimize and integrate the design of containment housings with the rotor design, discusses fragmentation characteristics of composite rotors, and outlines some preliminary design methods presently being developed for composite rotor containment.

INTRODUCTION

Developments of high performance energy storage flywheel systems that have been pursued in recent years have emphasized the optimization of the flywheel rotor component. As a result, advanced fibrous composites have been the choice for a number of rotor designs and weight-specific energies as high as 28.4 Whr/lb(1) at 0.311 Kw. hr. (laminated disk)(1) and 37.8 Whr/lb at 1.16 KWhr (wound rim)(2) have been attained with such materials. More recently, increased attention has been directed at evaluating the performance of flywheels as a system, and this has led to the awareness that systems considerations may play a deciding role in distinguishing optimum designs for commercial application. Prominent among such considerations is the safe containment of possible rotor bursts, and it is becoming evident that superior containment design techniques than are currently available will have to be applied in order to achieve the desired performance goals for flywheel systems. Other systems considerations include momentum transfer torques and forces that can be transmitted to the vehicle during a containment event, vehicle collision effects, maintenance of high vacuum in the flywheel housing, adequate noise suppression, repairability, and maintenance.

Important effects of containment on flywheel energy densities are discussed in Reference 3 for a variety of designs such as a multi-disk steel rotor, shaped steel rotor, and multi-rim composite rotors as contained by steel housings. The ratio of containment and rotor weights for these respective designs are reported to be 0.4, 5.0, and 1.6, the last value applying to a Kevlar/epoxy rim. In addition to showing the large weight contribution of containment to flywheel system weight, these values reflect several interesting effects of design configuration and materials: The relatively low penalty of the multi-disk steel rotor is due to the fact that only one of its constituent disks is assumed to rupture and more than a one disk-share of the containment structure acts to contain it. The high penalty of the shaped steel disk, on the other hand, is due to the requirement to contain the entire rotor. If containment for the laminated rotor were based on the requirement to contain a simultaneous burst of all its disks, its penalty might be as high as the shaped rotor. The value for the multi-rim composite rotor will depend on the number of constituent ring elements that can be expected to rupture simultaneously. If the number can be limited to a few rings, the penalty can be lower than those reported in Reference 3.

Containment must especially address the constraints of low weight, volume, and cost, because it does not contribute directly to the energy storage function. During the entire lifetime of the flywheel system, containment serves in the standby mode until it is called upon to perform in the uncertain event of rotor failure. Hence, containment serves an insurance rather than an active performance function and the containment designer is obliged to keep the cost of such "insurance" within reasonable bounds. Achievement of this goal will be greatly aided by early quantification of containment penalties relative to particular candidate flywheel constructions.

This program was sponsored by the U.S. Department of Energy through the Lawrence Livermore Laboratory; Dr. S. V. Kulkarni was the LLL Project Engineer.

CONTAINMENT PROCESSES

Metallic Rotors

When metallic rotors burst, relatively large fragments are released. Due to their hardness, sharp edges, relative narrowness and isotropic toughness, these fragments have great penetrating capability, and generally require heavy containment rings to resist them. The large ratio of containment-to-rotor weight (5:1) cited previously for the shaped steel disk dramatically exemplifies this point. Attempts have been made to design rotors so that in the event of failure smaller size, less damaging fragmentation is generated. A noteworthy example is the Rocketdyne Division constant strength disk(4) which is designed to fail in a narrow neck immediately inboard of its circumferential rim. Rupture of the neck completely around the circumference, as predicted by analysis, results in separation of the rim from the remainder of the disk in one piece. Since the rim supports much of its centrifugal stress as a hoop, high energy fragmentation is minimized. While it is to be hoped that such concepts can be proven to perform reliably and without significant penalty to rotor weight-specific energy, presently, metallic rotors invariably require very heavy containment structures. Reference 5 presents a survey of metallic rotor containment tests from which the great severity of containment is quite evident. Figure 1 shows the results of a containment test(6) involving a bladed steel rotor that has initially burst into two halves. The rotor had a blade tip diameter of 14.0 in. and weight 11.9 lbs. Burst speed was 19,900 rpm and energy of 25.9 Whr. The containment ring weighed 8.63 lbs. and contained the fragments. The ratio of containment-to-rotor weight was 0.73, which is impressively high, since the weight-specific energy of the rotor (2.19 Whr/lb) is very low in relation to the levels at which vehicle energy storage flywheels will operate.

Composite Rotors

Composite rotors, on the hand, release less destructive fragements, and require considerably lighter containment structures than equivalent metallic-rotors. There are several reasons for this. First, the heterogeneity of composites tends to inhibit the spread of fracture surfaces through large regions of the material. A local failure tends rather to induce delaminations, fiber breaks and debonds, all of which increase the energy involved in spreading the fracture zone. Especially in the case of uniaxial fiber reinforcement, a crack will tend to run parallel to fibers, thereby generating long fibrous fragments. Hence, a wound rim will tend to release circumferentially long, radially thin fragments which present relatively broad bearing surfaces to the containment device. Second, the composite fragments tend to break up into finer pieces upon impact. This is because the matrix, which may or may not already be damaged, cannot sustain the very high stresses produced during engagement with the containment ring. These stresses are due to impact during the initial engagement, to centrifugal forces induced as the fragments sweep rapidly along the curved containment surface, and to friction set up by the high centrifugal normal forces. The resulting frictional heating further degrades the matrix and fibers and accelerates the break-up process. Finally the same friction forces can rapidly decelerate the fragements in their circumferential motion and thereby reduce the radial impulse delivered to the containment ring.

The character of debris released by composite rotors depends on the construction of the composite, to material composition, and to the stress distribution. Debris obtained after bursts of composite rotors varies from a highly disrupted consistency as shown in Figure 2(7) to the large, rigid fragments shown in Figure 3(1). Although the burst associated with latter resulted in multiple breakup of a 0.25 inch thickness steel ring, the action was probably still greatly less severe than if the rotor had been metallic. The debris of the former example, on the other hand, might suggest a much more benign process than it actually was. As will be discussed later, completely fragmented material sweeping along the inner surface of a containment ring at speeds of 3000 fps will exert very high centrifugal pressures. Up to the present time, complete rotor bursts which have produced debris of this type (Figure 2) have been performed only in very thick steel containment housings, so the damage potential of such debris systems has not been assessed experimentally. Another point is that the housings have generally provided much larger radial clearances than will be utilized in typical vehicle systems. Hence, possibly destructive interferences between the debris and spinning rotor have been precluded in those tests.

Two tests in which radial clearances have been sufficiently small to permit debris interferences are illustrated in Figures 4b and 5. Figure 4 shows the pre-test and post-test conditions of a "Bandwrap" flywheel rotor(8). Although the radial clearance was larger than those suitable for operating systems, the debris accumulated in the clearance space such that a thick wedge of material was produced. The forces exerted by this wedge ultimately forced the rim away from the hub. A good indication that debris interference may be reducible to tolerable levels in practical designs is the post-test condition shown in Figure 5. The rotor was tested in a practical vehicular containment housing with a running clearance of perhaps 0.25 inch. Due to the fact that only a small portion of the outer rim failed, debris interference was sufficiently mild that no apparent damage resulted from it, although a significant torque (1100 lb/hr for 2 sec.) was transferred to the housing support.

CONTAINMENT DESIGN AND ANALYSIS METHODS

Metallic Rotors

A useful design method for metallic rotor containment is that of Hagg and Sankey$^{(10)}$. The method, which assumes quadrant sector rotor fragements, is applicable to circular rings with and without stiffening flanges. The containment event is considered to be a sequential, two-stage process. Stage 1 involves an inelastic impact and transfer of momentum to an effective portion of the containment ring. If the ring has sufficient compression and shear resistance to preclude direct perforation of the ring thickness, Stage 2 ensues. To survive Stage 2, the overall available plastic tensile strain energy of the ring must exceed the kinetic energy remaining after Stage 1. Results obtained from large-scale tests involving steel rotors and unflanged containment rings$^{(10)}$ are in very good agreement with predictions based on these criteria.

Extensive analytical studies of containment behavior and related dynamic structural response problems have been performed by the Aeroelastic and Structures Research Laboratory of Massachusetts Institute of Technology over the past 13 years$^{(11)}$. These studies include the development of useful computer programs for predicting the large deflection elastic-plastic transient response of metal ring structures to rotor-burst fragment impact. Experimental data obtained from rotor disk and blade containment tests and from simpler experiments involving steel-sphere impact against aluminum beams and panels have been used to assess the predictive accuracy of these analyses.

Composite Rotors

Design methods for composite rotors, on the other hand are not well developed. The program reported on herein required designing containment rings for composite flywheel rotors that were tested at the Union Carbide, Oak Ridge Y-12 Flywheel Evaluation Laboratory during 1980. This work led to the development of preliminary containment design methods for composite rotors of various conditions, including circumferentially wound and laminated disk types. Some of the approaches taken are described briefly in the following section.

The containment design has to be based on the description of the initial fragmentation released by the rotor at failure. Failure of a circumferentially wound rotor may involve separation of complete hoops or release of circumferentially oriented fragements. A laminated disk rotor may burst into circular sector fragments, involving the full laminate thickness, or individual plies. The damage capability of the initial fragemntation depends on its ability to remain intact for a significant fraction of the fundamental response times of the containment ring. Rapid break-up of the fragmentation reduces the damage potential.

a. Wound Rotor

Circumferentially long and relatively thin fragments are considered in the following treatment of a wound rotor or a rotor having a wound rim. The fragments are assumed to be released simultaneously from an entire circumferential layer at the rotor periphery so that upon contact with the ring they exert forces that are uniformly distributed along the circumference.

The initial position of a typical fragment portion at the instant it is released from a rotor spinning about point 0 with angular velocity ω is shown in Figure 6. The fragment has a radial thickness t, linear velocity V_o through and angular velocity ω about its mass center B, and initial clearance c. After the fragment has moved completely through the clearance space, it is assumed to impact the ring uniformly with radial velocity, $V_{R_o} = V_o \sin\theta$ and begins to slide along the ring surface with tangential velocity, $V_{T_o} = V_o \cos\theta$.

The design of the ring is determined by two sequential conditions:

1. Radial momentum transfer involving inelastic impact at initial velocity V_{R_o}.

2. Centrifugal pressure p exerted by the fragment moving with velocity V_{T_o} along a circular path of radius, R_{Co}. The centrifugal pressure, p produced in the fragment is:

$$p = \frac{\rho\omega_o^2}{3r}\,(r^3 - R_1^3),\; R_1 \leq r \leq R_{C_o} \qquad (1)$$

where ρ is the mass density of the fragment, R_1, the inner radius of the fragment, and r the radius to any point in the fragment. ω_o is equal to $V_{T_o}/\bar{r}$, where $\bar{r}$ is the radius to the fragment center of mass.

Equation (1) is used to determine the centrifugal pressures throughout the fragment and to compare them to the fragment transverse compression strength σ_{CT}. If $p_o < \sigma_{CT}$ throughout, the fragment is assumed to be rigid and the pressure at $r = R_{C_o}$ is imposed on the ring, or

$$p = \frac{\rho\omega_o^2}{3R_{C_o}}\,(R_{C_o}^3 - R_1^3),\; p_o \leq \sigma_{CT}, \qquad (2)$$

If instead $p_o > \sigma_{CT}$ over a portion of the fragment, say, between R and R_{C_o} then the fragment is considered to consist of two parts, namely a pulverized, quasi-fluid portion between R_{C_o} and R in which $p_o = \sigma_{CT}$ and a rigid portion between R and R_1, the latter having a mass M_R (see Figure 7). In this way, consideration of an excessively massive fragment, which would result in overdesign of the containment ring, is avoided.

The condition for containment is that the maximum radial displacement of the ring due to the above two conditions is less than the allowable displacement:

$$\delta_{C_{MAX}} < \delta_{C_{ALL}} .$$

The analyses for rigid and crushable fragments have been applied to containment rings that consist of a relatively thin metallic liner and a relatively thick Kevlar 29 fabric overwrap. Since the Kevlar fabric exhibits an almost linear load-deflection curve up to its failure strain (5 - 6%) and the raidal stiffness of the overwrap is much greater than the plastic stiffness of the liner, the resistance of the entire containment ring has been modeled by the elastic stiffness of the overwrap. The effect of fragment/ring interface friction has also been studied for rigid fragments. Results obtained so far indicate that accounting for fragment crushing and surface friction greatly reduces containment requirements relative to those for rigid fragments.

Laminated Disk Rotors

When laminated composite disk rotors fail, they release fragments, many of whose plies are radially oriented. For rotors that release fragments of the type shown in Figure 3, analysis(10) can be applied to obtain a conservative estimate of the containment requirements. For weight sensitive applications, however, it is especially necessary to account for break-up of the initial fragmentation. In designing the containment rings for Y-12 tests of laminated disk rotors, the longitudinal compression strength of the laminate was used as a basis for limiting the radial pressure that such fragments can exert on the containment ring. This approach resulted in defining an effective rigid fragment size, that was smaller than the initial size. This when input to the analysis(10) and to strength criteria resulted in much ligher containment ring designs.

It is our opinion that design methods for composite rotors must account for fragment break-up in order to include realistic design conditions. The energy levels of the initial predicted fragmentation are so large in some high performance flywheels that designs based on the assumption of fragmentation remaining intact during the entire process may be expected to be both excessively heavy and costly.

CONCLUSIONS AND RECOMMENDATIONS

Containment is a requirement that seriously compromises the performance of vehicular energy storage flywheel systems. Hence, it is very important to the viability of flywheel systems that optimum combinations of rotors and containment housings be identified.

Penalties due to containment are strongly affected by the following: (a) Rotor Design: The energy level of initial fragmentation must be minimized, (b) Fragmentation Behavior during containment: rapid breakdown of initial fragmentation is desirable, (c) Torque Transfer during containment: high levels must be avoided.

Present technology (design methods, fragmentation data, both from analysis and test, dynamic materials data, friction properties, etc.) is inadequate to obtain the desired degree of system optimization. Efforts are underway to apply design methods to analyze flywheel containment tests, considering observed fragmentation phenomena. Appropriate dynamic and friction data for composites and metals may have to be obtained from specially designed materials type tests.

REFERENCES

1. Kulkarni, S. V., Stone, R. G., and Toland, R. H., "Prototype Development of an Optimized, Tapered-Thickness Graphite/Epoxy Composite Flywheel," Lawrence Livermore Report No. UCRL-52623, November, 1978.
2. Satchwell, D. L. and Towgood, D. A., "High-Energy Density Composite Flywheel," AiResearch Manufacturing Company, Report No. SAND 79-7019, February 1980.
3. Towgood, D. A., "An Advanced Vehicular Flywheel System for ERDA Electric Powered Passing Vehicle," 1977 Flywheel Technology Symposium Proceedings, pp. 63-38, March 1978.
4. Davis, D. and Hodson, D., "Rocketdyne's High-Energy-Storage Flywheel Module for the U.S. Army," 1977, Flywheel Technology Symposium Proceedings, U.S. Department of Energy, Report No. CONF-7710-53, March 1978.
5. Coppa, A. P., Zweben, C. H., and Mirandy, L., "Flywheel Containment Technology Assessment," General Electric Space Division, Doc. No. 80SDS4202, January 1980.
6. Mangano, G. J., Salvino, J. T., and DeLucia, R. A., "Rotor Burst Protection Program: Experimentation to Provide Guidelines for the Design of Turbine Rotor Burst Fragment Containment Rings," from "Assessment of Technology for Turbojet Rotor Failure," Proceedings, MIT Workshop, March 29-31, 1974.
7. Nimmer, R., General Electric Company Corporate Research and Development Center, (private communication), 1979.
8. Steele, R., Union Carbide Corp., Oak Ridge Y-12 Plant (private communication), 1980.
9. Rowlett, B. H., "Burst and Containment Test Report for Flywheel Power System," AiResearch Manufacturing Company of California Report No. 78-15148 (DOE Contract EY-76-C-03-1213, July 12, 1978).
10. Hagg, A. C. and Sankey, G. O., "The Containment of Disk Burst Fragments by Cylindrical Shells," ASMA Journal of Power, April 1974.
11. Rodal, J. J. A., and Witmer, E. A., "Finite-Strain-Large - Deflection Elastic - Viscoplastic Finite - Element Transient Response Analysis of Structures," NASA Cr 159874, ASRL TR 154-15 (See References No. 14-21 and 23-31 listed therein), July, 1979.

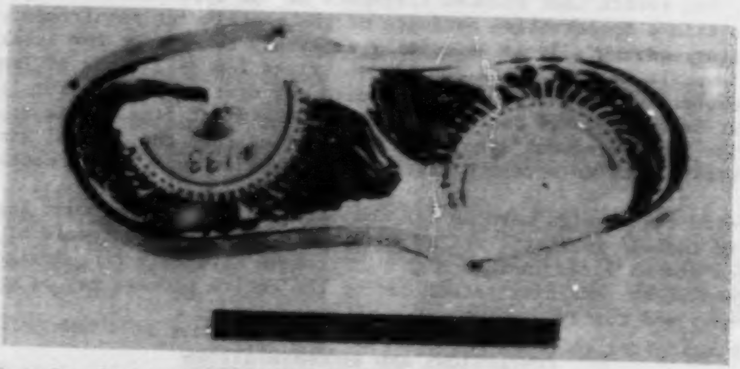

Figure 1. Test Results Showing a 2 Fragment Bladed Steel Rotor as Contained by a Steel Circular Ring(6)

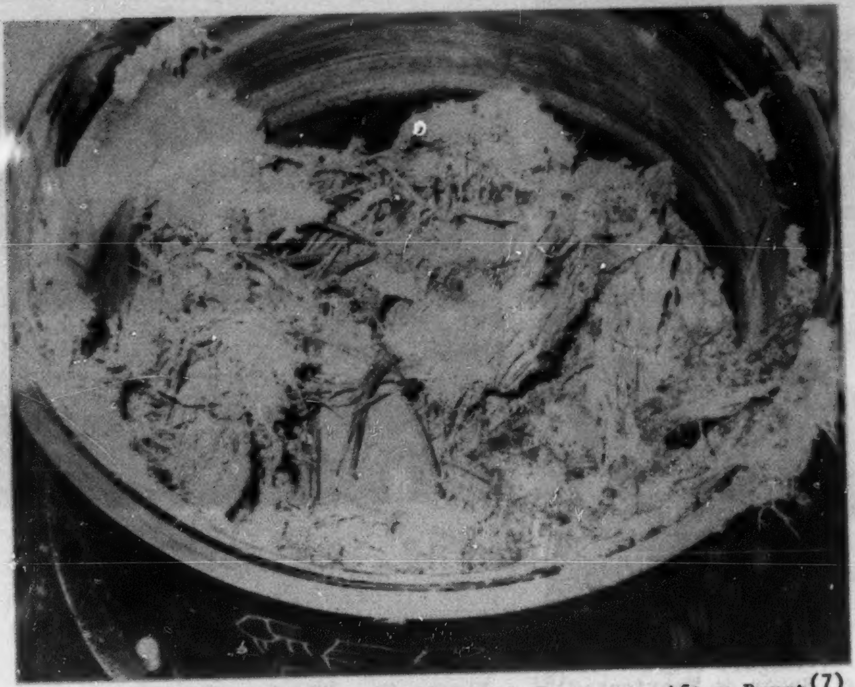

Figure 2. Glass/Epoxy Laminated Disk Fragments After Burst(7)

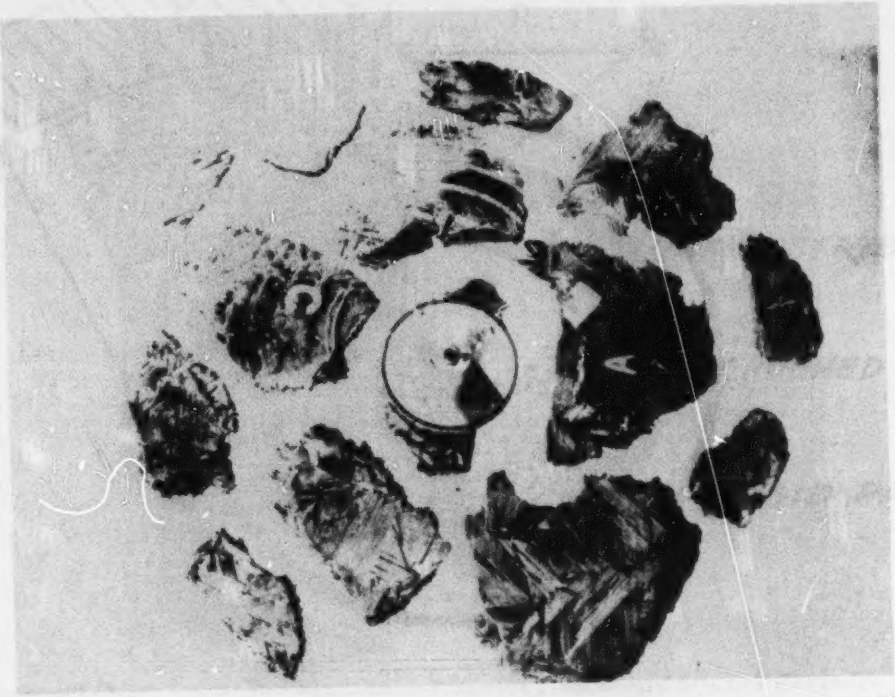

Figure 3. Graphite/Epoxy Laminated Profiled Thickness After Burst(1)

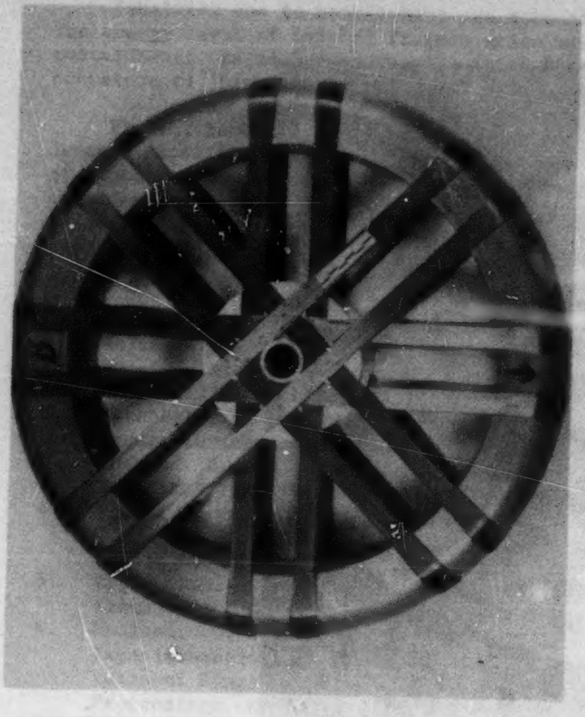

Figure 4a. "Bandwrap" Rotor as Fabricated(8)

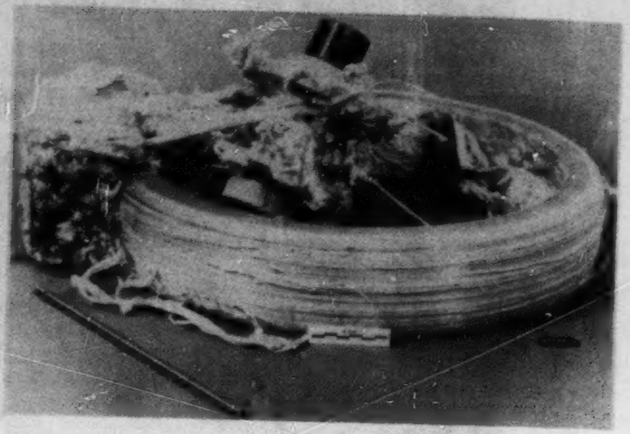

Figure 4b. "Bandwrap" After Failure, Showing Debris-Generated "Wedge"(8)

Figure 5. Wound Multi-Ring Kevlar/Epoxy Rotor After Failure

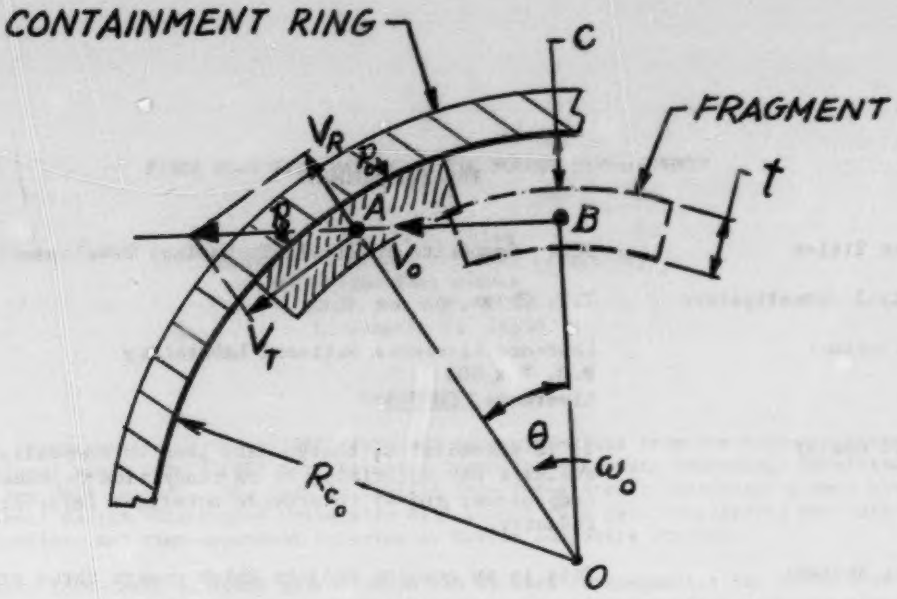
CONTAINMENT RING
C
FRAGMENT
t
V_R
P_A
δ
A
B
V_o
V_T
θ
ω_o
R_co
O

Figure 6. Fragment/Ring Contact: Rigid Fragment

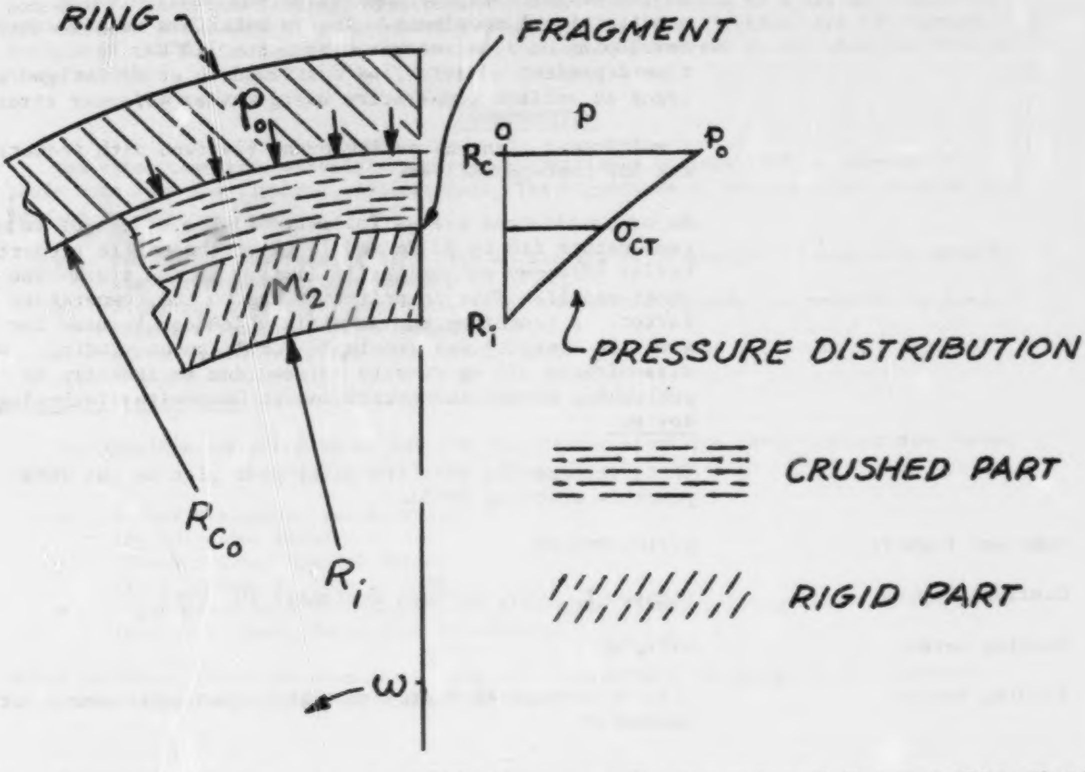
RING
FRAGMENT
P_o
M'_2
R_co
R_i
ω
p
o
R_c
P_o
σ_CT
R_i
PRESSURE DISTRIBUTION
CRUSHED PART
RIGID PART

Figure 7. Fragment/Ring Contact: Crushable Fragment, Showing Internal Pressure Distribution

PROJECT SUMMARY

Project Title:	Fiber Composite Materials Technology Development
Principal Investigator:	T.T. Chiao
Organization:	Lawrence Livermore National Laboratory P.O. Box 808 Livermore, CA 94550
Project Goals:	1) To establish an energy data base on composites; 2) to evaluate new materials; 3) to study time-dependent behavior of composites; and 4) to provide materials information to industry.
Project Status:	This is an ongoing project which covers three areas. In the area of data base, the effect of vacuum and temperature on the Kevlar 49/epoxy composites was studied using unidirectional specimens. In new materials we concentrated on developing an epoxy matrix system for 120°C. For time-dependent behavior, we continued to study fatigue and creep at ambient temperature using Kevlar 49/epoxy strands. A multi-year plan was outlined and reviewed with industrial and DOE representatives. Major conclusions are as follows: 1) The effect of vacuum and temperature (10 to 30 Pa and 75°C) on the static properties of Kevlar 49/epoxy composites is limited to the transverse and shear moduli. This is primarily due to the temperature factor. A promising epoxy matrix which can be used for 120°C with low toxicity was developed for filament winding. We have disseminated all up-to-date information to industry by publishing timely short articles in Composites Technology Review. It is recommended that the multi-year plan be put into practice starting FY-81.
Contract Number:	W-7405-ENG-48
Contract Period:	October 1, 1979, through September 30, 1980
Funding Level:	$434,000
Funding Source:	U.S. Department of Energy through Lawrence Livermore National Laboratory

FIBER COMPOSITE MATERIALS TECHNOLOGY DEVELOPMENT*

Mr. T. T. Chiao
Lawrence Livermore National Laboratory
7000 East Avenue
P.O. Box 808, L-388
Livermore, CA 94550

ABSTRACT

This paper summarizes the FY1980 technical accomplishments from the Lawrence Livermore National Laboratory (LLNL) for the Fiber Composite Materials Technology Development Task of the MEST Project. The task is divided into three areas: Engineering data base for flywheel design (Washington University will report this part separately) new materials evaluation, and time-dependent behavior of Kevlar composite strands.

We have formulated an epoxy matrix which can be used in composites for 120°C service with good processing and mechanical properties. Preliminary results on the time-dependent properties of the Kevlar 49/epoxy strands indicate: (1) Fatigue loading, as compared to sustained loading, drastically reduces the lifetime of a Kevlar composite; (2) the more the number of on-off load cycles, the less the lifetime; and (3) dynamic fatigue of the Kevlar composite can not be predicted by current damage theories such as Miner's Rule.

INTRODUCTION

The fiber composite materials program was initiated in late 1975 to provide the basic data base for flywheel applications. The objectives of the materials program have been to

- Develop an engineering data base on the static properties of composite materials for flywheel rotor designs.
- Study the time-dependent behavior of composites in order to predict the long-term performance of a flywheel rotor.
- Screen and develop new materials, fibers and matrices for potential flywheel applications.
- Disseminate information to the industry.

The specific technical scope and the responsible principal investigators are listed below:

- Matrix Evaluation and Formulation
  (Dr. J. Kolb, LLNL)
- Fibers & Other Special Topics
  (T. T. Chiao, R. Sherry, LLNL)
- Engineering Data On Composite Materials For Flywheel Design
  (Dr. T. H. Hahn, Washington University)

---

*Work performed under the auspices of the U. S. Department of Energy by the Lawrence Livermore Laboratory under Contract W-7405-Eng-48.

- Time-Dependent Behavior of Composites
  (Dr. E. M. Wu, LLNL)
- Information Dissemination to Industry
  (T. T. Chiao, LLNL)

In this paper, we summarize the technical progress made by Drs. Kolb and Wu in FY1980. The engineering data base will be covered by Dr. Hahn in a separate paper.

EPOXY MATRIX FOR 120°C SERVICE

System designers prefer to operate the flywheel in a vacuum chamber at as high a pressure as possible. This, in turn, may drive the service temperature of the rotor in excess of 120°C due to friction. This year we concentrated our matrix formulation work to meet this temperature requirement.

- Formulation

We studied four cycloaliphatic diamines and six imidazoles as the curing agent for the pure diglycidyl ether of bisthenol A diepoxide. The final formation selected (based on toxicity, processing factors, cured resin properties, and cost) is shown in Table 1.

Table 1. Epoxy Formulation

Base Resin	Dow DER 332
Curing Agent	Menthane Diamine
Wt. Ratio	100 Resin/24.5
Cure Cycle	2h from 23 to 150°C
	2h at 150°C

- Cost and Toxicity

Based on the above ratio, the resin system cost currently is $\$2^{+}$/lb which is approximately 80¢/lb more than the typical epoxies. This is mainly due to the low volume market of the menthane diamine. According to one manufacturer, there is no reason to believe why the typical volume-price relationship should not apply to menthane diamine. Nevertheless, cost for this resin system will be a drawback for some time to come. Chemically speaking, menthane diamine, being a member of the cycloaliphatic family should be much less toxic than the aromatic diamines. This is particularly true with regard to long-term toxicity.

- Processing Considerations

From the filament winding processing point of view, the viscosity is such that it requires little or no heating at ambient temperature (0.6 to 0.9 Pa's; and the potlife is such that is is adequate for wet-bath winding (gel time of 21h for 30-g mass at 25°C and 9.5h at 40°C). For composite processing, the recommended cure schedule is to gel the structure at 90°C or less, and a full cure for 2 hours at 150°C.

- Properties Of The Cured Resin

The cured resin, based on the conditions previously described, has a glass transition temperature of 153°C, and an equilibrium water absorption of 1% (ASTM - 570). The thermal coefficient of expansion (modified ASTM 228) can be represented by bilinear lines: 51.2×10^{-6} cm/cm/°C from 220 to 301K; 59×10^{-6} from 301 to 450K. The thermal conductivity (W/m·K) is 0.164 at 305K, 0.181 at 341K, and 0.218 at 418K.

The mechanical properties of the cured resin are summarized in Table 2.

Table 2. Mechanical Properties of the Cured Dow DER 332/MNDA

	25°C	75°C	125°C
Tensile Properties			
Modulus, GPa	2.8	2.4	1.9
Failure Stress, MPa	97.3	75.3	48.9
Failure Strain, %	7.0	6.4	6.9
Compressive Properties			
Stress at Max., MPa	124.2		
Compressive Modulus, GPa	0.04		
Strain at Max., %	6.4		
Shear Properties			
Failure Stress, MPa	62		
Shear Modulus			

Additional tests such as aging at 125°C in air and argon, and composite properties are in progress.

TIME DEPENDENT PROPERTIES OF KEVLAR 49/EPOXY COMPOSITE

Stress-rupture data of several composites have been summarized and published previously. Other than for the E-glass/epoxy composite, we consider that available data are adequate. Ongoing experiments using E-glass/epoxy strands are continuing at relatively low stress levels which have produced only few data points this year. In this paper, we summarize only Dr. Wu's work on Kevlar 49/epoxy strands in the area of stress-rupture and dynamic fatigue under tension.

The strand specimens are the basic building blocks for any flywheel designs. In our tensile stress-rupture and cyclic fatigue tests, fiber rupture controls the mode of failure of the specimens. We used Kevlar 49/epoxy strands from the same population to study the effect of load history on the lifetime of the composites. Preliminary data are summarized in Figures 1-3. In Figure 4 we compared the different load histories to show the trend.

Stress-rupture experiments were carried out under different constant tensions. This is essentially a one-cycle static fatigue test. Cyclic fatigue data were collected using square waves at different loading and resting ratios. Fatigue lifetime is the summation of all the times under load. From the data shown in Figures 1-4, preliminary conclusions are as follows:

- At a constant applied stress, cyclic loading is much more severe than sustained loading in damaging (in terms of drastically reduced lifetime) the longitudinal Kevlar 49/epoxy composite. (See Figures 1 and 2)

- The length of the rest periods in cyclic fatigue may also be an important factor affecting the lifetime of the longitudinal Kevlar composite. (See Figures 2, 3 and 4).

- Dynamic fatigue of longitudinal Kevlar composite can not be predicted by theories of cumulative damage such as Miner's Rule. (See Figure 4)

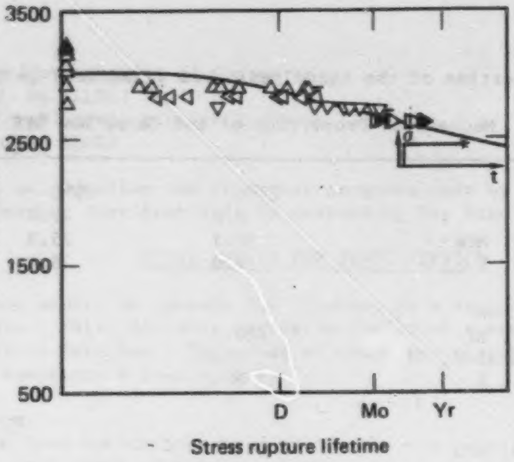

Fig. 1 Lifetime of Kevlar 49/Epoxy Strands Under Sustained Load

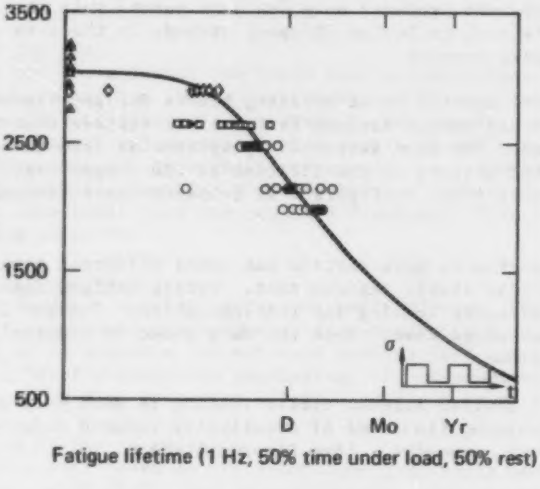

Fig. 2 Lifetime of Kevlar 49/Epoxy Strands Under Another Cyclic Load Condition

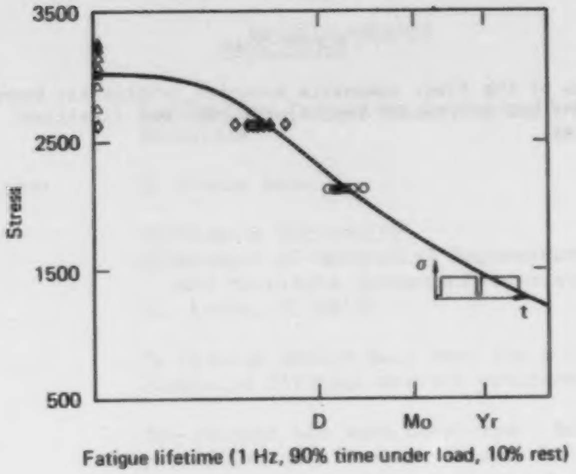

Fig. 3 Lifetime of Kevlar 49/Epoxy Strands Under One Cyclic Load Condition

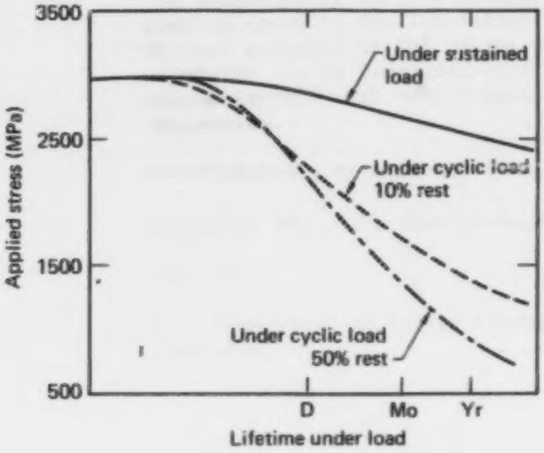

Fig. 4 Lifetime of Kevlar 49/Epoxy Strands Under Different Loading Conditions

FUTURE PLAN

A multi-year plan of the fiber composite material program has been completed, reviewed with industrial and government representatives, and finalized. We will put it into practice in FY1981.

PROJECT SUMMARY

Project Title:	Engineering Properties Determination for Fiber Composite Materials
Principal Investigator:	H. Thomas Hahn
Organization:	Washington University Department of Mechanical Engineering and Materials Research Laboratory St. Louis, MO 63130
Project Goals:	To develop design data base for a Kevlar 49/epoxy composite in simulated flywheel service environment.
Project Status:	The project has been completed. Both static and fatigue properties of a Kevlar 49/epoxy have been characterized in the laboratory environment and also in vacuum at 75°C. The epoxy, formulated at LLNL, was DER 332/Kelpoxy G293/Helox 68/Tonox 60-40(77/23/65/37.3) with a Tg of ~104°C. At 75°C both in air and in vacuum the longitudinal tensile strength was slightly higher than at the room temperature because of moisture desorption. The other strengths as well as the moduli showed only a small decrease. The longitudinal fatigue properties in vacuum at 75°C were as good as those in the laboratory environment. The median fatigue strength at 10^6 cycles was 70% of the average static strength. It is concluded that the composite can be used in vacuum at 75°C with only a minor loss in its mechanical properties.
Contract Number:	W-7405-ENG-48; Subcontract 6641009
Contract Period:	September 16, 1979, through September 15, 1980
Funding Level:	$50,835
Funding Source:	U.S. Department of Energy through Lawrence Livermore National Laboratory

ENGINEERING PROPERTIES DETERMINATION FOR COMPOSITE MATERIALS

H. Thomas Hahn and W. K. Chin
Materials Research Laboratory
Washington University
St. Louis, Missouri 63130

ABSTRACT

The purpose of this program was to determine the mechanical properties of a Kevlar 49/epoxy composite in a simulated flywheel service environment. The composite was filament-wound using an epoxy formulated at LLNL. The temperature and vacuum chosen were 75°C and $\sim 6 \times 10^{-3}$ torr, respectively. Specimens were preconditioned in the test environment for periods of 1 to 5 months before mechanical tests.

The simulated service environment seems beneficial for static strength while it has negligible effect on fatigue strength. Two factors seem responsible for such behavior: moisture desorption and lack of oxidation in vacuum. Thus, the elevated temperature of 75°C is no deterrent to the application of the Kevlar 49/epoxy composite in flywheels.

INTRODUCTION

Because of their high specific strength and nonhazardous failure modes, composite materials provide an excellent alternative to metals in the development of flywheel energy storage systems (1,2). The low mass density and high strength of composites make it possible for a flywheel made of composite material to store more kinetic energy per unit mass through increased speed. Since high-performance composites are relatively new, however, their reliability in service environments is not fully assessed yet. Therefore, we need to develop a solid data base for these materials before their full potential can be realized in flywheel applications.

Room temperature static properties, and a limited amount of stress rupture and fatigue properties, of composites suitable for flywheel applications have been characterized at LLNL. However, the design speed of a flywheel can be as high as 50,000 rpm, and therefore a vacuum near 10^{-4} torr is required to avoid excessive aerodynamic heating. Even so, the temperature can easily reach at least 75°C. Therefore, design data must be available on the mechanical performance of composites in such environment.

The combined effect of elevated temperature and vacuum on mechanical properties of composites, to the authors' knowledge, has not yet been characterized. Therefore, the objective of the present program is to develop a data base for a Kevlar 49/epoxy composite at 75°C in vacuum.

EXPERIMENTAL PROCEDURE

The composite studied was a unidirectional Kevlar 49/epoxy filament-wound at LLNL in the form of 254 mm x 305 mm panels. The epoxy was DER 332/Kelpoxy G293/Helox 68/Tonox 60-40 (77/23/65/37.3), and the composite was cured at 60°C for 4.5 h followed by a 3-h postcure at 130°C. The fiber volume content varied from 55 to 69%, and the nominal thickness was 0.5 mm. From the panels were cut $[0]_{2T}$ specimens 13 mm wide x 147 mm long with a 76-mm gage section.

Conditioning of some of the panels before mechanical tests was carried out in a vacuum oven at 75°C. Specimens, 13 mm wide x 33 mm long x 1 mm thick, were used to monitor the weight change as a function of the period of preconditioning.

At room temperature (RT), tensile tests were done either on an Instron or on an MTS machine. However, the Instron machine was exclusively used for elevated temperature (ET) tests. The loading rate was approximately 100N/s. Strain data were obtained by using strain gages.

Fatigue tests were performed on an MTS machine at a stress ratio of 0.1 and a loading frequency of 4 Hz. The fatigue tests at 75°C in vacuum were done inside a chamber designed at LLNL. A mechanical vacuum pump (Welch Duo-Seal Vacuum Pump) was used to maintain a vacuum of $6\sim8 \times 10^{-3}$ torr. The elevated temperature of 75°C was provided by electrical resistance heating.

RESULTS AND DISCUSSION

WEIGHT CHANGE DURING PRECONDITIONING

The weight change during preconditioning was monitored on two sets of specimens consisting of 15 specimens each. Each set was divided into 4 groups of equal number of specimens. Each group was then weighed on a rotational basis to minimize the possible moisture absorption during weight measurements. The results are shown in Figure 1. Note that after 11 months the weight loss is only 1.63%.

Two observations can be made of the results of Figure 1. First, the weight loss takes place at a faster rate in the beginning and then slows down. Second, the equilibrium weight loss is reached much earlier and to a lower value than reported elsewhere (3). The initial nonlinear diffusion can be caused by the frayed fibers along the cut edges. However, the second observation requires further explanation.

In the absence of voids, the equilibrium moisture content c of a composite can be determined from the equilibrium moisture contents of constituents by

$$c = (c_m v_m \rho_m + c_f v_f \rho_f)/(v_m \rho_m + v_f \rho_f)$$

Here the v's are volume fractions and the ρ's are mass densities. The subscripts m and f denote matrix and fiber, respectively.

In a typical laboratory environment where the relative humidity and temperature are ~50% and ~23°C, respectively, the equilibrium moisture contents are (3-6)

$$c_m = 2.3\%, \quad c_f = 3.2\%$$

Note that a typical value for most epoxies has been chosen for c_m.

The fiber volume fraction of the specimens used in Figure 1 is 0.7. Noting further that

$$\rho_m = 1.19, \quad \rho_f = 1.44$$

we finally calculate the equilibrium moisture content c to be 2.99%.

The calculated equilibrium moisture content is still larger than the experimentally measured. This observation in conjunction with the initial nonlinear diffusion leads to the conclusion that the moisture distribution at the start of the preconditioning was not uniform with higher moisture concentrations near the surfaces. Nevertheless, it can be concluded that the weight loss expected in a long-term exposure to the service environment is mostly caused by moisture desorption.

According to the results of Ref. (3), the time required for a 1.5 mm thick laminate to attain an equilibrium moisture content at 52% relative humidity and 23°C is about 14 months. The corresponding time required for the present specimens which are 0.5 mm thick is then one-ninth as long, or 1.6 months. Since the tests at room temperature were done at least 2 months after the panels had been fabricated, the moisture content in the specimens without preconditioning is expected to be an equilibrium value close to 3%.

STATIC PROPERTIES

At least ten specimens were tested in tension at each of the two temperatures (RT and 75°C) with and without preconditioning. The preconditioning was done for a period of 70-75 days. Since panels of various fiber volume contents were used, the data for failure stress and modulus were normalized to 65 volume percent of fiber using the rule of mixtures. For the failure strain and Poisson's ratio, the effect of fiber volume content is rather small for the range considered. Therefore, no modification was made of the data for these properties.

The static properties are summarized in Table 1. The Student t test applied to the failure stress data indicates with 95% confidence that the increase in failure stress after the preconditioning cannot be neglected. However, the difference between the RT and ET strengths is negligible both before and after the preconditioning. The modulus is lower at 75°C but it increases after the preconditioning.

The Kevlar fibers are known to suffer a loss in strength and modulus at 75°C in air (4). However, in atmosphere of N_2, the reduction in strength is almost negligible while the reduction in modulus is about the same as in air. Thus, the strength loss at 75°C in air is believed to be mostly caused by oxidation.

In the present composite laminate the fibers are protected by the matrix, and the large dimensions of specimens do not allow oxidation of a sufficient number of fibers to affect the composite strength in less than an hour required for static tests. Therefore, the resulting strength loss is expected to be small, as evidenced by the experimental data. One should note, however, that such minimal reduction in composite strength is in spite of ~50% strength reduction observed of an epoxy similar to the present one (7).

The increase in strength and modulus after the preconditioning is an encouraging sign for the application of the present composite in flywheels. In fact, a slight improvement of strength and modulus after drying was also observed in Ref. (3).

An exposure to 110°C in air for a period longer than 500 h has been shown to degrade the RT strength of a Kevlar 49/epoxy strand (8). In the present case, however, the temperature is lower although the preconditioning is more than three times as long. Yet, the combination of moisture desorption and lack of air seems to be mainly responsible for the improvement of properties after the preconditioning.

The specimens failed in a brush-like manner, as shown in Figure 2. Neither temperature nor preconditioning made any discernible differences. As the load was increased, longitudinal splits started at the tab ends and proceeded into the center section of specimen. Many longitudinal splits were observed before final failure.

Unlike brittle fibers such as graphite, boron, or glass, the Kevlar fibers fail by splitting along their length. The longitudinal splitting occurs because of poor laterial packing: the fibers consist of extended chains of macromolecules in lamellar form aligned along the fiber axis (9-11). This type of failure mode is certainly much less conducive to transverse crack propagation, and hence contribute to the brush-like failure of composite.

FATIGUE PROPERTIES

In general, fatigue life data were obtained at three different stress levels: 0.7 $\overline{X}$, 0.8 $\overline{X}$ and 0.9 $\overline{X}$. Here $\overline{X}$ is the average static strength in the same environment as the fatigue tests were run. A few more stress levels were chosen at room temperature.

The room-temperature fatigue data are shown in Figure 3. The general characteristics of the data are similar to those for graphite/epoxy and boron/epoxy composites (12). At 0.9 $\overline{X}$ the scatter is large. However, at lower stresses the scatter is smaller. Below 0.7 $\overline{X}$ no failures occur up to 10^6 cycles. A similar trend has been observed in the stress rupture of Kevlar 49/epoxy strands (13).

The results of elevated-temperature (ETV) fatigue tests in vacuum were obtained from those specimens that had been preconditioned for periods of 1 to 5 months. These ETV data in Figure 4 look very much like the RT data in Figure 3. Note that $\overline{X}$ in Figure 4 is the static strength at 75°C after the preconditioning, and hence larger than the one used in Figure 3.

At 100°C in air a considerable reduction in life has been observed in stress rupture of Kevlar 49/epoxy strands (13,14). Although obtained at a lower temperature of 75°C the present ETV data, however, shows no indication of significant degradation over the RT data, as will be shown later. Therefore, it is concluded that the accelerated failure at elevated temperature in air is caused by oxidation. In oxidative environment oxygen promotes breaking of molecular chains, thereby contributing to the cut growth, as observed in rubber (15). Such chain scission reactions are expected to occur in the fibers as well as in the matrix.

The macroscopic failure mode in fatigue was very similar to that in static tension regardless of preconditioning. The typical failure mode is as shown in Figure 2.

Both sets of fatigue data were fit by a two-parameter Weibull distribution of the form

$$R_f(N) = \exp\left[-\left(\frac{N}{N_o}\right)^{\alpha_f}\right]$$

The shape paraemter α_f and the characteristic life N_o were determined by the method of maximum likelihood. The results are listed in Table 2.

The shape parameter is smaller than unity at 0.9 $\overline{X}$ for both RT and ETV data. It increases with decreasing stress, becoming larger than unity at 0.7 $\overline{X}$. A similar variation of shape parameter with applied stress has been observed in the stress rupture data of Kevlar 49/epoxy strands (13). Thus, the failure process is believed to change from one controlled by initial defects to a wear-out failure as the fatigue stress is lowered from 0.9 $\overline{X}$ to 0.7 $\overline{X}$.

The ETV data are compared with the RT data in Figure 4 at two different survival probabilities. The RT data shows sharper downturn than the ETV data, indicating a possibility of the ETV environment being more beneficial in long-term applications. For practical purposes, however, there does not appear to be any difference between the two sets of data down to the fatigue stress of 0.7 $\overline{X}$.

CONCLUSIONS AND RECOMMENDATIONS

We have characterized the mechanical properties of a Kevlar 49/epoxy composite for flywheel applications. The composite was filament-wound using an epoxy formulated at LLNL. Two different environments were adopted: laboratory environment as a baseline, and a combination of 75°C and vacuum to simulate the flywheel service environment. Specimens were preconditioned in the test environment for periods of 1 to 5 months before mechanical tests. Fatigue tests were performed with a stress ratio of 0.1 and at a frequency of 4 Hz. The following conclusions can be drawn from the present study.

1. No unexpected weight loss has been caused by eleven months of exposure to the simulated service environment. A longer exposure is not likely to result in further weight loss. Most of the lost weight is moisture desorbed in vacuum.

2. The simulated service environment has been found to have no deleterious effects on static and fatigue strengths. Two factors seem responsible for such behavior: moisture desorption and lack of oxidation in vacuum.

3. The fatigue life expected at 70% of the average static strength is ~10^5 cycles for 95% survival probability.

4. The macroscopic failure mode is independent of the type of loading and also of the preconditioning. All specimens failed in a brush-like manner.

5. The elevated temperature of 75°C is no deterrent to the application of the present Kevlar 49/epoxy composite in flywheels. However, the possibility of increasing the service temperature to 150°C should be investigated.

REFERENCES

1. Proceedings of the 1975 Flywheel Technology Symposium, ERDA 76-85, ERDA and Lawrence Livermore Laboratory, 1975.
2. 1977 Flywheel Technology Symposium Proceedings, CONF-771053, Department of Energy, 1978.
3. E. M. Wu, "Strength Degradation of Aramid-Fiber/Epoxy Composites", AMMRC TR-80-19, April 1980.
4. Kevlar 49 Data Manual, DuPont de Nemours Chemical Company, Wilmington, Delaware, 1974.
5. R. DeIasi and J. B. Whiteside, "Effect of Moisture on Epoxy Resins and Composites", Advanced Composite Materials-Environmental Effects, ASTM STP 658, J. R. Vinson, Ed., 1978, p. 2.
6. L. Penn and F. Larsen, "Physiochemical Properties of Kevlar 49 Fiber", Preprint UCRL-79462, Lawrence Livermore Laboratory, June 1977.
7. J. A. Rinde, E. T. Mones, R. L. Moore, and H. A. Newey, "An Epoxy Resin-Elastomer System for Filament Winding", Proc. 34th Annual Conf. of the Reinforced Plastics/Composites Inst., SPI, 1979, 17-A.
8. L. Penn and R. J. Sherry, "Stress-Rupture Life and Strength Retention of an Aramid Fiber/Epoxy Composite Under Accelerating Conditions", Preprint UCRL-79449, Lawrence Livermore Laboratory, Nov. 1977.
9. C. C. Chiao and T. T. Chiao, "Aramid Fibers and Composites", Preprint UCRL-80400, Lawrence Livermore Laboratory, Dec. 1977.
10. A. R. Bunsell, "The Tensile and Fatigue Behavior of Kevlar-49 (PRD-49) Fibre", J. Mat. Sci., Vol. 10, 1975, p. 1300.
11. R. J. Morgan, E. T. Mones, W. J. Steele, and S. B. Deuttscher, "The Structure and Property Relationships of Poly (p-Phenylene Terephthalamide) Fibers", Preprint UCRL-84208, Lawrence Livermore Laboratory, April 1980.
12. H. T. Hahn, "Fatigue Behavior and Life Prediction of Composite Laminates", Composite Materials: Testing and Design (Fifth Conference), ASTM STP 674, S. W. Tsai, Ed., 1979, p. 383.
13. H. T. Hahn and T. T. Chiao, "Long-Term Behavior of Composite Materials", Advances in Composite Materials, Vol. 1, A. R. Bunsell, et al., Eds., Pergamon Press, 1980, p. 584.

14. C. C. Chiao, R. J. Sherry and N. W. Hetherington, "Experimental Verification of an Accelerated Test for Predicting the Lifetime of Organic Fiber Composites", J. Composite Materials, Vol. 11, 1977, p. 79.

15. A. N. Gent, "Some Chemical Effects in Fatigue Cracking of Vulcanized Rubbers", J. Applied Polymer Science, Vol. 6, 1962, p. 497.

Table 1. Static Properties (65 vol %)

	Without Preconditioning		With Preconditioning	
	RT	75°C	RT	75°C
Failure Stress Average, MPa C. V., %	1586(18) 4.12	1621(12) 3.44	1641(10) 3.93	1631(10) 2.14
Failure Strain Average, % C. V., %	2.09(5) 9.48	2.157(5) 3.29	2.023(5) 1.56	2.05(2) --
Modulus Average, GPa C. V., %	77.26(5) 3.94	75.06(5) 3.67	83.08(5) 2.79	77.56(5) 3.67
Poisson's Ratio Average, C. V., %	0.273 5.26	0.248 3.82	0.271 3.94	0.277 2.30

Table 2. Fatigue Properties

	RT		ETV	
Fatigue Stress/$\overline{X}$	α_f	N_o	α_f	N_o
0.7	1.994	1.295×10^6	1.254	1.297×10^6
0.8	1.183	4.643×10^5	0.997	2.832×10^5
0.9	0.373	1.821×10^4	0.429	4.658×10^4

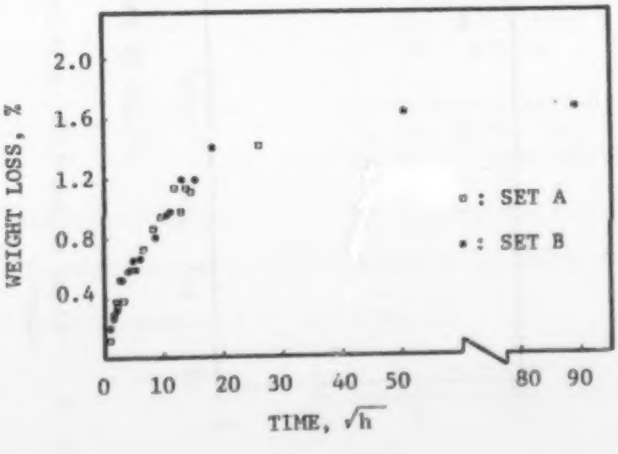

Fig. 1. Weight loss during preconditioning.

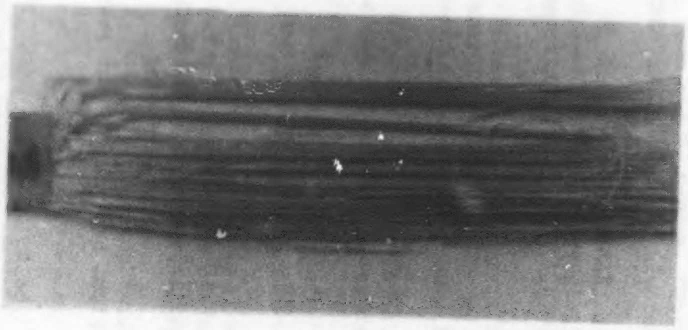

Fig. 2. A typical failure mode.

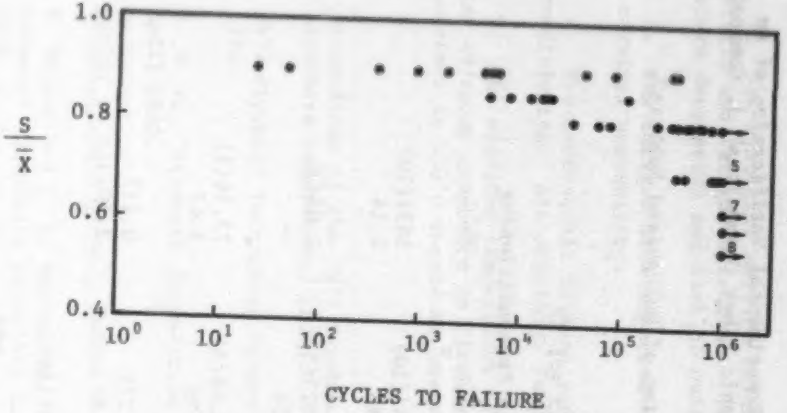

Fig. 3. Fatigue stress (S) - Life (N) relation at room temperature.

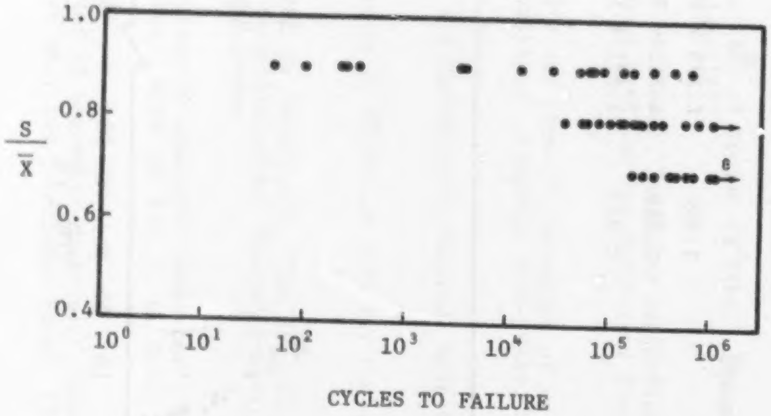

Fig. 4. Fatigue stress-life relation at 75°C in vacuum.

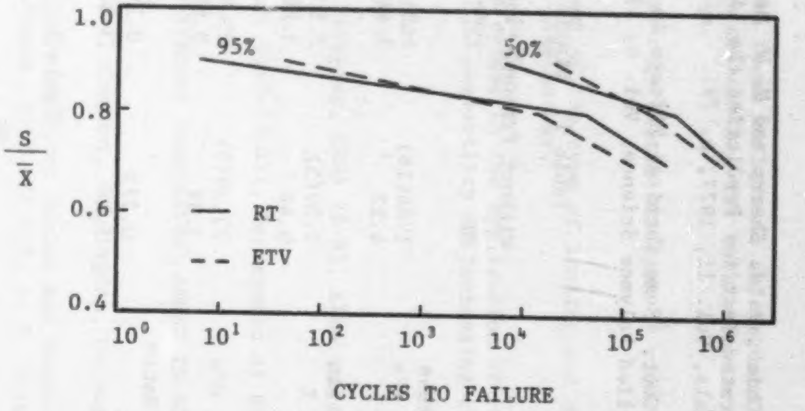

Fig. 5. Comparison between RT and ETV fatigue lives at 95% and 50% survival probabilities.

PROJECT SUMMARY

Project Title: Composite Flywheel Testing and Evaluation

Principal Investigator: Robert S. Steele, Jr., PhD

Organization:
Union Carbide Corporation
Nuclear Division
P. O. Box Y, 9998, MS-2
Oak Ridge, TN 37830
(615) 574-1837

Project Goal: The FY 1980 project goal was to evaluate for LLNL specific flywheels for maximum energy storage characteristics and to improve our capabilities based upon this experience in preparation for future, more comprehensive evaluation.

Project Status: Four flywheel evaluations with FY 1980 milestones are complete. Two others are in progress.

Major Findings are as follows:

1. The Garrett AiResearch sub-circular rim flywheel with graphite spokes achieved a maximum speed of 463 rev/sec and stored a maximum energy of 1.16 kW-h at 74.4 W-h/kg.

2. The William M. Brobeck composite rim with tension-balanced spokes achieved a maximum speed of 500 rev/sec and stored a maximum energy of .295 kW-h at 25.0 W-h/kg.

3. The Hercules pre-stressed graphite disk achieved a maximum speed of 372 rev/sec and stored a maximum energy of 0.85 kW-h at 37.5 W-h/kg.

4. The Rockwell-Rocketdyne Division graphite rim with twin disk hub achieved a maximum speed of 382 rev/sec and stored a maximum energy of 1.94 kW-h at 36.1 W-h/kg.

Other data regarding radial growth, resonant frequencies, failure modes, and other test observations are reported in detail test reports.

Contract Number: W-7405-eng-26, SANL/Request 803-039

Contact Period: December 10, 1979 through December 31, 1980

Funding Level: $385,000

Funding Source: U. S. Department of Energy through Lawrence Livermore National Laboratory.

COMPOSITE FLYWHEEL TESTING AND EVALUATION AT THE OAK RIDGE FLYWHEEL EVALUATION LABORATORY

R. S. Steele, Jr. and E. F. Babelay, Jr.
Union Carbide Corporation - Nuclear Division
P. O. Box Y
Oak Ridge, Tennessee 37830

ABSTRACT

This paper summarizes the results of spin tests conducted in the Oak Ridge Flywheel Evaluation Laboratory under a subcontract from Lawrence Livermore National Laboratory for the purpose of determining the ultimate energy density capabilities of the Garrett-AiResearch, William M. Brobeck and Associates, Hercules Aerospace, and Rockwell-Rocketdyne flywheel rotors built under subcontracts from Sandia National Laboratory, Albuquerque. A short description of each test is presented as well as data used to determine each failure mode. The conclusion was reached that each of these flywheels was limited by generic problems involving the attachment of a heavy rim to a central shaft.

INTRODUCTION

The Oak Ridge Flywheel Evaluation Laboratory (ORFEL), located in the Oak Ridge Y-12 Plant*, was established to comprehensively evaluate high performance composite flywheels. It is operated under a subcontract from the Mechanical Energy Storage Technology project at Lawrence Livermore National Laboratory (LLNL). The FY 1980 project goal has been to evaluate specific flywheels for maximum energy storage characteristics, while continuing to improve our analysis capabilities in preparation for future, more comprehensive evaluations. Flywheels evaluated during FY 1980 included four of the UCC-ND band-wrap design as partial fulfillment of facility qualification requirements, four that were built under Sandia National Laboratory Albuquerque (SNLA) subcontracts.[1] Evaluations of one each built by LLNL and General Electric are in progress. The results are summarized in Table 1. This paper will deal primarily with the results from the evaluation of the four SNLA subcontracted rotors.

GARRETT-AIRESEARCH FLYWHEEL TESTING RESULTS

The high-energy density composite flywheel[2] developed by Garrett-AiResearch employs the same sub-circular rim concept used successfully in their earlier flywheels. The primary new feature in this flywheel is the graphite composite hub which replaces an aluminum one and significantly reduces the weight of total flywheel with only minor reduction in total energy storage. Thus, the energy density is significantly increased. Figure 1 shows the flywheel tested at ORFEL.

The flywheel achieved a maximum speed of 463 rev/sec (27,780 rpm) and stored 1.16 kWhr at 74.6 Whr/kg (33.9 Whr/lb). Figure 2 is the runout plot for Run 21 of the Garrett flywheel. Each line is the locus of vectors whose components are the magnitude and phase angle of the radial eccentricity of a surface on the flywheel. Data were taken at approximately 5 rev/sec intervals in speed. The plot shows that between 430 and 450 rev/sec the rim eccentricities grew diametrically in opposite directions. That is, the rims had grown away from the 0° and 180° spokes. This was the predicted failure mode for the flywheel but it occurred at a speed slightly lower than the 504 rps (30,240 rpm) lift-off speed anticipated. Runout of the hub also grew rapidly at speeds above 450 rps. At 463 rps the dynamic instability became excessive and the test was terminated. During deceleration the flywheel stabilized, then became unstable again. The resulting instability grew until severe shaking caused the bond between the elastomer and the graphite hub to fail at 390 rev/sec. The flywheel then fell into the lip of a crash ring surrounding the wheel. The heat created by the subsequent rubbing caused the glow observed in the video record (Figure 3). Failure was complete within approximately 20 seconds after the drop. Figure 4 shows the base of the quill adaptor and the bond interface that failed.

---

*Operated for the Department of Energy by Union Carbide Corporation, Nuclear Division under Contract W-7405-eng-26.

WILLIAM M. BROBECK FLYWHEEL TESTING RESULTS

The William M. Brobeck Flywheel tested by ORFEL is shown in Figure 5. The flywheel design[3] featured a biannulated rim of S-2 fiberglas and Kevlar-49 with an aluminum hub supported by a Kevlar-49 overwrap. The rim and hub were joined by tension-balanced spokes designed to expand with the rim.

This flywheel failed while maintaining a constant 500 rev/sec (30,000 rpm). Total energy stored at that speed was 0.30 kWhr at 25 Whr/kg (11.35 Whr/lb). The phase reference is shown in Figure 6, along with the runout traces for the various probes monitoring the flywheel during the one second prior to catastrophic failure. These traces show that an asynchronous movement was developing in the hub and arbor but not in the rim. Figure 7 is a plot of the runout of the inner surface of the hub at various speeds approximately 1/2-in. up from the bottom. These figures show that the hub becomes elliptical with increasing speed as the tension-balanced spokes pinch opposite sides of a diameter. The axis of the ellipse will be different at each spoke location, and these plots are valid only at the lower spoke level. It is noted that in the 500 rps pattern, which was recorded just prior to failure, the axis shifted approximately 45°. These data indicate that failure was the result of a vibratory motion of the hub in relation to the rim. The most likely cause was a slightly earlier failure in one or more of the spokes.

HERCULES FLYWHEEL TESTING RESULTS

The Hercules Aerospace Flywheel was a circumferentially wrapped composite graphite disk subsequently machined to a specific contour. A polysulfone matrix was used to allow residual stresses to be economically generated in the disk during the winding process. The flywheel is shown in Figure 8.

Testing of this flywheel was terminated during the fourth run at the maximum speed of 372 rev/sec (22,320 rpm). Total energy stored was 0.85 kWhr at 37.5 Whr/kg (17.0 Whr/kg). The test was automatically terminated by a pressure rise caused by material slung from the outer surface of the flywheel (Figure 9). The flywheel was also experiencing circumferential cracking as seen by comparing the video pictures in Figures 10 and 11.

In the design summary[4] for this flywheel it is noted that the transverse strength of the composite was not as good as originally expected. Thus the circumferential cracking was the anticipated failure mode.

ROCKWELL-ROCKETDYNE TEST RESULTS

The Rockwell-Rocketdyne Flywheel[5] consisted of a graphite composite rim wound upon a mandrel that remained with the flywheel as an aluminum liner for the rim. The rim was supported by upper and lower disks machined to a uniform stress distribution design. These disks were centered in the mandrel by a total of 32 pins that were intended to maintain concentricity while the rim and mandrel grew away from the disk. Figure 12 is the Rockwell-Rocketdyne Flywheel tested by ORFEL. The 56.7 kg (125 lb) flywheel was the heaviest flywheel yet tested by ORFEL.

The maximum speed achieved was 383 rev/sec (22,980 rpm), 105% of the maximum design operating speed for the flywheel. Energy stored at this speed was 1.92 kWhr at 36.1 Whr/kg (16.4 Whr/lb). The maximum speed of the flywheel was limited by the fact that as speed increased the pins were unable to keep the disks centered in the hub within the test facility limits. Figures 13 and 14 show the gap between the hub disk and the rim at rest and near top speed during the final run. This gap appeared to be uniform about the circumference. What cannot be observed in the video signal is shown in the runout plot for the final run (Figure 15). Note that the runouts (twice the eccentricity) of the top disk and the bottom disk moved in opposite directions as the speed increased above 100 rev/sec. At the maximum speed the difference in these disk locations indicated a bending moment was being applied to the quill shaft above the safe allowable limit for the turbine. The visible symptoms which terminated the test were a growing instability and the eventual "bottoming out" of a damper. This series of tests identified a characteristic failure mode for this flywheel. The actual speed at which a test of this flywheel design is terminated will be dependent upon the clearance and locational tolerance of the particular test unit and the ability of the test facility to tolerate either a growing quill-tip couple force, as in this test, or a growing mass imbalance as would be the case for a double bearing suspension system.

CONCLUSIONS

This series of tests produced two composite flywheel records: 1) the highest energy density (by Garrett-AiResearch), and 2) the highest total energy stored (by Rockwell-Rocketdyne). The series also demonstrated that the generic problem of attaching a heavy rim to a central shaft still lacks an optimum solution, and all of the flywheels tested in ORFEL were limited by problems in this crucial area. Therefore, this is the problem that will have to be solved or eliminated before rim-type composite flywheels reach their full potential.

REFERENCES

1. "Sandia Activities Overview," R. O. Woods, Proceedings of the 1979 Mechanical and Magentic Energy Storage Contractor's Review Meeting, Conf-790854 (1979).
2. "High-Energy-Density Composite Flywheel," D. L. Satchwell, Dennis A. Towgood, SAND 78-7019 (February 1980).
3. "Fabrication of Two One-fifth Fiber Composite Flywheels - Final Report," William M. Brobeck and Associates, Berkley Ca., UCRL-15231 (April 1980).
4. "Design and Fabrication of a 5 kW-h Flywheel, Design Summary," AO-8472, Hercules Aerospace Division (12 February 1980).
5. "RPE-10 Composite Flywheel Final Report," RI/RD79-334, Rockwell International, Rocketdyne Division (October 1979).

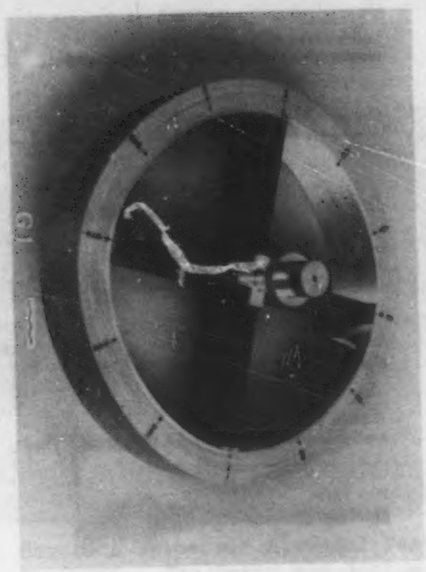

Fig. 1. Garrett-AiResearch Flywheel Tested by ORFEL. (193634)

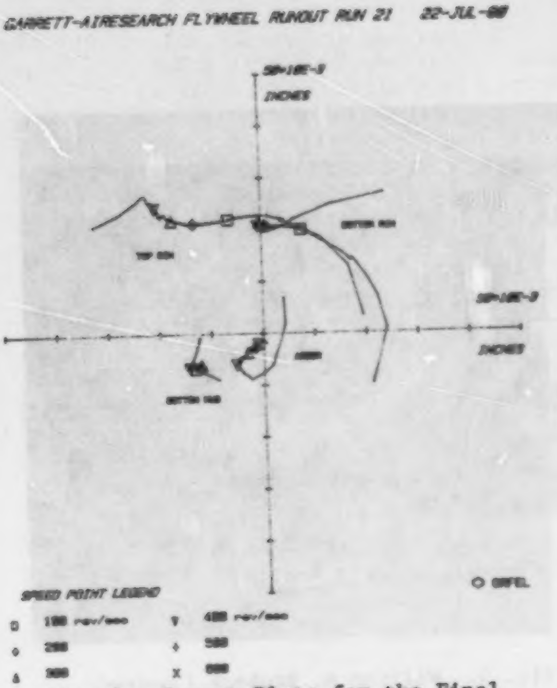

Fig. 2. Runout Plots for the Final Test Run of the Garrett-AiResearch Flywheel. (196592)

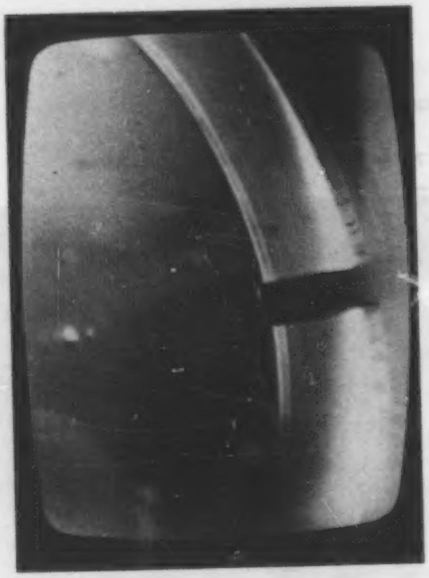

Fig. 3. Video Recording of the Garrett-AiResearch Flywheel Rubbing the Crash Ring During the Final Portion of the Failure. (195761)

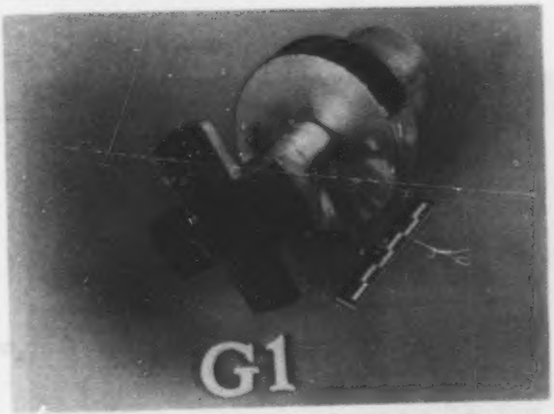

Fig. 4. Base of the Quill Adaptor at the Elastomer-Graphite Interface. (195746)

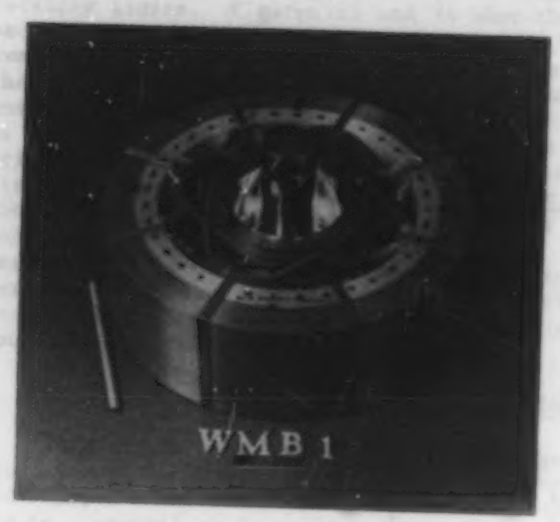

Fig. 5. William M. Brobeck Flywheel Tested at ORFEL. (194557)

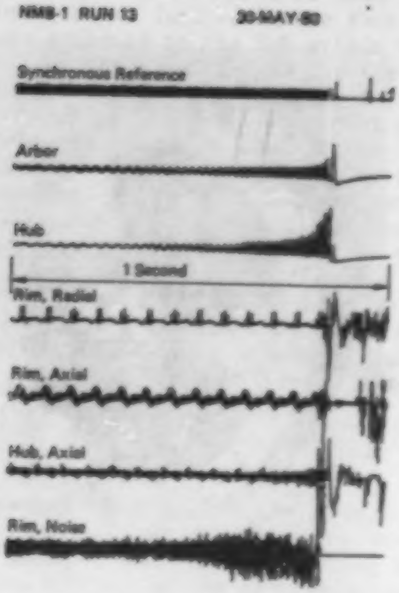

Fig. 6. Time-Domain Runout Traces During the Final One Second of Run 13.

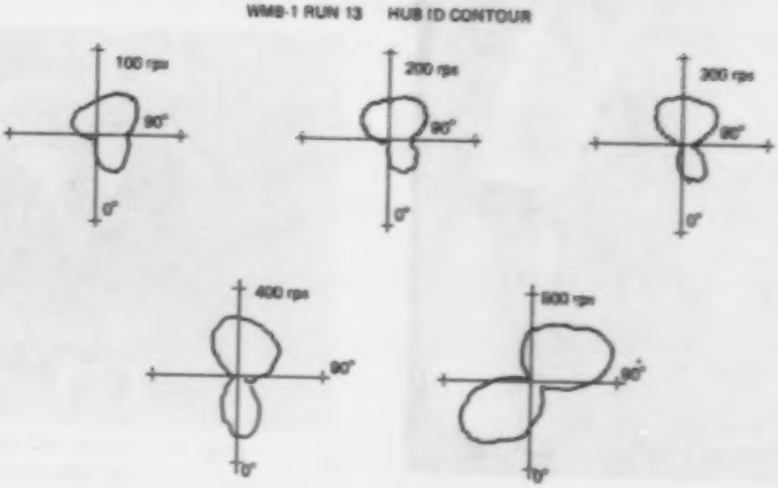

Fig. 7. Runout Pattern of the Innersurface of the William M. Brobeck Flywheel's Hub at Various Speeds.

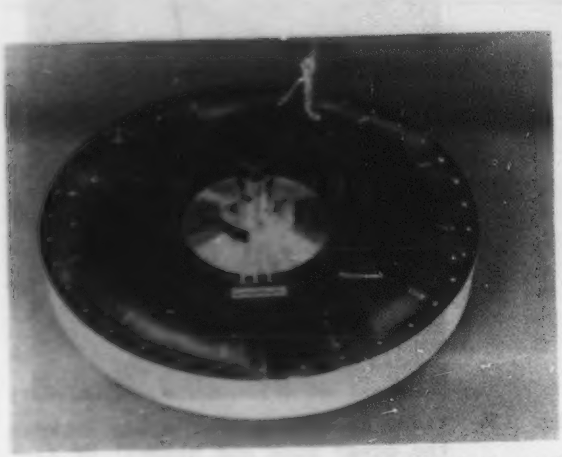

Fig. 8. Hercules Aerospace Flywheel Tested by ORFEL. The Outer and Bottom Surfaces Were Painted White. (195696)

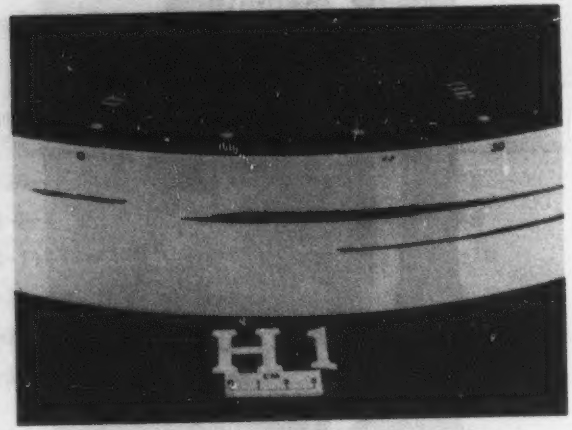

Fig. 9. Graphite Composite Slings From the Outer Surface. (196019)

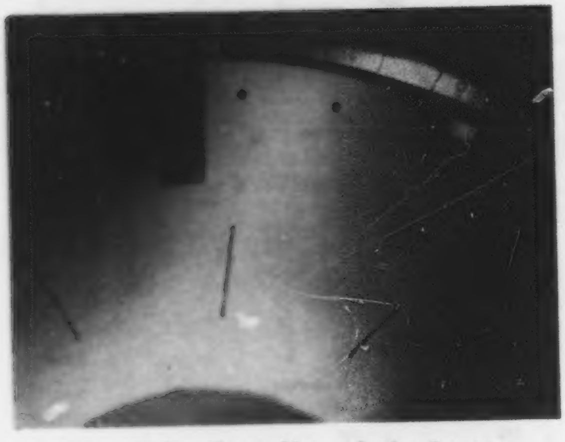

Fig. 10. Video Recording of the Lower Flywheel Surface at Rest Before Final Run. (196611)

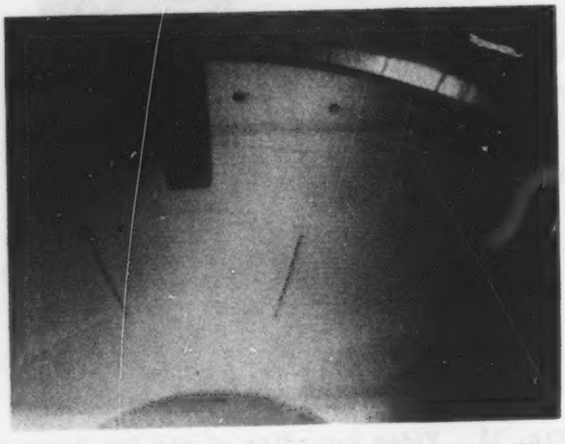

Fig. 11. Video Recording of the Lower Flywheel Surface Spinning at 350 rev/sec. (196610)

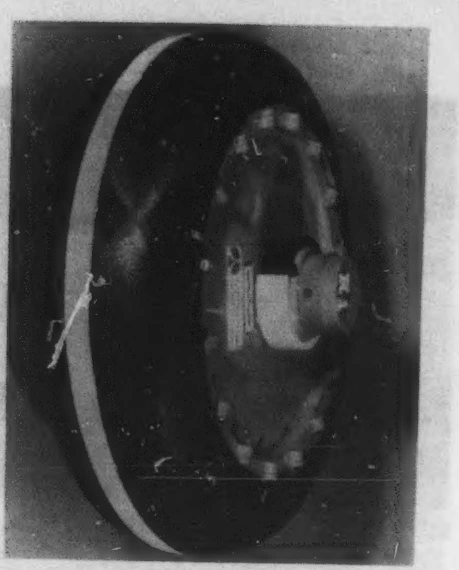

Fig. 12. Rockett-Rocketdyne Flywheel Tested by ORFEL. A Portion of the Outer Surface Was Painted White to Improve Radial Proximity Probe Sensitivity. (196051)

Fig. 13. Video Recording of the Gap Between the Lower Disk and Mandrel at Rest. (196609)

Fig. 14. Video Recording of the Gap Between the Lower Disk and Mandrel Near Top Speed. (196608)

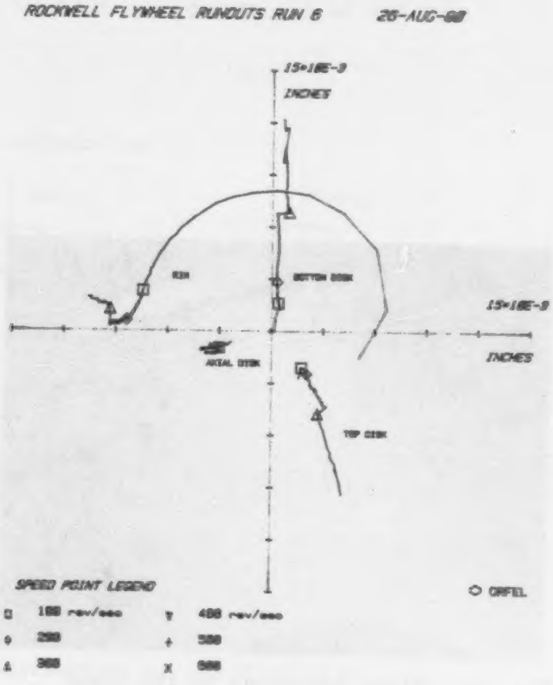

Fig. 15. Runout Plots for the Final Run. (196591)

Table 1

ORFEL FLYWHEEL TEST SUMMARY

Type	Designer Organization	Last Test Date	Results
Band Wrap	UCC-ND	9-10-79	Band Failure, 49 w-h/kg
Band Wrap	UCC-ND	11-8-79	Band Failure, 42 w-h/kg
Band Wrap	UCC-ND	12-11-79	Band Failure, 150 kft-lb
Band Wrap	UCC-ND	1-22-80	Band Failure, 5 kft-lb
Wagon Wheel	SNLA	2-14-80	Balanced, non-destructive
Tension Balanced Spokes	Brobeck	5-30-80	Hub/spoke failure, 25 w-h/kg
Sub-Circular Rim	AiResearch	7-2-80	Circular Rim, 74 w-h/kg
Prestressed Disk	Hercules	8-1-80	Circumferential cracking 37.5 w-h/kg
Twin-Disk Hub	Rockwell	8-20-80	Disk eccentricity, 36.1 w-h/kg

MECHANICAL, MAGNETIC, and UNDERGROUND ENERGY STORAGE 1980 ANNUAL CONTRACTORS' REVIEW

Washington, D.C.
November 10-13, 1980

United States Department of Energy
Office of Advanced Conservation Technology

Coordinated by Pacific Northwest Laboratory
Meeting Moderator: J.E. Minor

PRELIMINARY AGENDA

SUNDAY, NOVEMBER 9, 1980

6:00-9:00 pm	Registration/Reception	
9:00-10:00 pm	Review Committee Meeting	

MONDAY, NOVEMBER 10, 1980 (Grand Ballroom, Salons A, B, & C)

7:30-8:30 am	Registration (Continued)	
8:30-9:00 am	**Mechanical, Magnetic, and Underground Energy Storage Overview**	
	Introduction, Agenda, Announcements	J.E. Minor (PNL)
	DOE Headquarters Overview	J.A. Swisher (DOE)
	Seasonal Thermal Energy Storage (STES) Program	
9:00-9:40 am	*Program Overview* *International Activities in STES*	J.E. Minor (PNL)
	ATES PROJECTS	K. Fox, Moderator (PNL)
9:40-10:00am	*Bethel, Alaska, ATES Demonstration Project*	J. Cherne (TRW)
10:00-10:20 am	*Stony Brook, New York, ATES Demonstration Project*	L. Stern (D&M)
10:20-10:40 am	COFFEE BREAK	
10:40-11:00 am	*University of Minnesota ATES Demonstration Project*	W.E. Soderberg (Univ. of Minn.)
	STES SUPPORT PROGRAM	J.R. Eliason (PNL) Moderator
11:00-11:20 am	*Environmental Assessment*	H.E. McCartney (RM&A)
11:20-11:40 am	*Programmatic Environmental Assessment (Documentation)*	D. Lee (ORNL)
11:40-1:00 pm	LUNCHEON (Grand Ballroom, Salons D & E)	

1:00-1:20 pm	*Economic Assessment*	R.W. Reilly (PNL)
1:20-1:50 pm	*STES Technical Information System*	V. Hampel (LLL)
1:50-2:20 pm	*Field Test Facility*	F. Molz (Auburn)
2:20-2:50 pm	*Flow Facility Development and Laboratory Analysis*	C.H. Cooley (Terra Tek)
2:50-3:10 pm	COFFEE BREAK	
3:10-3:30 pm	*Numerical Simulation*	C.T. Kincaid (PNL)
3:30-4:00 pm	*ATES Simulation Studies*	C.F. Tsang (LBL)
4:00-4:20 pm	*Non-Aquifer STES Concepts*	D.E. Blahnik (PNL)

TUESDAY, NOVEMBER 11, 1980 (Grand Ballroom, Salons A, B, & C)

Compressed Air Energy Storage (CAES) Program

8:30-8:50 am	*CAES and UPHS Program Overview*	W.V. Loscutoff (PNL)
8:50-9:10 am	*Second-Generation Concepts Studies*	F.R. Zaloudek (PNL)
9:10-9:30 am	*CAES/FBC Studies*	R.D. Lessard (UTRC)
9:30-9:50 am	*Adiabatic CAES with Hard Rock Caverns*	C.L. Driggs (AAI)
9:50-10:10 am	*Adiabatic CAES with Aquifers*	S. Bahadur (AAI)
10:10-10:30 am	COFFEE BREAK	
10:30-10:50 am	*Champagne Effect*	D.S. Rowe (R&A)
10:50-11:10 am	*Reservoir Stability Studies*	L.D. Kannberg (PNL)
11:10-11:30 am	*Numerical Studies of Salt Cavities*	J. McNamara (SGI)
11:30-11:50 am	*Laboratory Studies of Salt*	R.L. Thoms (LSU)
11:50-1:00 pm	LUNCHEON (Buffet Style, Stirrup Cup Lounge)	
1:00-1:30 pm	*Hard Rock Studies*	A.F. Fossum (R/S)
1:30-1:50 pm	*Laboratory Studies of Aquifers*	J.A. Stottlemyre (PNL)
1:50-2:10 pm	*Aquifer Field Studies*	Neil Rudd (D&M)

Magnetic Energy Storage Program

2:10-2:25 pm	*Magnetic Energy Storage Program Overview*	M.O. Hoenig (MIT)
2:25-2:55 pm	*30MJ Superconducting Magnetic Energy Storage for BPA Transmission Line Stabilizer*	R.I. Schermer (Los Alamos)
2:55-3:10 pm	*30MJ Superconducting Coil Design and Fabrication*	J. Purcell (General Atomics)
3:10-3:25 pm	COFFEE BREAK	

3:25-3:40 pm	*Effects of SMES Units on Power System Stability*	J.A. Juves/ R.T. Byerly (Westinghouse)
3:40-3:55 pm	*Wire Rope Superconducting Cable for Diurnal Load Leveling SMES*	G. Costello (Univ. of Illinois)
3:55-4:15 pm	*Diurnal Energy Storage System's Design*	R.W. Boom (Univ. of Wisconsin)
4:15-4:30 pm	*Composite Conductor Development for Diurnal Energy Storage*	S. Van Sciver (Univ. of Wisconsin)
4:30-4:45 pm	*Development of NbTi for Diurnal Superconductive Magnetic Energy Storage*	D. Larbalestier (Univ. of Wisconsin)
5:30-7:00 pm	CASH BAR RECEPTION (Potomac & Bethesda Suites)	
7:00-9:00 pm	BANQUET (Salons A & B) *The Need for Annual Storage of Heat and Cold*	T.B. Taylor

WEDNESDAY, NOVEMBER 12, 1980 (Grand Ballroom, Salons A, B, & C)

8:00 am	**Flywheel Energy Storage Program**	
8:00-8:10 am	*Flywheel Energy Storage Program Overview*	T.M. Barlow (LLL)
8:10-8:30 am	*Mechanical Energy Storage Technology Application to Electric Vehicles*	E.P. Cornell (GE)
8:30-8:50 am	*Flywheel/Heat Engine Vehicle Applications Analysis*	A. Frank (Univ. of Wisconsin)
8:50-9:10 am	*Flywheel/Heat Engine Vehicle Design and Analysis*	I. Kains (Eaton Corp.)
9:10-9:30 am	*Elastomeric Energy Storage*	L.O. Hoppie (Eaton Corp.)
9:30-9:50 am	*Photovoltaic Energy System Applications of Flywheel Technology*	P.O. Jarvinen (MIT)
9:50-10:10 am	*Analysis of Fixed-Base Application of Mechanical Energy Storage*	D.B. Eisenhaure (Draper Lab)
10:10-10:30 am	COFFEE BREAK	
10:30-10:50 am	*Laboratory Development of a Variable Inertia Flywheel*	D. Ullman (Union College)
10:50-11:10 am	*Flywheel Applications of Cellulosic Materials*	D. Hagen (Univ. of Minnesota)
11:10-11:30 am	*The Alpha-Ply Laminated-Disc Flywheel Rotor*	R. Nimmer (GE)
11:30-11:50 am	*The Tapered-Thickness-Disc Flywheel Rotor*	S.V. Kulkarni (LLL)
11:50-1:20 pm	LUNCHEON (Buffet Style, Stirrup Cup Lounge)	

1:20-1:40 pm	*The Bidirectional Weave Disc-Type Rotor*	**A.D. Sapowith (AVCO Corp.)**
1:40-2:00 pm	*Flywheel Technology Development at APL*	**D.W. Rabenhorst (APL)**
2:00-2:20 pm	*Matched-Metal-Die Compression Molding: An Advanced Flywheel Fabrication Technology*	**F.Y. Soliman (Ewald Products)**
2:20-2:40 pm	*Compression Molded Low-Cost Composite Rotors*	**J.F. Kay (Owens Corning)**
2:40-3:00 pm	*Fabrication of High Performance, Filament-Wound Fiber Composite Rings*	**A.J. Hannibal (Lord Corp.)**
3:00-3:20 pm	COFFEE BREAK	
3:20-3:40 pm	*Review of Flywheel Containment Technology*	**A.D. Sapowith (AVCO Corp.)**
3:40-4:00 pm	*Review of Flywheel Containment Technology*	**A.P. Coppa (GE)**
4:00-4:20 pm	*Fiber Composite Materials Technology Development*	**T.T. Chiao (LLL)**
4:20-4:40 pm	*Engineering Properties Determination for Fiber Composite Materials*	**H.T. Hahn (Washington Univ.)**
4:40-5:00 pm	*Flywheel Tests-at the Oak Ridge Flywheel Evaluation Laboratory*	**R.S. Steele (Union Carbide)**
5:00 pm	*Closing Remarks*	**J.A Swisher (DOE)**

THURSDAY, NOVEMBER 13, 1980 (Potomac Suite)

8:30-10:00 am	Executive Session (Critique)
10:00-10:15 am	COFFEE BREAK
10:15 am	Review Committee Report and Closing

MECHANICAL, MAGNETIC, and UNDERGROUND ENERGY STORAGE 1980 ANNUAL CONTRACTORS' REVIEW

Washington, D.C.
November 10-13, 1980

LIST OF ATTENDEES

Michael Ambrosino
Ambrosino and DePinto
215 Lexington Avenue
New York, NY 10016

Donald E. Anderson
Fennix & Scisson
1401 South Boulder
Tulsa, OK 74119

Edwin F. Babelay, Jr.
Union Carbide
P.O. Box Y
Oak Ridge, TN 37830

Sher Bahadur
Acres American, Inc.
The Clark Building, Suite 329
Columbia, MD 20144

Thomas M. Barlow
Lawrence Livermore Lab.
P.O. Box 808, M/S L-388
Livermore, CA 94550

Don E. Blahnik
Pacific Northwest Labs
P.O. Box 999
Richland, WA 99352

Roger W. Boom
University of Wisconsin
531 Engr. Bldg. 1500 Johnson Dr.
Madison, WI 53706

Terje Brandshaug
RE/SPEC, Inc.
Box 725
Rapid City, SD 57709

C. Everett Brett
Univ. of Alabama
Engineering and Mines
University, AL 35486

Sibley C. Burnett
General Atomic Co.
P.O. Box 81608
San Diego, CA 92138

Sibley C. Burnett
General Atomic Co.
P.O. Box 81608
San Diego, CA 92138

Richard T. Byerly
Westinghouse Electric Corp.
700 Braddock Avenue
East Pittsburgh, PA 15112

Jack M. Cherne
TRW Energy Systems
One Space Park
Redondo Beach, CA 90278

T. T. Chiao
Lawrence Livermore Lab.
P.O. Box 808, L-338
Livermore, CA 94550

Anthony P. Coppa
General Electric Space Div.
P.O. Box 8555
Philadelphia, PA 19066

Don Cornish
Lawrence Livermore Labs
P.O. Box 808 L-550
Livermore, CA 94550

William T. Crothers
Lawrence Livermore Lab.
P.O. Box 808
Livermore, CA 94550

Roger Derby
Oak Ridge National Lab
P. O. Box Y Building 9204-1
Oak Ridge, TN 37830

Charles Driggs
Acres American, Inc.
Liberty Bank Building Main at Court
Buffalo, NY 14202

Jay R. Eliason
Pacific Northwest Labs
P.O. Box 999
Richland, WA 99352

David L. Chiang
ENTEC Research Associates
451 Hungerford Drive
Rockville, MD 20850

Craig H. Cooley
Terra Tek
Univ. Res. Park, 400 Wakara Way
Salt Lake City UT 84108

E.P. Cornell
General Electric Corp.
P.O. Box 43
Schenectady, NY 12301

George Costello
University of Illinois
Dept. of Applied Mechanics
Champaign, IL 61801

Donald E. Davis
Rockwell International
6633 Canoga Ave.
Canoga Park, CA 91304

Terry Doherty
Pacific Northwest Labs
P.O. Box 999
Richland, WA 99352

David B. Eisenhaure
Charles Stark Draper Lab
Mail Sta. #37, 555 Technology Square
Cambridge, MA 02139

Bob L. Erikson
Pacific Northwest Labs
P.O. Box 999
Richland, WA 99352

Harold E. Evans
NASA/GSFC
Greenbelt
Maryland 20770

Yehia Eyssa
University of Wisconsin
541 Engr. Res. Bldg. 1500 Johnson Dr.
Madison, WI 53706

Oswald C. Farquhar
University of Massachusetts
Department of Geology
Amherst, MA 01003

Arlo F. Fossum
Re/Spec, Inc.
P.O. Box 725
Rapid City, SD 57701

Kenneth Fox
Pacific Northwest Labs
P.O. Box 999
Richland, WA 99352

Andrew Frank
University of Wisconsin
Dept. of Electrical Engineering
Madison, WI 53706

Neil Frank
Lawrence Livermore Lab.
P.O. Box 808, L-388
Livermore, CA 94550

William A. Frier
Battelle-Columbus
2030 M St., N.W. Ste. 705
Washington, DC 20036

John Gahimer
Dept. of Energy, CS-AC
1000 Independence Ave.
Wash., DC 20585

Brian J. Gallagher
USDOE, OACT
600 E Street, N.W., Room 416
Washington, DC 20585

Albert J. Giramonti
United Technologies Corp.
Silver Lane
E. Hartford, CT 06001

Peter Graneau
M.I.T.
150 Albany Street
Cambridge, MA 02139

Michael Gurevich
Department of Energy
1000 Independence Ave.
Wash., D.C. 20585

David L. Hagen
University of Minnesota
111 Church Street, S.E.
Minneapolis, MN 55455

H. Thomas Hahn
Washington University
Campus Box 1087
St. Louis, MO 63130

Viktor E. Hampel
University of California
P.O. Box 808
Livermore, CA 94550

Alan J. Hannibal
Lord Corporation
P.O. Box 2051
Erie, PA 16152

Guran A. Hellstrom
Lawrence Berkeley Laboratory
One Cyclotron Road
Berkeley, CA 94720

Mitchell O. Hoenig
Massachusetts Inst. of Tech.
150 Albany Street, MW 14-2219 A
Cambridge, MA 02139

Jonathan W. Hurwitch
Battelle/Columbus
2030 M Street, Suite 700
Washington, DC 20036

Phillip O. Jarvinen
MIT Lincoln Laboratory
P.O. Box 73 -D337
Lexington, MA 02173

Ilmar Kalns
Eaton Corporation
26201 Northwestern Highway
Southfield, MI 48037

Lincoln B. Katter
Rocket Research Company
11441 Willows Road
Redmond, WA 98052

John F. Kay
Owens Corning Fiberglass
Technical Center
Granville, OH 43023

K. Theodore Hartwig
University of Wisconsin
543 Engr. Res Bldg. 1500 Johnson Dr.
Madison, WI 53706

Michael J. Hobson
Acres American, Inc.
The Clark Bldg., Suite 329
Columbia, MD 21044

Lyle O. Hoppie
Eaton Corporation
26201 Northwestern Highway
Southfield, MI 48037

William D. Jackson
Energy Consulting, Inc.
3590 McKinley Street, N.W.
Washington, DC 20015

Cordell K. Jee
ENTEC Research Associates
451 Hungerford Dr.
Rockville, MD 20850

Gabor M. Karadi
Univ of Wisconsin
2600 N. Cramer
Milwaukee, WI 53201

Donald L. Katz
University of Michigan
2042 East Engineering Bldg.
Ann Arbor, MI 48109

Richard H. Ketelle
Union Carbide Corp
P.O. Box Y
Oak Ridge, TN 37830

Charles T. Kincaid
Pacific Northwest Labs
P.O. Box 999
Richland, WA 99352

Satish V. Kulkarni
Lawrence Livermore Laboratory
P.O. Box 808, L-338
Livermore, CA 94550

Phillip J. Legendre
20030 Century Blvd.
Germantown
Maryland 20767

Walter V. Loscutoff
Pacific Northwest Labs
P.O. Box 999
Richland, WA 99352

Robert F. McAlevy, III
Robert F. McAlevy III & Assoc.
P.O. Box 300
Hampton Bays, NY 11946

Heather McCartney
Resource Man. & Assessment
P.O. Box 981
Everett, WA 98203

Charles A. McMonagle
Rowe and Associates
14400 Bellevue-Redmond Rd.
Bellevue, WA 98007

Bruce R. Meyer
Rensselaer Polytechnic Institute
Jonsson Engineering Center
Troy, NY 12181

Dennis M. King
Lawrence Livermore Laboratory
P.O. Box 808, L-388
Livermore, CA 94550

David C. Larbalestier
The Univerity of Wisconsin
1105 Eng. Bldg. 1500 Johnson Dr.
Madison, WI 53706

Robert D. Lessard
United Tech Research Center
Silver Lane
East Hartford, CT 06108

C. Lynn Marksberry
FluiDyne Engineering Corp
5900 Olson Memorial Highway
Minneapolis, MN 55422

Marianne B. McCarthy
MCC Associates, Inc.
1533 Red Oak Drive
Silver Spring, MD 20910

Arthur W. McGuigan
Westinghouse
700 Braddock Avenue
East Pittsburgh, PA 15112

John McNamara
Serata Geomechanics
1229 Eighth Street
Berkeley, CA 94710

Charles F. Meyer
Energy Program, GE-TEMPO
816 State St., P.O. Drawer QQ
Santa Barbara, CA 93103

Allan I. Michaels
Argonne National Laboratory
9700 South Cass Avenue, Bldg. 362
Argonne, IL 60439

James E. Minor
Pacific Northwest Labs
P.O. Box 999
Richland, WA 99352

Fred Molz
Auburn University
Engineering Experimental Sta.
Auburn, AL 36830

David A. Myers
Pacific Northwest Labs
P.O. Box 999
Richland, WA 99352

Brian R. Noton
Battelle
505 King Ave.
Columbus, OH 43201

A. David Parr
Auburn University
School of Engineering
Auburn, AL 36830

Jose C. Pereira
PB-KBB, Inc.
11999 Katy Freeway No. 600
Houston, TX 77079

Leigh S. Prater
Pacific Northwest Labs
P.O. Box 999
Richland, WA 99352

Barry L. Miller
Bonneville Power Administ.
1002 N.E. Holladay St. P.O.B. 3621
Portland, OR 97208

Al Mitchell
Fenix & Scisson, Inc.
1401 South Boulder
Tulsa, OK 74119

Milton L. Moon
Johns Hopkins University
Johns Hopkins Road
Laurel, MD 20810

Ronald P. Nimmer
General Electric Company
One River Rd., Bldg. 37, Rm. 304
Schenectady, NY 12309

Lawrence G. O'Connell
Lawrence Livermore National Lab
P.O. Box 808
Livermore, CA 94550

Joseph J. Peerson
Argonne National Laboratory
9700 South Cass Avenue
Argonne, IL 60439

Leigh S. Prater
Pacific Northwest Labs
P.O. Box 999
Richland, WA 99352

Don Provost
Department of Ecology
State of Washington
Olympia, WA 98504

John Purcell
General Atomics Company
P.O. Box 81608
San Diego, CA 92138

John R. Raymond
Pacific Northwest Labs
P.O. Box 999
Richland, WA 99352

Eberhart Reimers
Dept. of Energy, CS-66, ACT
1000 Independence Ave.
Washington, D.C. 20585

Donald S. Rowe
Rowe & Associates
14400 Bellevue-Redmond Rd.
Bellevue, WA 98007

Alan D. Sapowith
AVCO Systems Division
201 Lowell Street
Wilmington, MA 01887

Walter J. Schaetzle
Univ. of Alabama
P.O. Box 2908
University, AL 35486

Robert I. Schermer
Los Alamos Scientific Lab
Mail Stop 464
Los Alamos, NM 87575

David L. Schreiber
Consultant Hydraulic Engineer
P.O. Box 1087
Coeur d'Alene, ID 83814

David W. Rabenhorst
Applied Physics Laboratory
Johns Hopkins Road
Laurel, MD 20810

Raymond W. Reilly
Pacific Northwest Labs
P.O. Box 999
Richland, WA 99352

John D. Rogers
Los Alamos Scientific Lab
M/S 464
Los Alamos, NM 87545

Neilson Rudd
Dames and Moore
P.O. Box 588 Route 37
Mount Vernon, IL 62864

Harry A. Scarton
Renselear Polytechnical Inst.
Dept. of Mechanical Engineering
Troy, New York 12181

Robert B. Schainker
Electric Power Research Institute
3412 Hillview Ave., P.O. Box 10412
Palo Alto, CA 94303

Neil A. Schilke
General Motors Research Labs
GM Technical Center
Warren, MI 48089

Shosei Serata
Serata Geomechanics
1229 - 8th Street
Berkeley, CA 94710

Sharad K. Singh
Westinghouse Elect. Corp.
R & D Center, Beulah Rd.
Pittsburgh, PA 15235

Henry J. Sneck
Rensselaer Poly. Inst.
Troy
NY 12180

Al Sowards
Fennix & Scisson, Inc.
1401 South Boulder
Tulsa, OK 74119

Robert Steele
Union Carbide Corporation
P.O. Box Y
Oak Ridge, TN 37830

Louis I. Stern
Dames & Moore
Six Commerce Drive
Cranford, NJ 07016

Richard G. Stone
Lawrence Livermore Lab.
P.O. Box 808, L-123
Livermore, CA 94550

Donald J. Supkow
Dames & Moore
Six Commerce Drive
Cranford, NJ 07016

Theodore B. Taylor
Independent Consultant
10325 Bethesda Church Road
Damascus, MD 20750

William Skinner
Dames and Moore
6 Commerce Drive
Cranford, NJ 07016

Warren E. Soderberg
University of Minnesota
319 15th Avenue, S.E.
Minneapolis, MN 55455

Leo R. Spogen, Jr.
Lawrence Livermore Labs
P.O. Box 808
Livermore, CA 94550

David M. Stefonek
Bonneville Power Administration
12th & Penna. Ave, N.W., Rm. 3352
Washington, DC 20461

Katharine L. Stierhoff
Internat District Heating Assoc.
1735 Eye Street, N.W., Suite 611
Washington, DC 20006

James A. Stottlemyre
Pacific Northwest Labs
P.O. Box 999
Richland, WA 99352

James H. Swisher
U. S. Department of Energy
600 E Street NW
Washington, D.C. 20585

Philip A. Thompson
Dept. of Mechanical Engineering
Rensselaer Polytechnic Inst
Troy, NY 12181

Robert L. Thoms
Louisiana State University
Room 42, Atkinson Hall
Baton Rouge, LA 70803

Chin-Fu Tsang
Lawrence Berkeley Laboratory
One Cyclotron Road
Berkeley, CA 94720

David Ullman
Union College
Dept. of Mechanical Engineering
Schenectady, NY 12308

Gunnar E. Walmet
NY State Energy R&D Auth.
Agency Bldg, 2 Rockefeller Plz.
Albany, NY 12223

Howard R. Whitman
C.S. Draper Lab
555 Technology Square
Cambridge, MA 02139

Richard M Winar
Dames and Moore
1550 Northwest Highway
Park Ridge, IL 60068

George E. Wukelic
Battelle/Pacific Northwest Labs
Richland
WA 99352

Frank R. Zaloudek
Pacific Northwest Laboratory
P.O.Box 999
Richland, WA 99352

William F. Thorn
Rocket Research Company
11441 Willo
Redmond, WA 98052

Fred G. Turnbull
General Electric Co.
1 River Road
Schenectady, NY 12301

Steven W. Van Sciver
University of Wisconsin
529 Engr. Res Bldg. 1500 Johnson Dr.
Madison, WI 53706

Matt J. Walton
Minnesota Geological Survey
1633 Eustis St.
St. Paul, MN 55108

David C. Willett
Acres American, Inc.
900 Liberty Bank Bldg.
Buffalo, NY 14202

Thomas J. Wissing
Eaton Corp
P.O. Box 766
Southfield, Mich. 48037

DeMarquis D. Wyatt
National Academy of Sciences
2101 Constitution Ave., N.W.
Washington, DC 20418

☆U.S. GOVERNMENT PRINTING OFFICE: 1981 — 341-060/362

United States
Department of Energy
Washington, D.C. 20585

Official Business
Penalty for Private Use, $300

THIRD – CLASS MAIL
POSTAGE & FEES PAID
U.S. DEPT. OF ENERGY

PERMIT NO. G 20

THIRD CLASS MAIL